

TECHNICAL REPORT 93-22

Kristallin-I Safety Assessment Report

July 1994

TECHNICAL REPORT 93-22

Kristallin-I Safety Assessment Report

July 1994

The majority of the work documented in this report was performed by a project team consisting of E. Curti, R. Klos (both PSI), P. Smith, P. Zuidema (both Nagra) and T. Sumerling (Safety Assessment Management, U.K.).

Numerous other persons also contributed to this work, notably U. Berner, R. Grauer, J. Hadermann (all from PSI) and I.G. McKinley (Nagra), M. Hugi, M. Niemeyer (both Colenco) and D. Galson (Galson Sciences, U.K.).

The project was managed by P. Smith and P. Zuidema. P. Smith was also responsible for coordination of the calculations performed and for editorial work on the report; the overall responsibility for the project was with P. Zuidema.

"Copyright (c) by NAGRA, Wettingen (Switzerland). / All rights reserved.

All parts of this work are protected by copyright. Any utilisation outside the remit of the copyright law is unlawful and liable to prosecution. This applies in particular to translation, storage and processing in electronic systems and programs, microfilms, reproduction, etc."

ABSTRACT

This report presents a comprehensive description of the post-closure radiological safety assessment of a repository for vitrified high-level radioactive waste (HLW), sited in the crystalline basement of Northern Switzerland. The assessment considers a repository concept similar to that described in **Project Gewähr 1985**, but also takes account of a recent synthesis of information from geological investigations. The safety assessment, geological synthesis and an exploration study together form the Kristallin-I project; the last two studies are reported elsewhere. The aims of the Kristallin-I safety assessment are: to re-evaluate the crystalline basement of Northern Switzerland as a host rock for a HLW repository; to improve understanding of the performance of the engineered and geological barriers; to identify key geological characteristics and establish desirable ranges for corresponding parameters; to develop and test a more complete methodology and sets of models and computational tools.

The Kristallin-I safety assessment employs a hierarchy of deterministic calculations to investigate uncertainty in the geological environment and in the performance of the repository. In this, three types of uncertainty are distinguished:

- uncertainty in the selection and combination of relevant features, events and processes (FEPs); this is explored by performing calculations for a Reference Scenario and number of alternative scenarios;
- uncertainty in the way in which important FEPs are modelled; this is explored by performing calculations for a set of Reference Model Assumptions and a number of alternative model assumptions within the Reference Scenario;
- uncertainty in the rate and extent of important FEPs; this is explored by means of variations in the values assigned to model input parameters; parameter variations are performed around a Reference Case, which is based on the Reference Scenario and Reference Model Assumptions.

At each stage, conservatism is introduced. In modelling the Reference Scenario, some FEPs that could be beneficial to safety are not represented. Where alternative models are identified, the model leading to highest consequences is adopted in the Reference Model Assumptions. Data are also selected conservatively in the Reference Case.

The current interpretation of the geological situation indicates that conditions in the crystalline basement can provide a suitable environment for a safe repository for vitrified HLW. The peak annual individual dose calculated for the Reference Case is more than two orders of magnitude below the limit of 0.1 mSv y^{-1} established in Swiss regulatory guidelines and occurs more than 200 000 years after repository closure. All of the scenario, model and parameter variations calculated also lead to doses well below the regulatory guideline.

With the conservative model of geosphere transport appropriate to the current level of uncertainty in the hydrogeological regime and in the characteristics of water-conducting

features in the crystalline basement, the engineered barriers provide the principal constraint on radionuclide release and transport. Indeed, the engineered barriers alone, together with the expected dilution in the near-surface environment, are sufficient to ensure peak doses below the regulatory limit. In this case, the main role of the geological barriers is to provide an environment favouring the longevity and adequate performance of the engineered barriers. Such an environment gives mechanical protection, favourable geochemical conditions and sufficiently low groundwater flows. In future, a more detailed characterisation of the host rock, and of the water-conducting features therein, may allow a less conservative approach to geosphere-transport modelling. It may then be concluded that the host rock forms a very efficient additional safety barrier.

ZUSAMMENFASSUNG

Dieser Bericht enthält eine umfassende Beschreibung der Sicherheitsanalyse für die Nachbetriebsphase eines Endlagers für verglaste hochaktive Abfälle (HAA) im kristallinen Grundgebirge der Nordschweiz. Das in der Sicherheitsanalyse betrachtete Endlagerkonzept ist dem in **Projekt Gewähr 1985** vorgestellten Konzept ähnlich, berücksichtigt aber Informationen einer neuen Synthese der geologischen Untersuchungen. Die Sicherheitsanalyse, die geologische Synthese sowie eine Explorationsstudie bilden zusammen die verschiedenen Komponenten des Projektes Kristallin-I; die zwei letzteren werden in anderen Berichten dokumentiert. Ziele der Sicherheitsanalyse Kristallin-I sind: eine Neubewertung des kristallinen Grundgebirges der Nordschweiz als Wirtgestein für ein HAA-Endlager; ein verbessertes Verständnis für das Verhalten der technischen und geologischen Barrieren; die Evaluation wichtiger geologischer Eigenschaften sowie die Bestimmung von akzeptablen Wertebereichen für entsprechende Parameter; die Prüfung der umfassenderen Methoden, Modellsätze und Rechenprogramme auf ihre Anwendbarkeit für die Sicherheitsanalyse.

Die Sicherheitsanalyse zu Kristallin-I stützt sich auf breite Variationen deterministischer Berechnungen ab, um die Unsicherheiten bezüglich der geologischen Umgebung und dem Endlagerverhalten zu untersuchen. Drei Arten von Unsicherheiten werden dazu unterschieden:

- Unsicherheit in der Auswahl und der Kombination von relevanten Ereignissen und Vorgängen; diese wird anhand von Berechnungen für ein Referenzszenarium und eine Reihe von alternativen Szenarien untersucht;
- Unsicherheit in der Modellierung von wichtigen Ereignissen und Vorgängen; diese wird untersucht, indem Berechnungen für eine Reihe von Referenz-Modellannahmen und alternative Modellannahmen innerhalb des Referenzszenariums durchgeführt werden;
- Unsicherheit bezüglich dem Ausmass wichtiger Ereignisse und Vorgänge; dies wird mit Parameter-Variationen untersucht, vor allem für einen Referenzfall, der auf dem Referenzszenarium und den Referenz-Modellannahmen basiert.

Bei der Analyse wird konservativ vorgegangen: Bei der Modellierung werden vor allem wegen der Limitationen der zur Verfügung stehenden Modelle nicht alle Ereignisse und Vorgänge, die zur Sicherheit beitragen könnten, berücksichtigt und wo alternative Modelle identifiziert werden, wird das Modell mit den grössten Folgen verwendet. Die Inputparameter werden im Falle von Unsicherheiten konservativ ausgewählt.

Die gegenwärtige Interpretation der geologischen Situation zeigt, dass das kristalline Grundgebirge eine Umgebung für ein sicheres Endlager für verglaste HAA bieten kann. Die maximale jährliche Individualdosis, die für den Referenzfall errechnet wurde, liegt mehr als zwei Grössenordnungen unter dem Schutzziel von 0.1 mSv y^{-1} , wie er in den Richtlinien der Schweizer Behörden festgelegt wurde; diese Dosis tritt erst mehr als

200'000 Jahre nach dem Verschluss des Endlagers auf. Auch alle berechneten Variationen der Szenarien, Modelle und Parameter ergeben Dosen, die deutlich unter dem behördlichen Schutzziel liegen.

Bei Verwendung eines konservativen Modells der Geosphäre, das der gegenwärtigen Unsicherheit bezüglich den hydrogeologischen Bedingungen und den Eigenschaften der wasserführenden Systeme im kristallinen Grundgebirge Rechnung trägt, tragen die technischen Barrieren am meisten zur Nuklidrückhaltung bei. Schon die technischen Barrieren allein reichen aus, um das behördliche Schutzziel einzuhalten. Deshalb ist es eine Hauptaufgabe der geologischen Barriere, günstige Bedingungen für die technischen Barrieren zu bieten. Solche Bedingungen umfassen mechanischen Schutz, günstige geochemische Verhältnisse und ausreichend geringe Grundwasserflüsse. In der Zukunft sollte jedoch eine genauere Charakterisierung des Wirtgesteins und der darin enthaltenen wasserführenden Systeme ein weniger konservatives Vorgehen bei der Modellierung des Geosphärentransports erlauben. Dies kann durchaus dazu führen, dass sich die Geosphäre bei einer realistischeren Beschreibung als äusserst effiziente zusätzliche Sicherheitsbarriere erweist.

RÉSUMÉ

Ce rapport présente une description exhaustive de l'analyse de la sûreté radiologique après fermeture d'un dépôt final pour déchets vitrifiés de haute activité (DHA), implanté dans le socle cristallin du Nord de la Suisse. Cette évaluation considère un dépôt final de conception similaire à celle décrite dans le Projet garantie 1985, mais tient en outre compte d'une récente synthèse des informations recueillies lors des investigations géologiques. L'analyse de sûreté, la synthèse géologique et une étude d'exploration constituent ensemble le projet Cristallin I; les deux dernières études mentionnées font l'objet d'autres rapports. Les objectifs de l'analyse de sûreté Cristallin I sont: la réévaluation du socle cristallin du Nord de la Suisse comme roche d'accueil pour un dépôt final pour DHA; l'amélioration de la compréhension du comportement des barrières de sécurité ouvragées et géologiques; l'identification des caractéristiques clés et l'établissement des champs de valeurs acceptables pour les paramètres correspondants; le développement et la mise en application d'une méthodologie plus complète et d'ensembles de modèles et outils de calculs.

L'analyse de sûreté Cristallin I utilise une hiérarchie de calculs déterministiques pour investiguer les incertitudes de l'environnement géologique et du comportement du dépôt final. Pour cela on distingue trois types d'incertitudes:

- incertitudes dans la sélection et la combinaison des éléments caractéristiques significatifs, d'événements et de processus (FEPs); on explore ce domaine en réalisant les calculs pour un Scénario de référence et un nombre de scénarios alternatifs;
- incertitudes au sujet de la façon de modéliser les caractéristiques FEPs importantes; on explore ce domaine en réalisant les calculs pour un ensemble d'Hypothèses pour le modèle de référence et un nombre d'hypothèses pour les modèles alternatifs à l'intérieur du Scénario de référence;
- incertitudes quant à la fréquence et à l'extension d'importants FEPs; on explore ce domaine par la variation des valeurs assignées aux paramètres d'entrée des modèles; les variations de paramètres sont exécutées autour d'un Cas de référence, qui est basé sur le Scénario de référence et les Hypothèses du modèle de référence.

Des éléments de prudence sont introduits à chaque étape. Lors de la modélisation du Scénario de référence quelques caractéristiques FEPs qui pourraient être avantageuses pour la sûreté ne sont pas représentées. Lorsque des modèles alternatifs sont identifiés, celui d'entre eux menant aux conditions les plus sévères est adopté pour les Hypothèses du modèle de référence. Les données sont également sélectionnées avec prudence pour le Cas de référence.

L'interprétation actuelle de la situation géologique indique que les conditions dans le socle cristallin peuvent fournir un environnement adéquat pour un dépôt final sûr pour des déchets DHA vitrifiés. La dose annuelle individuelle de pointe calculée pour le Cas

de référence est située à plus de deux ordres de grandeur en-dessous de la limite de 0.1 mSv y⁻¹ figurant dans les prescriptions suisses et survient plus de 200'000 années après la fermeture du dépôt final. Tous les scénarios, modèles et variations de paramètres calculés mènent également à des doses situées bien en-dessous de celle figurant dans les prescriptions.

Avec le modèle prudent de transport dans la géosphère correspondant au niveau actuel des incertitudes relatives au régime hydrogéologique et aux caractéristiques des éléments aquifères du socle cristallin, les barrières ouvragées constituent l'obstacle principal au relâchement et au transport de radionucléides. En fait les barrières ouvragées, combinées avec la dilution prévue dans l'environnement proche de la surface, suffisent à elles seules pour garantir des doses maximales inférieures à la limite prescrite. Dans ce cas le rôle principal des barrières géologiques est d'assurer un environnement favorisant la longévité et les performances adéquates des barrières ouvragées. Un tel environnement assure une protection mécanique, des conditions géochimiques favorables et un apport d'eau souterraine suffisamment modeste. Dans le futur une caractérisation plus détaillée de la roche d'accueil et de ses éléments aquifères pourrait éventuellement permettre une approche moins entachée de conservatisme sur le plan de la modélisation du transport dans la géosphère. On pourrait alors conclure que la roche d'accueil constitue une barrière de sécurité supplémentaire très efficace.

EXECUTIVE SUMMARY

This report presents a comprehensive description of the post-closure radiological safety assessment of a repository for vitrified high-level radioactive waste (HLW), sited in the crystalline basement of Northern Switzerland. This assessment has been carried out as part of the Kristallin-I project, which also includes a synthesis of information from geological investigations and an exploration study. The Kristallin-I project is a milestone in the Swiss disposal planning programme, formally completing the regional investigation of potential siting areas in the crystalline basement. Engineering feasibility and operational management and safety studies do not form part of Kristallin-I and are not discussed.

The aims of the Kristallin-I safety assessment are:

- To re-evaluate the crystalline basement of Northern Switzerland as a host rock for a high-level radioactive waste repository and, using both moderately conservative arguments and robust arguments, to quantify the levels of safety that can reasonably be expected and can be relied on with confidence.
- To improve understanding of the roles of the engineered and geological barriers through quantitative analysis of their performances, including examination of the sensitivity of performance estimates to uncertainties.
- To make a detailed examination of the potential performance of the geological barriers, to identify key geological characteristics and to establish desirable ranges for corresponding parameters as input to the identification of sites for additional field work.
- To develop and test a more complete safety assessment methodology and an enhanced set of models and computational tools, including a scenario development methodology, new models of specific processes previously identified as important and new assessment computer codes.

The report presents the methodological and information bases, models, calculations and results for the Kristallin-I safety assessment.

In Chapter 1, the planning of the Swiss radioactive-waste management strategy and the milestones of the high-level and long-lived intermediate-level waste (HLW/TRU) programme are described. The aims of the Kristallin-I project and post-closure safety assessment are defined and the organisation of succeeding chapters is given.

In Chapter 2, the general aims of post-closure safety assessment of nuclear waste repositories are presented, with emphasis on specific regulatory protection objectives for a repository in Switzerland. The approach adopted to deal systematically with the unavoidable uncertainties that beset long-term safety assessment is also described, along

with the measures taken to achieve a sufficient level of confidence in the safety assessment. In addition, a brief overview is given of the progress of post-closure safety assessment studies in Switzerland since Project Gewähr 1985.

In Chapter 3, the information base for the Kristallin-I safety assessment is presented. The design performance of the engineered barriers and the expected contribution to long-term safety of the engineered and geological barriers - the Safety Concept - is described. The characteristics of the wastes, engineered barriers, host rock and surface environment are discussed, together with attendant uncertainties, and processes that could potentially affect radionuclide release and transport are identified. Finally, key data for the safety assessment models are presented based on this information.

In Chapter 4, the procedure for collating and screening this information is described, resulting in the identification of a set of safety-assessment calculations that reflects the uncertainty in the performance of the disposal system - Scenario Development. The application of the procedure to the Kristallin-I safety assessment is summarised. Relevant features, events and processes (FEPs) are discussed and a set of safety-assessment calculations is derived. Uncertainty in the selection and combination of relevant FEPs is explored by means of a Reference Scenario and a number of alternative scenarios. Uncertainty in the way in which important FEPs are modelled is explored by means of a set of Reference Model Assumptions and a number of alternative model assumptions within the Reference Scenario. In addition, calculations for a robust demonstration of safety are defined. FEPs that are not taken into account in Kristallin-I safety-assessment models, but would provide additional safety - reserve FEPs - are identified, as are unexpected FEPs that (if they occur) have the potential to compromise safety - open questions.

In Chapter 5, the model-development approach for long-term safety assessment is described, including a discussion of the different levels of detail at which modelling is performed. The underlying Reference Model Assumptions and mathematical formulations are presented for each of the principal assessment models - near field, geosphere and biosphere. The performance of the individual models is illustrated and their sensitivity to parameter variations investigated.

In Chapter 6, the key results relating to the safety of the overall system are presented. Results of model-chain calculations are described for the Reference Scenario, which represents a conservatively defined performance of the engineered barriers and a constant state of the geological barriers and of the surface environment, based on present-day conditions. Within this scenario, the effects of uncertainty in data and in the selection of conceptual models for key elements are investigated. Further model-chain calculations are presented for alternative scenarios, which consider a deep groundwater well, failure of repository seals and a number of climate-related scenarios. Safety is demonstrated by means of a scenario that takes a highly pessimistic view of uncertainties in the properties of the crystalline host rock.

In Chapter 7, key results and conclusions from the Kristallin-I safety assessment are presented. The primary conclusions are as follows:

- The engineered barriers as designed, emplaced in the low-permeability domain of the crystalline basement as currently characterised, can provide a sufficient level of safety. Even using the conservative models that are appropriate to currently available data, the calculated doses are well below the Swiss regulatory guideline of 0.1 mSv y^{-1} .
- A suite of calculations has been carried out that illustrates the effects of uncertainty in the characteristics of the engineered and geological barrier characteristics and in relevant processes that operate therein. Parameter variations have been performed, both for specific system components and for the whole system, and the effect of alternative model assumptions investigated. Alternative scenarios, covering uncertainty in the long-term evolution of the repository and environment have also been considered. The variations evaluated all lead to doses well below the regulatory guideline.
- The roles of the engineered and geological barriers in providing safety are relatively well understood. Uncertainty in the geological information now available requires a highly conservative representation of radionuclide transport in the geosphere; a robust demonstration of safety relies predominantly on the properties of the engineered barriers. The main role of the host rock in this case is to provide a suitable environment for the engineered barriers, i.e. mechanical protection, adequate geochemical conditions, and sufficiently low groundwater flowrates.
- In future, a more detailed characterisation of the host rock and the properties of its water-conducting features may allow a less conservative approach to geosphere-transport modelling. In this case, it may be concluded that the host rock forms a very efficient additional safety barrier. Such a characterisation will also provide information on the spatial and geometrical characteristics of major faults and will allow the repository layout to be optimised to take advantage of the natural safety barrier offered by the host rock.

Regarding confidence in the methodology and calculations that lead to these conclusions, attention is drawn to the following points:

- The scenario development procedure provides a structured and documented path by which the safety assessment calculations performed are justified. A number of reserve FEPs have been identified that could, if required, be mobilised to show even greater margins of safety. A number of open questions have also been identified. Most of these can, if necessary, be avoided by attention to detailed engineered-barrier design and siting. An exception is the effect of human intrusion into the repository; in this case, risk-probability arguments may need to be invoked to meet protection objectives.

- The present calculational tools are adequate, although enhancements could still be made. Codes have been tested and verified, including international intercomparison studies. Confidence has been built in the underlying conceptual models by a variety of means, particularly through the testing of models using data from field and laboratory experiments, and from analogue studies. The model input parameters are traceably derived and are defensible by reference to the underlying scientific data.

Overall it is concluded that, whereas considerable work is still to be done on the detailed characterisation of potential sites and optimisation of a repository layout and engineered barriers at a selected site, the crystalline basement of Northern Switzerland continues to offer good prospects as a host rock for a high-level radioactive waste repository.

TABLE OF CONTENTS

Abstract	I
Zusammenfassung	III
Résumé	V
Executive Summary	VII
Table of Contents.....	IX
1. INTRODUCTION.....	1
1.1 Scope of this Report	1
1.2 Swiss Radioactive Waste Management Planning.....	1
1.3 The HLW/TRU Programme.....	4
1.4 Aims of the Kristallin-I Project and the Safety Assessment	6
1.5 Organisation of this Report	8
2. SAFETY ASSESSMENT - AIMS AND APPROACH.....	11
2.1 Introduction.....	11
2.2 The International View.....	11
2.3 Regulatory Criteria.....	13
2.4 Treatment of Uncertainty	14
2.4.1 Approach in the Kristallin-I Safety Assessment.....	14
2.4.2 Uncertainty in Surface Environment Evolution	16
2.4.3 Treatment of Future Human Actions	17
2.5 Calculational Approach.....	19
2.5.1 Choice of Calculational Approach.....	19
2.5.2 Hierarchy of Calculations in Kristallin-I Safety Assessment	21
2.5.3 Interpretation of Results in relation to the protection objectives.....	25
2.6 Building a Robust Safety Case	25
2.7 Building Confidence in the Assessment.....	26
2.8 Status of Repository Safety Assessment in Switzerland	27
2.8.1 New Information.....	28
2.8.2 Development of Assessment Methodology and Models	28
2.8.3 Improved System Understanding.....	29
3. THE KRISTALLIN-I DISPOSAL SYSTEM.....	31
3.1 Introduction.....	31
3.2 The Safety Concept.....	33
3.3 Arisings of HLW and the Radionuclide Inventory.....	37
3.3.1 HLW Arisings and Vitrification.....	37
3.3.2 Model Radioactive Waste Inventory.....	38
3.3.3 Radionuclide Inventory for Safety Assessment	43
3.4 The Engineered Barriers.....	44
3.4.1 Thermal Constraints on Design	44

3.4.2	The Waste Matrix and Relevant Processes	47
3.4.2.1	Description and Function	47
3.4.2.2	Corrosion of the Glass	47
3.4.3	The Cast Steel Canister and Relevant Processes	48
3.4.3.1	Design and Performance.....	48
3.4.3.2	Steel Corrosion Processes	50
3.4.3.3	Localised Corrosion of the Steel.....	51
3.4.3.4	Hydrogen Evolution from Corrosion	52
3.4.3.5	Other Mechanisms for Evolution of Gas.....	53
3.4.4	The Bentonite Buffer and Relevant Processes.....	54
3.4.4.1	Design and Properties	54
3.4.4.2	Saturation and Swelling.....	54
3.4.4.3	Hydraulic Properties	55
3.4.4.4	The Short-Term Thermal Stability of Bentonite.....	55
3.4.4.5	Long-Term Stability of the Bentonite	56
3.4.4.6	Chemical Reactions with the Canister and Waste Matrix.....	58
3.4.4.7	Mechanical Interactions and Gas Dissipation	59
3.4.4.8	Bentonite Porewater Chemistry	59
3.4.4.9	Microbiological Activity.....	61
3.4.5	Backfill and Seals in Access Tunnels and Shafts	62
3.4.6	Radionuclide Retention and Transport in the Engineered Barriers.....	63
3.4.6.1	Effect of the Canister and Waste Matrix	63
3.4.6.2	Solubility Limits of Radionuclides in Bentonite Porewater.....	63
3.4.6.3	Diffusion and Retardation in Bentonite.....	64
3.5	Geology of the Crystalline Basement of Northern Switzerland.....	66
3.5.1	Introduction.....	66
3.5.2	Regional Geology and Siting.....	67
3.5.3	Water-Conducting Features in the Crystalline Basement.....	70
3.5.4	Hydrogeological Modelling.....	70
3.5.5	Groundwater Chemistry and Radionuclide Sorption	115
3.5.5.1	Groundwater Composition.....	115
3.5.5.2	Derivation of Sorption Constants for Geosphere Transport	115
3.5.5.3	Groundwater Colloids.....	80
3.6	The Surface Environment.....	81
3.6.1	Regional Description.....	81
3.6.2	Climate	82
3.6.3	Soils and the Natural Environment	82
3.6.4	Human Habitation and Economy	82
3.6.5	Land Use and Agriculture	83
3.6.6	Water Resources and Usage.....	83
3.7	Data for the Kristallin-I Safety Assessment Calculations	83
3.7.1	Overview of Safety Assessment Data	83
3.7.2	Inventories of Safety-Relevant Radionuclides	84
3.7.3	Element-Independent Data for the Engineered Barriers	86

3.7.4	Element-Dependent Data for the Engineered Barriers.....	88
3.7.5	Element-Independent Data for the Geological Barriers	89
3.7.5.1	Groundwater Flow Data for the Low-Permeability Domain	92
3.7.5.2	Groundwater Flow Data for the Major Water-Conducting Faults	96
3.7.6	Porosities and Geometrical Data for Water-Conducting Features.....	101
3.7.7	Element-Dependent Properties of the Geological Barriers	103
4.	SCENARIO DEVELOPMENT AND TREATMENT	104
4.1	Approach and Methodology	104
4.1.1	Uncertainty of Future Processes and Events	104
4.1.2	The Scenario Development Procedure.....	105
4.1.3	Application of the Procedure in the Kristallin-I Safety Assessment	108
4.2	The FEP Catalogue for Kristallin-I.....	110
4.2.1	Eliciting the System Understanding	110
4.2.2	Initiating the FEP Catalogue	110
4.2.3	Screening Arguments	111
4.2.4	Developing the System Concept.....	111
4.2.5	Audit Against International Experience	112
4.2.6	The Final FEP Catalogue for the Kristallin-I Assessment	113
4.3	Identification of Scenarios for Kristallin-I.....	118
4.3.1	The Reference Scenario	118
4.3.2	Developing Alternative Scenarios.....	121
4.3.3	FEPs Related to the Engineered Barriers	122
4.3.3.1	Mis-sealed or Unsealed Canister.....	124
4.3.3.2	Poor or Incomplete Emplacement of Buffer.....	124
4.3.3.3	Uncertainty in the Time of Canister Failure.....	124
4.3.3.4	Cracked Canister.....	125
4.3.3.5	Radiolytic Oxidation Front.....	125
4.3.3.6	Sorption and Co-precipitation with Iron Corrosion Products	126
4.3.3.7	Gas Production and Pressurisation	126
4.3.3.8	Release of Radioactive Gases	127
4.3.3.9	Degradation of Bentonite	128
4.3.3.10	Bentonite Erosion	128
4.3.3.11	Canister Sinking.....	129
4.3.3.12	Colloid Transport from the Waste	129
4.3.3.13	Transport along Tunnels and Shafts.....	130
4.3.4	FEPs Related to the Geological Barriers.....	130
4.3.4.1	Mechanisms for Radionuclide Transport.....	130
4.3.4.2	Mechanisms for Groundwater Flow.....	131
4.3.4.3	Transport Path Through the Geological Barriers	132
4.3.4.4	Characteristics of the Water-Conducting Features	133
4.3.4.5	Matrix Diffusion.....	134
4.3.4.6	Radionuclide Sorption.....	135
4.3.4.7	Transport with Groundwater Colloids	135

4.3.4.8	Effect of Repository Construction and Emplacement.....	136
4.3.4.9	Effect of the TRU silos	137
4.3.5	FEPs Related to Long-Term Geological Changes	137
4.3.5.1	Bounding Scenarios for Long-Term Geological Change	137
4.3.5.2	Regional Horizontal Movements	140
4.3.5.3	Regional Vertical Movements	140
4.3.5.4	Movement along Major Faults.....	140
4.3.5.5	Movement along Small-scale Faults.....	141
4.3.5.6	Seismic Activity and Stress Changes	141
4.3.5.7	Erosion and Denudation.....	141
4.3.5.8	Basement Alteration.....	142
4.3.5.9	Magmatic Activity (Plutonism and Volcanism)	142
4.3.5.10	Hydrothermal Activity.....	142
4.3.5.11	Summary of Impacts of Expected Geological Changes	143
4.3.6	FEPs Related to Long-Term Climatic Changes.....	144
4.3.6.1	Bounding Scenarios for Long-Term Climatic Changes.....	144
4.3.6.2	Recharge.....	145
4.3.6.3	Erosion	147
4.3.6.4	Groundwater Chemistry	147
4.3.6.5	Groundwater Discharge Zone	148
4.3.6.6	Permafrost and Ice-Sheet Effects.....	149
4.3.6.7	Climate State and Agricultural Practices.....	149
4.3.7	Human Actions and their Effect.....	150
4.3.7.1	Approach to Human Actions	150
4.3.7.2	Groundwater and Surface Water/Soil Pollution	151
4.3.7.3	Deep Groundwater Abstraction Wells	151
4.3.7.4	Water Management Schemes	151
4.3.7.5	Mining and Deep Drilling	152
4.3.7.6	Geothermal Exploitation	153
4.3.8	Summary of Evaluation and Treatment of Alternative Assumptions.....	154
4.4	Conclusions from Scenario Development for the Kristallin-I Assessment .	162
4.4.1	The Set of Safety Assessment Calculations.....	162
4.4.1.1	The Reference Scenario	162
4.4.1.2	Alternative Model Assumptions Within the Reference Scenario.....	163
4.4.1.3	Parameter Variations Within the Reference Scenario	164
4.4.1.4	Alternative Scenarios	165
4.4.2	Scenario for Robust Safety Demonstration	168
4.4.3	Reserve Features, Events and Processes	169
4.4.4	Open Questions.....	170
5.	REFERENCE MODEL ASSUMPTIONS AND THEIR EVALUATION	178
5.1	Introduction	178
5.1.1	Levels of Modelling	178
5.1.2	The Scope of Safety-Assessment Models in Kristallin-I	179
5.1.3	The Kristallin-I Safety-Assessment Model Chain	179

5.1.4	Definition of Assessment Calculation Cases.....	181
5.2	Near-Field Modelling	186
5.2.1	Model Assumptions	186
5.2.1.1	Features, Events and Processes	186
5.2.1.2	Simplifications and Additional Model Assumptions	189
5.2.2	Mathematical Representation	191
5.2.2.1	Release of Radionuclides from the Waste Matrix.....	193
5.2.2.2	Mass Balance at the Glass-Bentonite Interface and Diffusion through the Bentonite	195
5.2.2.3	Release to the Host Rock.....	196
5.2.3	Reference-Case Results and Model Sensitivity to Parameter Variations ...	196
5.2.3.1	Canister Lifetime.....	205
5.2.3.2	Glass-corrosion Rate.....	209
5.2.3.3	Elemental Solubility Limits.....	210
5.2.3.4	Effects of Shared Solubility Limits with Stable Isotopes	212
5.2.3.5	Sorption Constants in the Bentonite	214
5.2.3.6	Bentonite Thickness	214
5.2.3.7	Groundwater Flowrate at the Bentonite-Host Rock Interface	215
5.2.4	Summary of Near-Field Modelling and Performance.....	217
5.3	Geosphere Modelling	218
5.3.1	Model Assumptions	219
5.3.1.1	Features and Processes.....	219
5.3.1.2	Simplifications and Additional Model Assumptions	220
5.3.2	Mathematical Representation	222
5.3.2.1	Governing Equations.....	222
5.3.2.2	Initial Conditions and Boundary Conditions.....	225
5.3.2.2.1	Initial Conditions.....	225
5.3.2.2.2	Boundary Conditions - Model Conduit.....	225
5.3.2.2.3	Boundary Conditions - Porous Matrix	226
5.3.3	Solutions to the Model Equations.....	227
5.3.3.1	Linear Sorption	227
5.3.3.2	Non-Linear Sorption	227
5.3.3.3	Colloid Facilitated Radionuclide Transport.....	228
5.3.3.4	Simplified Solutions	229
5.3.4	Input Parameters.....	231
5.3.4.1	Advection	231
5.3.4.2	Dispersion.....	238
5.3.4.3	Matrix Diffusion.....	238
5.3.4.3.1	Diffusion Constant	238
5.3.4.3.2	Geometry and Porosity of Diffusion-Accessible Matrix.....	239
5.3.4.4	Sorption on Matrix Pore Surfaces	243
5.3.5	Parameter Uncertainty.....	245
5.3.5.1	The Geosphere Reference Case	246

5.3.5.2	Parameter Variations.....	250
5.3.6	Summary of Geosphere Modelling and Performance.....	257
5.4	Biosphere Modelling	261
5.4.1	Introduction.....	261
5.4.2	Model Assumptions	262
5.4.2.1	Features, Events and Processes	262
5.4.2.2	Simplifications and Additional Model Assumptions	266
5.4.3	Mathematical Representation	268
5.4.3.1	Compartment Model.....	268
5.4.3.2	Exposure pathways	272
5.4.4	Parameters for the Reference-Case Biosphere	273
5.4.5	Biosphere Results and Sensitivity Analysis	273
5.4.5.1	Behaviour of the Reference-Case Biosphere Model.....	273
5.4.5.2	Sensitivity to the Source of Irrigation Water.....	283
5.4.5.3	Sensitivity to Local Aquifer Thickness.....	283
5.4.5.4	Sensitivity to Local Erosion Rate	285
5.4.5.5	Sensitivity to Solid-Liquid Distribution Constants (Kds).....	285
5.4.6	Summary of Biosphere Modelling	287
6.	RESULTS AND THEIR INTERPRETATION	288
6.1	Introduction.....	288
6.2	The Reference Scenario	290
6.2.1	Reference Model Assumptions	290
6.2.1.1	Reference-Case Calculations	291
6.2.1.1.1	Parameter Values for the Reference Case	291
6.2.1.1.2	Reference-Case Results.....	292
6.2.1.1.3	Retention of Radionuclides in the Near field and Geosphere	293
6.2.1.2	Parameter Variations around the Reference Case.....	299
6.2.1.3	Alternative Reference Area for Repository Siting	306
6.2.2	Alternative Model Assumptions	310
6.2.2.1	Matrix Diffusion and Geometrical Representation of Water-Conducting Features	310
6.2.2.2	Radionuclide Migration Path.....	317
6.2.2.3	Sorption on Groundwater Colloids.....	319
6.2.2.4	Groundwater Flowrate Variability	322
6.3	Alternative Scenarios	327
6.3.1	Introduction.....	327
6.3.2	Deep Groundwater Well	327
6.3.3	Tunnel/Shaft Seal Failure	330
6.3.4	Alternative Climate-Related Scenarios.....	334
6.3.4.1	Results for Alternative Climate States	340
6.3.4.2	Climate-induced Changes in Near-Surface Conditions	341
6.4	The Robust Scenario.....	344

6.5	Summary of Results	347
6.5.1	The Reference Scenario	348
6.5.1.1	Reference Model Assumptions	348
6.5.1.1.1	Reference-Case Results	348
6.5.1.1.2	Results of Parameter Variations	348
6.5.1.2	Alternative Model Assumptions	350
6.5.2	Alternative Scenarios	353
6.5.3	The Robust Scenario	353
7.	SUMMARY AND CONCLUSIONS	356
7.1	Introduction	356
7.2	Overall System Performance	357
7.3	Performance of the Engineered and Geological Barriers	361
7.3.1	Relative Importance of Engineered Barriers, Geological Barriers and Biosphere.....	361
7.3.2	Performance of the Engineered Barriers	362
7.3.3	Performance of the Geological Barriers	364
7.3.4	Reserves of Performance in the Safety Case	365
7.4	Preferred Geological Characteristics of a Potential Site	366
7.4.1	Key Host-Rock Characteristics	366
7.4.2	Host-Rock Characteristics Providing a Favourable Environment for the Engineered Barriers.....	367
7.4.3	Host-Rock Characteristics Providing Adequate System Performance, Assuming Poor Performance of the Engineered Barriers.....	368
7.5	Safety Assessment Methods, Tools and Data.....	369
7.5.1	Developments in Methods and Tools for the Safety Case.....	369
7.5.2	Developments in Supporting Models and Databases	370
7.6	Building Confidence in Kristallin-I Assessment Conclusions	371
7.6.1	Introduction	371
7.6.2	Longevity of the Bentonite.....	373
7.6.3	Confidence in the Selection of Solubility Limits	374
7.6.4	Geosphere Transport Modelling	376
7.7	Suitability of the Crystalline Basement of Northern Switzerland	377
8.	REFERENCES.....	379

List of Figures

Fig.1.2.1: Overview of the sources of radioactive waste in Switzerland and the waste-management concepts considered

Fig. 13.1: Programme of planning for the disposal of high-level and long-lived intermediate-level waste (HLW/TRU)

- Fig. 2.5.1: The hierarchy of calculations performed in the Kristallin-I safety assessment, with the Reference Case indicated by shading
- Fig. 3.1.1: Possible layout for a deep repository for high-level and long-lived intermediate-level waste (HLW/TRU) in the crystalline basement of Northern Switzerland
- Fig. 3.2.1: The system of safety barriers for disposal of HLW in the crystalline basement of Northern Switzerland
- Fig. 3.3.1: Calculated total alpha and total beta-gamma activity content of the overall inventory
- Fig. 3.3.2: Calculated radiogenic heat output of a single flask of waste type WA-COG-1 as a function of time after unloading of fuel from the reactor
- Fig. 3.4.1: The engineered barrier system considered in the Kristallin-I safety assessment
- Fig. 3.4.2: Calculation of temperature evolution within the engineered barrier system
- Fig. 3.4.3: The Nagra reference cast steel canister for disposal of vitrified HLW
- Fig. 3.5.1: (a): the region of Northern Switzerland investigated in the regional field programme; (b): the locations of two potentially suitable siting areas in the crystalline basement, Area West and Area East
- Fig. 3.5.2: Principal tectonic units of Northern Switzerland and adjacent areas
- Fig. 3.5.3: Schematic section through the crystalline basement of Northern Switzerland in Area West, showing the main structural components affecting repository siting and groundwater flow
- Fig. 3.5.4: Water-conducting features in the crystalline basement, as observed in reality and as simplified for transport modelling
- Fig. 3.5.5: Schematic representation of the relationship between the hydrogeological conceptual model and numerical models of groundwater flow at regional, local and block (site) scales
- Fig. 3.5.6: Idealised meshes of major faults for groundwater flow modelling of Area West, based on a knowledge of the orientation of the main groups of first- and second-order faults
- Fig. 3.5.7: Two models for groundwater-flow of Area West
- Fig. 3.7.1: Derivation of input parameters for the near-field and geosphere models from the results of groundwater flow modelling of the low-permeability domain (LPD) of the crystalline basement in Areas West and East
- Fig. 3.7.2: Derivation of input parameters for the geosphere model from the results of groundwater flow modelling of major water-conducting faults (MWCF) within the crystalline basement
- Fig. 4.1.1: The central role of the scenario development procedure for a given repository design and a given database
- Fig. 4.1.2: The handling of FEPs in the Kristallin-I scenario development
- Fig. 4.2.1: Example of an influence diagram for one safety-relevant feature of the Kristallin-I disposal system - the vitrified waste form
- Fig. 4.3.1: Main features and processes considered in the Reference Scenario for Kristallin-I. (See also Section 3.2)
- Fig. 5.1.1: The Kristallin-I safety-assessment model chain (codes STRENG, RANCHMD and TAME) and supporting models
- Fig. 5.2.1: Modelling of the repository near field

- Fig. 5.2.2: Reference-Case radionuclide release rates from the near field (total repository) as a function of time
- Fig. 5.2.3: Maximum near-field release rates for selected radionuclides in the Reference Case and their sensitivity to parameter variations
- Fig. 5.2.4: The effect of solubility limit, S_E , on (a) the radionuclide concentration at the inner-boundary of the bentonite and (b) the release rate from the near field
- Fig. 5.2.5: The effect on the release rate from the near field of the sharing of solubility limits between stable isotopes and radio-isotopes, illustrated for the cases of (a) ^{79}Se and (b) ^{107}Pd
- Fig. 5.2.6: The effect of groundwater flowrate at the bentonite-host rock interface on radionuclide release from the near field
- Fig. 5.3.1: The dual-porosity transport model
- Fig. 5.3.2: Schematic representation of colloid facilitated transport
- Fig. 5.3.3: Geological, hydrogeological and hydrochemical input for geosphere transport modelling
- Fig. 5.3.4: Illustration of the water-conducting features intersected by the repository area and a geometrical description of the internal structure of the features
- Fig. 5.3.5: Alternative geometrical representations of the internal structure of water-conducting features
- Fig. 5.3.6: Retardation factor $R_p^{(i)}$ for matrix diffusion as a function of radio-Cs concentration $C_p^{(i)}$, with sorption modelled by a modified Freundlich isotherm
- Fig. 5.3.7: Comparison of Reference-Case geosphere results with simplified analytical solutions
- Fig. 5.3.8: Maximum annual individual dose from ^{79}Se for each of the geosphere parameter variations
- Fig. 5.3.9: Maximum annual individual dose from ^{99}Tc for each of the geosphere parameter variations
- Fig. 5.3.10: Maximum annual individual dose from ^{135}Cs for each of the geosphere parameter variations
- Fig. 5.3.11: Maximum annual individual dose from ^{237}Np for each of the geosphere parameter variations
- Fig. 5.3.12: Time development of the normalised ^{135}Cs flux from the geosphere low-permeability domain for each of the six geometric representations of the water conducting features
- Fig. 5.4.1: Schematic illustration of the reference biosphere region, indicating the main physical features and listing the exposure pathways considered in the calculations of annual individual dose
- Fig. 5.4.2: General arrangement of the compartments for a generic representation of the biosphere
- Fig. 5.4.3: Schematic representation of the exposure pathways modelled, indicating connections to the compartments in the dynamic part of the model (Figure 5.4.2), which act as sources for dose via ingestion or inhalation of contaminated material, or by direct γ -irradiation
- Fig. 5.4.4: Water-flux mass balance for the Kristallin-I Reference Case biosphere

- Fig. 5.4.5: Solid-material-flux mass balance for the Kristallin-I Reference-Case biosphere
- Fig. 5.4.6: Annual individual dose in the Kristallin-I Reference Case and in the hypothetical case of a constant geosphere release
- Fig. 5.4.7: Contribution of different exposure pathways to dose for individual radionuclides that contribute most to total dose at different times in the Kristallin-I Reference Case
- Fig. 5.4.8: Sensitivity of calculated dose to the source of irrigation water
- Fig. 5.4.9: Variation in the contribution of different exposure pathways for ^{135}Cs as a result of changing the source of irrigation water
- Fig. 5.4.10: Sensitivity of calculated dose to variation of the erosion rate
- Fig. 5.4.11: Sensitivity of calculated dose to variation of the solid-liquid distribution constants
- Fig. 6.2.1: Time development of the annual individual doses in the Reference Case and in the hypothetical case of direct release of radionuclides from the near field to the biosphere
- Fig. 6.2.2: (a), the release rate of ^{135}Cs from different components of the near field and (b), the distribution of inventory between these components as a function of time
- Fig. 6.2.3: (a), the release rates of ^{237}Np from different components of the near field and (b), the distribution of inventory between these components as a function of time
- Fig. 6.2.4: Time development of the annual individual doses in the Reference Case and in a parameter variation with "conservative" solubility limits
- Fig. 6.2.5: Time development of the annual individual doses in the extreme case of a combination of "conservative" near-field parameters
- Fig. 6.2.6: Time development of the annual individual doses for a repository located in Area East, with release in the Rhine valley; present-day climate and subsistence agriculture
- Fig. 6.2.7: Time development of the annual individual doses for a repository located in Area East, with release to a tributary valley of the Rhine; present-day climate and subsistence agriculture
- Fig. 6.2.8: Time development of annual individual dose for the six alternative representations of the geometry of water-conducting features
- Fig. 6.2.9: Comparison of the maximum annual individual doses arising from all the safety-relevant radionuclides for the three different representations of the internal geometry of water-conducting features (with unlimited matrix diffusion)
- Fig. 6.2.10: The effect of explicit consideration of transport in major water-conducting faults
- Fig. 6.2.11: The ratios of radionuclide flux maxima out of and into a geosphere model conduit ($F_{out}^{(i,max)}/F_{in}^{(i,max)}$) as a function of transit time to radionuclide half-life ratio ($T^{(i)}/T_{1/2}^{(i)}$), for transport through the low-permeability domain and for transport through major water-conducting faults
- Fig. 6.2.12: The effect of colloid-facilitated transport, assessed for each of the six representations of water-conducting feature geometry, for the $4N + 1$ chain ($^{237}\text{Np} \rightarrow ^{233}\text{U} \rightarrow ^{229}\text{Th}$)
- Fig. 6.2.13: (adapted from Figure 10-4 in THURY et al. 1994): Cumulative distribution of transmissive-element flowrate for the "sparse" hydrogeological model

- Fig. 6.2.14: Analysis of the effects of flowrate variability
- Fig. 6.3.1: Time development of annual individual dose for a scenario in which, rather than migrating through the low-permeability domain of the host rock, radionuclides migrate either (a) along the repository shaft backfill, or (b) through the excavation-disturbed zone surrounding a shaft
- Fig. 6.3.2: Comparison of the Reference Case, the case of transport through the shaft backfill and transport through the excavation-disturbed zone (EDZ)
- Fig. 6.3.3: Schematic representation of the water and solid-material fluxes used to model the Dry Climate State and the Humid Climate State (and the Reference Scenario; see also Figures 5.4.4 and 5.4.5)
- Fig. 6.3.4: System of compartments and water and solid-material fluxes used to represent of the Periglacial Climate State
- Fig. 6.3.5: Comparison of the results of the Reference Case (temperate climate) with those of the Dry Climate State and Humid Climate State
- Fig. 6.3.6: Doses arising in the Periglacial Climate State
- Fig. 6.3.7: Comparison of the results for Reference Case, with those for scenarios in which the gravel deposits are removed
- Fig. 6.4.1: Time development of annual individual doses in the Robust Scenario
- Fig. 6.5.1: The effect of varying the assumed groundwater flowrate on radiological impact
- Fig. 6.5.2: The effect of alternative assumptions regarding the geometrical representation of water-conducting features on radiological impact
- Fig. 6.5.3: The effect on radiological impact of alternative climate-related scenarios
- Fig. 7.2.1: Results of the Kristallin-I Reference-Case Calculations - annual individual dose as a function of time after repository closure
- Fig. 7.2.2: Results of the Kristallin-I safety assessment, compared those of other recent assessments
- Fig. A1.1: *Regions of Significance* for graphical results in the Kristallin-I assessment. Reference-Case results, showing the contributions of the actinide chains and activation/fission products to the overall radiological impact of the disposal
- Fig. A1.2: Results of the Kristallin-I Reference-Case calculations; annual individual dose as a function of time after repository closure
- Fig. A3.1: Kristallin-I directory structure and commands
- Fig. A3.2: The Kristallin-I log-file

List of Tables

- Tab. 1.2.1: The nuclear power plants currently operating in Switzerland
- Tab. 2.4.1: Summary of Conclusions from the NEA Working Group on Future Human Actions
- Tab. 2.5.1: Calculational approach in selected recent performance assessments of deep underground disposal of radioactive waste
- Tab. 3.3.1: Characteristics of a single flask of vitrified HLW - waste type WA-COG-1
- Tab. 3.3.2: Comparison of the glass composition by weight (%) of waste type WA-COG-1, as predicted by the Nagra model, with that given in the COGEMA specification

- Tab. 3.3.3: Average radionuclide content of a single HLW flask of waste type WA-COG-1 at reference time of vitrification - 4 years after unloading of fuel
- Tab. 3.4.1: Material inventory in the engineered barriers (per canister)
- Tab. 3.4.2: Bentonite porewater compositions calculated by modelling the interaction of two groundwaters, one representative of less saline and one of more saline groundwaters, with bentonite and accounting for reducing conditions due to iron corrosion products
- Tab. 3.4.3: Summary of the main considerations involved in the selection of solubility limits for specific elements
- Tab. 3.5.1: Features the crystalline basement of Northern Switzerland, together with those of adjacent and overlying sedimentary formations
- Tab. 3.5.2: Reference groundwater chemistries for the crystalline basement of Northern Switzerland
- Tab. 3.7.1: Inventories, activities and half-lives of safety-relevant radionuclides and inventories of stable isotopes of the same elements
- Tab. 3.7.2: Data for modelling of radionuclide release and transport in the engineered barriers - glass corrosion, geometry, canister failure, bentonite properties and water flow through repository
- Tab. 3.7.3: Element-dependent parameter values for modelling of radionuclide release and transport in the near field - solubility limits and sorption constants
- Tab. 3.7.4: Geometric and hydrogeological modelling results for safety assessment of Area West
- Tab. 3.7.5: Geometric and hydrogeological modelling results for safety assessment of Area East
- Tab. 3.7.6: Reference-Case assessment model parameters related to groundwater flow
- Tab. 3.7.7: Geometrical data and porosities for the three types of water-conducting features
- Tab. 3.7.8: Sorption constants and isotherm parameter values for modelling of radionuclide transport in the geosphere
- Tab. 4.2.1: Screening arguments for the Kristallin-I scenario development and examples of FEPs that were screened out by them
- Tab. 4.2.2: Features, events and processes (FEPs) considered in the Kristallin-I scenario development
- Tab. 4.3.1: Example section of a table which provides a map between relevant FEPs and the assumptions of the assessment model for the Reference Scenario, and identifies cases where alternative assumptions might be made
- Tab. 4.3.2: Bounding Scenarios for long-term geological change
- Tab. 4.3.3: Bounding Scenarios for long-term climatic change
- Tab. 4.3.4: Key Reference Model Assumptions and assumptions of the Reference Scenario, with possible alternative assumptions and their evaluation and consequent treatment in Kristallin-I safety assessment
- Tab. 4.4.1: Summary of scenarios for quantitative evaluation in Kristallin-I
- Tab. 4.4.2: Features, events and processes, not included in Kristallin-I assessment models, that might provide additional safety - reserve FEPs
- Tab. 4.4.3: Open questions identified from the scenario development process and comments on present assumptions and possible future work

- Tab. 5.1.1: Summary of the main features and processes represented in the Kristallin-I safety assessment model chain
- Tab. 5.1.2: A summary of calculations aimed at developing an understanding of the near-field, geosphere and biosphere models by means of parameter variations
- Tab. 5.1.3: A summary of calculations aimed at assessing repository performance
- Tab. 5.2.1: The near-field model and main parameters
- Tab. 5.2.2: Near-field parameters for Reference-Case and near-field sensitivity analysis calculations
- Tab. 5.2.3: Maximum releases, expressed as annual individual doses [mSv y^{-1}] (drinking-water consumption)
- Tab. 5.2.4: Data to assess for which elements the effects of solubility limits shared with stable isotopes from the waste are likely to be important
- Tab. 5.3.1: Parameters describing three alternative representations of the internal geometry of water-conducting features, spanning the variability observed in cores and surface exposures
- Tab. 5.3.2: Advection velocities u in the water-conducting features of the low-permeability domain (LPD) and major water-conducting faults (MWCF) for each of the three alternative geometrical representations described in Table 5.3.1
- Tab. 5.3.3: Parameters of the transport-model conduit and adjacent porous matrix (see Figure 5.3.1), used in the calculation of radionuclide transport through the six geometrical representations of water-conducting features
- Tab. 5.3.4: Geosphere model assumptions and parameters for Reference-Case calculations
- Tab. 5.3.5: Comparison of maximum annual individual doses, summed over all safety-relevant radionuclides, for the six geometrical representations of the water-conducting features of the low-permeability domain
- Tab. 5.3.6: Geosphere parameter variations, the geosphere transport processes which they affect and the associated dataset names
- Tab. 5.4.1: Summary of the biosphere scenarios considered
- Tab. 5.4.2: Data for the Kristallin-I Reference-Case biosphere
- Tab. 5.4.3: Water fluxes defined in the Reference-Case biosphere model (See Figure 5.4.4)
- Tab. 5.4.4: Solid-material fluxes defined in the Reference-Case biosphere model
- Tab. 5.4.5: Solid-liquid equilibrium distribution constants (K_d values) for the modelling of the biosphere in Kristallin-I
- Tab. 5.4.6: Processes considered and characteristic times (in years) for transport between compartments in the Reference-Case biosphere model
- Tab. 6.1.1: Structure of calculations performed in the Kristallin-I safety assessment
- Tab. 6.2.1: Principal near-field parameter values for Reference-Case calculations
- Tab. 6.2.2: Principal near-field parameter values for Reference-Case calculations
- Tab. 6.2.3: Summary of doses in the Reference Case
- Tab. 6.2.4: The percentage of the inventory of each radionuclide decaying within the near field (η_N) and the near field and geosphere combined (η_F)
- Tab. 6.2.5: Selected results from calculations investigating sensitivity of near-field and geosphere releases to parameter variations
- Tab. 6.2.6: Selected results from calculations investigating sensitivity of biosphere parameter variations

- Tab. 6.2.7: Combination of "conservative" near-field parameter values
- Tab. 6.2.8: Comparison of the biosphere parameters values used for the Rhine-valley (Reference-Case) biosphere and the tributary-valley biosphere
- Tab.6.2.9: Model Assumptions for the geological environment and for geosphere transport modelling and alternative model assumptions for which further calculations have been made
- Tab. 6.2.10: Variable parameters and dataset names for model-chain calculations exploring the effects of different representations of the geometry of water-conducting features and of limited matrix diffusion
- Tab. 6.2.11: Selected geosphere parameters for calculations illustrating the effects of explicit consideration of transport processes in major water-conducting faults
- Tab. 6.2.12: Groundwater flowrates for calculations used to illustrate the effects of flowrate variability
- Tab. 6.3.1: Alternative scenarios considered quantitatively
- Tab. 6.3.2: Summary of the potential radiological impact of drinking water from a deep well capturing all radionuclides released from the repository
- Tab. 6.3.3: Parameters for modelling transport along either the shaft or the surrounding excavation-disturbed zone (EDZ) for a scenario in which the shaft seals fail
- Tab. 6.3.4: Alternative climate-related scenarios
- Tab. 6.3.5: Parameter values used in the mass-balance schemes for modelling the Dry Climate State and Humid Climate State
- Tab.6.3.6: Summary of parameter values used for water and solid-material fluxes in modelling the Periglacial Climate State
- Tab. 6.4.1: Near-field and geosphere parameters for calculations within the Robust Scenario
- Tab. 6.5.1: Alternative model assumptions for geosphere transport and calculated maximum annual individual doses
- Tab. 6.5.2: Calculated maximum annual individual doses for the Reference Scenario and alternative scenarios
- Tab. A2.1: Dose index, defined as the ratio of drinking water dose to the regulatory guideline of 0.1 mSv y^{-1} , calculated for the activation/fission products
- Tab. A2.2: The radionuclides selected for consideration in the Kristallin-I assessment
- Tab. A4.1: Summary of the radionuclides considered in the Kristallin-I assessment runs
- Tab. A4.2: Dataset names for near-field calculations
- Tab. A4.3: Job matrix for the Kristallin-I near-field calculations. Each parameter is assigned a number (1-5). The letter (A-F) assigned to a particular parameter value corresponds to that in the parameter combinations of Table A4.2
- Tab. A4.4: Datasets for geosphere calculations
- Tab. A4.5: Job Matrix for the Kristallin-I geosphere calculations
- Tab. A4.6: Summary of calculations performed in the Kristallin-I assessment
- Tab. A6.1: Conversion factors based on the drinking-water dose per unit activity released directly to a gravel aquifer in the valley of the Rhine
- Tab. A7.1: Parameter values characterising the human behaviour and practices in the Reference-Case biosphere
- Tab. A7.2: Uptake and accumulation factors in the TAME exposure pathway model
- Tab. A7.3: Radionuclide half-life and dosimetric data

List of Appendices

- Appendix 1 Conventions for presentation of graphical results
- Appendix 2 Selection of Safety-Relevant Radionuclides
- Appendix 3 Quality Assurance and Traceability
- Appendix 4 Naming Conventions for Data sets
- Appendix 5 Quantification of near-field and geosphere performance
- Appendix 6 Dose conversion factors for near-field calculations
- Appendix 7 Generic Biosphere Data
- Appendix 8 Simplified analytical solutions for geosphere transport
- Appendix 9 The effect of a non-uniform flow around the bentonite

1. INTRODUCTION

1.1 Scope of this Report

This report presents a comprehensive description of the post-closure radiological safety assessment of a repository for vitrified high-level radioactive waste (HLW¹), sited in the crystalline basement of Northern Switzerland. This assessment has been carried out as part of the Kristallin-I project, which also includes a synthesis of information from geological investigations and an exploration planning study (THURY et al. 1994). The Kristallin-I project is a milestone in the Swiss HLW disposal planning programme, formally completing the regional investigation of the crystalline basement. Engineering feasibility and operational-safety studies do not form part of Kristallin-I and are not discussed in this report.

The following sections in this chapter discuss Swiss radioactive waste management planning, the milestones of the high-level and long-lived intermediate-level waste² (HLW/TRU) programme and the aims of the Kristallin-I project and post-closure safety assessment. Succeeding chapters present and discuss the methodology, information base, models, calculated results and conclusions of the Kristallin-I safety assessment.

1.2 Swiss Radioactive Waste Management Planning

Radioactive waste in Switzerland arises from the operation of nuclear power plants, from the fuel cycle of the power plants and from medicine, industry and research. With respect to waste volume, the planning of the waste management strategy is based on the arisings from the power plants currently operating (see Table 1.2.1), assuming a 40-year operational lifetime; this corresponds to a total nuclear power production of approximately 120 GW(e) years.

In Switzerland, the producers of radioactive waste are responsible for its safe management and disposal. With a view to carrying out their waste disposal responsibilities, the electricity supply utilities, which operate the nuclear power plants, and the Federal Government, which is responsible for the waste arising from medicine, industry and research, set up the National Cooperative for the Disposal of Radioactive Waste (Nagra) in 1972. Nagra is responsible for research and development work

¹ The German term, used in Switzerland, is HAA (hochaktive Abfälle).

² Long-lived intermediate-level waste, termed in German LMA (langlebige mittelaktive Abfälle), is broadly similar to the waste category referred to as TRU - transuranic-containing waste - even though the transuranics may not be the most safety-relevant radionuclides in such waste.

associated with final disposal. Other aspects of the waste management process, such as conditioning and interim storage, remain the responsibility of the individual waste producers or of organisations set up by the producers specifically for these purposes.

Plant	Reactor type	In operation since	Net power capacity [†] MW(e)
Beznau I	PWR	1969	350
Beznau II	PWR	1971	350
Mühleberg	BWR	1972	355
Gösgen	PWR	1979	940
Leibstadt	BWR	1984	990

Notes: † Status, January 1994.

BWR = boiling-water reactor, PWR = pressurised-water reactor.

Table 1.2.1: The nuclear power plants currently operating in Switzerland.

The current plan foresees the reprocessing of spent fuel abroad and the return of the resulting wastes to Switzerland. However, the option of direct disposal of spent fuel is kept open and incorporated into the planning of disposal strategies.

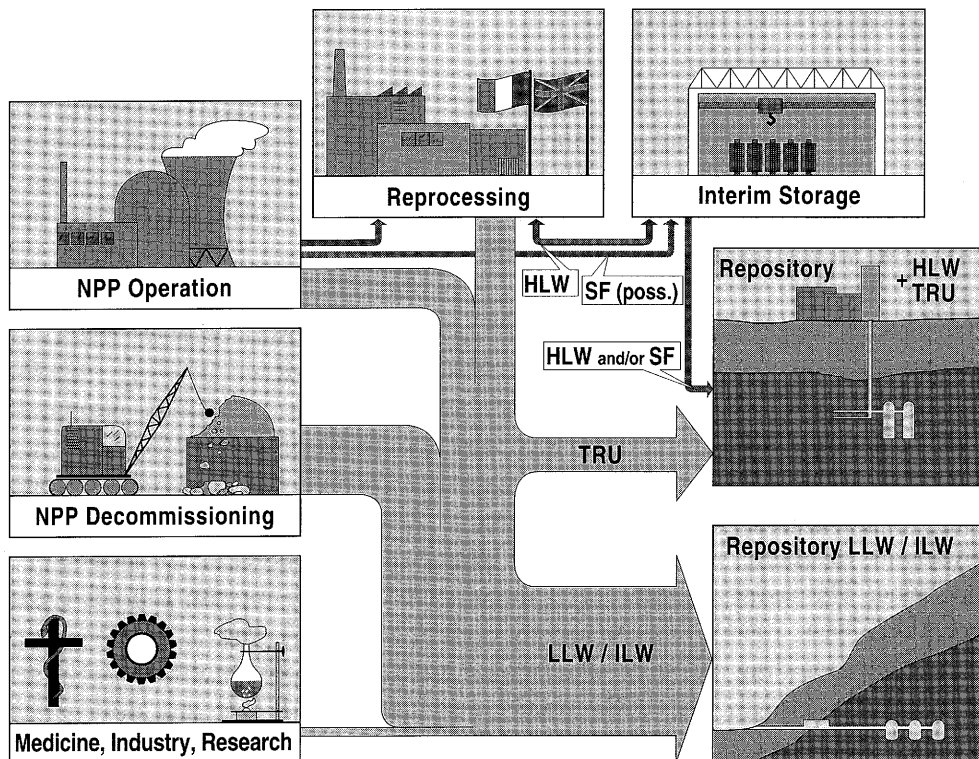
Two types of repository are foreseen:

- A L/ILW repository for low- and intermediate-level waste arising from the operation and decommissioning of Swiss nuclear power plants, from medicine, industry and research and low-level technological waste from reprocessing. The repository will consist of mined caverns with horizontal access, located in a suitable host rock. Wellenberg has been proposed as the site for this repository and the relevant application for a general licence has been submitted to the Federal Government on 29th June 1994. On 17th June 1994, a company was founded (GNW- "Genossenschaft für nukleare Entsorgung Wellenberg") that is responsible for construction and operation of the L/ILW repository.
- A HLW/TRU repository for vitrified high-level and long-lived intermediate-level waste, primarily resulting from fuel reprocessing, and for possible direct disposal of spent fuel elements. The repository will be located in a deep geological formation and will consist of a drift system for HLW or spent fuel and silos for long-lived

intermediate-level waste, with access via vertical shafts. In addition to the plan to dispose of these wastes within Switzerland itself, the option of disposal within the framework of foreign or international projects is also kept open.

Prior to disposal, HLW and spent fuel will be held in interim storage for a period of at least 40 years, in order to allow heat production from the waste to decrease. Because of the obligation to accept back waste from reprocessing abroad, completion of a centralised interim storage facility is a matter of high priority. The power plant operators have therefore set up the ZWILAG organisation, which is responsible for constructing and operating such a facility on a site near to the Paul Scherrer Institute, Würenlingen. In Summer 1993, the Federal Government granted a general licence for the interim storage project, but this decision still requires ratification by the Swiss Parliament. It is planned that the interim storage facility will become operational in 1998. The repository for high-level waste and spent fuel will not be required before the year 2020 at the earliest.

An overview of the sources of waste in Switzerland and the disposal concepts considered is presented in Figure 1.2.1. More detailed information on the organisation of nuclear waste disposal in Switzerland is given in NAGRA (1992).



Notes: NPP = nuclear power plant, HLW = high-level waste, TRU = transuranic-containing waste (long-lived intermediate-level waste; see footnote in text), ILW = intermediate-level waste, LLW = low-level waste, SF = spent fuel.

Figure 1.2.1: Overview of the sources of radioactive waste in Switzerland and the waste-management concepts considered.

1.3 The HLW/TRU Programme

The programme of planning for the disposal of HLW/TRU is shown schematically in Figure 1.3.1; work up to the end of the current decade can be summarised as follows:

- **Preparatory work:** As early as 1978, the Swiss electricity supply utilities and Nagra formulated the key aspects of the Swiss nuclear waste management concept in a landmark report (VSE et al. 1978). Both sediments (e.g. clay, marl, salt, anhydrite) and crystalline formations were identified as potential host rocks.
- **Project Gewähr 1985:** This Project (NAGRA 1985) was the result of a legal requirement to demonstrate the feasibility of safe disposal of all categories of radioactive waste, which was made a precondition to the further operation of existing nuclear power plants and the licensing of new plants (Federal Government Ruling on the Atomic Act, 1978). The host rock selected for examination in Project Gewähr 1985 for the disposal of HLW was the crystalline basement of Northern Switzerland and a regional field investigation programme, including seven deep boreholes and seismic surveys, was launched in the early 1980s. The deadline for submitting Project Gewähr 1985 fell before the completion of all field work (the Siblingen borehole was completed in 1989) and hence it was not possible to integrate a full interpretation of all geological data into the project.
- **Kristallin-I project:** The Kristallin-I project completes the evaluation of data collected in the regional field investigation programme and presents the results in the form of a synthesis. The project also includes an updated assessment of the post-closure safety of a HLW repository sited in the crystalline basement (cf. Section 1.4); the assessment forms the subject of this report.
- **Sediment study (interim reports 1988 and 1990, status review 1994):** In its decision on Project Gewähr 1985, which was handed down in 1987, the Federal Government required that sediments be investigated as alternative potential host rocks for the disposal of HLW. On the basis of existing data (from both its own and other programmes), Nagra's first step was to screen potential host-rock options and, as a result, Opalinus Clay (OPA) and the Lower Freshwater Molasse (Untere Süsswasser Molasse - USM) were identified as potential sedimentary host formations. The work carried out is documented in two interim reports (NAGRA 1988c; NAGRA 1991). The favoured option was OPA and a field-investigation programme, including seismics, was carried out for this potential host rock (seismic campaign 1991/1992). The USM option was also investigated in a desk study and with supplementary field data (e.g. Burgdorf geothermal field, Bassersdorf geothermal borehole). As part of the status review of 1994 (NAGRA 1994), the selection of the OPA as the favoured sediment option was confirmed by both Nagra and the authorities, with the USM being kept as a reserve option.

Programme fo HLW and TRU: Milestones

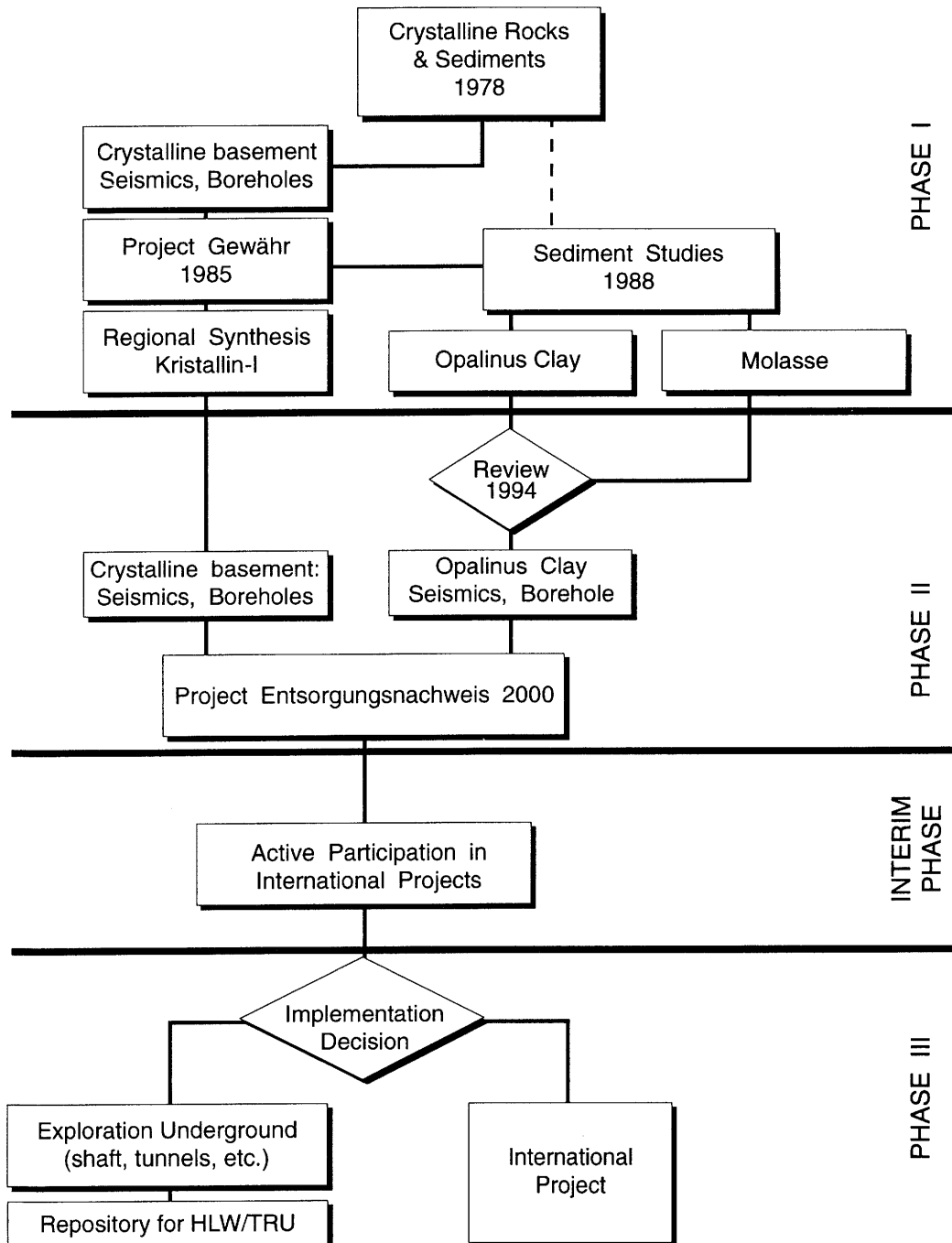


Figure 1.3.1: Programme of planning for the disposal of high-level and long-lived intermediate-level waste (HLW/TRU). The programme consists of three phases, in which initial regional studies (Phase I) lead to a more detailed investigation from the surface of a limited area (Phase II) and, eventually, underground characterisation of a potential site (Phase III).

- **Demonstration of siting feasibility (Standortnachweis):** Project Gewähr 1985 demonstrated the engineering feasibility and the safety of a repository, but the existence of sufficiently large blocks of crystalline basement with suitable properties was not demonstrated to the satisfaction of the authorities. The "Standortnachweis" (demonstration of siting feasibility) for the crystalline host-rock option is therefore still outstanding.
- For the sediment option, none of the three components (engineering feasibility, safety and the existence of a suitable site), which together make up an overall demonstration of disposal feasibility ("Entsorgungsnachweis") have been explicitly demonstrated as yet, although initial investigations of engineering feasibility and evaluation of long-term safety have been performed. Because of its homogeneity, there is a good possibility that the geological data necessary for a "Standortnachweis" in the case of the OPA option can be extrapolated from a relatively limited field programme (i.e. a single borehole and a seismic survey).

It is Nagra's intention to supplement the geological databases for both the crystalline basement and the OPA with further field work and, by the year 2000, to complete projects aimed at providing an overall demonstration of disposal feasibility for either one or both of the host-rock options. These will be considered by the authorities, who will be responsible for assessing whether "Standortnachweis" has been achieved. As a complement to this, studies are continuing on the feasibility and post-closure safety of disposal of long-lived intermediate-level waste and spent fuel.

Realisation of a repository for high-level waste, spent fuel and long-lived intermediate-level waste is foreseen by 2020 at the earliest. In the period between "Standortnachweis" and actual construction of the repository, the possibility of disposal within the framework of international or other national programmes will be examined in more detail.

1.4 Aims of the Kristallin-I Project and the Safety Assessment

The main objectives of the Kristallin-I project are as follows:

- To update and complement Project Gewähr 1985, with extended databases (particularly from the geological exploration), improved safety assessment tools and models, and further work on "open issues" identified in Project Gewähr 1985 and arising from its review by the authorities.
- To serve as a milestone in the HLW programme, formally completing Phase I by selection of areas for siting demonstration ("Standortnachweis"), developing a programme for Phase II field work and providing the background for a comparison of crystalline and sedimentary host rock options.

- To provide input for overall waste management planning, forming a benchmark for assessing inventory variants (vitrified HLW, spent fuel, various types of long-lived ILW) and design alternatives, allowing applied research and development priorities to be re-assessed in the context of integrated performance assessment and contributing to public information on the project.

The Kristallin-I project has three main components: a geological synthesis (THURY et al. 1994), a post-closure safety assessment (presented in this report) and an exploration planning study (THURY et al. 1994, Chapter 11). An overview of the entire Kristallin-I project is given in NAGRA (1994). The assessment consists of an evaluation of the post-closure safety of a HLW repository located in the crystalline basement of Northern Switzerland, building on the geological dataset derived from a synthesis of regional investigations. One particular focus of the assessment is the identification and quantification of the requirements placed on the geological environment in order to ensure acceptable repository performance. These geological requirements are, in turn, key input for the exploration planning study, in which the investigations required to assess whether a particular site would be acceptable are specified.

The aims of the Kristallin-I safety assessment are:

- To re-evaluate the crystalline basement of Northern Switzerland as a host rock for a high-level radioactive waste repository and, using both moderately conservative arguments and robust arguments, to quantify the levels of safety that can reasonably be expected and can be relied on with confidence.
- To improve understanding of the roles of the engineered and geological barriers through quantitative analysis of their performances, including examination of the sensitivity of performance estimates to uncertainties.
- To make a detailed examination of the potential performance of the geological barriers, to identify key geological characteristics and to establish desirable ranges for corresponding parameters as input to the identification of sites for additional (Phase II and III) field work.
- To develop and test a more complete safety assessment methodology and an enhanced set of models and computational tools, including a scenario development methodology, new models of specific processes identified as important in Project Gewähr 1985 (e.g. colloid facilitated radionuclide transport and non-linear sorption) and new assessment computer codes.

1.5 Organisation of this Report

This report presents the methodology, data, models, calculated results and conclusions of the Kristallin-I safety assessment.

In Chapter 2, the general aims of post-closure safety assessment of nuclear waste repositories are presented, with emphasis on specific regulatory protection objectives for a repository in Switzerland. The approach adopted to deal systematically with the unavoidable uncertainties that beset long-term safety assessment is also described, along with the measures taken to achieve a sufficient level of confidence in the safety assessment. In addition, a brief overview is given of the progress of post-closure safety assessment studies in Switzerland since Project Gewähr 1985.

In Chapter 3, the information base for the Kristallin-I safety assessment is presented. The design performance of the engineered barriers and the expected contribution to long-term safety of the engineered and geological barriers - the Safety Concept - is described. The characteristics of the wastes, engineered barriers, host rock and surface environment are discussed, together with attendant uncertainties, and processes that could potentially affect radionuclide release and transport are identified. Finally, key data for the safety assessment models are presented based on this information.

In Chapter 4, the procedure for collating and screening this information is described, resulting in the identification of a set of safety-assessment calculations that reflects the uncertainty in the performance of the disposal system - Scenario Development. The application of the procedure to the Kristallin-I safety assessment is summarised. Relevant features, events and processes (FEPs) are discussed and a set of safety-assessment calculations is derived. Uncertainty in the selection and combination of relevant features FEPs is explored by means of a Reference Scenario and number of alternative scenarios. Uncertainty in the way in which important FEPs are modelled is explored by means of a set of Reference Model Assumptions and number of alternative model assumptions within the Reference Scenario. In addition, calculations for a robust demonstration of safety are defined. FEPs that are not taken into account in Kristallin-I safety-assessment models, but would provide additional safety - reserve FEPs - are identified, as are unexpected FEPs that (if they occur) have the potential to compromise safety - open questions.

In Chapter 5, the model-development approach for long-term safety assessment is described, including a discussion of the different levels of detail at which modelling is performed. The underlying Reference Model Assumptions and mathematical formulations are presented for each of the principal assessment models - near field, geosphere and biosphere. The performance of the individual models is illustrated and their sensitivity to parameter variations investigated.

In Chapter 6, the key results relating to the safety of the overall system are presented. Results of model-chain calculations are described for the Reference Scenario, which

represents a conservatively defined performance of the engineered barriers and a constant state of the geological barriers and of the surface environment, based on present-day conditions. Within this scenario, the effects of uncertainty in data and in the selection of conceptual models for key elements are investigated. Further model-chain calculations are presented for alternative scenarios, which consider a deep groundwater well, failure of repository seals and a number of climate-related scenarios. Safety is demonstrated by means of a scenario that takes a highly pessimistic view of uncertainties in the properties of the crystalline host rock.

In Chapter 7, the conclusions from the Kristallin-I safety assessment are presented. This chapter is structured according to the aims of the assessment (Section 1.4) and thus consists of summaries of:

- the overall performance of the system, including a comparison to results of other recent safety assessment studies;
- the performance of the engineered and geological barriers, including identification of outstanding uncertainties and reserves of performance;
- the desired properties of potential sites in the crystalline basement of Northern Switzerland to ensure safety;
- the status of safety assessment methodologies, models and codes, and evidence and arguments leading to confidence in the Kristallin-I assessment results and conclusions.

Finally, a statement of the overall suitability of the crystalline basement of Northern Switzerland as a host rock for a repository for HLW is given.

2. SAFETY ASSESSMENT - AIMS AND APPROACH

2.1 Introduction

The purpose of this chapter is to describe the overall framework for post-closure safety assessment adopted in this report. This framework is based to a large extent on the international consensus that has developed in this field over the past 15 years. This consensus has been described most recently in a "Collective Opinion" published by the OECD Nuclear Energy Agency (NEA 1991a). The framework for Swiss safety assessments is influenced by the protection objectives for the disposal of radioactive waste specified by the national regulatory authorities (HSK & KSA 1993), and by the approach to demonstration of safety developed by Nagra (e.g., see McCOMBIE et al. 1991). In this chapter:

- the international view on safety assessment is summarised (Section 2.2);
- the regulatory criteria that a repository for radioactive waste in Switzerland must satisfy are noted (Section 2.3);
- the general approach to the treatment of uncertainties adopted in the Kristallin-I safety assessment is described and special comments are made on the treatment of uncertainties related to the surface environment and human activities in the far future (Section 2.4);
- possible calculational approaches (deterministic and probabilistic) are noted and the approach and hierarchy of deterministic calculations carried out in Kristallin-I are described (Section 2.5);
- the characteristics of a robust safety case are discussed (Section 2.6);
- the building of confidence in safety-assessment results is discussed (Section 2.7);
- the principal advances in Nagra performance assessment methodology and databases for assessments of HLW disposal in crystalline host rock since the completion of Project Gewähr 1985 (NAGRA 1985) are reviewed (Section 2.8).

2.2 The International View

The long-term safety of any disposal system for hazardous waste must be convincingly demonstrated prior to its implementation. For radioactive waste, safety assessments over timescales far beyond the normal horizon of social and technical planning have already

been conducted in many countries (e.g., KBS 1983; NAGRA 1985; AECL 1985; CEC 1988; SKI 1991c; SKB 1992; VIENO et al. 1992; PNC 1992). These assessments provide the principal means to investigate, quantify and explain long-term safety of the selected disposal concept and site. They are based on four main elements:

- definition of the features of the disposal system;
- identification of possible processes and events that determine the performance of the disposal system;
- quantification of potential future radiological impacts by numerical modelling;
- evaluation of the associated uncertainties.

The NEA Radioactive Waste Management Committee and the IAEA International Radioactive Waste Management Advisory Committee have examined the current scientific methods for safety assessment of radioactive waste disposal systems and have reviewed the experience now available from the application of these methods in many countries (NEA 1991a). While noting that collection and evaluation of data from proposed sites are the major tasks on which further progress is needed, the committees:

- confirmed that safety assessment methods are available to evaluate adequately the potential long-term radiological impact of a carefully designed radioactive waste disposal system on humans and the environment;
- considered that appropriate use of safety assessment methods, coupled with sufficient information from proposed sites, can provide the technical basis to decide whether a specific disposal system would offer a satisfactory level of safety for both current and future generations.

These conclusions have also been endorsed by the CEC Group of Experts on the Community Plan of Action in the field of radioactive waste management.

Clearly, a demonstration of safety cannot rely on direct observation over the timescales of concern. Rather, it is necessary to develop models of the engineered and natural components of the disposal system that can be used to illustrate the potential performance of individual subsystems - or of the overall system - taking account of uncertainties. It is important to note that safety assessment is not just a calculational framework for producing estimates of system performance. Safety assessment should be understood as a broad activity aimed at the following major goals (NEA 1991b):

- developing a sufficient understanding of the physical and chemical behaviour of a disposal system;

- quantifying this understanding in order to allow estimates of future system performance;
- evaluating uncertainties in the estimates;
- convincing all relevant groups (project staff, regulators and the public) of the adequacy of the analyses.

2.3 Regulatory Criteria

The principles and protection objectives that a final repository for radioactive waste in Switzerland must meet are defined in HSK Guideline R-21 (HSK & KSA 1993), issued jointly by the Swiss Federal Nuclear Safety Inspectorate (HSK) and the Federal Commission for the Safety of Nuclear Installations (KSA). Three protection objectives are defined:

– Protection Objective 1

The release of radionuclides from a sealed repository subsequent upon processes and events reasonably expected to happen, shall at no time give rise to individual doses which exceed 0.1 mSv per year.

– Protection Objective 2

The individual radiological risk of fatality from a sealed repository subsequent upon unlikely processes and events not taken into consideration in Protection Objective 1 shall, at no time, exceed one in a million per year.

– Protection Objective 3

After a repository has been sealed, no further measures shall be necessary to ensure safety. The repository must be designed in such a way that it can be sealed within a few years.

In Switzerland, no time cut-off is specified for post-closure assessments. The HSK/KSA suggest that "...dose and risk calculations should be carried out for the distant future, at least for the maximum potential consequences from the repository...". It is however recognised that dose calculations for the distant future are to be interpreted as indicators, and should be based on the use of " ... reference biospheres and a potentially effected population group with realistic, from a current point of view, living habits ... " (HSK & KSA 1993).

2.4 Treatment of Uncertainty

2.4.1 Approach in the Kristallin-I Safety Assessment

There is unavoidable uncertainty in estimates of repository performance attributable to the complex interaction of features and processes that may have a bearing on performance over the long timescales for which estimates of performance are required. These uncertainties can conveniently be grouped into three categories:

- uncertainty in the future evolution of the engineered barriers, geological barriers and surface environment, i.e. the features, events and processes that should be accounted for (often referred to as scenario uncertainty);
- uncertainty in what constitutes an appropriate model or models of the relevant features, events and processes (often referred to as model uncertainty or conceptual model uncertainty);
- uncertainty in the data and parameter values to be used in the models (often referred to as parameter uncertainty).

All of these types of uncertainty result in uncertainty or bias in the estimated performance of a disposal system; each is discussed further below, followed by a brief description of how their effect on estimates of performance has been examined in the Kristallin-I assessment.

Scenario uncertainty (uncertainty in selection and combination of FEPs):

For a high-level radioactive waste repository, due to the long half-lives of some safety-relevant nuclides, the timescales over which assessments are carried out may be up to several millions of years after closure. Over such timescales, both the natural environment and the engineered features will change due to natural processes, interaction of the natural environment with the repository and waste, and human actions (unrelated to the repository). Uncertainty in the future evolution of the disposal system is traditionally treated through the identification of features, events and processes (FEPs) potentially relevant to safety, and their incorporation into a limited set of *scenarios* for quantitative analysis (NEA 1992). There is uncertainty relating to the comprehensiveness of the initial list of FEPs and also in the selection of FEPs to be represented in scenarios for safety assessment. The scenario development procedure for the Kristallin-I assessment is discussed in Chapter 4.

Model uncertainty (uncertainty in representation of FEPs):

Quantitative assessments are conducted using a suite of models that describe the possible courses of evolution and performance of the various components of the disposal system. The term "models" here includes conceptual models (sets of assumptions), corresponding mathematical descriptions of the conceptual models, and numerical implementation of the mathematical models in computer codes. Conceptual models of a given subsystem may be developed at various levels of detail. For example, highly detailed, process-oriented research models that aim at realism may be constructed based on a theoretical framework, supported by laboratory and field studies. These research models and their associated databases may be simplified to form assessment models. Subsystem assessment models need to be linked to describe the overall performance of the disposal system. Further simplifications or assumptions may be introduced when assessment models are implemented in computer codes. The most significant uncertainties are considered to be related to the existence of plausible alternative conceptual models. The Reference Model Assumptions and corresponding computer codes used in the Kristallin-I assessment are described in Chapter 5.

Parameter uncertainty (uncertainty in model parameter values and the data from which they are derived):

There is uncertainty concerning the rate of change and physical extent of processes represented in the models. This may be due to temporal and spatial variability of natural and engineered material properties and to uncertainty in extrapolation from laboratory or analogue system data to repository conditions and timescales. In addition, safety assessment parameter values derived from experimental measurements may be strongly dependent on the model chosen to interpret the data (model uncertainty; see above). For example, experimental tracer break-through curves may generally be interpreted by a range of alternative models, in which different combinations of processes are assumed to be active. Alternative models may yield similar break-through curves, but require different sets of parameter values to do so.

The database for the Kristallin-I assessment has been developed over many years and considers the specific properties of the system and region under investigation. In principle, the characteristics of the engineered barriers are well defined, since they are specified by design, but there is uncertainty in the rates, or degree of effect, of relevant processes under repository conditions, e.g. corrosion and radionuclide sorption. The characteristics of the geological barriers are more uncertain at present. Although further information will be gained in time, it will never be possible to characterise the geological environment completely and some remaining uncertainty will be inevitable. In the case of missing site-specific field data - such as sorption data for the crystalline host rock - an evaluation of literature data has been performed taking into account the specific geochemical conditions and mineralogy. In the case of the engineered barriers, key data are conservatively selected so that it can be confidently considered that an engineered barrier system could be constructed with a performance at least as good as the calculated performance. Generic data, such as dose conversion factors, are taken from accepted

data compilations. The information on which the Kristallin-I assessment is based is summarised, and the assessment data presented, in Chapter 3.

2.4.2 Uncertainty in Surface Environment Evolution

The actual conditions that will exist in the surface environment at times in the far future (when releases might occur) are largely unpredictable. Specifically, it is not possible to predict the patterns of future human behaviour and local resource use that determine doses received by individuals or populations living in the future. Modelling of the surface environment and dose pathways (biosphere modelling) should thus be viewed only as a procedure to convert the estimated releases of radionuclides from the engineered and geological barriers to a common scale - annual individual dose (see Subsection 5.4.2.1) - that is accepted as an appropriate measure of radiological hazard. It must be stressed that the parameter calculated is not an estimate of actual dose that will be received by individuals at any future time, rather, it is an indicator of repository performance and, specifically, it is a quantity calculated for comparison with a regulatory guideline (HSK & KSA 1993).

Recognising the unavoidable limitations, and purpose, of biosphere modelling leads to the conclusion that it is neither possible nor necessary to treat uncertainties related to biosphere features, events and processes in the same way as uncertainties related to the performance of the engineered and geological barriers. For example, ICRP³ metabolic models and tissue weighting factors (ICRP 1979-82; ICRP 1991) are generally accepted as appropriate for estimating dose per unit intake for purposes of radiological protection, despite large uncertainties in the underlying metabolic and health-effect data. In the future it should be possible to define an approach to biosphere modelling that is, similarly, accepted as an appropriate method to calculate the quantity required for evaluation of overall performance of radioactive waste repositories. There is already considerable international consensus about the features, events and processes that should be considered in biosphere modelling for radioactive waste-disposal assessments, and there is an initiative to define a basis and procedure for the development of reference biospheres within the current BIOMOVS exercise (SSI 1993). For a given site, the biosphere model may then be constructed considering only those site-specific factors determined by the physical geographical characteristics of the potential future discharge zones, plus a model of human use of resources and exposure pathways defined by international consensus.

³ International Commission on Radiological Protection.

2.4.3 Treatment of Future Human Actions

It is acknowledged that possible future human actions may adversely affect even a deep underground radioactive-waste repository and constitute an important topic for consideration in safety assessments. Following a scientific workshop in 1989 (NEA 1989), the NEA established a Working Group on "Assessment of Future Human Actions at Radioactive Waste Disposal Sites" in which Nagra has participated. Table 2.4.1 summarises the conclusions of the group to be made in a NEA report now in preparation (NEA 1994).

Nagra concurs in broad terms with the points listed in Table 2.4.1. Specifically:

- Nagra agrees that intentional human intrusions into a closed repository should not be considered in safety analyses; such intrusions are ruled out by Swiss regulatory guideline (HSK & KSA 1993);
- estimates of impact that arise in the event of unintentional human intrusion, or actions significantly affecting the repository performance, are best presented separately (and in addition) to estimates of impact arising under assumptions of an evolution undisturbed by human actions;
- given the great uncertainty in future human technology and resource use, scenarios for future human actions can **only** be illustrative and it is justifiable to base these illustrations on current technology and practices.

For the Kristallin-I assessment, inadvertent future human actions that would adversely affect the repository performance are identified and discussed qualitatively in Subsection 4.3.7. Quantitative evaluation is not undertaken since the primary aim of Kristallin-I is to help guide geological investigations of a site in the crystalline basement. The overall characteristics of the host rock (crystalline basement under sedimentary cover in Northern Switzerland) are believed to be such as not to attract inadvertent human intrusion. Given the essentially unpredictable nature of possible future intrusion episodes, should they occur, the detailed characteristics of the host rock, such as will be determined by site investigation, are unlikely to affect estimates of likelihood of impact. Certain findings at a site, e.g. economic mineral deposits or an exploitable geothermal anomaly, would certainly be negative factors in a site-selection process; however, here the issue would be one of conflict of resources not radiological impact. Quantitative evaluation has been focused on the performance of the geological barrier assuming an evolution in which human actions do not compromise the engineered and natural barriers.

Quantitative analyses of radiological impact from future human actions will be required at a later stage of the HLW/TRU programme. In particular, the comparison between estimated consequences and probabilities of human actions for different potential host rocks or waste management concepts may be of interest. However, the importance which should be given to such results, relative to estimates for undisturbed performance, is still to be decided.

A. Framework for Consideration of Future Human Actions (FHA)

- FHA can adversely impact radioactive waste disposal systems and must therefore be considered in siting, design and assessment of safety.
- FHA committed intentionally, rather than inadvertently, can be considered the responsibility of the society that takes these actions.
- When quantitative analyses of FHA are undertaken, it may be helpful to present the results separately from results of undisturbed evolution of the disposal system.

B. Considerations Bearing on Quantitative Analysis

- The general quantitative framework developed for safety assessments involving naturally occurring events and processes is also appropriate for the analysis of FHA.
- The analysis of FHA can only be representative and never complete.
- Probabilities of scenarios of FHA are bound to be subjective and these probabilities should be termed "degrees-of-belief" to distinguish them from empirically determined frequencies.
- A range of possible scenarios should be considered in risk and uncertainty analyses.
- FHA scenarios have to be viewed as illustrations based on sets of assumptions; the consequence analyses are thus also illustrative for the purpose of informing decision makers and other stakeholders.
- Site- and system-specific scenarios could be based on the principle that assumed societal development should correspond to current practice at the repository location and at similar locations elsewhere.

C. Countermeasures

- The most effective countermeasure to inadvertent disruptive FHA is active institutional control of the surface above and for some distance around the disposal site; however, such controls cannot be relied on over the timescales for which the waste presents a hazard.
- Other possible countermeasures discussed by the Working Group included:
 - siting away from areas of known subsurface resource potential,
 - isolation from the human environment, e.g. the depth of disposal is an important mitigating factor,
 - criteria on design to mitigate consequence of disruptive FHA,
 - conservation and communication of information about the repository,
 - durable physical markers at or near the site,
 - physical barriers to deter attempted intrusion.

Table 2.4.1: Summary of Conclusions from the NEA Working Group on Future Human Actions. (Taken from NEA 1994).

2.5 Calculational Approach

2.5.1 Choice of Calculational Approach

Two distinct approaches to the calculation of repository performance and safety have been applied and reported in the various assessment programmes, generally termed:

deterministic calculations - by which it is meant that calculations are performed one-by-one, with a single value of each input parameter used to produce a single value (or function of time/space) of each output parameter, and

probabilistic calculations - by which it is meant that a range of values or probability distribution is assigned to selected (or all) input parameters and a number of calculations are made, e.g. by random sampling of the input ranges or distributions, to achieve a distribution of the output parameter.

Early probabilistic calculations tended to use simplified models to represent the total disposal system. More recently, more detailed models have been applied in a probabilistic mode to simulate a limited part of the system, where the complexity of the features and processes is important. Examples are:

- calculations of groundwater flow and tracer transport through a set of statistically-generated fields of variable hydraulic conductivity;
- calculations of radiological performance using a set of time-dependent boundary conditions to a hydrogeological model, generated by a separate model of environmental change.

Relative advantages, disadvantages and appropriate conditions for use of deterministic and probabilistic calculations have been widely discussed in the literature and debated, for example, within the framework of the NEA Performance Assessment Advisory Group (PAAG). Table 2.5.1 provides a brief analysis of the calculational approach in selected recent integrated performance assessment studies. It is accepted that the approach to be taken should depend on the quality and extent of information available, the regulatory criteria and the purpose of the calculations. For example, integrated assessments may be aimed at bounding analysis for the purpose of safety demonstration or at detailed quantitative understanding of the uncertainties in order to evaluate specific design and siting options.

As in Project Gewähr 1985, the Kristallin-I safety assessment is based entirely on deterministic calculations. This approach is adopted for the following reasons.

- Currently available data are insufficient to provide statistically justified ranges or distributions for many of the most safety-relevant parameters.

Country	Study (reference)	Calculational Approach
Canada	AECL Post-closure assessment for EIA (GOODWIN et al. 1994)	Deterministic calculations using median value of PDFs of input parameters used to illustrate radiological system behaviour. Probabilistic calculations used to calculate risk for comparison to regulatory target.
Finland	TVO 92 (VIENO et al. 1992)	Deterministic calculations (only) used to illustrate radiological system behaviour and calculate performance measures and dose for comparison to dose criterion.
Japan	H-3 (PNC 1992)	Deterministic calculations (only) used to illustrate radiological system behaviour and calculate performance measures and dose.
Sweden	SKI Project 90 (SKI 1991c)	Deterministic calculations used to illustrate system behaviour. Probabilistic calculations used to evaluate releases from near-field and geosphere models, principally to provide a sensitivity analysis.
	SKB 91 (SKB 1992)	Deterministic calculations used to illustrate near-field behaviour. Evaluation of groundwater travel times based on conditioned simulation of groundwater flow field, accounting for spatial variability. System performance calculated by deterministic calculations of near-field release, coupled with sampled location of failed canisters and characteristics of flow paths taken from groundwater simulations.
United Kingdom	Dry Run 3 (SUMERLING (ed.) 1992)	Deterministic calculations used to guide nuclide selection, and to illustrate environmental and radiological system behaviour. Probabilistic calculations used to calculate risk including simulations for time-varying boundary conditions generated by Markov model of environmental change, plus sensitivity analyses.
United States	WIPP 1992 (WIPP PAD 1992)	Probabilistic calculation of cumulative release to accessible environment required by regulations, considering natural evolution and human intrusion (drilling) scenarios. Groundwater travel times and dispersion in the overlying aquifer sampled from results of particle tracking in conditioned simulations of the aquifer transmissivity field, accounting for spatial variability.
	TSPA 1991 (BARNARD et al. 1992)	Probabilistic calculation of cumulative release to accessible environment required by regulations, considering several scenarios.

Note: Abbreviations not defined elsewhere:

EIA = environmental impact assessment

PDF = probability density function

WIPP PAD = Waste Isolation Pilot Plant Performance Assessment Department

TSPA = total system performance assessment (Yucca Mountain Project)

Table 2.5.1: Calculational approach in selected recent performance assessments of deep underground disposal of radioactive waste.

- It is likely that simultaneous random sampling of multiple parameters, where the ranges or distribution of values arise largely from ignorance, will lead to unrealistic combinations which must then be identified and rejected retrospectively. In particular, unless correlations between parameters are taken into account, physically impossible input data sets may be sampled.
- Although sampling techniques allow the consequences of uncertainties within the bounds of the selected scenario and conceptual and numerical model to be quantified, it is believed that, at the current stage of site and process information, there is greater uncertainty associated with the selection and representation of the relevant processes (see Subsection 2.4.1). It is the latter uncertainties that are more relevant at this stage.
- Deterministic calculations, with single values assigned to each input parameter, provide more transparent illustrations of system performance and sensitivity and are thought to be more instructive at this stage.

The hierarchy of deterministic calculations carried out in Kristallin-I (described in Subsection 2.5.2), is aimed at a systematic investigation of uncertainties related to FEP selection (alternative scenarios), FEP representation (alternative model assumptions) and selection of parameter values, as introduced in Subsection 2.4.1. However, conservatism is introduced at each stage, so that the deterministic output results are not to be regarded as best or central estimates of performance. Rather, they tend towards upper-bound estimates of performance of the system for the stated assumptions of a particular scenario.

This approach is appropriate at this stage of the HLW programme. As more site-specific data becomes available, and optimisation of repository design is considered, then it may be desirable to reduce the conservatism and also to introduce more explicit representations of uncertainty and variability through probabilistic simulation techniques. Random sampling tools are available and (limited) experience has been gained in the PSACOIN exercises within the Swiss programme (NEA 1993). It is noted that sampling approaches may be particularly useful to explore uncertainty within complex models in order to identify high consequences arising from combinations of parameter values that may not be obvious from prior reasoning.

2.5.2 Hierarchy of Calculations in Kristallin-I Safety Assessment

The Kristallin-I assessment methodology employs a hierarchy of deterministic calculations (see Figure 2.5.1) to investigate the different types of uncertainty discussed in Subsection 2.4.1.

A **Reference Scenario** is defined that includes the key phenomena expected to determine the performance of the disposal system, i.e. features, events and processes (FEPs). In the Kristallin-I safety assessment, the Reference Scenario is based on a conservatively defined performance of the engineered barriers and a constant state of the geological barriers based on present-day conditions. The latter assumption is possible because the engineered barriers and the safety-relevant characteristics of the geological barriers in the vicinity of the repository are not greatly affected by the expected environmental changes over relevant timescales ($\sim 10^6$ years), see Subsection 4.3.4.

The Reference Scenario includes most phenomena that are relevant to the long-term radiological performance of the system. However, some beneficial phenomena are deliberately excluded, e.g. because the necessary models and data to represent these phenomena are not available; these phenomena are termed "reserve" FEPs. Within the Reference Scenario, a range of alternative conceptual models is identified for key phenomena. Where equally likely alternative conceptual models are identified for components of the disposal system, the model leading to the highest consequences is incorporated in the **Reference Model Assumptions**.

A conservative approach is also adopted in deriving a set of **Reference Parameters**. Some parameters are kept constant in all calculations. These parameters are either (i) known with a high degree of confidence (e.g. radionuclide half-lives), (ii) imposed by the technical design of the repository (e.g. the number of canisters and the radionuclide inventory per canister) or (iii) taken from data compilations accepted as appropriate for use in such analyses (i.e. dose per unit ingestion or inhalation). Other parameters, the values of which are less certain but which may have an important effect on radionuclide release, transport or doses, are varied. In general, for these parameters, two values have been defined⁴.

- A **"realistic-conservative" value** - this is a value which, according to current understanding of the process or feature being represented, is realistically supported by the available data. Where there is uncertainty, numerical values are selected such that higher radiological consequences arise from the choice. The term "best estimate", employed in some other assessments, is therefore not used in Kristallin-I.
- A **"conservative" value** - this is a value which is confidently believed to yield an upper bound for the consequences, in terms of repository safety, of the particular process or feature being considered. It is intended to represent pessimistic but possible conditions. Often, the selection takes account of a situation where some unlikely detrimental process or event has reduced the effectiveness of a safety-relevant feature or process.

⁴ For some key parameters (for example the flowrate of groundwater through the host rock), several values have been examined in the calculations.

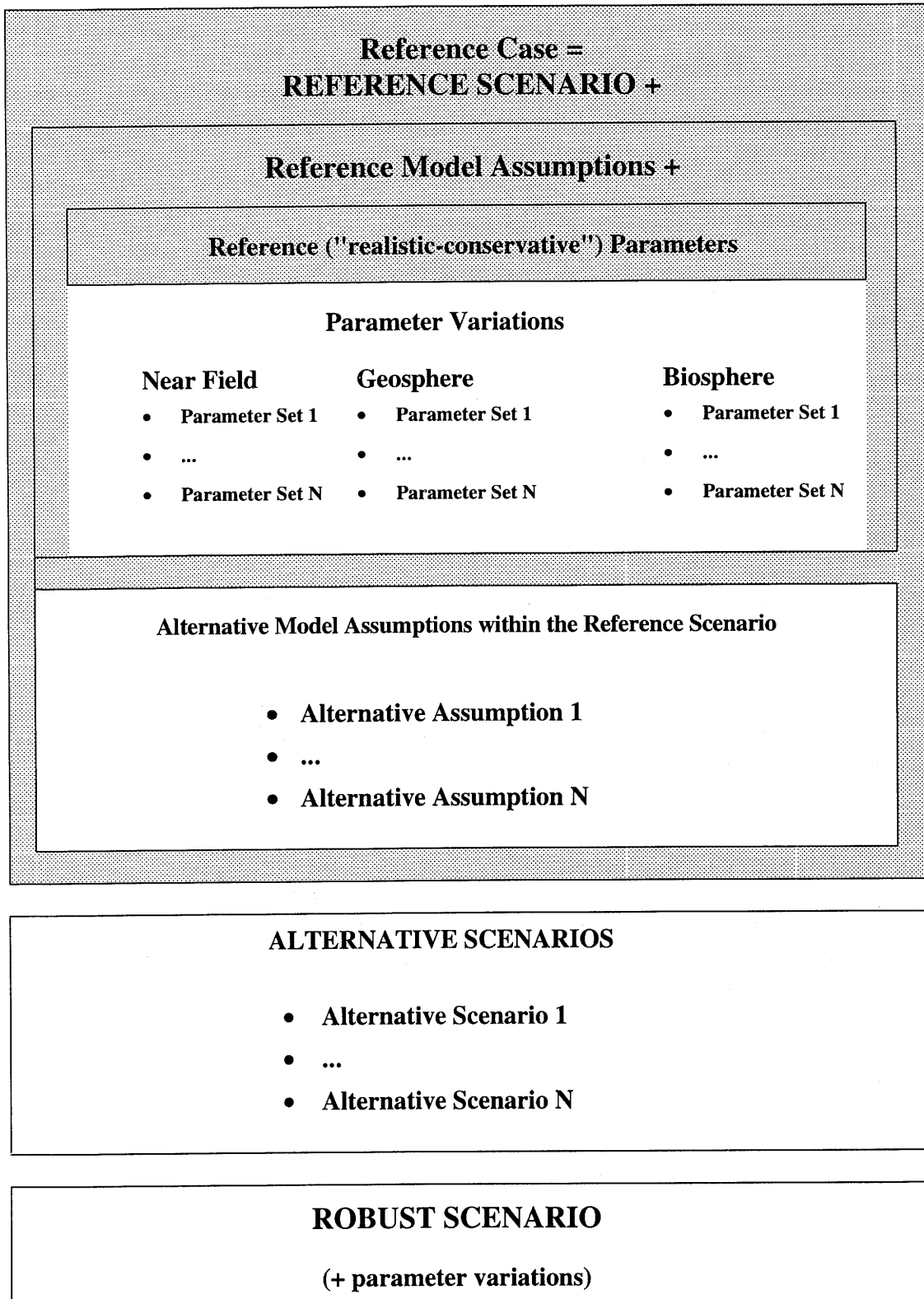


Figure 2.5.1: The hierarchy of calculations performed in the Kristallin-I safety assessment, with the Reference Case indicated by shading.

The combination of the Reference Scenario, Reference Model Assumptions and Reference (i.e. "realistic-conservative") Parameters is termed the **Reference Case**. Sensitivity to parameter uncertainty within the Reference Scenario (and with the Reference Model Assumptions) is examined by varying individual parameter values, typically in a pessimistic sense, to account for maximum likely variations. The results of these sensitivity analyses are given in Chapter 5.

Results of calculations are presented in Chapter 6 for:

- the **Reference Case** (Reference Scenario, Reference Model Assumptions, Reference Parameters);
- a set of alternative model assumptions within the Reference Scenario;
- a set of alternative scenarios;
- a **Robust Scenario**.

The last provides results that are confidently expected to overestimate the radiological impact, thus quantifying of the minimum level of safety that can be relied upon.

This hierarchy of calculations is designed to cover uncertainty related to FEP selection and model representation and to provide the basis for a **robust safety case**, discussed further in Section 2.6.

Results in this report are given over very long timescales. Furthermore, doses have been calculated which, in many cases, are far too small to be measured or to have any discernible radiological effect. The way in which results are presented in the figures in the following chapters is designed to help put these long timescales and low doses in perspective; the basis for this presentation is discussed in Appendix 1. The selection of safety-relevant radionuclides for which calculations are performed is described in Appendix 2.

Quality assurance and traceability of model-chain calculations are discussed in Appendix 3. The names assigned to the input and output datasets used in individual calculations, together with the Kristallin-I directory structure, facilitate the traceability of results to their corresponding scenarios, model assumptions and input data. The nomenclature for datasets is described in Appendix 4. All parameter values can be traced from the dataset name; for example, *SA_60ALA* is the dataset name for the Reference-Case calculations.

2.5.3 Interpretation of Results in Relation to the Protection Objectives

In this assessment, estimates of overall performance of the disposal system are presented in terms of annual individual dose to be compared with HSK Protection Objective 1 (see Section 2.3). However, because of various conservatisms introduced at the stages of FEP, model and data selection, these results should be interpreted as lower-bound estimates of performance within the stated assumptions of the relevant scenario (see Subsection 2.5.2.).

At this stage, no attempt is made to assess the likelihood of occurrence of, and the degree of belief in, the various scenarios, or to assess probabilities reflecting uncertainty in the corresponding models and datasets. Hence, all results are presented as bounding estimates for scenarios that, given present uncertainties, may occur, i.e. all results are presented as if the probability of occurrence is one. As understanding improves, it may be possible to assign probabilities (or degrees of belief) to scenarios, models or datasets, in which case it may be possible to weight results according to probability, and to estimate risks for comparison with HSK Protection Objective 2. However, this is only likely to be of value for scenarios that have rather low probability of occurrence, e.g. human intrusion, or would affect only a small part of the repository and release, e.g. quality control failures. In this assessment such scenarios are identified (see Chapter 4) but, for the most part, not analysed quantitatively.

In accordance with HSK Protection Objective 3, it is assumed, in all calculations, that the repository will be sealed after completion of disposal operations and no account is taken of any further measures to ensure safety.

2.6 Building a Robust Safety Case

A **robust safety case** is one based on an assessment with the following characteristics (see also McCOMBIE et al. 1991):

- A description (conceptual model) of all key FEPs and construction of scenarios from selected FEPs.
- Representation of selected FEPs and their interconnection by means of models and parameter values (or ranges) that are either well justified through direct evidence or are demonstrably conservative.
- Examination of uncertainty in FEP selection and representation through, for example, a hierarchy of deterministic calculations (see Subsection 2.5.2). In this methodology, uncertainty is replaced by conservatism in a step-wise process, the final stage of which is the definition of a Robust Scenario in which quantitative consideration is limited to:

- all potentially detrimental processes within a specified domain of relevance⁵;
- only those positive (impact-reducing) processes for which a sufficiently high degree of confidence can be attributed to the results of their analysis.

This simplification in modelling reality can decrease the difficulty in finding adequate data and assist in the building of confidence in the assessment (see Section 2.7).

- Support for (or "validation" of) both models and data from laboratory, field and analogue studies.

The conclusions derived from such an assessment are, within established ranges, insensitive to changes in conceptualisation and parameters. This is facilitated if the disposal system is itself robust. In a **robust disposal system**, most phenomena that could be detrimental to safety are excluded or forced to very low probability or consequence by the repository design and siting concept. In the Kristallin-I disposal concept, the use of large quantities of relatively well understood materials within the system of engineered barriers reduces the potential impact of detrimental processes. Furthermore, the siting of a repository in a stable, deep geological unit effectively isolates the engineered barriers from variations due to surface environmental processes and the possibility that future natural events and processes will lead to detrimental consequences for repository performance is thereby reduced.

Finally, a robust safety case can also be used to derive goals for site characterisation. For example, one focus of site characterisation would be to seek supporting evidence for assumptions that form part of the robust case. In particular, attention would be given to the examination of detrimental influences (e.g., identification of high-permeability zones).

2.7 Building Confidence in the Assessment

The measures that might be adopted to establish confidence in the use of models within a repository safety case include:

⁵ Some processes may be beyond the reasonable scope of concern of a specific assessment; see Subsection 4.2.3.

- systematic and transparent approaches to model development and consideration of alternative conceptual models, including a full description of the judgements and assumptions made in model development and application;
- use of laboratory and field tests as well as natural analogues to test the models;
- iteration between model development, safety assessment and collection of experimental data, either in the laboratory or in the field;
- use of natural analogues and palaeohydrogeological models to evaluate uncertainties arising from the temporal scales of concern;
- ongoing critical peer review through presentations, publications in open literature and participation in international projects and workshops.

All of these activities are, in broad terms, concerned with "validation", defined in the Swiss programme as "Providing confidence that a computer code used in safety analysis is applicable for the specific repository system." (HSK & KSA 1993). Confidence in a computer code implies confidence in the underlying model assumptions and data. Much of the controversy in the area of validation arises from alternative interpretations of the term itself. These range from an inherently unachievable "proof of truth"⁶ to the more pragmatic emphasis in the Swiss programme on the subjective assessment of whether models and data are "good enough" (see, for example, McCOMBIE & McKINLEY 1993).

A "good model" is one which describes a large class of observations (from laboratory, field and natural analogue studies), contains only a few arbitrary elements, and makes definite predictions about the results of future observations (HAWKING 1990). A prediction need not be an exact forecast of the value that a measured quantity will take, but may also be a bounding estimate of the behaviour of a system. The question then is whether there is confidence that model and data are "good enough" for a particular (site- and concept-specific) application. The answer to this question can only be provided on a case-by-case basis after detailed examination of the supporting arguments. For the purpose of safety assessment, these arguments must demonstrate that models and parameters err (if at all) on the side of conservatism, i.e. will underestimate performance and, thereby, overestimate consequences, such as radionuclide release or dose to humans.

2.8 Status of Repository Safety Assessment in Switzerland

Within the Nagra programme, activities related to post-closure repository safety assessment have been ongoing for more than 15 years, covering model development,

⁶ A predominant view of the philosophy of science holds that proof of validity in a strict sense is not possible; models can only be falsified (POPPER 1959).

testing and application as well as experimental work to derive relevant model input parameters. The models developed in the Swiss programme have been tested within international intercomparison studies such as INTRACOIN (SKI 1984; SKI 1986), HYDROCOIN (SKI 1992), INTRAVAL (SKI 1993), BIOMOVs (SSI 1991; SSI 1993) and PSACOIN (NEA 1993) and have been applied in a variety of studies.

Eight years have passed since the previous assessment of a repository for the final disposal of HLW in the crystalline basement of Northern Switzerland reported in Project Gewähr 1985. During this period, there have been considerable advances as a result of new information (see Chapter 3), improvements in the scenario-development methodology (see Chapter 4) and models (see Chapter 5), and improved understanding of the overall disposal system (see Chapters 6 and 7). Improvements in the Kristallin-I safety assessment compared to Project Gewähr 1985 are summarised below.

2.8.1 New Information

- There is a completed synthesis of the geological, hydrogeological and hydrochemical situation in Northern Switzerland (THURY et al. 1994), supported by new data (e.g. from completion of the deep borehole investigations at Leuggern in 1985 and Siblingen in 1989), providing a more complete, and more traceable, database of geological information.
- Final specifications for the vitrified high-level waste have been issued both by COGEMA and BNFL, which have been judged to be appropriate within formal waste-acceptance procedures ("Vorabklärungsgesuche").
- Ongoing studies on the characteristics of the engineered barriers, including the glass matrix, the canister and the bentonite, have essentially confirmed the assumptions made in Project Gewähr 1985.
- There is a larger body of international experience and information available. In particular, use has been made of thermodynamic and sorption data from outside Switzerland.

2.8.2 Development of Assessment Methodology and Models

- A systematic methodology has been developed for managing information on features, events and processes that may influence repository performance. This methodology has been used to track information and assumptions, to develop scenarios and, more generally, to specify the calculations that must be carried out to demonstrate safety.

- A new thermodynamic database, more rigorously defined, is used in the selection of solubility limits for near-field calculations.
- A new near-field release and transport model now explicitly takes account of radionuclide retention in the bentonite.
- A better and more transparent link between field information, especially the detailed characteristics of water-conducting features in the crystalline basement, and input parameters of the geosphere transport model is now available. Furthermore, the geosphere transport model now includes an option to treat non-linear sorption and can treat colloid-facilitated radionuclide transport.
- A new model that better represents the movement of radionuclides in the surface environment and dose pathways to man is now available.
- There is enhanced confidence in the suite of assessment models (and the underlying databases), based on information from the deep boreholes in Northern Switzerland, from the *in situ* migration experiments conducted at the Grimsel Test Site, from laboratory experiments, and from participation in various international or multilateral collaborative exercises, such as INTRAVAL and the Poços de Caldas natural analogue study.

2.8.3 Improved System Understanding

- The relative roles of the engineered barriers (glass matrix, cast steel container, bentonite) and the geological barriers (host rock, overlying geological units) in demonstrating safety has been further investigated and is better understood.
- The relative significance of various processes (and corresponding data) to a demonstration of safety is better understood.
- There is more international assessment experience available, the general conclusions of which are supportive of those reached in this study (NEALL (ed.) 1994).
- The results of assessments conducted by Nagra for other projects are now available (NAGRA 1988a; NAGRA 1988b; NAGRA 1988c; NAGRA 1993); the Kristallin-I assessment can be seen as consistent with, and building upon, the methodologies and understanding developed for these projects.

3. THE KRISTALLIN-I DISPOSAL SYSTEM

3.1 Introduction

The term "disposal system" is used here to describe the combination of engineered and geological barriers which are designed and selected to provide for the long-term safe disposal of radioactive waste. The disposal system analysed in Kristallin-I is the same as that developed for HLW in Project Gewähr 1985 (NAGRA 1985), except for the total quantity of waste considered. However, a significant step forward relative to Project Gewähr 1985 is that a more extensive characterisation of the geological environment is now available.

A major finding from the geological synthesis (THURY et al. 1994) has been that the structure of the crystalline basement of Northern Switzerland is more complex than originally expected, due to the higher frequency of large-scale sub-vertical faults. Faults would be avoided in repository siting, both because of their poor mechanical properties and because some, termed major water-conducting faults, will act as the principal conduits for groundwater flow at depth. The existence of low-permeability blocks in the crystalline basement has been demonstrated, but the size of these blocks is limited by the spacing of faults; difficulties may be encountered in finding a single block of crystalline host rock of sufficient extent for locating an entire repository on a single level. The Project Gewähr 1985 reference layout has been reassessed accordingly and a new layout devised in which the emplacement tunnels are grouped into a small number of panels, separated by major faults. An example of a repository layout is illustrated in Figure 3.1.1. An alternative option would be a multi-layer repository in a single block.

The feasibility of construction has been demonstrated, and operational aspects of the system assessed, in Project Gewähr 1985. Further rock-mechanics studies have investigated the practicality of tunnelling through large-scale faults (OBAYASHI 1993a). In the present report, attention focuses on features and properties relevant to the long-term performance of the system.

Before describing the disposal system in detail, it is instructive to describe the safety function that the various elements of the system are expected to perform. Thus, attention is drawn to the most safety-relevant characteristics, which are also the characteristics that are represented in assessment models. In Section 3.2, the system of engineered and geological barriers is defined and their safety functions summarised. Descriptions of the major elements (waste, engineered barriers, host rock and surface environment), and of the processes relevant to safety that operate therein, are given in Sections 3.3 to 3.6; key input data for the Kristallin-I safety assessment derived from this information is summarised in Section 3.7.

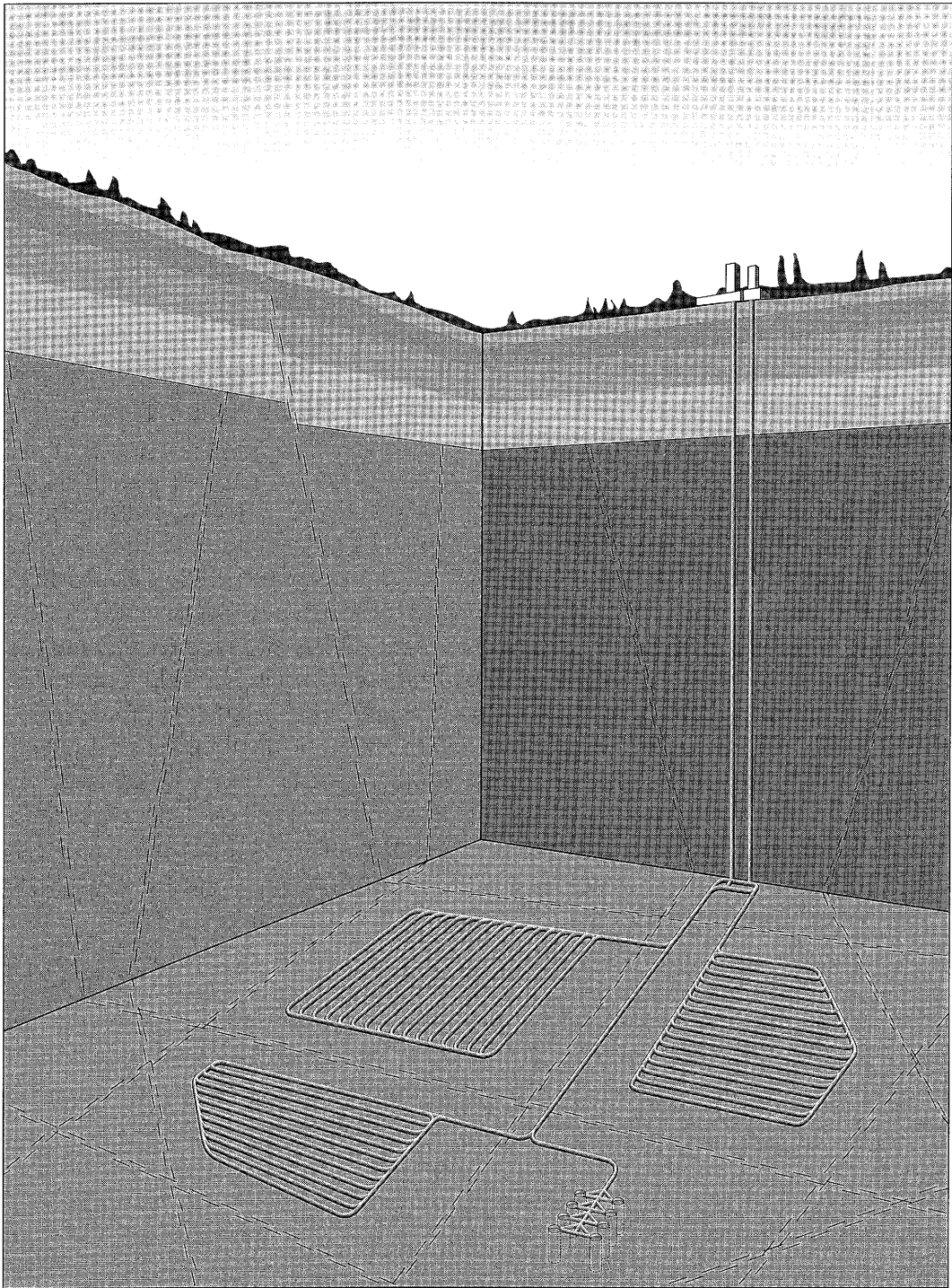


Figure 3.1.1: Possible layout for a deep repository for high-level and long-lived intermediate-level waste (HLW/TRU) in the crystalline basement of Northern Switzerland. Panels for emplacement of HLW and silos for long-lived intermediate-level waste are located in blocks of low-permeability rock avoiding major faults. Major faults are here assumed to separate access shafts and silos for long-lived intermediate-level waste from the HLW emplacement panels.

3.2 The Safety Concept

The Nagra concept for disposal of HLW provides for safety by a combination of engineered and natural geological barriers. The engineered barriers, which employ large quantities of materials with well-known (and favourable) properties and predictable performance, provide the primary containment of the wastes; it is expected that most radionuclides will decay to insignificant levels within the engineered barriers. The geological barriers provide a stable and protected environment for the engineered barriers, ensuring their longevity; they also provide retardation (with consequent radioactive decay) of any radionuclides that eventually escape from the engineered barriers. This is achieved through the siting of the repository in a low-permeability host rock, with favourable groundwater chemistry, in a tectonically stable location. The siting of the repository at depth in the crystalline basement, which has no significant mineral resources, reduces the probability of future human disturbance.

Figure 3.2.1 provides an overview of the system of engineered and geological barriers for HLW disposal in crystalline basement.

The barriers consist of:

- a glass matrix incorporating the high-level waste, encapsulated in a thin, stainless steel flask;
- a massive steel canister;
- a surrounding compacted bentonite clay buffer⁷;
- a low-permeability crystalline host rock block;
- adjacent geological units (i.e. faults, high-permeability crystalline rock, overlying sedimentary formations).

The majority of radionuclides from the reprocessing of spent nuclear fuel are incorporated in a glass matrix, which is contained in thin stainless steel flasks. The flasks are assigned no long-term safety function, but the glass is expected to provide a physically and chemically homogeneous matrix, and to offer resistance to aqueous corrosion. Because radionuclides are homogeneously distributed throughout this matrix, their release rate is limited by the rate of corrosion of the glass, which is likely to be very low in the chemical environment created by the surrounding engineered barriers (see below). Complete corrosion of the glass is expected to take over 150 000 years following contact by water.

⁷ The term "backfill" was used in Project Gewähr 1985 and is also commonly employed in the literature. However, use of the term "buffer" in the present report is intended to recognise the safety function of the bentonite.

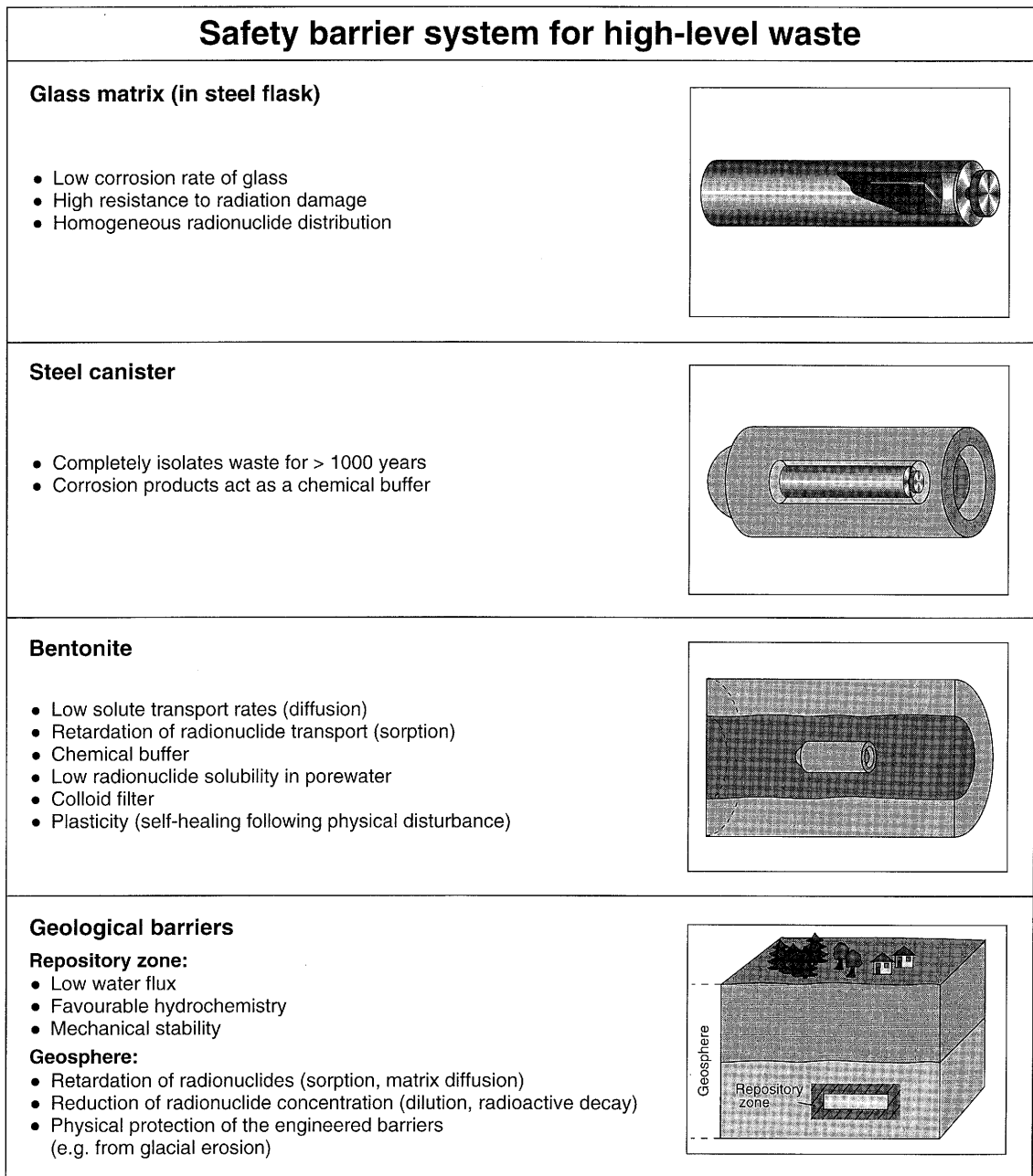


Figure 3.2.1: The system of safety barriers for disposal of HLW in the crystalline basement of Northern Switzerland.

Each flask, containing the vitrified waste, will be placed inside a cast steel canister. The primary function of the canister following repository closure will be to prevent water access to the waste during the period of significant radiogenic heat generation. The mechanism by which canister integrity will eventually be lost is likely to be mechanical failure following weakening by corrosion. The thickness of the canister is sufficient to withstand the maximum load that might develop within the buffer and includes an additional corrosion allowance, which ensures that the canister will remain unbreached

for at least 1000 years after emplacement. During this time, temperatures throughout the engineered barriers will fall to values close to ambient rock temperature and all unsupported, shorter-lived radionuclides, notably ^{90}Sr and ^{137}Cs , will decay to insignificant levels. In addition, the canister will act as a radiation shield during this period, preventing significant radiolysis in the surrounding bentonite porewater (which would otherwise lead to less favourable chemical conditions).

In the safety assessment, it is assumed that, after failure, the canister offers no further physical resistance to water ingress or radionuclide release, although, in reality, mechanical failure is likely to be local, with the cracking around the internal void space, and some physical resistance may continue. The canister does, however, fulfil an important chemical role after failure; the iron corrosion products provide a low oxidation potential around the waste, which ensures low solubility of many of the radionuclides. The iron corrosion products may also provide a good substrate for retention of radionuclides by sorption and co-precipitation processes, but this is not taken into account in the safety case at present.

The thick layer of saturated compacted bentonite surrounding the canister is a key feature of the safety concept for HLW as considered in Kristallin-I. Important features of the saturated bentonite are:

- its low permeability;
- its homogeneous fine pore structure;
- the chemical buffering reactions which occur therein;

Furthermore the expected long-term stability (longevity) of the bentonite, in a suitable geological environment, will ensure that these features are maintained over a long timescale ($\sim 10^6$ years or more).

Low permeability will result in negligible water flow through the bentonite itself. Furthermore, the plasticity and swelling capability of the bentonite will ensure that there are no open cracks or fissures within the bentonite through which water may flow⁸. The low water flow prevents significant advective transport of radionuclides and, along with the chemical buffering reactions, will result in a stable chemical environment.

An important function of the homogeneous and micro-porous structure is to prevent the movement of colloids incorporating radionuclides away from the waste. Colloids may be produced by primary glass corrosion and precipitation processes and could potentially provide a means of transport for radionuclides to the surface environment with reduced retardation (see also Subsection 3.5.4).

⁸ The plasticity of the bentonite may also protect the canister from movements along small faults intercepting the emplacement tunnels.

Aqueous diffusion is thus expected to be the only significant mechanism for radionuclide transport through the bentonite. Many radionuclides will be sorbed on clay mineral surfaces during transport, which will ensure a slow release to the host rock, allowing further radioactive decay to occur.

The zone of host rock immediately around the disposal tunnels, the excavation disturbed zone (EDZ), may have an increased permeability compared to the undisturbed rock, resulting from the opening of joints due to stress relief during repository construction. This zone, if continuous, may provide a conduit for advective transport of radionuclides and other solutes along the length of the tunnels. For this reason, high integrity seals are placed in access tunnels that would otherwise provide potential pathways for radionuclide transport between the emplacement tunnels and regions of higher-permeability rock. The tunnel sealing measures are designed to ensure that transport of radionuclides from the repository can take place only along a path through the low-permeability host rock.

The low-permeability of the undisturbed host rock will result in a low groundwater flowrate in the repository region, which will ensure that the chemical and physical properties of the bentonite are maintained over a very long period (probably greater than one million years; see Subsection 3.4.4.5), and will restrict the rate of advective transport through the host rock of any radionuclides released from the repository. The host rock porewater is reducing, with a nearly neutral pH, and contains no species in concentrations sufficiently high to have significant deleterious effects on the bentonite over the timescales of concern.

Radionuclide transport in the low-permeability host rock is expected to take place by slow advection through networks of water-conducting features. Diffusion into stagnant porewater and sorption onto pore surfaces will further retard radionuclide transport and will allow further radioactive decay to take place.

The crystalline basement of Northern Switzerland is intersected by sub-vertical faults, some of which may be significant conduits for water flow and hence provide paths for relatively fast radionuclide transport. A design criterion for this study was therefore that waste emplacement tunnels should at no point be closer than 100 metres to any such feature. The faults are expected to act as foci for possible future tectonic movement, making significant displacements within the low-permeability host rock blocks highly unlikely. In addition, if water-conducting, the faults may reduce the hydraulic gradients across the repository host rock blocks.

The upper part of crystalline basement in Northern Switzerland has a higher permeability than the potential host rock. This higher-permeability domain of the crystalline basement and the overlying sedimentary rocks (which include significant aquifers and aquitards) substantially isolate the low-permeability crystalline host rock from surface environmental changes, including human activities, climatic changes and glacial effects. The higher-permeability domain cannot be relied on to offer a significant barrier to

radionuclide transport because of the relatively rapid water flows therein. The higher-permeability domain and major water-conducting faults may contribute some dilution, but this would be less than that available in near-surface aquifers.

Any radionuclides that reach the near-surface environment may be a source of radiation exposure to man. The near-surface environment is not considered as a safety barrier. However, groundwaters flowing through the crystalline basement of Northern Switzerland are most likely to be discharged in a region of the Rhine valley where substantial dilution with recent meteoric water can be expected to occur in the fluvio-glacial valley sediments. In addition, any contamination entering the Rhine will be substantially diluted in the river water, so that concentrations downstream in the fluvial system, and hence possible radiation doses, will be extremely small. Therefore, individual radiation doses need only be calculated for hypothetical critical groups living in the immediate vicinity of the possible groundwater discharge.

3.3 Arisings of HLW and the Radionuclide Inventory

3.3.1 HLW Arisings and Vitrification

The waste stream considered in this assessment is the highly radioactive residue from nuclear fuel reprocessing, termed HLW. This contains most of the radionuclides from the irradiated fuel, but is significantly depleted of uranium and plutonium, which are separated for re-use, and volatile components such as iodine. For Kristallin-I, it is assumed that all fuel is reprocessed, although there is an option for direct disposal of spent fuel.

The high-level waste from reprocessing, in the form of highly active liquor, is evaporated, calcined and mixed at high temperature with borosilicate glass-forming additives. Quality control of the glass manufacture ensures a homogeneous glass-waste matrix, in particular avoiding macroscopic phase separation or significant recrystallization. The molten glass is poured into thin, stainless steel fabrication flasks which are then sealed. To allow for differential expansion and to avoid spillage, a void space is left at the crown of each flask.

Initially, the vitrified waste generates significant heat due to radioactive decay of short-lived radionuclides. To keep the temperature in the repository sufficiently low (see Subsection 3.4.1), the waste will be stored to allow radiogenic heat output to decline to an acceptable level; at present, a period of at least 40 years is planned between unloading of fuel from the reactors and emplacement of HLW in the repository.

The current disposal concept for HLW is based on the present-day Swiss nuclear energy production capacity of 3 GW electrical power (GW(e)) (see Section 1.2), which is assumed to continue over a period of 40 years, i.e. 120 GW(e) years, total. Assuming pressurised-water reactor (PWR) fuel with a nominal burn-up of 33 000 MWd/tU (megawatt days per tonne of elemental uranium), this corresponds to approximately 3600 tU at an average 3.5 % enrichment. However, vitrified waste returned to Switzerland for disposal will include waste from the reprocessing of a mixture of fuels, where the quantity of glass returned will be calculated on an equivalent activity basis.

3.3.2 Model Radioactive Waste Inventory

The radionuclide inventory assumed for vitrified HLW in this assessment is based on a single waste type, considered to be representative of all possible vitrified HLW types that might be disposed. The characteristics of the representative waste type, denoted as WA-COG-1, are based on the reprocessing of a COGEMA reference PWR fuel with a burn-up of 33 000 MWd/tU, specifications of which have been issued by COGEMA (COGEMA 1986). The fuel is assumed to be reprocessed 3 years after unloading from the reactor, and vitrified 4 years after unloading. WA-COG-1 differs only slightly from the waste type WA-1 considered in Project Gewähr 1985. The characterisation of WA-1 was based on the preliminary COGEMA specification then available.

In addition to the COGEMA specification for WA-GOG-1, British Nuclear Fuels Limited (BNFL) has issued specifications for a range of vitrified HLW types, each with an assumed burn-up, according to the type of spent fuel reprocessed:

- Magnox fuel;
- PWR fuel;
- blended fuels.
- advanced gas-cooled reactor (AGR) fuel;
- BWR fuel;

However, the radiological characteristics of glass, loaded with residues of these different fuels, are very similar and the stainless steel flasks containing the glass are the same. Hence, the adoption of a single waste type for this assessment is not considered to introduce any significant bias.

The model radionuclide inventory used in this assessment is derived from an independent characterisation of a nominal HLW flask by Nagra (ALDER & MCGINNES 1994). The COGEMA specification is not used directly because the radionuclide inventory therein is incomplete. The Nagra model inventory includes components not accounted for in the COGEMA specification: e.g. gadolinium and its activation products, which are present in boiling-water reactor (BWR) fuel. The Nagra model and COGEMA specification differ in some aspects, but not in those data most relevant for post-closure safety analysis. Table 3.3.1 shows the characteristics of a single flask of vitrified HLW. Table 3.3.2 compares the glass composition by weight in the Nagra model and COGEMA specification.

Reprocessing of a nominal 3600 tU reference fuel in the 120 GW(e) year scenario, gives rise to approximately 485 m³ of vitrified HLW that can be contained in about 2700 flasks⁹. For the Kristallin-I assessment, 2693 canisters are considered¹⁰ each containing vitrified waste from the reprocessing of 1.37 tU. Table 3.3.3 shows the average radionuclide content per flask at 4 years after unloading of fuel from the reactor, corresponding to the assumed time of vitrification. These data are from the Nagra model inventory, accounting for radioactive decay, calculated using the ORIGEN 2 code (CROFF 1980).

Figures 3.3.1 and 3.3.2 show the calculated activity content of the total repository (2693 containers of waste type WA-COG-1) and the calculated radiogenic heat production of a single waste container, respectively, as a function of time after unloading from the reactor.

Overall volume of flask [†]	0.18 m ³						
Glass volume [†]	0.15 m ³						
Weight of glass [†]	412 kg						
Initial heavy metal equivalent [†]	1.37 tU						
Radioactivity content:	beta / gamma			alpha			
4 years after fuel unloading	2.8 × 10 ¹⁶ Bq			1.1 × 10 ¹⁴ Bq			
40 years after fuel unloading	7.1 × 10 ¹⁵ Bq			5.2 × 10 ¹³ Bq			
Radiogenic heat output:							
Time after fuel unloading [years]	4	40	50	100	300	600	1000
Heat output [watts]	2810	589	469	161	21.6	12.9	7.3

Note: † indicates data directly from COGEMA specification, other data are specific to the Nagra model inventory.

Table 3.3.1: Characteristics of a single flask of vitrified HLW - waste type WA-COG-1. (From ALDER & McGINNES 1994).

⁹ In Project Gewähr 1985, it was assumed that the currently envisaged 120 GW(e) y scenario would double, giving rise to a correspondingly larger volume of waste.

¹⁰ In calculating the number of canisters required to contain vitrified waste with an initial heavy metal equivalent of 3591 tU (rounded to 3600 in the text), a rounded value for the amount of waste per container was used: 0.73 canisters per tU (1.37 tU per canister) was "rounded" to 0.75 canisters per tU (1.33 tU per canister).

Component	Nagra model	COGEMA specification
SiO ₂	45.36	45.1
B ₂ O ₃	14.04	13.9
Al ₂ O ₃	4.50	4.9
Na ₂ O	9.19	9.8
CaO	4.01	4.0
Fe ₂ O ₃	2.75	2.9
NiO	0.39	0.4
Cr ₂ O ₃	0.49	0.5
P ₂ O ₅	0.29	0.3
Li ₂ O	2.01	2.0
ZnO	2.47	2.5
Fission product oxides	10.87	11.1
Zr oxides [†]	0.98	1.0
Metallic particles	0.67	0.7
Actinide oxides	0.86	0.9
	98.88	
Other components [‡]	1.12	
	100.0	100.0

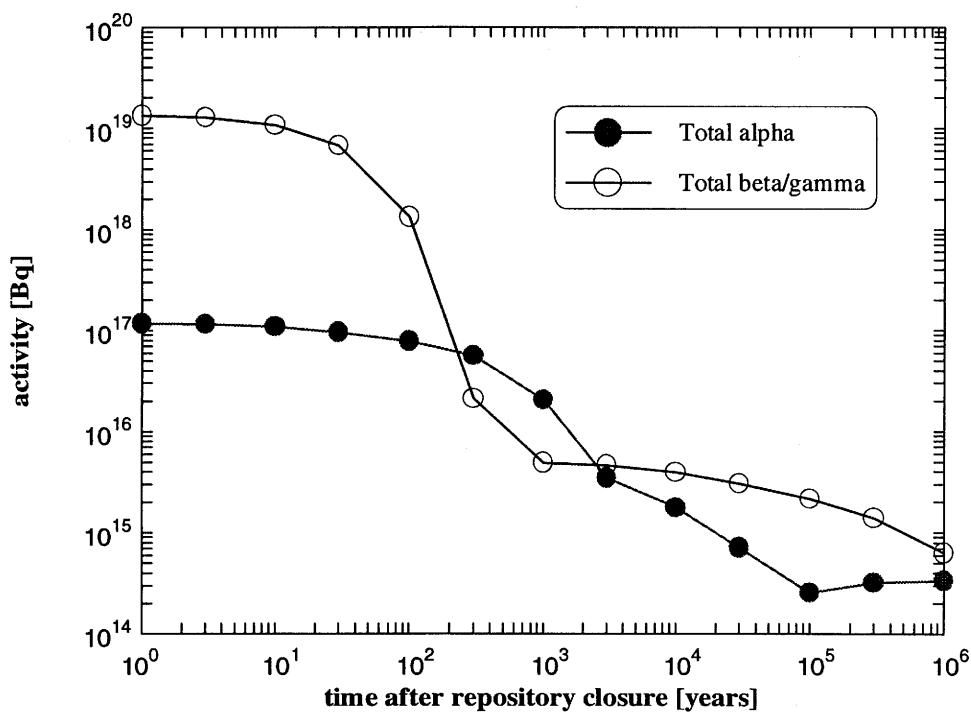
Notes: † Excluding Zr from fission.

‡ Activation products arising from impurities in the fuel 0.12 %; Gd activation products 0.96 %; Inconel fines from the structural material of the fuel assembly 0.04 %.

Table 3.3.2: Comparison of the glass composition by weight (%) of waste type WA-COG-1, as predicted by the Nagra model, with that given in the COGEMA specification. (From ALDER & McGINNES 1994).

Radionuclide	Activity (Bq)	Radionuclide	Activity (Bq)	Radionuclide	Activity (Bq)
¹⁰ Be	2.2×10^5	¹²⁹ I	1.6×10^6	²²⁸ Th	2.8×10^8
¹⁴ C	4.3×10^7	¹³⁴ Cs	1.9×10^{15}	²²⁹ Th	5.3×10^3
⁴¹ Ca	9.4×10^6	¹³⁵ Cs	1.9×10^{10}	²³⁰ Th	3.1×10^6
⁴⁵ Ca	4.8×10^7	¹³⁷ Cs	4.8×10^{15}	²³¹ Th	1.6×10^6
⁵⁴ Mn	5.5×10^9	^{137m} Ba	4.4×10^{15}	²³² Th	3.2
⁵⁵ Fe	3.3×10^{11}	¹⁴⁴ Ce	1.6×10^{15}	²³⁴ Th	2.5×10^7
⁵⁹ Fe	1.1×10^1	¹⁴⁴ Pr	1.6×10^{15}	²³¹ Pa	8.7×10^5
⁵⁷ Co	3.7×10^{10}	¹⁴⁷ Pm	2.5×10^{15}	²³³ Pa	1.6×10^{10}
⁵⁸ Co	1.6×10^6	¹⁴⁷ Sm	1.9×10^5	^{234m} Pa	2.5×10^7
⁶⁰ Co	5.8×10^{12}	¹⁵¹ Sm	1.8×10^{13}	²³² U	1.6×10^6
⁵⁹ Ni	1.9×10^9	¹⁵² Eu	2.5×10^{11}	²³³ U	7.8×10^4
⁶³ Ni	2.5×10^{11}	¹⁵⁴ Eu	3.8×10^{14}	²³⁴ U	9.4×10^7
⁶⁵ Zn	1.0×10^{11}	¹⁵⁵ Eu	1.8×10^{14}	²³⁵ U	1.6×10^6
⁷⁹ Se	2.1×10^{10}	^{166m} Ho	2.0×10^8	²³⁶ U	2.1×10^7
⁹⁰ Sr	3.5×10^{15}	¹⁸² Ta	1.5×10^9	²³⁸ U	2.5×10^7
⁹⁰ Y	3.5×10^{15}	²⁰⁹ Pb	5.3×10^3	²³⁷ Np	1.6×10^{10}
⁹³ Zr	9.4×10^{10}	²¹⁰ Pb	4.4×10^2	²³⁹ Np	7.4×10^{11}
^{93m} Nb	2.2×10^{10}	²¹⁴ Pb	5.4×10^3	²³⁶ Pu	4.7×10^7
⁹⁴ Nb	1.0×10^8	²¹⁰ Bi	4.4×10^2	²³⁸ Pu	9.4×10^{11}
⁹⁵ Nb	2.5×10^{10}	²¹³ Bi	5.3×10^3	²³⁹ Pu	1.1×10^{11}
⁹³ Mo	3.9×10^7	²¹⁴ Bi	5.4×10^3	²⁴⁰ Pu	2.0×10^{11}
⁹⁹ Tc	6.7×10^{11}	²¹⁰ Po	1.4×10^6	²⁴¹ Pu	3.8×10^{13}
¹⁰⁶ Ru	1.6×10^{15}	²¹³ Po	5.2×10^3	²⁴² Pu	5.9×10^8
¹⁰⁶ Rh	1.6×10^{15}	²¹⁴ Po	5.4×10^3	²⁴⁴ Pu	1.2×10^2
¹⁰⁷ Pd	5.3×10^9	²¹⁸ Po	5.4×10^3	²⁴¹ Am	3.3×10^{13}
^{108m} Ag	6.2×10^8	²¹⁷ At	5.3×10^3	²⁴² Am	3.4×10^{11}
^{110m} Ag	3.3×10^{12}	²²² Rn	5.4×10^3	^{242m} Am	3.5×10^{11}
^{119m} Sn	2.1×10^{11}	²²¹ Fr	5.3×10^3	²⁴³ Am	7.4×10^{11}
^{121m} Sn	9.4×10^9	²²⁵ Ra	5.3×10^3	²⁴² Cm	4.6×10^{12}
¹²³ Sn	7.1×10^{10}	²²⁶ Ra	5.4×10^3	²⁴³ Cm	7.8×10^{11}
¹²⁶ Sn	3.9×10^{10}	²²⁵ Ac	5.3×10^3	²⁴⁴ Cm	6.8×10^{13}
¹²⁵ Sb	2.5×10^{14}	²²⁷ Ac	1.1×10^5	²⁴⁵ Cm	5.8×10^9
^{125m} Te	6.3×10^{13}			²⁴⁶ Cm	1.1×10^9
Total alpha			1.1×10^{14} Bq		
Total beta-gamma			2.8×10^{16} Bq		

Table 3.3.3: Average radionuclide content of a single HLW flask of waste type WA-COG-1 at reference time of vitrification - 4 years after unloading of fuel. (From ALDER & MCGINNES 1994).



Notes: The repository contains 2693 flasks of waste type WA-COG-1.

Figure 3.3.1: Calculated total alpha and total beta-gamma activity content of the overall inventory. (Data from ALDER & MCGINNES 1994).

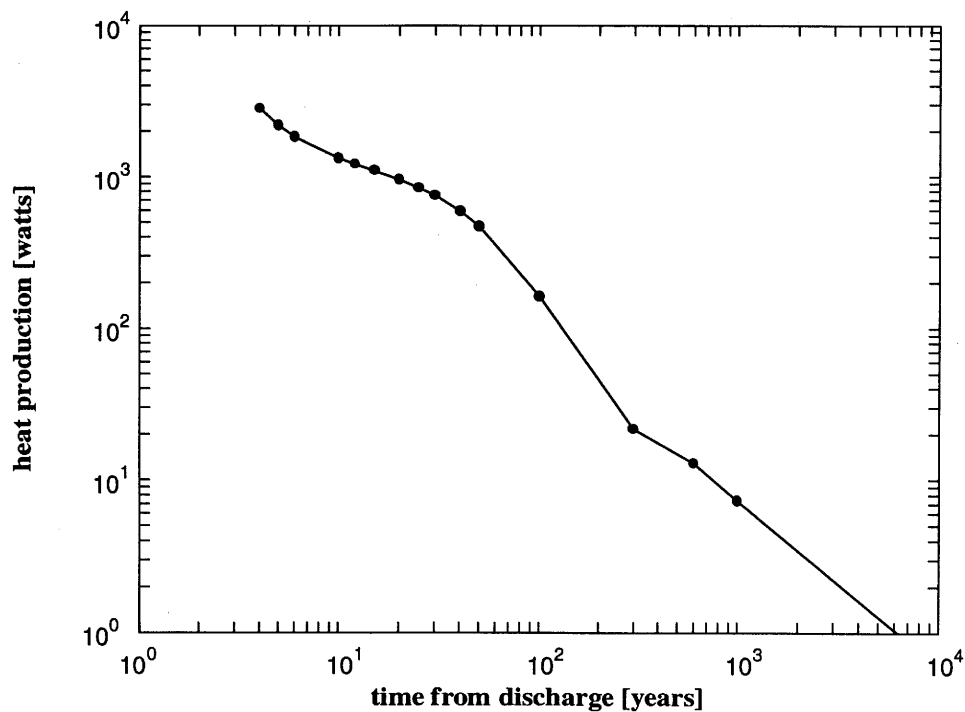


Figure 3.3.2: Calculated radiogenic heat output of a single flask of waste type WA-COG-1 as a function of time after unloading of fuel from the reactor. (Data from ALDER & MCGINNES 1994).

3.3.3 Radionuclide Inventory for Safety Assessment

For safety assessment it is necessary to identify those radionuclides that might have some potential to give rise to significant radiation doses following disposal of the waste in the repository, or the parents of such radionuclides. It is also necessary to consider stable isotopes of these elements, since these can influence effective solubilities of radionuclides.

In order to identify safety-relevant radionuclides, a simple analysis has been carried out that takes account of:

- the design lifetime of the waste canister;
- the rate of glass corrosion;
- dilution in a near-surface aquifer;
- drinking of aquifer water.

Retention in the engineered and geological barriers, further dilution/concentration processes in the surface environment and other dose pathways have been neglected. The model is described in Appendix 2 and the drinking water doses from all radionuclides, calculated using this model, are presented. It is assumed that only radionuclides for which the calculated dose is greater than 10^{-4} mSv y^{-1} (or long-lived parents of such radionuclides) are relevant to long-term radiological safety. This dose level is one thousandth of the Swiss regulatory dose limit of 0.1 mSv y^{-1} . As a result, five fission/activation products and the members of four actinide chains have been selected as the radionuclides for more detailed consideration in the Kristallin-I safety assessment. In addition, ^{59}Ni and ^{107}Pd have been included, in spite of their low calculated drinking water doses, in order that the Kristallin-I assessment covers all radionuclides calculated in Project Gewähr 1985. The actinide decay chains can be simplified for the purpose of assessment modelling by neglecting the shorter-lived members of each chain (see Appendix 2), although all the chain-members have been considered in the final calculation of dose. The calculated inventory of each of the selected radionuclides and stable isotopes of the same elements are given in Table 3.7.1 for the reference canister failure time of 1000 years after repository closure (1040 years after unloading of the fuel from the reactor). Decay and ingrowth of the inventory given in Table 3.3.3 during the period up to 1000 years after closure are accounted for using the code RAPIDE (GRINDROD et al. 1990a).

3.4 The Engineered Barriers

The engineered barrier system considered in Kristallin-I is identical to that described for vitrified HLW in Project Gewähr 1985 (Volume 4 of NAGRA 1985) and is illustrated in Figure 3.4.1. In this concept, relatively small volumes of waste are surrounded by large quantities of materials (Table 3.4.1), which maintain the stability of the chemical and physical properties of the engineered system for long periods of time. Since Project Gewähr 1985, understanding of some of the relevant processes acting within the engineered system has developed further; this understanding has enhanced confidence in the modelling of the repository near field for safety assessment.

Material	Volume (m ³)	Mass (kg)
Glass	0.15	412
Stainless steel (fabrication flask)	0.01	75
Fabrication void	0.03	-
Cast steel (canister) [†]	1.2	8.4 × 10 ³
Bentonite:	52.8	-
(a) dry material	32.7	9.0 × 10 ⁴
(b) pore space (water-filled)	20.1	2.0 × 10 ⁴

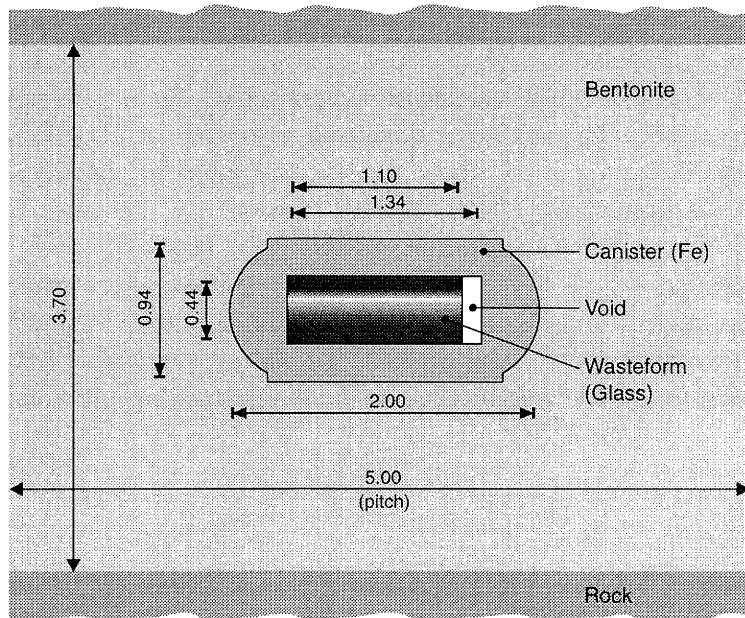
Note: † This volume includes internal spacers, shielding etc. (see Figure 3.4.3)

Table 3.4.1 Material inventory in the engineered barriers (per canister).

3.4.1 Thermal Constraints on Design

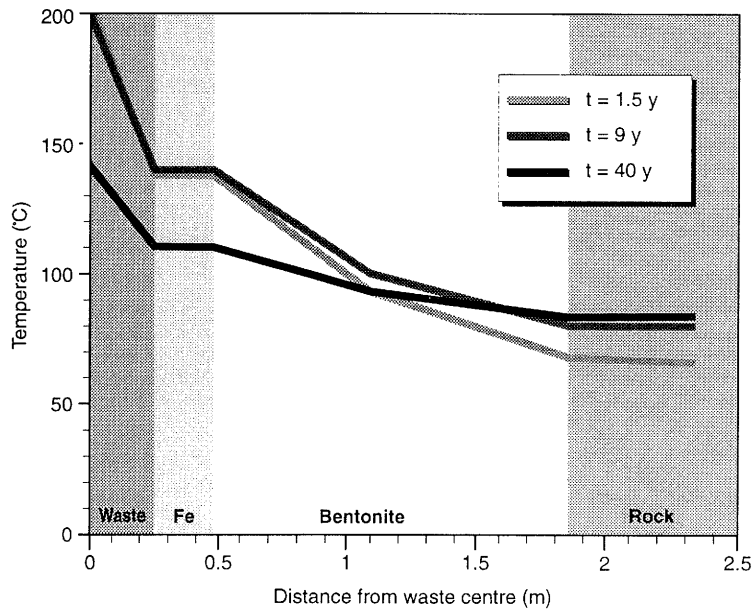
Many of the processes occurring within the engineered barriers are temperature dependent. In particular, to assure the required properties of the bentonite, it is desirable that a significant thickness of bentonite does not experience temperatures above 100 °C. Model results for the thermal evolution of the repository in Project Gewähr 1985 (Volume 4 of NAGRA 1985; HOPKIRK & WAGNER 1986) showed sensitivity to the assumptions made concerning the resaturation of the bentonite; several different calculations were carried out based on the variable bentonite porewater content, the existence or not of air gaps within the bentonite and the thermal properties of such air gaps. The results of these calculations have been confirmed as part of a joint project with the Obayashi Corporation of Japan (OBAYASHI 1993b); the more recent calculations also investigate alternative tunnel spacings and uncertainties concerning the thermal properties of the bentonite buffer. Assuming conservative values for the thermal

conductivity and heat capacity of the bentonite, a porewater content which varies as a function of temperature between 7% at 30 °C and 0% at ≥ 150 °C, an ambient rock temperature of 55 °C and a reference tunnel separation of 40 m (the reference tunnel separation in Project Gewähr 1985), a maximum temperature of 150 °C would be reached at the canister-bentonite interface, but less than half the thickness of bentonite would experience temperatures above 100 °C; moreover, the period of elevated temperatures would be rather short (less than 50 years). The assumption of a reduced emplacement tunnel spacing of 20 m leads to a similar temperature evolution (shown in Figure 3.4.2). More realistic assumptions (higher thermal conductivity and heat capacity) give significantly lower temperatures in the bentonite. However, higher temperatures are calculated for further hypothetical reductions in the tunnel spacings (to 5 and 10 m).



Note: Dimensions are given in units of metres.

Figure 3.4.1: The engineered barrier system considered in the Kristallin-I safety assessment. The vitrified HLW is emplaced in a thick cast steel canister surrounded by precompacted bentonite blocks in horizontal emplacement tunnels.



Note: Analysis 8 from OBAYASHI 1993b: 20 m emplacement tunnel spacing, no air gaps between bentonite blocks and temperature-dependent bentonite porewater content in the range 0 to 7% by weight.

Figure 3.4.2: Calculation of temperature evolution within the engineered barrier system.

3.4.2 The Waste Matrix and Relevant Processes

3.4.2.1 Description and Function

The composition of the waste matrix, which is a borosilicate glass loaded with residues from the reprocessing of nuclear fuel, is given in Subsection 3.3.2.

The function of the glass is to provide a corrosion-resistant solid matrix for the waste. After canister failure, water contacts the glass, which begins to corrode. The glass is assumed to be cracked due to stresses induced during cooling and minor handling shocks; the surface area of the glass available for corrosion or leaching is therefore greater than the surface of a monolithic block. A surface area increase by a factor of 12.5 is considered to be appropriate for the purpose of safety assessment (GRAUER 1983).

3.4.2.2 Corrosion of the Glass

The corrosion rate of the glass is determined by its composition and temperature, as well as the composition and pH of the solution with which it has contact (GRAUER 1985). Selective leaching of alkali and alkaline earth ions is a transient phenomenon at repository temperatures and influences the corrosion process for only a few days to weeks. This phenomenon is therefore unimportant in safety assessment. At longer times, non-selective glass-matrix corrosion occurs, giving congruent radionuclide release. Although their release is congruent, many glass components (heavy metals, the actinides and lanthanides) have a low solubility and are retained in secondary products at the glass surface. Therefore, not all elements pass completely into solution at the same rate.

If glass composition, temperature and pH are fixed, the most important parameter which influences glass corrosion is the silicic acid concentration at the glass surface. The corrosion rate follows first-order kinetics with respect to silicic acid (GRAUER 1985; VERNAZ & DUSSOSSOY 1992). This has been confirmed in numerous experiments, which can be described quantitatively using this concept (see, for example, CURTI et al. 1993). However, critical model parameters cannot be determined with sufficient accuracy to allow a long-term extrapolation (CURTI 1991). The reaction rates used in the safety assessment are therefore conservative estimates based on the experimental evidence and supported by investigations of natural basalt glasses.

The chemical corrosion of highly radioactive borosilicate nuclear waste glass has been investigated in the international JSS project, the results of which are summarised in WERME et al. 1990. Experimental data for times up to 1.5 years indicate that, after saturation with silica is attained, the corrosion rate of COGEMA glass is in the order of 10^{-4} kg m⁻² y⁻¹. This rate is confirmed by the interim results of on-going experiments in the Swiss programme, which, after 548 days, also indicate a corrosion rate in the order

of 10^{-4} kg m⁻² y⁻¹ at 90 °C (ZWICKY et al. 1992) and thus support the choice of the reference glass-corrosion rate in Project Gewähr 1985 of 4×10^{-4} kg m⁻² y⁻¹ (10^{-7} g cm⁻² day⁻¹). A reference value of 4×10^{-4} kg m⁻² y⁻¹ is therefore also adopted for the Kristallin-I safety assessment calculations, giving a lifetime for each fractured glass block of 1.5×10^5 years (see Subsection 5.2.2.1).

Natural basalt glasses have a SiO₂ content (ca. 50 %) similar to that of the waste glasses (although they contain effectively no boron or lithium). Since the SiO₂ content is one of the most important parameters determining the stability of a glass, such basalts are possible natural analogues for borosilicate glasses. Investigations of natural glasses have provided support for very low long-term corrosion rates of waste glasses (e.g. WERME et al. 1990; PETIT 1991; MILLER et al. 1994).

In the Kristallin-I safety assessment, in order to cover uncertainties in this rate, a very conservative value of 4×10^{-2} kg m⁻² y⁻¹ is used in parameter variations, with a corresponding lifetime for a glass block of 1.5×10^3 years following failure of the canister.

3.4.3 The Cast Steel Canister and Relevant Processes

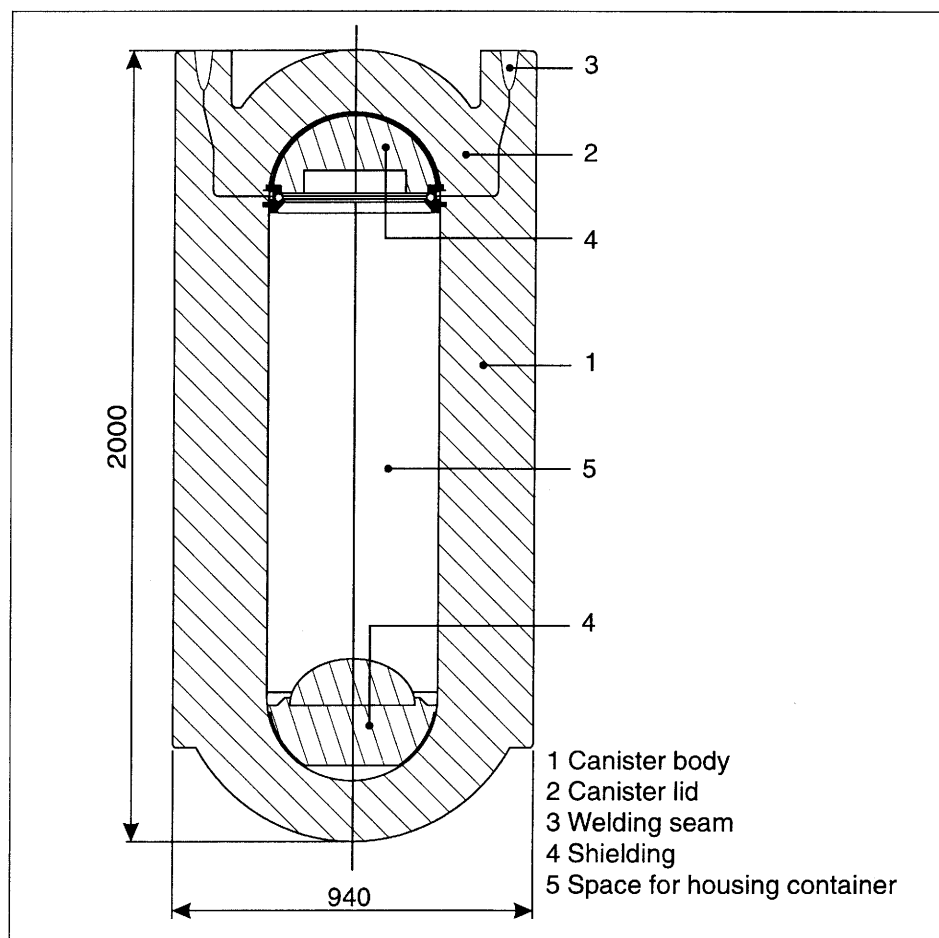
3.4.3.1 Design and Performance

The thin stainless steel flask containing the vitrified HLW acts only as a mould for the molten glass and a primary container prior to disposal; it is not relied upon to provide any barrier function after disposal.

The design criteria placed on the cast steel canister include a maximum acceptable dose at the canister surface for the operational period and the requirement that the canister should remain unbreached for at least 1000 years after repository closure. In particular, it should be able to withstand an external isostatic pressure of 30 MPa, corresponding to the sum of the maximum swelling pressure of the compacted bentonite (see Subsection 3.4.4.2) and hydrostatic pressure. These requirements are the same for Kristallin-I as for Project Gewähr 1985 (Volume 4 of NAGRA 1985), as are the canister material and design.

The evaluation of the canister material is discussed in NAGRA (1984) and design carried out at the time of Project Gewähr 1985 is documented in STEAG & MOTOR-COLUMBUS (1985). This report describes a canister made of cast steel GS 40 and consisting of a thick-walled self-supporting cylindrical shell with hemispherical ends (see Figure 3.4.3). The wall thickness is 250 mm in the cylindrical body and 150 mm in the

hemispherical ends (a lid, which is welded onto the main body of the canister, and a base, which is cast together with the main body as a single unit); additional shielding is provided on the inside of the canister ends. The total weight of the canister, when loaded with a vitrified waste flask, is 8.9 tonnes. Fabrication quality is ensured through, for example, a simple sand-mould casting production method and ultrasonic inspection of the completed canister, lid and weld.



Note: Dimensions of the canister are given in units of millimetres.

Figure 3.4.3: The Nagra reference cast steel canister for disposal of vitrified HLW.

The canister was designed according to the American Society of Mechanical Engineers (ASME) code, and its performance evaluated by the FEABL-1 computer model (STEAG & MOTOR-COLUMBUS 1985). These stress and stability analyses were carried out assuming uniformly and unevenly corroded canisters (i.e. with wall thicknesses reduced by up to 50 mm, giving a thickness of 200 mm) and, for the design external isostatic pressure of 30 MPa, show that the safety margins are higher than required by the ASME code. The analysis tool and methods have been verified and tested

against experiments, including the prediction of failure of scale-model canisters, in the CEC COMPAS exercise (OVE ARUP 1990; ATTINGER & DUIJVESTIJN 1994).

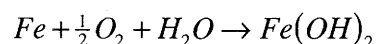
The extent of corrosion allowed for in the above analyses (a maximum of 50 mm) is greater than the maximum corrosion in 1000 years of about 30 mm due to pessimistically calculated reactions with oxygen, sulphides and anaerobic reaction with water (see Subsection 3.4.3.2). The reference canister wall thickness of 250 mm thus provides a more than sufficient allowance for corrosion, significant uneven corrosion being ruled out (see Subsection 3.4.3.3).

For Kristallin-I, the design lifetime of 1000 years following repository closure is conservatively adopted as a Reference-Case time for canister failure; the same as that adopted in Project Gewähr 1985. Realistically, the canister lifetime may far exceed this value. A more realistic estimate of canister lifetime is not, however, adopted in the Reference Case, because of uncertainties in estimating the rate and distribution of corrosion, the mechanical loads that may be imposed, and the modes of failure. The effects of a longer canister lifetime are investigated in a parameter variation (see Subsection 5.2.3.1) and shown to be small.

3.4.3.2 Steel Corrosion Processes

In Project Gewähr 1985, three corrosion processes were considered (Volume 4 of NAGRA 1985):

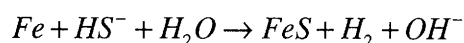
- (i) Reaction with trapped oxygen, enclosed at the time of emplacement;



– *estimated extent of corrosion in 1000 years, < 1 mm.*

The estimated amount of metal corrosion caused by oxygen trapped during the operational phase is less than 1 mm. This estimate assumes that the entire volume of oxygen enclosed at the time of emplacement is available and is completely consumed within the specified period (NAGRA 1984). The conditions are such that, after a short period of time, the oxygen corrosion becomes less significant than corrosion induced by reaction with water.

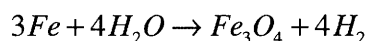
- (ii) Reaction with dissolved sulphides produced from reduction of sulphates in the groundwater;



– *estimated extent of corrosion in 1000 years, 9 mm.*

When considering corrosion by sulphides, the extremely conservative assumption was made that the total amount of sulphate reaching the canister is reduced to sulphide. This would only be possible if sulphate-reducing bacteria and a sufficient amount of reductant were encountered (GRAUER 1991).

(iii) Anaerobic reaction with water;



– *estimated extent of corrosion in 1000 years, 20 mm.*

The estimate of 20 mm in 1000 years for the anaerobic reaction of steel with water is derived from a conservative corrosion rate of $20 \mu\text{m y}^{-1}$; this value is based on experimental data and includes an allowance for non-uniform corrosion (NAGRA 1984).

The estimated extent of corrosion by all three processes combined is < 30 mm, compared with the canister-wall corrosion allowance of 50 mm. In their evaluation of Project Gewähr 1985, HSK considered that the corrosion allowance of 50 mm for the canister wall thickness was sufficient to withstand these processes (HSK 1987). However, HSK felt it was necessary to carry out further investigations on the extent of any localised corrosion.

3.4.3.3 Localised Corrosion of the Steel

Corrosion of large surfaces is generally uneven, mainly due to differences in surface composition or slight local variations in the corrosive medium. This fact was taken into account when determining the conservative rate for anaerobic reaction with water of $20 \mu\text{m y}^{-1}$ (NAGRA 1984). In the course of time, non-uniform corrosion will even out to some extent. An increase in corrosion rate also means an increased production of solid corrosion products. The corrosion products have a greater volume than the metal, and therefore tend to seal the corroding location, leading to a slower corrosion rate.

One form of corrosion that cannot be dealt with by the corrosion-allowance approach is stress corrosion cracking (SCC). SCC is a possible mechanism for more rapid corrosion in areas with high residual stresses, e.g. due to welding. The SCC process requires a certain minimum stress level before it can occur. The model results of ATTINGER & DUIJVESTIJN (1994) show that the calculated residual tensile stresses around the weld of the Nagra canister lid (Figure 3.4.3) may reach the yield limit. Experimental evidence suggests that a reduction in these stresses to 50% of the yield strength should be sufficient to prevent SCC (MARSH et al. 1986). The calculations in ATTINGER & DUIJVESTIJN (1994) show that it should be possible to achieve this reduction by

means of stress-relief heat treatment after welding, thus avoiding the problem of SCC. The possibility of SCC could also be avoided by bolting or screwing the canister lid.

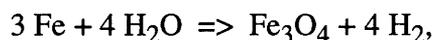
Strongly localised corrosion also occurs if cathodic and anodic partial reactions are spatially separated, as would be the case if aeration cells are present. Local oxygen concentration gradients along the surface of the canister are unlikely to form because any oxygen present would be removed by diffusion through the bentonite (GRAUER 1993). Furthermore, aeration cells cause local differences in pH, which reduces their likelihood of formation and their stability in buffered solutions, such as will be maintained in bentonite porewater. The electrolyte conductivity, the ratio of cathode to anode surface and the rate of oxygen supply determine the extent of localised corrosion by such aeration cells. With a water content of 30%, the bentonite has a specific resistance of 10^4 Ohm cm (GRAUER 1986). The risk that aeration cells will form at this resistance is low and, in practice, with resistances of this order, cathodic corrosion protection can generally be dispensed with (BAECKMANN & SCHWENK 1980).

The effects on the canister of radiolysis, high-temperature creep and hydrogen embrittlement have been considered and are expected to be negligible for a cast steel canister (GRÄFEN & HEITZ 1984; ROSSELET 1984)

3.4.3.4 Hydrogen Evolution from Corrosion

The production of hydrogen by corrosion of steel is relevant to repository safety because of the disturbance to the bentonite which might occur if a high-pressure free gas phase were to form. Gas dissipation is discussed in Subsection 3.4.4.7.

Hydrogen is evolved during the anaerobic reaction of water with steel. According to the reaction



the hydrogen evolution per micrometre of metal removal amounts to 0.188 moles of hydrogen per square metre. With the corrosion rate of $20 \mu\text{m y}^{-1}$ used for estimating the canister lifetime (see Subsection 3.4.3.2), the hydrogen production rate would be $3.8 \text{ mol m}^{-2} \text{ y}^{-1}$ (or 22.6 mol y^{-1} per canister). However, the value of $20 \mu\text{m y}^{-1}$ is very conservative (NAGRA 1984), since:

- it contains an allowance for uneven metal corrosion, which is appropriate when deriving a conservative canister lifetime, since the canister may fail locally, but not relevant when assessing hydrogen evolution from the entire canister surface;
- it takes account of the relatively wide scatter in experimental measurements of weight loss;

- it is based on the measured, initial corrosion rate, which is much higher than the stationary rate attained after formation of a layer of corrosion products.

Gravimetric experiments show that, after initial rapid corrosion, the corrosion rate drops to $5 \mu\text{m y}^{-1}$ and lower (ANANTATMULA et al. 1984; NAGRA 1984; SIMPSON & VALLOTTON 1986). It is not, therefore, appropriate to base the long-term hydrogen evolution rate on measurements of the initial value. In order to obtain a more realistic estimate, hydrogen evolution has been determined directly for corroding samples by both gas chromatography (SCHENK 1988; SIMPSON 1989) and manometer measurements (KREIS 1991). Corrosion of unalloyed, refined steel in deep Böttstein (1326 m) and Säckingen waters and in chloride solutions was investigated.

The gas chromatography measurements were carried out for a temperature range of 25 to 80 °C, with typical measurement periods of around 200 hours. Initially, hydrogen evolution rates in the order of 6 to $30 \text{ mol m}^{-2} \text{ y}^{-1}$ were measured (corresponding to 30 to $160 \mu\text{m y}^{-1}$). Steady-state conditions were reached after around 100 hours when, independent of temperature, the hydrogen evolution rate was typically in the range 0.18 to $0.47 \text{ mol m}^{-2} \text{ y}^{-1}$ (corresponding to a corrosion rate of 1 to $2.5 \mu\text{m y}^{-1}$). However, in isolated cases, $0.9 \text{ mol m}^{-2} \text{ y}^{-1}$ was evolved.

The manometer measurements were carried out over several thousand hours at ambient temperature. The hydrogen evolution values, measured after around 100 hours, were about $0.1 \text{ mol m}^{-2} \text{ y}^{-1}$ (corresponding to $0.5 \mu\text{m y}^{-1}$). After around 4000 hours, the production rate had dropped to typical values of 0.01 to $0.02 \text{ mol m}^{-2} \text{ y}^{-1}$ (corresponding to 0.05 to $0.1 \mu\text{m y}^{-1}$).

Thus, a hydrogen evolution rate of $3.8 \text{ mol m}^{-2} \text{ y}^{-1}$ appears significantly too high. For the purpose of estimating hydrogen evolution, where an allowance for uneven corrosion is not required, a long-term corrosion rate for the canister in the repository in the order of 0.1 to $1 \mu\text{m y}^{-1}$ appears to be realistic, particularly considering the thick layers of corrosion products that form with time. This corresponds to a long-term rate of hydrogen evolution of 0.02 to $0.2 \text{ mol m}^{-2} \text{ y}^{-1}$, or about 0.1 to 1.2 mol y^{-1} per canister under repository conditions.

3.4.3.5 Other Mechanisms for Evolution of Gas

Following canister failure, hydrogen will also be formed by radiolytic decomposition of water close to the glass. However, the maximum rate of production is estimated at about $0.01 \text{ moles y}^{-1}$ per canister at 1000 years, conservatively assuming no recombination of radiolysis products (McKINLEY 1985), and will decline as the activity of the wastes decreases. This rate is very small compared to the estimated rate of hydrogen evolution from anaerobic canister corrosion and can be neglected.

No significant gas production due to organic degradation is expected because of the negligible amount of organic material present in HLW disposal tunnels. The small quantity of helium from alpha decay will readily dissipate from a failed canister.

3.4.4 The Bentonite Buffer and Relevant Processes

3.4.4.1 Design and Properties

Bentonite is the geological term for clays produced by hydrothermal alteration of volcanic rocks, usually tuff and ash. Bentonite is rich in swelling clays (smectites), mainly montmorillonites. These clays have a very wide range of uses and are commercially available in many forms.

In Project Gewähr 1985, Volclay MX-80, as mined in Wyoming and South Dakota (USA), was taken as the reference material for the HLW repository, primarily because of the comparatively large volume of experimental data which was available. This bentonite is retained in Kristallin-I, although other bentonites could fulfil the necessary functions in the planned repository equally well. MX-80 is a bentonite with about 75% montmorillonite content. Na is the major exchangeable cation. The most important additional components are quartz (15%) and feldspar (5 to 8%); carbonates (1.4%), pyrite (0.3%) and organic carbon (0.4%) are also present (GRAUER 1986).

It is planned to emplace the bentonite in the form of precompacted blocks with a dry density of 1650 to 1750 kg m⁻³, in order to provide a swelling pressure in the order of 4 to 18 MPa (PUSCH 1980b; PUSCH 1983).

3.4.4.2 Saturation and Swelling

After emplacement, groundwater will slowly penetrate the bentonite, which will swell and seal gaps between the blocks, at the bentonite-host rock interface and at the bentonite-canister interface, so that a homogenous mass is formed (see, for example, PUSCH et al. 1987). The time taken for bentonite to saturate depends on the hydraulic and thermal properties of both the bentonite and the surrounding rock. This coupled problem is difficult to solve because of the effects of the thermal pulse from the waste and perturbation of the host rock caused by tunnel construction. Modelling studies indicate that saturation times may range from less than 100 years to greater than 1000 years (ANDREWS et al. 1986). However, the resaturation time is conservatively neglected (assumed to be instantaneous) in estimating the canister lifetime.

Although access of the water from the host rock to the bentonite will be localised, modelling studies indicate that the infiltration front in the bentonite will even out because of the temperature field from radiogenic heat production (CARNAHAN 1988).

A significant volume increase in the bentonite as it saturates is prevented by the restricted volume of the tunnels. The swelling pressure of the bentonite may close fissures and cracks in the neighbouring rocks to some extent, but this effect is neglected in the safety assessment. In order to avoid fracturing of the host rock, the dry density of the bentonite is selected so that the swelling pressure will not lead to excessive fracturing of the rock.

3.4.4.3 Hydraulic Properties

The hydraulic conductivity of smectite-rich clays as a function of density has been intensively investigated and reported in the literature (see, for example, PUSCH 1980a; SCHMIDT et al. 1994). Hydraulic conductivities of 3×10^{-6} to 3×10^{-7} m y⁻¹ (10^{-13} to 10^{-14} m s⁻¹) have been measured for pure bentonites, under expected repository conditions, using high-pressure techniques. Measurements of the hydraulic conductivity in compacted bentonite using an ultracentrifuge technique give results below the detection limit (10^{-16} m s⁻¹) in all samples (CONCA et al. 1993). This means that, once water saturation is reached, the bentonite is practically water-impermeable and any solute transport can only occur by diffusion (see Subsection 3.4.6.3).

Colloids, containing radionuclides, may be produced as the glass degrades. These are, however, prevented from being transported away from the glass by the micro-porous structure of the bentonite buffer.

3.4.4.4 The Short-Term Thermal Stability of Bentonite

The calculated temperature at the canister-bentonite interface, though slightly dependent on the model assumptions, peaks at about 150 °C and then drops to below 100 °C after 50 years (OBAYASHI 1993b; see also Figure 3.4.2). The temperature at the rock wall depends less on model assumptions and, assuming a reference 40 m tunnel spacing, reaches a maximum of about 75 °C. Up to a third of the thickness of the bentonite is exposed to temperatures in excess of 100 °C for a period of a few tens of years (see Figure 3.4.2). In this zone, the interlayer water of unsaturated montmorillonite is easily expelled. At 105 °C, a layer of water remains intact, but, between 130 and 150 °C, all the water is removed (PUSCH & KARNLAND 1990). However, such dehydration is reversible. Shrinkage cracks can form if the bentonite dries out, but it has been shown that these cracks heal in the presence of water (OSCARSON et al. 1990). Only if the cation-exchange capacity of the montmorillonite is saturated with potassium ions does

drying-out at 110 °C lead to irreversible layer collapse. Saturation with potassium can, however, be ruled out by the low rate of supply of this element (see Subsection 3.4.4.5), and the temperature, which is maintained at around 100 °C for only few decades, is insufficient for significant illitisation. This is supported by investigations of natural smectites which were exposed to higher temperatures (MÜLLER-VONMOOS & KAHR 1985; PUSCH 1985; PUSCH & KARNLAND 1988).

There are indications that the interaction of water vapour with bentonite can cause cementation, with relatively rapid loss of swelling capacity (the "Couture effect"; see COUTURE 1985). This has been interpreted in terms of silica cementation (MEIKE 1989; PUSCH & KARNLAND 1988; PUSCH & KARNLAND 1990). However, such cementation is weak and does not have significant effects in highly compacted bentonite (SHARLAND 1991).

The following text is taken from Appendix C of OECD (1993):

A set of hydrothermal field tests on the resaturation of compacted clay have been conducted, in part to test this concept and impact of cementation. The tests were conducted for up to 4 years at a maximum 170-180 °C and a gradient of 13 °C cm⁻¹ (PUSCH et al. 1992). They find that there was considerable cementation of the clay, causing brittleness and loss of expansivity within a few centimetres of the steel surface of the heat source. Clay samples from further away showed slight to negligible changes in properties. There was no evidence of increased iron content in the clay near the steel heater, indicating that iron compounds were not the cause of the cementation. In the hottest region, anhydrite and probably hexahydrate¹¹ were precipitated, probably attributable to their retrograde solubility (i.e. these phases are less soluble at higher temperatures): Slightly further away from this hottest zone, new amorphous silica-aluminium phases formed in this slightly cooler region. The mobilisation and deposition of these phases may be attributable to their prograde solubility in a thermal gradient or to cyclic evaporation/condensation that takes place in a resaturating clay under a thermal gradient.

It thus seems probable that any cementation that occurs is limited to the zone immediately around the canister, leaving a thick annulus of unaffected bentonite. Even if the loss of swelling is more extensive, it should be noted that, following water vapour treatment, the swelling capacity of bentonite is reduced but is not completely lost (COUTURE 1985). For the emplacement densities considered, the remnant (inter-crystalline) swelling is sufficient to ensure that the bentonite has an adequately low permeability (GRAUER 1990a).

3.4.4.5 Long-Term Stability of the Bentonite

In order to determine the long-term stability of bentonite at repository temperature, the existing literature on the subject has been evaluated (GRAUER 1986; GRAUER 1990a;

¹¹ The term hexahydrate is used in mineralogy to denote MgSO₄ · 6H₂O.

Appendix C in OECD 1993). The most likely possible alteration process appears to be the transformation of montmorillonite to illite, which would reduce the swelling potential and the cation-exchange capacity of the buffer. Alteration to chlorite occurs only in waters with high magnesium concentrations, which are not found in the crystalline basement of Northern Switzerland (see Table 3.5.2).

Two conditions have to be fulfilled simultaneously for illite to form from montmorillonite, namely (i) an increase in the (tetrahedral) layer charge of the clay; and (ii) replacement of the interlayer ions by potassium ions. The transition from montmorillonite to illite occurs naturally via intermediate stages of illite and montmorillonite interlayers. Increasing the layer charge alone does not affect the swelling capability, which is lost only if the interlayer ions are exchanged for potassium.

For the hypothetical case that supply of potassium ions to the repository controls illite formation, the extent of alteration can be estimated from the potassium supply from the groundwater and the cation exchange capacity of the bentonite. For Project Gewähr 1985 conditions, total conversion of montmorillonite to illite was calculated to take longer than 10 million years ($\sim 7 \times 10^7$ years based on calculations in NAGRA 1985 and $\sim 4 \times 10^7$, as calculated in McKINLEY 1985). This was for an assumed groundwater flowrate of 0.7 litres per canister per year and a potassium concentration in groundwater of 1.15 mM. For Kristallin-I, the reference water (Area West) contains 0.22 mM K^+ (see Table 3.5.2), while the reference flowrate through the repository is $3 \text{ m}^3 \text{ y}^{-1}$, equivalent to 1.1 litres per canister per year (see Table 3.7.2). In the Reference Case, therefore, montmorillonite to illite conversion times longer than 10^8 years are indicated. Even for the most conservative groundwater flowrates, two orders of magnitude higher than the Reference-Case value (see Table 3.7.2), and assuming that all potassium in groundwater is taken up in the alteration process, a montmorillonite "lifetime" of greater than one million years can still be justified.

If it is assumed that the increase in the layer charge, rather than the supply of potassium ions, is rate-determining in illite formation (i.e. postulating an unlimited supply of potassium ions), data on the kinetics of alteration from montmorillonite to illite have to be included. With a low water flux, this reaction occurs isochemically, with around two illite layers and silicic acid being produced from three montmorillonite layers. This alteration occurs extremely slowly and the kinetics can only be investigated in the laboratory under hydrothermal conditions (temperatures greater than 250 °C). Extrapolation to the repository temperature also results in a montmorillonite "lifetime" of around one million years. However such an extrapolation is problematic because of uncertainty regarding the activation energies.

Natural analogue investigations of montmorillonite-rich clay sediments are a useful tool for assessing the long-term stability of these materials. For example, the clays in the Gulf of Mexico have been studied in considerable depth in connection with oil exploration. These sediments have been deposited continuously over a 200 million year period. Studies of drill cores indicate that, even in old sediments (30 million years), significant

illitisation occurs only at temperatures in excess of 80 °C. Independent of geological age, the maximum illite component is in the order of 80%. The temperature required for illitisation to begin is between 60 and 90 °C and alteration to 70 to 80% illite occurs in the temperature range 90 to 140 °C (FREED & PEACOR 1989). Evaluation of the large number of investigations carried out on natural analogues leads to the conclusion that, with a long-term temperature within the bentonite close to that of the host rock (55 °C; see Figure 3.4.2), there will be no drastic change in swelling capability, hydraulic conductivity or cation exchange capacity of the bentonite in time periods well in excess of one million years. The formation of mixed illite-montmorillonite layers during the course of time cannot be ruled out, but complete illitisation can be.

Finally, although the alteration to illite may reduce the swelling capacity and cation-exchange capacity of the buffer, illite has many of the favourable properties required of a buffer material, i.e. low permeability and microporous structure that will prevent colloid transport. Illite has also been considered as a potential buffer material (BROOKINS 1984).

3.4.4.6 Chemical Reactions with the Canister and Waste Matrix

Corrosion of the steel canister under anaerobic conditions produces magnetite. There is very little information on potential interactions between this corrosion product and the bentonite and the thermodynamic data required for making a reliable evaluation are lacking. However, experiments with iron- and magnetite-bentonite mixtures at 80 °C show, after 27 and 29 weeks respectively, that there is no adverse change in the bentonite properties (MÜLLER-VONMOOS et al. 1991).

Potential interactions between magnetite and montmorillonite have been discussed in detail on the basis of chemical and crystal-chemistry data (GRAUER 1990a). The most likely of these reactions leads to the formation of new iron silicate phases; the formation of chamosite, greenalite or nontronite is considered likely and these reaction products have only a limited swelling capability. However, given the quantity ratios in the repository (see Table 3.4.1), a complete reaction of this type could alter only a limited amount of the montmorillonite. Furthermore, as clay minerals, the reaction products are micro-crystalline and the sorption capacity of the bentonite would be virtually unaffected.

Any possible effects that the products of glass corrosion may have on the bentonite would be of secondary importance, given the relative quantities in the repository. The glass is spatially separated from the bentonite by the canister corrosion products, so that, at most, the formation of iron silicate phases would be expected.

3.4.4.7 Mechanical Interactions and Gas Dissipation

If the bentonite is to be effective as a safety barrier, retarding solute transport and preventing the movement of colloids, it must continue to completely surround the steel canister over a long period of time. If the canister were able to sink through the bentonite under gravity, then the effectiveness of the bentonite barrier could be lost. Calculations of canister sinking have been carried out in which it is assumed that the bentonite is fully saturated, the clay is modelled using conventional soil-mechanical creep-strain equations (MITCHELL et al. 1968) and data are taken from short-term compression tests on bentonite (BÖRGESSON et al. 1988). Results indicate a maximum sinking of 1 to 5 mm in 10 000 years, with a rate of sinking that decreases with time (WHITTLE & ARISTORENAS 1991). This amount of canister displacement is negligible for safety assessment. However, confirmation that the creep-strain equations are applicable over the very long periods required for repository safety assessment is lacking and, if future work does not rule out significant canister sinking, then design modifications, e.g. incorporation of a sand-rich layer around the canister or use of stone supports beneath the canister, could be considered to avoid the effect.

The formation of magnetite from iron causes a doubling of the volume, which has the effect of dilating the canister and potentially increasing stresses in the bentonite. Though the results are likely to depend strongly on the local stress field, mechanical analyses of canisters emplaced in various diameter boreholes and tunnels have shown that, in the case of 100 cm tunnels or greater, the dilation is likely to be accommodated within the bentonite and thus host rock fracturing will not occur (SAOTOME et al. 1991).

In Project Gewähr 1985, a high production rate of hydrogen from the anaerobic corrosion of steel of $3.8 \text{ mol m}^{-2} \text{ y}^{-1}$ was pessimistically assumed (Volume 4 of NAGRA 1985). More recent long-term corrosion experiments in which hydrogen evolution is measured indicate much lower rates of evolution, which justify the assumption of a long-term hydrogen generation rate in the range 0.02 to $0.2 \text{ moles m}^{-2} \text{ y}^{-1}$ (see Subsection 3.4.3.4). Since the possible rate of loss of hydrogen by aqueous diffusion at the canister surface is estimated at about 0.2 moles y^{-1} per canister ($\sim 0.02 \text{ moles m}^{-2} \text{ y}^{-1}$; ANDREWS 1993), it is uncertain whether or not a gas phase will form. However, if a gas phase does form around the canister surface, this is itself likely to reduce the rate of corrosion and the rate of production of further hydrogen. If future studies reveal that the rate of hydrogen generation will exceed the rate at which hydrogen can diffuse from the surface, it may be necessary to consider special design features, such as the incorporation of a sand capillary-breaking layer (NERETNIEKS 1985a) to provide additional buffer volume and surface area for hydrogen dissolution; this topic is also mentioned in Subsection 4.3.3.6.

3.4.4.8 Bentonite Porewater Chemistry

The chemical composition of the porewater in the buffer and contacting the wastes is assumed to be dominated by the equilibration of groundwater with bentonite and canister corrosion products.

A range of bentonite porewaters has been defined using an empirical model of groundwater reaction with bentonite that assumes both ion exchange (based on the model of WANNER 1986) and saturation equilibria with mineral phases (CURTI 1993). Reference crystalline basement groundwaters are given in Table 3.5.2 for each of the two areas currently under consideration in Northern Switzerland (Area West and Area East; see Section 3.5). For bentonite porewater definition, however, two groundwaters having a wider range of compositions are selected - one representative of less saline and one of more saline groundwaters (CURTI 1993). The resulting bentonite porewaters are presented in Table 3.4.2. Eh values are defined by canister corrosion products, assuming thermodynamic equilibrium between magnetite-hematite or magnetite-goethite.

Several models, with significantly different conceptual bases, can equally well simulate experimental bentonite porewater chemistry data and hence such models must be interpreted with caution. In parallel, therefore, independent estimates have been made by GRAUER (1993) to establish expected constraints on key parameters such as pH and carbonate concentration. The Eh / pH range specified in Table 3.4.2, which is used in the selection of elemental solubility limits, is consistent with both the modelling and literature studies in view of the uncertainties involved.

Properties of the reducing porewater formed by the interaction of groundwater with bentonite:		
	Low-salinity groundwater	High-salinity groundwater
T (C)	50	50
pH	8.97	8.49
pe	-6.18	-5.72
Eh (mV)	-396	-367
	Species concentrations (millimoles per litre, mM)	
Na ⁺	78	240
K ⁺	0.17	0.57
Ca ²⁺	0.011	0.055
Mg ²⁺	0.067	0.48
HCO ₃ ⁻	52	18
Cl ⁻	3.0	187
F ⁻	0.70	0.19
SO ₄ ²⁻	4.5	16
Al ³⁺	0.10	0.036
Si _{total}	0.26	0.19

Note: Although the temperature of the bentonite is close to that of the surrounding rock ($\leq 55^{\circ}\text{C}$) after about 100 years, a temperature of 50°C has been assumed in estimating the porewater composition. The effect of this difference in temperature is likely to be negligible.

Table 3.4.2: Bentonite porewater compositions calculated by modelling the interaction of two groundwaters, one representative of less saline and one of more saline groundwaters, with bentonite and accounting for reducing conditions due to iron corrosion products. (From CURTI 1993).

In Kristallin-I, near-field solubility limits¹² of elements are based on the reference bentonite porewater chemistry, taking account of the redox conditions provided by the canister. In principle, solubility limits could also be evaluated in borosilicate glass leachate or in pore fluids within the canister corrosion products. However, solubility limits can be more reliably calculated for the well-buffered conditions in the bentonite. In addition, if the solubilities of radionuclides were higher immediately adjacent to the wastes then precipitation would occur as the radionuclides moved into the bentonite and, if lower, then the use of solubility limits based on bentonite porewater is conservative.

3.4.4.9 Microbiological Activity

Even in the harsh conditions expected in the engineered barriers of a HLW repository, microbiological activity cannot be precluded (McKINLEY et al. 1985). Microbiological activity, with the associated production of organic complexants, could reduce the effectiveness of the engineered barriers by increasing near-field solubilities and decreasing sorption (see also the discussion of the corrosion of the canister by sulphides - Subsection 3.4.3.2). However, the maximum extent of such activity is tightly constrained by the low rates of supply of some key elements and low availability of usable energy for microbial growth in this extremely oligotrophic (nutrient-poor) environment. The relative simplicity of the disposal system allows these constraints to be quantified from the rates of nutrient supply and the maximum rate of supply of chemical energy from redox reactions.

The maximum steady-state biomass production calculated for Kristallin-I repository conditions is 10^{-5} kg (dry) y^{-1} per waste package (McKINLEY & HAGENLOCHER 1993). In the worst possible case, this high biomass production would be balanced by a similar rate of production of organic by-products, available for complexation. This source of organic carbon would be large when compared to the rate of supply from groundwater (10^{-8} kg y^{-1} per waste package). Furthermore, assuming an average molecular weight of 10^3 daltons - corresponding to a typical size of siderophores, which are extremely strong specific complexants for some radionuclides (BIRCH & BACHOFEN 1990; BRAINARD et al. 1992), these organic by-products would be mobile in the bentonite pores. However, even the pessimistic assumption that all organics complex solely with actinides would only approximately double the maximum release rate, since the production rate (10^{-5} moles y^{-1}) is roughly equivalent to the total, solubility-limited release rate of actinides to the bentonite. Such an increase is

¹² The term "solubility limit" here denotes a near-field model parameter defining the maximum concentration in solution which can be reached for a given element; any further addition of the element is considered to result in precipitation of a solid phase. The values chosen are not necessarily based on thermodynamic solubility products of specific phases, but generally reflect an appraisal of the calculated solubilities of a range of solid phases, supported by chemical analogues, experimental data and assessment of source term restrictions (see Subsection 3.4.6.2).

insignificant with respect to other uncertainties involved in the estimation of solubility limits. This worst case is, of course, likely to be over-pessimistic as:

- The calculated microbial activity is a maximum value, assuming all available energy is used by micro-organisms.
- All biomass production is assumed to be balanced by a similar production of organic by-products, available for complexation; in reality, carbon is expected to be efficiently recycled in such an oligotrophic environment and would thus be unavailable for complexation.
- All the organic by-products which are available to complex with radionuclides are assumed to be highly mobile; in reality, only a small fraction of by-products would have molecular weights less than 10^3 daltons and organics larger than this size would be immobile due to the microporous structure of compacted bentonite and could thus have a net positive effect in retarding radionuclide transport.
- All organic complexant is assumed to make soluble the most radio-toxic components of the waste; in reality, there will be competition with other metals present at much larger concentrations (particularly iron).

Furthermore, field observations in soil indicate siderophore concentrations of mM level only where very high microbial activities exist; nM concentrations are more likely in oligotrophic environments (BRINARD et al. 1992). Natural analogue studies strongly link microbial populations at redox fronts with trapping of trace elements, which suggests that the net effect of microbiological activity in such an environment will be catalysis of redox reactions and the formation of secondary minerals, thus tending to reduce radionuclide releases (e.g. HOFMANN 1989).

Taking all these points together, the net consequences of microbial activity in terms of complexant production can be safely neglected.

3.4.5 Backfill and Seals in Access Tunnels and Shafts

Access tunnels and shafts will connect the various repository elements and may cross higher-permeability rock zones in the crystalline basement (see Figure 3.1.1). The orientation of the access tunnels may be arranged so that access to a given block is only from one direction, thus minimising the likelihood of significant flow along access tunnels. At closure, the tunnels and shafts will be backfilled and, at certain locations, high-quality seals will be emplaced (STUDER et al. 1984).

Seals will be designed to isolate hydraulically the individual HLW panels and ILW silos from each other and from higher-permeability zones in the host rock. Investigation

boreholes in the low-permeability host rock will also be sealed. The seals may consist of short sections of the access tunnels and shafts filled with a low-permeability material (e.g. compacted bentonite blocks) and contained, on either side, by thick plugs (e.g. concrete). Bentonite can be altered by alkaline solutions (cement porewater). However, only a limited thickness of bentonite adjacent to the concrete plugs is expected to be affected, due to the limited extent of diffusion of such solutions into the bentonite.

The practicality and effectiveness of seals for boreholes, shafts and tunnels has been investigated (PUSCH et al. 1987). The seals are expected to provide complete hydraulic isolation of the repository panels, so that the only route for radionuclide transport is by movement through the undisturbed low-permeability host rock (GRAY 1993).

3.4.6 Radionuclide Retention and Transport in the Engineered Barriers

3.4.6.1 Effect of the Canister and Waste Matrix

Even after the canister has failed, its physical presence may restrict access of water to the glass and also restrict radionuclide release (see, for example, NERETNIEKS 1993). Similarly, it is possible that the limited access of water to the surfaces of the cracked glass might offer some transport resistance. These effects are neglected in the Kristallin-I assessment. However, continuing corrosion of the unreacted iron of the canister and buffering by corrosion products exerts an influence on the chemistry of the water in contact with the waste glass. The most critical process is buffering of the oxidation potential. Such buffering is assumed in the evaluation of solubility limits (see Subsection 3.4.6.2).

The concentration of many radionuclides in aqueous solution adjacent to the glass will be limited by the solubilities of radionuclide-bearing solids formed by the interaction of glass and bentonite pore fluid. In addition, radionuclides may be sorbed or co-precipitated with these secondary glass phases and iron corrosion products. For simplicity, these latter processes are conservatively ignored in the Kristallin-I safety assessment and the solubility limits are determined for the reference bentonite porewater.

3.4.6.2 Solubility Limits of Radionuclides in Bentonite Porewater

The low solubility of many key radionuclides is an important constraint limiting their concentrations and hence their rate of diffusion through the bentonite. Because of the limitations of current models/databases for quantifying solubility limits, a number of simplifications are made in deriving a solubility database:

- Solubility limits are defined for a water chemistry which would correspond to bentonite porewater with redox conditions buffered by canister corrosion products. Although based on the reference bentonite porewater compositions (pH range 8.5 to 9.0; see Table 3.4.2), uncertainties in groundwater composition are also taken into account.
- A chemical thermodynamic model is used to assess solubility limits for a range of pure mineral phases which could potentially form under the expected conditions.
- The output of the thermodynamic model is reviewed in terms of literature data on the formation of identified minerals and measured concentrations of the element of interest in relevant natural and laboratory systems.
- The likelihood of formation of pure phases is assessed in terms of the relative inventories of elements with similar chemical properties in the waste.
- Bearing in mind the intention to err on the side of conservatism in the derivation of parameters values (i.e. overprediction of solubility limits), expert judgement is used to select elemental solubility limits which are defensible as "realistic-conservative" and "conservative" values¹³.

The procedure and results of this selection procedure are documented in BERNER (1994); a simplified overview of the main considerations involved in the selection of solubility limits for specific elements is given in Table 3.4.3. The resultant solubility limits for the safety assessment are listed in Table 3.7.3.

3.4.6.3 Diffusion and Retardation in Bentonite

The diffusion of radionuclides in compacted bentonite is described by an element-specific apparent diffusion constant. The apparent diffusion constant is usually expressed as the quotient of a pore diffusion constant and a retention factor. The pore diffusion constant takes account of radionuclide retardation due to the tortuosity and constrictivity of the pore space and of processes such as ion exclusion. An effective diffusion constant (the product of the pore diffusion constant and the porosity) within the saturated bentonite at 55 °C of $6.3 \times 10^{-3} \text{ m}^2 \text{ y}^{-1}$ ($2 \times 10^{-10} \text{ m}^2 \text{ s}^{-1}$) and a porosity of 0.38 are assumed, as in Project Gewähr 1985. The retention factor includes retardation due to chemical interaction (sorption) of the radionuclide with the mineral surfaces in the bentonite.

Apparent diffusion constants for compacted bentonite are primarily functions of the composition of the pore solution, its redox state and the physical properties of the pore

¹³ See Subsection 2.5.2 for definitions of the terms "realistic-conservative" and "conservative".

space. These factors are taken into account when selecting the element-specific diffusion constants for Kristallin-I safety analysis (STENHOUSE 1994). In cases where measurements have been carried out under conditions appropriate to Kristallin-I, direct use is made of apparent diffusion constants. Sorption constants are calculated from the apparent diffusion constants (and the assumed pore diffusion constant¹⁴) and compared with sorption constants determined directly in batch experiments. The values of sorption constants selected for the safety analysis are always the lesser of the values obtained by the two methods.

Element	Rationale for setting solubility limits
Cs, Ni	Very high solubility expected in the absence of co-precipitation processes (arbitrary "high" value selected which could be set as 1M).
Pa, Sn, Tc, Th, U, Zr, Np, Pu	Main constraint on solubility taken to be formation of the metal oxides (or hydroxides); selected solubilities based on evaluation of uncertainties in thermodynamic data, solid phase crystallinity, laboratory measurements and the likely formation of mixed oxides.
Pd	Expected to be effectively insoluble but, conservatively, solubility assessed assuming control by Pd (OH) ₂ .
Se	Assumed to be set by Fe Se ₂ although coprecipitation with S might be expected in reality.
Am	Assumed to be set by Am OH (CO ₃).
Cm, Ra	Assumed to co-precipitate with chemically similar elements present in much higher quantities (Am and Ba/Sr/Ca, respectively).

Table 3.4.3: Summary of the main considerations involved in the selection of solubility limits for specific elements. The selection procedure is fully documented in BERNER (1994).

The sorption constants presented in Table 3.7.3 give both a "realistic-conservative" and a "conservative" value for each chemical element. The "realistic-conservative" value is appropriate for sorption under the reference conditions specified after canister failure and is a value which can be realistically supported from the available data. For the corresponding "conservative" sorption constant, the scatter of values measured under reference conditions, as well as some feasible perturbations of the reference conditions that are likely to have the maximum effect on the sorption behaviour of that element, are considered.

¹⁴ In STENHOUSE (1994), a pore diffusion constant of $1.75 \times 10^{-2} \text{ m}^2\text{y}^{-1}$ is assumed. For an effective diffusion constant of $6.3 \times 10^{-3} \text{ m}^2\text{y}^{-1}$, this corresponds to a porosity of 0.36. The difference between this porosity value and the Project Gewähr 1985 value of 0.38, used in the near-field transport calculations, is not significant.

3.5 Geology of the Crystalline Basement of Northern Switzerland

3.5.1 Introduction

Project Gewähr 1985 was carried out at a relatively early stage in the regional characterisation of the crystalline basement of Northern Switzerland and was based on an analysis of very limited information (mainly data from the Böttstein borehole). For Kristallin-I, information from 7 deep boreholes has been analysed. Additional information is available, mainly from seismic surveys, regional surface geological mapping and hydrochemical and hydrogeological analysis. THURY et al. (1994) provide an integration of all relevant information produced to date. Developments in the geological, geochemical and hydrogeological databases and supporting models since the completion of Project Gewähr 1985 are outlined below.

- A much improved structural model of the region has been developed, which allows potential siting sub-regions (Areas West and East; see Figure 3.5.1) to be delineated. Understanding of the distribution of major faults within these areas has been formalised in a statistical model.
- A new suite of hydrogeological models has been developed, based on a synthesis of more extensive measurements and taking account of the structural model.
- A detailed characterisation of water-conducting features observed in the deep boreholes has been carried out, which has been synthesised into model representations of three classes of such features. These descriptions are supported by new literature studies to quantify sorption and diffusion parameters and laboratory studies to investigate the extent of connected matrix porosity.
- Hydrochemical and isotopic data have been synthesised on a regional basis, providing a fairly consistent picture of slow chemical evolution of the groundwater due to rock-water interaction. This information is used:
 - to confirm general groundwater flow patterns in the basement predicted by the hydrogeological models;
 - to form a basis for the definition of reference waters for the two potential siting areas.
- Analysis of potential long-term geological evolution scenarios has underpinned the two bounding scenarios presented in Project Gewähr 1985, particularly with regard to the quantification of expected uplift, erosion and movement along faults of various sizes in the areas of interest.

3.5.2 Regional Geology and Siting

The major tectonic movements of the Alpine orogeny, which are responsible for the present mountainous terrain of Switzerland, occurred in the time interval 100 to 10 million years before present (b.p.). The last major tectonic event directly related to the Alpine orogeny was the thrusting and folding of the Jura mountains some 10 million years b.p. The principal tectonic units of Northern Switzerland and adjacent areas are shown in Figure 3.5.2. In addition to the Alpine influence, Northern Switzerland was affected by the Tertiary rifting of the Rhine Graben (starting about 40 million years b.p.) and by differential vertical movements (THURY et al. 1994). Differential vertical movements, namely the uplift of the Alps and of the Black Forest massif, are still continuing today with rates in the order of 1 mm per year. While the present stress field in the crystalline basement of Northern Switzerland is still related to the Alpine orogeny (maximum horizontal stress is oriented NW-SE, i.e. perpendicular to the Alpine chain), it is unclear whether compressive movements are still operative or whether the orogeny is completed.

The requirement that a potential site for a HLW repository should be far from areas of major uplift and associated faulting led to focusing of geological investigations by Nagra in a selected region of Northern Switzerland (THURY 1980), see Figure 3.5.1. The region has a low seismic activity compared with other regions in Switzerland. Features of the crystalline basement, together with those of adjacent and overlying sedimentary formations, are summarised in Table 3.5.1. During the Phase I regional investigation programme, the presence of a large trough filled with Permo-Carboniferous sediments (the Permo-Carboniferous Trough of Northern Switzerland) was identified; this both increased the complexity of the regional geological picture and reduced the area that could be considered for repository siting. As a result of the synthesis of information from geological investigations in Kristallin-I, two areas of potentially suitable crystalline basement have been identified, termed Area West and Area East. These are delimited by the Permo-Carboniferous Trough to the south and the Swiss national border to the north.

A schematic north-south section through the crystalline basement of Northern Switzerland in Area West is shown in Figure 3.5.3. In the region of interest, which lies between the river Rhine and the Permo-Carboniferous Trough, the basement is covered by Mesozoic sediments. The crystalline basement itself can be divided into an upper domain, several hundred metres thick, with a generally higher hydraulic conductivity (the higher-permeability domain) and a lower domain with generally lower hydraulic conductivity (the low-permeability domain). Both domains are intersected by major regional faults, with hydraulic conductivities similar to that of the higher-permeability domain. These faults limit the size of blocks within the low-permeability domain, which would be considered suitable for emplacement of HLW. In Area East, the existence of the low-permeability domain is not well established, with two possible interpretations of the available borehole data - see hypotheses 1 and 2, Subsection 3.5.3.

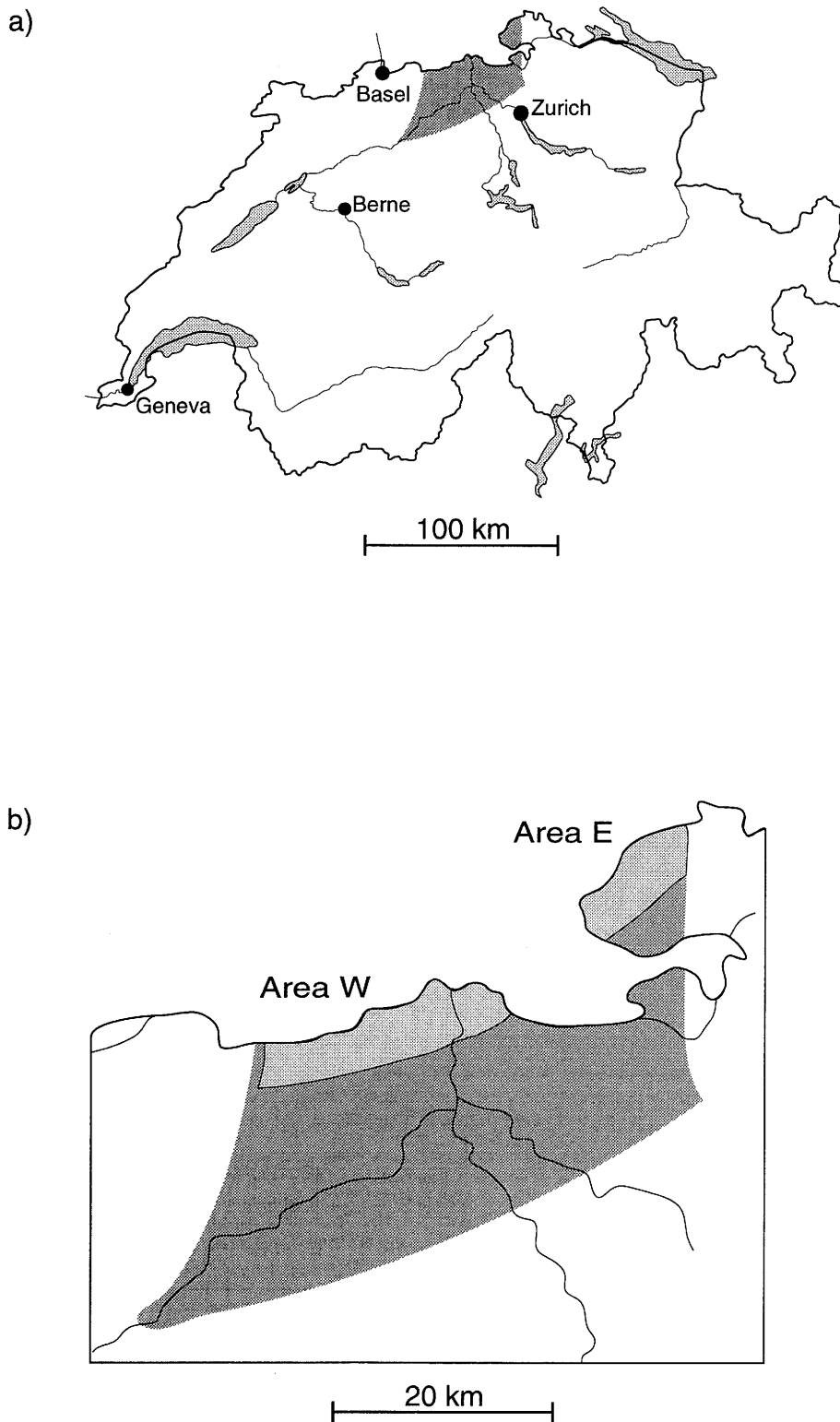


Figure 3.5.1: (a): the region of Northern Switzerland investigated in the regional field programme; (b): the location of two potentially suitable siting areas in the crystalline basement, Area West and Area East.

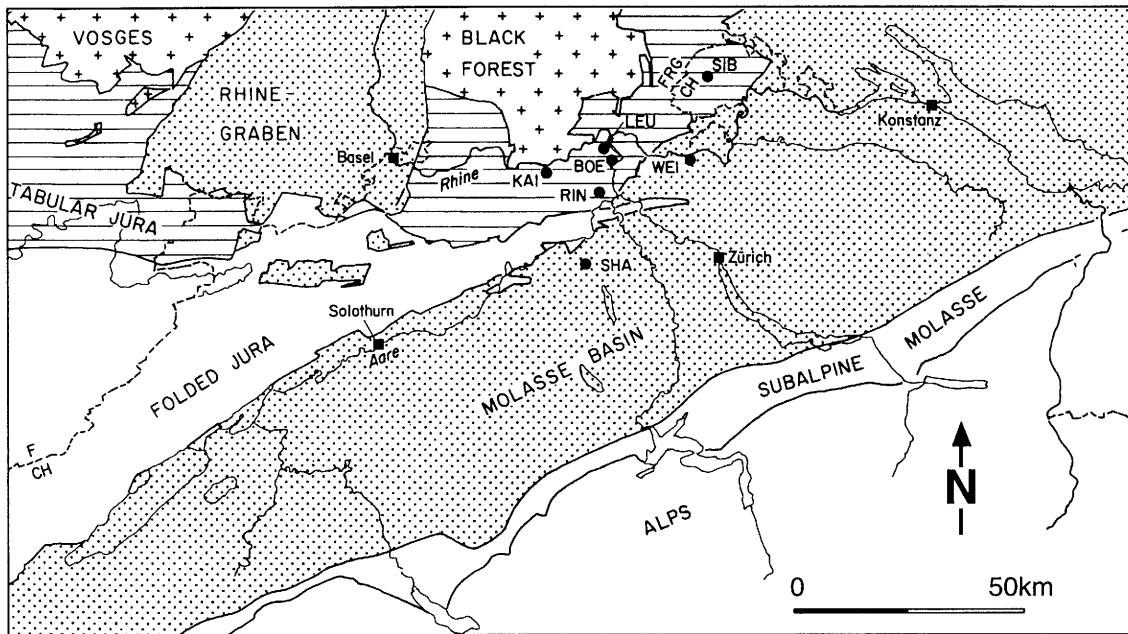


Figure 3.5.2: Principal tectonic units of Northern Switzerland and adjacent areas. The positions of the Nagra boreholes are indicated: BOE - Böttstein, KAI - Kaisten, LEU - Leuggern, RIN - Riniken, SHA - Schafisheim, SIB - Siblingen, WEI - Weiach.

Crystalline Basement	Gneisses with Variscan (mainly granitic) intrusions; crops out in the Alps and Black Forest.
Permo-Carboniferous	ENE-trending trough up to several kilometres deep.
Mesozoic	Covers the Crystalline Basement and Permo-carboniferous trough from the Black Forest to the Alps; slightly faulted in the Tabular Jura, folded and thrust (mainly in the late Tertiary) in the Folded Jura.
Tertiary	Detrital sediments up to several kilometres thick in the Molasse Basin and Rhine Graben.
Quaternary	Tills covering large areas of the Molasse Basin; glacial, fluvio-glacial and lacustrine deposits filling valleys.

Table 3.5.1: Features the crystalline basement of Northern Switzerland, together with those of adjacent and overlying sedimentary formations.

3.5.3 Water-Conducting Features in the Crystalline Basement

As illustrated in Figure 3.5.3, all domains of the crystalline basement contain a series of small-scale discontinuities which provide preferential paths for groundwater flow (water-conducting features) and are classified as (i) cataclastic zones, (ii) open joints and (iii) fractured aplite/pegmatite dykes and aplitic gneisses. For geosphere transport modelling, a description of the small-scale structure of these features is required. The results of a detailed examination of cores from both areas, as well as of surface exposures in the Southern Black Forest, are summarised in Figure 3.5.4 (taken from THURY et al. 1994). The figure shows observed features (fractures, channels, infill material, altered and unaltered wallrock), each displaying natural complexity, and also simplified representations, on which calculations of geosphere transport are based (see Section 5.3). The porosities of the fracture infill, altered wallrock and unaltered wallrock are given in Table 3.7.7, together with a summary of geometrical data relevant to transport modelling. Mineralogies of each component of the water-conducting features are given in THURY et al. (1994). On the basis of available information, there is no justification for assuming that the small-scale structure of water-conducting features differs between the two areas and hence the data presented in Figure 3.5.4 and Table 3.7.7 are applicable to both.

3.5.4 Hydrogeological Modelling

To investigate the hydrogeological regime, groundwater-flow modelling has been carried out on regional, local and block scales, with the larger-scale models providing boundary conditions for the smaller-scale models (Figure 3.5.5). Regional-scale modelling suggests a pattern of regional groundwater flow in the crystalline basement with recharge in the Southern Black Forest and discharge in the Rhine valley. This results in flow generally south-westwards then north-westwards through Area West (a view which is also supported by regional hydrochemical and isotopic analyses). A similar pattern is indicated in Area East, although there is some evidence of a water divide, with eastward flow in the eastern part of the area (THURY et al. 1994).

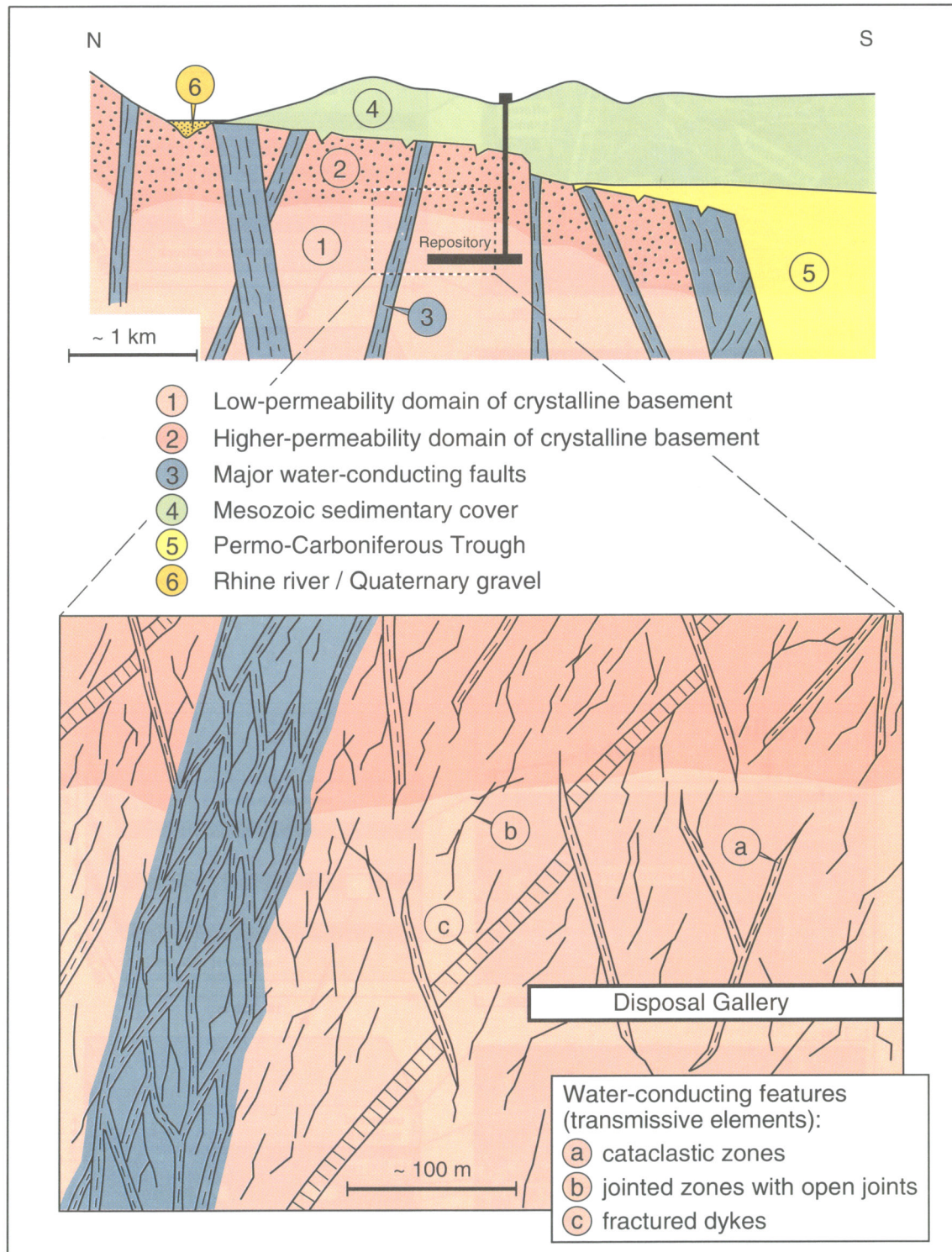


Figure 3.5.3: Schematic section through the crystalline basement of Northern Switzerland in Area West, showing the main structural components affecting repository siting and groundwater flow. In Area East, the existence of the low-permeability domain is not well established, with two possible interpretations of the available borehole data - see Subsection 3.5.3.

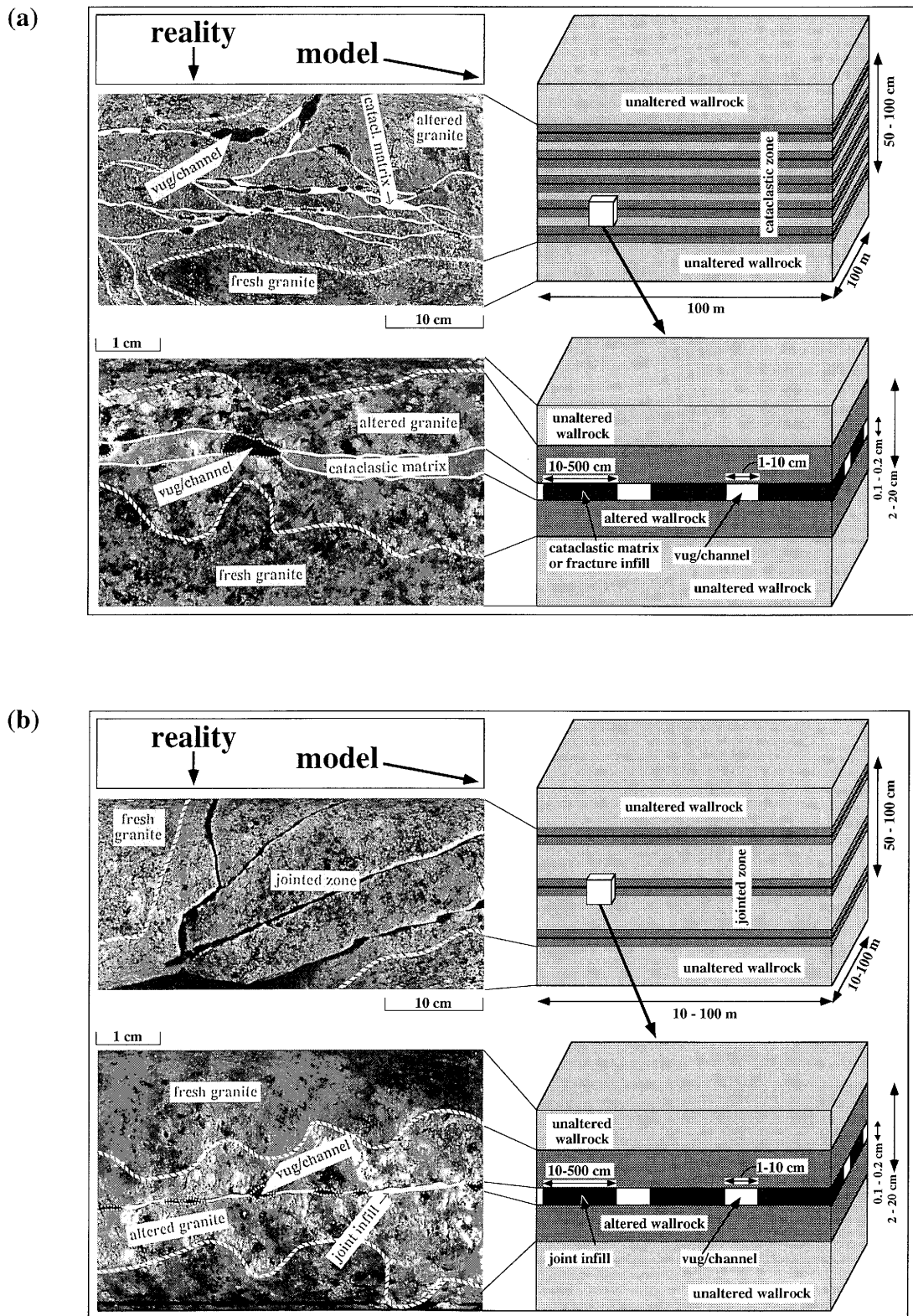


Figure 3.5.4: Water-conducting features in the crystalline basement, as observed in reality and as simplified for transport modelling. (a) Cataclastic zones; (b) jointed zones.

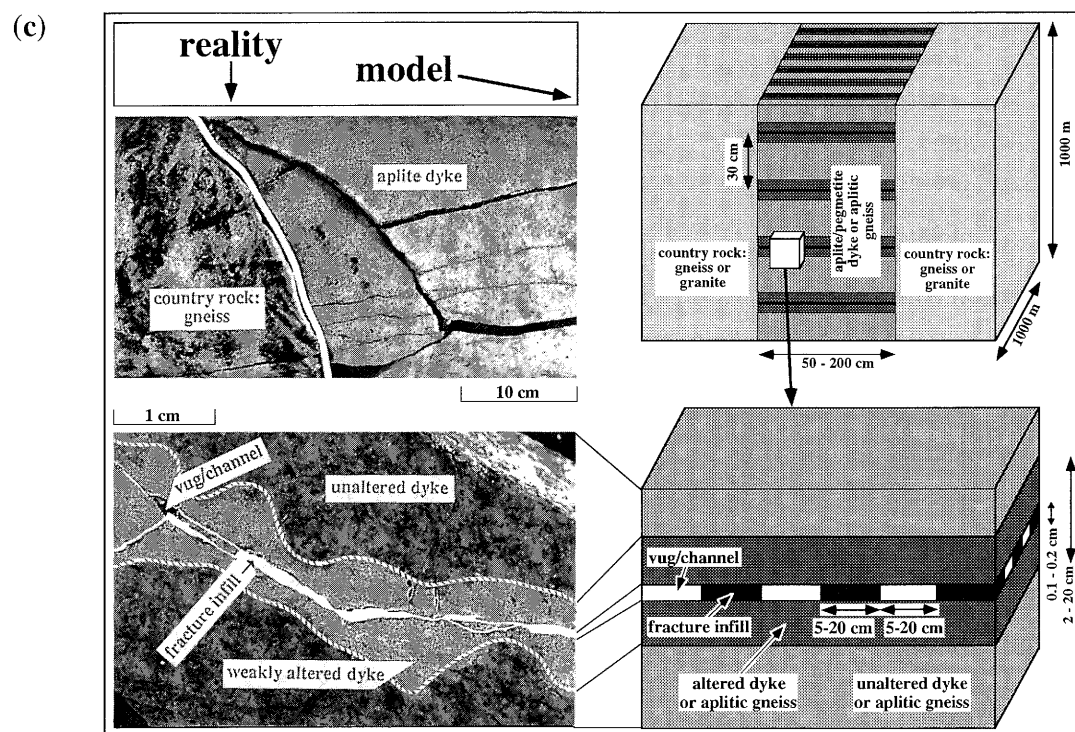


Figure 3.5.4: (Continued). Water-conducting features in the crystalline basement, as observed in reality and as simplified for transport modelling. (c) Fractured aplite/pegmatite dykes and aplitic gneisses.

For Area West, regional structural features are predominantly defined by extrapolation of detailed mapping of the outcrops in the Southern Black Forest, supported by limited data from boreholes and seismic studies. From a knowledge of the orientation of the main groups of regional (first- and second-order¹⁵) faults, idealised fault zone meshes can be derived (see Figure 3.5.6). These meshes, coupled to hydraulic data from boreholes, form the basis for local-scale models of groundwater flow in Area West, which represent the blocks between faults as equivalent porous media and also include specific representation of the faults as two and three-dimensional features. An open question is the degree to which these faults are hydraulically active. This uncertainty is handled by considering a range of models, of which the extremes are the "Full Model", in which all first- and second-order faults are active ("major water-conducting faults"), and the "Sparse Model", in which very few second-order faults are hydraulically active (see Figure 3.5.7)¹⁶.

¹⁵ This classification of faults in the basement is defined in Thury et al. (1994). To summarise, first-order faults are of length > 10 km and have widths in the range 100 m to 1 km (generally in several fault branches). Second-order faults are several km to ca. 10 km in length and have widths in the range of several m to 100 m.

¹⁶ The terms "Full Scenario" and "Sparse Scenario" are used in THURY et al. (1994). However, "Full Model" and "Sparse Model" are more consistent with the terminology adopted for the safety assessment reported here.

Based on such groundwater-flow modelling (described in more detail in Chapter 8 of THURY et al. 1994), the expected flowrates through a block of low-permeability domain are calculated for a range of hydraulic parameter values. Throughout the crystalline basement, flow occurs predominantly in water-conducting features (Figure 3.5.4), which are represented by a statistical distribution of two-dimensional transmissive elements in a fracture-network model. The results of such analyses are summarised in Table 3.7.4. The groundwater flowrates thus calculated provide boundary conditions for the near-field release model, as well as input for the geosphere transport analysis.

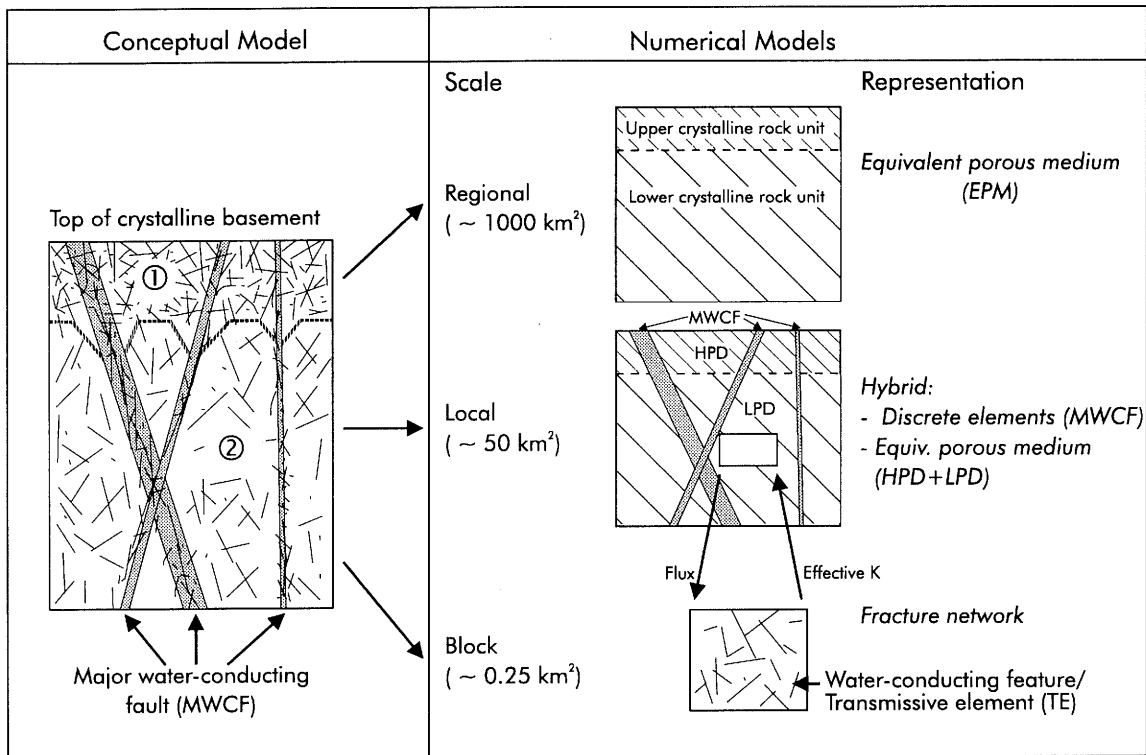
Area East is less well defined due to the relative scarcity of information in this region. Nevertheless, the main structural features are expected to be generally similar to those in the Area West. Estimation of representative hydraulic data for Area East is complicated by the fact that data are only available from one borehole (Siblingen), in which the crystalline basement at depth appears to be more permeable than observed in the boreholes in Area West. Two separate hypotheses are thus considered:

Hypothesis 1: Data from the Siblingen borehole are representative for the whole of Area East and the deep crystalline basement in Area East is more permeable than that in the Area West, with no clear distinction between low- and higher-permeability domains.

Hypothesis 2: The Siblingen data are a special case and hence data for Area West are also of relevance to the determination of the properties of low- and higher-permeability domains in Area East.

The resultant hydraulic data for each of the two hypotheses are summarised in Table 3.7.5.

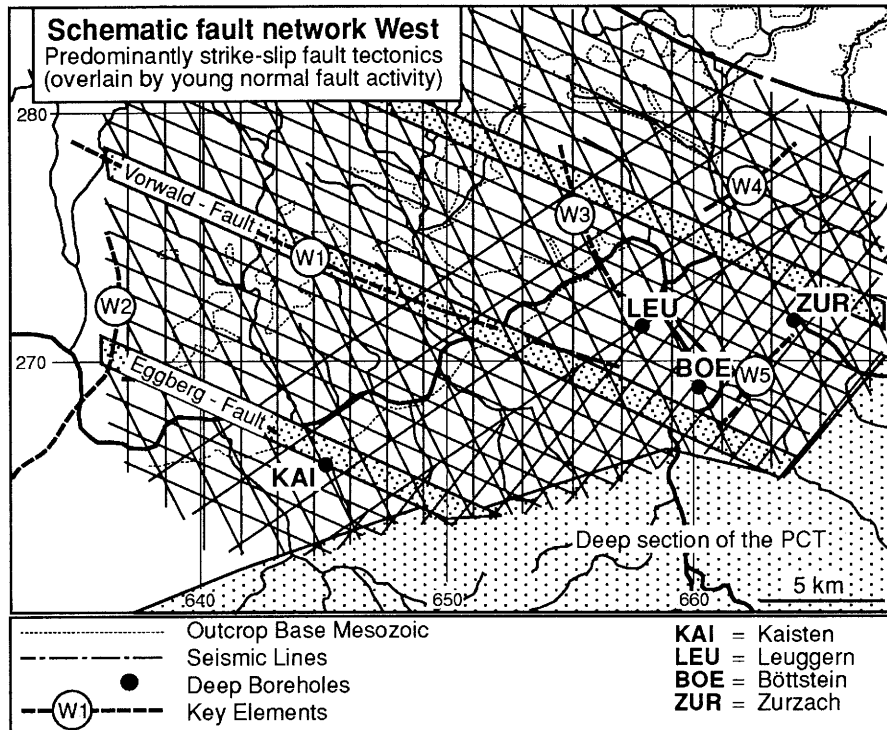
In order to assess geosphere transport in the low-permeability domain and major water-conducting faults, key inputs from groundwater-flow modelling are the density of water-conducting features (the total trace length of water-conducting features - or transmissive elements - in a hypothetical plane of unit area), which provide conduits for advective radionuclide transport, and the flowrate of water through these features. It is assumed that radionuclides reaching the higher-permeability domain are transported rapidly to the biosphere; no calculations of transport in this domain are made (see also Subsection 5.3.1). For biosphere modelling, key geological input are the location of the discharge area of any groundwater flowing through the repository and the extent of dilution occurring along the pathway from the repository to the surface environment. Groundwater flow modelling suggests that, for present conditions, discharge occurs predominantly into gravel aquifers in the Rhine valley, which give very significant dilution (factors of about 10^6 to 10^7 , see "dilution ratio, $Q_{\text{bio}}/Q_{\text{r}}$ " in Table 3.7.4). This is true for both Area West and Area East, with equal degrees of dilution in each case. For Area East only, a possible alternative scenario is discharge into a tributary valley, with a consequently smaller dilution (see also Subsection 4.3.6.6).



- ① Upper crystalline rock domain; designated as higher-permeability domain (HPD) in area West
 ② Lower crystalline rock domain; designated as low-permeability domain (LPD) in area West

Note: MWCF = major water-conducting fault.

Figure 3.5.5: Schematic representation of the relationship between the hydrogeological conceptual model and numerical models of groundwater flow at regional, local and block (site) scales.



Note: PCT = Permo-Carboniferous Trough.

Figure 3.5.6: Idealised meshes of major faults for groundwater flow modelling of Area West, based on a knowledge of the orientation of the main groups of first- and second-order faults.

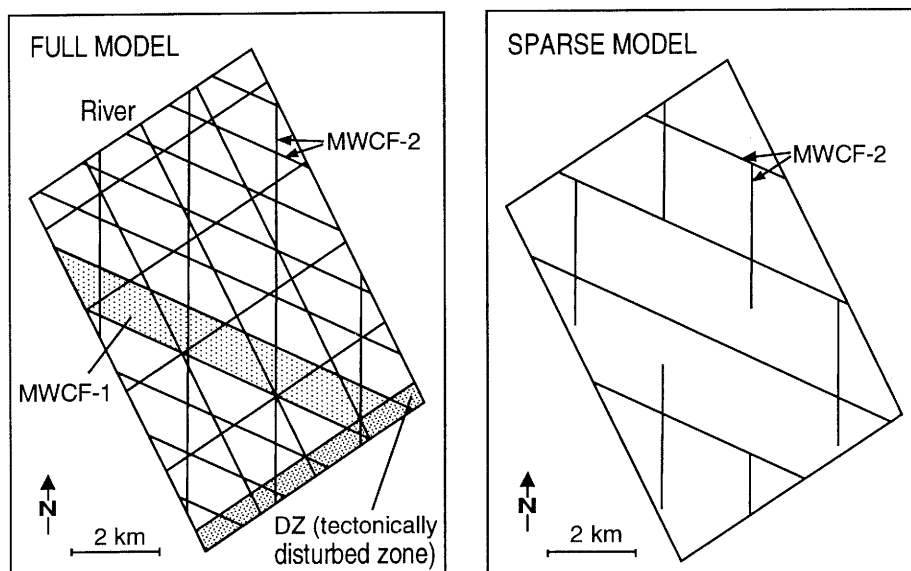


Figure 3.5.7: Two models for groundwater-flow of Area West. (i) the Full Model, in which all first- and second-order faults (MWCF-1 and MWCF-2, respectively) are active; (ii) the Sparse Model, in which no first-order faults and very few second-order faults are hydraulically active. (From THURY et al. 1994).

3.5.5 Groundwater Chemistry and Radionuclide Sorption

3.5.5.1 Groundwater Composition

On the basis of a regional synthesis of groundwater chemistry, the predominant groundwater in the low-permeability domain of the Area West is considered to be of the Na-SO₄-(Cl-HCO₃) type, with about 1 g l⁻¹ total dissolved solids (PEARSON & SCHOLTIS 1993). The composition of this reference water is given in Table 3.5.2. Two samples of more saline water of different chemical types were collected from the Leuggern borehole at 923 m depth and from the Böttstein borehole at 1326 m depth. These waters are also discussed in THURY et al. (1994). The water from the Böttstein borehole provided a basis for the reference water for the safety assessment calculations in Project Gewähr 1985. It is of the Na-(Ca)-Cl-(SO₄) type and has a 13 g l⁻¹ total dissolved solids. The water from the Leuggern borehole is of the Na-Ca-SO₄ type and has 5 g l⁻¹ total dissolved solids.

Despite the limited availability of data, both regional hydrochemistry and the expected hydrogeological regime argue for a less mineralised water in the crystalline basement of Area East, which is consistent with measurements at Siblingen. A reference water of the Na-HCO₃-SO₄-(Cl) type is defined with 0.5 g l⁻¹ dissolved solids (see Table 3.5.2).

3.5.5.2 Derivation of Sorption Constants for Geosphere Transport

When modelling radionuclide transport in groundwater, it is generally assumed that sorption is fast, reversible and can be represented by a concentration-independent distribution coefficient (sorption constant K_d), equal to the equilibrium radionuclide concentration in the sorbed phase, divided by the concentration in the aqueous phase. In this case, a constant retardation factor can be defined which quantifies the degree to which advective radionuclide transport is retarded relative to the flow of groundwater.

The basic premise in deriving sorption constants for Kristallin-I is that values should be appropriate to the rock-water systems of the site being investigated. Thus, heterogeneities within the rock mass are taken into consideration via the reference mineralogies for different types of water-conducting features within the crystalline rock, including infill and altered rock materials (THURY et al. 1994). In addition, reference groundwater characteristics, including chemical composition, pH and Eh, are provided, based on measurements of these parameters (see Table 3.5.2).

Radionuclide partitioning in specific rock-water systems can be determined experimentally. However, because of the limited data available for relevant conditions, it is necessary to complement measurements made on samples of Swiss crystalline rock with an appraisal of the wider sorption literature.

	Area West		Area East	
pH	7.66		7.68	
pe	-2.72		-0.52	
Eh (volts)	-0.18		-0.03	
Formation temp. (C)	55		55	
Density (g ml ⁻¹)	0.999		1.0005	
TDS (mg l ⁻¹)	969		543	
IS (molality)	0.021		0.0103	
	mg l⁻¹	molality	mg l⁻¹	molality
Lithium (Li ⁺)	1.1	1.59 × 10 ⁻⁴	0.64	9.22 × 10 ⁻⁵
Sodium (Na ⁺)	323.8	1.41 × 10 ⁻²	177	7.70 × 10 ⁻³
Potassium (K ⁺)	8.5	2.18 × 10 ⁻⁴	4.2	1.07 × 10 ⁻⁴
Rubidium (Rb ⁺)	0.055	6.45 × 10 ⁻⁷	<0.05	<5.85 × 10 ⁻⁷
Caesium (Cs ⁺)	0.043	3.24 × 10 ⁻⁷	0.05	3.76 × 10 ⁻⁷
Ammonium (NH ₄ ⁺)	0.14	7.78 × 10 ⁻⁶	<0.005	2.77 × 10 ⁻⁷
Beryllium (Be ²⁺)	5 × 10 ⁻⁴	5.56 × 10 ⁻⁸	--	--
Magnesium (Mg ²⁺)	0.3	1.24 × 10 ⁻⁵	1.1	4.53 × 10 ⁻⁵
Calcium (Ca ²⁺)	14.0	3.50 × 10 ⁻⁴	11.5	2.87 × 10 ⁻⁴
Strontium (Sr ²⁺)	0.46	5.26 × 10 ⁻⁶	0.35	3.99 × 10 ⁻⁶
Barium (Ba ²⁺)	0.05	3.65 × 10 ⁻⁷	0.08	5.48 × 10 ⁻⁷
Radium (Ra ²⁺)	7 × 10 ⁻¹⁰	3.10 × 10 ⁻¹⁵	1.7 × 10 ⁻⁷	7.52 × 10 ⁻¹³
Chromium (Cr)	8.5 × 10 ⁻⁴	1.64 × 10 ⁻⁸	--	--
Manganese (Mn ²⁺)	0.037	6.75 × 10 ⁻⁷	<0.005	<9.10 × 10 ⁻⁸
Iron (Fe ²⁺)	0.007	1.26 × 10 ⁻⁷	<0.01	<1.79 × 10 ⁻⁷
Nickel (Ni ²⁺)	<5 × 10 ⁻⁴	<8.53 × 10 ⁻⁹	<0.01	<1.70 × 10 ⁻⁷
Cobalt (Co ²⁺)	1.5 × 10 ⁻⁴	2.55 × 10 ⁻⁹	--	--
Copper (Cu ²⁺)	<0.002	<3.15 × 10 ⁻⁸	0.01	1.57 × 10 ⁻⁷
Zinc (Zn ²⁺)	0.004	6.13 × 10 ⁻⁸	<0.03	<4.59 × 10 ⁻⁷
Zirconium (Zr)	1.5 × 10 ⁻⁴	1.65 × 10 ⁻⁹	--	--
Palladium (Pd)	<1 × 10 ⁻⁴	<9.42 × 10 ⁻¹⁰	--	--
Tin (Sn)	6 × 10 ⁻⁴	5.07 × 10 ⁻⁹	--	--
Lead (Pb)	2.5 × 10 ⁻⁴	1.21 × 10 ⁻⁹	<0.005	<2.41 × 10 ⁻⁸
Aluminium (Al)	0.012	4.46 × 10 ⁻⁷	0.012	4.35 × 10 ⁻⁷
Uranium (U)	1.3 × 10 ⁻⁴	5.47 × 10 ⁻¹⁰	3 × 10 ⁻⁴	1.26 × 10 ⁻⁹
Thorium (Th)	5 × 10 ⁻⁴	2.16 × 10 ⁻⁹	--	--
Fluoride (F ⁻)	12.2	6.43 × 10 ⁻⁴	11.8	6.21 × 10 ⁻⁴

Notes: TDS = total dissolved solids. IS = Ionic Strength.

Molality values given are calculated from measured concentrations in mg l⁻¹; precision of this data should be judged from precision of the measured concentration data.

Where values are presented as maxima, this reflects either the detection limit of the apparatus or the presence of contamination (for example, drilling fluid).

Table 3.5.2: Reference groundwater chemistries for the crystalline basement of Northern Switzerland. (Data from PEARSON & SCHOLTIS 1993).

	Area West		Area East	
	mg l ⁻¹	molality	mg l ⁻¹	molality
Chloride (Cl ⁻)	128	3.62 × 10 ⁻³	26	7.33 × 10 ⁻⁴
Bromide (Br ⁻)	0.72	9.03 × 10 ⁻⁶	0.2	2.50 × 10 ⁻⁶
Iodide (I ⁻)	0.01	7.90 × 10 ⁻⁸	<0.01	<7.88 × 10 ⁻⁸
Sulphate (SO ₄ ²⁻)	296	3.09 × 10 ⁻³	135	1.41 × 10 ⁻³
Phosphate (as P)	0.04	1.29 × 10 ⁻⁶	<0.02	<6.46 × 10 ⁻⁷
Nitrate (NO ₃ ⁻)	<0.1	<2.00 × 10 ⁻⁶	<0.9	<1.45 × 10 ⁻⁵
Arsenite (As ³⁺)	0.12	1.60 × 10 ⁻⁶	--	--
Arsenate (As ⁵⁺)	0.035	4.68 × 10 ⁻⁷	--	--
Total Arsenic (As)	0.16	2.07 × 10 ⁻⁶	0.0065	8.68 × 10 ⁻⁸
Selenium (Se)	0.1	7.89 × 10 ⁻⁷	--	--
Molybdenum (Mo)	0.005	3.13 × 10 ⁻⁸	--	--
Tungsten (W)	0.7	2.83 × 10 ⁻⁶	--	--
Alkalinity as HCO ₃ ⁻	291	4.78 × 10 ⁻³	268	4.39 × 10 ⁻³
Bicarbonate (HCO ₃ ⁻)	285	4.67 × 10 ⁻³	262	4.29 × 10 ⁻³
Carbonate (CO ₃ ²⁻)	2.7	4.51 × 10 ⁻⁵	2.2	3.67 × 10 ⁻⁵
Total Sulphide (H ₂ S)	<0.005	<1.50 × 10 ⁻⁷	--	--
Silica (H ₂ SiO ₃)	46.1	5.91 × 10 ⁻⁴	46	5.93 × 10 ⁻⁴
Borate (B(OH) ₃)	3.4	5.51 × 10 ⁻⁵	0.9	1.46 × 10 ⁻⁵
Total Iron	0.026	4.66 × 10 ⁻⁷	--	--
Organic carbon	0.04	3.34 × 10 ⁻⁶	<6	<5.00 × 10 ⁻⁴
Oxygen (O ₂)	<5 × 10 ⁻⁴	<1.56 × 10 ⁻⁸	<0.008	<2.50 × 10 ⁻⁷
Nitrogen (N ₂)	33	1.18 × 10 ⁻³	31	1.11 × 10 ⁻³
Methane (CH ₄)	0.017	1.06 × 10 ⁻⁶	<0.01	<6.24 × 10 ⁻⁷
Hydrogen (H ₂)	<5 × 10 ⁻⁴	<2.43 × 10 ⁻⁷	<7 × 10 ⁻⁴	<3.40 × 10 ⁻⁷
Argon (Ar)	0.88	2.21 × 10 ⁻⁵	1.0	2.50 × 10 ⁻⁵
Carbon Dioxide (CO ₂)	7.7	1.75 × 10 ⁻⁴	7	1.59 × 10 ⁻⁴

Notes: Data for carbon dioxide in Area East is not given in PEARSON and SCHOLTIS (1993), but may be found in THURY et al. (1994).

Molality values given are calculated from measured concentrations in mg l⁻¹; precision of this data should therefore be judged from precision of the concentration data

Where values are presented as maxima, this reflects either the detection limit of the apparatus or the presence of contamination (for example, drilling fluid).

Table 3.5.2: (Continued). Reference groundwater chemistries for the crystalline basement of Northern Switzerland. (Data from PEARSON and SCHOLTIS 1993).

In comparison to the review used to derive the sorption database for Project Gewähr 1985 (McKINLEY & HADERMANN 1985), which focused on measurements on rock samples, the Kristallin-I review (STENHOUSE 1994) considers a wider range of measurements, including those carried out on pure minerals. For each element, sorption data representative of the individual minerals are combined according to the corresponding contribution (percentage volume) of each to the reference mineralogies. This approach, in which sorption on rocks is determined by adding contributions from their constituent minerals, is preferred because of its transparency - it indicates which minerals contribute most to sorption. The approach is made possible by the improved specification of the minerals accessible to sorption within the water-conducting features and the expanded literature on sorption on pure minerals. Experimental sorption data from the literature are reviewed in detail and only those data that are relevant to the reference mineralogies (THURY et al. 1994) and groundwaters (Table 3.5.2) are considered further.

In the summary table of sorption parameters (Table 3.7.8), recommendations are provided for "realistic-conservative" and "conservative" K_d values. The "realistic-conservative" K_d for each element is considered to quantify sorption under the reference conditions specified. The corresponding "conservative" K_d dataset considers some possible perturbation of the reference conditions that is likely to have the maximum effect on the sorption behaviour of that element. For example, a change in redox conditions (Eh) would affect redox-sensitive elements such as Tc, Np and U. For actinides other than Np and U, a pH variation was considered most likely to lead to a maximum change in sorption behaviour. Similarly, either an increase in ionic strength or concentration of competing ions was considered as the perturbation most likely to influence the extent of sorption by ion exchange.

Although the distribution of many elements in natural rock-water systems between the sorbed phase and the aqueous phase is known to show some concentration dependence, of the elements with safety-relevant isotopes, only caesium has been studied sufficiently to justify sorption being represented by an empirical Freundlich isotherm (see also Subsection 5.3.4.4).

3.5.5.3 Groundwater Colloids

Colloids, which are present in all groundwaters, may have an influence on the transport of radionuclides through the host rock. Whether colloids act to retard radionuclides (e.g. by sorption of aqueous species and subsequent filtration) or enhance transport (e.g. by sorption of aqueous species and transport with flowing groundwater along fractures and with exclusion from matrix pores) is unclear and depends on the characteristics of the colloids and the water-conducting features. The Reference Model Assumptions for the geosphere do not include colloid-facilitated radionuclide transport (see Subsection 5.3.1). However, a simple model for colloid-facilitated transport is presented in

Subsection 5.3.3.3 and results of calculations are presented in the discussion of alternative model assumptions within the Reference Scenario (see Subsection 6.2.2.3).

The most important additional parameters for modelling of colloid-facilitated transport are the colloid concentration and the sorption constants for radionuclides on colloids. For the groundwater chemistry of Area West, an upper bound for the colloid concentration is 0.1 ppm (see Chapter 10 in THURY et al. 1994). Sorption on colloids can be quantified by the parameter $K_c = 10^4 \text{ m}^3 \text{ kg}^{-1}$, representing an upper bound for sorption of tetravalent Np, U and Th (DEGUELDRE 1994). The value of K_c is large in comparison to the K_d values, because of the very large specific surface area available for sorption on colloids.

3.6 The Surface Environment

3.6.1 Regional Description

Any radionuclides released from the repository which have not decayed during transport through the engineered and natural barriers would be likely to reach the surface environment in the region of the Rhine valley, broadly corresponding to the northern border of Switzerland. The Rhine here flows from east to west towards the city of Basel. The elevation is 250 to 650 m above sea level and the topography of the Rhine valley is characterised by relatively gently sloping valley bottoms, with river terraces developed over gravels laid down in the Quaternary period. Slopes found in tributary valleys are steeper.

The river Rhine forms the major drainage feature in the region and also the main transport path for radionuclides in the surface environment away from the potential discharge areas. Other major rivers in the region (e.g. the Aare) have similar flowrates, so that attention can focus on the Rhine as a suitable representative river. Additionally, the geological evidence is that the releases from the upper (higher-permeability domain) crystalline basement are most likely to occur in the vicinity of the Rhine. For Area East, a much less probable scenario, which cannot, however, be completely excluded, is release to the valley of a Rhine tributary.

The volumetric water flow in the river Rhine is around $3 \times 10^{10} \text{ m}^3 \text{ y}^{-1}$ (Hydrologisches Jahrbuch der Schweiz 1979) and the sub-surface water flow in the gravels (from the slopes towards the river) is typically in the order of $6 \times 10^6 \text{ m}^3 \text{ y}^{-1}$ (STÄUBLE 1993). In the tributary valleys, the flux of river water is estimated from the size of the catchment area and the specific flowrate in the sub-surface gravels, which is similar to that in the Rhine valley bottom: see Table 6.2.8.

3.6.2 Climate

Over the long timescales considered in safety assessment, climatic changes are expected. These are discussed in Subsections 4.3.4. However, the present-day climate and surface environmental conditions are taken as a starting point from which to define reference biosphere conditions.

The present climate of the region is temperate and shows little spatial variation along the section of the Rhine valley of interest in this study. Temperature and precipitation data are based on those of Basel (KLIMAATLAS DER SCHWEIZ 1982-1991), at the western end of the region; the nearest meteorological station for which complete data are available. The variation in the mean annual temperature is 8 to 12 °C and the annual mean rainfall is 790 mm y⁻¹, but both show considerable seasonal variation. The annual evapotranspiration rate is approximately one-third of the annual precipitation rate.

3.6.3 Soils and the Natural Environment

In the region of interest, the predominant soils are neutral "Parabraunerde" (parabrownearths) in the valley bottoms and weakly acidic "Braunerde" (brownearths) in the valley sides (ATLAS DER SCHWEIZ 1965-1990). Since the expected release area is the Rhine valley, the Parabraunerde are of most interest in this study. The Parabraunerde have coarse particle sizes, being derived from the terraces and moraines, have good drainage and exhibit translocation of clay. In addition, both soil types contain pockets of reduced iron minerals (pseudogley).

At present, natural vegetation is almost entirely absent from the region. The present rural landscape is the result of human cultivation over the past few thousand years. On the basis of soil types and topography, the natural vegetation would be deciduous forests (e.g. beech and oak).

3.6.4 Human Habitation and Economy

The human population has had a large influence on the regional environment. In this study the human life-style modelled is that of subsistence agriculture¹⁷, which has been practised in the region until comparatively recent times. The present day population

¹⁷ In the biosphere model, the assumption of subsistence agriculture means that no account is taken of dilution resulting from consumption of uncontaminated food from outside the region by the critical group.

density varies between 50 and 500 persons km⁻² (ATLAS DER SCHWEIZ 1965-1990). However, lower population densities would be expected in the case of subsistence agriculture. The data relating to the distribution of present-day human settlements are therefore not relevant to the biosphere modelling for the safety assessment (see Section 5.4 for a description of the Reference Biosphere methodology adopted here). At present, the regional non-agricultural economy consists mainly of small businesses and light industry with a strong service sector (ATLAS DER SCHWEIZ 1965-1990).

3.6.5 Land Use and Agriculture

Agriculture is important to the regional economy (ATLAS DER SCHWEIZ 1965-1990). This includes animal husbandry, arable farming and forestry (mainly conifer plantations). Between 15 % and 45 % of the open agricultural land is devoted to arable and fruit production, with the remainder being used for livestock grazing (pasture land) or for growing animal foodstuffs (predominantly maize).

3.6.6 Water Resources and Usage

The near-surface hydrology is determined by climate and water flows in the Quaternary deposits. In the region of interest, these include fluvio-glacial gravels in the valley bottoms, which comprise important local aquifers. Historical records show extensive use of these water resources (STÄUBLE 1993); they would be likely water sources for subsistence agricultural communities, such as those considered in the biosphere model employed in this assessment.

There are several extraction sites, with flowrates up to 5000 litres min⁻¹ from gravel aquifers in the region (ATLAS DER SCHWEIZ 1965-1990). In addition, there are a number of mineral and thermal water sources, where water is extracted from the upper part of the crystalline basement (e.g. Zurzach with a flowrate of 600 litres min⁻¹).

3.7 Data for the Kristallin-I Safety Assessment Calculations

3.7.1 Overview of Safety Assessment Data

This section gathers the principal data for the Kristallin-I safety-assessment calculations, based on the information and data presented in Sections 3.3 to 3.6. Much of this data is used directly in the safety assessment models described in Chapter 5. For the modelling of the biosphere, other data are required which are not specific to the disposal concept or site; these are presented in Section 5.4 and Appendix 7.

The data presented here consists of:

- inventories of safety-relevant radionuclides, selected as described in Appendix 2 (Subsection 3.7.2);
- element-independent properties of the engineered barriers relevant to the modelling of radionuclide release and transport in the engineered barriers (Subsection 3.7.3);
- element-dependent parameters (solubility limits and sorption constants) for modelling radionuclide release and transport in the engineered barriers (Subsection 3.7.4);
- hydrogeological modelling results for Area West and Area East and the corresponding element-independent properties of the geological barriers (Subsection 3.7.5), relevant to the modelling of transport in both the engineered and geological barriers;
- geometrical parameters and porosities for the three types of water-conducting features which provide preferential paths for groundwater flow through the geological barriers of the crystalline basement (Subsection 3.7.6);
- element-dependent parameters (sorption constants and isotherm parameters) for modelling radionuclide transport in the geological barriers (Subsection 3.7.7).

For several parameters "realistic-conservative" and "conservative" values are presented. The distinction, and methodological basis for this, is discussed in Subsection 5.1.4.

3.7.2 Inventories of Safety-Relevant Radionuclides

The Nagra model radioactive waste inventory is discussed in Section 3.3. The inventories, activities and half-lives of safety-relevant radionuclides and inventories of stable isotopes, calculated at 1000 years after repository closure, are presented in Table 3.7.1.

Nuclides	Inventory per Waste Canister		Half-Life
	(moles)	(Bq)	(years)
Activation/fission products (including stable isotopes)			
Ni (stable)	2.32×10^1	-	-
^{59}Ni	1.07×10^{-2}	1.88×10^9	7.50×10^4
Se (stable)	8.83×10^{-1}	-	-
^{79}Se	1.07×10^{-1}	2.18×10^{10}	6.5×10^4
^{93}Zr	1.06×10^1	9.20×10^{10}	1.53×10^6
^{99}Tc	1.04×10^1	6.48×10^{11}	2.13×10^5
Pd (stable)	1.40×10^1	-	-
^{107}Pd	2.56	5.20×10^9	6.50×10^6
Sn (stable)	9.52×10^{-1}	-	-
^{126}Sn	2.78×10^{-1}	3.67×10^{10}	1.00×10^5
^{135}Cs	3.30	1.90×10^{10}	2.30×10^6
4N + 1 chain (neptunium chain)			
^{245}Cm	3.43×10^{-3}	5.33×10^9	8.50×10^3
^{241}Am	2.13×10^{-1}	6.51×10^{12}	4.32×10^2
^{237}Np	3.49	2.16×10^{10}	2.14×10^6
^{233}U	1.06×10^{-3}	8.84×10^7	1.59×10^5
^{229}Th	2.23×10^{-6}	4.01×10^6	7.34×10^3
4N + 2 chain (uranium chain)			
^{246}Cm	3.38×10^{-4}	9.45×10^8	4.73×10^3
^{242}Pu	1.72×10^{-2}	6.04×10^8	3.76×10^5
^{238}U	8.11	2.40×10^7	4.47×10^9
^{234}U	1.11×10^{-2}	6.01×10^8	2.45×10^5
^{230}Th	4.58×10^{-5}	7.87×10^6	7.54×10^4
^{226}Ra	2.38×10^{-7}	1.97×10^6	1.60×10^3
4N + 3 chain (plutonium chain)			
^{243}Am	3.85×10^{-1}	6.90×10^{11}	7.38×10^3
^{239}Pu	2.52×10^{-1}	1.39×10^{11}	2.41×10^4
^{235}U	9.22×10^{-2}	1.73×10^6	7.04×10^8
^{231}Pa	2.10×10^{-6}	8.48×10^5	3.28×10^4
4N chain (thorium chain)			
^{240}Pu	1.68×10^{-1}	3.40×10^{11}	6.54×10^3
^{236}U	5.82×10^{-2}	3.29×10^7	2.34×10^7
^{232}Th	4.89×10^{-6}	4.60	1.41×10^{10}

Note: Selection of the radionuclides is according to a simple conservative screening model described in Appendix 2. In the biosphere calculations, some short lived decay products (not shown here) are calculated explicitly.

Table 3.7.1: Inventories, activities and half-lives of safety-relevant radionuclides and inventories of stable isotopes of the same elements. Data are for one canister of vitrified HLW, waste type WA-COG-1 (the repository is assumed to contain 2693 such canisters - see Section 3.3), calculated at the reference canister failure time of 1000 years after repository closure (1040 years after unloading of fuel from the reactor).

Special notes on half-life of ^{230}Th :

For some radionuclides, there is some uncertainty or inconsistency between different data on half-life. In the Kristallin-I assessment calculations for ^{230}Th , slightly different half lives have been adopted for different model elements as a result of different base references being consulted.

A value of 7.54×10^4 years (ANTONY 1992; SCHÖTZIG & SCHRADER 1993) was adopted in calculations of the radionuclide inventory, in STRENG (near field) calculations and dose conversion factors for STRENG results (Appendix 6).

A value of 7.7×10^4 years (ICRP 1983) was adopted in RANCHMD (geosphere) and TAME (biosphere) calculations.

The discrepancy of about 2%, though undesirable, has no significant effect on calculated releases and doses.

3.7.3 Element-Independent Data for the Engineered Barriers

Element-independent properties of the engineered barriers are summarised in Table 3.7.2. Corrosion of the cast steel canister, leading to eventual canister failure, is discussed in Subsection 3.4.3. Corrosion of the glass waste matrix, together with the increase in glass surface area as a result of fracturing, is discussed in Subsection 3.4.2. The glass block volume (0.15 m^3 per canister) is given in Subsection 3.3.2, corresponding to a circular cylinder of diameter of 0.43 m and a length of 1.03 m. The "volume for dissolution" is a concept introduced for modelling solubility-limited radionuclide release and is described further in Subsection 5.2.1. Diffusion through the bentonite is described in Subsection 3.4.6.3. Modelling transport across the bentonite-host rock interface using the "mixing-tank" boundary condition (see Subsections 5.2.1 and 5.2.2) requires a value for groundwater flow through the repository area. Groundwater flowrate is assessed through hydrogeological modelling (see Subsection 3.5.3); selection of flowrate values for safety assessment is discussed below in Subsection 3.7.5, where the concept of "repository area" is also defined.

Parameter	"Realistic-conservative" value	Variations
Time of canister failure, $t=0$	10 ³ years after repository closure	10 ⁵ years, 10 ² years
Glass corrosion rate, R	$3.8 \times 10^{-4} \text{ kg m}^{-2} \text{ y}^{-1}$	$3.8 \times 10^{-2} \text{ kg m}^{-2} \text{ y}^{-1}$
Length of glass blocks, h	$2.77 \times 10^3 \text{ m}$ (2693 blocks of length 1.03 m)	-
Initial diameter of glass block, d_0	0.43 m	-
Glass density, ρ_g	2750 kg m^{-3}	-
Factor for glass surface area increase due to fracturing	12.5	-
Volume for dissolution, V_R^\dagger	99 m^3 (0.037 m^3 for each block)	-
Inner bentonite radius, r_a	0.47 m	-
Outer bentonite radius, r_b	1.85 m	0.67 m
Bentonite porosity, ϵ	0.38	-
Bentonite solid density, ρ_b	2760 kg m^{-3}	-
Effective diffusion constant in bentonite, D_e	$6.3 \times 10^{-3} \text{ m}^2 \text{ y}^{-1}$	-
Groundwater flowrate through repository area, Q (see Table 3.7.6)	Mixing tank boundary condition applied: $Q = 3 \text{ m}^3 \text{ y}^{-1}$	(i) Mixing tank boundary condition applied: Area West, $Q = 0.3, 30, 300 \text{ m}^3 \text{ y}^{-1}$; Area East, $Q = 100 \text{ m}^3 \text{ y}^{-1}$ (ii) Zero-concentration boundary condition applied

Notes: † The volume for dissolution is the total volume of a set of hypothetical water-filled annular regions of 2.5 cm thickness surrounding the glass blocks; results of near-field calculations are insensitive to the value assigned to this volume over a broad range.

Table 3.7.2: Data for modelling of radionuclide release and transport in the engineered barriers - glass corrosion, geometry, canister failure, bentonite properties and water flow through repository.

3.7.4 Element-Dependent Data for the Engineered Barriers

Element-dependent properties of the engineered barriers are given in Table 3.7.3 for those elements of which the safety-relevant radionuclides are isotopes. The solubility limits of radionuclides in bentonite porewater are discussed in Subsection 3.4.6.2. Sorption on pore surfaces in the bentonite is discussed in Subsection 3.4.6.3.

Element	Solubility limit, S_E (1,2) (M)		Sorption constant, K_d (3) (m ³ kg ⁻¹)	
	"Realistic- conservative" value	"Conservative" value	"Realistic- conservative" value	"Conservative" value
Ni	high	high	1	0.1
Se	1×10^{-8}	6×10^{-7}	0.005	0.001
Zr	5×10^{-9}	5×10^{-7}	1	0.1
Tc	1×10^{-7}	high	0.1	0.05
Pd	1×10^{-11}	1×10^{-6}	1	0.1
Sn	1×10^{-5}	1×10^{-5}	1	0.1
Cs	high	high	0.01	0.001
Ra	1×10^{-10}	1×10^{-10}	0.01	0.001
Th	5×10^{-9}	1×10^{-7}	5	0.5
Pa	1×10^{-10}	1×10^{-7}	1	0.1
U	1×10^{-7}	7×10^{-5}	5	0.5
Np	1×10^{-10}	1×10^{-8}	5	0.5
Pu	1×10^{-8}	1×10^{-6}	5	0.5
Am	1×10^{-5}	1×10^{-5}	5	0.5
Cm	6×10^{-8}	1×10^{-5}	5	0.5

Notes: (1) Solubility limits from BERNER (1994).

(2) "high" indicates that no solubility limit is set in the near-field model calculations.

(3) Sorption constants for bentonite from STENHOUSE (1994).

Table 3.7.3: Element-dependent parameter values for modelling of radionuclide release and transport in the near field - solubility limits and sorption constants.

3.7.5 Element-Independent Data for the Geological Barriers

The geology of the crystalline basement of Northern Switzerland, including hydrogeological modelling, is discussed in Section 3.5. Hydrogeological modelling results for Areas West and East are summarised in Tables 3.7.4 and 3.7.5, respectively. In deriving parameters for the modelling of radionuclide transport in the geosphere (and transport across the bentonite-host rock interface using the "mixing-tank" boundary condition in the near-field model), some further interpretation is required; this is discussed below.

Type of input/result	Value/range	Remarks	Value in P.A. Ref. Case
Selected input parameters and results (local-scale and regional-scale)			
1. Transmissivity (T) of water-conducting features (WCF) in low-permeability domain (LPD)[m ² /s]	Arithmetic mean: 9.4E-10 Mean logT: -9.24; Standard deviation logT: 0.4	Table 8-2	-
2. Effective hydraulic conductivity (K-eff) of LPD [m/s]	4.2E-11	Fig. 8-14; locally, over an interval of a few decimetres, the value could be up to 5E-10 m/s (see Fig. 8-2).	4E-11
3. T of WCF in higher-permeability domain (HPD) [m ² /s]	Arithmetic mean: 4.4E-6 Mean logT: -6.17; Standard deviation logT: 1.1	Table 8-2	-
4. K-eff HPD [m/s]	2.8E-7	Fig. 8-14; see comment 2. above, value could be up to 5E-6 m/s (see Fig. 8-2).	-
5. T of WCF in major water-conducting faults (MWCF)[m ² /s]	Arithmetic mean: 4.1E-6 Mean logT: -6.32; Standard deviation logT: 0.9	Table 8-2	-
6. K-eff of MWCF first order [m/s]	3.2E-7	Fig. 8-14	3E-7
7. T of MWCF second order [m ² /s]	6.4E-6	Fig. 8-14	-
8. Transmissive element length per unit cross-sectional area of major water conducting faults [m ⁻¹]	0.08 - 0.12	Section 10.2.1	0.1
9. Darcy flux - LPD [m/s]	Mean: 1E-12 - 3.2E-12 Range: 5E-14 - 3E-11	Table 8-5	-
10. Darcy flux - MWCF [m/s]	Mean: 1.9E-9 - 6.7E-9 Range: 9E-11 - 5E-8	Table 8-5	6.7E-9
11. Darcy flux - Rhine alluvia [m/s]	Eastern part of area West: 1E-5 Frick Valley: 1E-4	Section 10.2.1	-
12. Volumetric flux - Rhine alluvia [m ³ /s]	section in Laufenburg: 0.05 section near Stein: 0.65 section in Frick valley: 0.36	Section 10.2.1	0.17 (=5.5E+6 m ³ /y)
13. Volumetric flux - Rhine [m ³ /s]	1000	Section 10.2.1	1000 (=3.2E+10 m ³ /y)

Note: *Mean* is mean of full-model distribution - mean of sparse-model distribution, *Range* is from lower end of full-model distribution to upper end of sparse-model distribution.

Table 3.7.4: Geometric and hydrogeological modelling results for safety assessment of Area West. Figures and tables referenced under "Remarks" are found in THURY et al. (1994). Transmissive elements (TEs) are equivalent to the water-conducting features in the assessment calculations.

Type of input/result	Value/range	Remarks	Value in P.A. Ref. Case
Results from block-scale models: Geometry			
1. Number of transmissive elements (TEs) that intersect a 500 m tunnel segment	Range: 6 - 20 Mean: 13.7	See Section 8.6.2 and Fig. 8-20.	14
2. Trace lengths of single TEs that intersect a 500 m tunnel segment [m]	Range: <1 - 72 Average: 21.7; Most: 20 - 30	See Section 8.6.2 and Fig. 8-20. A value of 25 was recommended for P.A. reference case calculations.	25
3. Length of direct flowpath, LPD to HPD or MWCF [m]	Minimum: defined by SA Maximum: Value depends on position of emplacement caverns and local hydrogeologic conditions.	Flowpath direction may be predominantly vertical or horizontal.	100
4. Ratio, actual flowpath length to direct one	Range: 1.2 - appr. 3 Most: 1.4 - 2.0	For conservatism, assume ratio = 1	2
5. Number of TEs in a flowpath	—	For conservatism, assume 1	1
Results from block-scale models: Hydraulics			
	Range: 2.5%-97.5%	Geometric mean / Arithmetic mean	
1. Hydraulic gradient/LPD [-]: - Horizontal component - Vertical component - Absolute	0.002 - .09 <E-3 - 0.07 .0055 - .12	N.A. / 0.009 - .03 N.A. / 0.005 - .03 N.A. / .01 - .05	See Section 8.5 and Figure 8-15. -
2. Normalised flux [m ² /s] in TEs in LPD (i.e., flux per unit length)	6E-13 - 2E-10	5.7E-12 - 2E-11 / 9.4E-12 - 4E-11	Fig. 10-3 and notes below. 2E-11
3. Conductance of TEs in LPD [m ³ /s]	3E-10 - 3.8E-8	5E-9 / 9E-9	Fig. 8-20 and notes below. -
4. Flux through single TEs intersecting a 500-m tunnel segment in LPD, Q _{TE} [m ³ /s]	3E-12 - 2E-9	5.3E-11 - 1.8E-10 / 1.1E-10 - 4.8E-10	Fig. 10-4 and notes below. -
5. Total flux through a 500-m tunnel segment in LPD, Q _t [m ³ /s]	4E-11 - 3E-8	7E-10 - 2.4E-9 / 1.5E-9 - 6.6E-9	Fig. 10-5 and notes below. -
6. Total flux through repository, Q _r [m ³ /y] [Q _r = 30 Q _t]	0.04 - 28.4	0.65 - 2.3 / 1.4 - 6.2	Assumes 30 tunnels and vertical flow; see note 2 below and Section 10.2.1 -
7. Dilution ratio, Q _{MWCF} /Q _{LPD}	E+2 - E+3	—	Section 10.2.1 -
8. Dilution ratio, Q _{HPD} /Q _{LPD}	E+2 - E+3	—	Section 10.2.1 -
9. Dilution ratio, Q _{bio} /Q _r	7E+5 - 5E+8	9E+6 - 3E+7 / 3.3E+6 - 1.5E+7	Biosphere is Rhine River alluvium at section near Stein; see 12. above. -

Notes: *Mean* is mean of full-model distribution - mean of sparse-model distribution, *Range* is from lower end of full-model distribution to upper end of sparse-model distribution, *Most* is used for the trace length distribution in a qualitative sense, since the distribution is highly skewed.

The study by LANYON & HOCH (1993) indicates that fluxes derived considering the flow dynamics can be up to 10 times lower than the ones derived from the geometric approach (cf. Chapter 10 in THURY et al. 1994).

N.A. = not available, SA = safety assessment.

Table 3.7.4: (Continued). Geometric and hydrogeological modelling results for safety assessment of Area West.

Type of input/result	Value/range						
	Hypothesis 1 (SIB data are representative)				Hypothesis 2 (SIB data are not representative)		
	Range	Mean		Value in P.A. Ref. Case	Range	Mean	
		Geom.	Arith.			Geom.	Arith.
Selected input parameters							
1. Transmissivity of TEs in LPD [m ² /s]	Mean of logT = -6.9 Std. deviation of logT = 0.5			-	see Table 10-1		
2. Effective hydraulic conductivity of LPD [m/s]	1E-8			-	see Table 10-1		
Geometry							
1. Number of TEs intersected in a 500 m tunnel segment.	32 - 47	N.A.	40.8	40.8	6-20	N.A.	13.7
2. Trace lengths of single TEs in a 500 m tunnel segment [m]	0.2-136 Most values: 20-25	N.A.	22.8	22.8	0.5 - 72 Most values: 20-30	N.A.	21.7
3. Length of direct flowpath within a block in the Lower Unit [m]	Not determined	-	-	200	Not determined	-	-
4. Ratio, actual flowpath length to direct flowpath length	Not determined: For conservatism, assume ratio = 1.0						
5. Number of TEs along a flowpath	Not determined For conservatism, assume number = 1						
Hydraulics							
1. Hydraulic gradient: - Hor. component - Vert. component - Absolute (see sect. 8.7)	< 0.0004 - .006 < .0001 - .006 < .0004 - .007	N.A. N.A. N.A.	0.0028 .0013 .0033	-	0.002 - 0.032 0 - .022 .003 - 0.033	N.A.	0.004 - .020 .001 - .007 .004 - .022
2. Normalised flux [m ² /s] in TEs (per unit length)	2E-11 - 5E-9	3.4E-10	8.7E-10	2.8E-10	3E-13 - 7E-11	2E-12 - 1E-11	4E-12 - 2E-11
3. Conductance of TEs [m ³ /s]	5E-8 - 2E-5	1.2E-6	2.7E-6	-	3E-10 - 4E-8	5E-9	9E-9
4. Flux through single TEs intersecting a 500 m tunnel segment [m ³ /s]	1E-10 - 5E-8	3.3E-9	1.1E-8	-	1E-12 - 1E-9	2.1E-11 - 1.1E-10	4.2E-11 - 2.1E-10
5. Total flux through 500 m tunnel segment, Q _t [m ³ /s]	4E-9 - 2E-6	1.3E-7	4.2E-7	-	2E-11 - 1E-8	2.7E-10 - 1.4E-9	5.7E-10 - 2.9E-9
6. Total flux through repository, Q _r [m ³ /y] [Q _r = 30 Q _t]	3.8 - 1.9E+3	123	396	-	0.02-9.45	0.25-1.3	0.55 - 2.7
7. Dilution ratio, Q _{bio} /Q _r : Q _{bio} =Rhine valley alluvium	1.1E+4-5.4E+6	1.7E+5	5.2E+4	-	2.2E+6-1E+9	1.6E+7-8.2E+7	7.6E+6 - 3.7E+7

Note: For Hypothesis 2, Mean is mean of full-model distribution - mean of sparse-model distribution, Range is from lower end of full-model distribution to upper end of sparse-model distribution; for both Hypothesis 1 and Hypothesis 2, in the case of hydraulic results it corresponds to 2.5% to 97.5% of the cumulative.

Table 3.7.5: Geometric and hydrogeological modelling results for safety assessment of Area East. (From THURY et al. 1994).

For the purposes of assessment modelling, the basement rock is assumed to comprise three main elements at a macroscopic scale (see Subsection 3.5.1): (i) a higher-permeability domain, (ii) a low-permeability domain and (iii) major water-conducting faults. Radionuclide transport is modelled explicitly through the low-permeability domain and through the major water-conducting faults (see Section 5.3). Model parameters must therefore be specified for these two elements of the basement rock. It is, however, assumed that radionuclides reaching the higher-permeability domain are transported rapidly through the higher-permeability domain to the biosphere (see Subsection 5.3.1); the properties of this element of the basement rock are not considered further here.

3.7.5.1 Groundwater Flow Data for the Low-Permeability Domain

The method used to derive assessment model parameters for the low-permeability domain (applicable to both Area West and Area East) is illustrated in Figure 3.7.1. The parameters themselves are presented in Table 3.7.6(a).

Data quantifying groundwater flow in the low-permeability domain can be divided into the following four categories:

A. Data related to repository siting

Direct flowpath length - in Area West and Area East, the minimum geometrical distance from any part of the repository tunnel system to either the nearest major water-conducting fault or the lower boundary of the higher-permeability domain is currently planned to be 100 m.

Ratio of actual flowpath length to direct flowpath length - in Area West, a range from 1.2 to approximately 3 has been calculated for this ratio (see Table 3.7.4); a value of 2 is adopted for the Kristallin-I Reference Case, with a conservative parameter variation of 1.

B. Geometrical data for water-conducting features

The results of a detailed examination of water-conducting features identified in both Areas are summarised in Figure 3.5.4 and Table 3.7.7; data presented in the figure and table are applicable to both areas. The three types of water-conducting features each consist of a set of partially infilled parallel fractures, with discrete channels within which groundwater flow is confined. Geometrical parameters relevant to safety assessment calculations are:

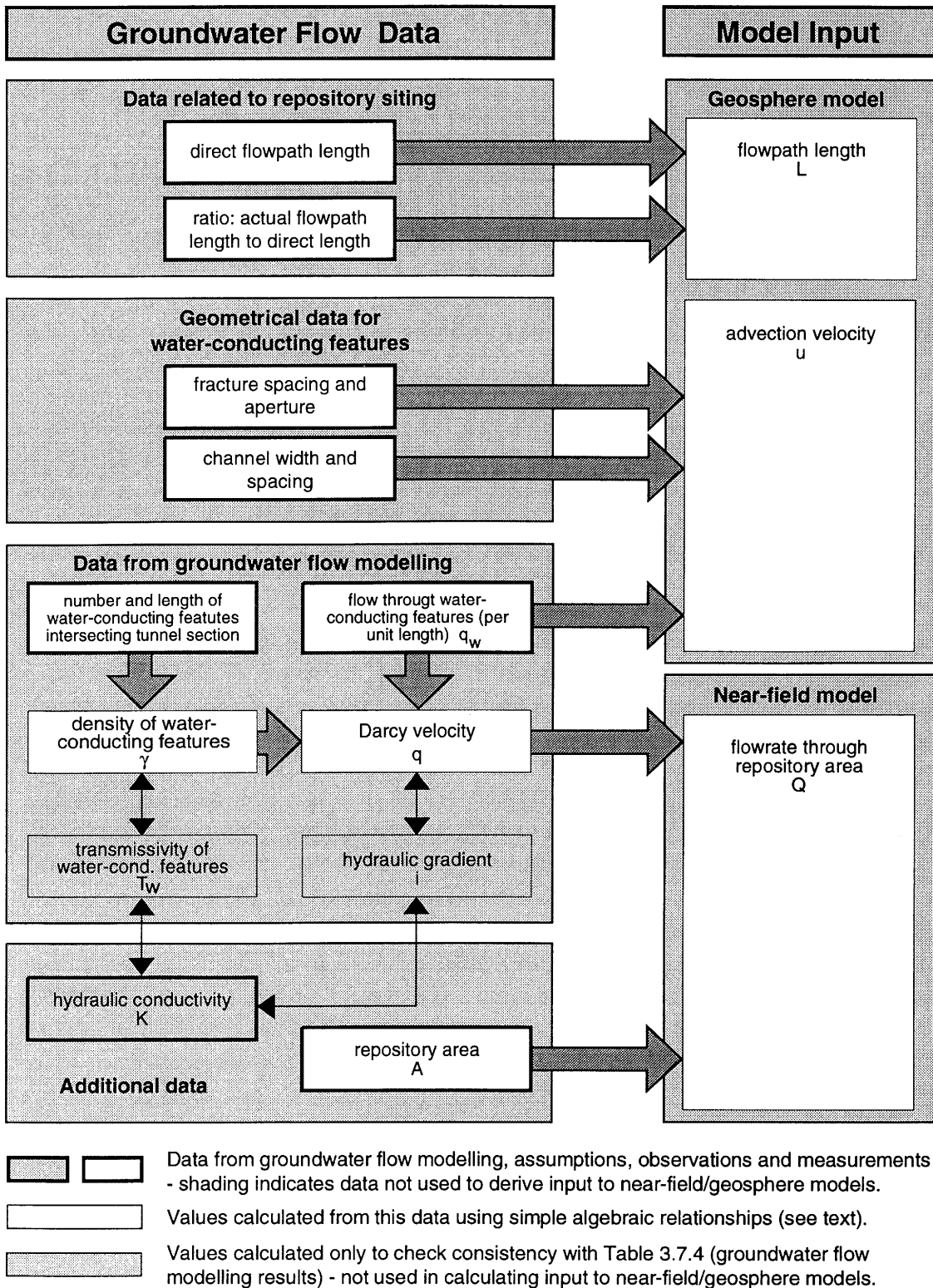


Figure 3.7.1: Derivation of input parameters for the near-field and geosphere models from the results of groundwater flow modelling of the low-permeability domain (LPD) of the crystalline basement in Areas West and East.

Fracture spacing and aperture - see Table 3.7.7.

Channel width and spacing within a fracture - channel width and the width of fracture infill between channels are given in Table 3.7.7.

The selection of values for safety assessment from the ranges given in Figure 3.5.4 and Table 3.7.7 is discussed in Subsection 5.3.4.1 (see, in particular, Table 5.3.1).

C. Data from groundwater flow modelling

Number and length of water-conducting features intersecting a tunnel section - in the groundwater flow model reported in THURY et al. (1994), a hypothetical 500 m tunnel section is considered. This is assigned a square cross section, each side having a length of 5 m. The number of water-conducting features intersecting the tunnel section is taken to be 14 in Area West (a mean value of 13.7 is given in Table 3.7.4) and 41 in Area East (a mean value of 40.8 is given in Table 3.7.5). The mean length of a single feature along the tunnel wall is taken to be 25 m in Area West (the value recommended for safety assessment in Table 3.7.4) and 23 m in Area East (a mean value of 22.8 m is given in Table 3.7.5).

Flow through water-conducting features (per unit length) q_w [$\text{m}^2 \text{y}^{-1}$] - the flowrate through a single water-conducting feature, divided by the length of the feature (trace length of the feature in a plane normal to the flow direction), is taken to be the geometric mean of the flowrate distribution obtained from groundwater flow modelling. In Area West, the more conservative (higher flowrate) "Sparse Model" is assumed and similarly, in Area East, the more conservative "Hypothesis 1", in which data from the Siblingen borehole is assumed to be representative of the area, is assumed (see Subsection 3.5.3). A value of $6 \times 10^{-4} \text{ m}^2 \text{y}^{-1}$ (a geometric mean of $2 \times 10^{-11} \text{ m}^2 \text{s}^{-1}$ is given as the "normalised flux in TEs" in Table 3.7.4) is therefore taken for Area West. For Area East, a geometric mean flux through the hypothetical 500 m tunnel section of $1.3 \times 10^{-7} \text{ m}^3 \text{s}^{-1}$ is given in Table 3.7.5. Assuming half of the features carry water into the tunnel section, with the remaining half carrying water out, this flux is distributed between $40.8/2$ features of mean length 22.8 m (see above), giving a flow per unit length of $10^{-2} \text{ m}^2 \text{y}^{-1}$ ($2.8 \times 10^{-10} \text{ m}^2 \text{s}^{-1}$). As noted in Table 3.7.4, the geometric approach used to derive these values may give values up to 10 times higher than a more realistic approach considering the flow dynamics (see also Subsection 5.3.4.1). A parameter variation, in which the flowrate is decreased by a factor of 10, is therefore considered for Area West. Parameter variations with flowrate increased by factors of 10 and 100 are also considered in order to cover uncertainty and variability in flowrate (see also Subsection 6.2.2.4).

Density of water-conducting features γ [m^{-1}] - the density of water-conducting features is defined here as the total length of features intersecting a hypothetical plane of unit area (see also Subsection 5.3.4.1). As indicated in Figure 3.7.1, this is derived from the number and length of features intersecting the hypothetical tunnel section of square

cross-section, with four 5 m sides and a length of 500 m (see C, above). Multiplying the number and length of water conducting features intersecting the tunnels section and dividing by the area of the tunnel wall gives densities of 0.04 m^{-1} and 0.1 m^{-1} for Areas West and East, respectively.

Darcy velocity q [m y^{-1}] - as indicated in Figure 3.7.1, the Darcy velocity is related to q_w , the flow through the water-conducting features (per unit length), and γ , the density of water-conducting features, through the expression $q = q_w \gamma$. This gives Darcy velocities of $2 \times 10^{-5} \text{ m y}^{-1}$ (Reference Case) and 10^{-3} m y^{-1} for Areas West and East, respectively.

Transmissivity of water-conducting features T_w [$\text{m}^2 \text{ y}^{-1}$] - the transmissivity of the water-conducting features is related to K , the hydraulic conductivity (see D, below), and γ , the density of water-conducting features, through the expression $T_w = K / \gamma$. This gives transmissivities of $0.03 \text{ m}^2 \text{ y}^{-1}$ and $3 \text{ m}^2 \text{ y}^{-1}$ for Areas West and East, respectively, which are consistent with the mean transmissivities given in Tables 3.7.4 and 3.7.5 (the transmissivity of water-conducting features is not directly used to derive input for the assessment models).

Hydraulic gradient i [-] - the hydraulic gradient can be derived from K , the hydraulic conductivity, and q , the Darcy velocity, through the expression $i = q / K$. This gives hydraulic gradients of 0.02 and 0.003 for Areas West and East, respectively, which are consistent with the arithmetic means of absolute gradient given in Tables 3.7.4 and 3.7.5 (the hydraulic gradient is not directly used to derive input for the assessment models).

D. Additional data

Hydraulic conductivity K [m y^{-1}] - the hydraulic conductivities for Areas West and East are taken directly from Tables 3.7.4 and 3.7.5. The values taken are 10^{-3} m y^{-1} ($4.2 \times 10^{-11} \text{ m s}^{-1}$ in Table 3.7.4) and 0.3 m y^{-1} (10^{-8} m s^{-1} in Table 3.7.4) for Areas West and East, respectively (the hydraulic conductivity is not directly used to derive input for the assessment models).

Repository area A [m^2] - the repository area is taken to be the sum of the areas of a set of hypothetical horizontal planes intersecting the repository emplacement tunnels and their surrounding excavation disturbed zones, as illustrated in Figure 5.3.4. Each tunnel has a diameter of 3.7 m and the excavation disturbed zone is expected to extend to a distance in the order of one tunnel diameter beyond the tunnel wall; each of the hypothetical planes is therefore assigned a width of 10 m. There are 2693 waste packages, with a separation along the tunnel axis of 5 m; the repository area is therefore $10 \text{ m} \times 5 \text{ m} \times 2693 = 1.35 \times 10^5 \text{ m}^2$.

The data given above are combined to provide input to the Kristallin-I assessment models. In the case of the low-permeability domain of the crystalline basement of Areas West and East, input is provided for both the near-field and geosphere models, as shown in Figure 3.7.1 and described below:

E. Input to assessment models

Flowpath length L [m] - a flowpath length must be specified as input to the geosphere model (see also Subsection 5.3.4.1); for Area West, the Reference Case flowpath length is set to 200 m, the product of the minimum direct flowpath length and the ratio of the actual flowpath length to direct flowpath length (see A, above). The same flowpath length is assumed for Area East. Parameter variations with flowpath length decreased to 100 m (corresponding to a unit ratio of actual to direct flowpath length) and increased to 500 m are also considered.

Advection velocity u [m y⁻¹] - an advection velocity must also be specified as input to the geosphere model. Derivation of the advection velocity requires geometrical data for water-conducting features (B, above) and a value for flowrate through the features (C, above). The derivation is described in Subsection 5.3.4.1 (see, in particular, Table 5.3.2).

Flowrate through the repository area Q [m³ y⁻¹] - a flowrate through the repository area, A , (see D, above, for definition of repository area) must be specified as input to the near-field model, as indicated in Table 3.7.2; this flowrate can be derived from A and q , the Darcy velocity (C, above). These quantities are related through the expression $Q = q A$, which gives flowrates of 3 m³ y⁻¹ (Reference Case) and 100 m³ y⁻¹ for Areas West and East, respectively.

3.7.5.2 Groundwater Flow Data for the Major Water-Conducting Faults

The derivation of assessment model parameters for the major water-conducting faults (data available only for Area West) is illustrated in Figure 3.7.2. The parameters themselves are presented in Table 3.7.6(b).

As for the low-permeability domain, data quantifying groundwater flow can be divided into the four categories:

A. Data related to repository siting

Repository depth - the minimum geometrical distance from any part of the repository tunnel system, located in the low-permeability domain, to the overlying higher-permeability domain is currently planned to be 100 m. This also gives an indication of the flowpath length within major water-conducting faults, should radionuclides be conveyed (horizontally) to the faults, rather than (vertically) through the low-permeability domain to the higher-permeability domain (see the discussion of possible pathways from the repository to the biosphere in Subsection 5.3.1.1).

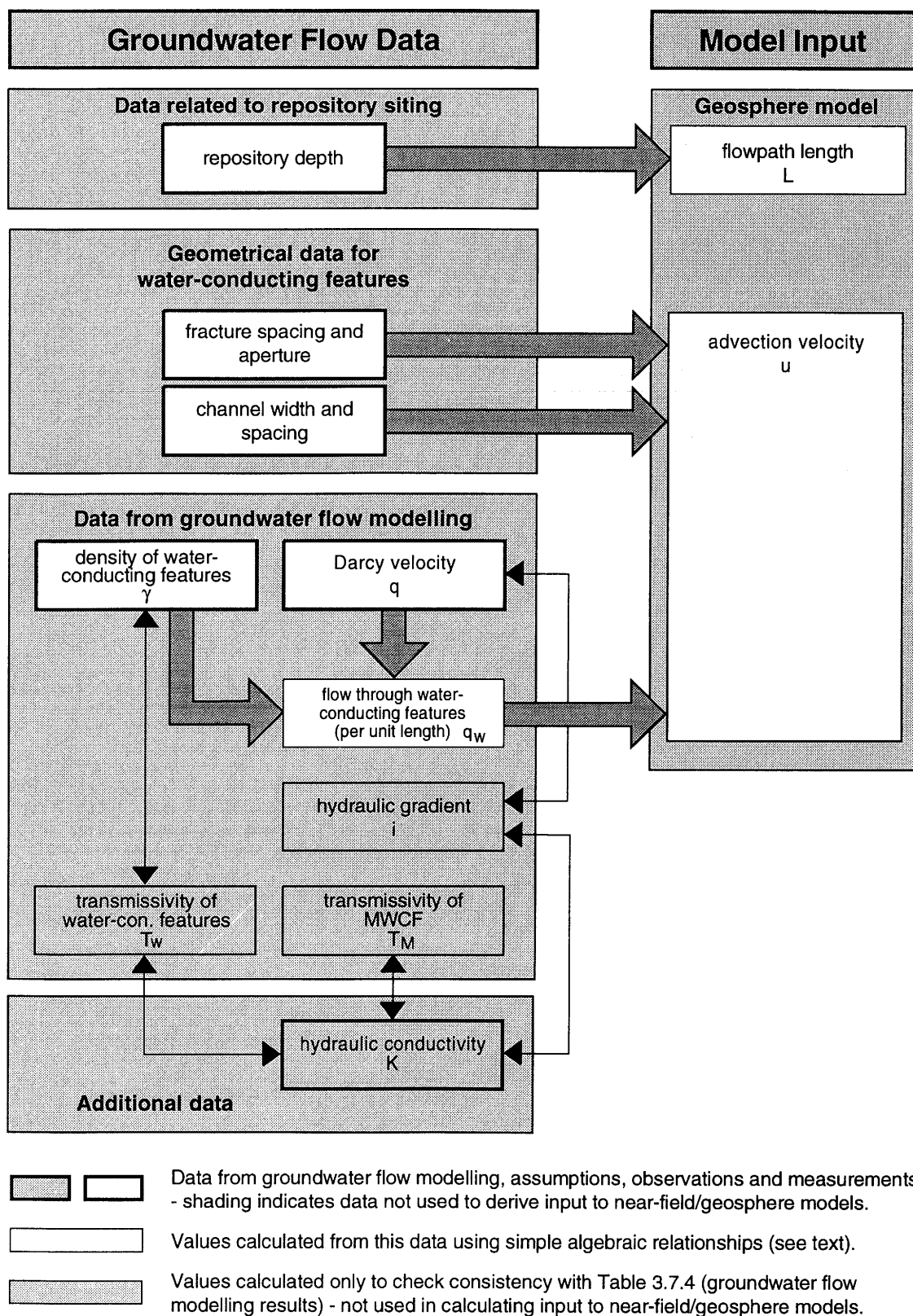


Figure 3.7.2: Derivation of input parameters for the geosphere model from the results of groundwater flow modelling of major water-conducting faults (MWCF) within the crystalline basement.

A: Data related to repository siting			
		Area West	Area East
Direct flowpath length	[m]	>100	-
Ratio of actual flowpath length to direct length	[-]	2	-
B: Geometrical data for water-conducting features			
Fracture spacing and aperture		See Figure 3.5.4 and Table 3.7.7	
Channel width and spacing			
C: Data from groundwater flow modelling			
Number and mean length of water-conducting features intersecting a 500 m hypothetical tunnel section	[-], [m]	14, 25	41, 23
Flow through water-conducting features (per unit length)	[m ² y ⁻¹]	(6×10 ⁻⁵), 6×10 ⁻⁴ , (6×10 ⁻³), (6×10 ⁻²)	10 ⁻²
Density of water-conducting features	[m ⁻¹]	0.04	0.1
Darcy velocity	[m y ⁻¹]	(2×10 ⁻⁶), 2×10 ⁻⁵ , (2×10 ⁻⁴), (2×10 ⁻³)	10 ⁻³
Transmissivity of water-conducting features	[m ² y ⁻¹]	0.03	3
Hydraulic gradient	[-]	0.02	0.003
D: Additional data			
Hydraulic conductivity	[m y ⁻¹]	10 ⁻³	0.3
Repository area	[m ²]	10 ⁵	10 ⁵
E: Input to assessment models			
Flowpath length	[m]	(100), 200, (500)	200
Advection velocity	[m y ⁻¹]	See Table 5.3.2	
Flowrate through repository area	[m ³ y ⁻¹]	(0.3), 3, (30, 300)	10 ²

Table 3.7.6: Reference-Case assessment model parameters related to groundwater flow. (a): data for the crystalline basement of Area West (low-permeability domain) and Area East. Parameter variations around the Reference Case are shown in parentheses. Data are presented to one significant figure.

A: Data related to repository siting		
Repository depth below higher-permeability domain	[m]	> 100
B: Geometrical data for water-conducting features		
Fracture spacing and aperture		See Figure 3.5.4
Channel width and spacing		
C: Data from groundwater flow modelling		
Density of water-conducting features	[m ⁻¹]	0.1
Darcy velocity	[m y ⁻¹]	0.2
Flow through water-conducting features (per unit length)	[m ² y ⁻¹]	2
Hydraulic gradient	[-]	0.02
Transmissivity of water-conducting features	[m ² y ⁻¹]	100
Transmissivity of major water-conducting faults	[m ² y ⁻¹]	200
D: Additional data		
Hydraulic conductivity	[m y ⁻¹]	10
E: Input to assessment models		
Flowpath length	[m]	200
Advection velocity	[m y ⁻¹]	See Table 5.3.2

Table 3.7.6: (Continued). Reference-Case assessment model parameters related to groundwater flow. (b): data for the major water-conducting faults of the crystalline basement in Area West. Data are presented to one significant figure.

B. Geometrical data for water-conducting features

The geometrical data relevant to safety assessment calculations, the **fracture spacing and aperture** and the **channel width and spacing within a fracture** are the same as for the low-permeability domain.

C. Data from groundwater flow modelling

Density of water-conducting features γ [m^{-1}] - the density of water-conducting features (the total length of features intersecting a hypothetical plane of unit area) is taken to be 0.1 m^{-1} ; a range of "average TE length per unit cross sectional area of major water-conducting faults" of $0.08 - 0.12 \text{ m}^{-1}$ is given in Table 3.7.4.

Darcy velocity q [m y^{-1}] - the Darcy velocity is taken to be the mean of the distribution obtained from groundwater flow modelling assuming the more conservative (higher flowrate) "Sparse Model" - 0.2 m y^{-1} (a mean "Darcy flux" of $6.7 \times 10^{-9} \text{ m s}^{-1}$ is given in Table 3.7.4).

Flow through water-conducting features (per unit length) q_w [$\text{m}^2 \text{ y}^{-1}$] - as indicated in Figure 3.7.2, the flowrate through a single water-conducting feature, divided by the length of the feature normal to the flow direction, is related to q , the Darcy velocity, and γ , the density of water-conducting features, through the expression $q_w = q / \gamma$. This gives a flow per unit length of $2 \text{ m}^2 \text{ y}^{-1}$.

Hydraulic gradient i [-] - the hydraulic gradient is related to K , the hydraulic conductivity (see D, below), and q , the Darcy velocity, through the expression $i = q / K$. This gives a hydraulic gradient of 0.02, which is consistent with the arithmetic mean of absolute gradient given in Tables 3.7.4 (the hydraulic gradient is not directly used to derive input for the assessment models).

Transmissivity of water-conducting features T_w [$\text{m}^2 \text{ y}^{-1}$] - the transmissivity of the water-conducting features is related to K , the hydraulic conductivity (see D, below), and γ , the density of water-conducting features, through the expression $T_w = K / \gamma$. This gives a transmissivity of $100 \text{ m}^2 \text{ y}^{-1}$, consistent with the mean transmissivity for water-conducting features within major water-conducting faults given in Table 3.7.4 (the transmissivity of water-conducting features is not directly used to derive input for the assessment models).

Transmissivity of major water-conducting faults T_M [$\text{m}^2 \text{ y}^{-1}$] - the transmissivity of the major water-conducting faults is related to K , the hydraulic conductivity, and an assumed width for the faults of 20 m, through the expression $T_M = K \times 20 \text{ m}$. This gives a transmissivity of $200 \text{ m}^2 \text{ y}^{-1}$ (the transmissivity of major water-conducting faults is not directly used to derive input for the assessment models).

D. Additional data

Hydraulic conductivity K [m y^{-1}] - the hydraulic conductivity of major water-conducting faults is taken to be 10 m y^{-1} ($3.2 \times 10^{-7} \text{ m s}^{-1}$ in Table 3.7.4) (the hydraulic conductivity is not directly used to derive input for the assessment models).

The data given above are combined to provide input to the Kristallin-I geosphere model, as shown in Figure 3.7.2 and described below:

E. Input to assessment models

Flowpath length L [m] - for major water-conducting faults, the flowpath length is set to 200 m. This is a factor of 2 larger than that suggested by the minimum specified repository depth below the higher-permeability domain (see A, above), and is therefore a non-conservative selection. However, the geosphere calculations in which transport through major water-conducting faults is considered aim to show an upper-limit to the barrier effect which the faults might provide (see Subsection 6.2.2.2); in the Reference Model Assumptions (see Subsection 6.2.1), retardation and decay in major water-conducting faults is neglected.

Advection velocity u [m y^{-1}] - derivation of the advection velocity requires geometrical data for water-conducting features (B, above) and a value for flowrate through the features (C, above). The derivation is described in Subsection 5.3.4.1 (see, in particular, Table 5.3.2).

3.7.6 Porosities and Geometrical Data for Water-Conducting Features

The water-conducting features, that are present throughout all domains of the crystalline basement and provide preferential paths for groundwater flow, are described in Subsection 3.5.2. Water-conducting features are classified as cataclastic zones, open joints and fractured aplite/pegmatite dykes and aplitic gneisses; the internal structure of each is shown in Figure 3.5.4 (taken from THURY et al. 1994). Each type of water-conducting feature has an internal structure consisting of partially infilled fractures with channels through which water may flow and wallrock, which may be altered in a band adjacent to the fractures. The geometrical data and porosities are given in Table 3.7.7. Two crystalline rock types are distinguished - granite and gneiss - and two types of alteration - high temperature alteration and argillic alteration (THURY et al 1994).

	Cataclastic Zones				Jointed Zones				AD
Channel width, $2x_1$	1 - 10 cm				1 - 10 cm				5 - 20 cm
Width of fracture infill between channels, $2(x_2-x_1)$	10 - 500 cm				10 - 500 cm				5 - 20 cm
Fracture aperture, $2y_1$	0.1 - 0.2 cm				0.1 - 0.2 cm				0.1 - 0.2 cm
Extent of altered zone (both sides of fracture), $2y_2$	2 - 20 cm				2 - 20 cm				2 - 20 cm
Width of water-conducting feature, $2W$	50 - 100 cm				50 - 100 cm				50 - 200 cm
Fracture spacing, $2y_3$	13 - 25 cm				25 - 50 cm				30 cm
	altered / unaltered wallrock				altered / unaltered wallrock				
	granite		gneiss		granite		gneiss		
	high T.	arg.	high T.	arg.	high T.	arg.	high T.	arg.	
Porosity of altered wallrock	4%	5%	1.5%	5%	4%	5%	1.5%	5%	1%
Porosity of unaltered wallrock	0.25%	1%	1%	2%	0.25%	1%	1%	2%	0.5%
Porosity of fracture infill	3%				3%				2%

Notes: AD = fractured aplite/pegmatite dykes and aplitic gneisses, high T. = high temperature alteration, arg. = argillic alteration.

Table 3.7.7: Geometrical data and porosities for the three types of water-conducting features.

3.7.7 Element-Dependent Properties of the Geological Barriers

Element-dependent properties of the geological barriers are given in Table 3.7.8 for those elements of which the safety-relevant radionuclides are isotopes. The derivation of sorption constants (and, in the case of Cs, Freundlich isotherm parameters) is discussed in Subsection 3.5.5.

Element	"Realistic-conservative" value K_d ($m^3 kg^{-1}$)	"Conservative" value K_d ($m^3 kg^{-1}$)
Ni	0.5	0.05
Se	0.01	0.001
Zr	1	0.1
Tc [†]	0.5 (West); 0.05 (East)	0.05 (West); 0.0 (East)
Pd	0.5	0.05
Sn	0.5	0.05
Ra	0.5	0.1
Th [§]	1	0.1
Pa	1	0.1
U ^{†§}	1	0.10 (West); 0.05 (East)
Np [§]	1	0.05
Pu	5	0.5
Am	5	0.5
Cm	5	0.5

Element	"Realistic-conservative" value	"Conservative" value
Cs [‡]	$K = 2.0 mol^{0.3} kg^{-1} l^{0.7}$	$K = 0.4 mol^{0.3} kg^{-1} l^{0.7}$
Freundlich parameters	$N = 0.70$	$N = 0.70$

Notes: † For Tc and U, different K_d values are adopted, taking into account of differing redox conditions in Area West and Area East.

‡ Non-linear sorption of Cs is modelled by a Freundlich isotherm (see Subsection 5.3.3.2) with the parameters shown. The stable elemental Cs concentration assumed is $3.2 \times 10^{-7} M$ for Area West and $3.8 \times 10^{-7} M$ for Area East.

§ Sorption on a background population of groundwater colloids (0.1 ppm) is quantified by a parameter K_c , which takes a value of $10^4 m^3 kg^{-1}$ for tetravalent Np, U and Th (see Subsection 3.5.4.3).

Table 3.7.8: Sorption constants and isotherm parameter values for modelling of radionuclide transport in the geosphere. (From STENHOUSE 1994).

4. SCENARIO DEVELOPMENT AND TREATMENT

4.1 Approach and Methodology

A key element of the assessment of the post-closure safety of an underground repository is the identification of the possible future evolutions of the disposal system and selection of features, events and processes to be analysed - this process is called scenario development.

4.1.1. Uncertainty of Future Processes and Events

Over the timescales considered in radioactive waste disposal assessment (in the order of a million years or more), both the natural environment and the engineered features will change due to natural processes, human actions (unrelated to the disposal), and interactions of the repository and wastes with the natural environment. Hence, there will be large and unavoidable uncertainty about the future state or evolution of the system due to the following:

- uncertainty about the importance or rate of various processes which will act on the system, e.g. degradation processes;
- uncertainty about the timing or frequency of certain natural events and processes, e.g. climatic change and tectonic processes;
- uncertainty about human activities in the far future, e.g. groundwater and mineral resource use.

This uncertainty is handled by carrying out safety-assessment calculations for a number of simplified or stylised descriptions of future states or evolutions, termed scenarios. The SKI, HSK, SSI Working Group on regulatory guidance (SKI et al. 1990) described scenarios as:

".... future evolutions ..., each of them being a hypothetical, but physically possible, sequence of processes and events that influence the release and transport of radionuclides from the repository to the biosphere and the exposure to humans. The set of scenarios defined for a particular repository and which will be considered in the performance assessment should form an envelope within which the future evolution of the repository system is expected to lie."

For a repository in Switzerland, the appropriate regulatory agencies have advised (see HSK & KSA 1993):

" ... the applicant has to show what processes and events could affect the repository system over the course of time and then derive potential evolution scenarios from these. Processes and events with extremely low probability of occurrence or with considerably more serious non-radiological consequences, as well as intentional human intrusion into the repository system, are not required to be considered in the safety analysis."

The SKI, HSK, SSI Working Group's definition of scenarios implies a set of scenarios that are realistic or encompass the expected future evolution and performance. However, in the Kristallin-I safety assessment the focus is on evaluation of safety, not prediction of performance. In this case, scenario development is the means by which the importance of processes and events are discussed and, where necessary, scenarios are defined and calculations performed to quantify the impact of omission or inclusion of particular processes and events. This is in accord with HSK, KSA guidance, as given above.

4.1.2 The Scenario Development Procedure

The aim of scenario development, within the Nagra assessment methodology, is to identify the features, events and processes (FEPs) that will be included in assessment calculations and to define a set of scenarios that investigate the uncertainty related to the selection of FEPs (see Subsection 2.4.1).

The scenario development procedure determines the safety calculations to be made in the immediate phase of assessments. It also identifies and keeps track of

- issues which may adversely affect safety, but are not adequately dealt with at present - termed "open questions";
- phenomena that are beneficial to safety but are not taken account of in current models - termed "reserve FEPs"¹⁸.

The procedure should give guidance on how to address such open questions or mobilise reserve FEPs in the safety assessment. For example, will an open question be resolved by obtaining additional data or can the repository design or siting be constrained so that safety is insensitive to the possible effects of the insufficiently understood process or feature? The procedure must also provide a traceable record of the understanding of

¹⁸ This may be because of lack of data, or, sometimes, for reasons of mathematical or modelling convenience. Exclusion of a reserve FEP from a model will tend to make the resulting model conservative, though the degree of conservatism may be difficult to assess. Such FEPs may be the target of future research and/or model development.

relevant processes, data and key assumptions so that each assessment phase can build on the experience gained in previous phases. Hence, the scenario development procedure is seen as an active tool for managing information and specifying paths by which a demonstration of safety can be made, see Figure 4.1.1.

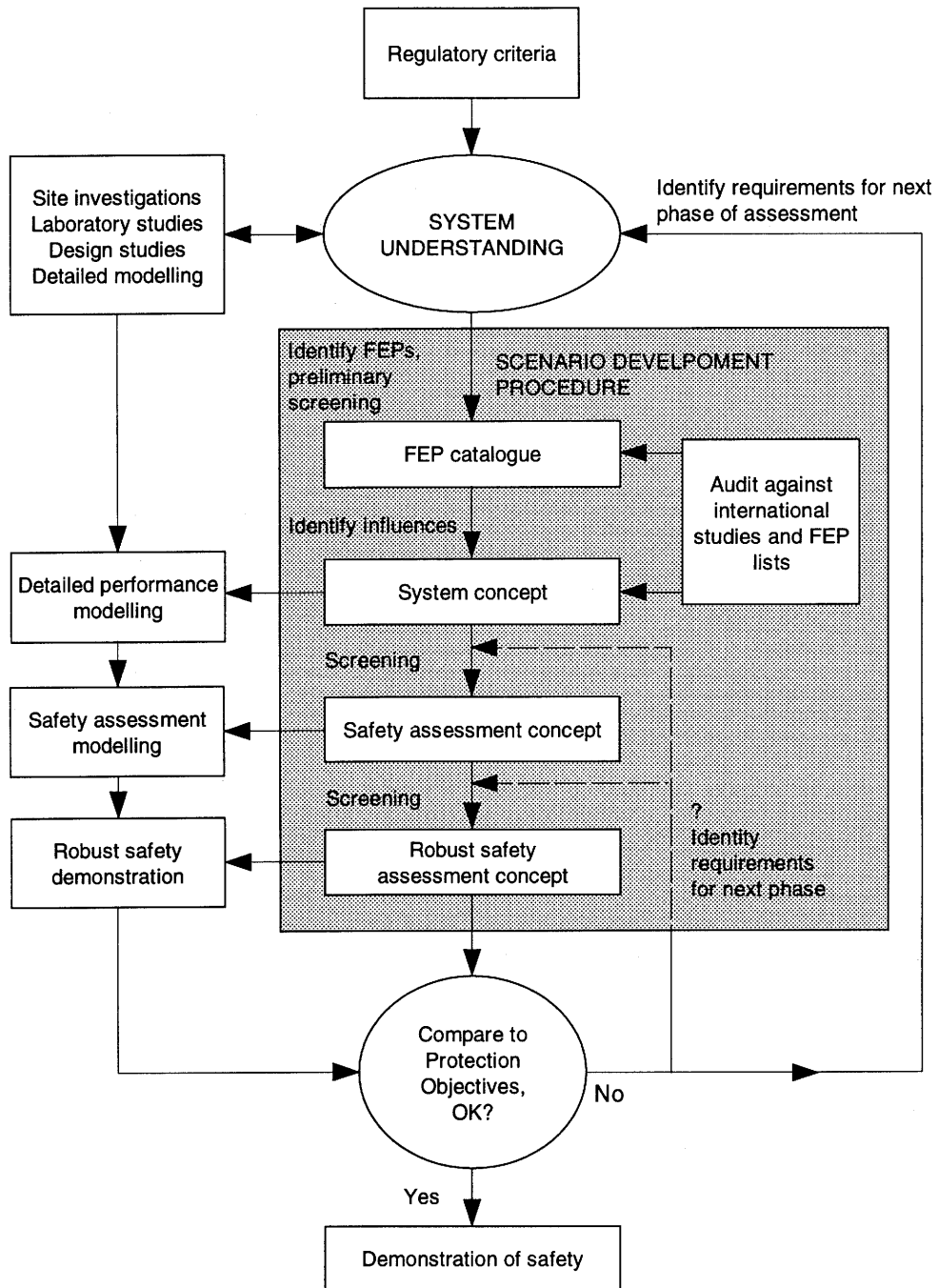


Figure 4.1.1: The central role of the scenario development procedure for a given repository design and a given database.

The procedure includes the following generic stages (SUMERLING et al. 1993) :

1. For the defined disposal system, document understanding of the system and processes relevant to its behaviour, and identify the basic characteristics that are expected to ensure long-term safety.
2. Develop a catalogue of all potentially relevant features, events and processes (FEPs) based on current understanding of the system and audit this against international experience.
3. Develop the System Concept - a description of the behaviour of the repository and its environment, incorporating scientific understanding and indicating the interactions of all relevant FEPs.
4. Develop the Safety Assessment Concept - a conceptual model of all FEPs to be taken into account in assessment calculations; compare this with the assessment models available and identify any important FEPs that cannot be analysed using existing models; define the Reference Scenario and alternative scenarios for safety assessment calculations.
5. Develop the Robust Safety Assessment Concept - including only those FEPs that can be relied upon to enhance safety, plus consideration of all detrimental FEPs; define the calculations required for a robust safety case.

As indicated in Figure 4.1.1, various stages of the scenario development will make use of results of detailed performance calculations and safety assessment calculations.

The scenario development is iterative. First, the processes believed to be most relevant to the performance of the repository according to its design function are considered. These are usually the expected processes of barrier degradation and radionuclide release, transport and exposure pathway processes. In the case of a deep repository, long-term environmental changes may be neglected at this stage as the objective of siting a repository deep underground is to minimise the impact of such changes. A Reference Scenario is developed based on this consideration.

The additional expected processes and events, and uncertainty associated with their degree or extent, are then considered. Alternative scenarios for safety assessment are defined where qualitative considerations or scoping calculations lead to the conclusion that estimates of repository performance may be markedly altered (especially made worse) by inclusion of the additional process or event. Finally, more unlikely or extreme events and processes are considered, especially those that might lead to significant detrimental changes in the disposal system or its performance.

The Reference Scenario is represented by an assessment model chain. Within this scenario, alternative conceptual models of key features or processes may be developed, and these may be treated by parameter variation or substitution of submodels within the assessment model chain. Alternative scenarios may also be represented by the same model chain by means of changes in parameter values, alternative submodels or boundary conditions, or by entirely different models. Unlikely events may be similarly treated or simply be discussed qualitatively and dismissed from further consideration.

4.1.3 Application of the Procedure in the Kristallin-I Safety Assessment

For the Kristallin-I safety assessment, a Reference Scenario is developed based on the Safety Concept for a HLW repository in the crystalline basement, as described in Section 3.2. In this scenario, the effects of long-term geological and climatic changes are neglected, even though such changes are expected. In addition, certain processes that are expected to be beneficial to safety (reserve FEPs) are neglected. Thus, the scenario is not to be considered the most likely nor even, necessarily, a realistic scenario. The Reference Scenario is developed as a group of assumptions underlying a set of calculations intended to provide a conservative estimate of repository performance. Subsequent evaluation of expected processes and events, which are neglected in the Reference Scenario, will indicate whether the results of calculations based on the Reference Scenario can be accepted as conservative estimates, or if additional processes and events must be considered quantitatively in the demonstration of safety.

Figure 4.1.2 shows how, in the Kristallin-I scenario development, all FEPs are first screened and then categorised as unimportant, reserve, open question or included in safety assessment calculations; those included are represented in the Reference Scenario (which includes alternative model assumptions and parameter variations) or in alternative scenarios covering the realistically expected future conditions and also unexpected or unlikely conditions.

The primary aim of the Kristallin-I safety assessment is to investigate the performance of a high-level waste disposal system in the crystalline basement of Northern Switzerland, with special emphasis on the role of the geosphere. This is in order to put the information gained from the regional investigations (THURY et al. 1994) in context, and to help define geological investigation requirements for future phases of site characterisation. A final demonstration of disposal system safety is not the objective of the project at this stage.

This aim has conditioned the selection of scenarios for quantitative evaluation in Kristallin-I. In particular:

- a number of detrimental FEPs, which could potentially affect the engineered barriers, are identified but not evaluated quantitatively at this stage since it is believed they can be avoided by design and attention to quality control;

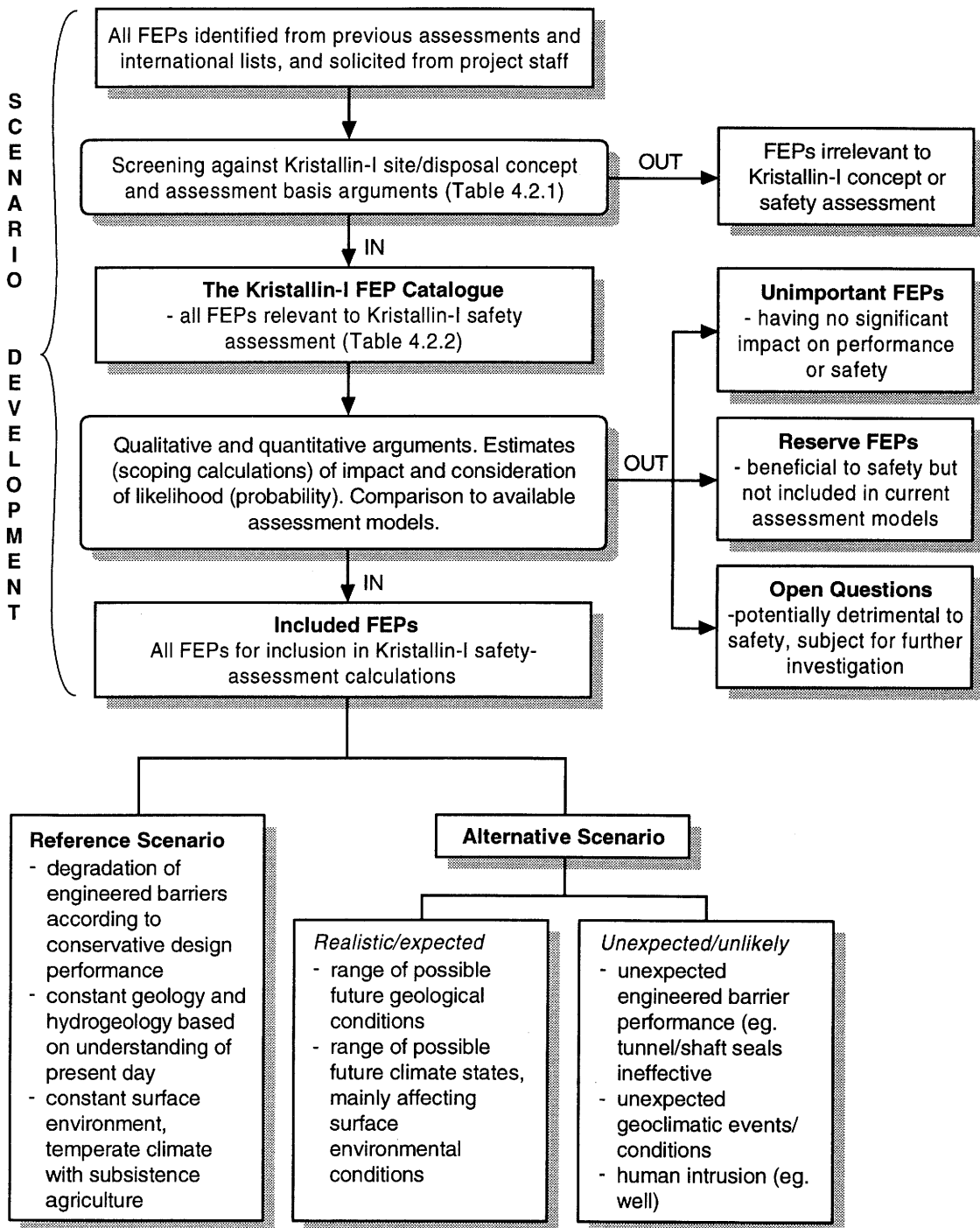


Figure 4.1.2: The handling of FEPs in the Kristallin-I scenario development. Screening arguments are used to reject FEPs that are irrelevant to the disposal concept or post-closure safety assessment. Relevant FEPs are evaluated by qualitative and quantitative arguments, with regard to model capabilities, and classified as unimportant, reserve, open question or included. The last category are represented in Kristallin-I safety-assessment calculations within a Reference Scenario and/or alternative scenarios.

- future human actions that could potentially by-pass or be detrimental to the engineered and geological barriers are identified and discussed qualitatively, but no quantitative analysis is undertaken at this stage (see discussion in Subsection 2.4.3);
- for the stage of robust safety assessment, a scenario is devised that is robust with regard to the transport properties of the geological barrier; it is accepted that the scenario does not include all detrimental processes as discussed in Subsection 2.6.2.

The application of the scenario development procedure in Kristallin-I is fully documented in SUMERLING & GROGAN (1994). The following sections summarise the main points and results of the application.

4.2 The FEP Catalogue for Kristallin-I

4.2.1 Eliciting the System Understanding

The scenario development acts as a focus for the available knowledge about the site, engineered barriers and relevant processes. The most detailed and accurate knowledge of the relevant processes will be that held by the various staff and contractors involved in the project. It is important that this knowledge resource is fully exploited. In the scenario development for Kristallin-I, structured tables were used to elicit a comprehensive list of relevant FEPs from the project staff.

Initially, the elicitation was focused on the basic characteristics of the disposal system that are expected to ensure long-term safety. It is important first to understand the features and processes that are expected to provide the necessary safety so that processes and events that may compromise safety, i.e. that damage or affect those safety features and processes, can be considered against this background.

4.2.2 Initiating the FEP Catalogue

A preliminary FEP catalogue was established, based on experience established during Project Gewähr 1985 (NAGRA 1985) and associated work. This was developed iteratively. Additions and modifications to the catalogue were discussed with and reviewed by the Kristallin-I project staff. For convenience, the FEPs were classified under headings of the main safety-relevant features of the Kristallin-I disposal concept plus the main external influences, i.e.:

Main safety-relevant features:

1. Vitrified waste form
2. Canister
3. Bentonite

4. Bentonite-host rock interface
5. Low-permeability domain of the crystalline basement rock
6. Major water-conducting faults
7. Higher-permeability domain of the crystalline basement
8. Biosphere

Main external influences:

9. Geological processes and events
10. Climatic processes and events
11. Human activities

For each FEP, a name or abbreviated title, a short description of the FEP, references and/or the source of the description of the FEP and any additional comments, e.g. the need for an improved description or an additional reference, was recorded. As the scenario development progressed, further information was added, such as how the FEP is classified or treated in the assessment.

4.2.3 Screening Arguments

Screening arguments were used to define the limits of the assessment in broad terms. Two groups of screening arguments were applied:

- Site and Disposal Concept - these allow phenomena that are physically impossible or irrelevant for the specific disposal concept to be screened out.
- Assessment Basis or "Ground Rules" - these define the scope of the safety assessment and allow phenomena outside that scope to be screened out.

Table 4.2.1 summarises the screening arguments applied in the Kristallin-I scenario development and indicates examples of FEPs that were screened out, so excluding them from consideration. If FEPs were rejected in this way, then the text of the screening argument was checked, and in some cases amended, to ensure its consistency with the required scope of the assessment.

4.2.4 Developing the System Concept

Besides recording individual FEPs, it is important to understand the possible relations between them. The System Concept is the overall conceptual model of the repository and its environmental setting, specifying all possibly relevant FEPs and their interactions.

Taking one main safety-relevant feature at a time, all the FEPs pertaining to the feature were examined. Links between the FEPs were noted and a set of influence diagrams was developed to record the links. Figure 4.2.1 shows an example of one such influence diagram. These served as a focus for discussion with project staff with the best understanding of the individual processes and subsystems. The development of the System Concept and influence diagrams led to the discovery of several inconsistencies in the FEP descriptions, and to the identification of additional FEPs. The FEP catalogue was updated accordingly.

Screening arguments		Examples of FEPs screened out
1.	Site and Disposal Concept:	
1.1	Waste form and packaging	FEPs relating to other waste forms etc.
1.2	Waste emplacement and repository	cementitious backfill FEPs
1.3	Host rock (crystalline basement)	salt diapirism
1.4	Local and regional surface environment	estuarine and marine FEPs
1.5	Geographical location	sea level rise/fall etc.
2.	Assessment Basis:	
2.1	Appropriate repository design & closure	repository left unsealed
2.2	No consideration of global and regional disasters	nuclear war, meteorite impact
2.3	No consideration of malicious acts	terrorism
2.4	No consideration of deliberate intrusion	recovery of wastes
2.5	No consideration of future human society and technology	futuristic technologies, cure for cancer
2.6	Limitation to post-closure radiological assessment	non-radiological impacts
2.7	No consideration of future evolution of man and other species	changed radio-sensitivity of man; new crop/animal species

Note: The full texts of the screening arguments are given in SUMERLING & GROGAN (1994).

Table 4.2.1: Screening arguments for the Kristallin-I scenario development and examples of FEPs that were screened out by them.

4.2.5 Audit Against International Experience

Whereas the understanding and knowledge of project staff and contractors is the primary basis for the scenario development, it is also important to draw in wider expertise and experience, for example, through participation in the AECL/PNC/Nagra/TVO/SKB crystalline assessment group and NEA-PAAG working groups.

In addition, a formal audit process can give confidence in the comprehensiveness of considerations. The Kristallin-I FEP catalogue was audited against a combined list of

over 1000 FEPs identified in other assessment and scenario development studies (e.g. CRANWELL et al. 1982; ANDERSSON (ed.) 1989; GOODWIN et al., in press; NEA 1992; THORNE 1992).

The process of audit consisted of:

- screening out of FEPs irrelevant to the Kristallin-I disposal concept, site or assessment scope from the international FEP lists according to the arguments listed in Table 4.2.1;
- mapping of remaining FEPs to the Kristallin-I FEP catalogue and identification of any relevant FEP not included.

Only a few relevant processes were identified that were not already included in some form in the Kristallin-I catalogue. Some additions were made to the catalogue and the text descriptions as a result. No critical omissions were identified.

4.2.6 The Final FEP Catalogue for the Kristallin-I Assessment

Table 4.2.2 shows the final list of features, events and processes which were considered in the Kristallin-I scenario development. The catalogue of descriptions of the FEPs, references and specifications of treatment are documented in SUMERLING & GROGAN (1994). It is important to note that the list and catalogue are not regarded as complete or closed; rather, it is expected that they will be developed and augmented in future assessment phases. However, it is not expected that additional FEPs that might significantly compromise the overall safety of the disposal system will be identified. This is because, as demonstrated by the results of the consequence analysis in Chapter 6, the safety of the system is primarily provided by a few reliable processes, e.g. solubility limits and diffusion, operating within the engineered barriers, the properties of which can be well controlled with current technology.

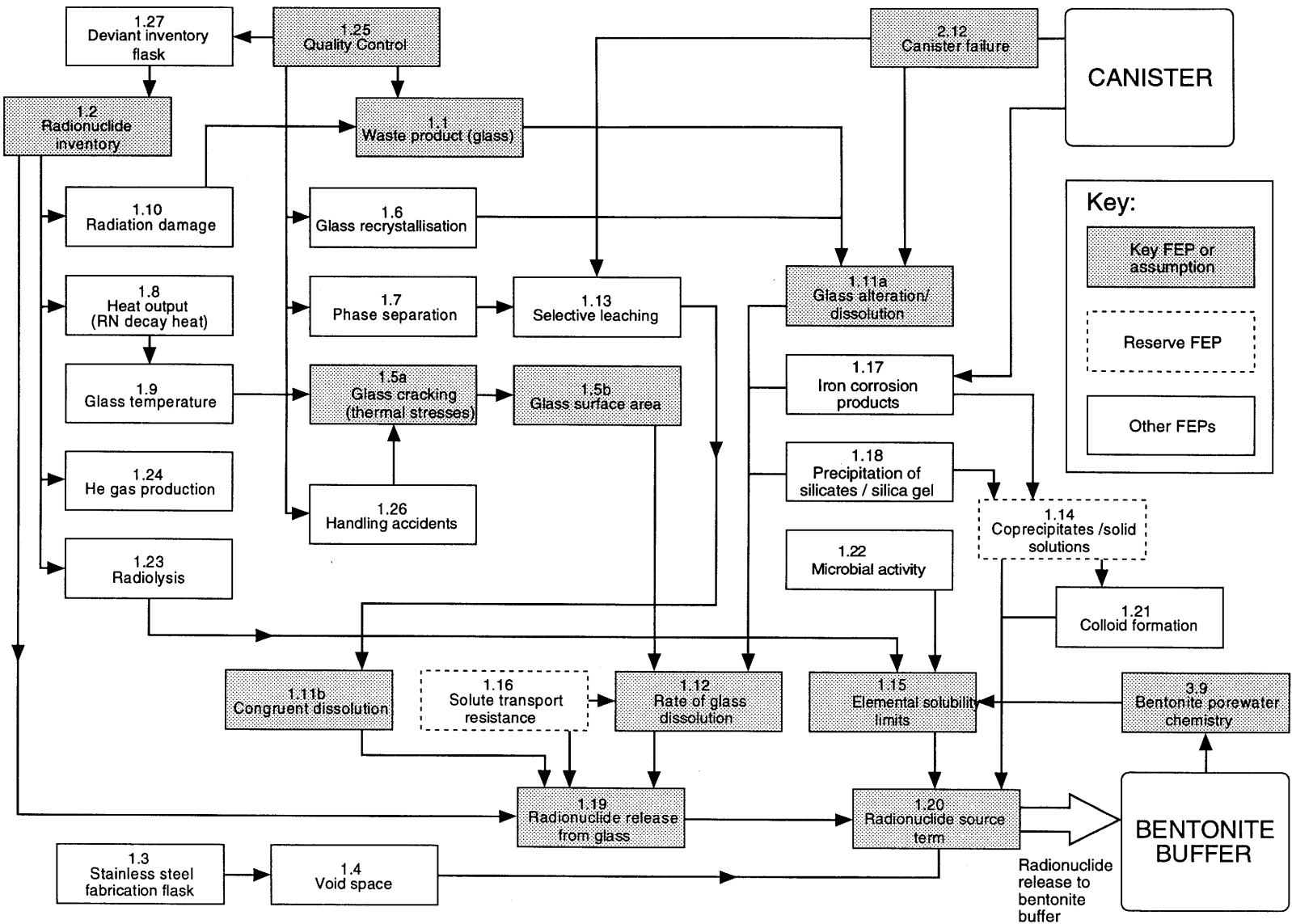


Figure 4.2.1: Example of an influence diagram for one safety-relevant feature of the Kristallin-I disposal system - the vitrified waste form.

0.	RADIONUCLIDES (RN)		
0.1	Radioactive decay	0.2	Speciation (inc. gases/volatiles)
1.	GLASS		
1.1	Waste product (glass)	1.14	Coprecipitates/solid solutions
1.2	Radionuclide inventory	1.15	Elemental solubility limits
1.3	Stainless steel fabrication flask	1.16	Solute transport resistance
1.4	Void space	1.17	Iron corrosion products
1.5a	Glass cracking	1.18	Precipitation of silicates/silica gel
1.5b	Glass surface area	1.19	Radionuclide release from glass
1.6	Glass recrystallisation	1.20	Radionuclide source term
1.7	Phase separation	1.21	Colloid formation
1.8	Heat output (RN decay heat)	1.22	Microbial activity
1.9	Glass temperature	1.23	Radiolysis
1.10	Radiation damage	1.24	He gas production
1.11a	Glass alteration/dissolution	1.25	Quality control
1.11b	Congruent dissolution	1.26	Handling accidents
1.12	Rate of glass dissolution	1.27	Deviant inventory flask
1.13	Selective leaching		
2.	CANISTER		
2.1	Cast steel canister	2.13	Residual canister (crack/hole effects)
2.2	Canister thickness	2.14	Chemical buffering (canister corrosion products)
2.3	Corrosion on wetting	2.15	Radionuclide sorption and co-precipitation
2.4	Oxic corrosion	2.16	Hydrogen production
2.5	Microbially mediated corrosion	2.17	Effect of hydrogen on corrosion
2.6	Anoxic corrosion	2.18	Corrosion products (physical effects, including volume increase)
2.7	Localised corrosion	2.19	Canister temperature
2.8	Total corrosion rate	2.20	Radionuclide transport
2.9	Stress corrosion cracking	2.21	Quality control
2.10	Canister integrity (other effects)	2.22	Mis-sealed canister
2.11	Radiation shielding		
2.12a	Canister failure (alternative modes)		
2.12b	Canister failure (reference)		
3.	BENTONITE		
3.1	Bentonite emplacement and composition	3.14	Canister/bentonite interaction
3.2	Thermal evolution	3.15	Gas permeability
3.3	Bentonite saturation	3.16	Radionuclide transport through buffer
3.4	Bentonite swelling pressure	3.17	Microbial activity
3.5	Bentonite plasticity	3.18	Elemental solubility/precipitation
3.6	Bentonite erosion/colloid formation	3.19	Radiolysis
3.7	Canister sinking	3.20	Interaction between canisters
3.8	Buffer impermeability	3.21	Inhomogeneities (properties and
3.9	Bentonite porewater chemistry	3.22	Quality Control
3.10	Radionuclide retardation	3.23	Poor emplacement of buffer
3.11	Colloid filtration	3.24	Organics/contamination of bentonite
3.12	Mineralogical alteration	3.25	Interaction with cement components
3.13	Bentonite cementation		

Table 4.2.2: Features, events and processes (FEPs) considered in the Kristallin-I scenario development. FEPs related to radionuclides, glass, canister and bentonite.

4.	BENTONITE-HOST ROCK INTERFACE AND REPOSITORY	
4.1	Excavation-disturbed zone (EDZ)	4.10 Elemental solubility
4.2	Natural radionuclides/elements	4.11 Gas transport/dissolution
4.3	Desaturation/resaturation of EDZ	4.12 Colloids
4.4	Effect of bentonite swelling on EDZ	4.13 Radionuclide release from EDZ
4.5	Geochemical alteration	4.14 HLW panels (siting)
4.6	Groundwater chemistry	4.15 TRU silos (siting)
4.7	Water flow at the bentonite/host rock interface	4.16 Access tunnels and shafts
		4.17 Shaft and tunnel seals
4.8	Radionuclide migration	4.18 Oil or organic fluid spill
4.9	Radionuclide retardation	4.19 TRU silos high pH plume
5.	LOW-PERMEABILITY DOMAIN OF THE CRYSTALLINE BASEMENT (LPD)	
5.1	LPD effective hydraulic properties	5.14 Regional stress regime
5.2	Water-conducting features (types)	5.15 Natural colloids
5.3	Groundwater flow in LPD	5.16 Solubility limits/colloid formation
5.4	Groundwater flowpath	5.17 Gas pressure effects
5.5	Radionuclide transport through LPD	5.18 Hydraulic gradient changes (magnitude, direction)
5.6	Matrix diffusion	
5.7	Mineralogy	5.19 Influx of oxidising water
5.8	Groundwater chemistry	5.20 TRU alkaline or organic plume
5.9	Sorption	5.21 Organics
5.10	Non-linear sorption	5.22 Microbial activity
5.11	Intrusion of saline groundwater	5.23 Dilution of radionuclides in ground- water (LPD to HPD or MWCF)
5.12	Density-driven groundwater flow (thermal)	5.24 Geogas
5.13	Geothermal regime	5.25 Exploratory boreholes (sealing)
6.	MAJOR WATER-CONDUCTING FAULTS (MWCF)	
6.1	MWCF effective hydraulic properties	6.14 Regional stress regime
6.2	Water-conducting features (types)	6.15 Natural colloids
6.3	Groundwater flow in MWCF	6.16 Solubility limits/colloid formation
6.4	Groundwater flowpath	6.17 Gas pressure effects
6.5	Radionuclide transport through MWCF	6.18 Hydraulic gradient changes (magnitude, direction)
6.6	Matrix diffusion	6.19 Influx of oxidising water
6.7	Mineralogy	6.20 TRU alkaline or organics plume
6.8	Groundwater chemistry	6.21 Organics
6.9	Sorption	6.22 Microbial activity
6.10	Non-linear sorption	6.23 Dilution of radionuclides in groundwater (MWCF to HPD and Biosphere)
6.11	Intrusion of saline groundwater	
6.12	Density-driven groundwater flows (thermal)	6.24 Geogas
6.13	Geothermal regime	

Table 4.2.2: (Continued). Features, events and processes (FEPs) considered in the Kristallin-I scenario development. FEPs related to the bentonite-host rock interface, low-permeability domain and major water-conducting faults.

7	HIGHER-PERMEABILITY DOMAIN OF CRYSTALLINE BASEMENT (HPD)	
7.1	HPD effective hydraulic properties	7.8 Groundwater chemistry
7.2	Mesozoic sedimentary cover	7.9 Radionuclide sorption
7.3	Permo-Carboniferous Trough	7.10 Stress regime
7.4	Groundwater flow	7.11 Erosion
7.5	Boundary conditions for flow	7.12 Hydraulic gradient (magnitude, regional direction)
7.6	Groundwater flow path	
7.7	Dilution of radionuclides in HPD	7.13 Density-driven groundwater flows (temperature/salinity differences)
8.	BIOSPHERE	
8.1	Present-day biosphere	8.23 Sedimentation
8.2	Future biosphere conditions	8.24 Soil formation
8.3	Exfiltration to local aquifer	8.25 Soil
8.4	Exfiltration to surface waters	8.26 Surface water bodies
8.5	RN accumulation in sediments	8.27 Atmosphere
8.6	Radionuclide accumulation in soils	8.28 Interface effects
8.7	Water resource exploitation	8.29 Precipitation
8.8	Filtration	8.30 Evapotranspiration
8.9	Uptake by crops	8.31 Capillary rise
8.10	Uptake by livestock	8.32 Percolation
8.11	Uptake in fish	8.33 Irrigation
8.12	Radionuclide volatilisation/aerosol/dust production	8.34 Surface run-off
8.13	Exposure pathways	8.35 Bioturbation
8.14	Human lifestyle	8.36 Suspended sediment transport
8.15	Radiation doses	8.37 Earthworks (human actions, dredging, etc.)
8.16	Food chain equilibrium	8.38 Ploughing
8.17	Radionuclide sorption	8.39 Agricultural processes
8.18	Secular equilibrium of RN chains	8.40 Natural and semi-natural environments
8.19	Surface water flow (river Rhine)	
8.20	Groundwater flow (alluvium of Rhine valley)	8.41 Hunter/gathering lifestyle
8.21	Dilution of radionuclides (alluvium to river)	8.42 Contaminated products (non-food)
8.22	Erosion/deposition (changes)	8.43 Removal mechanisms
		8.44 Consumption of uncontaminated products
		8.45 Radon pathways and doses
9	GEOLOGICAL PROCESSES AND EVENTS	
9.1	Regional horizontal movements	9.7 Erosion/denudation
9.2	Regional vertical movements	9.8 Basement alteration
9.3	Movements along major faults	9.9 Magmatic activity (volcanism and plutonism)
9.4	Movements along small-scale faults	
9.5	Seismic activity	9.10 Hydrothermal activity
9.6	Stress changes - hydrogeological effects	9.11 Extraterrestrial events

Table 4.2.2: (Continued). Features, events and processes (FEPs) considered in the Kristallin-I scenario development. FEPs related to the higher-permeability domain, biosphere and geological processes and events.

10	CLIMATIC PROCESSES AND EVENTS	
10.1	Present-day climatic conditions	10.10 Greenhouse effect
10.2	Effective moisture (amount)	10.11 Fluvial erosion/sedimentation
10.3	Seasonality of climate	10.12 Surface denudation
10.4	Future climatic conditions	10.13 Permafrost
10.5	Tundra climate	10.14 Glacial erosion/sedimentation
10.6	Glacial climate	10.15 Glacial-fluvial erosion/sedimentation
10.7	Warmer climate - arid	10.16 Ice sheet effects (loading, melt water recharge)
10.8	Warmer climate - seasonal humid	
10.9	Warmer climate - equable humid	
11	HUMAN ACTIVITIES	
11.1	Exploratory drilling	11.7 Groundwater pollution
11.2	Mining activities	11.8 Surface pollution (soils, rivers)
11.3	Geothermal exploitation	11.9 Human-induced climate change
11.4	Liquid waste injection	11.10 Repository records, markers
11.5	Deep groundwater abstraction	11.11 Planning restrictions
11.6	Water management schemes	

Table 4.2.2: (Continued). Features, events and processes (FEPs) considered in the Kristallin-I scenario development. FEPs related to climatic processes and events and human activities.

4.3 Identification of Scenarios for Kristallin-I

4.3.1 The Reference Scenario

The primary assumptions adopted for the Kristallin-I Reference Scenario are as follows:

- the siting of the repository in low-permeability crystalline basement with overlying higher-permeability basement and sedimentary layers effectively isolates the engineered barriers and their immediate geological surroundings from significant variations due to natural surface-environmental processes, human activities and geological events and processes;
- the engineered barriers behave essentially as they have been designed to behave; and
- humans will be present in the region of eventual releases of radionuclides to the surface environment at the time that any such release occurs.

The main characteristics of the Reference Scenario in terms of the three "fields" or regions of the disposal system (see Chapter 5) are:

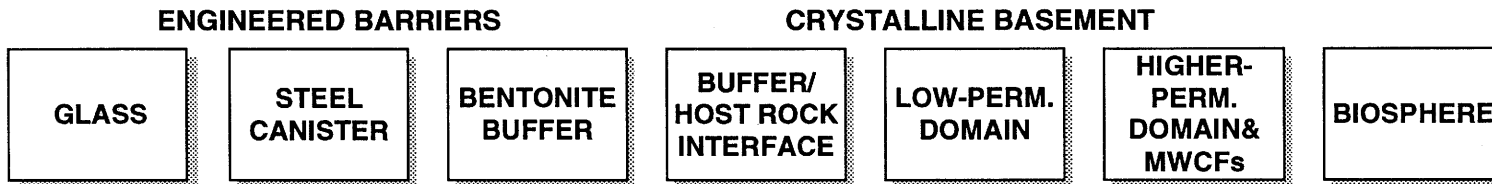
- for the near field - a conservative (pessimistic) degradation and performance of engineered barriers, but respecting the design function of the barriers;
- for the geosphere - constant geological and hydrogeological regime, based on understanding of present-day conditions;
- for the biosphere - present-day topography, hydrology and climate, with a subsistence community (conservative behaviour) located at the region of geosphere discharge.

Figure 4.3.1 illustrates the main safety-relevant features, key environmental processes and radionuclide release and transport processes considered within the Reference Scenario. In addition, some of the Reference Model Assumptions are noted in the figure. The processes considered, and the evolution of the system, are those identified and discussed in the description of the Safety Concept in Section 3.2.

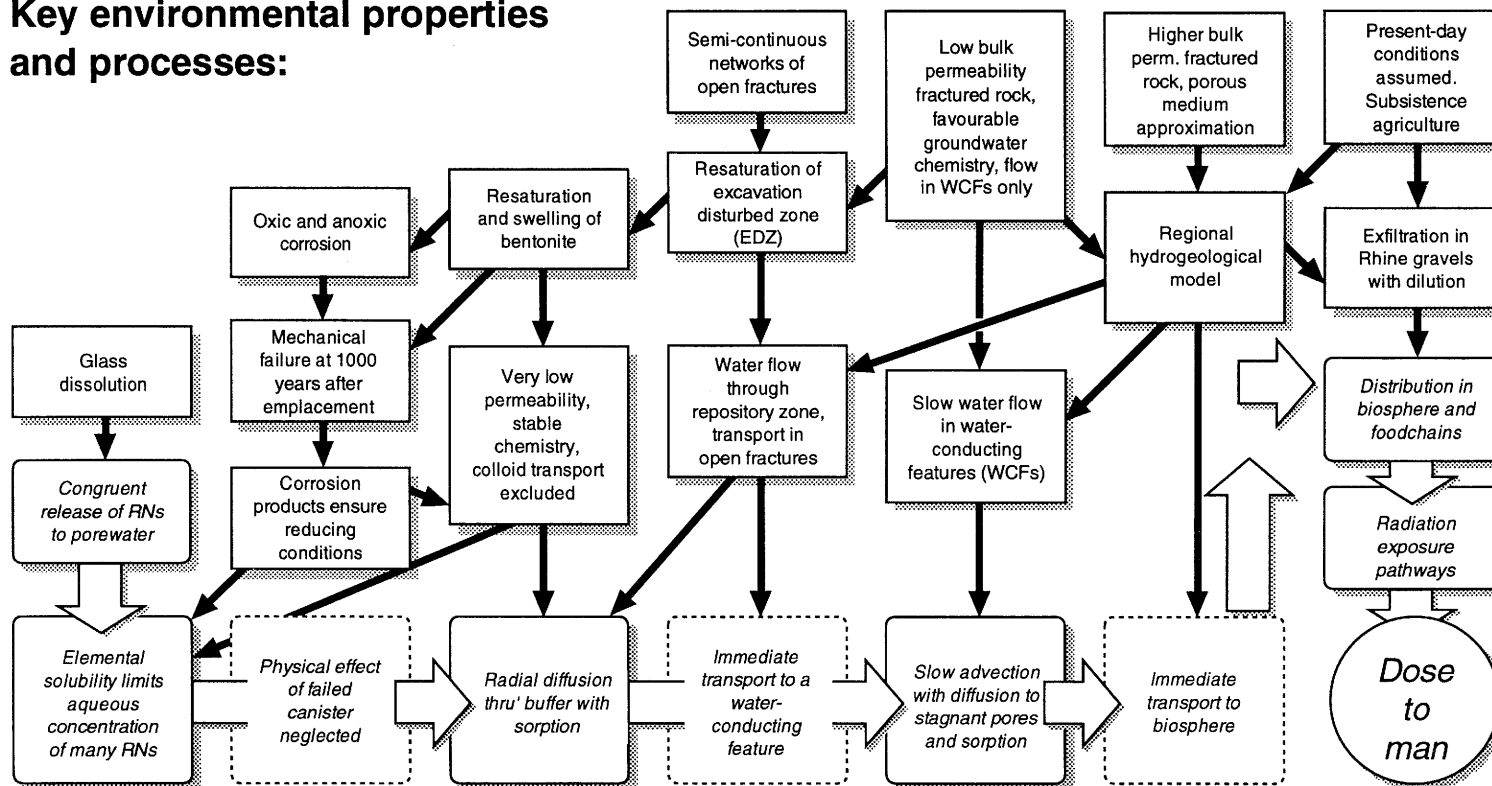
In summary, the Reference Scenario assumes:

- resaturation of the bentonite following repository closure;
- canister corrosion and failure not earlier than 1000 years after closure, at which time stable chemical and thermal conditions will have been established in the bentonite;
- corrosion of the glass matrix with congruent release of radionuclides, for which the concentrations in aqueous solution are limited by elemental solubility limits, determined for reducing conditions;
- diffusion of radionuclides through the bentonite, with sorption on bentonite pore surfaces;
- advection of radionuclides away from the bentonite-host rock interface and through the water-conducting features of the low-permeability domain, with matrix diffusion and sorption on matrix pore surfaces;
- relatively rapid transport of radionuclides to the surface, emerging in the gravel aquifers of the Rhine valley;
- distribution in the biosphere and exposure to man by various dose pathways.

Main safety relevant features:



Key environmental properties and processes:



Key radionuclide release and transport processes and assumptions

Note: Certain Reference Model Assumptions are also included in the figure (canister failure at 1000 years and neglect of radionuclide transport in major water-conducting faults).

Figure 4.3.1: Main features and processes considered in the Reference Scenario for Kristallin-I. See also Section 3.2.

4.3.2 Developing Alternative Scenarios

The engineered barriers are massive and relatively simple and this gives confidence that the evolution of the repository system and the associated radionuclide release/transport processes will take place in the manner described by the Reference Scenario. In this case, alternative scenarios arising out of uncertainty in near-field processes can be identified by examining, in turn, the various assumptions made in constructing the Reference Scenario and checking for credible alternative assumptions.

The geosphere and biosphere are affected by external geological and climatic processes and events which do not occur as independent processes, but as linked sequences with interactions. In this case, it is necessary to define realistic geological and climatic evolutions, and then to determine the impact that these possible futures will have on the characteristics of the disposal system and assumptions governing radionuclide release/transport/exposure. However, for radiological assessment, it is only necessary to make calculations for scenarios in as much as they affect the radionuclide release/transport/exposure pathways. In some cases, widely different geo-climatic evolutions may have rather similar, or little, effect on these pathways as represented by the assessment models, or can be represented by parameter value changes.

Human activities in the far future will be linked to other factors such as climatic change and will depend on social and technological development. However, given the very limited knowledge about future human actions, it is appropriate to treat such actions as independent processes and events. Scenarios due to possible future human actions that directly compromise the engineered and geological barriers are identified and discussed but are not assessed quantitatively in Kristallin-I (see Subsection 2.4.3).

The following procedure was applied to record, and promote the comprehensiveness of, considerations leading to the identification of alternative scenarios.

1. All the assumptions made (explicitly or implicitly) in constructing the Reference Scenario were recorded. This included the assumptions that are made in the assessment codes and in arriving at key data for the models represented by these codes (the Reference Model Assumptions, which are recorded in Subsections 5.2.1, 5.3.1 and 5.4.1).
2. For each assumption, the relevant FEPs were noted and their status within the Reference Scenario assigned, i.e. whether the FEP was important/included, reserve or judged unimportant/unlikely in the assessment model of the scenario.
3. Each of the assumptions was then considered in turn and a judgement made of confidence in the validity of the assumption.
4. Where possible, alternative assumptions were postulated for each of the assumptions of the Reference Scenario (and Reference Model Assumptions). In the case of

geological and climatic scenarios, the alternative assumptions were supplied by consideration of the possible realistic evolutions of the geo-climatic system.

5. As a result, cases were identified where there was a credible alternative assumption that might lead to significantly different radiological performance of the disposal system.

Table 4.3.1 shows a small section of the resulting table which provides a map between the assumptions of the assessment model chain, FEPs identified in Table 4.2.2 and cases where alternative assumptions might be made. The potential alternative models and scenarios which are thus derived may arise from uncertainty in a FEP already included in the Reference Scenario (or Reference Model Assumptions) or the inclusion of a FEP excluded from the Reference Scenario (or Reference Model Assumptions). Often, an alternative model or scenario will involve a combination of both factors or consideration of several FEPs together.

The following subsections discuss the possible alternative assumptions and FEPs with the capacity to give rise to alternative models and scenarios, and identify those that require quantitative treatment in Kristallin-I. They are discussed in three groups:

- FEPs related to the engineered barriers and radionuclide transport therein (Subsection 4.3.3);

FEPs related to the geology and hydrogeology, as they are understood to exist at present, and radionuclide transport therein (Subsection 4.3.4);

- FEPs related to long-term geological changes and their effects (Subsection 4.3.5)
- FEPs related to long-term climatic changes and their effects (Subsection 4.3.6)
- FEPs related to future human actions and their effects (Subsection 4.3.7);

The process of identifying potential scenarios also leads to the identification of reserve FEPs and open questions. These are discussed in Subsections 4.4.3 and 4.4.4, respectively.

4.3.3 FEPs Related to the Engineered Barriers

The following FEPs or alternative assumptions have been identified by the method described in Subsection 4.3.2 and illustrated in Table 4.3.1.

ASSUMPTIONS OF THE REFERENCE SCENARIO	FEATURES, EVENTS AND PROCESSES CONSIDERED AND STATUS WITHIN THE REFERENCE SCENARIO			ASSESSMENT OF REFERENCE ASSUMPTION, POSSIBLE ALTERNATIVE ASSUMPTIONS AND POTENTIAL FOR ALTERNATIVE SCENARIOS (AS) OR NEED FOR DISCUSSION (D)		
	Important/ included	Reserve	Unimportant or unlikely	Confidence (bias, if any)	Comment or alternative assumption	AS or D
The waste radionuclides are mixed uniformly in a homogeneous borosilicate glass matrix.	1.1 Waste product (glass) 1.25 Quality control		1.7 Phase separation	High	None	No
The glass is solidified in thin steel fabrication flasks each containing 150 litres of glass	1.3 Stainless steel fabrication flask		1.4 Void space	High	None	No
The glass is amorphous but cracked so that the surface area is 12.5 times greater than that of 150 l block.	1.5a Glass cracking (thermal stresses) 1.5b Glass surface area		1.6 Glass recrystallization 1.26 Handling accidents	Acceptable (conservative)	A value of 12.5 is conservative for long-term safety assessment. Some glass blocks may be less cracked. Handling accidents which might cause greater cracking are not expected.	No
The radionuclide inventory of each flask is determined according to the COGEMA specification and assuming 40y cooling post reactor discharge.	0.1 Radioactive decay 1.1 Waste product (glass) 1.2 Radionuclide inventory 1.25 Quality control		0.2 Gaseous/volatile RNs 1.27 Deviant inventory flask	Acceptable	Actual inventories may differ slightly but the HLW waste specification guarantees a maximum value.	No
There are a total of 2693 flasks for disposal in the repository.	1.2 Radionuclide inventory			Acceptable (Assessment basis)	The actual number will depend on the Swiss power programme. This number based on 120GW(e) years is adopted as basis for Kristallin-I.	No
The heat output of the glass at disposal is about 590W per canister.	1.8 Heat output 1.9 Glass temperature 1.24 Quality control		1.26 Deviant flask inventory	Acceptable	Depends on waste specification and time of disposal relative to time of unloading of fuel. A maximum value can thus be guaranteed.	No
The glass and fabrication flask are contained in a massive cast steel canister with 250mm thick walls.	2.1 Cast steel canister 2.21 Quality control		2.22 Mis-sealed canister	High	The case of an individual poorly sealed container should be discussed.	Yes Dis- cuss
The canisters are emplaced co-axially in 3.7m diameter disposal tunnels surrounded by precompressed bentonite blocks.	3.1 Buffer emplacement and composition 3.20 Quality control			High (Assessment basis)	3.7m is the reference diameter for Kristallin-I defined from thermal considerations. Smaller diameter tunnels could be assessed.	No
There will be an excavation disturbed zone of the host rock about the tunnels which may have higher hydraulic conductivity and become desaturated and oxidised to some degree during construction/operation.	4.1 Excavation disturbed zone 4.3 Desaturation/resaturation of EDZ		4.5 Geochemical alteration	Acceptable (conservative)	If the disturbed zone is not significant then resaturation may be more uneven (and possibly reduced). Eventual diffusive release of radionuclides through the bentonite may also be reduced.	Yes Dis- cuss

Table 4.3.1: Example section of a table which provides a map between relevant FEPs and the assumptions of the assessment model for the Reference Scenario, and identifies cases where alternative assumptions might be made.

4.3.3.1 Mis-sealed or Unsealed Canister

It is possible that a canister is not properly sealed or the welding or closing of the lid is sufficiently faulty to lead to failure immediately after emplacement. The probability of occurrence is very low since the waste flask will be loaded into the canister at the surface where the sealing could be checked and remedied if faulty. If the event does occur, water may penetrate to the waste earlier than would otherwise be the case, and dissolution of the glass may be initially slightly more rapid than in the Reference Case, due to the higher temperature. However, the earliest time at which the waste can be contacted by significant quantities of water will be limited by the time taken for resaturation of the bentonite, which is estimated to be of the order of 100 to 1000 years (see Subsection 3.4.4.2). During this time, the steel canister will have been in a damp, warm atmosphere, so that significant corrosion will have taken place and anoxic conditions already established in the bentonite buffer.

Although the event is very unlikely and should be detected by quality control procedures, it is relatively straight forward to assess the importance of this event by parameter variation within the Reference Scenario (see Subsection 5.2.3.1).

4.3.3.2 Poor or Incomplete Emplacement of Buffer

The precompacted bentonite blocks will be emplaced around canisters remotely and there may be some chance of mis-emplacements, e.g. gaps between vertical walls of blocks or inability to fit a last block in place. Serious deviations are likely to be recognised by the operators, but remedial action may not be taken. If the gaps were too large to be closed successfully by swelling of the bentonite; this could leave higher permeability pathways for radionuclide transport through the bentonite.

For Kristallin-I, it is assumed that the buffer is emplaced as intended. Alternative methods of buffer and canister emplacement could be considered if the current emplacement technique was found to be problematic. The FEP is identified as an open question for design and operation studies.

4.3.3.3 Uncertainty in the Time of Canister Failure

One of the Reference Model Assumptions made in modelling the Reference Scenario is that all the massive steel canisters fail at 1000 years. That all canisters fail at the same time is not at all likely, but is mathematically convenient and will tend to be conservative, since peak releases from all canisters occur simultaneously and are summed. The assumption that the canisters fail at 1000 years is also conservative, since this implies very high corrosion rates (see Subsection 3.4.3). More realistically, canisters may fail over a range of times and most canisters are expected to remain intact for much longer than 1000 years.

The importance in canister lifetime can be explored by parameter variation within the Reference Scenario (see Subsection 5.2.3.1). The processes following canister failure are the same and therefore no new scenario is created. The investigation of the importance of canister lifetime also provides guidance on whether alternative canister designs or materials, which could provide longer lifetimes, deserve consideration.

4.3.3.4 Cracked Canister

If the canister fails locally, e.g. by a crack or due to mis-sealing (see Subsection 4.3.3.1), then the access of bentonite porewater to the waste and subsequent transport of released radionuclides may be restricted. The Reference Scenario conservatively assumes that, after failure, the canister offers no transport resistance. The effect that more realistic assumptions can have on calculated releases from the bentonite has been investigated by scoping calculations (McKINLEY et al. 1992b). If the crack is assumed to be water filled, the release is rather insensitive to crack width and releases are little changed with respect to the Reference Scenario. However, if the crack is assumed to be filled with bentonite (or canister corrosion products), then the resistance to transport imposed by the crack can dominate the total near-field transport resistance and releases may be reduced by several orders of magnitude, depending on the crack width.

The physical resistance that a failed, e.g. cracked, canister may offer to radionuclide releases is identified as a reserve FEP and is not included in Kristallin-I safety analyses.

4.3.3.5 Radiolytic Oxidation Front

A potentially detrimental aspect of localised failure of a canister (e.g. by cracking), with only limited corrosion having taken place, is that oxidants produced by radiolytic action may diffuse out through the cracked canister and into the bentonite. This is important because the solubility limits that are used in the safety-assessment calculations are based on solubility limits in reducing bentonite porewaters (see Subsection 3.4.6.2).

The progress of an oxidising front into the bentonite has been calculated for a pessimistic case in which the following assumptions are made: a high value for the rate of production of radiolytic oxidant, which does not decrease with time, is assumed; the products of alpha radiolysis are H_2 , which is chemically inert and lost from the near field, and O_2 , which is reactive; the inner surfaces of the canister and the hypothetical crack are coated with a non-reactive layer, e.g. Fe_2O_3 ; the oxidant is consumed only by reaction with aqueous $Fe(II)$ in bentonite porewater, originating from groundwater. For the expected concentrations of $Fe(II)$, 10^{-6} to 10^{-7} M, only very limited penetration of the oxidation front into the bentonite is predicted, and, even for very low $Fe(II)$ concentrations in porewater, 10^{-8} M, the redox front does not penetrate more than halfway into the buffer (McKINLEY et al. 1992b).

Realistically, the oxidation potential of the steel canister and corrosion products will ensure reducing conditions and there is no need to consider the case of oxidising conditions in the near field in assessment calculations.

4.3.3.6 Sorption and Co-precipitation with Iron Corrosion Products

Iron oxides of the type formed by corrosion of the steel canister are well known scavengers of many trace elements and are used as such in many industrial and analytical methods. The association of a range of trace elements with iron oxy-hydroxide coatings in a wide range of geological environments is also well documented. Mass balance calculations indicate that expected levels of uptake on the corroded canister may be capable of immobilising the entire inventory of many safety-relevant elements (see McKINLEY et al. 1992a). In the Reference Scenario, these effects are neglected due to lack of the required data.

Radionuclide sorption and/or co-precipitation with iron corrosion products is identified as an important reserve FEP and is not included in Kristallin-I assessment calculations.

4.3.3.7 Gas Production and Pressurisation

The production of hydrogen by the anaerobic corrosion of the steel canisters is the most important mechanism for gas production in the engineered barriers (see Subsection 3.4.3.4). At the time of Project Gewähr 1985, a very conservative corrosion rate of $20 \mu\text{m y}^{-1}$ was used for estimation of canister lifetime, which would give rise to production of hydrogen at a rate of $3.8 \text{ mol m}^{-2} \text{ y}^{-1}$ (NAGRA 1985). Taking account of more recent experimental work, a long-term corrosion rate in the range 0.1 to $1 \mu\text{m y}^{-1}$, giving rise to an evolution of 0.02 to $0.2 \text{ mol m}^{-2} \text{ y}^{-1}$ of hydrogen, appears to be realistic (see Subsection 3.4.3.4).

The maximum rate of loss of hydrogen from the canister surface by aqueous diffusion is estimated at about 0.2 mol y^{-1} per canister, i.e. about $0.02 \text{ mol m}^{-2} \text{ y}^{-1}$ (ANDREWS 1993). Thus, it is uncertain whether the hydrogen evolved during corrosion could be dissipated by aqueous diffusion, without the formation of a free gas phase. However, if a free gas phase does form, it is likely to form first in larger pore spaces immediately around and within the steel canister and corrosion products, rather than in the finer pore spaces of the bentonite. This may have the effect of suppressing further hydrogen production. Furthermore, if future studies reveal that the rate of hydrogen generation will exceed the rate at which hydrogen can diffuse from the surface, a sand capillary-breaking layer (NERETNIEKS 1985a) could be considered as one way to provide additional buffer volume and surface area for hydrogen dissolution; the gas would be expected to occupy the large pore spaces in this layer to create a gas "pillow" surrounding the canister.

If gas continues to be generated, then the gas pressure close to the canister will rise. At low gas pressures, the gas permeability of the bentonite is low, but a 100 fold increase in permeability occurs at gas pressures around 30 to 70% of swelling pressure (PUSCH et al. 1985), the low gas permeability being restored when gas pressure is relieved. This is interpreted as escape of gas by "channelling" through connected pore spaces. Experimental evidence (e.g. DeCANNIERE et al. 1993) indicates that, when gas pressures are applied across clay plugs, only a tiny fraction of the pore space is evacuated prior to gas breakthrough; indeed, it is often impossible to detect the gas flowpaths except by X-ray tomography. Recent modelling studies (e.g. GRINDROD et al. 1994) are able to reproduce this behaviour and indicate that gas can overcome the capillary forces and hydrostatic pressure to pass through larger connected capillary pores of typically 10 nm, which is consistent with the estimate of minimum effective diameter of connected porosity in the bentonite buffer (McKINLEY 1988). Thus it is likely that no significant physical disturbance of the clay is involved and no degradation of the bentonite hydraulic properties or colloid retention properties is expected due to the passage of the gas.

It is concluded that hydrogen in excess of that which can be dissipated by aqueous diffusion may escape in gas phase with no implications for aqueous radionuclide transport; alternatively, the presence of a gas phase at the canister may even be beneficial to safety by suppressing further corrosion. Hence, quantitative evaluation of radionuclide release taking account of gas production is not required and not included in Kristallin-I. However, the study of hydrogen evolution and capacity for dissipation in aqueous and gas phases under repository conditions is identified as a topic to be kept under review. In particular, it is an open question whether a sand capillary-breaking layer is necessary or could be introduced to improve performance.

4.3.3.8 Release of Radioactive Gases

If hydrogen from canister corrosion escapes in the gas phase, as described above, then it may carry other gaseous species with it. However, release of radioactive gases is not a concern for vitrified HLW because gaseous fission products, e.g. krypton isotopes, and fission products with the potential to form gases, e.g. carbon and iodine isotopes, are present in only small quantities as they are driven off from the HLW residues during reprocessing. Carry-over fractions assumed for carbon and iodine in the Kristallin-I inventory are 1.5×10^{-3} and 1.0×10^{-3} , respectively (ALDER & MCGINNES 1994); these are maximum carry-over fractions, actual quantities present are expected to be even smaller. Radon isotopes will grow in from their respective actinide parents, especially ^{222}Rn from ^{226}Ra in the $4N + 2$ chain, but will be of no significance if released separately, unsupported by parent concentrations, because of their very short half-lives (4 days for ^{222}Rn).

It is concluded that release of radioactive gasses from the HLW repository can be ruled out from further consideration.

4.3.3.9 Degradation of Bentonite

A number of processes have been identified that might lead to some alteration of montmorillonite (which is the principal component of the bentonite) at temperatures above about 100 °C (see Subsection 3.4.4.4). However, the rates of reaction are slow and the thermal phase is short so that no significant alteration is expected. In any case, less than half the thickness of bentonite will experience temperatures in excess of 100 °C (see Figure 3.4.2), leaving a thick annulus of bentonite unaffected.

In the long-term, the most likely process for degradation of the bentonite is the alteration of montmorillonite to illite, which occurs by an increase in the (tetrahedral) layer charge followed by reaction with potassium from groundwater (see Subsection 3.4.4.5). Conservative calculations, in which all the potassium in groundwater passing the repository is taken up by this process, indicate a time of about one hundred million years for complete illitisation for the Reference-Case groundwater flowrate, and over one million years even for the most pessimistic groundwater flowrates. Evaluation of natural analogues also leads to the conclusion that, with a repository temperature of 60 °C or less, there will be no large change in swelling capability, hydraulic conductivity or cation exchange capacity of the bentonite in time periods well in excess of a million years. The formation of mixed illite-montmorillonite layers during the course of time cannot be ruled out, but complete illitisation can be (see Subsection 3.4.4.5).

It is concluded that any degradation of the bentonite will be insignificant over relevant timescales. However, some additional safety assessment calculations have been performed to investigate the effects of a loss of performance of part of the bentonite (see Subsection 5.2.3.6).

4.3.3.10 Bentonite Erosion

It has been postulated that bentonite may be physically eroded by groundwater flow. The rate of bentonite erosion has been calculated and shown to be trivial for well emplaced bentonite and the low water flows expected (NAGRA 1987; BRENNER 1988). It is, however, possible that bentonite erosion might become significant, as a result of poor or incomplete backfill emplacement or in the case of bentonite placed near to a high-permeability, water-conducting zone. The likelihood of either of these circumstances will be low due to quality control and investigations during tunnel excavation and before emplacement.

It is concluded that, for the expected conditions in the crystalline basement, provided attention is paid to identifying and avoiding high-permeability water-conducting zones, significant bentonite erosion can be avoided.

4.3.3.11 Canister Sinking

The mass divided by volume of the steel canister as emplaced is a factor of between three and four greater than the density of the compacted saturated bentonite. Hence, there is a potential for the canister to sink through the bentonite. Calculations indicate a maximum sinking of only 1 to 5 mm, occurring over a period of 10 000 years, at a rate that tends to zero with time (WHITTLE & ARISTORENAS 1991). These calculations model the behaviour of clay using conventional soil-mechanical creep-strain equations under the assumption that the bentonite is fully saturated and employing data from short-term compression tests on bentonite. Radionuclide transport calculations indicate that, for a displacement of 20 % (20 cm), there is negligible change of the total diffusive flux from the buffer and even a displacement of 50 % (i.e. sinking of 70 cm) leads to an increase of only 20 % in total flux (McKINLEY et al. 1992b). Hence, the effect on radionuclide release from the degree of sinking calculated by WHITTLE & ARISTORENAS (1991) will be negligible. However, confirmation that compacted bentonite can be modelled as a solid with strain-hardening properties over very long timescales is lacking. If, for example, the rate of sinking were to be low but constant, the canister could, in time, sink through the bentonite to contact the disposal tunnel floor.

The present understanding is that sinking will not occur, or be so slow as to be unimportant. Design modifications could be introduced to prevent or reduce the potential for sinking if required. For example, inert silica sand could be mixed with the bentonite surrounding the canister or stone supports could be placed in the bentonite beneath the canister. The FEP is identified as a topic deserving further consideration in the future.

4.3.3.12 Colloid Transport from the Waste

Colloids, containing radionuclides, may be produced as the glass degrades/dissolves and also by precipitation and co-precipitation at geochemical transitions around the wastes and canisters. Any colloids produced are expected to be trapped near the canister by the fine pore structure of the bentonite (see Subsection 3.4.4.3). However, if the colloid filtration function of the bentonite buffer is lost, for example, by incomplete emplacement of the bentonite or by canister sinking, then colloids, if stable, may provide a transport mechanism for radionuclides through the damaged buffer, and subsequently through the geosphere, with potentially much reduced retardation (see Subsection 4.3.4.7).

The present understanding is that, provided the buffer is correctly emplaced (which can be assured by quality control), such a sequence of events cannot happen and the scenario is excluded from quantitative assessment in Kristallin-I.

4.3.3.13 Transport along Tunnels and Shafts

Low-permeability tunnel seals will be installed (see Subsection 3.4.5) to hydraulically isolate the individual HLW panels and TRU silos from each other and also from major water-conducting faults in the host rock. Similarly, seals will be placed in the various shafts and investigation boreholes. However, if the seals are ineffective in the long term, the backfilled tunnels and shafts may offer potentially higher-permeability pathways for water flow and radionuclide transport than the undisturbed host rock. In addition, some dilation of fractures is expected in an excavation disturbed zone of host rock immediately surrounding the tunnels (including the emplacement tunnels) and shafts, and it is possible that continuous, or semi-continuous, networks of open fractures in this zone may also provide transport pathways.

The potential importance of the higher-permeability pathways that could be formed if tunnel and shaft seals are not effective is investigated in an alternative scenario. Two bounding cases are distinguished:

- transport along backfilled tunnels and shafts;
- transport along an excavation-disturbed zone, assumed to be continuous.

These calculations are discussed in Subsection 6.3.3.

4.3.4 FEPs Related to the Geological Barriers

In this subsection, FEPs related to the present-day geology and hydrogeological regime, and transport of radionuclides through the geological barrier, are discussed. FEPs related to future geological changes are discussed in Subsection 4.3.5.

4.3.4.1 Mechanisms for Radionuclide Transport

The predominant mechanism by which radionuclides released from the engineered barriers are expected to be transported through the host rock is by diffusion and advection in groundwater in aqueous solution. Transport in association with groundwater colloids may also be important (see Subsection 4.3.4.7).

It has been suggested that natural gas may provide a carrier for gaseous species released from a repository (SKI 1991a; SKI 1991b). However, vitrified HLW does not include significant inventories of potentially gaseous elements (see Subsection 4.3.3.8). It is possible that human actions, e.g. deep drilling, could result in direct transport of solid materials (e.g., wastes, contaminated bentonite or host rock) to the surface; this is discussed in Subsection 4.3.7.

A special case that is not considered in the Kristallin-I assessment is the transport of the noble gas radon (^{222}Rn), produced from decay of radium (^{226}Ra). The natural concentrations of radon in groundwater in the crystalline basement are typically one thousand times greater than that of the parent radium (see SCHASSMANN et al. 1992), since radon may emanate from the disintegrations of radium atoms, incorporated in a mineral (solid) phase. A similar effect can be expected in the case of a plume of $4N + 2$ actinide-chain radionuclides, including ^{226}Ra , originating from the repository. Transport of dissolved radon cannot be important in the geosphere because of the low groundwater flows in the crystalline basement and the short half-life (4 days) of ^{222}Rn . However, emanation and transport of radon may be important in the near-surface environment and at geosphere discharge zones; in particular, the potential for doses due to radon and its short-lived daughters from radon in well waters and emanating from soil should be examined in future.

It is concluded that, neglecting direct intrusion by humans, groundwater-mediated transport is the only significant mechanism for transfer of radionuclides released from the engineered barriers to the biosphere. The case of dissolved and gaseous transport of radon in the near-surface environment (geosphere-biosphere interface) may deserve special consideration.

4.3.4.2 Mechanisms for Groundwater Flow

Hydrogeological modelling carried out in Kristallin-I (Chapter 8 in THURY et al. 1994) only considers topographically-driven flows (although the southern boundary of the regional model is a no-flow boundary defined, to some extent, by the presence of mostly stagnant, highly mineralised water in the low-permeability sediments of the Permo-Carboniferous Trough). Groundwater flows may also be modified by density driven differences due to thermal effects (repository and geothermal heat) and salinity.

Thermal effects on groundwater flow due the presence of the repository (i.e. convection cells) may be neglected because the heat output of the wastes rapidly becomes insignificant (see Figures 3.3.2 and 3.4.2) and any initial disturbance will be restored long before any radionuclides are released from the engineered barriers.

The boundary fault at the margin of Permo-Carboniferous Trough has been noted as a possible conduit for upward convection of geothermal waters from depth and has been invoked to help explain the occurrence of the observed geothermal anomaly by RYBACH et al. (1987). They proposed a volumetric flow equivalent to an input of flow of $10^{-7} \text{ m}^3 \text{ s}^{-1}$ per metre of fault. This flow was represented in some of the hydrogeological model simulations (Chapter 8, THURY et al. 1994). However, the results from these simulations predict salinities in the crystalline basement that are much higher than those actually measured. This indicates the groundwater flow proposed by

RYBACH et al. is too high; only model runs with no imposed fluxes gave estimates of salinity consistent with the hydrochemical evidence, which justifies the assumption of the deep Permo-Carboniferous Trough acting as a no-flow boundary for the investigated region.

The dissolved solids (salinity) in the groundwater of the crystalline basement (typically 1 g l^{-1} in Area West; see Table 3.5.2) are believed to arise primarily from the long contact time with local rock minerals. Hydrochemical evidence suggests that the composition of most groundwater in the crystalline basement is the result of chemical evolution entirely within the crystalline rock itself. However, some saline groundwater, occurring in isolated zones of the low-permeability domain in Area West (e.g. Böttstein), has chemical characteristics that are similar to those of groundwater in the sediments of the Permo-Carboniferous Trough. This occurrence indicates that, in the past, some saline groundwater could have flowed from the Permo-Carboniferous Trough and mixed with the crystalline-rock groundwater. Water in the upper unit has been interpreted by SCHASSMANN et al. (1992) as being principally crystalline-rock water with recharge in the southern Black Forest that could contain only very small amounts of saline water. It is believed that the effect of the generally rather low salinities in the crystalline basement will not significantly modify the topographically-driven flows and can be neglected.

It is concluded that the neglect of temperature and salinity effects in the groundwater modelling carried out for Kristallin-I is unlikely to have significantly biased the results, but these effects may deserve consideration in future hydrogeological modelling studies.

4.3.4.3 Transport Path Through the Geological Barriers

Radionuclides released from the engineered barriers will be carried by groundwater in discrete water-conducting features in the crystalline rock; detail characteristics of these are discussed in 4.3.4.4. Groundwater modelling studies (Chapter 8, THURY et al. 1994) indicate that, within the low-permeability crystalline basement blocks, groundwater flow will tend to be mainly vertically upwards, but may be sub-horizontal, towards the nearest major water-conducting fault, in the immediate vicinity of such faults. Flow in the more permeable major water-conducting faults and upper crystalline unit are expected to be mainly sub-horizontal and generally follow the regional hydraulic gradients, leading to groundwater discharge in the Rhine valley.

Thus, two alternative groundwater pathways are identified for transport of radionuclides from the repository:

- transport through the low-permeability domain directly to the higher-permeability domain, which is adopted as a Reference Model Assumption, and

- transport through the low-permeability domain to a major water-conducting fault, and thence to the higher-permeability domain, which is treated as an alternative model assumption within the Reference Scenario.

Groundwater from the crystalline basement in both Area West and Area East is expected to emerge, and mix with more recent waters, in the gravel deposits of the Rhine valley. For a repository in Area East, where a groundwater divide may exist (THURY et al. 1994), there is a possibility that groundwaters from the crystalline basement will emerge in the Wutach valley, a tributary of the Rhine to the north of Area East. In this case, the basic processes of dilution and subsequent water use (e.g. in agricultural production) would be similar, but the volume for dilution would be smaller. The expected case of discharge to the gravels of the River Rhine is treated as a Reference Model Assumption within Kristallin-I Reference Scenario. The case of discharge to a smaller valley in Area East (only) is treated as an alternative model assumption, calculated by means of biosphere parameter variations.

4.3.4.4 Characteristics of the Water-Conducting Features

A regional analysis of permeable zones (inflow points) in the boreholes within the crystalline basement (Chapter 6, THURY et al. 1994) results in classification of three types of water-conducting features:

- cataclastic zones;
- jointed zones;
- fractured aplite/pegmatite dykes and aplitic gneisses.

These have been discussed in Subsection 3.5.2 and data for performance assessment has been presented in Subsection 3.7.6.

Water-conducting feature of all types contain sets of partially infilled fractures, with discrete open channels within which groundwater flow is confined, and zones of altered wallrock immediately adjacent to the fractures. These components exhibit ranges of geometrical and mineralogical characteristics. Available data on the spatial orientation of the water-conducting features indicate that, although there is a slight bias towards a steeply dipping orientation, the range is very large. All water-conducting features are assumed to be interconnected; this assumption is corroborated by larger-scale observations in surface outcrops in the Black Forest as well as by the largely homogenous water chemistry within each borehole (THURY et al. 1994).

Because of this good interconnection, it seems unlikely that radionuclides released from the repository would remain in the same type of water-conducting feature throughout their transit of the crystalline basement. However, in the Kristallin-I assessment

calculations, it is assumed that transport does occur through a single type of water-conducting feature, with a fixed set of geometrical and mineralogical characteristics. Separate calculations are performed to investigate the transport implications of the different types of features and of the range of characteristics within a single type of feature. This approach is a convenient modelling simplification, and is believed to be justified at this stage because:

- if, in reality, transport occurs through a network of linked features, then the overall transport behaviour is expected to lie within the range of results obtained by separately considering each of the alternative model descriptions of the water-conducting features;
- the modelling of transport along a pathway consisting of a network of linked water-conducting features, with a range of characteristics, would require better information than is currently available on statistical occurrence, connection and importance to flow of the different water-conducting features.

4.3.4.5 Matrix Diffusion

Evidence from field studies (see, for example, results of the migration experiment at the Grimsel Test Site: FRICK et al. 1991; ALEXANDER et al. 1992; FRICK et al. 1992) has shown that tracers are significantly retarded relative to the velocity of groundwater in fractured rock, even in the absence of sorption. This retardation has been attributed to the process of matrix diffusion, whereby elements dissolved in aqueous phase diffuse into stagnant porewater within fracture infill material and/or within the wallrock adjacent to the fractures.

In modelling matrix diffusion in the water-conducting features of the crystalline basement, two alternative model assumptions are investigated:

- that matrix diffusion occurs only in a spatially-limited region of fracture infill and altered rock immediately adjacent to the fracture ("limited" matrix diffusion);
- that matrix diffusion is "unlimited", and radionuclides may also diffuse into unaltered crystalline rock.

These two assumptions, combined with variability in the characteristics of water-conducting features discussed above (section 4.3.4.4), lead to a number of possible alternative geometrical representations of the internal structure of water-conducting features. These are considered as alternative model assumptions within the Reference Scenario of Kristallin-I, and are discussed further in Subsection 5.3.4.

4.3.4.6 Radionuclide Sorption

The approach to modelling interaction of dissolved radionuclides with solid mineral phases, and related data, has been discussed in Subsection 3.5.5. In the Kristallin-I assessment, sorption is assumed to be rapid and completely reversible. With the exception of Cs, data for sorption of all elements is given in the form of linear isotherms (sorption constant, K_d); Cs sorption is described by a Freundlich isotherm (see Subsection 5.3.4.4).

The assumption that sorption is rapid and reversible (i.e. reaction kinetics can be disregarded) is consistent with the sorption database used (data comes mainly from relatively short-term experiments, in which the sorption processes operative are those with rapid kinetics). It is possible that, on longer time-scales, other sorption processes, especially irreversible sorption processes, might become important. However, the effect of these would be to further retard radionuclide release hence, in modelling transport of dissolved radionuclides, it is conservative to neglect them (see, however, Subsection 4.3.4.7).

4.3.4.7 Transport with Groundwater Colloids

As well as transport in aqueous phase, it is recognised that radionuclides may also be transported in association with (sorbed to) groundwater colloids and this has been observed to be a significant effect under some circumstances (see, for example, RYAN & GSCHWEND 1990). The effect may be significant because colloids have high a specific surface area and are thus efficient at sorbing radionuclides and also, because of electrical-charge and size effects, may be carried efficiently with flowing groundwater in open channels and excluded from the stagnant water in smaller pores. Thus, the retarding process of matrix diffusion (see Subsection 4.3.4.5) is negated. In addition, the sorption of radionuclides on groundwater colloids may reduce the radionuclide concentration in solution at the bentonite-host rock interface and increase the concentration gradient across the engineered barriers, leading to increased radionuclide releases.

Factors affecting the importance of colloid-facilitated transport are discussed in SMITH (1993a). Colloid-facilitated transport will be insignificant in the following cases.

- Where the concentration of groundwater colloids is too low to sorb a significant fraction of dissolved radionuclides and the effect can be neglected; this is effectively a Reference Model Assumption in the Kristallin-I assessment.
- Where, even at relatively high concentrations of colloids, radionuclides are poorly sorbed and are not significantly affected by association with colloids.

For well-sorbed radionuclides, e.g. Np, U, Th, and at higher colloid concentrations, sorption on colloids may be significant. Whether this results in enhanced or diminished radionuclide transport depends on the nature of the sorption process (reversible or irreversible) and of the processes by which mobile colloids enter into, and are removed from, the flowing groundwater:

- (a) Radionuclides may be reversibly sorbed, so that there is a dynamic population of radionuclides in aqueous phase and sorbed on colloids; the population of colloids may also be dynamic, resulting from continuous processes of generation, dissolution and filtration/entrapment. Exclusion of colloids from matrix pores could, in this case, lead to enhanced radionuclide transport.
- (b) Radionuclides may be irreversibly sorbed to colloids, in which case it is expected that the process of colloid filtration/entrapment would deplete the population of radionuclide-bearing colloids and lead to reduced releases. It is, however, possible that a fraction of colloids with irreversibly-sorbed radionuclides could be transported through the crystalline basement experiencing little or no delay compared to groundwater transit times.

Case (a) is considered as a Alternative Model Assumption within the Reference Scenario and is further discussed in Subsection 6.2.2.3. Case (b) is retained as a open question, deserving attention in future assessments. Although it considered more likely that irreversible sorption on colloids will reduce, rather than enhance transport, there is currently insufficient knowledge about the behaviour of colloids in the water-conducting features of the crystalline basement to justify categorising this as a reserve FEP.

4.3.4.8 Effect of Repository Construction and Emplacement

The construction of tunnels within the crystalline basement, and associated pumping and ventilation during the operational phase, are expected to have a significant local effect on the hydrological regime, with water flow into the open tunnels due to the large hydraulic head difference and, possibly, disturbance of redox conditions in the host rock. In the Kristallin-I assessment, it is assumed that these changes are temporary, with both hydrogeological and hydrochemical parameters returning to pre-emplacement values within a few years of repository closure.

During tunnel and shaft construction, some stress relief, leading to dilation of joints and fractures, is expected in an axial zone of up to one diameter width surrounding the tunnels and shafts; this is termed the excavation-disturbed zone (EDZ). The characteristics and long-term importance of this zone are very uncertain. It is possible that the swelling pressure of the bentonite may restore dilation of open joints, so that the long-term effect is negligible. On the other hand, the zone may remain as a higher-permeability zone and hence act as a preferential path for both water flow and radionuclide transport (see also 4.3.3.13).

In the Kristallin-I groundwater-flow modelling, the effect of an EDZ is not considered. This is equivalent to assuming that the zone (if it exists at all) is not continuous over more than a few metres and hence does not modify local groundwater flows, which is believed to be realistic. In the Kristallin-I safety assessment, however, it is assumed that there is connectivity in this zone, so that radionuclides diffusing to the periphery of the engineered barriers are advected away with a mean groundwater flow.

4.3.4.9 Effect of the TRU silos

The TRU (long-lived intermediate-level waste) silos contain large quantities of cementitious backfill and structural material, as well as small quantities of organic material within the disposed wastes. Over time, the interactions of groundwater with the silos will lead to a plume of cementitious species, which is expected to alter the mineralogy of water-conducting features in its path.

In the Kristallin-I reference design (see Figure 3.1.1), the TRU silos are sited in a separate block of low-permeability crystalline basement. They are thus separated from any HLW emplacement panels by a major fault zone that may be either non-conductive (acting as a barrier to groundwater flow) or water-conducting (acting as a source of dilution). In the Kristallin-I assessment, it is assumed that the TRU silos could be sited so that there would be no hydrological or hydrochemical effect on the HLW panels. The relative siting of the TRU silos and HLW panels is a subject that will require further consideration on a site-specific basis.

4.3.5 FEPs Related to Long-Term Geological Changes

4.3.5.1 Bounding Scenarios for Long-Term Geological Change

Prognoses for the future evolution of the geological regime of Northern Switzerland over the next one million years can be made under the assumption that those processes that are currently active and, from geological evidence, have been active in the recent geological past (last few million years), will continue to operate. However, there is uncertainty:

- in the details of the present-day situation, due to sparse sampling (e.g. limited number of boreholes) and to uncertainty in the interpretation of measurements;
- in the processes that may have been active in the past, due to the limited geological record and to uncertainty in its interpretation.

It is not, therefore, possible to make detailed quantitative predictions of future geological change, but it is possible to develop plausible scenarios, the extreme variants of which bound the expected future geological developments.

Bounding scenarios for geological change in Northern Switzerland have been developed based on interpretation of neotectonic studies (i.e., studies dealing with the movement of the Earth's crust) of the region from the Upper Rhine Graben rift zone to the Alpine Chain (see Figure 3.5.2). The data available, which comes from studies of geology, geomorphology, analysis of drainage patterns, measurements of the recent stress field, regional geodesy (precision-levelling surveys), seismicity and seismotectonics, is summarised and interpreted in Chapter 9 of THURY et al. (1994). Based on this data, two bounding scenarios are defined which, in principle, are those derived by DIEBOLD & MÜLLER (1985) at the time of Project Gewähr 1985, but have been updated and refined based on the wealth of new data now available.

Table 4.3.2 summarises the key features of bounding scenarios for long-term geological change.

- In Scenario A, it is assumed that the Alpine orogeny is largely completed and that active crustal shortening is no longer expected in Northern Switzerland. The only major processes occurring would be decreasing crustal movements in the form of isostatic uplift.
- In Scenario B, it is assumed that Alpine tectonics are continuing, with corresponding stresses in the crust of Northern Switzerland. This causes active movements at fault zones and further folding in the Folded Jura. The basement will be increasingly involved in the compressive tectonic regime.

Considering the long-term nature of the tectonic processes causing Alpine uplift, Scenario B is the more likely. Based on current understanding, Scenario A is rather unlikely, but can be thought of as an extreme of cases in which uplift continues, but at a reduced rate.

For the purpose of repository safety assessment, it is necessary to consider scenarios that cover the widest range of expected future evolution. The Reference Scenario (see Subsection 4.3.1) assumes no change in geology, hydrogeological regime and surface environment. Relative to the Reference Scenario, Bounding Scenario B, with continuing Alpine tectonics and orogeny, provides the greatest potential for change (e.g. movement on faults, stress changes, seismicity, uplift and erosion). Bounding Scenario A, with declining tectonic activity and orogeny, represents an intermediate case. For this reason, and also because Scenario B seems more probable, Scenario A is not discussed further, and a prognosis for possible geological change over the next one million years is developed based on Scenario A, i.e. the case of **Continuation of Alpine Orogeny**.

The following Subsections (4.3.5.2 to 4.3.5.10) discuss the various geological processes and events, identified in Section 9 of Table 4.2.2, under the assumption that Alpine orogeny is continuing. The key implications, i.e. changes that could affect the long-term radiological performance of a HLW repository in the crystalline basement of Northern Switzerland, are summarised in Subsection 4.3.5.11.

	Bounding Scenario A	Bounding Scenario B
Alpine orogeny	The Alpine orogeny is complete and active crustal shortening no longer occurs. Driving forces between the Alps and the Upper Rhine Graben are sub-crustal and thermal processes: rifting and isostatic movements. The regional uplift of the Alps: continuing isostatic compensation for the pronounced Tertiary thickening of light crustal material beneath the Alps. Uplift fading in time; maximum amount ca. 5-7 km in 10 Ma. No further decollement in the foreland.	Crustal convergence and compression is continuing in the Alps and foreland. Advance of the alpine front, narrowing of the Molasse plateau by ca. 30 km in 10 Ma. Uplifting of the central massifs by > 10 km of the Molasse wedge and Jura by 1-3 km / 10 Ma. Compression and continued shear in the crust along trans-current faults and thrusts (crystalline basement wedges and future massifs). Inversion of the Permo-Carboniferous troughs, possibly including the PCT. Decollement of the foreland sedimentary cover and Jura folding continue; dislocation of about 500 m in 1 Ma. Accelerated erosion in uplift areas.
Upper Rhine Graben and uplift of the Black Forest	The continuing updoming of the Southern Black Forest is associated with rifting in the Upper Rhine Graben and is primarily of thermal origin (Mantle diapir). Although a long-term continuing process, the uplift will slowly die out; maximum expected uplift ca. 2 km. Maximum uplift in the potential siting regions of the order of 200 m in Area West and 500 m in Area East in 1 Ma.	The thermal anomaly around the Upper Rhine Graben (thin crust, rifting) ensures continuing uplift in the region. The Graben itself undergoes transpressive shearing, which causes some segments to be uplifted and others to subside (seismic activity). Thermal and compressive updoming of the Black Forest and the Upper Rhine Graben marginal segments of up to several km in 10 Ma. Regional uplift for next 1 Ma similar to Scenario A.
Stress field	The present-day stress field is not an expression of active compressive tectonics, but rather a residual stress which will decrease with time.	The regional stress field is a result of continuing orogenic activity and will prevail in the future.
Regional structures in the crystalline basement of Northern Switzerland	Reactivation of existing fault zones as extensional structures: jointing and normal faulting (kairites). Preferred strike: Hercynian (WNW-ESE) and also Rhenish (NNE-SSW) in the West.	Reactivation of existing fault zones as (1) normal faults around the Black Forest dome (horst and graben structures) and (2) as ca. NW-SE-striking dextral and ca. NNE-SSW-striking sinistral shear zones.
Local structures in potential repository regions	Moderate reactivation of small-scale structures with no formation of new systems. Undisturbed blocks remain stable.	Continuing slight displacements at fault and joint systems; some overprinting of whole segments and blocks. Movements orientated along existing structures

Table 4.3.2: Bounding Scenarios for long-term geological change. (From THURY et al. 1994).

4.3.5.2 Regional Horizontal Movements

Within the zone of influence of the Jura overthrust, the sedimentary cover will continue to shear horizontally northwards relative to the basement (THURY et al. 1994). The movement is likely to be not more than 500 m in the next million years and this horizontal movement of sediments will not significantly influence repository safety. Regional horizontal movements in the basement, relative to other formations, are likely to be less than about 100 m in the next million years, and are expected to be absorbed by movement along existing first- and second-order faults.

4.3.5.3 Regional Vertical Movements

The up-doming of the crystalline basement in the Southern Black Forest region (which has continued over the last several tens of million years) will lead to a maximum uplift of 200 m and 400 m in the next one million years in Area West and Area East, respectively (THURY et al. 1994). The relative movement will be absorbed by movement on existing major faults. As a result of the up-doming, there will be a southwards shift of the river Rhine, with consequent shortening of the groundwater flowpath in the higher-permeability domain of the basement for Area West, but a lengthening in Area East. Flowpaths in the low-permeability domain will not be directly affected, although hydraulic gradients may be changed, especially in Area East.

4.3.5.4 Movement along Major Faults

Movements along faults will occur due to the updoming of the Southern Black Forest and the existing compressive stress field in the crystalline basement resulting from the Alpine orogeny. The relative movement along any fault will lie in the range 0 to 100 m in one million years. The faults are heterogeneous and the properties of the faults are a result of past movements; continuing movement will therefore not change their average range of properties, although previously conductive zones may become less conductive and vice versa.

Movement on major faults that intercept access tunnels connecting the repository panels, or repository shafts, may cause relative displacement of the tunnels in adjacent blocks. This will not be significant if tunnel seals remain intact. Although the movement might adversely affect seals near to such a fault, it is expected that this can be avoided by attention to the choice of seal locations and design.

4.3.5.5 Movement along Small-scale Faults

A fraction of the deformation will be absorbed by minor faults such as the cataclastic zones intercepting emplacement tunnels. The displacement is likely to be of the order of a few tens of centimetres and not exceed 1 m in one million years. Provided canisters are placed away from such faults, which should be detectable during repository excavation, then the displacement would not have any significant effect from the point of view of repository safety.

4.3.5.6 Seismic Activity and Stress Changes

Seismic activity is low in the potential repository siting areas in Northern Switzerland and the corresponding risk to safety is considered negligible (THURY et al. 1994). Direct disturbance of a sealed repository by seismic activity can practically be ruled out. In addition, earthquake magnitudes to be expected in Switzerland will never be sufficient to cause serious damage to a deep underground tunnel system during the operational phase (see DIEBOLD & MÜLLER 1985; BERGER 1987).

It has been observed that stress changes due to fault movement can have a hydrogeological effect, changing the aperture of fractures within a rock mass to cause expulsion or drawing in of water (MUIR-WOOD & WOO 1992). MUIR-WOOD & WOO concluded that the most significant hydrological response is found to accompany major normal fault earthquakes, involving an increase in spring and river discharge to a peak a few days after the earthquake, the excess flow being sustained for periods typically of around 8 months. In contrast, hydrological changes accompanying reverse fault earthquakes are either undetected or else involve falls in well levels and spring flows.

It is concluded that, for a sealed and backfilled repository, seismic events are unlikely to have any direct effect through ground movement. Any hydrogeological "pulse" would be a transient effect not affecting long-term water-borne radionuclide transport. The changes in aperture are expected to remain within the range of apertures of present-day water-conducting features in the crystalline basement and hence be covered already by the Reference Scenario.

4.3.5.7 Erosion and Denudation

The updoming of the Southern Black Forest is expected to be largely balanced by continuing erosion (see Chapter 9 in THURY et al. 1994). The sedimentary cover of the crystalline basement to the south of the Upper Rhine is currently subject to erosion and denudation processes. In this area, as uplift and erosion continue, the crystalline basement may be exposed on the south side of the present-day course of the Rhine along a strip 100 m to 2 km in extent within the next one million years. The Rhine may also downcut into the uplifting basement. Certain fault zones may thus lose their sedimentary

cover, which may modify the hydrogeological regime in the basement. The rates of erosion will depend on rates of uplift and climate; climatic influences are discussed in Subsection 4.3.6.

4.3.5.8 Basement Alteration

Local removal of the sedimentary cover and the southward shift of the Rhine may result in changes to the hydrogeological regime in the basement, especially in the higher-permeability domain. The nearer-surface crystalline basement has been progressively altered in the past as a result of stress relief and rock-water interactions, especially hydrothermal alteration, which has been more significant in the higher-permeability domain than in the low-permeability domain (THURY et al. 1994, Ch. 12). In future, as the overlying sediment, or the basement itself, is eroded, then the depth of the transition from higher-permeability domain to low-permeability domain might move downwards. This effect is only expected to be significant in areas where the basement is directly exposed at the surface, for example, near to the river Rhine. In the areas for potential repository siting, the basement is presently overlain by sediments and alteration of the basement is expected to be negligible within the next one million years.

4.3.5.9 Magmatic Activity (Plutonism and Volcanism)

Magmatic activity in the repository region could have a major impact on the system. For example, a magma dyke intersecting the repository could force molten rock along the zones of weakness created by the disposal tunnels and associated excavation-disturbed zones; severe alteration and disturbance of the bentonite buffer would result.

Conditions and consequences of magmatic activity, in the form of intrusions and volcanic activity, have been discussed in detail by DIEBOLD & MÜLLER (1985). They have confirmed that a direct intrusion or extrusion of magma is extremely unlikely in Northern Switzerland during the next ten million years. Magmatic activity is not, therefore, considered further.

4.3.5.10 Hydrothermal Activity

A relationship between the increased geothermal gradient in Northern Switzerland and the Permo-Carboniferous Trough has been postulated on several occasions (see, for example, DIEBOLD & MÜLLER 1985). The fault systems at the margin of the trough appear to promote the rise of deep groundwaters (see also Subsection 4.3.4.2). The thermal waters cause an overprinting of the conductive heat flux by that due to convection. Clear indications of hydrothermal activity are the thermal springs to the north and south of the Permo-Carboniferous Trough (e.g. at Zurzach). Hydrothermal activity may result in changes in fracture characteristics through hydrothermal neo-mineralisation and, conversely, formation of solution cavities in cataclastic zones (THURY et al. 1994).

The pattern of hydrothermal activity in the region is not expected to change significantly over the next million years. It is also expected that significant geothermal anomalies can be avoided by repository siting. Therefore, the process is not included in Kristallin-I assessment calculations, but is identified as a topic for consideration in site investigation studies.

4.3.5.11 Summary of Impacts of Expected Geological Changes

The expected scenario for geological change is a Continuation of Alpine Orogeny: see Subsection 4.3.5.1. Based on the above discussion, the following are identified as maximum expected changes that could affect the long-term radiological performance of a HLW repository in the crystalline basement of Northern Switzerland over the next one million years.

- Regional vertical movements will lead to maximum uplift of 400m in Area East and 200 m in Area West. This may increase hydraulic gradients, especially in Area East.
- The uplift is, however, expected to be largely balanced by erosion, leading to a reduction, or removal, of sedimentary cover, which may also affect the hydrogeological regime.
- The updoming, centred in the Black Forest region, will lead to a maximum southward shift of the River Rhine by about 2 km, thus decreasing the groundwater flowpath length in the higher-permeability domain for a repository in Area West and increasing the flowpath length in the higher-permeability domain for a repository in Area East, if the repository is sited to the south of any possible future groundwater divide in the area (see, however, Subsection 4.3.6.5).

Hydrogeological modelling has been performed for a range of boundary conditions representing possible future geological situations (see Chapter 8 of THURY et al 1994). The results of the modelling indicates that flowpaths and conditions in the higher-permeability domain can change markedly. However, these have no impact on safety-assessment calculations because of the very conservative treatment of the higher-permeability domain in the Reference Model Assumptions (immediate transport through this unit). The model results indicate that conditions in the low-permeability domain are not strongly affected. Indeed, the estimated changes in hydraulic gradient fall within the range considered as parameter variations within the Reference Scenario .

It is concluded that Continuation of Alpine Orogeny should be identified as an alternative scenario because it is the expected geological evolution, but it is not necessary to carry out additional safety-assessment calculations, since the expected changes fall within the range of parameter variations considered in the Reference Scenario.

4.3.6 FEPs Related to Long-Term Climatic Changes

4.3.6.1 Bounding Scenarios for Long-Term Climatic Changes

Bounding scenarios for long-term climatic change in Northern Switzerland over the next one million years can be developed based on analogy with the climate over the last few million years, which is in turn based on an analysis of regional and global indicators, as preserved in the geological record, and on atmospheric and climate modelling studies.

The climatic evolution of the Earth has been strongly influenced, since the Middle Miocene (approximately 15 million years b.p.), by the Antarctic ice sheet. The beginning of glaciation in Greenland took place more recently, 3 to 4 million years b.p., and extensive glaciation of the Arctic has been occurring since the Middle Pliocene (2.5 million years b.p.). The last 2 million years of the Quaternary has been characterised by glacial-interglacial cycling.

High-resolution measurements of stable oxygen isotopes on carbonate shells collected from deep oceans cores, and on water samples from ice cores from the two poles, give a consistent pattern of cyclic global temperature changes. Further, there is a marked correlation between global temperature indicators, atmospheric CO₂ concentration indicators and perturbations of the Earth's orbital parameters described by MILANKOVITCH (1930). It is thus hypothesised that the periodicity of glacial-interglacial conditions is related to variations in solar insolation, determined by the Earth's orbital variations (see, for example, IMBRIE et al. 1984). Between 900 000 and 600 000 years b.p., there was a gradual change from a 41 000 year dominated cycle to a 100 000 year dominated cycle, which, it is presumed, was due to tectonic changes in the Earth's ocean basins affecting the distribution of heat through the large ocean currents. Thus, while the occurrence of future glacial-interglacial cycles can be forecast from periodicity of Milankovitch cycles, the exact occurrence is uncertain and may be affected by other factors.

In the natural course of events, the next ice age is expected to begin within the next 20 000 years and the next glacial maximum will occur within the next 80 000 years. Regional evidence indicates that, in the last 600 000 years, ice build-up has occurred gradually over long periods of time, interrupted by several complete retreats of the Alpine glaciers. The transition from an interglacial to a glacial period appears to occur as a relatively rapid drop in temperature and transition from temperate to tundra vegetation types over the course of a few hundred years; ice build-up occurs more slowly, over several hundred or thousands of years, which, in the case of Northern Switzerland, could lead to complete glaciation of the Alpine Foreland. The transition from a glacial to an interglacial state may be even more rapid; stable isotope measurements on ice cores indicate a maximum rate of temperature rise of 7 °C in 50 years at the end of the last glaciation.

A significant uncertainty is the effect of man's activities, especially the postulated trend towards global warming due to the introduction of CO₂ and other gases into the

atmosphere - the greenhouse effect. The most likely prognosis is that man's activities may cause some temporary minor warming, but that the capacity of the deep ocean waters to absorb excessive heat and CO₂ will be sufficient that the orbitally-driven glacial-interglacial cycling observed over the past million years will persist. However, a less likely possibility is that glacial-interglacial cycling will be disrupted and the global climate will shift to some other quasi-equilibrium state.

Thus, two bounding scenarios are defined for future climatic evolution.

- **Glacial-interglacial cycling** - the pattern of glacial-interglacial cycling that has been experienced in the last one million years continues, with up to 25 glaciations expected in the next one million years. The current, temperate climate is representative of an interglacial period; future interglacials could be somewhat warmer or cooler. A much cooler climate will develop during periglacial periods.
- **Continuous warm climate** - glacial-interglacial cycling ceases, with establishment of a stable climate that is expected to be warmer than, or similar to, that of the present-day. Three alternative climate states are possible in this case: equable humid, seasonal humid, and arid; the last is considered least likely.

Table 4.3.3 summarises the key characteristics of the two bounding scenarios for climate evolution and climate state alternatives, especially with regard to hydrology and erosion potential. The first scenario is considered to be more likely than the second. This is, however, a subject of current scientific debate. Both bounding scenarios are therefore considered further. The following subsections examine the various climatic processes, identified in Section 10 of Table 4.2.2, for both cases.

4.3.6.2 Recharge

Recharge of the groundwater system is influenced by climate-dependent factors, such as temperature, humidity and vegetation cover. In the glacial/interglacial cycling case, the availability of water for recharge may increase (relative to present-day) during cooler boreal climates, due to reduced evaporation and transpiration, but decrease during colder tundra climates, when precipitation is reduced. If permafrost develops, then the groundwater may be partially or completely isolated from recharge (see also Subsection 4.3.6.6). In the continuous warm case, there will be a marked increase (relative to present-day) in effective moisture during humid climate states and a very marked decrease during the arid climate state.

	Glacial-interglacial cycling Alternating cold and warm periods	Continuous warm climate Alternative climate states		
	Glacials and interglacials	Humid	Seasonal humid	Arid
Climate and vegetation	Marked long-term alternation between cold periods with permafrost/tundra/cold deserts/ice cover and warm periods with close vegetation cover and a humid-temperate climate similar to present-day.	Humid-temperate to warm-wet climate with permanent cover.	Short-term alternating rainy and dry periods. Disperse vegetation.	Dry climate with episodic precipitation. Vegetation minimal to absent.
Hydrology	Glacial: separation of surface and groundwater in permafrost areas; braided streams with high bedload. Glacial/interglacial transition: meltwater streams, high discharge, high bedload. Interglacial: (see seasonal humid).	Fixed drainage network, high discharge, low bedload. Steady groundwater table, infiltration of meteoric waters.	Shifting drainage network, high discharge, low bedload. Strongly fluctuating groundwater tables, episodic infiltration.	Shifting, rudimentary drainage pattern (wadi type), sheet floods with extreme bedloads. Evaporation-dominated groundwater regime.
Erosion type	Glacial abrasion and deep scouring during ice ages; very marked fluvial erosion at cold-warm period transition due to glacial melt-waters. Average erosion and moderate denudation during warm periods.	Average fluvial erosion. Intensive deep weathering. Moderate denudation.	Seasonally marked erosion effects, both linear and denudative. No over-deepening; dynamic groundwater regime with strongly fluctuating water tables.	Denudation (uniform erosion) due to aeolian erosion and episodic rainfalls (sheet floods). Ascending ground water circulation (due to net evaporation).
Erosion effects	Large weathering and erosion potential. Glacial scouring up to several 100 m deep, in places to below erosion base level. Fluvial erosion rate can greatly exceed the rate of regional uplift. Denudation (uniform erosion) maximum 100m / 1 Ma.	Low to average denudation rates < 50 m in 1 Ma. Uplift could be compensated by erosion only in high mountain areas.	Seasonally high; denudation rate < 100 m in 1 Ma. Fluvial erosion continually compensates uplift.	Marked denudation, but generally less than regional uplift. Fluvial erosion along pre-existing valleys.

Table 4.3.3: Bounding Scenarios for long-term climatic change. (From THURY et al. 1994).

However, recharge to the crystalline basement is limited by its relatively low hydraulic conductivity, which will not change. Therefore, in general, the groundwater flow in the crystalline basement is not expected to change greatly; this is confirmed by hydrogeological modelling (Chapter 8 in THURY et al. 1994). A possible exception is the case of sub-glacial meltwater recharge, which is discussed in Subsection 4.3.6.6.

4.3.6.3 Erosion

Two types of erosion are distinguished: **uniform erosion or denudation**, which results in an overall lowering of land surface, this may be due to transport of wind-borne particulates (dust) or particulates in surface run-off; **linear erosion or downcutting**, which occurs along particular courses, usually river courses by fluvial action but also, for example, due to glacial abrasion and sub-glacial melt-water rivers.

In humid and glacial climates, linear erosion dominates. Assuming the Alpine orogeny continues, with associated uplift in Northern Switzerland, the maximum fluvial erosion (downcutting) by the Rhine is estimated at 200 m in one million years; erosion by tributary rivers draining the Southern Black Forest (e.g. the Wutach) will be greater, up to 500 m. Surface denudation will not exceed 100 m. There will thus be an accentuation of the relief, with a deepening of the valleys in the Southern Black Forest and less marked effects in the Tabular Jura. During a glacial period, unconsolidated deposits in the river valleys may be scoured out several times. However, the glacial retreat is likely to be accompanied by deposition of glacial tills and gravels.

There will also be significant lateral erosion due to the southward shift of the Rhine. The lateral erosion by the river will vary locally depending on resistance of rock formations. In some places, a shift of the river bed of up to 2 km to the south may be expected. The shift of the river Rhine towards the south will result in the old Rhine bed, which is filled with glacial gravels, being abandoned. In the case of a humid climate, which is not interrupted by ice ages, there will be no alluvial build-up and, if erosion is sufficient to remove overlying sediments, the river Rhine may flow directly over the crystalline basement. Thus groundwater from the crystalline basement could discharge directly into the river.

In the case of an arid climate, with very low precipitation, in-situ weathering will dominate. The material remains in place until it is transported away by episodic heavy rainstorms. Uniform surface denudation then dominates over linear erosion, but should not exceed 50 m in one million years.

4.3.6.4 Groundwater Chemistry

The most important parameters of groundwater chemistry for radionuclide transport (e.g. sorption) are Eh/pH and ionic strength. These parameters are determined (buffered) to a large extent by the rock mineralogy. Only arid conditions are expected to have a significant influence on the key parameters. In arid conditions, near-surface waters

evaporate and become increasingly saline. At repository depth, changes in groundwater composition caused by changes in the near-surface groundwater conditions will be minor and will only occur after a delay of several tens of thousands of years. Hence, changes due to individual climate-state changes, e.g. due to glacial/interglacial cycling, are expected to have no impact the low-permeability host rock.

An exceptional case would be if changes in the hydrogeological regime were sufficient to allow saline waters from the Permo-Carboniferous Trough to intrude into the crystalline basement in the region of a repository. This should be considered as a geological event, since climate-induced changes in surface recharge alone seem unlikely to be able to induce such a change. In Kristallin-I it is assumed that the repository can be situated such that this event can be ruled out. It may, however, need to be considered, and evaluated if necessary, on a site-specific basis.

4.3.6.5 Groundwater Discharge Zone

In the Reference Scenario, it is assumed that radionuclides are transported in groundwater through the crystalline basement and discharged to the Quaternary gravels of the Rhine valley (see Subsection 4.3.4.3). This is the expected discharge zone, given present-day conditions in Northern Switzerland. Based on the above discussion, two alternative scenarios are identified.

- (i) The gravels presently filling the Rhine valley could be removed. This is considered most likely to occur after 100 000 years due to continuous erosion if glacial cycling ends and a long-term humid climate becomes established. The condition may also arise as a transient phenomenon during the early stages of an interglacial, after glacial and fluvio-glacial action have eroded the gravels and before significant redeposition takes place. In the latter circumstances, the condition would only persist for up to a few thousand years. In some stretches, the river Rhine currently runs directly over the basement. If the gravels are absent, then groundwater will exfiltrate directly to the river Rhine (with immediate dilution) and also, possibly, to adjacent low-lying areas of basement. If soils have developed on these areas, then exposure through agricultural pathways may occur. This scenario is possible for a repository in both Area West and Area East.
- (ii) For a repository in Area East only, where a groundwater divide is possible (THURY et al. 1994), exfiltration to a tributary valley of the river Rhine is possible (e.g. the Wutach, to the north of Area East). This is possible following down-cutting of the tributary into the basement, so groundwaters may exfiltrate to the smaller valley rather than to the river Rhine. This case would be particularly severe if significant deepening and southward migration of the Wutach valley occurred, possibly resulting in rather short flowpaths and high hydraulic gradients.

4.3.6.6 Permafrost and Ice-Sheet Effects

As the climate cools, air temperatures will fall substantially below freezing point for much of the year. If these conditions are sustained, then permafrost (permanently frozen ground) may develop. The depth to which permafrost will penetrate depends on the average surface temperature, geological conditions (thermal conductivity and geothermal flux) and the period of sustained low temperature (DAMES & MOORE 1991). In Arctic and Antarctic regions, permafrost of several kilometres thickness has developed in places. However, modelling and geological evidence suggest that, in currently temperate regions, permafrost of depths up to a maximum of only a few hundred metres is possible over the period of a future glaciation (BOULTON & PAYNE 1993). If summer temperatures remain above freezing point, then a zone of seasonally unfrozen ground will remain above the permafrost layer, which may support migratory animals and nomadic herdsman. Thus, the biosphere may be partially isolated from the deep groundwater system. However, significant groundwater discharge zones and the courses of major rivers and lakes are liable to remain as open "taliks", free from permafrost due to the heat from discharging groundwater and insulating effect of large water bodies. Thus, while the presence of permafrost may tend to reduce recharge (to high ground), it may focus groundwater discharge to the remaining unfrozen zones (McEWEN & DeMARSILY 1991).

A scenario that has been postulated in other studies (e.g. see Volume 3 of SUMERLING (Ed.) 1992) is that, as the ice sheet advances then recharge will occur from the meltwater formed under pressure at the base of the ice sheet. In the case of a static or retreating ice sheet, this water may escape as sub-glacial rivers between the ice and ground. However, in the case of an advancing ice sheet a sealed front may be created by the ice sheet advancing over permafrost so that the meltwater is forced downward into the underlying rock. This situation has been modelled for the case of the Fennoscandinavian ice sheet during the last glaciation (BOULTON & PAYNE 1993). Assessments of a site in the UK have shown the effects can be significant to radiological performance of a repository (SUMERLING (Ed.) 1992).

In the case of a repository in the crystalline basement of Northern Switzerland, this scenario would only be significant if permafrost were to develop throughout the overlying sediments and higher-permeability domain, so that water flow in the low-permeability domain is increased. However, this is not thought to be possible because of the great depth implied for permafrost formation (~500m) and the significant geothermal gradient in the crystalline basement. Studies have indicated a likely depth of permafrost penetration in advance of a glacial advance in Northern Switzerland of only 100 m (ANON 1994).

4.3.6.7 Climate State and Agricultural Practices

The alternative climate states that might arise in Northern Switzerland have been identified in THURY et al. 1994 as:

- a temperate climate, similar to present-day conditions, during interglacial periods;
- a significantly cooler (tundra) climate during the approach to and after glacial periods (during the period of glacial ice sheet cover in the region, there are assumed to be no humans present and therefore no agriculture or exposure pathways);
- a warmer climate than the present-day, which may be equable humid, seasonal humid or arid, and may arise during a future interglacial period, or if glacial/interglacial cycling ceases.

The temperate climate is assumed in the Reference Scenario. Three alternative climate states are therefore selected for treatment as alternative biosphere scenarios:

- A periglacial (tundra) climate - The food chains and exposure pathways would be significantly different to the present-day situation. Agriculture is assumed to be based on herding of cattle or reindeer, with no significant arable crops.
- A warm humid climate - The food chains and exposure pathways are assumed to be similar to the present-day. However, the extent of certain processes will differ, e.g. vegetative yield will increase.
- A warm dry climate - The food chains and exposure pathways are assumed to be similar to the present-day. Again, the extent of certain processes will differ, e.g. use of irrigation will increase.

4.3.7 Human Actions and their Effect

4.3.7.1 Approach to Human Actions

In the Kristallin-I safety assessment, a number of screening arguments (see Table 4.2.1) are used to restrict the range of human actions considered. Phenomena related to assumptions about changes in human behaviour and futuristic technologies are screened out, because it is not possible to predict these changes in any defensible manner. Phenomena related to future deliberate human intrusion into the repository are also excluded on regulatory advice (HSK & KSA 1993; see Subsection 4.1.1). Future inadvertent human actions with some capacity to by-pass or significantly alter the performance of the engineered and/or geological barriers are discussed below, considering a range of human activities that are realistic from a current point of view. In the following discussions, it is assumed that records of the repository or its location have been lost or neglected. This is only possible far in the future, e.g. beyond a few hundred or thousand years, or following some serious social or technical disruption.

4.3.7.2 Groundwater and Surface Water/Soil Pollution

Human activity unrelated to the repository may result in pollution of the groundwaters, surface waters, soils and sediments. In the case of groundwater pollution, contaminants could change the geochemistry of the higher-permeability domain basement rock, and hence affect the speciation, solubility and sorption of radionuclides released from the repository. In the Reference Scenario, radionuclide solubility limits and sorption processes are not accounted for in this unit, therefore no further calculations are required. In the case of surface and near-surface pollution, the speciation, solubility and sorption of radionuclides in the biosphere may be affected, as may the agricultural or fisheries potential of contaminated units. It is considered that the main effect of serious pollution would be to decrease any radiological impacts through lessening of local agricultural potential. Changes in sorption in the biosphere due to pollution are within the parameter variations already considered within the Reference Scenario. However, an effect of surface and near-surface groundwater pollution may be to make the extraction of deeper groundwaters more likely, see below.

4.3.7.3 Deep Groundwater Abstraction Wells

The crystalline basement could be considered as a water source and wells sunk to extract the groundwater, especially in the future if, for example, nearer-surface groundwater and surface waters become polluted. This would provide a direct pathway to man for radionuclides in the groundwater of the crystalline basement.

If pollution and water quality were a concern, then it is likely that the water would be analysed for natural and artificial contamination before use. Unless radioanalyses are performed, however, the presence of chemically tiny quantities of radionuclides that might originate from the repository would not be detected. The yield of a well in the crystalline basement will, in general, be rather low and, hence, the water would be insufficient for extensive irrigation, for example. Therefore, only drinking water is considered as a realistic exposure pathway for water abstracted from the crystalline basement. The consumption of drinking water abstracted from a deep groundwater well is treated as an alternative biosphere scenario in Kristallin-I.

4.3.7.4 Water Management Schemes

Water is a valuable resource and elaborate water management schemes may be devised to control and protect it. Significant water management is already practised along the Rhine valley in Northern Switzerland for hydro-electric power. Although such schemes may impact the point of exfiltration of contaminated groundwater and its dilution, it is considered that no processes would result that are not already covered by the Reference Scenario and alternative biosphere scenarios.

4.3.7.5 Mining and Deep Drilling

Based on present-day technologies, the following activities could inadvertently lead to disturbance of the repository or the host rock:

- exploration for minerals, especially oil and gas in the Permo-Carboniferous Trough;
- exploration for geothermal energy;
- investigation for waste disposal.

The crystalline basement of Northern Switzerland has no known mineral resources that are likely to attract mining activities (THURY et al. 1994). Furthermore, exploitation of the crystalline basement itself as a mineral source is highly unlikely because alternative sources of similar crystalline rock can be found in much more accessible locations, e.g. at outcrops in the Black Forest region.

Geological formations in proximity to the crystalline basement may attract exploratory drilling in the region. Deep drilling for oil and gas is possible, recognising the proximity of the Permo-Carboniferous Trough; however, such drilling would cease on interception of the crystalline rock. The Molasse Basin has been considered as a potential geothermal resource, but here the main interest is in confined sedimentary aquifer units. This is discussed in Subsection 4.3.7.6.

The only known examples of deep boreholes into the crystalline basement at present are those undertaken as part of the Nagra investigation programme. It is assumed that, if similar investigations for waste disposal are undertaken in future beyond the time at which specific records of the site are lost, then those undertaking the investigation will be aware of the possibility of earlier disposal operations and plan the investigation accordingly.

If deep drilling is undertaken in the crystalline basement in the future, e.g. for scientific or geothermal investigation, then, depending on the target depth and the drilling activity, the repository may or may not be detected. If the repository is detected, it is assumed that the necessary remedial action will be taken and the borehole will be sealed. Due to their limited diameter and spacing, inadvertent interception of the emplacement tunnels themselves is less likely than interception of the excavation-disturbed zone (possibly extending up to one tunnel diameter around the tunnels) or water-conducting features that are hydraulically connected to the repository.

Doses to geological investigators due to examination of core material following a direct hit on a high-level waste or spent-fuel canister have been variously calculated at between 40 mSv (NORDMAN & VIENO 1989) and 20 to 90 Sv (PRIJ et al. 1989), where the probabilities of these events were estimated at 10^{-8} y^{-1} (NORDMAN & VIENO 1989) and 2 to $60 \times 10^{-9} \text{ y}^{-1}$ (PRIJ et al. 1989). This indicates that the doses received may be very high and certainly exceed the regulatory dose criterion. However, the estimated annual probabilities are sufficiently low that the annual risk criterion of 10^{-6} , specified in HSK Protection Objective 2, would not be exceeded regardless of the dose.

4.3.7.6 Geothermal Exploitation

The potential for extraction of geothermal energy in Northern Switzerland has been discussed in RYBACH (1992a) and RYBACH (1992b). Two categories are considered:

- a) natural resources (thermal spring and stratiform aquifers)
- b) resources for artificially aided heat extraction (vertical heat exchanger and Hot Dry Rock systems)

Confined aquifers in the Molasse Basin (to the south of the crystalline basement units considered in Kristallin-I; see figure 3.5.1) are considered to be the most likely targets for extraction of natural geothermal waters, especially the Obere Meeresmolasse and Muschelkalk formations at depths of ca. 500 and 3500 m below ground. RYBACH notes the possibility of extraction from the upper weathered parts of the crystalline basement "at greater depth", i.e. lying below the Molasse Basin sediments at depths ca. 4000 m below ground.

Two distinct methods of artificially aided heat extraction are possible: vertical heat exchanger (VHE) and hot dry rock (HDR) systems.

The VHE is a closed circuit device for a fluid to take heat from the first tens/hundreds of metres of the ground and to feed the cold side (evaporator) of a heat pump. Up to now, over 8000 VHE systems have been installed in Switzerland in a range of geological media. The depth of such systems is generally rather shallow, only requiring a sufficient temperature to evaporate the pumped fluid, and hence VHE installations will not affect a deep repository.

The hydraulic properties of the crystalline basement of Northern Switzerland (low permeability and porosity) would necessitate heat extraction by HDR technology (i.e. introduction of water from the surface via a borehole with pumped circulation through natural or artificially stimulated fractures (hydrofracturing) in the rock, before return of the steam or steam/hot water to the surface via a second or more boreholes, see RYBACH 1992a; RYBACH 1992b).

Moderate geothermal gradients are observed in the crystalline basement of Northern Switzerland, in the range 35 to 45 °C km⁻¹, and the ambient rock temperature at a depth of 1200 m is expected to be a maximum of 60 °C (THURY et al. 1994). With existing technology, a viable geothermal energy scheme would require a source temperature of 150 to 200 °C; this could only be found by drilling to depths of about 3 to 5 km, i.e. well below the repository depth. Thus, an HDR-type geothermal installation at or near repository depth is considered very unlikely.

If, however, a HDR system were installed in a crystalline-basement block housing repository panels, this would provide a direct route for return of radionuclides to the biosphere. In the longer-term, after abandonment or closure of the thermal project, the higher permeability introduced by stimulated fractures would continue to be a factor leading to enhanced flow of water and possible transport of radionuclides in the affected zone. A particular feature of this unlikely scenario is that, if an installation were made, the repository may not be detected until after the drilling and hydrofracturing had been conducted and that, if detected afterwards, effective remedial action may not be possible.

It is concluded that, considering both the current technologies for geothermal exploitation and the local geothermal conditions, VHE installations would be too shallow to intercept the crystalline basement rocks and HDR installations would be too deep to affect the performance of a repository. It is, however, an open issue whether the possible future exploitation of the crystalline basement as a geothermal energy source should be considered as a factor against the siting of a repository in crystalline basement in principle, i.e. conflicting use of natural resources.

4.3.8 Summary of Evaluation and Treatment of Alternative Assumptions

As described in Subsection 4.3.2, the process of developing alternative scenarios applied in Kristallin-I is formalised in terms of identifying credible alternative assumptions to those adopted in the Reference Scenario. Various FEPs which give rise to scope for alternative assumptions have been discussed in Subsections 4.3.3 to 4.3.7.

Table 4.3.4 lists the key, or relevant, Reference Model Assumptions and assumptions of the Reference Scenario, summarises the alternative assumptions, and notes the evaluation (as discussed in previous sections) and consequent treatment in Kristallin-I safety assessment. The alternative assumptions are evaluated as:

- to be treated quantitatively in safety assessment calculations by means of parameter variation, alternative model assumptions or alternative scenarios (as indicated in the table) and discussed further in Subsection 4.4.1;
- reserve FEPs or open questions, and discussed further in Subsections 4.4.3 and 4.4.4 respectively;
- requiring no further investigation or discussion at present.

Key Reference Model Assumptions and Assumptions of the Reference Scenario	Possible Alternative Assumptions	Evaluation and Consequent Treatment
<i>Engineered barriers and radionuclide transport path (see Subsection 4.3.3)</i>		
1. Canisters are correctly sealed and thus do not fail earlier than 1000 years after emplacement.	One or more canister may be mis-sealed, possibly leading to early failure. <i>See Subsection 4.3.3.1.</i>	Low probability for any individual canister, controlled by quality control. Effect of early canister failure is examined by parameter variation . <i>See Subsection 5.2.3.1.</i>
2. The bentonite buffer is emplaced as planned, without significant problems.	Gaps or misplacement may be possible. <i>See Subsection 4.3.3.2.</i>	Problems should be identified by quality control. Achieving the required standard of emplacement is an open question for operation studies.
3. All canisters fail at the same time; failure at 1000 years after emplacement is a Reference Model Assumption.	Canister can be expected to fail over a range of times and, in general, might be remain unbreached for much longer than 1000 years. <i>See Subsection 4.3.3.3.</i>	The assumption of simultaneous failure at 1000 years is conservative. The effect of later failure is examined by parameter variation . <i>See Subsection 5.2.3.1.</i>
4. After failure, the canister has no physical effect on radionuclide releases.	If the canister fails by cracking or limited penetration, the crack or hole may offer resistance to radionuclide releases. <i>See Subsection 4.3.3.4.</i>	Scoping calculations indicate the effect may be important if the crack is filled with bentonite and/or canister corrosion products. Consider as a reserve FEP .
5. Reducing conditions will be ensured by infiltration of reducing groundwater and corrosion of the steel canister (and this is relied on in estimating solubility limits in the near field).	Radiolysis may be sufficient to provide oxidising conditions, especially in the case of a canister that fails locally, with little general corrosion, i.e. cracked canister. <i>See Subsection 4.3.3.5.</i>	Scoping calculations indicate that the reducing capacity of infiltrating groundwater is sufficient to ensure reducing conditions throughout most of the bentonite. No further consideration is needed.
6. Concentrations of radionuclides in solution close to the waste are limited by elemental solubility limits.	Concentrations in solution may be significantly reduced by sorption and co-precipitation with canister corrosion products. <i>See Subsection 4.3.3.6.</i>	Insufficient knowledge as to the important processes and solid phases; required thermodynamic data lacking. Identified as a reserve FEP .

Table 4.3.4: Key Reference Model Assumptions and assumptions of the Reference Scenario, with possible alternative assumptions and their evaluation and consequent treatment in Kristallin-I safety assessment.

Key Reference Model Assumptions and Assumptions of the Reference Scenario	Possible Alternative Assumptions	Evaluation and Consequent Treatment
7. Hydrogen generated by corrosion of steel canister will be dissipated and not affect radionuclide releases.	Hydrogen gas will not be dissipated and may either suppress canister corrosion or channel through the bentonite, in either case with some potential for affecting radionuclide releases. <i>See Subsection 4.3.3.7.</i>	Experimental evidence and modelling indicates there will probably be no significant effect on radionuclide releases due to the escape of a gas phase. A sand capillary-breaking layer could provide additional capacity for gas dissipation. Identified as an open question deserving future attention.
8. Radionuclides are released and transported through the engineered barriers by water-mediated processes.	Some radionuclides might be released and transported in gaseous forms. <i>See Subsection 4.3.3.8.</i>	The HLW inventory does not include significant quantities of radionuclides able to form gaseous phases. No further consideration is needed.
9. The bentonite will retain the required properties (e.g. low hydraulic conductivity, high swelling capacity, plasticity, cation-exchange capacity, filtration of colloids) over the period of assessment (at least 10 ⁶ years).	Some degradation of properties may occur either due to short-term (thermal) effects or long-term geochemical alteration. <i>See Subsection 4.3.3.9.</i>	Detailed consideration and calculations (see Subsection 3.4.4) indicate that significant alteration will not occur in such a massive buffer in the conditions of the crystalline basement. However, the effect of a performance loss in parts of the bentonite is examined by parameter variation . <i>See Subsection 5.2.3.6.</i>
10. The bentonite buffer will remain physically intact over the period of the assessment (at least 10 ⁶ years).	Flowing groundwater could physically erode the bentonite. <i>See Subsection 4.3.3.10.</i>	Calculations indicate that the maximum rate of erosion is trivial for the expected groundwater flowrates. No further consideration is needed.
11. The steel canister will remain approximately central within the bentonite buffer over the period of assessment (at least 10 ⁶ years).	The canister may sink through the buffer under gravity. <i>See Subsection 4.3.3.11.</i>	Calculations indicate that the canister will sink by only a few millimetres, but there is some uncertainty in the conceptual model. The FEP is identified as an open question deserving future attention.

Table 4.3.4: (Continued). Key Reference Model Assumptions and assumptions of the Reference Scenario, with possible alternative assumptions and their evaluation and consequent treatment in Kristallin-I safety assessment.

Key Reference Model Assumptions and Assumptions of the Reference Scenario	Possible Alternative Assumptions	Evaluation and Consequent Treatment
12. Radionuclides will be transported through the bentonite buffer in aqueous solution (only).	Radionuclides could be transported associated with colloids from glass dissolution or near-field precipitation processes. <i>See Subsection 4.3.3.12.</i>	This is prevented by the microporous structure of the bentonite (and potential alteration products) except under conditions of faulty emplacement or complete sinking, see 2 and 11 above.
13. Tunnels and shafts will be backfilled and sealed at closure, so that the only significant route for radionuclide release will be through the intact rock of the low-permeability domain.	The tunnels and shafts may provide an alternative route for radionuclide transport if tunnel seals prove ineffective. <i>See Subsection 4.3.3.13.</i>	To investigate the importance of such pathways, two cases - transport along backfilled tunnels and shafts, and transport along the associated excavation disturbed zone - are treated as an alternative scenario . <i>See Subsection 6.3.3.</i>
<i>Geological barriers and radionuclide transport path (see Subsection 4.3.4)</i>		
14. Radionuclides will be transported through the geosphere by groundwater mediated processes only.	Radionuclides could be transported by: (a) gas phase (b) human activity <i>See Subsection 4.3.4.1.</i>	(a) The HLW inventory does not include significant quantities of radionuclides able to form gaseous phases. However, the special case of radon at the geosphere-biosphere interface is an open question that deserves evaluation in future. (b) Human actions are considered in Subsection 4.3.7 and below.
15. Groundwater flow is topography driven.	Density differences due to thermal effects and salinity may modify groundwater flows. <i>See Subsection 4.3.4.2.</i>	The effects are expected to be small and are not considered in hydrogeological modelling for Kristallin-I. This is an open question deserving attention in future hydrogeological modelling studies.

Table 4.3.4: (Continued). Key Reference Model Assumptions and assumptions of the Reference Scenario, with possible alternative assumptions and their evaluation and consequent treatment in Kristallin-I safety assessment.

Key Reference Model Assumptions and Assumptions of the Reference Scenario	Possible Alternative Assumptions	Evaluation and Consequent Treatment
<p>16. The expected pathway for groundwater-mediated radionuclide transport is through the low-permeability domain of the crystalline basement to the higher-permeability domain and thence to discharge in gravel aquifers of the Rhine valley.</p>	<p>Alternatively, radionuclides may be carried</p> <p>(a) from the low-permeability domain to a major water-conducting fault and thence to the higher-permeability domain and/or</p> <p>(b) be discharged to a smaller valley (Area East only).</p> <p><i>See Subsection 4.3.4.3.</i></p>	<p>(a) Transport through a major-water-conducting fault is treated as an alternative model assumption.</p> <p><i>See Subsection 6.2.2.2.</i></p> <p>(b) The case of discharge to a small valley is identified as an alternative scenario (for Area East only) but is treated by biosphere parameter variation.</p> <p><i>See Subsection 6.2.1.3.</i></p>
<p>17. Radionuclides are advected through a single type of water-conducting feature, with characteristics which are constant in time and space. Matrix diffusion transports radionuclides within stagnant pore water of fracture infill material and wallrock.</p>	<p>Radionuclides are likely to be advected through a network of interconnected water-conducting features, with different and spatially-variable characteristics. The extent of diffusion-accessible matrix is uncertain.</p> <p><i>See Subsections 4.3.4.4 and 4.3.4.5.</i></p>	<p>Three alternative geometrical representation of water-conducting features, each with two alternative assumptions for the extent of diffusion-accessible matrix (six geometries in all), are treated as alternative model assumptions.</p> <p><i>See Subsection 6.2.2.1</i></p> <p>A case in which groundwater flow is distributed between water-conducting features is also treated as alternative model assumptions.</p> <p><i>See Subsection 6.2.2.4</i></p>
<p>18. Radionuclides are sorbed on matrix pore surfaces according to linear sorption isotherms, except in the case of Cs, for which sufficient data are available to define a Freundlich isotherm. In the Reference Case, non-linear Cs sorption is modelled implicitly, by conservative choice of a linear isotherm.</p> <p><i>See Subsection 5.3.4.4.</i></p>	<p>Sorption may be non-linear, with slow kinetics or partial irreversibility.</p> <p><i>See Subsection 4.3.4.6.</i></p>	<p>Non linear sorption of Cs can be treated explicitly using code RANCHMDNL. This may be regarded as a parameter variation of the exponent of the Freundlich isotherm.</p> <p><i>See Subsection 5.3.5.2.</i></p> <p>Enhanced long-term and irreversible sorption on matrix pores is identified as a reserve FEP.</p>

Table 4.3.4: (Continued). Key Reference Model Assumptions and assumptions of the Reference Scenario, with possible alternative assumptions and their evaluation and consequent treatment in Kristallin-I safety assessment.

Key Reference Model Assumptions and Assumptions of the Reference Scenario	Possible Alternative Assumptions	Evaluation and Consequent Treatment
19. Radionuclides will be transported through the geosphere in aqueous phase (only).	Radionuclides could be transported sorbed to naturally occurring colloids or colloids from bentonite-host rock interface interactions. <i>See Subsection 4.3.4.7.</i>	Reversible sorption of radionuclides on colloids is treated as an alternative model assumption , i.e. concentration of colloids is zero in Reference Case and is set at a conservative value in the alternative case. <i>See Subsection 6.2.2.3.</i> If sorption is irreversible, the effect of colloids on radionuclide transport will depend on the degree of colloid filtration/entrapment; this is an open question deserving future attention.
20. The effects of repository construction and emplacement on the long-term hydrogeological regime can be neglected.	An excavation-disturbed zone around the disposal tunnels may induce a significant modification of groundwater flow within the host-rock blocks. <i>See Subsection 4.3.4.8.</i>	(A) The zone is expected to be discontinuous and hence not induce significant modifications; this is, however, an open question for future hydrogeological modelling. (B) The zone is, conservatively, assumed to be continuous in radionuclide-transport calculations but, if discontinuous, then releases from the near field may be reduced, i.e. reserve FEP .
21. The existence of TRU silos in a neighbouring host-rock block can be neglected.	A cementitious (high pH) plume from the silos could modify the geochemistry of transport pathways from the HLW panels. <i>See Subsection 4.3.4.9.</i>	It is assumed that the silos can be sited so that there is no interaction with the HLW panels or radionuclide transport paths; this is retained as an open question for future site-specific studies.

Table 4.3.4: (Continued). Key Reference Model Assumptions and assumptions of the Reference Scenario, with possible alternative assumptions and their evaluation and consequent treatment in Kristallin-I safety assessment.

Key Reference Model Assumptions and Assumptions of the Reference Scenario	Possible Alternative Assumptions	Evaluation and Consequent Treatment
<i>Long-Term Geological and Climatic Changes</i>		
<p>22. Future (expected) geological and climatic changes can be neglected and the geological and hydrogeological regime remains as currently observed for the whole period of assessment.</p>	<p>(A) Future expected geological changes must be considered. A realistic prognosis is that Alpine orogeny will continue, with associated:</p> <ul style="list-style-type: none"> - regional uplift, - movement on existing faults, - stress changes and seismicity - erosion and denudation, - basement alteration. <p style="text-align: center;"><i>See Subsection 4.3.5.1.</i></p>	<p>This is defined as an alternative scenario in Kristallin-I, although, in practice, the calculations required fall within the Reference Scenario. The relevant processes have been considered (see Subsections 4.3.5.2-10) and it is concluded (see Subsection 4.3.5.11) that, given the conservative treatment of the higher-permeability domain in the assessment models, the only significant effect could be to change groundwater flowrate in the low-permeability domain, within the bounds of parameter variations for the Reference Scenario.</p>
	<p>(B) Future expected climatic changes must be considered. Possible alternative prognoses are that</p> <ol style="list-style-type: none"> 1. glacial-interglacial cycling will continue, or 2. a continuous warm climate will develop. <p>In either case changes may occur in:</p> <ul style="list-style-type: none"> - recharge, - erosion (uniform and linear), - groundwater chemistry, - groundwater discharge zone, - agriculture practices. <p style="text-align: center;"><i>See Subsection 4.3.6.1.</i></p>	<p>The relevant processes have been considered (see Subsections 4.3.6.2-7) and it is concluded that the major effects will be in the biosphere, where the effects can be scoped by considering alternative scenarios, namely:</p> <ul style="list-style-type: none"> - Dry Climate State, - Humid Climate State, - Periglacial Climate State, - Rhine Gravels Absent. <p style="text-align: center;"><i>See Subsection 6.3.4</i></p> <p>In addition:</p> <ul style="list-style-type: none"> - exfiltration to small valley is identified as an alternative scenario (but treated by parameter variation within the Reference Scenario) for Area East only. <p style="text-align: center;"><i>See Subsection 6.2.1.3</i></p>

Table 4.3.4: (Continued). Key Reference Model Assumptions and assumptions of the Reference Scenario, with possible alternative assumptions and their evaluation and consequent treatment in Kristallin-I safety assessment.

Key Reference Model Assumptions and Assumptions of the Reference Scenario	Possible Alternative Assumptions	Evaluation and Consequent Treatment
<p>23. Future (unexpected) geological changes can also be neglected.</p>	<p>The following are identified as potentially most important unexpected processes:</p> <p>(a) Changes in hydrothermal activity (which may modify groundwater flow and transport properties of water-conducting features).</p> <p><i>See Subsection 4.3.5.10.</i></p> <p>(b) Saline water intrusion from the PCT (which may affect fluid density and geochemistry).</p> <p><i>See Subsection 4.3.6.4.</i></p>	<p>(a) It is expected that potential zones of excessive hydrothermal activity can be avoided by siting.</p> <p>(b) Similarly, it is expected that the repository can be sited to avoid such effects.</p> <p>Both are identified as open questions for site investigation studies.</p>
<p>24. Future (unexpected) climate-induced changes can also be neglected.</p>	<p>Permafrost and ice sheet effects (meltwater recharge and ice loading) may cause modification of deep groundwater regime.</p> <p><i>See Subsection 4.3.6.6.</i></p>	<p>Current estimates indicate that permafrost in Northern Switzerland will not be deep enough to force ice sheet meltwater to the depth of the low-permeability domain. Identified as open question deserving future attention.</p>
<p><i>Future Human Actions</i></p>		
<p>25. The engineered and geological barriers are not significantly disturbed or degraded by future human actions.</p>	<p>The relevant processes have been considered and the following are identified as potentially most important:</p> <p>(a) water may be extracted from a deep well, by-passing expected near-surface dilution processes;</p> <p>(b) direct intrusion into the repository e.g. by drilling;</p> <p>(c) geothermal exploitation by Hot Dry Rock techniques within the crystalline basement.</p> <p><i>See Subsections 4.3.7.2-6.</i></p>	<p>(a) A deep well, which is used as a source of drinking water, is considered as an alternative scenario.</p> <p><i>See Subsection 6.3.2.</i></p> <p>(b) Doses to intruders may be high but the probability of intrusion will be very low, so that an annual risk of 10^{-6} will not be exceeded.</p> <p>(c) Geothermal exploitation of the crystalline basement is unlikely given there are other more promising targets in Northern Switzerland, but effect on repository performance could be significant.</p> <p>Both (b) and (c) are identified as open questions for future assessment studies.</p>

Table 4.3.4: (Continued). Key Reference Model Assumptions and assumptions of the Reference Scenario, with possible alternative assumptions and their evaluation and consequent treatment in Kristallin-I safety assessment.

4.4 Conclusions from Scenario Development for the Kristallin-I Assessment

Table 4.3.4 indicates how a critical examination of the key Reference Model Assumptions and assumptions of the Reference Scenario leads to the identification of FEPs that will be investigated in safety-assessment calculations (via alternative scenarios, alternative model assumptions or parameter variations) plus FEPs that are not treated quantitatively because they are either unimportant, reserve (believed to be beneficial to safety, but not included in current models) or open questions (potentially detrimental, although believed to be either unimportant or avoidable by design or siting, but still requiring attention in the future); see also Figure 4.1.2.

The following subsections:

- summarise the set of safety-assessment calculations defined by the scenario development and intended to investigate the uncertainty due to selection and representation of FEPs (Subsection 4.4.1);
- define a scenario for robust safety demonstration, to illustrate the level of safety that can be confidently expected, even given the present level of uncertainty (Subsection 4.4.2);
- comment on reserve FEPs, including those identified from more detailed considerations, evaluate these and identify the most important (Subsection 4.4.3);
- comment on the open questions identified in Table 4.3.4 and indicate the general type of future work that might allow them to be resolved (Subsection 4.4.4).

4.4.1 The Set of Safety Assessment Calculations

4.4.1.1 The Reference Scenario

The Reference Scenario has been defined in section 4.3.1 and is based on the Safety Concept described in Section 3.2; the scenario takes advantage of the following factors.

- The careful engineering and use of large quantities of well understood materials in the engineered barriers limits the possibilities for detrimental processes to act, so that the evolution of the near field is most likely to follow the course described in the Safety Concept (see Section 3.2 and Figure 4.3.1).
- The siting of the repository at depth in low-permeability, geologically stable, basement rock also protects and ensures the stability of the engineered barriers.

- The significant thicknesses of overlying higher-permeability basement and sediments effectively buffer the host rock from surface environmental changes associated with changes in climate.
- The conservative treatment of certain processes in modelling the Reference Scenario (in particular, instantaneous radionuclide transport through the major water-conducting faults and higher-permeability domain of the basement) avoids the need to make detailed consideration of the time-dependent response of the hydrogeological system to environmental change.
- Inadvertent human intrusion into the repository is unlikely due to its siting in crystalline basement with no known mineral resources.

The main characteristics of the Reference Scenario in terms of the three "fields" or regions of the disposal system (see Chapter 5) are:

- for the near field - a conservative (pessimistic) degradation and performance of engineered barriers, but respecting the design function of the barriers;
- for the geosphere - constant geological and hydrogeological regime, based on understanding of present-day conditions;
- for the biosphere - present-day topography, hydrology and climate, with a subsistence community (conservative behaviour) located at the region of geosphere discharge.

4.4.1.2 Alternative Model Assumptions Within the Reference Scenario

Within the Reference Scenario, there is uncertainty about how to treat certain key FEPs and this is explored through alternative model assumptions. These are identified from Table 4.3.4 as follows:

- **Radionuclide transport through a major water-conducting fault:** The Reference Model Assumption within the Reference Scenario is immediate transport of radionuclides emerging from the low-permeability domain to the biosphere. To investigate the significance of major-water-conducting faults to radionuclide transport, these are represented explicitly in an alternative model assumption (see Subsection 6.2.2.2).
- **Alternative water-conducting feature geometries:** The effect of variability in the geometrical properties of water-conducting features is investigated in calculations of three, alternative geometrical representations (see Subsection 6.2.2.1).

- **Limited and unlimited matrix diffusion:** Uncertainty in the extent of matrix diffusion is represented by two alternative assumptions, applied to all three of the alternative geometrical representations, to form six alternative cases in all (see Subsection 6.2.2.1).
- **Distribution of groundwater flow in water-conducting features:** The Reference Model Assumption in the Reference Scenario is that all water-conducting features involved in radionuclide transport carry the same groundwater flow, based on the mean Darcy velocity. The effect of variability in the transmissivity of the water-conducting features, leading to a distribution in the rate of radionuclide transport between water-conducting features, is investigated as an alternative model assumption (see Subsection 6.2.2.4).
- **Transport of radionuclides with groundwater colloids:** The Reference Model Assumption in the Reference Scenario is that sorption on groundwater colloids can be neglected; only transport in the aqueous phase is modelled. Radionuclide sorption and transport of radionuclides on groundwater colloids is modelled explicitly as an alternative model assumption (see Subsection 6.2.2.3).

4.4.1.3 Parameter Variations Within the Reference Scenario

Table 4.3.4 also identifies some uncertainties that should be investigated by parameter variations, specifically:

- early canister failure, e.g. due to faulty canister sealing;
- later canister failure, i.e. failure at times later than the reference time of 1000 years after closure;
- loss of performance of the bentonite over part of its thickness, e.g. due to alteration affecting part of (but not the whole of) the bentonite;
- the effect of non-linear sorption of Cs, which can be treated explicitly by the computer code RANCHMDNL - this can be regarded as a parameter variation in the exponent of the Freundlich isotherm for Caesium sorption (which is assigned a reference value of unity).

However, a much greater range of uncertainties also needs to be treated by parameter variation to investigate data uncertainties which are not discussed in this chapter. Reference ("realistic-conservative") and alternative (usually "conservative") model parameter values have been derived in Section 3.7 and their impact is evaluated in Chapter 5.

4.4.1.4 Alternative Scenarios

In the Kristallin-I safety assessment, alternative scenarios are defined to investigate the impact of FEPs that are not included in the Reference Scenario. From Table 4.3.4, the only alternative scenarios that are considered both reasonably likely to occur, and have some potential impact on repository performance so as to warrant quantitative evaluation in the Kristallin-I safety assessment, are identified as follows.

- **Transport in Tunnels and Shafts** - The importance of radionuclide transport along tunnels and shaft, such as might occur if tunnel/shaft seals are ineffective, is considered as an alternative scenario. Two cases are distinguished and treated as alternative model assumptions within the scenario: transport along the backfilled tunnels and shafts and transport along an associated excavation disturbed zone assumed to be continuous.
- **Exfiltration to Small Valley** - This is a possibility for a repository in Area East only. It may occur (but is considered unlikely) under present-day conditions, and it is also possible in future following uplift of the Southern Black Forest region and downcutting of rivers, e.g. the Wutach, that drain the region. It will affect initial dilution in the biosphere.
- **Continuation of Alpine Orogeny** - This is the expected geological evolution and may lead to some hydrogeological changes compared to the present day. However, given the conservative treatment of the radionuclide transport through the major-water-conducting faults and higher-permeability domain of the basement in assessment models, it can be assessed by a change in the groundwater flowrate in the low-permeability domain which is within the parameter variations that are carried out within the Reference Scenario.
- **Alternative Climate-related Scenarios** - number of alternative scenarios are defined that span the range of conditions that may arise due to long-term climate changes.
 - **Dry Climate State** - This affects conditions in the biosphere, notably soil water balance and rate of irrigation.
 - **Humid Climate State** - This affects conditions in the biosphere, notably soil water balance and vegetative yield.
 - **Periglacial Climate State** - This affects conditions in the biosphere, notably soil water balance, available foodstuffs, human habits and diet. The biosphere may also be isolated from deep groundwater by continuous permafrost.

- **Rhine Gravels Absent** - This is possible due, for example, to glacial erosion, and is a condition existing at present on some stretches of the river Rhine. In this scenario, discharge may occur either to the river Rhine (with immediate dilution) or to deep soil lying directly above the basement.
- **Deep Groundwater Well** - A deep well in the crystalline basement is considered unlikely with present-day conditions since water is more readily available from other sources. The scenario may be more likely in future if near-surface water sources are polluted. The scenario is investigated because it provides a case of minimum dilution of radionuclides. However, drinking water is the only exposure pathway considered.

The main characteristics of these scenarios relative to the Reference Scenario are summarised in Table 4.4.1, where they are reordered according to the order of discussion in Chapter 6.

The majority of scenarios are treated by an appropriate selection of parameter values within the assessment model chain (codes STRENG, RANCHMD and TAME - see Chapter 5). In the case of the scenario **Continuation of Alpine Orogeny**, the parameter values necessary to represent the scenario are within the range of the parameter sensitivity study carried out for the Reference Scenario. Specifically, the effects of continued Alpine orogeny with most potential radiological impact are (i) change in the path length through the higher-permeability domain of the crystalline basement and (ii) slightly higher groundwater flows at repository depth. The former is irrelevant within the Reference Model Assumptions, where transport through the higher-permeability domain is considered to be instantaneous (see Subsection 5.3.1), and the latter is covered by parameter variations within the Reference Scenario. No specific reference to **Continuation of Alpine Orogeny** is therefore made in Chapter 6.

Several of the alternative scenarios (**Exfiltration to a Small Valley** and the Alternative Climate-related Scenarios) only affect the modelling of the biosphere although, in these cases, the TAME input datasets are substantially modified. In the case of **Periglacial Climate State**, with continuous permafrost developed, the biosphere is isolated from further input of contaminants from the geosphere.

Only two scenarios involve a significant change in the assessment model chain. A simple alternative geosphere model is used to represent Transport in Tunnels and Shafts (hereafter referred to as **Tunnel/Shaft Seal Failure**) and, for the **Deep Groundwater Well**, the biosphere is replaced by a drinking water model, taking account of the daily fluid intake by an individual and ICRP radionuclide ingestion to dose factors (see Subsection 6.3.2).

Scenario	Main characteristics	Represented by
Reference Scenario	<ul style="list-style-type: none"> - Expected near-field evolution. - Radionuclide release and transport in groundwater. - Constant hydrogeology and biosphere based on present day. - Agricultural subsistence group. (see Figure 4.3.1) 	Reference Assessment Model Chain: STRENG, RANCHMD & TAME. (See Chapter 5).
Continuation of Alpine Orogeny (included within the Reference Scenario in the following chapters)	Erosion and southward movement of river Rhine lead to changed flowpath in HPD and changed groundwater flow in the LPD.	Parameter variations in STRENG and RANCHMD: Increased groundwater flow at repository depth. (Covered by parameter variations within the Reference Scenario in Chapter 6).
Exfiltration to Small Valley (included within the Reference Scenario in the following chapters)	For Area East only, exfiltration to gravel aquifer of a small tributary valley.	Parameter changes in TAME. (Covered by separate calculations within the Reference Scenario in Chapter 6).
Deep Groundwater Well	Well abstracting water directly from the crystalline basement. Exposure by drinking water only.	TAME biosphere model replaced by simple drinking water dose model.
Tunnel/Shaft Seal Failure	<ul style="list-style-type: none"> - Tunnel/shaft seals ineffective after repository closure. - Radionuclide movement along tunnels and shafts and/or associated EDZ. 	Simple model for transport from near field to biosphere replaces geosphere model. (See Subsection 6.3.3).
Alternative Climate-Related Scenarios		
• Dry Climate State	Increased evap. and decreased ppt. Increased irrigation. Agricultural subsistence group.	Parameter changes in TAME.
• Humid Climate State	Increased ppt. and evap. Agricultural subsistence group.	Parameter changes in TAME.
• Periglacial Climate State	Decreased ppt. and evap. Reduced flow in river/local aquifer. Subsistence group based on herding. Continuous permafrost developed.	Parameter changes in TAME. Isolation of biosphere from further contaminant input.
• Rhine Gravels Absent	No local aquifer. Exfiltration directly to river Rhine or to deep soil directly overlying basement.	Parameter changes in TAME.

Note: Because of the simplifications of the assessment models, the Reference Scenario, as represented by the models, is sufficiently broad to represent a range of scenarios for future evolution - in particular, Continuation of Alpine Orogeny and Exfiltration to a Small Valley.

Abbreviations: ppt. = precipitation; evap. = evapotranspiration;
 LPD = low-permeability domain of the crystalline basement;
 HPD = higher-permeability domain of the crystalline basement;
 EDZ = excavation disturbed zone.

Table 4.4.1: Summary of scenarios for quantitative evaluation in Kristallin-I safety assessment.

4.4.2 Scenario for Robust Safety Demonstration

Subsection 4.3.3 indicates that, whereas there is uncertainty concerning processes that might affect the evolution and performance of the engineered barriers, the effect of these is minimised by the massive nature of the barriers, and the deleterious events and processes that have been identified can be avoided by attention to design, siting and quality control. There is considerably greater uncertainty pertaining to the characteristics of the geological barrier at this stage of investigation, since only general characteristics of the crystalline basement and properties measured at individual boreholes are known. In addition, some of the processes occurring in the geological barriers are not well understood (for example, colloid dynamics and the reversibility of radionuclide sorption on colloids). The conditions within the surface environment and man's future use of the environment are very uncertain, and uncertainties related to the latter are essentially irreducible. However, these uncertainties should not be a determining factor in safety assessment or taken as an obstacle to the planning and development of a repository system. Hence, whereas uncertainties in the performance of the engineered and geological barriers should be fully explored in safety assessment, models of the surface environment and human behaviour (biosphere) should be representative (see also Subsections 2.4.2 and 2.4.3).

The following case is therefore selected as suitable to illustrate the level of safety that can be confidently expected, even given the present level of uncertainty.

- The **evolution and performance of the engineered barriers according to their design function** (safety concept) should be assumed (see Section 3.2). As has been noted in Section 3.4 and Subsection 4.3.3, the engineered barriers may realistically perform better than this, and current models neglect a number of key processes that might further reduce radionuclide releases (see Subsection 4.4.3).
- The **most pessimistic possible representation of the geological barriers** should be assumed. That is, radionuclides reaching the bentonite-host rock interface should be assumed to be transported immediately to the biosphere, neglecting any retarding effects of the geological barriers; this covers uncertainty in the characteristics of the transport pathway (i.e. the characteristics of the water-conducting features) and also uncertainty in processes (e.g. the possible significance of irreversible sorption on colloids). Thus radionuclide release from the near-field model should be input directly to the biosphere model. In this case, the only requirements placed on the geological barriers are favourable geochemical conditions and mechanical and hydraulic protection of the engineered barriers, including assurance of low groundwater flow which is an important boundary condition to the near field model. As a variant, the case of a zero concentration boundary at the bentonite-host rock interface should be tested (this represents a case in which radionuclides are removed from aqueous solution at the interface, e.g. by sorption on colloids).

- The **present-day surface environment and conservative human behaviour** should be assumed. Thus the biosphere should be represented by the model as defined for the Reference Scenario (see Section 5.4). This model includes realistic near-surface dilution, a range of potential accumulation processes and exposure pathways, plus conservative assumptions concerning human diet and behaviour.

4.4.3 Reserve Features, Events and Processes

A reserve FEP is a feature, event or process that has beneficial effects for the safety of the disposal system but is not incorporated in the current assessment models. This may be because of lack of data, or, sometimes, for reasons of mathematical or modelling convenience. Exclusion of a reserve FEP from a model will tend to make the resulting model conservative, though the degree of conservatism may be difficult to assess. Such FEPs may be the target of future research and/or model development.

In order to qualify as a *significant* reserve FEP, two requirements should be met.

- First, **it must be possible for the FEP to be relied upon**, that is, by some means (e.g. scientific research, measurement, siting or design), the information could be acquired or the repository system arranged so that the FEP could be justifiably included in assessment models. FEPs related to human behaviour, for example, are unlikely to qualify, since no research or measurement can be devised that would allow reliance to be placed on assumptions about human behaviour in the far future.
- Second, if taken account of in assessment models **it should offer some additional degree of safety**. There are two aspects to safety: performance and confidence in performance. For example, it is expected that the steel canister may remain unbreached for times far exceeding the 1000 years of the Reference Model Assumptions. If it could be assured that the canister would remain intact for 10 000 years then, in the case of the Kristallin-I disposal concept, this would not offer much additional performance (see Subsection 5.2.3.1). However, it might offer confidence that, even in the event of some very unlikely degradation of the buffer, releases could not occur at early times.

Table 4.4.2 identifies and makes summary comments and evaluation of reserve FEPs in the Kristallin-I assessment. These include the reserve FEPs identified in Table 4.3.4, plus those identified from more detailed consideration (SUMERLING & GROGAN 1994). Those which are thought to be most important, i.e. have the potential to reduce, significantly delay or dilute radionuclide releases to the biosphere, are indicated by bold type in the table and are as follows.

- **Immobilisation or co-precipitation with glass secondary minerals and/or canister corrosion products** - Solubility limits close to the waste are presently assessed for pure phases; retention of radionuclides in or with other solids/gels could considerably reduce concentrations in aqueous solution near to the wastes.

- **Natural concentrations of safety-relevant radionuclides in groundwater** - The natural concentration of radionuclides at the bentonite-host rock interface is neglected at present but, if considered, would reduce the calculated concentration gradient across the bentonite, notably for uranium isotopes.
- **Effect of bentonite swelling and the limited extent of the excavation-disturbed zone (EDZ)** - Fractures within the EDZ around the emplacement tunnels are expected to dilate due to stress relief during construction and operation of the repository. The EDZ is currently assumed to be continuous and to act both as a uniform boundary condition for diffusion through the bentonite and as a higher-permeability conduit for radionuclide advective transport from the outer boundary of the bentonite to water-conducting features in the host rock. The continuity of the EDZ is not known, but, following closure, the swelling pressure of the bentonite may be sufficient to close (restore the dilation of) all or some of these fractures, making it more likely to be discontinuous. If this is taken into account, then some axial as well as radial diffusion must be required for radionuclides to reach water-conducting features in the host rock. Furthermore, the radionuclides released from each canister may reduce the concentration gradients seen by neighbouring canisters.
- **Connectivity and variability of path through water-conducting features in the low-permeability domain** - At present, variability in hydraulic and geometrical characteristics along the length of individual water-conducting features, and the variability between one feature and another, is neglected. A single set of constant characteristics is selected conservatively; if variability along the path is considered, this conservatism can be relaxed and calculated radionuclide transport reduced; if this variability is taken in conjunction with a limited extent of the EDZ (above), then the range of characteristics of water-conducting features could be taken into account, i.e., only a small proportion of canisters will be connected to more transmissive features.

4.4.4 Open Questions

An open question is a feature, event or process that is not dealt with within the current safety assessment but is recognised as having some potential to adversely affect the safety of the repository. The reason for omission at this stage is usually that it is believed to have a low probability of occurrence or may be avoided by some means. The lack of quantitative investigation at this stage may also be related to a lack of data or appropriate models.

Table 4.4.3 lists key open questions that have been identified during the scenario development process (see Table 4.3.4) and have already been discussed in the sections indicated; the comments describe the assumption or treatment in the Kristallin-I assessment and indicate the general type of future work which might allow the open question to be resolved.

Reserve FEPs and evaluation (1)	Comments
<p>Glass cracking and surface area (1.5a/b)</p> <p>Effect may be marginal, but could be tested mathematically.</p>	<p>The glass is likely to crack into relatively few large fragments plus small shards, but is modelled as though is it cracked into a large number of equal volume (spherical) units with total initial surface area 12.5 times that of the monolithic block. This may be over conservative at long times when only the large fragments are left to dissolve.</p>
<p>Glass solute transport resistance (1.16)</p> <p>No reliable data are currently available.</p>	<p>To dissolve the glass, water must penetrate into the cracks between fragments. As dissolution proceeds, these will be filled with alteration products/silica gels. Similarly, radionuclides must diffuse out along these constricted paths. This may retard the glass dissolution process and also nuclide release.</p>
<p>Co-precipitates/solid solutions (1.14)</p> <p>Potentially very important.</p>	<p>Radionuclides could be co-precipitated or immobilised in glass alteration layers, with release to aqueous solution much delayed or prevented.</p>
<p>Elemental solubility limits (1.15)</p> <p>May be important for some radionuclides but requires more detailed calculations and/or experiments to justify concentrations of elements in pore fluids close to the wastes.</p>	<p>Maximum concentrations of radionuclides close to the wastes are calculated taking account of sharing of solubility limits but only considering stable element inventories from the dissolved glass. Consideration of stable element concentrations originating from groundwater and canister corrosion could reduce effective solubility limits for some radionuclides, e.g. Ni isotopes due to stable nickel from the stainless steel fabrication flask.</p>
<p>Total canister corrosion rate (2.8)</p> <p>Within a wide range, the time of mechanical canister failure, which follows weakening by corrosion, does not significantly affect the time (or magnitude) of peak release from the engineered barriers, which is limited by the dynamics of diffusion through the bentonite (see Subsection 5.2.3.1).</p>	<p>The Reference Case assumes canister failure at 1000 years, which implies corrosion of at least 50 mm in the same period to reduce canister wall thickness to 200 mm. Even allowing maximum reactions with oxygen and sulphide to account for 10 mm this implies a rate of $40 \mu\text{m y}^{-1}$ for anaerobic corrosion compared to the rates of 1 to $5 \mu\text{m y}^{-1}$ that could probably be justified from experimental data. This indicates a canister lifetime of 8000 to 40 000 years, or even longer, since assumptions for canister failure are also pessimistic, see below.</p>
<p>Canister failure (2.12a)</p> <p>Questions of uneven stresses, including those due to canister corrosion products may be difficult to resolve.</p>	<p>Calculations indicate that the canister will easily withstand an external isostatic pressure of 30 MPa (i.e. the hydrostatic pressure plus the bentonite swelling pressure) even after significant corrosion (calculated stresses = a factor of 5 less than tensile strength). Hence, provided corrosion is low (see 2.8, above) the canister may remain unbreached considerably longer.</p>

- Notes: 1. Assessment of the likelihood that the FEP could be proved, or additional safety could result from incorporation.
2. FEPs indicated in **bold** are those estimated to be most important.
3. FEPs are numbered (in brackets) according to the scheme in Table 4.2.2.

Table 4.4.2: Features, events and processes, not included in Kristallin-I assessment models, that might provide additional safety - reserve FEPs.

Reserve FEPs and evaluation (1)	Comments
<p>Residual canister (2.13)</p> <p>Although the canister may fail by cracking or local penetration, the subsequent behaviour, e.g. crack extension and opening under mechanical stresses, is uncertain.</p>	<p>The canister is expected to fail by cracking or local penetration by corrosion and will therefore pose a residual transport barrier to water ingress and radionuclide release. Calculations indicate diffusive transport from radially cracked canister is not markedly lower than that assuming no canister, unless the crack is filled with bentonite or corrosion products. In this case, a considerable reduction in release is calculated.</p> <p>(Note: chemical buffering effect (2.14) is included in Kristallin-I assessment).</p>
<p>Radionuclide sorption and co-precipitation (2.15)</p> <p>Potentially very important.</p>	<p>Radionuclides are likely to be sorbed and co-precipitated with canister corrosion products, but this is neglected in the Kristallin-I assessment. The effect could reduce concentrations of radionuclides in solution, reducing the source concentration for diffusion in the bentonite. The effect is only beneficial if it brings concentrations below the solubility limits already applied.</p>
<p>Effect of hydrogen production on corrosion (2.17)</p> <p>No reliable data are currently available to model this process.</p>	<p>In the Kristallin-I assessment, no account is taken of the effect on the rate of canister corrosion of the possible formation of a hydrogen gas phase. If a gas phase forms, then this may suppress further corrosion by limiting the access of water to the canister surface, thus leading to a longer canister lifetime.</p>
<p>Corrosion products (physical effects) (2.18)</p> <p>(a) Potentially a very long canister lifetime would result, but argument is difficult to sustain.</p> <p>(b) Continuity of layer cannot be guaranteed, especially following canister failure.</p>	<p>As corrosion proceeds, a continuous layer of corrosion products (e.g. magnetite) is expected to develop.</p> <p>(a) For corrosion to be sustained, water must be able to diffuse through this layer. At repository pressures, the amount of free water in the corrosion product layer may be limited, hence, the rate of corrosion will drop or even cease.</p> <p>(b) If a continuous corrosion product layer exists, then outward radionuclide transport would also be retarded, especially if sorption is considered (see 2.15 above).</p>

- Notes:
1. *Assessment of the likelihood that the FEP could be proved, or additional safety could result from incorporation.*
 2. *FEPs indicated in **bold** are those estimated to be most important.*
 3. *FEPs are numbered (in brackets) according to the scheme in Table 4.2.2.*

Table 4.4.2: (Continued). Features, events and processes, not included in Kristallin-I assessment models, that might provide additional safety - reserve FEPs.

Reserve FEPs and evaluation (1)	Comments
<p>Colloid filtration (3.11)</p> <p>No reliable data available and probably less effective than 1.14 and 2.15 above.</p>	<p>If stable colloids that incorporate or sorb radionuclides form close to the wastes and these are filtered/entrapped in the bentonite, then a reduction in radionuclide concentration in solution, and hence in the source term for aqueous diffusion, is achieved.</p>
<p>Radionuclide transport through the buffer (3.16) - effect of bentonite between canisters.</p> <p>This effect may be small (see 2.13 above) unless the excavation-disturbed zone is discontinuous (see 4.7 below).</p>	<p>Present calculations assume 1D diffusion with radial symmetry, i.e. neglecting diffusion into bentonite between canisters.</p>
<p>Interaction between canisters (3.20)</p> <p>Relies on proving low groundwater flows parallel to the tunnel axis at the bentonite-host rock interface.</p>	<p>The 'plume' of radionuclides released from one canister may reduce the concentration gradient across the bentonite adjacent to neighbouring canisters.</p>
<p>Natural radionuclides (4.2)</p> <p>Potentially important for uranium decay series.</p>	<p>The naturally occurring concentrations of radionuclides, notably the uranium decay series, in groundwater will reduce the concentration gradient across the bentonite.</p>
<p>Effect of bentonite swelling on the excavation-disturbed zone (4.4)</p> <p>Potentially important (see also 4.7 and 4.8 below).</p>	<p>The swelling pressure may be sufficient to close (restore dilation of) fractures that are expected to dilate due to stress changes during the excavation and open period. Hence the EDZ may not act as a conduit for groundwater flow and radionuclide transport as assumed in the Kristallin-I assessment.</p>
<p>Water flow at the bentonite-host rock interface (4.7)</p> <p>Radionuclide migration (4.8)</p> <p>Accounting for the spatial distribution of water flow at the interface is potentially very important since, for the majority of canisters,</p> <p>(a) the gradient driving diffusion is decreased and</p> <p>(b) the distance for diffusion is increased.</p>	<p>The Kristallin-I assessment assumes that radionuclides diffusing across the outer boundary of the bentonite are conveyed instantaneously (by axial advection along the EDZ) to water-conducting features within the host rock, which are typically 10 to 20 m apart. This requires flow along the bentonite-host rock interface (EDZ). If axial flow were, however, negligible or discontinuous, then radionuclides would have to diffuse axially, either through the bentonite or through the host rock, as well as radially. The results would be that:</p> <p>(a) canister plumes would be more likely to interact and the gradients driving diffusion would be reduced;</p> <p>(b) the distance through which radionuclides would have to diffuse before reaching a water-conducting feature would be increased.</p>

- Notes:
1. *Assessment of the likelihood that the FEP could be proved, or additional safety could result from incorporation.*
 2. *FEPs indicated in **bold** are those estimated to be most important.*
 3. *FEPs are numbered (in brackets) according to the scheme in Table 4.2.2.*

Table 4.4.2: (Continued). Features, events and processes, not included in Kristallin-I assessment models, that might provide additional safety - reserve FEPs.

Reserve FEPs and evaluation (1)	Comments
<p>LPD effective hydraulic properties (5.1)</p> <p>Not possible to determine conductivity or connectivity over the 100m scale directly (by field measurements) in such a low-permeability medium, and therefore it would be difficult to prove a lower estimate.</p>	<p>The estimated hydraulic conductivity of the low-permeability domain (LPD) used in hydrogeological modelling is based on borehole measurements. These measure conductivity over the range of a few metres. On a larger scale, limited connectivity of water-conducting features in the LPD may mean that the average conductivity over the (~ 100 m) scale which is relevant to modelling is considerably lower.</p>
<p>Water-conducting features types (5.2) and Radionuclide transport through LPD (5.5)</p> <p>Potentially very important, although requiring a relatively detailed site-specific investigation of the characteristics of water-conducting features to prove.</p>	<p>The Kristallin-I assessment assumes the most conservative treatment of water-conducting features (the assumed continuity of the EDZ - see 4.7, above - allows releases from all canisters potential access to a path with the most conservative transport characteristics). If the repository is treated as a spatially extensive body with limited or no axial transport along the excavation-disturbed zone, then the variation in characteristics of the water-conducting features becomes significant, with different sectors of repository accessing features of differing characteristics. In addition, at present, a path of constant characteristics is assumed, whereas the actual path may consist of several water-conducting features in series, each with variation along their length.</p>
<p>Radionuclide transport through the major water-conducting faults (MWCF) (6.5)</p> <p>Uncertainty in properties of MWCF leads to conservative approach chosen.</p>	<p>This is neglected at present since even somewhat non-conservative calculations indicate that possible retardation in the MWCF is negligible compared to that in the low-permeability domain.</p>
<p>Filtration (8.8)</p> <p>Limited importance</p>	<p>Water for animal consumption is assumed not to be filtered, i.e. concentration includes suspended particulates.</p>
<p>Irrigation (8.33)</p> <p>Undoubtedly conservative but any alternative assumption might be criticised as arbitrary.</p>	<p>Irrigation is an important transfer path from aquifer to soil in the Kristallin-I reference biosphere model. An area of agricultural soil is assumed to be continuously irrigated, causing radionuclides to build up (for some radionuclides, over thousands of years). Such continuous irrigation and agricultural use seems unlikely.</p>
<p>Consumption of uncontaminated products (8.44)</p> <p>An assessment basis decision.</p>	<p>Dose is calculated for an individual obtaining their total dietary and water intake from a limited area of land, coinciding with the area assumed to be affected by any release from the repository. Such a situation is rarely observed today in developed cultures.</p>

- Notes: 1. *Assessment of the likelihood that the FEP could be proved, or additional safety could result from incorporation.*
2. *FEPs are numbered (in brackets) according to the scheme in Table 4.2.2.*

Table 4.4.2: (Continued). Features, events and processes, not included in Kristallin-I assessment models, that might provide additional safety - reserve FEPs.

Open Questions	Comments
<p>Poor emplacement of buffer (3.23)</p> <p>(discussed in Subsection 4.3.3.2)</p>	<p>It is assumed the precompacted bentonite blocks can be placed remotely around the HLW canister without significant problems.</p> <p>Engineering feasibility tests will be necessary to confirm this before final implementation.</p> <p>However, these need not be undertaken until after design optimisation studies.</p>
<p>Hydrogen production (2.16) and bentonite gas permeability (3.15)</p> <p>(discussed in Subsection 4.3.3.7)</p>	<p>It is assumed that hydrogen from the canister corrosion will be able to dissipate or channel through the bentonite backfill without significant implications for long-term radiological performance of the near field.</p> <p>Recent experimental and modelling work under the CEC MEGAS project could be reviewed and modelling or calculations specific to the Nagra concept undertaken. In particular, the extent to which gas dissipation can be affected by a capillary breaking layer (or other engineered features) should be modelled.</p>
<p>Canister sinking (3.7)</p> <p>(discussed in Subsection 4.3.3.11)</p>	<p>It is assumed that the compacted bentonite will behave as a solid with strain-hardening properties so that sinking will be negligible.</p> <p>Alternative models for long-term behaviour of bentonite should be considered. In addition, possible design measures to reduce or prevent sinking, and their implications for safety, should be reviewed and quantified.</p>
<p>Radon pathways and doses (8.45)</p> <p>(discussed in Subsection 4.3.4.1)</p>	<p>Radon (^{222}Rn) and its short-lived daughters are not considered explicitly in the Kristallin-I assessment; the $4N+2$ radionuclide chain is simplified, as shown in Appendix 2 (Table A2.2).</p> <p>The potential for transport of radon across the geosphere-biosphere interface, and also possible dose pathways due to radon and its short-lived daughters, should be examined by scoping calculations.</p>
<p>Density-driven flows (7.13)</p> <p>(discussed in Subsection 4.3.4.2)</p>	<p>Kristallin-I hydrogeological modelling considers topographically-driven flows only (the effect of water influx along the boundary representing the Permo-Carboniferous Trough, which may be thermally driven, has also been tested). The modifying effects of density differences due to groundwater temperature and salinity should be examined by scoping calculations.</p>

Note: FEPs are numbered (in brackets) according to the scheme in Table 4.2.2.

Table 4.4.3: Open questions identified from the scenario development process and comments on present assumptions and possible future work

Open Questions	Comments
<p>Irreversible radionuclide sorption on groundwater colloids (5.9/5.15/6.9/6.15)</p> <p>(discussed in Subsection 4.3.4.7)</p>	<p>It is assumed that radionuclides do not become irreversibly sorbed to groundwater colloids. Such radionuclides might not be subject to the important retardation processes of matrix diffusion and sorption on matrix pores. It is probable that filtration/entrapment would deplete the population of radionuclide-bearing colloids and lead to reduced radionuclide releases. It is, however, possible that a fraction of colloids with irreversibly-sorbed radionuclides would be transported relatively rapidly through the crystalline basement. Illustrative calculations of radiological impact can be made; an extremely pessimistic assumption, in which transport through the geosphere is considered instantaneous, is adopted in the Kristallin-I Robust Scenario.</p>
<p>Hydrogeological effect of the excavation-disturbed zone (4.1/4.7)</p> <p>(discussed in Subsection 4.3.4.8)</p>	<p>The presence of disposal tunnels and excavation-disturbed zone is neglected in hydrogeological modelling, which is equivalent to assuming that the zone is not continuous. The hydrogeological effect of the disposal tunnels and excavation-disturbed zone should be investigated by scoping calculations.</p>
<p>TRU silos and high pH plume (4.15/4.19)</p> <p>(discussed in Subsection 4.3.4.9)</p>	<p>It is assumed that the TRU silos can be sited so that there is no interaction with the HLW panels or radionuclide transport paths. The relative siting of the TRU silos and HLW panels should be investigated as part of site-specific optimisation studies.</p>
<p>Hydrothermal activity (9.10)</p> <p>(discussed in Subsection 4.3.5.10)</p>	<p>It is expected that zones of excessive hydrothermal activity can be avoided by siting. Scoping calculations could be made of possible impacts of hydrothermal activity on the hydrogeological regime.</p>
<p>Intrusion of saline groundwater (5.11/6.11)</p> <p>(discussed in Subsection 4.3.6.4)</p>	<p>It is expected that the repository can be sited far enough away from the Permo-Carboniferous Trough for saline intrusion from this source to be ruled out.</p> <p>Evidence for (non)occurrence of saline intrusion episodes should be sought as part of the next phase of site investigations.</p> <p>In addition, scoping calculations could be made of possible impacts of saline intrusion on host-rock geochemistry, the bentonite buffer and the hydrogeological regime.</p>

Note: FEPs are numbered (in brackets) according to the scheme in Table 4.2.2.

Table 4.4.3: (Continued). Open questions identified from the scenario development process and comments on present assumptions and possible future work

Open Questions	Comments
<p>Permafrost (10.13) and ice-sheet effects (10.16)</p> <p>(discussed in Subsection 4.3.6.6.)</p>	<p>It is estimated that future permafrost in Northern Switzerland will not be deep enough to channel ice-sheet melt water to the depth of the low-permeability domain.</p> <p>If estimates are not already available from detailed modelling (e.g. see ANON 1994), scoping calculations should be made to estimate the range of future permafrost thicknesses in Northern Switzerland and hydrogeological modelling should be undertaken to estimate the maximum extent of deep groundwater flow modifications. In addition, paleohydrogeological studies may indicate the extent to which deep groundwaters have been affected by past glacial episodes.</p>
<p>Exploratory drilling (11.3)</p> <p>(discussed in Subsection 4.3.7.5)</p>	<p>It is estimated that the probability of future exploratory drilling in the crystalline basement (apart from that undertaken as part of repository siting) is very low, so that a risk limit will not be exceeded.</p> <p>Illustrative assessments of potential radiological impacts could be made, including direct impact to intruders and effects of open bore holes in the low-permeability domain.</p>
<p>Geothermal exploitation (11.3)</p> <p>(discussed in Subsection 4.3.7.6)</p>	<p>Geothermal exploitation of the crystalline basement is unlikely given that there are other more promising geothermal targets in Northern Switzerland.</p> <p>The specific characteristics of possible geothermal exploitation in the rather low temperatures of the crystalline basement at repository depth should be estimated and feasibility assessed. Illustrative calculations of radiological impact could also be made.</p>

Note: FEPs are numbered (in brackets) according to the scheme in Table 4.2.2.

Table 4.4.3: (Continued). Open questions identified from the scenario development process and comments on present assumptions and possible future work.

5. REFERENCE MODEL ASSUMPTIONS AND THEIR EVALUATION

5.1 Introduction

As noted in Chapter 2, appropriate models and datasets are required to quantify the performance of radioactive waste disposal systems. These models and datasets must represent the relevant features, events and processes at an appropriate level of detail and remain flexible enough to represent a range of alternative conditions that cover uncertainties in possible future conditions and in the nature of the relevant processes.

5.1.1 Levels of Modelling

Models are used in safety assessments in several complementary ways:

- (i) to interpret experimental data and, in so doing, to build up and demonstrate an understanding of individual processes, such as the corrosion of a steel canister for given geochemical conditions, or the interaction between dissolved radionuclide species and solid surfaces, and to determine appropriate parameter values for these processes;
- (ii) to investigate boundary conditions for safety-assessment model subsystems, for example, modelling the thermal field due to radiogenic heat generation, or the groundwater flow as affected by the possible alternative assumptions for media properties and the distribution of fault zones;
- (iii) to describe and understand subsystem performance in isolation, such as radionuclide retention in the near field or transport of radionuclides through the geosphere for different assumptions of pathway characteristics and boundary conditions;
- (iv) to estimate the overall performance of the waste disposal system, by linking together models of the individual subsystems.

Models at level (i) are often considered to belong to the realm of underlying research and are usually developed and applied to assist understanding of laboratory and field experiments. Models at level (ii) are essential to the understanding of the elements of the disposal system and, for the Kristallin-I assessment, the understanding gained from these models is largely incorporated in the development of safety-assessment scenarios as described in Chapter 4. This chapter is primarily concerned with models at level (iii), i.e. understanding individual subsystems relevant to radionuclide release from the repository and transport to the human environment. In Chapter 6, results of analyses are presented, linking together the models described in this chapter, in order to estimate the overall performance of the disposal system, i.e. modelling at level (iv).

5.1.2 The Scope of Safety-Assessment Models in Kristallin-I

The various scenarios for which it is necessary to carry out safety-assessment calculations have been identified in Chapter 4 and are summarised in Table 4.4.1. They all describe the release and transport of radionuclides in groundwater according to the natural flow regime. Although scenarios considering repository gas effects and human actions which may disturb the repository are identified and discussed in Chapter 4, it is concluded that none of these scenarios is sufficiently probable or pertinent to the question of further site investigation to warrant quantitative treatment within Kristallin-I.

A chain of safety-assessment models has been developed to represent the processes of radionuclide release, transport in groundwater and exposure to man, considering three "fields" or regions of the disposal system: near field, geosphere and biosphere.

These regions are defined as follows:

- the **near field** consists of the vitrified waste form, engineered barriers and that region of the host rock that significantly affects the performance of the engineered barriers (the excavation-disturbed zone and about 10 m of undisturbed rock);
- the **geosphere** is defined as the undisturbed host rock plus any geological formations that contain potential paths for radionuclide transport to the biosphere;
- the **biosphere** is the surface environment and associated natural and man-made (e.g. agricultural) systems, including near-surface aquifers and unconsolidated sediments and soils, that provide the human habitat, water and dietary resources.

5.1.3 The Kristallin-I Safety-Assessment Model Chain

A sequence of models is used to describe each of the three regions of interest:

- a near-field code, **STRENG** (GRINDROD et al. 1990b), which models radionuclide release following canister failure and transport through the bentonite buffer and into the host rock immediately surrounding the emplacement tunnels;
- a geosphere code, **RANCHMD** (JAKOB 1992), which models radionuclide transport in water-conducting features of the crystalline basement rock;
- a biosphere code, **TAME** (KLOS et al. 1994), which models radionuclide dilution in near-surface aquifers, distribution in soils, sediments and water bodies, and the radiological exposure pathways to man.

The main features and processes included in each code are summarised in Table 5.1.1.

Near field	Geosphere	Biosphere
STRENG	RANCHMD	TAME
<p>Radionuclide decay (single RNs and chains).</p> <p>Canister failure at specified time.</p> <p>Glass corrosion at a constant rate (per unit area of exposed surface) with congruent release of RNs.</p> <p>RN precipitation/re-dissolution near to the glass, constrained by elemental solubility limits.</p> <p>Diffusion through bentonite with instantaneous, linear, reversible sorption on the bentonite pore surfaces.</p> <p>Alternative BCs at the bentonite-host rock interface.</p> <p><i>Further details in Section 5.2.</i></p>	<p>Radionuclide decay (single RNs and chains).</p> <p>Water-conducting features of various geometries.</p> <p>Solute advection and dispersion in water-conducting features.</p> <p>Diffusion into stagnant porewater of the rock matrix, with instantaneous, linear, reversible sorption on matrix pore surfaces[†].</p> <p><i>Further details in Section 5.3.</i></p>	<p>Radionuclide decay (single RNs and chains).</p> <p>Accumulation by sorption on soils and sediments.</p> <p>Transport in solid and aqueous phases.</p> <p>Dilution in a near-surface aquifer and/or river.</p> <p>RN uptake in plants and animals.</p> <p>Doses to man from:</p> <ul style="list-style-type: none"> - ingestion (water and foods); - inhalation (particles); - external exposure (soils and sediments). <p><i>Further details in Section 5.4.</i></p>

Notes: RN = radionuclide; BC = boundary condition;

† A variant, RANCHMDNL, allows for non-linear (Freundlich) sorption.

Table 5.1.1: Summary of the main features and processes represented in the Kristallin-I safety assessment model chain.

Other models have been used to account for certain specific processes or subsystems at a greater level of detail or by more mechanistic concepts. These models either provide input to the assessment model chain or affirm the validity, or conservatism, of underlying assumptions made in the assessment calculations. Figure 5.1.1 illustrates the Kristallin-I safety-assessment model chain and supporting models. A summary of the capabilities of, and examples of the application of, the STRENG-RANCHMD-TAME model chain is given in Sections 5.2 to 5.4.

5.1.4 Definition of Assessment Calculation Cases

The Kristallin-I **Reference Case** is a description of the **Reference Scenario**, defined in Chapter 4, which uses **Reference Model Assumptions** and **Reference Parameters** (generally, "realistic-conservative" parameter values) (see also Subsection 2.5.2). This calculation is thought to yield a moderately conservative result in view of the conservative assumptions in the models and partial conservatism of the data. The sensitivity of the calculation to parameter uncertainty is investigated using modified parameter values (parameters values are modified either individually or in groups), combined with "realistic-conservative" values of all other variable parameters. This is done primarily to understand model sensitivity and to identify key parameters. The results are considered to be pessimistic where the modified parameters are set to their "conservative" values. For the biosphere, only selected parameters that are most important to the performance of the biosphere model are varied.

Table 5.1.2 summarises the calculations made, according to the above approach, which are described in the following sections of this chapter. These calculations are primarily concerned with developing an understanding of the individual components of the disposal system. Table 5.1.3 summarises calculations described in Chapter 6, which are aimed at assessing overall repository performance. The latter calculations consider **alternative model assumptions** for the Reference Scenario and also the **alternative scenarios** identified in Chapter 4.

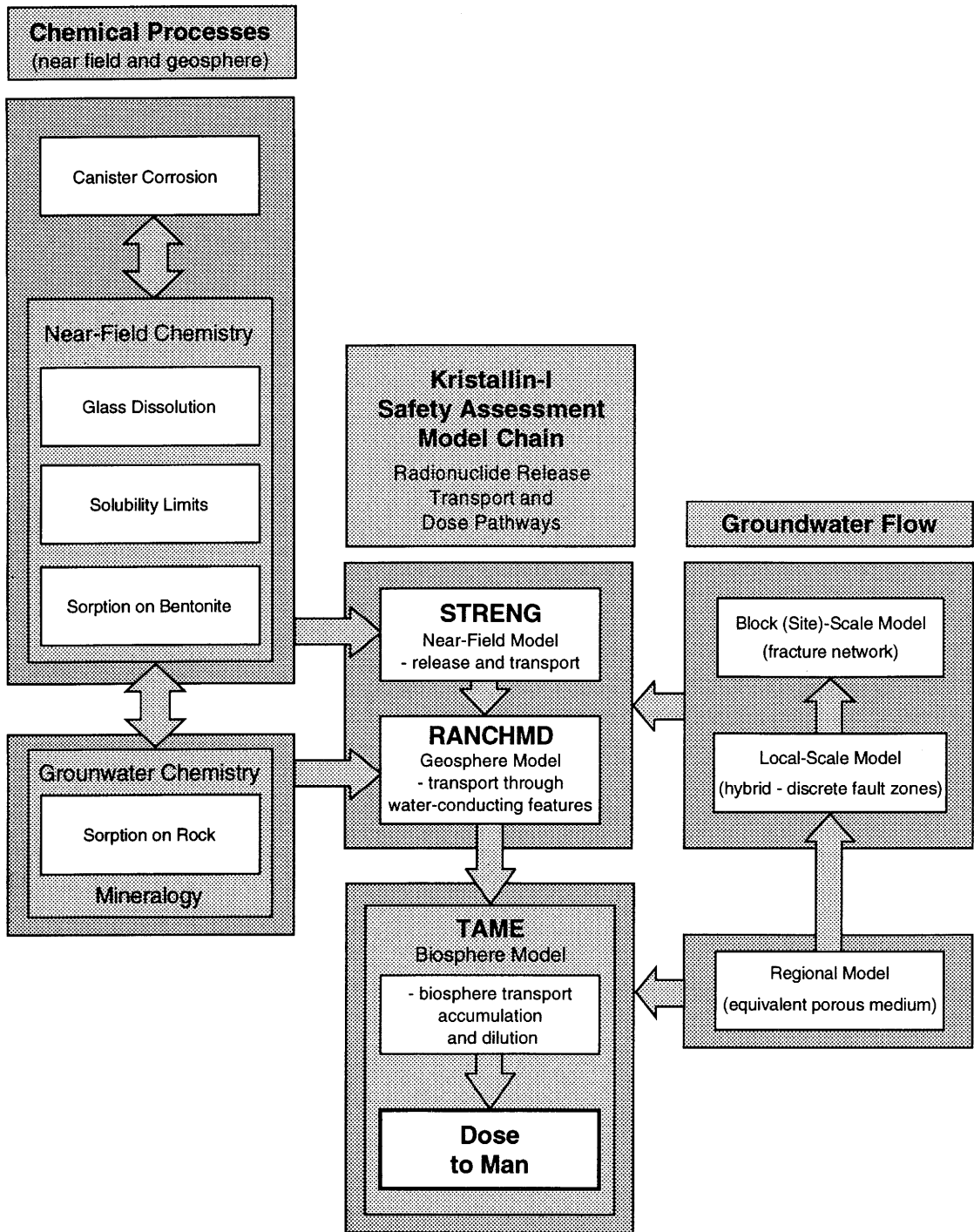


Figure 5.1.1: The Kristallin-I safety-assessment model chain (codes STRENG, RANCHMD and TAME) and supporting models.

Scenario	Model Assumptions	Parameter Values
Reference-Case Calculations (see Sections 5.2, 5.3 and 5.4)		
Reference Scenario.	Reference Model Assumptions (near field, geosphere and biosphere) - geometry 6 (see Subsection 5.3.4) used to describe internal structure of water-conducting features.	Reference Parameters (near field, geosphere and biosphere).

Near-field Parameter Variations (see Section 5.2)		
Reference Scenario.	Reference Model Assumptions (near field).	Increased canister lifetime. Reduced canister lifetime.
		Increased glass corrosion rate.
		"Conservative" solubility limits.
		Sharing the elemental solubility limits with stable isotopes not taken into account.
		"Conservative" K_d values.
		Reduced bentonite thickness.
		10-fold decrease in LPD flowrate. 10-fold increase in LPD flowrate. 100-fold increase in LPD flowrate. Zero-concentration boundary condition at the bentonite outer edge.

Geosphere Parameter Variations (see Section 5.3)		
Reference Scenario.	Reference Model Assumptions for the near field; geosphere calculations with 6 alternative model assumptions for the internal structure of water-conducting features - see also Table 5.1.3.	Modified advection velocity, geometrical parameters for the conduit, matrix porosity and extent.
	Reference Model Assumptions (near field, geosphere) - geometry 6 used in geosphere.	Reduced LPD path length.
		Increased LPD path length.
		"Conservative" K_d values.
		"Conservative" diffusion constant.
		Increased longitudinal dispersivity (reduced Peclet number). Reduced longitudinal dispersivity.
		"Conservative" matrix diffusion depth.
		10-fold decrease in LPD flowrate. 10-fold increase in LPD flowrate. 100-fold increase in LPD flowrate.
	Non-linear sorption accounted for explicitly in the geosphere using code RANCHMDNL.	Cs sorption described by modified Freundlich isotherm.

Biosphere Parameter Variations (see Section 5.4)		
Reference Scenario.	Reference Model Assumptions (near field, geosphere and biosphere) - geometry 6 used to describe the internal structure of water-conducting features.	Biosphere K_d values reduced by a factor of 10.
		Biosphere K_d values increased by a factor of 10.
		All irrigation water obtained from the river Rhine.
		All irrigation water obtained from the aquifer in the Rhine gravel sediments.
		Soil turnover reduced by a factor 10.
		Soil turnover increased by a factor 100.
		Gravel aquifer thickness decreased by a factor 10.
		Gravel aquifer thickness increased by a factor 100.

Note: LPD = low-permeability domain of the crystalline basement.

Table 5.1.2: A summary of calculations aimed at developing an understanding of the near-field, geosphere and biosphere models by means of parameter variations. The Reference-Case calculations, around which variations are made, are based on the Reference Scenario discussed in Chapter 4, together with Reference Model Assumptions and Reference Parameters ("realistic-conservative" physico-chemical data) described in Chapter 3.

Scenario	Model Assumptions	Parameter Values
Reference-Case Model-Chain Calculations and Calculations for Alternative Siting Area (see Subsection 6.2.1)		
Reference Scenario.	Reference Model Assumptions (near field, geosphere and biosphere).	Reference Parameters (Area West). Near-field, geosphere parameters for Area East - Reference-Case biosphere. Near-field, geosphere parameters for Area East - release to a tributary valley.
Alternative Model Assumptions (see Subsection 6.2.2)		
Reference Scenario.	Alternative water-conducting feature geometries: - Cataclastic/jointed zones with narrow, closely-spaced channels. - Aplite/pegmatite dykes and aplitic gneisses. - Cataclastic/jointed zones with broad, widely-spaced channels.	Modified model conduit aperture/radius, matrix extent and porosity.
	Unlimited matrix diffusion - both altered and unaltered wallrock accessible to diffusion.	Modified matrix extent and porosity.
	Radionuclides transported through the low-permeability domain to major water-conducting faults; transport through faults included in calculations.	Reference Parameters for two-layer geosphere model.
	Radionuclides sorb onto a constant background population of groundwater colloids; calculations for 6 alternative descriptions of the internal geometry of water-conducting features.	Colloid concentration and sorption properties of radionuclides on colloids.
	Groundwater flow is distributed between three groups of water-conducting features according to a probability distribution derived from groundwater flow modelling.	Calculations performed with both reference and increased flowrates.
Alternative Scenarios (see Section 6.3)		
Deep groundwater well.	Modified (simple) biosphere model.	Reduced biosphere data.
Tunnel/shaft seal failure.	Model of transport from near field to biosphere along shaft replaces geosphere model.	Modified near-field data (flowrate at bentonite outer boundary) and modified geosphere data.
Alternative climate-related scenarios: - Dry Climate State, - Humid Climate State, - Periglacial Climate State, - Rhine Gravels Absent.	Modified biosphere model.	Modified biosphere data.
Robust Scenario (see Section 6.4)		
Robust Scenario.	Modified geosphere model (immediate transport to biosphere).	Reference-Case near-field and biosphere parameters.
		Zero-concentration boundary condition at bentonite-host rock interface.
		"Conservative" K_d values, solubility limits and glass-corrosion rate in the near field.

Note: For the alternative climate-related scenarios, input data are assumed not to be time dependent, i.e. no attempt has been made to model a time-dependent climate. It is assumed that the near field and geosphere are unaffected by climatic conditions.

Table 5.1.3: A summary of calculations aimed at assessing repository performance. In addition to Reference-Case calculations, parameter variations, alternative model assumptions and alternative scenarios are examined. Results are presented in Chapter 6.

5.2 Near-Field Modelling

In Section 5.2, the near-field modelling assumptions are described (Subsection 5.2.1) and the governing equations presented (Subsection 5.2.2). In Subsection 5.2.3, the sensitivity of near-field performance to parameter variations is discussed; the parameters varied include canister lifetime, glass-corrosion rate, solubility limits, sorption constants in the bentonite, thickness of the bentonite and flowrate at the bentonite-host rock interface. In Subsection 5.2.4, the results are summarised and analysed.

The Kristallin-I engineered barriers consist of the vitrified waste form, contained in massive steel canisters, surrounded by bentonite and emplaced horizontally in disposal tunnels, see Figure 3.4.1. The characteristics of these elements have been described in Section 3.4 and their safety function discussed in Section 3.2.

The Reference Scenario - resaturation of the bentonite, failure of the steel canisters, dissolution of the glass matrix, release of radionuclides and their diffusion, in aqueous phase, through the bentonite - has been described in Section 4.3. In the following subsection, only the assumptions directly relevant to safety-assessment modelling of the near field will be re-stated, as well as additional simplifying assumptions that are made in order to facilitate the mathematical modelling.

5.2.1 Model Assumptions

The safety-assessment model for the near field is concerned only with the release of radionuclides from the glass matrix following canister failure, along with transport through the bentonite and release from the latter to the host rock.

5.2.1.1 Features, Events and Processes

The following assumptions are made about the physical and chemical processes actually occurring. The background to, and justification of, these assumptions are discussed in Chapters 3 and 4:

- The radionuclides are mixed uniformly in a homogeneous borosilicate glass matrix.
- During cooling of the glass, cracks form so that the surface area of the glass at the time of emplacement will be greater than that of the original moulded block.
- The glass is solidified in thin steel fabrication flasks, each containing 150 litres of glass. Together with the glass, these are then put into massive, cast-steel canisters. The flasks provide **no** barrier function, but the canisters are designed to remain unbreached for at least 1000 years following closure.

- The Nagra model radionuclide inventory in each flask at disposal time is based on the COGEMA specification and assumes disposal 40 years following unloading of fuel from the reactor.
- There are a total of 2693 flasks for disposal in the repository.
- Canisters fail (at times greater than 1000 years following repository closure) due to mechanical loads, following some degree of weakening by corrosion.
- The 0.94 m-diameter canisters are emplaced co-axially in 3.7 m-diameter tunnels and are surrounded by precompacted bentonite blocks.
- The canisters are maintained approximately centrally within the disposal tunnels by the compacted bentonite over the period of the assessment, i.e., canister sinking is negligible.
- There is a continuous excavation-disturbed zone along the axial direction in the host rock surrounding the emplacement tunnels¹⁹
- At the time of canister failure:
 - the thermal output from the waste is negligible and the near field is at rock ambient temperature,
 - the bentonite is fully resaturated and forms a homogeneous low-permeability barrier around the canisters,
 - the near-field porewater reaches a chemical equilibrium determined predominantly by the interaction between groundwater, bentonite and iron corrosion products at the glass-bentonite interface.
- The reducing effect of the iron canister material and corrosion products on porewater chemistry is accounted for.
- The safety-relevant properties of the bentonite remain unchanged over the period of the assessment.
- Hydrogen may be produced by anoxic corrosion of the iron canisters, but is assumed to have no effect on the release or transport of radionuclides.

¹⁹ This is a conservative assumption; in practice the zone may be discontinuous or absent. However, the assumption allows the near-field and geosphere models to be decoupled and allows simplification of the geometry of the near-field model (see Subsection 5.2.1.2).

- Following failure of the canisters, water contacts the glass matrix, which begins to corrode; corrosion is assumed to occur at a rate proportional to the glass surface area (which decreases with time).
- As the glass corrodes, radionuclides are released congruently to the aqueous solution immediately surrounding the glass fragments within the failed canisters. Any transport resistance due to internal fracturing of the glass and diffusion through alteration products is conservatively neglected.
- Colloids may be produced within the failed canisters (for example, by the corroding glass); however, they do not move away from the waste because of filtration by the micro-porous structure of the bentonite.
- The concentration of radionuclides in the solution adjacent to the glass will be limited by elemental solubilities, shared (where appropriate) with all isotopes of the element (stable and radioactive) present in the vitrified waste. Background concentrations in the intruding pore water are conservatively ignored²⁰.
- Secondary phases, precipitated due to saturation being reached, redissolve to maintain radionuclide concentration at solubility limits as the supply from dissolution of the glass decreases or ceases altogether.
- Radionuclides may sorb on or co-precipitate with glass secondary minerals and canister corrosion products; however, this is conservatively neglected in the calculations.
- Solubility limits are applied to radionuclides leached from the glass and are estimated for conditions in the bentonite porewater. They are applied at the glass-bentonite interface, but not within the bentonite, and radioactive ingrowth may cause the concentration of some chain members to exceed the elemental solubility limits leading to a conservative over-estimate of the release.
- Radionuclide migration through the bentonite occurs exclusively by diffusion in aqueous solution; advection is negligible due to the very low bulk permeability of the saturated bentonite and colloid transport is prevented as mentioned above.
- Radionuclide diffusion through the bentonite is retarded by element-specific sorption, represented as an instantaneous, concentration-independent, reversible process; selection of sorption constants accounts for the dependence of accessible porosity in the bentonite on radionuclide speciation.

²⁰ The contribution of nuclides in the bentonite and canister should, in most cases, be negligible. Furthermore, the background concentrations in the groundwater are in most cases almost zero, with the possible exception of Se, Cs, Th and U.

- Radionuclides reaching the bentonite-host rock interface are conservatively assumed to be transferred directly to the water-conducting features of the crystalline basement which intersect the tunnels.
- Microbial activity and the effect of organic material in the near field is assumed to be negligible.

The transport of radionuclides within the water-conducting features is the concern of the geosphere transport model (see Section 5.3).

5.2.1.2 Simplifications and Additional Model Assumptions

The left-hand side of Figure 5.2.1 illustrates the main features of the repository near field, in which the processes described above occur. Some further simplifications and assumptions are required to facilitate the mathematical representation (see also the right-hand side of Figure 5.2.1):

- All canisters are assumed to fail simultaneously at 1000 years after repository closure.
- Calculations of radionuclide release begin at the time of canister failure; only radionuclide decay and ingrowth are accounted for at earlier times.
- After failure, the canisters provide no physical resistance to water or solute transport.
- For the calculation of glass corrosion and radionuclide release, glass fragments are represented as a number of spheres of equal size, with total volume equal to the total volume of glass. The initial surface area is set to a value which accounts for the increase in surface area due to cracking. The surface area decreases with time as the glass corrodes.
- Radionuclides released from the corroding glass enter the surrounding porewater, represented by a hypothetical "volume for dissolution", where precipitation and redissolution maintain radionuclide concentrations at, or below, the solubility limit (results of near-field calculations are insensitive to the value assigned to this volume over a broad range).
- The radionuclide concentration in the volume for dissolution provides an inner boundary condition for diffusion through the bentonite.

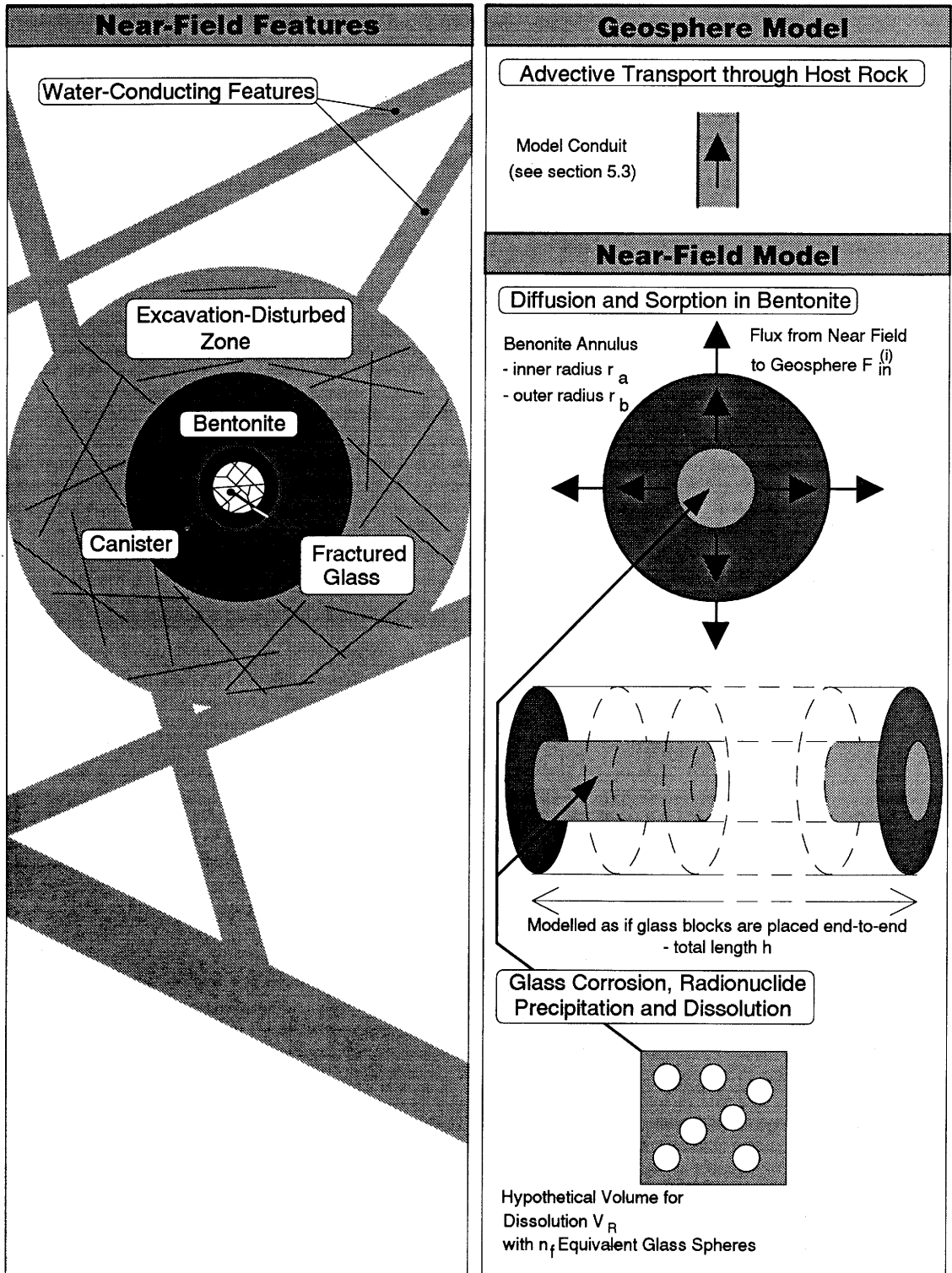


Figure 5.2.1: Modelling of the repository near field. A cross-section through a single emplacement tunnel is shown on the left-hand side, with important features indicated. The model representation of these features, together with processes relevant to radionuclide release and transport, are shown on the right-hand side.

- For the calculation of diffusion through the bentonite, the geometry of the system is simplified in such a way that only one-dimensional radial diffusion is considered, i.e. the axial diffusion of radionuclides into the bentonite separating the canisters is conservatively neglected. The release from the total repository is thus calculated as though the waste packages were arranged end-to-end in a continuous cylinder.
- Two alternative outer boundary conditions for diffusion are considered:
 - (a) the concentration and its gradient are set such that the rate of radionuclide release by diffusion across the boundary is equal to the rate of radionuclide advection in flowing groundwater in the geosphere ("mixing-tank" boundary condition),
 - (b) a zero concentration boundary condition.

Condition (a) tends to condition (b) at high groundwater flowrates, i.e. when flow is sufficient to reduce radionuclide concentrations at the bentonite-host rock interface to negligible levels. In order to preserve the one-dimensional geometry of the near-field model, non-uniformity in the groundwater flow around the outer boundary of the bentonite is neglected when applying condition (a). The effects of non-uniformity around this boundary at a given position along the tunnel axis are likely to be small, as discussed in Appendix 9. The effects of non-uniformity in the axial direction depend largely on the properties of the excavation disturbed zone (see the discussion of reserve FEPs in Subsection 4.4.3).

FEPs represented in the near-field model and its main parameters are summarised in Table 5.2.1 (features in Table 5.2.1(a), processes in Table 5.2.1(b)).

5.2.2 Mathematical Representation

The near-field model, described above, has been formalised in the computer code STRENG. The program calculates:

- the release of radionuclides from the waste matrix;
- the diffusive transport of radionuclides through the bentonite;
- the release of radionuclides to groundwater at the bentonite-host rock interface.

A complete description of STRENG, including the underlying formalism, parameter description and an overview of model testing can be found in GRINDROD et al. (1990b). Here, emphasis is placed on the safety-analysis results, and on the selection of values for the most important parameters. Therefore, only a concise description of the governing equations is given below. The symbols used in this description are defined in Table 5.2.1.

Features	Model Parameters			Comments
Glass waste form	V_0	[m ³]	initial glass matrix volume	The volume V_0 and length h are summed over all waste blocks - radionuclide release is modelled as if all waste blocks were packed end-to-end, without intermediate spacing.
	d_0	[m]	initial diameter	
	n_f	[-]	number of equivalent spheres	
	ρ_g	[kg m ⁻³]	glass density	
	$C_g^{(i)}$	[mol m ⁻³]	concentration of radionuclide i in the glass	
	h	[m]	axial length of glass waste blocks	
	r_f	[m]	initial radius of equivalent spheres	
Hypothetical volume for dissolution	V_R	[m ³]	volume for dissolution	
	$M^{(i)}$	[mol]	inventory of radionuclide i	
	$\theta_E^{(i)}$	[-]	the ratio of the inventory of radionuclide i to the inventory summed over all isotopes (including stable isotopes) of the element E of which the radionuclide i is an isotope	
Bentonite	r_a	[m]	inner radius	1-D radial geometry. Surface area through which radionuclides diffuse out of the near field (excluding intermediate spacing between waste packages).
	r_b	[m]	outer radius	
	ρ_b	[kg m ⁻³]	solid density	
	ϵ	[-]	porosity	
	A_{ben}	[m ²]	external surface area: $A_{ben} = 2\pi r_b h$	
	$C^{(i)}$	[mol m ⁻³]	concentration of radionuclide i in porewater	

Note: The parameters defined in this table are used in the mathematical expressions found in the following sections of the report.

Table 5.2.1: The near-field model and main parameters. (a): features represented.

Processes	Parameters			Comments
Radioactive decay	$\lambda^{(i)}$	$[y^{-1}]$	decay constant for radionuclide i	
Glass corrosion	R	$[kg\ m^{-2}\ y^{-1}]$	corrosion rate	
Radionuclide precipitation / dissolution	S_E	$[mol\ m^{-3}]$	elemental solubility limit	Shared by all isotopes of the element E .
Diffusion in bentonite	D_e	$[m^2\ y^{-1}]$	effective diffusion constant	$D_e = \varepsilon D_p$, where D_p is the pore diffusion constant for bentonite
Radionuclide sorption in bentonite	$K_d^{(i)}$	$[m^3\ kg^{-1}]$	sorption constant for radionuclide i	Rapid, linear and reversible.
Groundwater flow in the host rock	Q	$[m^3\ y^{-1}]$	groundwater flowrate through repository area A	The repository area A is defined in Subsection 3.7.4.1
Radionuclide release to the geosphere	$F_{in}^{(i)}$	$[mol\ m^{-2}\ y^{-1}]$	Flux of radionuclide i entering the geosphere from the near field	

Note: The parameters defined in this table are used in the expressions found in the following sections of the report.

Table 5.2.1: The near-field model and main parameters. (b): processes represented.

5.2.2.1 Release of Radionuclides from the Waste Matrix

For the i th radionuclide in the chain $1 \rightarrow 2 \rightarrow \dots \rightarrow i \rightarrow \dots$, with decay constant $\lambda^{(i)}$, the rate of change of radionuclide concentration $C_g^{(i)}$ in the glass due to radioactive decay and ingrowth is given by

$$\frac{dC_g^{(i)}}{dt} = -\lambda^{(i)}C_g^{(i)} + \lambda^{(i-1)}C_g^{(i-1)}. \quad (5.2.1)$$

t [y] is defined such that $t = 0$ corresponds to the time of canister failure.

Radionuclides are released as the glass corrodes. Based on the model assumption that the glass is in the form of a single continuous cylinder, the initial volume of the glass, V_0 , is given by:

$$V_0 = \frac{\pi d_0^2 h}{4}. \quad (5.2.2)$$

The glass-corrosion rate is proportional to the surface area of the glass. The surface area is increased by a factor of 12.5 to account for fracturing due to thermo-mechanical stresses on cooling (see Subsection 3.4.2.1 and Table 3.7.2). The initial surface area of all 2693 waste blocks, A_0 [m²], is given by:

$$A_0 = 12.5 \pi d_0 \left(h + 2693 \frac{d_0}{2} \right) \quad (5.2.3)$$

(note that, in Table 5.2.1(a), h is defined as the sum of lengths of all 2693 waste blocks). Following the approach adopted in Project Gewähr 1985 (NAGRA 1985; HARTLEY 1985), the fractured waste matrix is represented by n_f equivalent spheres of equal volume. The radius of the spheres, r_f [m], is fixed by the requirement that the initial ratio of glass volume to surface area is the same for the spheres as for the cracked glass block:

$$r_f = \frac{3V_0}{A_0} \equiv \frac{3}{25} \left(\frac{hd_0}{2h + 2693d_0} \right). \quad (5.2.4)$$

In order that the total volume of the spheres equals the glass volume, the number of spheres is given by:

$$n_f = \frac{3V_0}{4\pi r_f^3}. \quad (5.2.5)$$

Using the values in Table 3.7.2, this corresponds to approximately 3700 spheres for each of the 2693 glass blocks, each sphere with a radius of 2.1 cm. The assumption of a constant glass-corrosion rate leads to a decrease in the radius of the spheres which is proportional to time, so that the lifetime of the blocks is given by τ [y]:

$$\tau = \frac{\rho_g r_f}{R}. \quad (5.2.6)$$

This is equal to 1.5×10^5 years in the case of the "realistic-conservative" glass-corrosion rate given in Table 3.7.2 and 1500 years using the "conservative" rate. $V(t)$ [m³], the time-dependent volume of glass summed over all waste blocks, is then:

$$V(t) = V_0 \left(1 - \frac{t}{\tau} \right)^3 \quad : \quad 0 < t < \tau \quad (5.2.7)$$

$$V(t) = 0 \quad : \quad t \geq \tau. \quad (5.2.8)$$

5.2.2.2 Mass Balance at the Glass-Bentonite Interface and Diffusion through the Bentonite

As the glass dissolves, the radionuclides become free to move. In the model, the released radionuclides enter a hypothetical "volume for dissolution", which has a radionuclide inventory, $M^{(i)}$, varying in time according to:

$$\frac{dM^{(i)}}{dt} = -\lambda^{(i)}M^{(i)} + \lambda^{(i-1)}M^{(i-1)} - C_g^{(i)} \frac{dV}{dt} + 2\pi r_a h D_e \left. \frac{\partial C^{(i)}}{\partial r} \right|_{r=r_a}, \quad (5.2.9)$$

where r [m] is radial distance. The terms on the right-hand side represent, respectively, radioactive decay and ingrowth, release from the dissolving glass and diffusion into the bentonite. The time development of the radionuclide concentration in the bentonite porewater is described by the equation:

$$\frac{\partial C^{(i)}}{\partial t} = \frac{D_e}{\varepsilon R_b^{(i)}} \frac{1}{r} \frac{\partial}{\partial r} \left(r \frac{\partial C^{(i)}}{\partial r} \right) - \lambda^{(i)} C^{(i)} + \frac{R_b^{(i-1)}}{R_b^{(i)}} \lambda^{(i-1)} C^{(i-1)}, \quad (5.2.10)$$

with equilibrium, reversible, linear sorption accounted for in Equation 5.2.10 by the retardation factor $R_b^{(i)}$ [-]:

$$R_b^{(i)} = 1 + \rho_b K_d^{(i)} \left(\frac{1-\varepsilon}{\varepsilon} \right). \quad (5.2.11)$$

The boundary condition at the inner surface of the bentonite is fixed by the radionuclide concentration in the hypothetical volume for glass dissolution:

$$C^{(i)} \Big|_{r=r_a} = \frac{M^{(i)}}{V_R} \quad (5.2.12)$$

when the solubility limit S_E is not exceeded and:

$$C^{(i)} \Big|_{r=r_a} = \theta_E^{(i)} S_E \quad (5.2.13)$$

when the total concentration of element E exceeds the elemental solubility limit, S_E .

5.2.2.3 Release to the Host Rock

At the bentonite-host rock interface, two alternative boundary conditions may be applied:

- a) a "mixing-tank" boundary condition, in which the concentration and gradient are set such that the rate of radionuclide release by diffusion across the boundary is equal to the rate of radionuclide advection in the geosphere:

$$QC^{(i)}\Big|_{r=r_b} = -A_{\text{ben}}D_e \frac{\partial C^{(i)}}{\partial r}\Big|_{r=r_b} \quad (5.2.14)$$

- b) a zero concentration boundary condition:

$$C^{(i)}\Big|_{r=r_b} = 0 \quad (5.2.15)$$

The total radionuclide flux $F_{in}^{(i)}$ entering the geosphere, which is assumed to be distributed across the repository area A (see definition in Subsection 3.7.4.1), is given by

$$F_{in}^{(i)} = -D_e \frac{A_{\text{ben}}}{A} \frac{\partial C^{(i)}}{\partial r}\Big|_{r=r_b} \quad (5.2.16)$$

5.2.3 Reference-Case Results and Model Sensitivity to Parameter Variations

Sensitivity of near-field modelling results to uncertainty in parameter values is explored by defining a Reference Case, around which parameter variations are made. Results of the Reference Case and an investigation of the sensitivity of radionuclide releases to parameter variations are presented in this section. Key input parameters are discussed in Chapter 3 and summarised in Section 3.7; the groundwater flowrate for the Reference Case is based on Area West, which is better characterised and may provide more favourable conditions for the siting of a repository. The Reference-Case values of all variable parameters (Reference Parameters) and variations on these values are given in Table 5.2.2. The selection of radionuclides for safety assessment has been discussed in Appendix 2; the inventory of safety-relevant radionuclides at 1000 years post-closure (the Reference-Case time for canister failure) is presented in Table 3.7.1.

Figures 5.2.2a to c present the Reference-Case radionuclide release rates from the near field for the activation/fission products and for the four actinide chains. In the case of the actinide chains, the shorter-lived initial members of the chain do not appear on the figures because they decay to insignificant levels within the near field and releases are negligible.

Maximum release rates of all radionuclides are well below 0.1 mol y^{-1} . The highest release rate is for ^{135}Cs , with a peak of about 0.05 mol y^{-1} released from the total repository. Peak releases of other radionuclides lie in the range 10^{-8} to $10^{-3} \text{ mol y}^{-1}$. These releases correspond to activities ranging from negligible values (less than 1 Bq y^{-1} for ^{246}Cm , ^{240}Pu and ^{241}Am) to a maximum of $2 \times 10^8 \text{ Bq y}^{-1}$ for ^{135}Cs .

Table 5.2.3 shows the maximum near-field release rates, irrespective of time of occurrence, for both the Reference-Case calculations and calculations of parameter variations. In order to express the results for different radionuclides on a radiologically comparable scale, the release rates are converted to annual individual doses, using a set of simple conversion factors for the drinking-water consumption pathway, assuming radionuclides are released directly to a gravel aquifer in the valley of the river Rhine (see Appendix 6) and allowing for subsequent dilution therein. Parameter variations which either increase or decrease the maximum release by a factor of 10 or more are indicated by bold type and shading.

Parameter	Reference Values	Parameters in Sensitivity-Analysis Calculations	
		Variations	Datasets
Time of canister failure, $t = 0$ (see Table 3.7.2)	10^3 y	$10^2 \text{ y}, 10^5 \text{ y}$	1, 2
Glass-corrosion rate, R (see Table 3.7.2)	$3.8 \times 10^{-4} \text{ kg m}^{-2} \text{ y}^{-1}$ (glass lifetime 150 000 y)	$3.8 \times 10^{-2} \text{ kg m}^{-2} \text{ y}^{-1}$ (glass lifetime 1500 y)	3, 14
Solubility limits, S_E (see Table 3.7.3)	Element-dependent "realistic-conservative" values	Element-dependent "conservative" values	4, 12, 14
Distribution of elemental solubility between isotopes (incl. stable isotopes) in glass	Inventory of stable isotopes taken into account	Total elemental solubility limit is assigned to each isotope (inventory of stable isotopes set to zero)	5
Sorption constants in bentonite (see Table 3.7.3)	Element-dependent "realistic-conservative" values	Element-dependent "conservative" values	6, 13, 14
Thickness of bentonite $r_b - r_a$ (see Table 3.7.2)	1.38 m	0.2 m - assumed as a "conservative" value	7
Groundwater flowrate Q (see Table 3.7.2)	$3 \text{ m}^3 \text{ y}^{-1}$	(i) mixing-tank boundary condition: $Q = 0.3 \text{ m}^3 \text{ y}^{-1}$ $Q = 30 \text{ m}^3 \text{ y}^{-1}$ $Q = 300 \text{ m}^3 \text{ y}^{-1}$	8 9, 12, 13 10
		(ii) zero-concentration boundary condition	11, 14

Notes: In all datasets other than 12, 13 and 14, only a single parameter is varied with respect to its Reference-Case value.

Table 5.2.2: Near-field parameters for Reference-Case and near-field sensitivity analysis calculations. The parameter values for the Reference Case are compared with the corresponding values used in each of the fourteen parameter variations examined. The column on the right-hand side of the table shows dataset identification numbers for calculations in the near-field sensitivity analysis; these correspond to the results shown in Table 5.2.3.

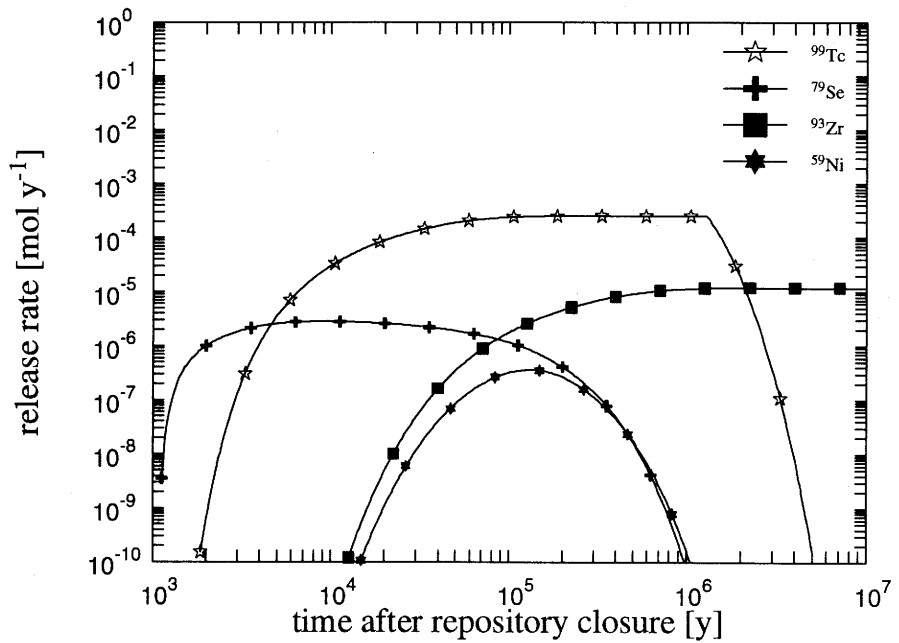
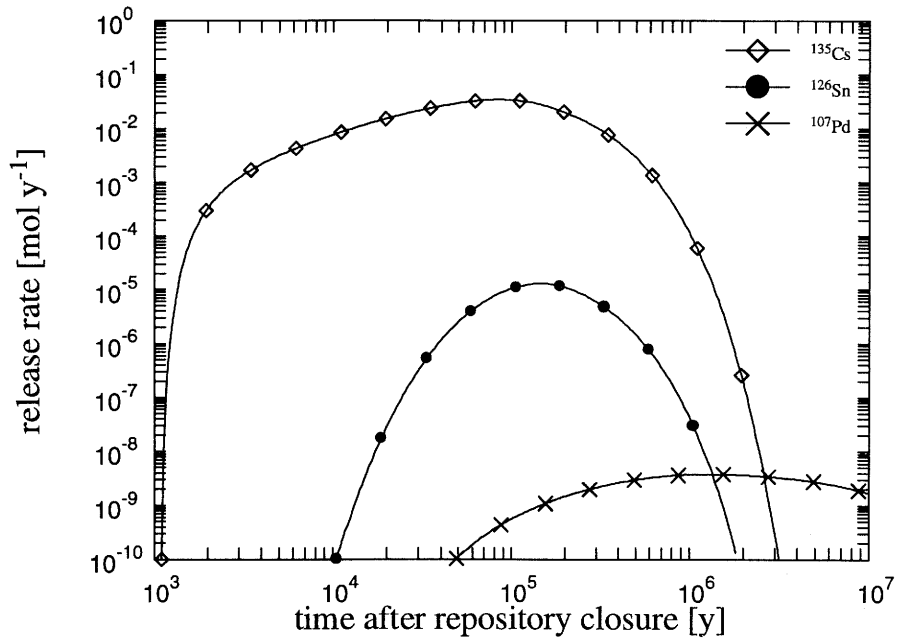
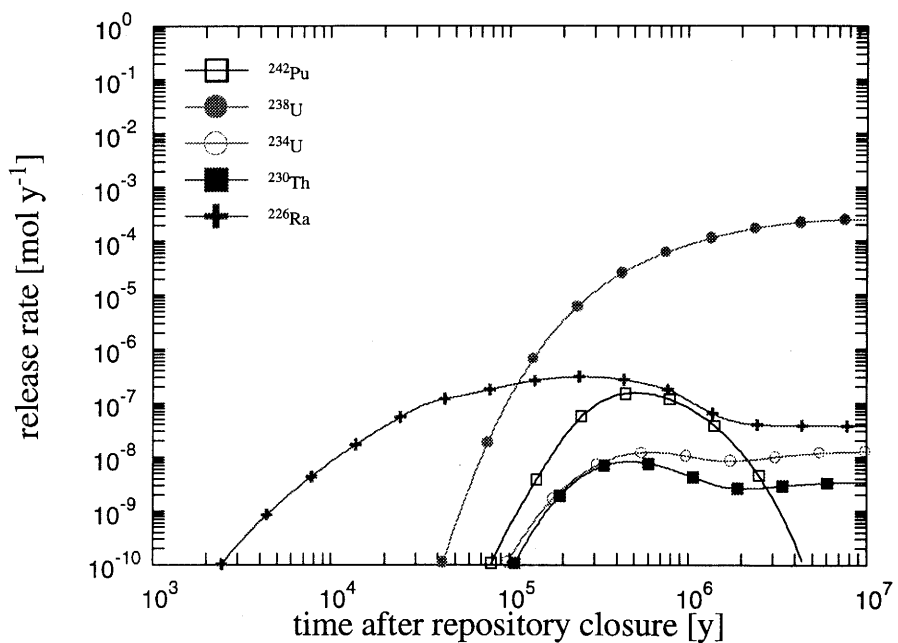
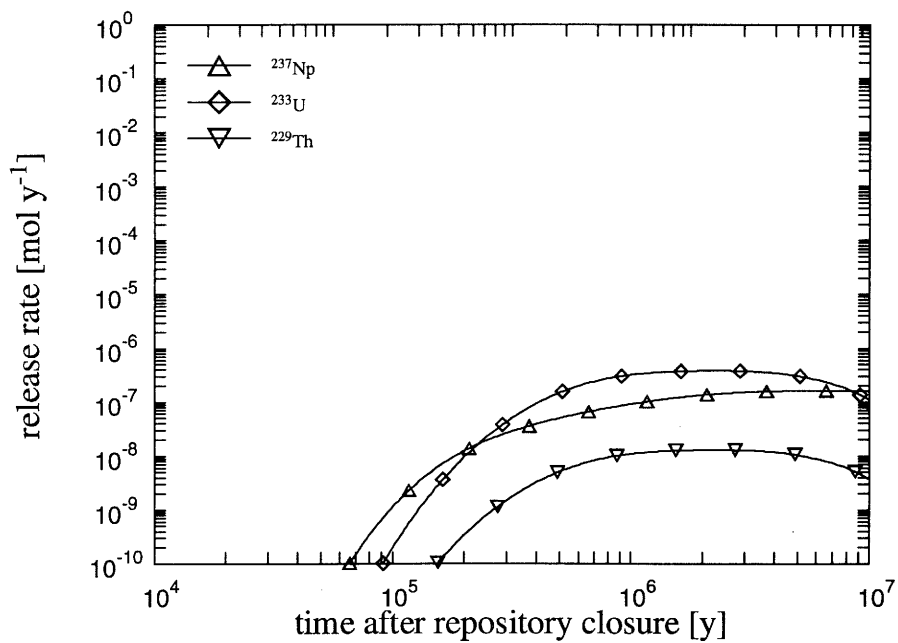
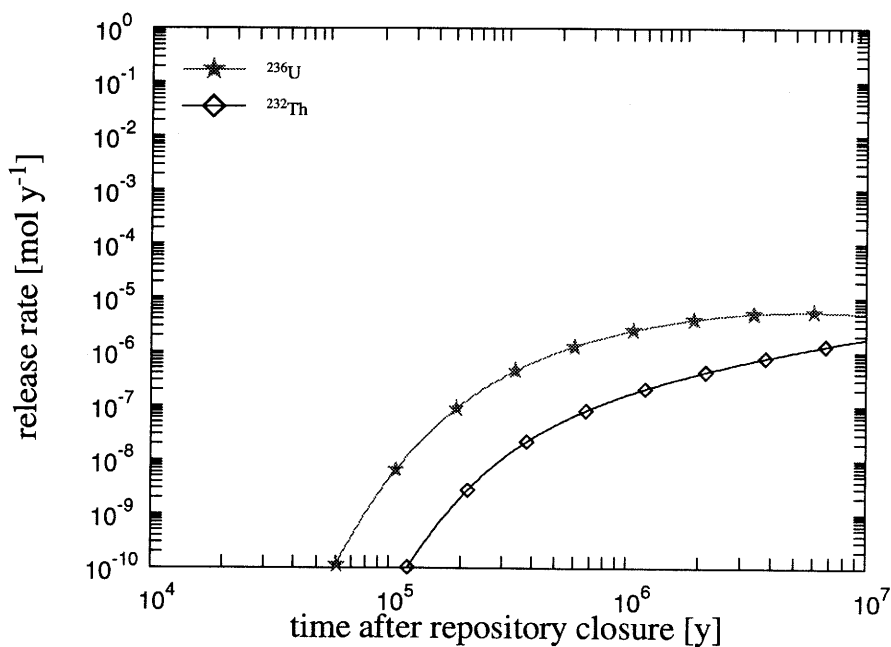
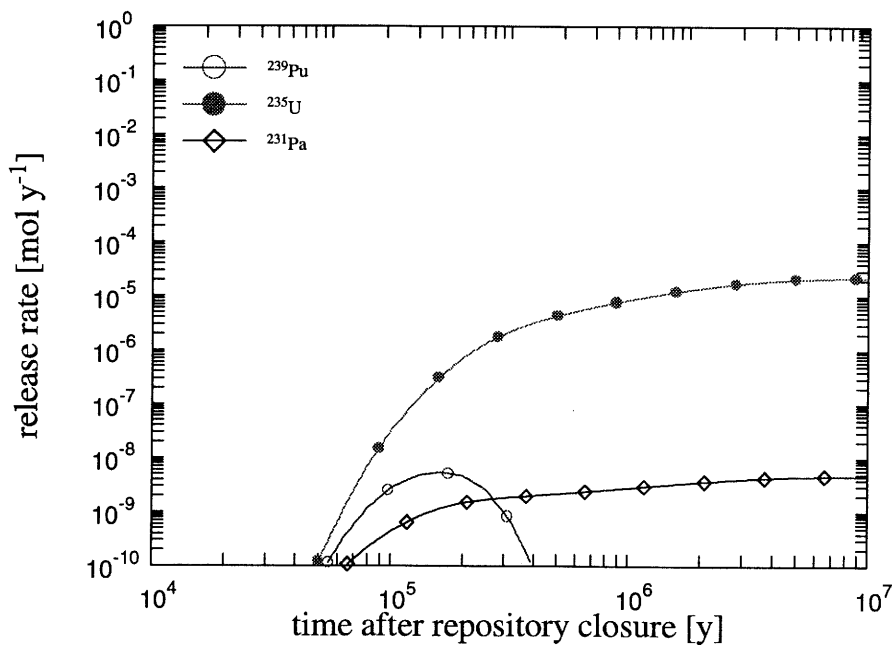


Figure 5.2.2: Reference-Case radionuclide release rates from the near field (total repository) as a function of time for the activation and fission products.



Note: Some of the shorter-lived actinide parents decay to insignificance and hence do not appear in this figure.

Figure 5.2.2: (Continued). Reference-Case radionuclide release rates from the near field (total repository) as a function of time for the 4N + 1 (above) and 4N + 2 (below) actinide chains.



Note: Some of the shorter-lived actinide parents decay to insignificance and hence do not appear in this figure.

Figure 5.2.2: (Continued). Reference-Case radionuclide release rates from the near field (total repository) as a function of time for the 4N + 3 (above) and 4N (below) actinide chains.

	Radionuclides						
	¹³⁵ Cs	¹²⁶ Sn	⁵⁹ Ni	⁹⁹ Tc	¹⁰⁷ Pd	⁷⁹ Se	⁹³ Zr
Reference Case	4.5×10 ⁻⁵	1.2×10 ⁻⁶	4.8×10 ⁻¹⁰	7.3×10 ⁻⁷	3.9×10 ⁻¹⁴	1.7×10 ⁻⁷	1.9×10 ⁻⁸
1. Reduced canister lifetime	4.5×10 ⁻⁵	1.2×10 ⁻⁶	4.8×10 ⁻¹⁰	7.3×10 ⁻⁷	3.9×10 ⁻¹⁴	1.7×10 ⁻⁷	1.9×10 ⁻⁸
2. Increased canister lifetime	4.3×10 ⁻⁵	5.9×10 ⁻⁷	1.8×10 ⁻¹⁰	7.3×10 ⁻⁷	3.9×10 ⁻¹⁴	5.2×10 ⁻⁸	1.9×10 ⁻⁸
3. Increased glass-corrosion rate	7.1×10 ⁻⁵	1.6×10 ⁻⁶	7.3×10 ⁻¹⁰	7.3×10 ⁻⁷	3.9×10 ⁻¹⁴	1.7×10 ⁻⁷	1.9×10 ⁻⁸
4. "Conservative" solubility limits	(a)	(b)	(a)	3.3×10⁻⁵	3.9×10⁻⁹	1.0×10⁻⁵	1.9×10⁻⁶
5. Sharing of elemental solubility with stable isotopes not taken into account	(c)	(d)	(d)	(c)	2.2×10⁻¹²	1.7×10⁻⁶	(c)
6. "Conservative" sorption on bentonite	1.3×10 ⁻⁴	2.0×10⁻⁵	9.3×10⁻⁹	7.7×10 ⁻⁷	4.4×10 ⁻¹⁴	1.9×10 ⁻⁷	2.2×10 ⁻⁸
7. Reduced bentonite thickness	1.5×10 ⁻⁴	2.9×10⁻⁵	1.4×10⁻⁸	8.5×10 ⁻⁷	4.6×10 ⁻¹⁴	2.0×10 ⁻⁷	2.3×10 ⁻⁸
8. 10-fold decrease in groundwater flowrate	6.4×10 ⁻⁶	1.2×10⁻⁷	4.8×10⁻¹¹	7.5×10 ⁻⁸	4.0×10 ⁻¹⁵	1.8×10 ⁻⁸	1.9×10⁻⁹
9. 10-fold increase in groundwater flowrate	1.4×10 ⁻⁴	1.1×10 ⁻⁵	4.5×10 ⁻⁹	5.6×10 ⁻⁶	3.0×10 ⁻¹³	1.3×10 ⁻⁶	1.5×10 ⁻⁷
10. 100-fold increase in groundwater flowrate	1.9×10 ⁻⁴	6.6×10⁻⁵	2.7×10⁻⁸	1.7×10⁻⁵	9.4×10⁻¹³	4.1×10⁻⁶	4.6×10⁻⁷
11. Zero-concentration boundary condition	2.1×10 ⁻⁴	1.5×10⁻⁴	6.6×10⁻⁸	2.3×10⁻⁵	1.3×10⁻¹²	5.4×10⁻⁶	6.2×10⁻⁷
12. 10-fold increase in groundwater flowrate + "conservative" solubility limits	(a)	1.1×10 ⁻⁵	(a)	2.4×10⁻⁴	3.0×10⁻⁸	8.0×10⁻⁵	1.4×10⁻⁵
13. 10-fold increase in groundwater flowrate + "conservative" sorption on bentonite	2.0×10 ⁻⁴	(d)	7.5×10⁻⁸	(d)	(d)	(d)	(d)
14. Glass-corrosion rate, solubility limits and sorption constants set to "conservative" values, zero-conc. Boundary condition	1.5×10⁻²	4.1×10⁻³	2.0×10⁻⁶	9.1×10⁻³	1.3×10⁻⁷	3.3×10⁻⁴	6.4×10⁻⁵

Notes: (a) no solubility limit given (Table 3.7.3).
 (b) no distinction between "realistic-conservative" and "conservative" values (Table 3.7.3).
 (c) no inventory of stable isotopes given (Table 3.7.1).
 (d) not calculated.

Table 5.2.3: Maximum releases, expressed as annual individual doses [mSv y⁻¹] (drinking-water consumption). (a): activation/fission products. Parameter variations which give doses differing from the Reference Case by a factor of 10 or more are indicated by bold type. Darker background shading indicates those variations which *decrease* dose by a factor of 10 or more. Lighter background shading indicates those which *increase* dose by a factor of 10 or more.

	Radionuclides						
	4N Chain			4N+3 Chain			
	²⁴⁰ Pu	²³⁶ U	²³² Th	²⁴³ Am	²³⁹ Pu	²³⁵ U	²³¹ Pa
Reference Case	7.2×10^{-11}	2.7×10^{-8}	5.1×10^{-10}	1.7×10^{-9}	3.7×10^{-7}	3.7×10^{-9}	1.7×10^{-6}
1. Reduced canister lifetime	4.5×10^{-11}	1.6×10^{-8}	3.0×10^{-10}	1.8×10^{-9}	3.9×10^{-7}	3.7×10^{-9}	1.7×10^{-6}
2. Increased canister lifetime	7.2×10^{-15}	2.7×10^{-8}	5.1×10^{-10}	1.0×10^{-13}	4.8×10^{-8}	3.7×10^{-9}	1.7×10^{-6}
3. Increased glass-corrosion rate	8.6×10^{-11}	2.7×10^{-8}	5.2×10^{-10}	9.6×10^{-9}	1.2×10^{-6}	3.7×10^{-9}	1.7×10^{-6}
4. "Conservative" solubility limits	3.0×10^{-10}	3.6×10^{-8}	5.0×10^{-10}	1.7×10^{-9}	8.2×10^{-7}	4.0×10^{-9}	1.9×10^{-6}
5. Sharing of elemental solubility with stable isotopes not taken into account	(c)	(c)	(c)	(c)	(c)	(c)	(c)
6. "Conservative" sorption on bentonite	5.5×10^{-6}	3.3×10^{-8}	2.1×10^{-9}	1.4×10^{-4}	3.6×10^{-4}	3.8×10^{-9}	1.7×10^{-5}
7. Reduced bentonite thickness	1.9×10^{-4}	3.6×10^{-8}	1.7×10^{-9}	1.4×10^{-3}	1.3×10^{-3}	3.9×10^{-9}	2.7×10^{-5}
8. 10-fold decrease in groundwater flowrate	7.2×10^{-12}	2.8×10^{-9}	9.8×10^{-11}	1.7×10^{-10}	3.7×10^{-8}	3.9×10^{-10}	1.8×10^{-7}
9. 10-fold increase in groundwater flowrate	7.1×10^{-10}	2.1×10^{-7}	1.2×10^{-9}	1.6×10^{-8}	3.7×10^{-6}	2.7×10^{-8}	1.2×10^{-5}
10. 100-fold increase in groundwater flowrate	6.4×10^{-9}	6.9×10^{-7}	1.9×10^{-9}	1.5×10^{-7}	3.2×10^{-5}	7.8×10^{-8}	4.9×10^{-5}
11. Zero-concentration boundary condition	7.2×10^{-8}	9.3×10^{-7}	2.2×10^{-9}	1.4×10^{-6}	2.1×10^{-4}	1.0×10^{-7}	1.1×10^{-4}
12. 10-fold increase in groundwater flowrate + "conservative" solubility limits	3.0×10^{-9}	3.2×10^{-7}	9.8×10^{-10}	1.6×10^{-8}	8.1×10^{-6}	3.5×10^{-8}	1.6×10^{-5}
13. 10-fold increase in groundwater flowrate + "conservative" sorption on bentonite	(d)	(d)	(d)	(d)	(d)	(d)	(d)
14. Glass-corrosion rate, solubility limits and sorption constants set to "conservative" values, zero-conc. boundary condition	1.0×10^{-1}	3.4×10^{-5}	1.4×10^{-9}	2.9×10^{-1}	6.2×10^{-1}	2.5×10^{-6}	2.8×10^{-4}

Notes: (c) no stable isotopes (Table 3.7.1).
(d) not calculated.

Table 5.2.3: Maximum releases, expressed as annual individual doses [mSv y^{-1}] (drinking-water consumption). (b): the 4N and 4N + 3 actinide chains. Parameter variations which give doses differing from the Reference Case by a factor of 10 or more are indicated by bold type. Darker background shading indicates those variations which *decrease* dose by a factor of 10 or more. Lighter background shading indicates those which *increase* dose by a factor of 10 or more.

	Radionuclides				
	²⁴⁵ Cm	²⁴¹ Am	²³⁷ Np	²³³ U	²²⁹ Th
Reference Case	3.6×10^{-11}	1.9×10^{-11}	1.5×10^{-7}	3.0×10^{-7}	3.3×10^{-6}
1. Reduced canister lifetime	3.8×10^{-11}	2.1×10^{-11}	1.5×10^{-7}	3.0×10^{-7}	3.4×10^{-6}
2. Increased canister lifetime	9.7×10^{-15}	5.2×10^{-15}	1.5×10^{-7}	2.9×10^{-7}	3.2×10^{-6}
3. Increased glass-corrosion rate	1.9×10^{-10}	1.0×10^{-10}	5.9×10^{-7}	3.1×10^{-7}	3.4×10^{-6}
4. "Conservative" solubility limits	3.6×10^{-11}	1.9×10^{-11}	1.4×10^{-5}	1.7×10^{-6}	1.9×10^{-5}
5. Sharing of elemental solubility with stable isotopes not taken into account	(c)	(c)	(c)	(c)	(c)
6. "Conservative" sorption on bentonite	1.7×10^{-6}	1.1×10^{-6}	3.2×10^{-7}	2.7×10^{-6}	6.0×10^{-5}
7. Reduced bentonite thickness	1.4×10^{-5}	1.1×10^{-5}	4.3×10^{-7}	4.9×10^{-6}	6.1×10^{-4}
8. 10-fold decrease in groundwater flowrate	3.6×10^{-12}	1.9×10^{-12}	1.5×10^{-8}	3.0×10^{-8}	3.3×10^{-7}
9. 10-fold increase in groundwater flowrate	3.5×10^{-10}	1.9×10^{-10}	1.2×10^{-6}	3.8×10^{-6}	4.3×10^{-5}
10. 100-fold increase in groundwater flowrate	3.2×10^{-9}	1.7×10^{-9}	4.4×10^{-6}	3.5×10^{-5}	4.0×10^{-4}
11. Zero-concentration boundary condition	3.1×10^{-8}	3.1×10^{-8}	6.5×10^{-6}	1.2×10^{-4}	1.9×10^{-3}
12. 10-fold increase in groundwater flowrate + "conservative" solubility limits	3.5×10^{-10}	1.9×10^{-10}	1.2×10^{-4}	1.6×10^{-5}	1.8×10^{-4}
13. 10-fold increase in groundwater flowrate + "conservative" sorption on bentonite	(d)	(d)	(d)	(d)	(d)
14. Glass-corrosion rate, solubility limits and sorption constants set to "conservative" values, zero-concentration boundary condition	3.0×10^{-3}	3.0×10^{-3}	1.4×10^{-3}	1.7×10^{-3}	2.6×10^{-2}

Notes: (c) no stable isotopes (Table 3.7.1).
(d) not calculated.

Table 5.2.3: Maximum releases, expressed as annual individual doses [mSv y^{-1}] (drinking-water consumption). (c): the 4N + 1 actinide chain. Parameter variations which give doses differing from the Reference Case by a factor of 10 or more are indicated by bold type. Darker background shading indicates those variations which *decrease* dose by a factor of 10 or more. Lighter background shading indicates those which *increase* dose by a factor of 10 or more.

	Radionuclides					
	²⁴⁶ Cm	²⁴² Pu	²³⁸ U	²³⁴ U	²³⁰ Th	²²⁶ Ra
Reference Case	6.3×10^{-14}	6.6×10^{-7}	6.5×10^{-9}	6.3×10^{-9}	1.1×10^{-8}	7.2×10^{-4}
1. Reduced canister lifetime	7.1×10^{-14}	6.3×10^{-7}	6.6×10^{-9}	6.3×10^{-9}	1.1×10^{-8}	2.1×10^{-4}
2. Increased canister lifetime	3.2×10^{-20}	5.6×10^{-7}	6.5×10^{-9}	6.3×10^{-9}	1.1×10^{-8}	6.7×10^{-4}
3. Increased glass-corrosion rate	5.5×10^{-13}	6.7×10^{-7}	6.5×10^{-9}	6.3×10^{-9}	1.1×10^{-8}	7.2×10^{-4}
4. "Conservative" solubility limits	6.3×10^{-14}	6.9×10^{-7}	7.1×10^{-9}	3.6×10^{-8}	8.6×10^{-8}	9.3×10^{-4}
5. Sharing of elemental solubility with stable isotopes not taken into account	(c)	(c)	(c)	(c)	(c)	(c)
6. "Conservative" sorption on bentonite	4.7×10^{-8}	1.6×10^{-5}	6.8×10^{-9}	7.0×10^{-9}	9.4×10^{-8}	6.7×10^{-4}
7. Reduced bentonite thickness	8.6×10^{-7}	2.7×10^{-5}	6.9×10^{-9}	7.2×10^{-9}	2.9×10^{-6}	1.3×10^{-3}
8. 10-fold decrease in groundwater flowrate	6.3×10^{-15}	6.6×10^{-8}	7.0×10^{-10}	6.7×10^{-10}	1.2×10^{-9}	9.4×10^{-6}
9. 10-fold increase in groundwater flowrate	6.2×10^{-13}	6.2×10^{-6}	4.7×10^{-8}	4.6×10^{-8}	8.1×10^{-8}	6.3×10^{-3}
10. 100-fold increase in groundwater flowrate	5.7×10^{-12}	4.0×10^{-5}	1.4×10^{-7}	3.8×10^{-7}	1.9×10^{-6}	2.9×10^{-2}
11. Zero-concentration boundary condition	7.3×10^{-11}	1.1×10^{-4}	1.9×10^{-7}	9.9×10^{-7}	6.4×10^{-6}	4.7×10^{-2}
12. 10-fold increase in groundwater flowrate + "conservative" solubility limits	6.2×10^{-13}	6.5×10^{-6}	6.2×10^{-8}	3.5×10^{-7}	8.2×10^{-7}	8.2×10^{-3}
13. 10-fold increase in groundwater flowrate + "conservative" sorption on bentonite	(d)	(d)	(d)	(d)	(d)	(d)
14. Glass-corrosion rate, solubility limits and sorption constants set to "conservative" values, zero-conc. boundary condition	1.7×10^{-4}	2.1×10^{-3}	6.4×10^{-6}	1.5×10^{-4}	1.1×10^{-4}	4.3×10^{-2}

Notes: (c) no stable isotopes (Table 3.7.1).
(d) not calculated.

Table 5.2.3: Maximum releases, expressed as annual individual doses [mSv y^{-1}] (drinking-water consumption). (d): the 4N + 2 actinide chain. Parameter variations which give doses differing from the Reference Case by a factor of 10 or more are indicated by bold type. Darker background shading indicates those variations which *decrease* dose by a factor of 10 or more. Lighter background shading indicates those which *increase* dose by a factor of 10 or more.

Figure 5.2.3 summarises the effect of varying single parameters (with all other parameters held at their Reference-Case values) on the peak release rates for a set of representative radionuclides. The four histograms show release rates expressed (a,c) in moles per year and (b,d) according to a dose index, defined as the ratio of annual individual dose (obtained from the dose-conversion factors given in Appendix 6, using the drinking-water consumption pathway) to the HSK R-21 regulatory guideline of 0.1 mSv y^{-1} (see Protection Objective 1 - Section 2.3). In no case does the index exceed unity, suggesting that the guideline can be met, even with no account taken of retardation and decay in the geosphere.

The guideline can be exceeded only in the most extreme case of a combination of "conservative" values for glass-corrosion rate, solubility limits and sorption constants, together with a zero-concentration boundary condition at the bentonite-host rock interface, corresponding to an unlimited groundwater flowrate (see results for ^{243}Am , ^{240}Pu and ^{239}Pu in Table 5.2.3).

Each of the variations of single parameters is discussed in more detail below.

5.2.3.1 Canister Lifetime

In the Reference Case, it is assumed that all canisters fail simultaneously at 10^3 years following emplacement. If it can be ensured that all the canisters are correctly sealed, this assumption is likely to be conservative. Although the probability of occurrence of even a single mis-sealed or unsealed canister is thought to be low (Subsection 4.3.3.1), in order to delimit the consequences of this FEP, calculations have been carried out under the extreme assumption that all canisters fail at an earlier time and glass corrosion begins at 10^2 years after emplacement. In these calculations, the bentonite is assumed to be completely resaturated at 10^2 years, although the actual resaturation time is highly uncertain (see Subsection 3.4.4.2). No account is taken of the effect of the higher temperatures on the rate of glass corrosion or the possibility that reducing conditions may not have become established throughout the near field, although, at 10^2 years, the temperature of the glass will have dropped to about $80 \text{ }^\circ\text{C}$ (Figure 3.4.2) and it is likely that most of the oxygen in the system will have been consumed by reaction with the canister.

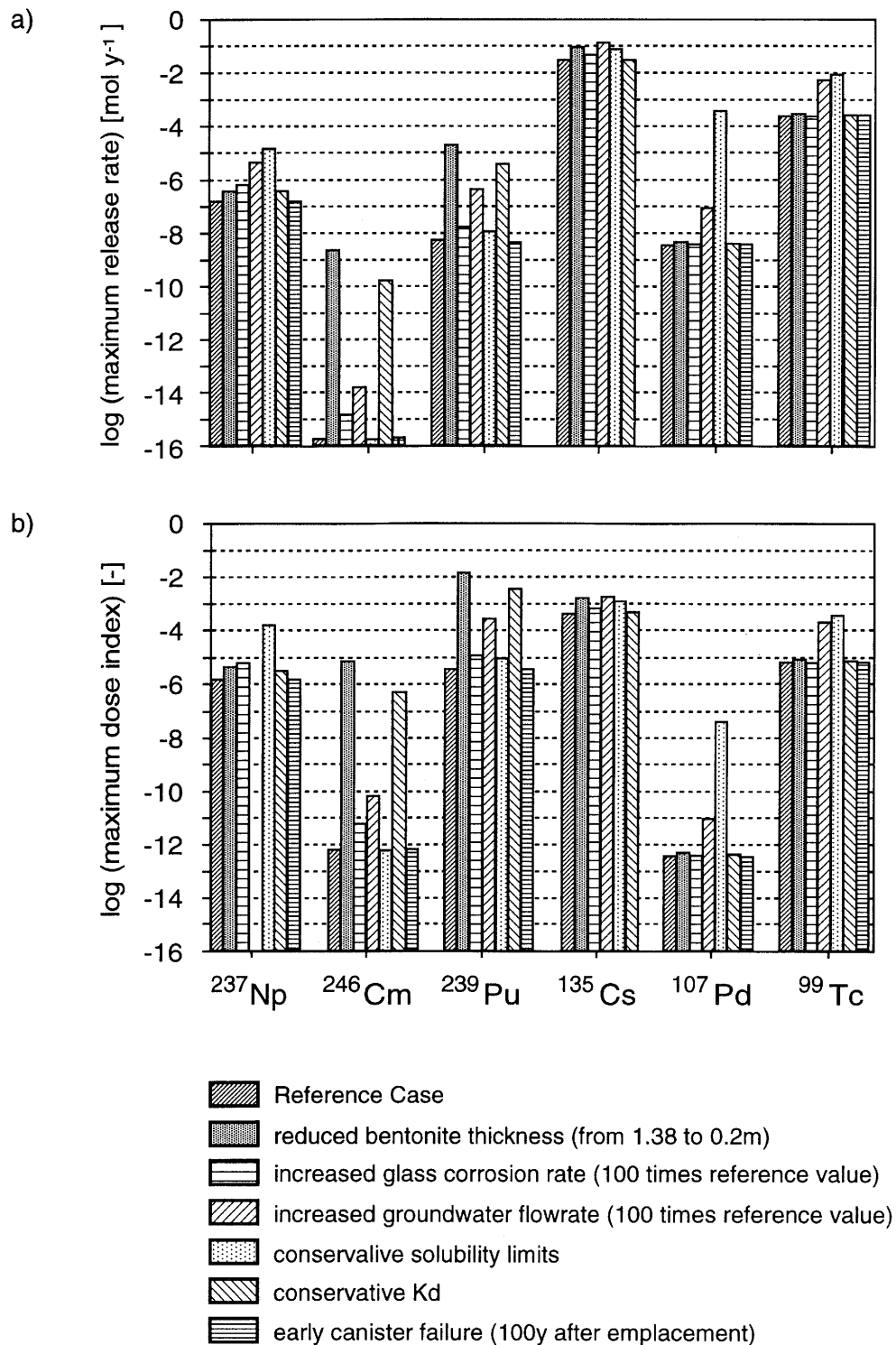


Figure 5.2.3: Maximum near-field release rates for selected radionuclides in the Reference Case and their sensitivity to parameter variations. Release rates are expressed in (a) moles per year from the total repository and (b) as a dose index (see text for definition).

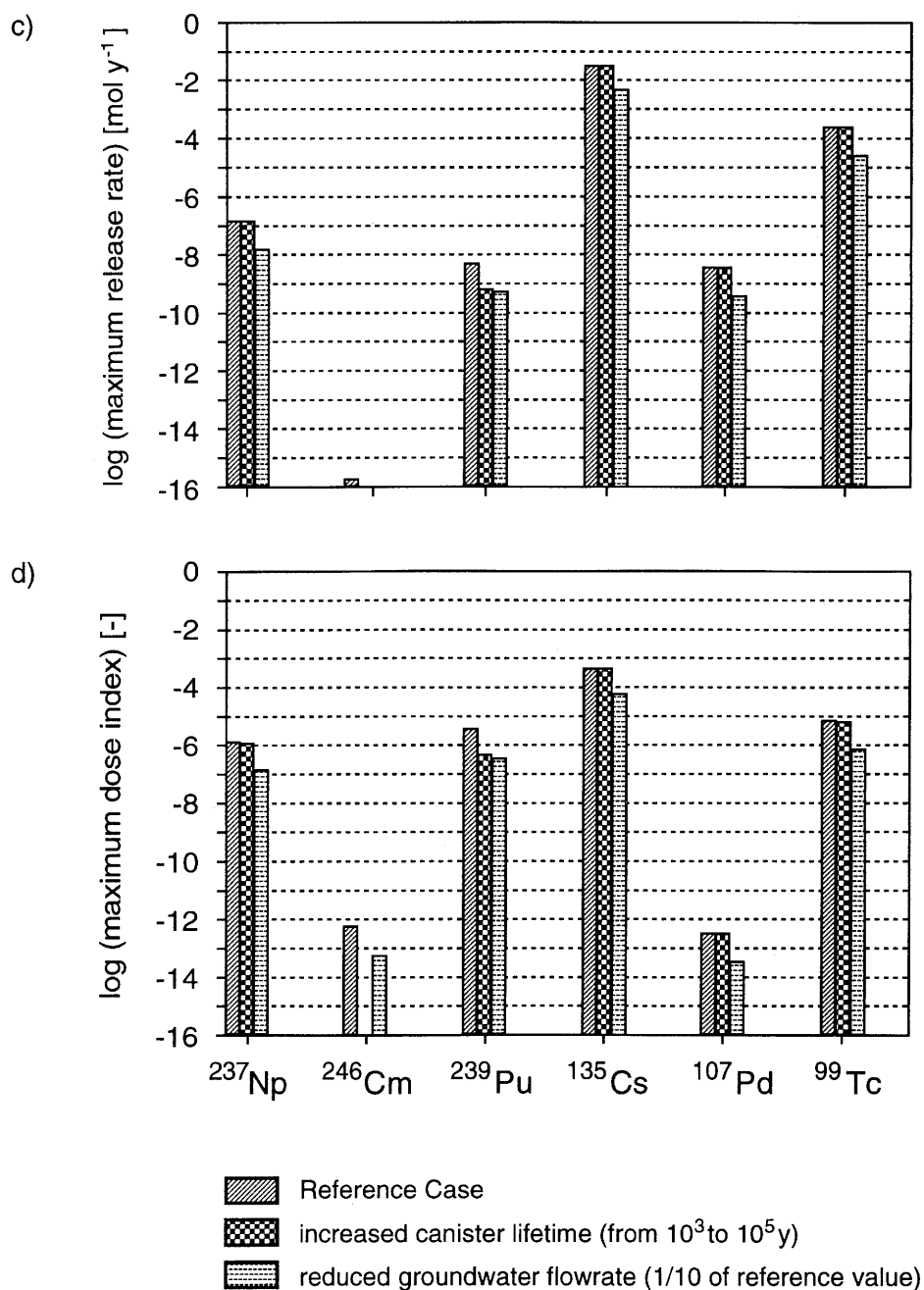


Figure 5.2.3: (Continued). Maximum near-field release rates for selected radionuclides in the Reference Case and their sensitivity to parameter variations. Release rates are expressed as (c) moles per year from the total repository and (d) as a dose index (see text for definition).

Safety-relevant radionuclides are identified in Appendix 2 on the assumption of a 10^3 -year canister lifetime. Many of the radionuclides listed in the inventory in Table 3.3.3, which is calculated for a time of 4 years after unloading of the fuel, decay to insignificance by this canister failure time. However, if a reduced canister lifetime is assumed, other radionuclides may need to be considered. A full re-assessment of safety-relevant radionuclides has not been carried out for a reduced time of complete isolation of 10^2 years, but two additional radionuclides which are most likely to be affected, ^{137}Cs (half-life 30.17 years) and ^{90}Sr (half-life 28.50 years), are included in the calculations²¹.

In general, if shorter-lived parent members of the actinide chains decay to insignificance by 10^3 years, their release and transport is not calculated; only truncated decay chains are considered (see Table A2.2). However, in the Reference-Case calculations, ingrowth resulting from the decay of these parent radionuclides *is* considered in deriving the inventory at 10^3 years (Table 3.7.1) from that at 4 years after unloading of the fuel (Table 3.3.3). This ingrowth is neglected in the calculations with a reduced canister lifetime, where the inventories of members of the truncated decay chains are taken directly from Table 3.3.3. The effect is apparent in the results shown in Table 5.2.3. In particular, in the case of the $4N$ chain ($^{240}\text{Pu} \rightarrow ^{236}\text{U} \rightarrow ^{232}\text{Th}$), calculated doses for the reduced canister lifetime are found to be *lower* than in the Reference Case; an artefact which arises because ingrowth from ^{244}Cm (half-life 18.11 years) is neglected.

The effect of a 10^2 -year canister lifetime on the calculated dose maxima is generally small, with results differing only slightly from those of the Reference Case. For the two additional radionuclides considered, the maximum calculated release rates and annual individual doses (from the drinking-water pathway; Appendix 6) are:

- ^{90}Sr : maximum release rate = $3.6 \times 10^{-10} \text{ mol y}^{-1}$;
maximum annual individual dose = $7.4 \times 10^{-7} \text{ mSv y}^{-1}$;
- ^{137}Cs : maximum release rate = $9.3 \times 10^{-10} \text{ mol y}^{-1}$;
annual individual dose = $6.5 \times 10^{-7} \text{ mSv y}^{-1}$.

The maximum doses from these radionuclides are thus comparable to, for example, those of ^{99}Tc and ^{126}Sn , but more than an order of magnitude below that of ^{135}Cs .

In reality, because of the conservative assumptions made in quantifying canister corrosion, the canister lifetime is likely to exceed by far the Reference-Case value of 10^3 years (Subsection 4.3.3.3). In order to investigate the influence of a longer canister lifetime on near-field releases, calculations have been carried out for the extreme

²¹ The solubility limit of Sr in the near field is estimated to be $2 \times 10^{-6} \text{ M}$, assuming that it is controlled by the mineral strontianite (SrCO_3) - the least soluble of the common, simple Sr minerals. However, this value is not of critical importance since, during the course of the calculations, the solubility limit is never reached. Sorption of Sr within the bentonite is conservatively neglected.

assumption of a 10^5 year lifetime. Comparison of the results of these calculations with those of the Reference Case (Table 5.2.3) indicates a significant reduction in the maximum release rates for only a few short-lived radionuclides, i.e. ^{246}Cm , ^{245}Cm , ^{243}Am , ^{241}Am and ^{240}Pu . The flux maxima of all other radionuclides remain largely unaffected by the increased canister lifetime. The assumption of a prolonged canister lifetime leads to reduced maximum release rates when *all* of the following criteria are met:

- the radionuclide half-life is shorter than or comparable to the assumed canister lifetime,
- the radionuclide has no long-lived, abundant precursor,
- the solubility limit is not attained during the calculations.

For instance, the increased canister lifetime has no effect on the ^{226}Ra peak flux, in spite of its short half-life (1.6×10^3 y), because this radionuclide is in radioactive equilibrium with the slowly decaying and abundant precursor ^{238}U . On the other hand, large effects are found for the short-lived first members of each chain, for which the maximum release rates are decreased by up to 4 orders of magnitude.

It is concluded that, even under extreme assumptions with regard to either decreased or increased canister lifetimes, doses from the most safety-relevant radionuclides (those that contribute most to the total dose when looking at overall system performance; see Chapter 6) are little affected. For an increased canister lifetime, a pronounced decrease is observed in the maximum releases of a few shorter-lived radionuclides. For a reduced canister lifetime, doses from radionuclides which would, in the Reference Case, decay to insignificance before canister failure, may contribute to the overall dose to a similar degree as some of the safety-relevant radionuclides identified in Appendix 2. They do not, however, dominate the overall dose. Furthermore, because of their relatively short half-lives, they would be likely to decay considerably during their passage through the geosphere.

5.2.3.2 Glass-corrosion Rate

A range of 3.8×10^{-4} kg m⁻² y⁻¹ to 3.8×10^{-2} kg m⁻² y⁻¹ has been defined for the glass-corrosion rate. From Equation 5.2.6, these values imply times for complete corrosion of the waste matrix ranging from 150 000 to 1500 years following canister failure. The effects of varying this parameter from "realistic-conservative" to "conservative" values

have been calculated for all radionuclides listed in Table 3.7.1. However, referring to Table 5.2.3, in no case does the variation greatly affect the near-field maximum release²².

The lack of sensitivity of peak release arises partly because most of the radionuclides are solubility limited. The solubility limit fixes the maximum concentration in solution near the waste matrix; only the time taken to reach this concentration can be affected by the glass-corrosion rate. However, the time taken for radionuclides to diffuse through the bentonite effectively masks any time-dependent behaviour near the waste matrix. Non-solubility limited radionuclides (⁵⁹Ni and ¹³⁵Cs) also show insensitivity to variations in this parameter. Here again, the time taken for radionuclides to diffuse through the bentonite is sufficient to mask the duration of release from the glass.

It can thus be concluded that the uncertainty in the glass-corrosion rate is not of critical importance in determining the near-field performance if the waste form is protected by engineered barriers evolving as expected. The integrity of the waste would be of concern only if the bentonite were to lose its safety relevant properties (i.e. effective sorption of radionuclides and colloid filtration).

5.2.3.3 Elemental Solubility Limits

"Realistic-conservative" and "conservative" values of solubility limits are presented in Table 3.7.3. Table 5.2.3 shows that the maximum release from the near field is significantly affected by the adoption of "conservative" solubility limits for ²³⁷Np, ⁹⁹Tc, ¹⁰⁷Pd, ⁷⁹Se and ⁹³Zr, to the extent that the calculated dose maxima for ²³⁷Np, ⁹⁹Tc and ⁷⁹Se are comparable to that of non-solubility limited ¹³⁵Cs. As an example of sensitivity to the solubility limit selected, Figure 5.2.4 shows the release rates of ⁹⁹Tc from the near field as a function of time for the Reference Case (broken curve) compared to the case in which the Tc solubility limit is set to a "conservative" high value, not reached in the calculation. In the Reference Case, the solubility limit of 10⁻⁷ M is reached at the inner boundary of the bentonite soon after canister failure, resulting in a fixed Tc concentration thereafter (Figure 5.2.4(a)). After approximately 100 000 years, steady-state diffusion through the bentonite is established, as indicated by the constant release rates from that time up to about 2 million years (Figure 5.2.4(b)). Later, as the isotope decays and the precipitated Tc disappears, the concentration and release rates decrease to negligible values. If a high solubility limit is set, then the model indicates considerably higher release rates up to one million years after canister failure. The maximum release rate at about 100 000 years is almost two orders of magnitude higher than in the solubility-limited case (see also Table 5.2.3(a)).

²² For ¹³⁵Cs, a significant effect is observed, but this is principally in the timing of the peak flux rather than its magnitude. For this radionuclide, the peak flux is increased by only 60 % when the conservative glass corrosion rate is selected, but the peak flux occurs much earlier, at about 3 000 years after closure, compared with 80 000 years after closure in the Reference Case.

The relative insensitivity of the maximum release rate of ^{238}U to variation in the solubility limit arises principally because of the high sorption constant for U in the bentonite (with respect, say, to Tc). Diffusion is sufficiently retarded by this sorption that the precipitated secondary phase solid disappears before steady-state conditions become established within the bentonite.

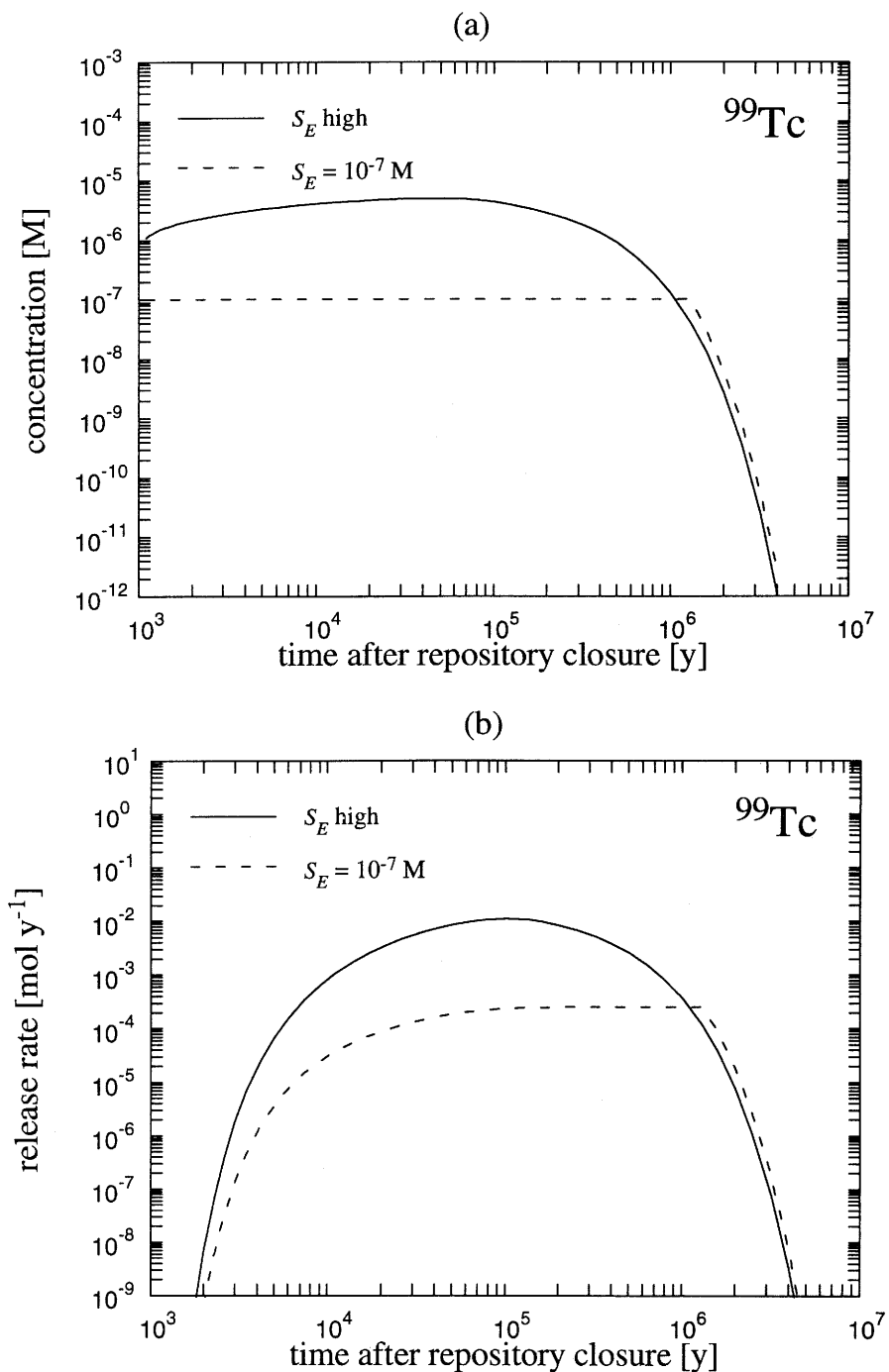


Figure 5.2.4: The effect of solubility limit, S_E , on (a) the radionuclide concentration at the inner boundary of the bentonite and (b) the release rate from the near field. Data for the case of ^{99}Tc .

Changes in the solubility limits have a pronounced effect for most safety-relevant solubility-limited radionuclides (^{237}Np , ^{99}Tc , ^{79}Se). Solubility limits are thus of key importance in near-field performance.

5.2.3.4 Effects of Shared Solubility Limits with Stable Isotopes

In the analyses for Project Gewähr 1985, solubility limits were distributed between isotopes of the same element, but taking into account only the radio-isotopes present. In the case of elements for which there is a significant inventory of stable isotopes in the waste, neglecting the presence of stable isotopes may lead to overly conservative results. This is the case for a number of activation/fission products, as illustrated by the data in Table 5.2.4, derived from values in Tables 3.7.1 and 3.7.3.

	Ratio of isotope inventory to total elemental inventory (including stable isotopes) at 1000 years	Ratio of elemental concentration in the volume for dissolution (calculated assuming complete, instantaneous waste dissolution) to "realistic-conservative" solubility limit.
^{59}Ni	0.05%	less than 1
^{79}Se	11%	2.7×10^6
^{107}Pd	15%	4.5×10^{10}

Note: Conservatively, only stable isotope inventories released from the glass waste are considered, with those of the stainless steel fabrication flask (in particular, Ni), the canister, the bentonite and the porewater neglected.

Table 5.2.4: Data to assess for which elements the effects of solubility limits shared with stable isotopes from the waste are likely to be important. (See text for explanation).

Hypothetical elemental concentrations in the volume for dissolution are here calculated assuming instantaneous dissolution of the waste matrix (the ratio of total elemental inventory, including stable isotopes, to the volume for dissolution V_R). For Ni, this concentration is less than the "realistic-conservative" solubility limit assumed in the calculations, even though there is a significant inventory of stable Ni. Sharing of solubility limits can therefore have no effect on the release of the radio-isotope ^{59}Ni . The sharing of solubility limits is, however, relevant for ^{79}Se and ^{107}Pd . In order to investigate the magnitude of this effect, calculations with no account taken for stable isotopes have been performed for ^{79}Se and ^{107}Pd . The maximum releases are shown in Table 5.2.3 and release vs. time is plotted in Figure 5.2.5; the maximum release is greater than the Reference Case by two orders of magnitude for ^{107}Pd and by an order of magnitude for ^{79}Se . This difference is related to the ratio of the radio-isotope inventory

to the stable inventory, which increases with time as the radio-isotope decays. Hence, the reduction in release rate is greater than the ratios at 1000 years, shown in Table 5.2.4, would indicate.

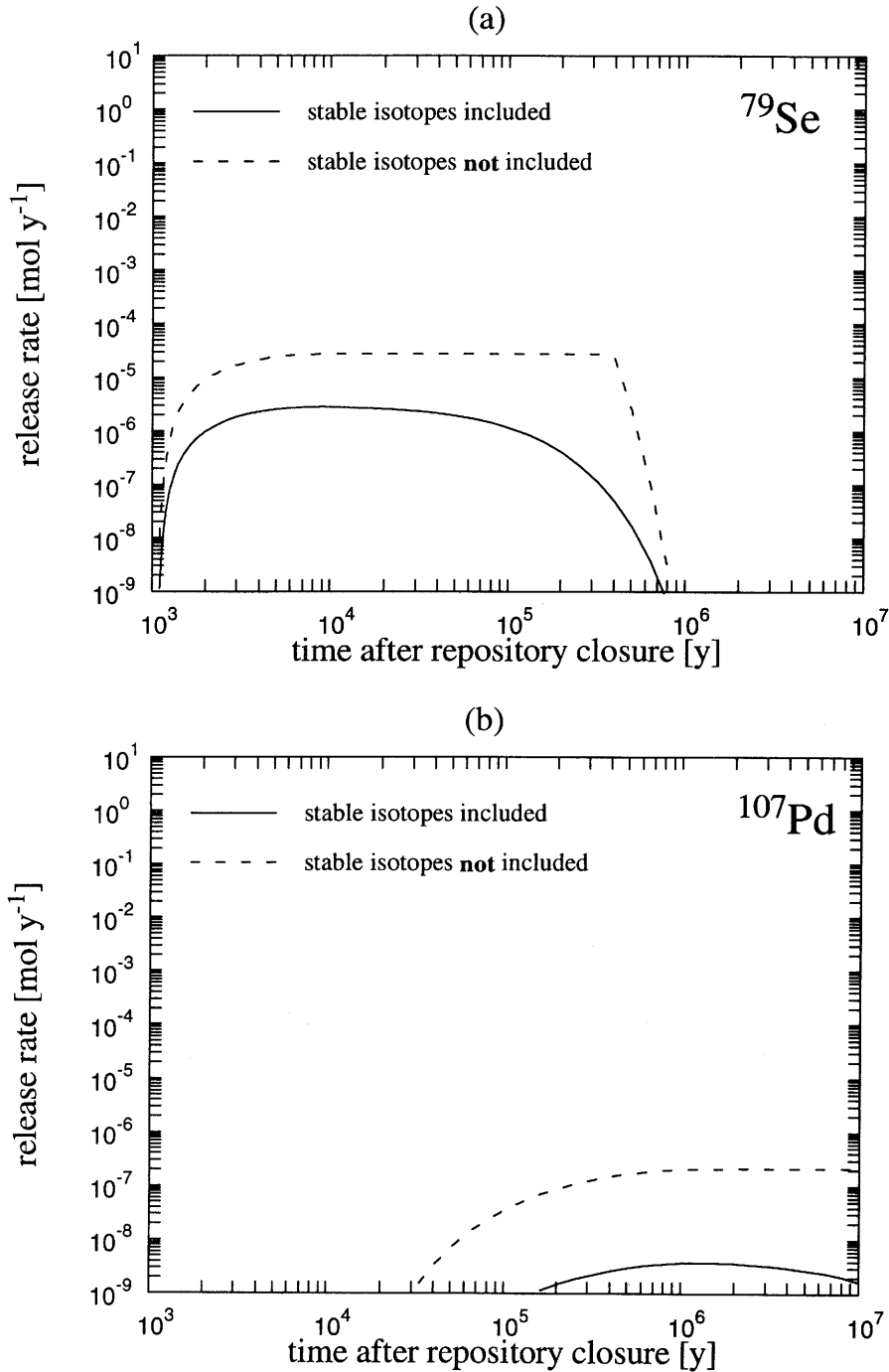


Figure 5.2.5: The effect on the release rate from the near field of the sharing of solubility limits between stable isotopes and radio-isotopes, illustrated for the cases of (a) ^{79}Se and (b) ^{107}Pd . This feature of the near field was not included in the modelling for Projekt Gewähr 1985. Since that time, its status has been changed from that of a reserve FEP to an active FEP in the new near-field model (code STRENG).

5.2.3.5 Sorption Constants in the Bentonite

Sorption has the effect of prolonging the transport times of solutes through the bentonite. For radioactive solutes, increased decay will occur during transport. In Project Gewähr 1985, only limited account was taken of sorption in the bentonite: strongly retarded radionuclides with relatively short half-lives (e.g. ^{137}Cs , ^{90}Sr , ^{245}Cm , ^{241}Am), which could be shown to decay to insignificant levels during transit, were excluded from further consideration. The Kristallin-I near-field code STRENG, however, allows sorption in the bentonite to be modelled explicitly. "Realistic-conservative" and "conservative" sorption constants are presented in Table 3.7.3. Table 5.2.3 shows that the maximum release from the near field is significantly affected by the adoption of "conservative" sorption constants for a limited number of the safety-relevant radionuclides:

- the activation/fission products ^{59}Ni and ^{126}Sn ;
- the actinide-chain members ^{246}Cm , ^{245}Cm , ^{243}Am , ^{241}Am , ^{242}Pu , ^{240}Pu , ^{239}Pu , ^{231}Pa , and ^{229}Th .

The release rates of the longer-lived radionuclides, i.e. ^{99}Tc , ^{79}Se , ^{135}Cs and ^{237}Np , which tend to dominate dose, are increased by less than an order of magnitude when "conservative" sorption constants are applied.

5.2.3.6 Bentonite Thickness

Calculations have been performed assuming a reduction in the bentonite thickness from 1.38 to 0.2 m, in order to investigate whether the performance of the engineered barriers would still be acceptable. The main aim of these calculations is to illustrate the role of the bentonite as an effective barrier, by examining an extreme case in which the thickness of the bentonite is much less than the design value. The variation can also be thought of as representative of such situations as incorrect emplacement of the canisters, the sinking of the canisters (see Subsection 4.3.3.11) or the loss of performance of part of the bentonite due to the partial alteration of montmorillonite (see Subsection 4.3.3.9). These situations are considered to be unlikely. Even though an increase in the inner radius of the bentonite might be a more appropriate model, particularly of the latter effect, the reduction of the bentonite thickness is in fact modelled by a decrease in the outer radius; however, the difference between these two approaches (i.e. the effect of the curvature of the bentonite annulus) is likely to be small.

The effect of decreased bentonite thickness is similar to that of adopting "conservative" sorption constants: the impact is large for short-lived radionuclides, such as the first members of the actinide chains, e.g. ^{246}Cm and ^{239}Pu ; see Table 5.2.3. The calculations show that the releases from the near field would be significantly higher for these

radionuclides. On the other hand, the release rates of the longer-lived activation/fission products and actinides (e.g. ^{99}Tc , ^{107}Pd , ^{79}Se , ^{135}Cs and ^{237}Np , ^{238}U , ^{235}U , respectively) are increased by less than one order of magnitude. Since these longer-lived radionuclides tend to dominate dose for the overall system, this indicates that a reduced bentonite thickness would still provide sufficient performance within the overall disposal system.

5.2.3.7 Groundwater Flowrate at the Bentonite-Host Rock Interface

Increasing the groundwater flowrate at the bentonite-host rock interface reduces radionuclide concentrations at the interface, leading to steeper concentration gradients in the bentonite and increased release rates to the host rock. The sensitivity of near-field releases to flowrate variation has been investigated by performing calculations with the Reference-Case flowrate decreased by a factor of 10 and also increased by factors of 10 and 100. These variations span the variability and uncertainty in the groundwater flow calculations (see the discussion in Subsection 6.2.2.4). A further, highly conservative variation has been calculated: that of a zero-concentration boundary condition at the interface, which, as noted in Subsection 5.2.1.2, corresponds to unlimited advective transport away from the bentonite.

The results given in Table 5.2.3 show that the maximum releases of all the safety-relevant radionuclides are moderately sensitive to this parameter. With the exception of ^{135}Cs , releases vary approximately proportionately to flowrate up to a 10-fold increase, but are less sensitive if the flowrate is increased to still higher values. At the higher flowrate values, the concentration at the outer boundary of the bentonite is reduced almost to zero. Further increases in flowrate therefore have little effect on the concentration gradient across the bentonite and on the diffusive flux across the outer boundary of the bentonite. ^{135}Cs release is relatively insensitive to flowrate increase, but is reduced by a factor of 7 for a 10-fold decrease in flowrate. With the exception of a few of the actinide-chain members (e.g. ^{243}Am , ^{240}Pu), there is little difference in results between the 100-fold flowrate increase and the zero-concentration boundary condition. Figure 5.2.6 illustrates the effect of varying the flowrate on release-rate vs. time curves for two radionuclides: ^{79}Se and ^{135}Cs .

It can be concluded that the groundwater flowrate at the bentonite-host rock interface is an important parameter determining near-field performance.

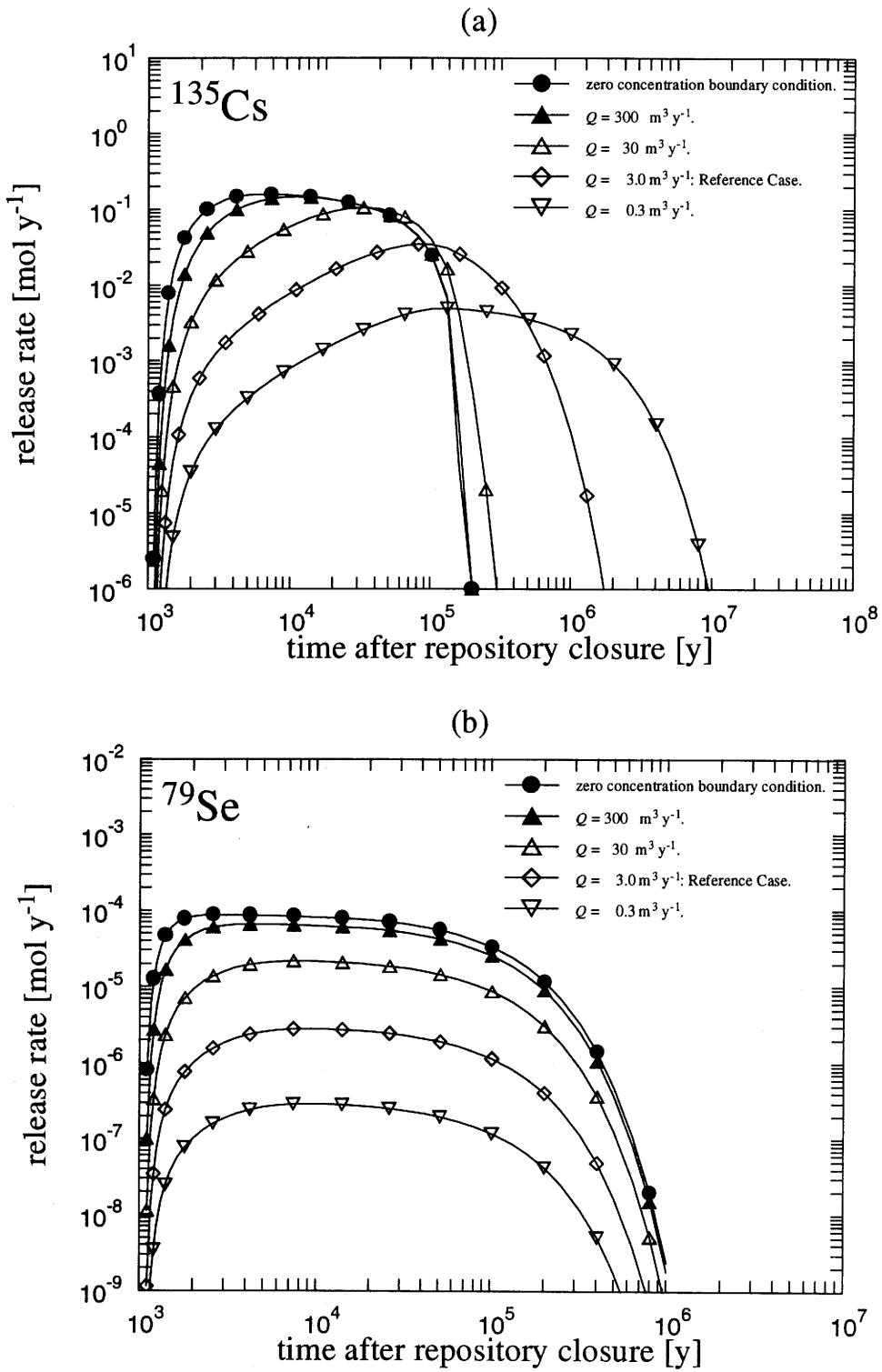


Figure 5.2.6: The effect of groundwater flowrate at the bentonite-host rock interface on radionuclide release from the near field. Results are shown for (a) ^{135}Cs and (b) ^{79}Se .

5.2.4 Summary of Near-Field Modelling and Performance

The principal components of the engineered barriers of the near field are:

- the glass matrix;
- the massive steel canister;
- the thick, compacted bentonite clay buffer.

A conceptual model of this system has been developed; the model includes several conservative assumptions, in particular:

- the massive steel canister containing the vitrified waste is assumed to fail (in Reference-Case calculations) at 1000 years after repository closure and thereafter offers no physical resistance to water ingress and radionuclide transport;
- no account is taken of radionuclide sorption on, and co-precipitation with, glass secondary minerals and canister corrosion products, which are known to be effective scavengers of many key radionuclides.

Further conservatism arises from simplifications that have been made to facilitate mathematical treatment and from the selection of parameter values for the Reference-Case calculations. Nevertheless, an examination of the Reference-Case results shows that the engineered barriers are highly effective. The calculated annual individual dose maxima indicate that the near field alone reduces radionuclide fluxes sufficiently to meet the regulatory guideline of 0.1 mSv y^{-1} , even without account being taken of retardation and decay in the geosphere.

Examination of the sensitivity of results to parameter variations shows that the most important factor is that the solubility limits for many of the longer-lived radionuclides are low within the well-controlled chemical conditions of the near field and limit the maximum source concentration for diffusion to the bentonite. The role of the solubility limits is linked to the effectiveness of the bentonite as a colloid filter; the bentonite ensures that precipitated species are retained within the engineered barriers.

Sorption within the bentonite (and the thickness of the bentonite) affects the release of shorter-lived radionuclides, but these are, in any case, likely to decay considerably during geosphere transport. Finally, the results show that a reduction in the groundwater flowrate at the bentonite-host rock interface can significantly enhance the calculated performance of the engineered barriers.

5.3 Geosphere Modelling

In this section, the geosphere modelling assumptions are first described (Subsection 5.3.1), the governing equations (Subsection 5.3.2) and their solutions (Subsection 5.3.3) are then discussed and the input parameters are listed (Subsection 5.3.4). In Subsection 5.3.5, the sensitivity of geosphere performance to parameter variations is discussed; the parameters varied include the groundwater flowrate, flowpath length, longitudinal dispersion length and matrix properties (diffusion and sorption constants, geometry and extent of diffusion-accessible matrix). In Subsection 5.3.6, the results are summarised.

The geological and hydrogeological features relevant to the safety of the Kristallin-I repository are described in Section 3.5. Briefly, the crystalline basement of Northern Switzerland comprises a low-permeability domain²³; overlain by a higher-permeability domain and intersected to below repository depth by major faults, some of which may be water conducting (Figure 3.5.3). Groundwater flow through the host rock occurs within a network of water-conducting features which extends throughout the crystalline basement. Some features will inevitably be intersected by the repository tunnel system, thus providing a route by which radionuclides released from the repository near field may be transported to the biosphere. Groundwater flow and advective transport within the rock matrix between water-conducting features is considered to be negligible.

The repository emplacement tunnel system may be divided into panels, each located within a single block of the low-permeability domain (see Figure 3.1.1). Depending on the location of their source within the repository and on the hydrogeological regime, radionuclides released from a repository panel would be transported to the higher-permeability domain, and thence to the biosphere, either directly through the low-permeability domain, or via both the low-permeability domain and major water-conducting faults. In either case, the dominant transport mechanisms are considered to be advection of radionuclides in solution through channels within the water-conducting features and diffusion from these channels into the stagnant pore waters of the adjacent rock matrix - the resulting division of porosity into flow porosity and matrix porosity is termed the dual-porosity concept (see, for example, HADERMANN & RÖSEL 1985). Radionuclide sorption onto pore surfaces must also be taken into account. Furthermore, colloids, which can be present in groundwater, may influence transport if they sorb radionuclides significantly and the colloid concentration is sufficiently high (see, for example, AVOGADRO & DE MARSILY 1984; SMITH 1993a).

The Reference Scenario has been described in detail in Chapter 4. In the following subsection, only the assumptions within the Reference Scenario directly relevant to safety assessment modelling of the geosphere will be restated, together with additional simplifying assumptions which are made to facilitate mathematical modelling.

²³ In Area East, the existence of the low-permeability domain is less well established than in Area West, with two possible interpretations of the available borehole data - see hypotheses 1 and 2 in Subsection 3.5.3.

5.3.1 Model Assumptions

The safety-assessment model for the geosphere described below considers groundwater mediated transport of radionuclides from the near field to the biosphere through the host rock. A possible alternative transport path is along access drifts and shafts; this is considered as an alternative scenario in Chapter 6.

5.3.1.1 Features and Processes

The following assumptions are made concerning the physical and chemical features and processes to be considered. The background to, and justification of, these assumptions is discussed in Chapters 3 and 4 and in THURY et al. (1994).

- The crystalline basement rock is heterogeneous at all scales considered. For the purpose of safety-assessment modelling, the basement rock in Area West is assumed to comprise three main elements at a macroscopic (local) scale (see Figure 3.5.5):
 - 1: Low-permeability domain, with average large-scale hydraulic conductivity of the order of 10^{-3} m y^{-1} ($4 \times 10^{-11} \text{ m s}^{-1}$), some hundreds of metres below the top of the crystalline basement.
 - 2: Higher-permeability domain overlying the low-permeability domain, with large-scale average hydraulic conductivity of the order of 10 m y^{-1} ($3 \times 10^{-7} \text{ m s}^{-1}$).
 - 3: Major water-conducting faults - predominantly sub-vertical faults, of 1st or 2nd order (see Figure 3.5.5), intersecting both low- and higher-permeability domains with hydraulic conductivity identical to that of the higher-permeability domain ($10 \text{ m}^3 \text{ y}^{-1}$).

In Area East, the existence of the low-permeability domain is not well established, with two possible interpretations of available borehole data (hypotheses 1 and 2, see Subsection 3.5.3). For safety assessment-modelling of Area East, the more conservative "Hypothesis 1" is assumed, in which data from the Siblingen borehole are assumed to be representative, giving an average large-scale hydraulic conductivity in basement of the order of 0.3 m y^{-1} (10^{-8} m s^{-1}) and no clear distinction between low- and higher-permeability domains.

- The repository panels are sited at a depth of about 1000 m below ground, at least 100 m from any major water-conducting faults and, in Area West, at least 100 m below the interface between the low- and higher-permeability domains.
- The possible pathways to the biosphere considered for radionuclides released from a repository in Area West are:

- through the low-permeability domain to a major water-conducting fault, upwards to the higher-permeability domain and thence to the biosphere;
- through the low-permeability domain directly (upwards) to the higher-permeability domain and thence to the biosphere.

For a repository in Area East, transport through major water-conducting faults is not explicitly modelled.

- On a smaller (block) scale (see Figure 3.5.5), groundwater flow and radionuclide transport in the crystalline basement (low-permeability domain, major water-conducting faults and higher-permeability domain) occurs in a network of discrete, water-conducting features.
- These smaller water-conducting features are divided into three types (Figure 3.5.4) - (i) cataclastic zones, (ii) jointed zones, (iii) fractured aplite/pegmatite dykes and aplitic gneisses - with different geological and mineralogical characteristics. Each type consists of a set of sub-parallel, partially infilled fractures. Water flows through channels within the fracture infill.
- Radionuclides are advected in solution (or sorbed on groundwater colloids - see below) along the channels within the water-conducting features. Radionuclides in solution may diffuse into stagnant matrix porewaters of the adjacent wallrock/fracture infill (the dual-porosity concept).
- Solubility limits appropriate to the groundwater chemistry are assumed not to be exceeded in the geosphere.
- Radionuclides sorb onto the surfaces of the channels and matrix pores. The degree of sorption is influenced by mineralogy and groundwater chemistry.

Radionuclides reaching the higher-permeability domain are transported rapidly to the biosphere (the valley of the river Rhine).

The dilution of radionuclides in the near-surface environment and subsequent processes are considered in the biosphere model: see Section 5.4.

5.3.1.2 Simplifications and Additional Model Assumptions

The following simplifications and additional assumptions are made in order to model the above features and processes:

- The channels within the small-scale water-conducting features are modelled by a single, representative parallel-walled conduit (planar geometry) or tubular conduit (cylindrical geometry) of specified dimensions: flowpath length L [m], aperture $2b$ [m] or radius r_0 [m]. The selection of either planar or cylindrical geometry is based on the dimensions of the channels in the conceptual model of the water-conducting features (Figure 5.3.5) and is explained in Subsection 5.3.4.3.
- Advection is calculated along the conduit with a velocity u [m y^{-1}], obtained from the flowrate through, and internal geometric structure of, the water-conducting features.
- Interconnections between water-conducting features and their internal variability give rise to mechanical dispersion. Hydrodynamic dispersion, the combined effect of mechanical dispersion and molecular diffusion within the conduits, is modelled as a Fickian diffusion process in the longitudinal (flow) direction. Transverse dispersion is conservatively neglected.
- Hydrodynamic dispersion is quantified by a longitudinal dispersion length a_L [m], with the implicit assumption that the coefficient of longitudinal hydrodynamic dispersion is proportional to the advection velocity (see Equation 5.3.1). This assumption is supported by many experimental measurements (see, for example, Figure 6.6 in BEAR & VERRUJT 1987), given that the velocity is high enough that mechanical dispersion is large with respect to molecular diffusion, but not so high that flow becomes turbulent.
- Matrix diffusion, quantified by a pore diffusion constant D_p [$\text{m}^2 \text{y}^{-1}$], is calculated normal to the direction of flow into a region of connected porosity (porosity ϵ_p [-], solid density ρ [kg m^{-3}]) of limited extent adjacent to the conduit. The thickness of this "porous matrix" is $y_p - b$ [m] for planar geometry and $r_p - r_0$ [m] for cylindrical geometry (see Figure 5.3.1).
- Reversible, equilibrium sorption is assumed to take place on the pore surfaces of the matrix. Sorption onto the surfaces of the conduits themselves is conservatively neglected.
- Except in the case of Cs, sorption is assumed to be linear and is quantified by element-specific sorption constants. For Cs, sorption is described by a non-linear Freundlich isotherm.
- Advection velocity, longitudinal dispersion length, pore diffusion constant, parameters for sorption isotherms and matrix porosity are all assumed to be uniform in space and time.
- Two alternative assumptions are applied to the transport of radionuclides in the major water-conducting faults of Area West:

- Radionuclide transport time in the major water-conducting faults is neglected; radionuclides are assumed to be transported instantaneously to the higher-permeability domain on exiting the low-permeability domain (a conservative approach, adopted as a Reference Model Assumption for the geosphere).
- Radionuclide transport through water-conducting features in the major water-conducting faults is modelled explicitly, taking account of the same processes as in the low-permeability domain, but with modified parameters (treated as an alternative model assumption within the Reference Scenario - see Subsection 6.2.2.2).

As mentioned above, for a repository in Area East, transport through major water-conducting faults is not explicitly modelled.

- Radionuclides reaching the higher-permeability domain are conservatively assumed to be transported instantaneously to the biosphere.

Radionuclides are transported through the geosphere either in solution, or sorbed on groundwater colloids. However, the lack of empirical data, which would be required by a more complete model, has led to a highly simplified treatment of colloid transport. Colloid facilitated radionuclide transport is not included in the Reference Model Assumptions for the geosphere, but is treated as an alternative model assumption within the Reference Scenario - see Subsection 6.2.2.3.

5.3.2 Mathematical Representation

The dual-porosity transport model is illustrated in Figure 5.3.1 for the two alternative transport-model representations of the channels within the water-conducting features. For planar geometry, a Cartesian co-ordinate system (x,y,z) is adopted. The x,z -plane is located in the centre of the fracture, with the z -axis in the direction of water flow. For cylindrical geometry, a polar co-ordinate system (r,z) is used, with z following the axis of the tubular conduit.

5.3.2.1 Governing Equations

The mathematical formulation of the transport model is based on mass balance, carried out over a representative elementary volume. Neglecting for the moment the presence of colloids, transport within the model conduit is governed by the equation:

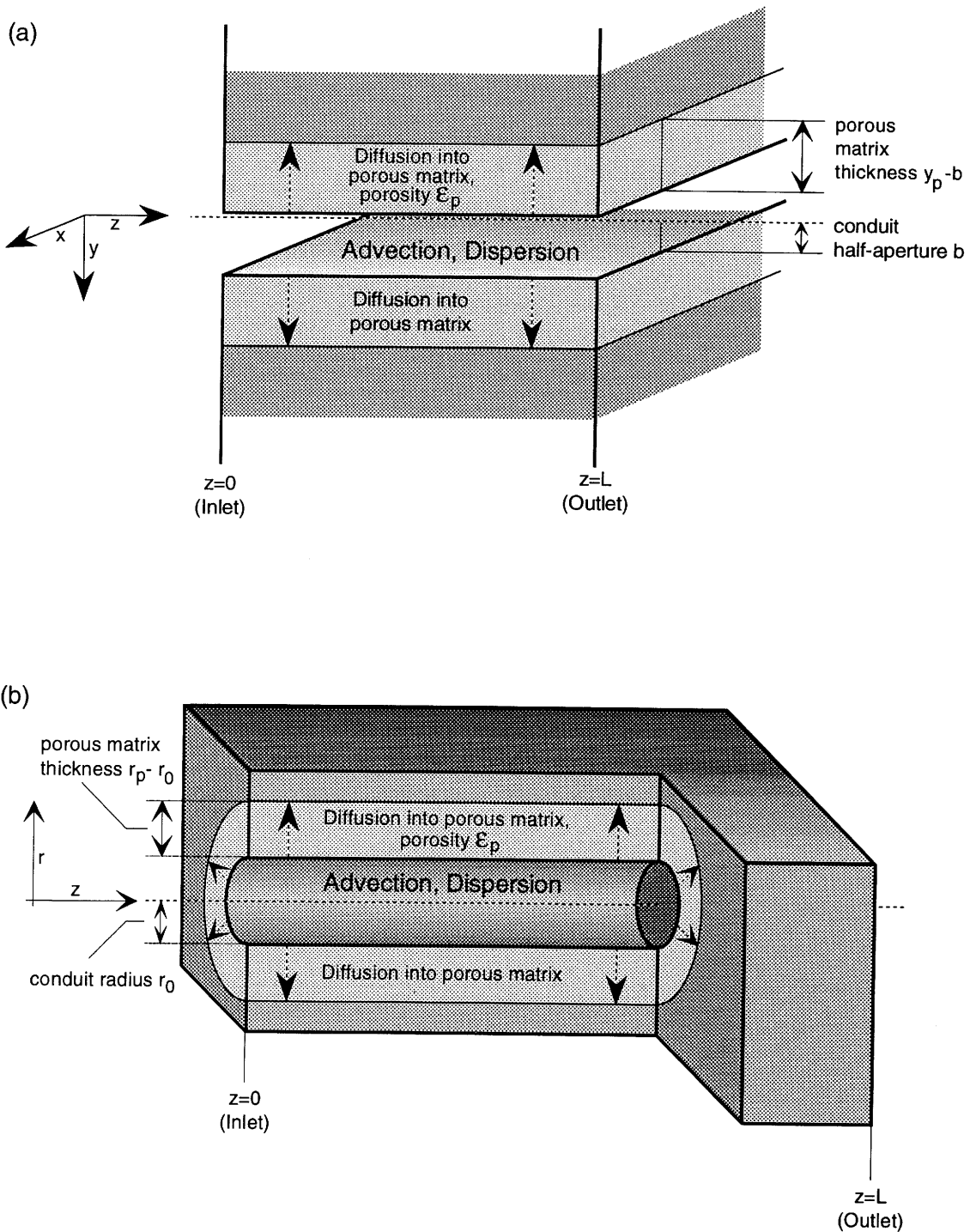


Figure 5.3.1: The dual-porosity transport model. Advection and longitudinal dispersion are modelled within either (a) a parallel-walled conduit (planar geometry) or (b) a tubular conduit (cylindrical geometry). One-dimensional, spatially-limited matrix diffusion normal to the advection-dispersion direction is also considered.

$$\frac{\partial C_f^{(i)}}{\partial t} = \frac{1}{R_f^{(i)}} \left[-u \frac{\partial C_f^{(i)}}{\partial z} + a_L u \frac{\partial^2 C_f^{(i)}}{\partial z^2} + \tilde{R}_f^{(i-1)} \lambda^{(i-1)} C_f^{(i-1)} - \tilde{R}_f^{(i)} \lambda^{(i)} C_f^{(i)} \right] + \frac{1}{R_f^{(i)}} \begin{cases} \left. \frac{1}{b} \varepsilon_p D_p \frac{\partial C_p^{(i)}}{\partial y} \right|_{y=b} & \text{planar geometry} \\ \left. \frac{2}{r_0} \varepsilon_p D_p \frac{\partial C_p^{(i)}}{\partial r} \right|_{r=r_0} & \text{cylindrical geometry} \end{cases} \quad (5.3.1)$$

where, on the right-hand side, the terms represent, respectively, advection, hydrodynamic dispersion, radioactive ingrowth and decay and diffusion into the porous matrix. Within the porous matrix itself,

$$\frac{\partial C_p^{(i)}}{\partial t} = \frac{1}{R_p^{(i)}} \left[\tilde{R}_p^{(i-1)} \lambda^{(i-1)} C_p^{(i-1)} - \tilde{R}_p^{(i)} \lambda^{(i)} C_p^{(i)} + \right] + \frac{D_p}{R_p^{(i)}} \begin{cases} \frac{\partial^2 C_p^{(i)}}{\partial y^2} & \text{planar geometry} \\ \frac{\partial^2 C_p^{(i)}}{\partial r^2} + \frac{1}{r} \frac{\partial C_p^{(i)}}{\partial r} & \text{cylindrical geometry.} \end{cases} \quad (5.3.2)$$

Here, the terms on the right-hand side represent ingrowth, decay and diffusion. The symbols used in these equations are defined in Subsection 5.3.1.2 and below:

$C_f^{(i)}$ and $C_p^{(i)}$ [mol m⁻³] are the concentrations in solution, within the conduit and the matrix porewater, respectively, of the *i*th radionuclide in the chain 1 → 2 → ... → *i* → ...,

$\lambda^{(i)}$ [y⁻¹] is the decay constant for radionuclide *i*,

$R_f^{(i)}$ and $R_p^{(i)}$ [-] are the retardation factors for advection and dispersion within the model conduit ($R_f^{(i)} = 1, \forall i$, since sorption on the conduit walls is not considered in the present analysis) and for matrix diffusion, respectively (see Subsection 5.3.3),

$\tilde{R}_f^{(i)}$ and $\tilde{R}_p^{(i)}$ [-] are also defined in Subsection 5.3.3 and are used to generalise the governing equations to deal with non-linear sorption; they are identical to the retardation factors $R_f^{(i)}$ and $R_p^{(i)}$ when sorption is linear.

5.3.2.2 Initial Conditions and Boundary Conditions

5.3.2.2.1 Initial Conditions

It is assumed that radionuclide concentrations in the geosphere are initially zero. Defining $t = 0$ as the time of canister failure and writing $C_f^{(i)} = C_f^{(i)}(z, t)$, $C_p^{(i)} = C_p^{(i)}(y, z, t)$ (for planar geometry) and $C_p^{(i)} = C_p^{(i)}(r, z, t)$ (for cylindrical geometry),

$$C_f^{(i)}(z, t) = 0 \quad ; \quad \forall z, \quad t \leq 0 \quad (5.3.3)$$

$$C_p^{(i)}(y, z, t) = 0 \quad ; \quad \forall z, \quad |y| \geq b, \quad t \leq 0 \quad \text{planar geometry} \quad (5.3.4)$$

$$C_p^{(i)}(r, z, t) = 0 \quad ; \quad \forall z, \quad r \geq r_0, \quad t \leq 0 \quad \text{cylindrical geometry} \quad (5.3.5)$$

5.3.2.2.2 Boundary Conditions - Model Conduit

As described in Subsection 5.3.1, two alternative assumptions are made concerning the modelling of the major water-conducting faults in Area West: radionuclides are either considered to enter the higher-permeability domain directly on exiting the low-permeability domain, or are considered to pass through the major water-conducting faults before entering the higher-permeability domain. In both cases, transport calculations for the low-permeability domain are carried out.

Additional transport calculations for the major water-conducting faults are required for the second of the alternative assumptions. In calculations for which the model conduit represents channels in the low-permeability domain, the boundary condition at the upstream end of the conduit is obtained by equating the advective and dispersive flux entering the conduit to the radionuclide flux from the near field (Equation 5.2.16). Where the conduit represents channels in the major water-conducting faults, this boundary condition equates the flux into the conduit to the flux from the low-permeability domain. In either case this flux is denoted by $F_{in}^{(i)}(t)$ [mol m⁻² y⁻¹], given by

$$F_{in}^{(i)}(t) = q \left[C_f^{(i)}(0,t) - a_L \frac{\partial C_f^{(i)}}{\partial z} \Big|_{z=0} \right] \quad ; \quad t > 0 \quad (5.3.6)$$

where q [m y^{-1}] is the Darcy velocity (for the low-permeability domain, $Q = qA$). At the downstream end of the conduit, a zero concentration boundary condition is assumed, corresponding to high dilution in either the major water-conducting faults or the higher-permeability domain:

$$C_f^{(i)}(L,t) = 0 \quad ; \quad \forall t. \quad (5.3.7)$$

$F_{out}^{(i)}(t)$ [$\text{mol m}^{-2} \text{y}^{-1}$], the radionuclide flux from the model conduit is given by

$$F_{out}^{(i)}(t) = -qa_L \frac{\partial C_f^{(i)}}{\partial z} \Big|_{z=L}. \quad (5.3.8)$$

Where transport through the major water-conducting faults is modelled, $F_{out}^{(i)}(t)$ from the calculation of transport in the low-permeability domain is equated to $F_{in}^{(i)}(t)$ for the subsequent calculation of transport in the faults.

5.3.2.2.3 Boundary Conditions - Porous Matrix

Solute concentration is continuous across the boundary between the conduit and the adjoining matrix, as described by the equation

$$C_f^{(i)}(z,t) = \begin{cases} C_p^{(i)}(b,z,t) & \text{planar geometry} \\ C_p^{(i)}(r_0,z,t) & \text{cylindrical geometry} \end{cases} \quad ; \quad \forall z, \forall t \quad (5.3.9)$$

A boundary condition of zero diffusive flux is imposed at the outer boundary of the porous matrix.

$$\frac{\partial C_p^{(i)}}{\partial y} \Big|_{y=y_p} = 0 \quad \text{for planar geometry} \quad (5.3.10)$$

$$\frac{\partial C_p^{(i)}}{\partial r} \Big|_{r=r_p} = 0 \quad \text{for cylindrical geometry}$$

5.3.3 Solutions to the Model Equations

5.3.3.1 Linear Sorption

In the modelling study for Kristallin-I, radionuclide sorption on the channel surface is conservatively neglected

$$R_f^{(i)} = \tilde{R}_f^{(i)} = 1 \quad (5.3.11)$$

and instantaneous sorption equilibrium is assumed on the surfaces of matrix pores. When this sorption is linear, described by a sorption constant $K_d^{(i)}$ [$\text{m}^3 \text{kg}^{-1}$], the retardation factors in the governing Equations 5.3.1 and 5.3.2 are independent of concentration and are given by

$$R_p^{(i)} = \tilde{R}_p^{(i)} = 1 + \frac{1 - \varepsilon_p}{\varepsilon_p} \rho K_d^{(i)}. \quad (5.3.12)$$

The linear governing equations may be solved numerically using the code RANCHMD (HADERMANN & RÖSEL 1985; JAKOB 1992). Solutions are obtained by first deriving a set of time-dependent ordinary differential equations using the Lagrange interpolation technique and then integrating using Gear's method for stiff sets of equations. RANCHMD has been extensively tested (SKI 1984; SKI 1986) and is used in the Kristallin-I geosphere calculations unless otherwise stated.

5.3.3.2 Non-Linear Sorption

Where data are available, specifically for the radionuclide ^{135}Cs , a few calculations have been carried out to examine the effect of non-linear sorption, described by a Freundlich isotherm. In the definition of the Freundlich isotherm (see, for example, TRAVIS & ETNIER 1981), the amount of a particular element sorbed onto a unit mass of material is equal to KC^N , where C [mol m^{-3}] is the concentration in solution and N [-] and K [$\text{mol}^{1-N} \text{kg}^{-1} \text{m}^{3N}$] are empirical constants. C is the sum of concentrations of all isotopes of a particular element, including stable isotopes naturally present in the groundwater. Denoting the latter by C_{min} [mol m^{-3}], and assuming this to be constant in time and space, the retardation factors in Equations 5.3.1 and 5.3.2 are then given by Equation 5.3.11 and

$$R_p^{(i)} = 1 + \frac{1 - \varepsilon_p}{\varepsilon_p} \rho NK \left(C_p^{(i)} + C_{min} \right)^{N-1} \quad (5.3.13)$$

$$\tilde{R}_p^{(i)} = 1 + \frac{1 - \varepsilon_p}{\varepsilon_p} \rho K \frac{(C_p^{(i)} + C_{\min})^N - C_{\min}^N}{C_p^{(i)}}. \quad (5.3.14)$$

The derivation of these retardation factors is given in JAKOB et al. (1989)²⁴. The governing non-linear equations are solved numerically using an extension of RANCHMD, code RANCHMDNL, also described in JAKOB et al. (1989).

5.3.3.3 Colloid Facilitated Radionuclide Transport

The model described above may be extended to deal with linear or non-linear sorption on a background concentration of colloids in the geosphere (SMITH 1993a). The processes which are incorporated in the current transport model are illustrated in Figure 5.3.2. The following model assumptions are made, in addition to those described in Subsection 5.3.1:

- Colloids are present naturally in the groundwater (colloids may also be generated by erosion of the bentonite; as discussed in Subsection 4.3.3.10, this process is considered a negligible source of colloids). A concentration of colloids χ [kg m^{-3}] (mass of colloids per unit volume of water), constant in space and time, is assumed, based on measured concentrations of natural colloids. An equilibrium is implicitly assumed between colloid loss (by filtration, dissolution, coagulation) and generation.
- Colloids are transported in the model conduit with an advection velocity u_c [m y^{-1}].
- Colloids are (conservatively) assumed not to diffuse into matrix pores due to their size and charge.
- Colloids may interact with the conduit walls; a fixed ratio K_a [m] is assumed between the surface concentration of colloids reversibly attached to the conduit walls and the volume concentration of mobile colloids advected along the model conduit.
- Radionuclides sorb reversibly onto and are transported by colloids. Instantaneous linear equilibrium sorption is assumed. K_c [$\text{m}^3 \text{kg}^{-1}$] is a sorption constant for radionuclides on colloids (the amount sorbed onto a unit mass of colloidal material is equal to $K_c C$, where C [mol m^{-3}] is the radionuclide concentration in solution).

²⁴ Equation 5.3.14 has a slightly different form to that given in JAKOB et al. (1989); the modification was recommended in a private communication by Dr. W. Heer, Paul Scherrer Institute, Würenlingen and Villigen, Switzerland.

In order to describe the effect of colloids on transport, parameters of both the near-field and geosphere models must be modified. In the near-field model (Section 5.2), the radionuclide concentration in solution at the bentonite-host rock interface is reduced by sorption onto colloids. This affects the concentration gradient controlling diffusion across the bentonite and is taken into account by replacing the flowrate Q by an "effective flowrate" Q' [$\text{m}^3 \text{y}^{-1}$], defined below. In the geosphere model, a similar substitution, with q' [m y^{-1}] replacing q , is made for the Darcy velocity in the boundary condition at the upstream end of the model conduit (Equation 5.3.6) and in the expression for radionuclide flux at the downstream end (Equation 5.3.8). Furthermore, the advection velocity u in Equation 5.3.1 is replaced an "effective velocity" u' [m y^{-1}]. The retardation parameters $R_f^{(i)}$ and $\tilde{R}_f^{(i)}$ must also be appropriately defined. Equation 5.3.2 for diffusion of radionuclides within the matrix is unchanged, since colloids are assumed to be excluded from matrix pore space.

Where sorption on colloids is non-linear, u' , Q' , q' , $R_f^{(i)}$ and $\tilde{R}_f^{(i)}$ are all functions of radionuclide concentration. In the Kristallin-I safety assessment, however, because available data are insufficient for non-linear isotherms to be defined, only linear sorption on colloids is considered. In this special case, the five parameters are concentration-independent and are given by the following equations:

$$R_f^{(i)} = \tilde{R}_f^{(i)} = 1 + \chi K_c \left(1 + \frac{K_a}{b} \right) \quad (5.3.15)$$

$$\frac{u'}{u} = \frac{Q'}{Q} = \frac{q'}{q} = 1 + \frac{u_c}{u} \chi K_c. \quad (5.3.16)$$

The derivation of these equations is given in SMITH (1993a). Since the transport equations are identical in form to those in which colloid transport is not considered, they may be solved using codes STRENG (with a modified flowrate in the mixing-tank boundary condition) and RANCHMD (with a modified advection velocity and retardation factor).

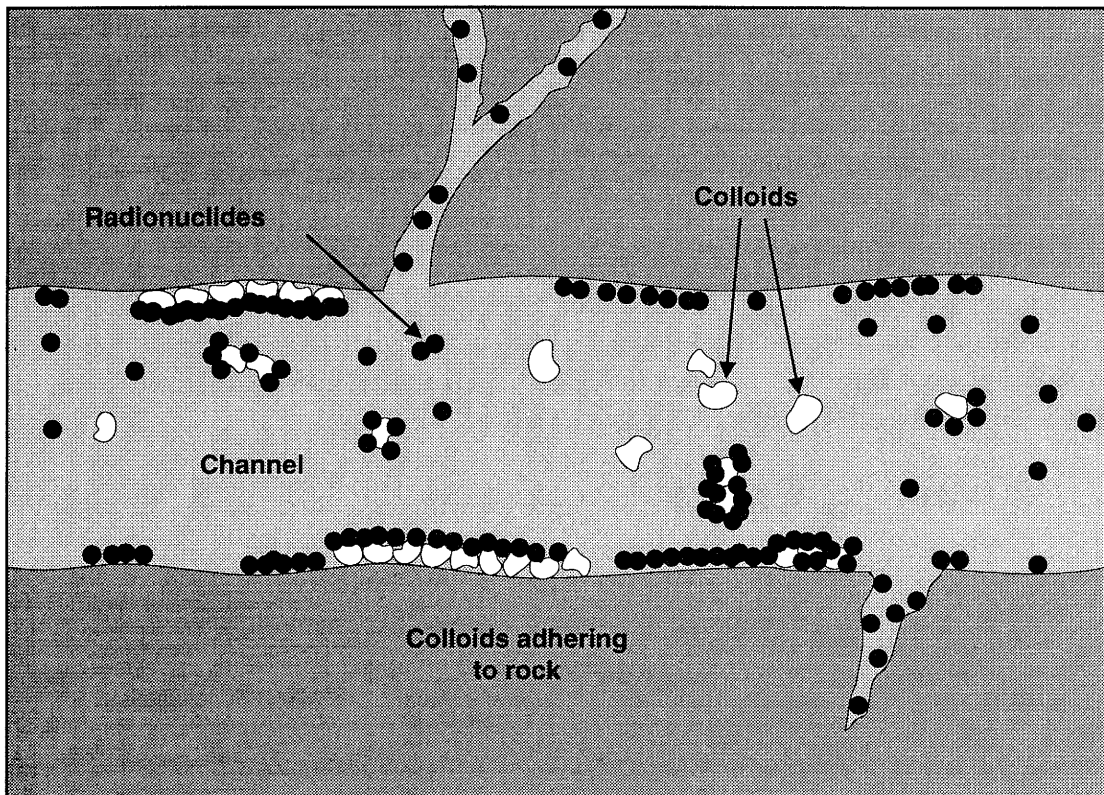
5.3.3.4 Simplified Solutions

Analytical solutions to special cases of the governing equations are, because of their transparency, useful in interpreting the more general numerical solutions and exploring the sensitivity of the system to parameter variations. Two such solutions are:

- a steady-state solution, applicable when the release from the near field is slowly varying with respect to the transit time through the geosphere and radioactive ingrowth is negligible;

- equilibrium between radioactive decay and ingrowth of decay-chain daughters, applicable when the transit time through the geosphere is sufficiently long with respect to half-life for equilibrium to be attained.

These solutions are given in Appendix 8; in Subsection 5.3.5, it is shown that they approximate well the behaviour of many safety-relevant radionuclides.



Note: The size of radionuclides with respect to colloids, and that of colloids with respect to the fracture, are exaggerated; the pore structure is simplified.

Figure 5.3.2: Schematic representation of colloid facilitated transport. An individual channel within a water-conducting feature conveys radionuclides both in solution and sorbed onto groundwater colloids. Radionuclides also diffuse into matrix pores and sorb onto pore surfaces. In modelling this system, it is conservatively assumed that colloids are excluded from all matrix pores. They may interact with the walls of the channel, although an equilibrium is assumed between colloid loss and generation.

5.3.4 Input Parameters

The values of the various input parameters for the geosphere transport model are specified and discussed in this subsection. The geological, hydrochemical and hydrogeological data which are required to quantify the processes included in the model are summarised in Figure 5.3.3. There is a considerable degree of uncertainty associated with many of these data. As with the near-field model, sensitivity of geosphere modelling results to this uncertainty is explored by defining a Reference-Case, based on the better-characterised Area West, around which parameter variations are made. In the Reference-Case, *physico-chemical* parameters are assigned "realistic-conservative" values, with one or more additional values defining the range of uncertainty. In defining the *geometry* of the model conduit, however, it is not appropriate to specify a single "realistic-conservative" parameter set, based on the observed internal structure of water-conducting features. The results of such observations, summarised in Figure 3.5.4, reveal a high degree of variability, which the geosphere model, being limited to relatively simple geometrical representations, is unable to incorporate in a single set of parameters. Instead, a set of alternative conduit geometries is defined, which spans this variability in a manner appropriate to compensate for the limitations of the model. The sensitivity of geosphere model calculations to the choice of geometrical representation of the model conduit and to uncertainty in the physico-chemical parameters is described in Subsection 5.3.5.

5.3.4.1 Advection

As indicated in Figure 5.3.3 (see also Figure 3.7.1), in order to quantify the process of advection through either the low-permeability domain or the major water-conducting faults, the flowpath length L (discussed in Subsection 3.7.5) and advection velocity u must be determined. Radionuclides are advected through channels within small-scale water-conducting features and, in order to derive the advection velocity, the necessary information is:

- the total volume of the channels within a water-conducting feature (requiring a geometrical description of the internal structure of the water-conducting features);
- the total flow of water through a water-conducting feature.

Water-conducting features have been classified into three types, present in all domains of the crystalline basement in both Area West and Area East:

- cataclastic zones;
- jointed zones;
- fractured aplite/pegmatite dykes and aplitic gneisses.

For geosphere transport modelling, each type has been assigned a separate, simplified geometrical description (see Figures 3.5.4a, b and c). These simplified descriptions have several common features; each consists of a set of partially infilled parallel fractures, with discrete open channels within which groundwater flow is confined, and a zone of altered wallrock immediately adjacent to the fractures.

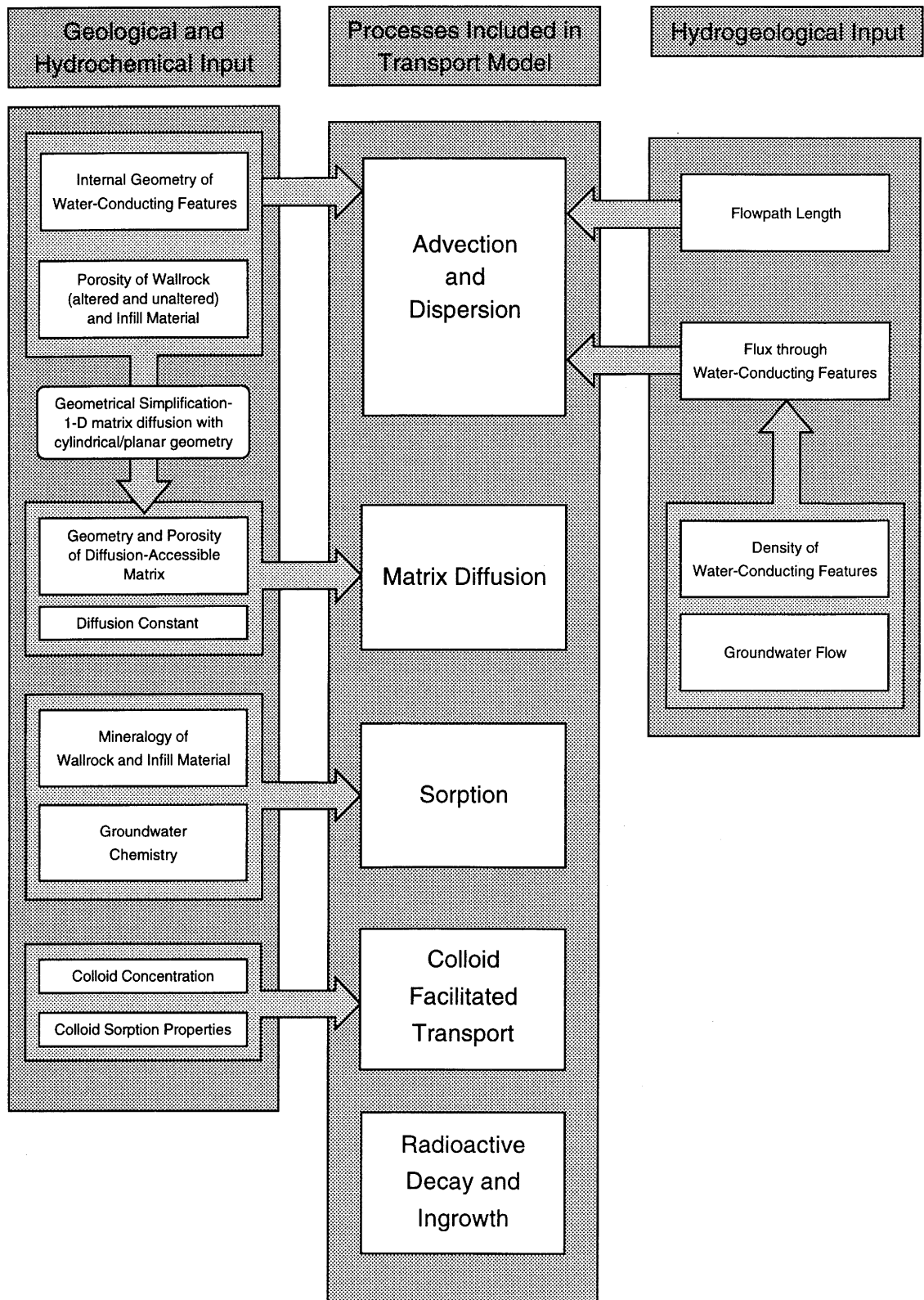


Figure 5.3.3: Geological, hydrogeological and hydrochemical input for geosphere transport modelling.

Consider a hypothetical plane normal to the flow direction (examples of such hypothetical planes are shown, for both the low-permeability domain and a major water-conducting fault, in Figure 5.3.4). The plane intersects a number of small-scale water-conducting features, the fractures contained within the water-conducting features and the channels contained within the fractures. The similarity between the different types of water-conducting features allows a single system of notation (see also Figure 5.3.4) to be adopted for the geometrical description of the internal structure of all three types of water-conducting feature:

- γ [m^{-1}] defines the total trace length of features intersected by a plane of unit area, the density of water-conducting features (see Subsection 3.7.5).
- Each feature has a width $2W$ [m] and consists of a set of fractures with aperture $2y_1$ [m] and separation $2y_3$ [m]; the total trace length of fractures, per unit trace length of water-conducting feature, is therefore equal to W/y_3 .
- Each fracture contains a set of channels. The channels have width $2x_1$ [m] and are separated by a distance $2x_2$ [m] in the fracture plane; the total trace length of channels, per unit length of fracture, is therefore equal to x_1/x_2 .

Combining the above, ϕ [-], defined as the total trace length of channels within a water-conducting feature of unit trace length in a hypothetical plane, is given by:

$$\phi = \frac{x_1}{x_2} \cdot \frac{W}{y_3} \quad (5.3.17)$$

and H [m^{-1}], defined as the total trace length of channels intersected by unit area of a hypothetical plane, is given by:

$$H = \phi\gamma. \quad (5.3.18)$$

The quantity H , which may be regarded as an average "density" of open channels within a domain of the host rock, is a key characteristic of the host rock (see Section 7.4) and is, for example, identical to the "specific surface area for matrix diffusion" defined in the SKB 91 assessment (SKB 1992).

The advection velocity within the channels is then given by:

$$u = \frac{q}{2Hy_1} = \frac{q_w}{2\phi y_1} = \frac{q_w}{2y_1} \cdot \frac{x_2}{x_1} \cdot \frac{y_3}{W}, \quad (5.3.19)$$

where q_w (defined in Section 3.7) is the flowrate through a single water-conducting feature of unit trace length in the hypothetical plane.

A description of the internal structure of water-conducting features, from which values of x_1 , x_2 , y_1 and y_3 are derived, is obtained from a detailed examination of cores and surface exposures, the results of which are summarised in Figure 3.5.4 and in Table 3.7.7. The figure and table show that the width of the channels ($2x_1$) and their separation within the fracture plane ($2x_2$) display a particularly high degree of variability²⁵. Maximum and minimum values of $2x_1$ and $2(x_2-x_1)$ range from 1 cm to 10 cm and from 10 cm to 500 cm, respectively. It is, however, the ratio $x_2:x_1$ which is of importance in the transport model (see Equation 5.3.19). The two quantities are correlated with, for example, large values of x_1 accompanying large values of x_2 (see Chapter 10 in THURY et al. 1994). Accounting for this correlation reduces the variability in $x_2:x_1$; narrow, widely-spaced channels and broad, closely-spaced channels need not be considered since they are not observed in rock samples. For cataclastic zones and jointed zones, the maximum and minimum values of this ratio then differ by a factor of 5 (i.e. values of the ratio ranging from 10 to 50). Two extreme cases (narrow, closely-spaced channels and broad, widely-spaced channels) have been selected in order to examine the influence of this variability on radionuclide transport. A single case is assumed to be sufficient to represent fractured aplite/pegmatite dykes and aplitic gneisses, since the ratio $x_2:x_1$ when both x_1 and x_2 take their maximum values is the same as when both quantities take their minimum values. The geometrical parameters relevant to the modelling of radionuclide advection for all three cases are given in Table 5.3.1.

The flowrate through the water-conducting features is obtained from the results of groundwater flow modelling (see Subsection 3.7.15; Table 3.7.6). It should be noted that, in selecting values for the geosphere Reference Case, the following conservative assumptions are made (see also Subsection 3.5.3):

- For Area West, results from the "Sparse Model" are taken; in this hydrogeological model, only a few of the first and second-order faults are hydraulically active. Assuming that the overall flow pattern is broadly unaffected, this model leads to higher gradients (and thus higher flowrates) than the alternative "Full Model".
- For Area East, data from the Siblingen borehole are assumed to be representative of the whole area (Hypothesis 1). This assumption implies that the crystalline basement is more permeable in Area East than in Area West.

Furthermore, in the geometric approach used in groundwater flow modelling, the gradient assigned to each water-conducting feature is independent of its transmissivity. In reality, for a network of water-conducting features, highly transmissive features would experience lower gradients than less transmissive features. A preliminary study of fracture networks, taking account of this dynamic interdependence, indicates that the present method may over-estimate groundwater flow in the water-conducting features by up to a factor of 10 (see Chapter 10 in THURY et al. 1994).

²⁵ The fracture aperture ($2y_1$) shows far less variability and is assigned the same value (1 mm) in each geometrical representation of the water-conducting features. Model results are, in any case, insensitive to the value of this parameter.

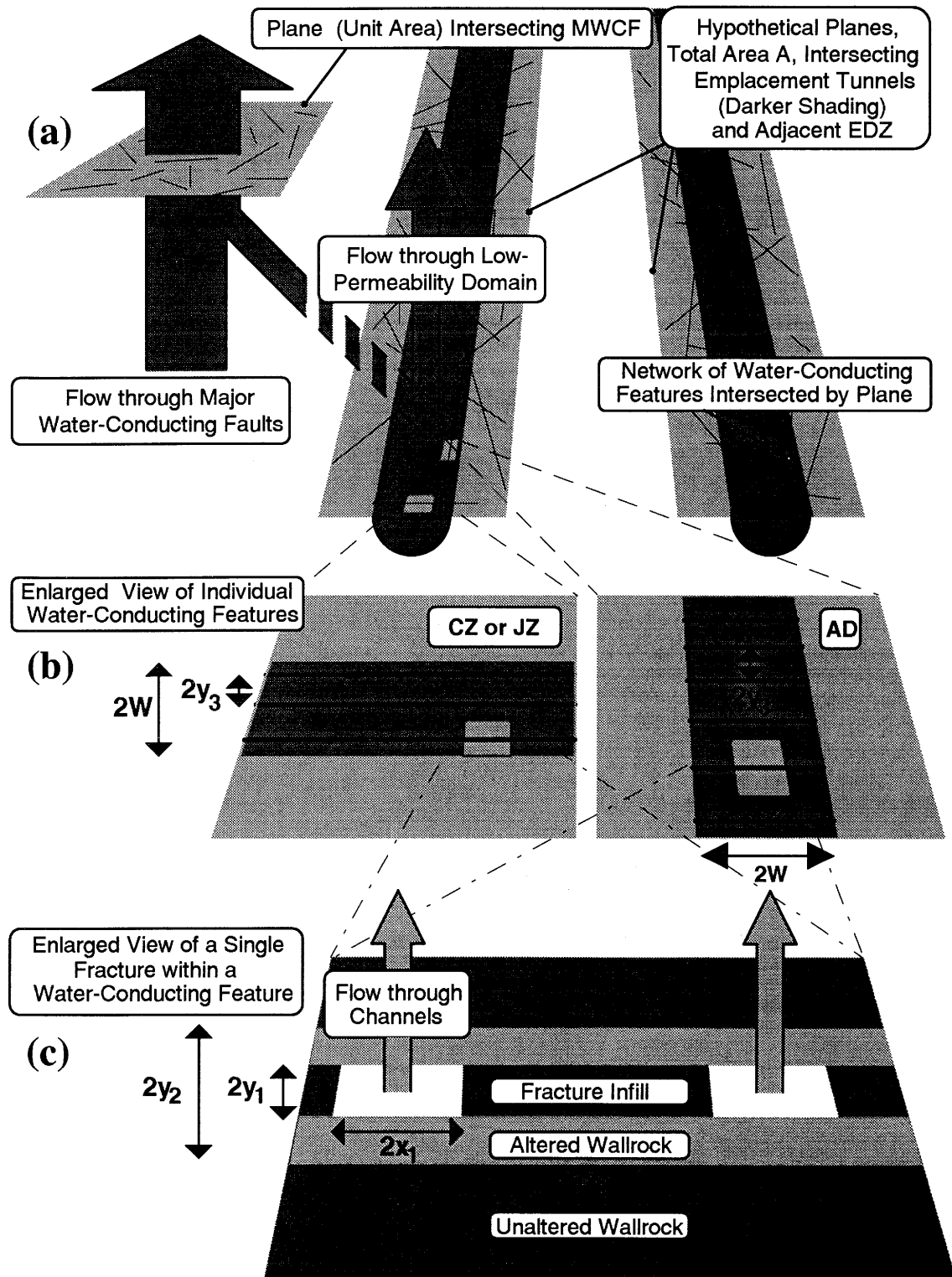


Figure 5.3.4: Illustration of the water-conducting features intersected by the repository area and a geometrical description of the internal structure of the features. (a) The repository is located in the low-permeability

domain of the crystalline basement. The repository area is defined as the sum of areas of a set of hypothetical planar cross-sections passing centrally through the emplacement tunnels and their surrounding excavation-disturbed zones (see also Subsection 3.7.5). Water-conducting features which pass through the repository area are considered to convey any radionuclides released from the repository through the low-permeability domain either directly to the higher-permeability domain of the crystalline basement, or to a major water-conducting fault. (b) The water-conducting features, of thickness W , are of three types (CZ - cataclastic zones, JZ - jointed zones and AD - fractured aplite / pegmatite dikes and aplitic gneisses). All three types contain sets of parallel fractures, of spacing $2y_3$. The fractures lie in the plane of the water-conducting features in the cases of CZ and JZ, and normal to the plane in the case of AD. (c) A common system of notation may be adopted to describe the internal structure of all three types of water-conducting feature. Channels within individual fractures have a width $2x_1$ and a separation $2x_2$ within the fracture plane. The channels (and also the fractures) have an aperture $2y_1$. Each fracture has an adjoining zone of altered rock extending a distance $y_2 - y_1$ from the fracture walls, beyond which the rock is unaltered.

The geometrical parameters given in Table 5.3.1, together with the flowrates through the water-conducting features of Areas West (low-permeability domain and major water-conducting faults) and Area East given in Table 3.7.6, give the advection velocities in each domain using Equation 5.3.19. Advection velocities, calculated using the Reference-Case flowrates, are presented in Table 5.3.2 (the flowrates through water-conducting features - per unit length - are, from Table 3.7.6, $6.3 \times 10^{-4} \text{ m}^2 \text{ y}^{-1}$ and $8.8 \times 10^{-3} \text{ m}^2 \text{ y}^{-1}$ for Area West - low-permeability domain - and Area East, respectively, and $2.1 \text{ m}^2 \text{ y}^{-1}$ for major water-conducting faults in Area West). In each case, the total trace length of channels intersected by unit area of a hypothetical plane is also presented in the table.

	Cataclastic / Jointed Zones		Fractured Aplite/Pegmatite Dykes and Aplitic Gneisses
	(narrow, closely-spaced channels)	(broad, widely-spaced channels)	
$2x_1$ [mm]	10	10^2	$x_2 \cdot x_1 = 1$
$2x_2$ [mm]	10^2	5×10^3	
$2y_1$ [mm]	1	1	1
$2y_3$ [mm]	3.8×10^2	3.8×10^2	3×10^2
W/y_3 [-]	3	3	3.3
ϕ [-]	2.7×10^{-1}	5.9×10^{-2}	1.7

Note: As a further geometrical simplification, use is made of the observation that there is very little difference of relevance to transport modelling between cataclastic zones and jointed zones. The only differences in the simplified representations in Figures 3.5.4a and b are the lateral extent of the water-conducting features - irrelevant in the present context - and the number of parallel fractures within a water-conducting feature - 5 in the case of cataclastic zones and 3 in the case of jointed zones. In the modelling study, no distinction is made between cataclastic zones and jointed zones, with 3 parallel fractures assumed for both, giving $W/y_3 = 3$. $2y_3$, for both types of water-conducting feature, is taken to be the mid-value in the range given in Table 3.7.7 for jointed zones (i.e. 37.5 cm).

Table 5.3.1: Parameters describing three alternative representations of the internal geometry of water-conducting features, spanning the variability observed in cores and surface exposures. Parameters are defined in Figure 5.3.4 and in Equation 5.3.17.

Domain	Reference Area	Parameter	Cataclastic / Jointed Zones		Fractured Aplite/Pegmatite Dykes and Aplitic Gneisses
			(narrow, closely-spaced channels)	(broad, widely-spaced channels)	
LPD	West ($\gamma = 0.04 \text{ m}^{-1}$)	H [m^{-1}] u [m y^{-1}]	1.1×10^{-2} 2.3	2.4×10^{-3} 1.1×10^1	6.6×10^{-2} 3.8×10^{-1}
	East ($\gamma = 0.1 \text{ m}^{-1}$)	H [m^{-1}] u [m y^{-1}]	2.7×10^{-2} 32.6	5.9×10^{-3} 1.5×10^2	1.7×10^{-1} 5.2
MWCF	West ($\gamma = 0.1 \text{ m}^{-1}$)	H [m^{-1}] u [m y^{-1}]	2.7×10^{-2} 7.8×10^3	5.9×10^{-3} 3.6×10^{-4}	1.7×10^{-1} 1.3×10^3

Table 5.3.2: Advection velocities u in the water-conducting features of the low-permeability domain (LPD) and major water-conducting faults (MWCF) for each of the three alternative geometrical representations described in Table 5.3.1. The advection velocity is dependent on flowrate and on H , the trace length of channels per unit area of a plane normal to the flow direction. γ is the trace length per unit area of water-conducting features, which contain the channels.

5.3.4.2 Dispersion

Several field-scale tracer tests in porous and fractured media have indicated that the longitudinal dispersion length is not a constant, but rather depends on the mean travel distance. A review of field-scale dispersion in aquifers has been reported in GELHAR et al. (1992). The data do not show any significant difference between the longitudinal dispersion lengths measured in porous media and those measured at the same scale in fractured media; a Peclet number $Pe = L/a_L = 10$ is adopted as a "realistic-conservative" value for the present study. The uncertainty involved in estimates of longitudinal dispersivity is apparent in the review by GELHAR et al. (1992); the authors of the review caution against routinely adopting a fixed Peclet number. In the present study, parameter variations of $Pe = 2$ and $Pe = 50$ are considered to cover this uncertainty²⁶. The range is based on the Peclet numbers presented in NERETNIEKS (1985b) for experiments on fractured crystalline rocks. Results from particle tracking studies carried out during hydrogeological modelling for Kristallin-I indicate an effective dispersivity of about 1/20th of the total travel length ($Pe = 20$, see VOMVORIS et al. 1993), which is covered by the range of parameter variation.

5.3.4.3 Matrix Diffusion

Figure 5.3.3 indicates that, in order to model the process of matrix diffusion, information is required on the diffusion constant (Subsection 5.3.4.3.1) and the extent and porosity of the diffusion-accessible matrix (Subsection 5.3.4.3.2).

5.3.4.3.1 Diffusion Constant

A diffusion constant $D_p = 10^{-3} \text{ m}^2 \text{ y}^{-1}$ ($3 \times 10^{-11} \text{ m}^2 \text{ s}^{-1}$) for all radionuclides is considered a "realistic-conservative" parameter value for the rock fabrics and porosities under consideration, with a "conservative" parameter value of $D_p = 2 \times 10^{-4} \text{ m}^2 \text{ y}^{-1}$ ($6 \times 10^{-12} \text{ m}^2 \text{ s}^{-1}$). The values are selected on the basis of a survey of experimentally determined diffusion constants for crystalline rocks (FRICK 1993). This survey shows that the sample preparation and the prevalence of small samples for diffusion experiments may produce a bias towards artificially increased values. However, these effects are probably small and more than compensated for by the fact that most experiments are performed with anions which, unlike cations, may have a substantially reduced mobility in narrow pores with negatively-charged surfaces.

²⁶ Peclet number is defined as the ratio of advective to dispersive flux. In writing $Pe = L/a_L$, it is assumed that longitudinal hydrodynamic dispersion can be represented as a Fickian process and that dispersive flux is proportional to the advection velocity (as stated in Subsection 5.3.1). It should be noted, however, that, at a Peclet number of 2, the assumption that dispersion can be represented as a Fickian diffusion process may no longer be reasonable; the assumption is applicable only at a few dispersion lengths away from the boundaries and, for a Peclet number of 2, the distance between the boundaries is of the same order of magnitude as the dispersion length.

5.3.4.3.2 Geometry and Porosity of Diffusion-Accessible Matrix

Simplifications in treatment of matrix diffusion within the geosphere transport model result in the following limitations:

- matrix diffusion is restricted to one dimension in space, directed normally to the surface of the model (parallel-walled or tubular) conduit;
- matrix diffusion occurs in a spatially-limited region of connected porosity adjacent to the model conduit. The cross-section of this region is thus either rectangular (planar geometry) or annular (cylindrical geometry);
- the properties of the diffusion-accessible matrix are uniform.

These transport-model limitations require that the conceptual model of the water-conducting features (Figure 5.3.4(c)) be further simplified.

In Table 5.3.1, three representations of the water-conducting features are described (quantified by different values of the geometrical parameters defined in Figure 5.3.4(c)), which span the observed variability in channel dimensions. These representations are illustrated in Figure 5.3.5, with corresponding model conduits and surrounding diffusion-accessible matrix for geosphere transport modelling. Ranges of porosities for altered and unaltered wallrock and fracture infill are taken from Table 3.7.7.

Two sets of transport model parameters are assigned to each of the three representations: one where the assumption is made that fracture infill and both altered and unaltered wallrock are accessible by diffusion ("unlimited" matrix diffusion²⁷; Geometries 1,2 and 3), and a second, where matrix diffusion is assumed to be confined to the fracture infill and altered wallrock only ("limited" matrix diffusion; Geometries 4, 5 and 6). Parameters describing all six geometries are given in Table 5.3.3, together with the dimensions of the corresponding conduits and matrix porosities for geosphere transport modelling. The relationship between the transport-model parameters - b , y_p , r_0 , r_p and ε_p - and the observed properties of the water-conducting features - x_1 , x_2 , y_1 , y_2 and porosities of infill and altered/unaltered wallrock - is discussed below for all six geometries.

Geometries 1 and 4:

A cylindrical geometry is selected to model cataclastic zones/jointed zones with narrow, closely-spaced channels (Geometries 1 and 4), since the dimensions of the channels are small with respect to the distance available for matrix diffusion in the xy -plane (the plane

²⁷ Though termed "unlimited", matrix diffusion is limited in the transport model by geometrical constraints: for example, the spacing of adjacent, parallel fractures.

of Figure 5.3.5). The ratio of channel volume ($4x_1y_1L$) to surface area ($(4x_1+4y_1)L$) is conserved in the model conduit. For the model conduit, the ratio of volume to surface area is equal to $r_0/2$. Thus, the inner radius of the annular region of diffusion-accessible matrix in the transport model is given by:

$$r_0 = \frac{2x_1y_1}{x_1 + y_1}, \tag{5.3.20}$$

which is approximately equal to the observed fracture aperture $2y_1$ if the fractures are narrow ($y_1 \ll x_1$). Where unlimited matrix diffusion is assumed (as in Geometry 1), the outer radius of the diffusion-accessible matrix is constrained either by the separation of channels within a fracture plane (the x -direction), or by the separation of the fracture planes themselves (the y -direction):

$$r_p = \min(x_2, y_3) \tag{5.3.21}$$

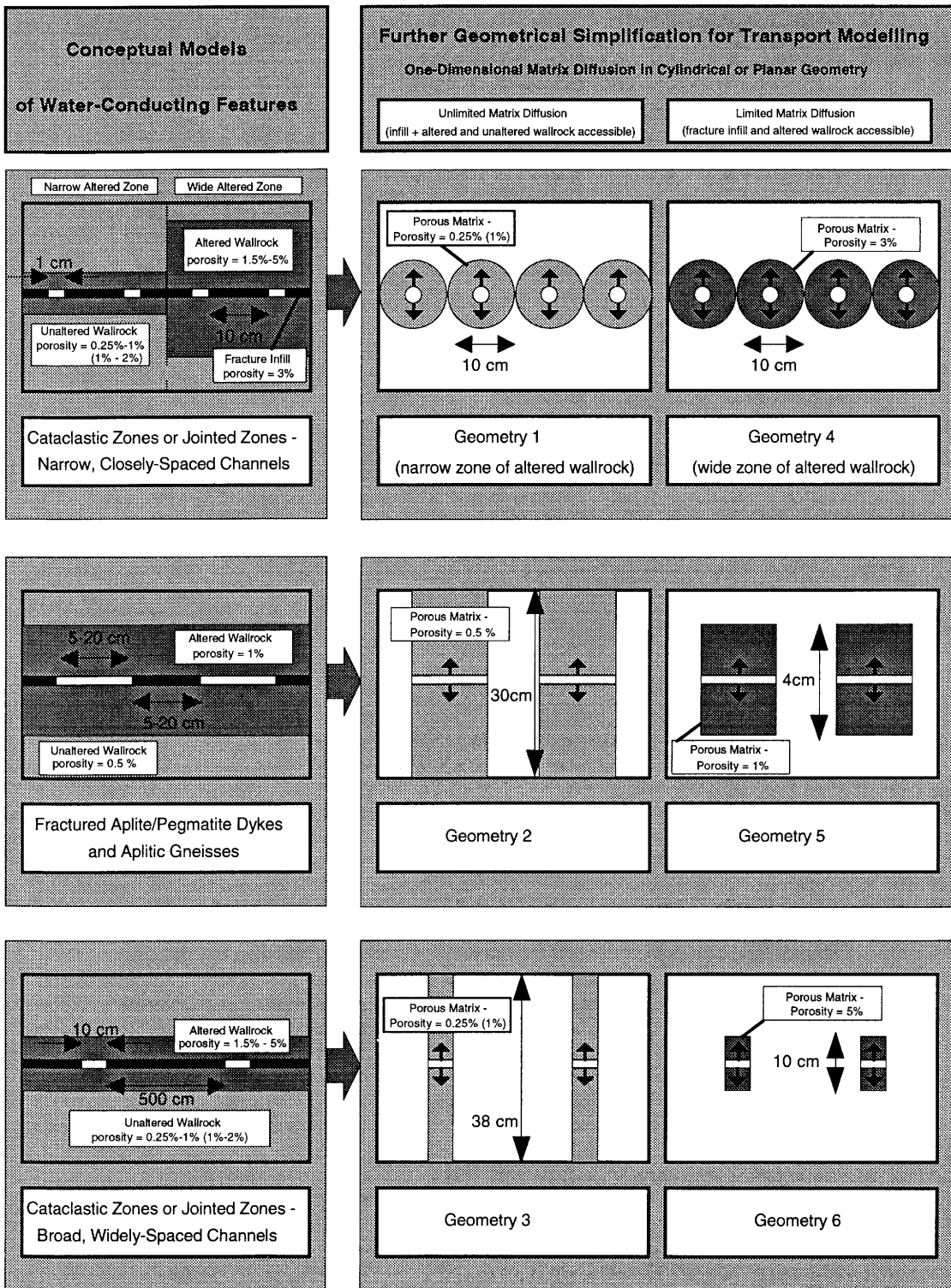
parameter	Geometry					
	1	2	3	4	5	6
	cylindrical	planar	planar	cylindrical	planar	planar
b [mm]	-	0.5	0.5	-	0.5	0.5
y_p [mm]	-	150	188	-	20	50
r_0 [mm]	1	-	-	1	-	-
r_p [mm]	50	-	-	50	-	-
ϵ_p [%]	0.25 (1)	0.5	0.25 (1)	3	1	5

Notes: Geometries 1 and 4 are representative of either cataclastic zones or jointed zones with narrow, closely-spaced channels. 2 and 5 are representative of fractured aplite/pegmatite dykes. 3 and 6 are representative of either cataclastic zones or jointed zones with broad, widely-spaced channels. Matrix diffusion is allowed throughout the wallrock in Geometries 1, 2, 3 (unlimited matrix diffusion), but is restricted to the altered wallrock and fracture infill only in Geometries 4, 5, 6 (limited matrix diffusion).

For Geometries 1 and 4, r_p is limited by x_2 (see Equations 5.3.21 and 5.3.22 and accompanying text). Referring to Table 5.3.1, r_p should properly have been assigned a value of 55 mm (i.e. $x_2 - x_1$) in each case, whereas a value of 50 mm is, in fact, assigned. Though undesirable, this discrepancy is both small and conservative.

Figures in brackets apply to major water-conducting faults.

Table 5.3.3: Parameters of the transport-model conduit and adjacent porous matrix (see Figure 5.3.1), used in the calculation of radionuclide transport through the six geometrical representations of water-conducting features. Where a planar geometry is adopted in the transport model, the conduit has an aperture $2b$ and the porous matrix has a thickness $y_p - b$. Where cylindrical geometry is adopted, the conduit has a radius r_0 and the porous matrix has a thickness $r_p - r_0$. The matrix has porosity ϵ_p .



Note: Porosities in parentheses apply to features within major water-conducting faults.

Figure 5.3.5: Alternative geometrical representations of the internal structure of water-conducting features. The representations are simplified to allow transport modelling with the codes RANCHMD and RANCHMDNL;

the codes impose the limitation of one-dimensional matrix diffusion in cylindrical or planar geometry. Geometries 1, 2 and 3 incorporate the assumption of unlimited matrix diffusion (i.e. diffusion into both altered and unaltered wallrock). Geometries 4, 5 and 6 incorporate the assumption of matrix diffusion limited to the altered wallrock only. Shading indicates regions accessible to matrix diffusion. In Geometries 1 and 4, the extent of these regions is limited by the separation of the channels within each fracture. The difference in the two cases lies in the porosity assigned to the matrix: assumed equal to that of the unaltered wallrock for Geometry 1 (appropriate if the region of alteration is narrow) and equal to that of the altered wallrock for Geometry 4.

For the dimensions specified in Table 5.3.1, r_p is limited by x_2 , the separation of the channels. If it is assumed that the zone of altered wallrock is narrow, such that $y_2 < x_2$, then the diffusion-accessible matrix consists of infill material and both altered and unaltered wallrock. It is then conservative to set the matrix porosity to 0.25% in the low-permeability domain and 1% in major water-conducting faults, since these values lie at the low end of the range for unaltered wallrock and are smaller than those of either the altered wallrock or the infill material²⁸.

Where matrix diffusion is limited to the altered wallrock and infill material (as in Geometry 4), the outer radius of the diffusion-accessible matrix is constrained either by the separation of channels within a fracture plane, or by the thickness of the altered wallrock:

$$r_p = \min(x_2, y_2) \quad (5.3.22)$$

In this case, if it is assumed that the zone of altered wallrock is broad, such that $y_2 > x_2$, then r_p is limited by x_2 (as in Geometry 1) and the diffusion-accessible matrix consists of infill material and altered wallrock, but not unaltered wallrock. The value assigned to the matrix porosity, which is the only difference between Geometries 1 and 4, is 3%. This represents an average value for the altered wallrock and is equal to that of the infill material.

Geometries 2, 3, 5 and 6:

Planar geometry is selected to model the remaining cases, since the dimensions of the channels cannot be considered small with respect to the distance available for diffusion in

²⁸ A low porosity is "conservative", since it is one of the factors which controls the flux of radionuclides from water-conducting features into the adjoining matrix and, for isotopes of sorbing elements in particular, the rate at which radionuclides diffuse within the matrix. Where porosity is low, radionuclide penetration into the matrix will be small and less will be sorbed. Consequently, retardation will be low, leading to an earlier release.

the xy -plane. Diffusion in the infill material is conservatively neglected and the aperture of the model conduit is equal to the fracture aperture:

$$b = y_1. \quad (5.3.23)$$

Where unlimited matrix diffusion is assumed (Geometries 2 and 3), the extent of diffusion-accessible matrix is constrained by the separation of the fracture planes themselves:

$$y_p = y_3, \quad (5.3.24)$$

whereas, for matrix diffusion limited to altered wallrock (Geometries 5 and 6):

$$y_p = y_2. \quad (5.3.25)$$

Values of y_3 for Geometries 2 and 3, 150 mm and 188 mm, respectively, are taken from Table 5.3.1. y_2 is assigned values of 20 mm and 50 mm in Geometries 5 and 6, respectively; these values lie within the ranges given in Figure 3.5.4 and Table 3.7.7. In Subsection 5.3.5, a parameter variation is also described in which only a part of the altered wallrock is considered accessible by diffusion ($y_p = 10$ mm). This is a lower limit to the matrix depth accessible by diffusion, derived on the basis of natural analogue U-Th-decay-series disequilibrium studies (ALEXANDER et al. 1990; MILLER et al. 1994).

For Geometry 2, matrix porosity is taken to be that of the unaltered wallrock (0.5%), since this is smaller than that of the altered wallrock and diffusion may take place in both materials. Similarly, for Geometry 3, matrix porosities are set equal to 0.25% in the low-permeability domain and 1% in major water-conducting faults, since these values lie at the low end of the range for unaltered wallrock and are below the range for altered wallrock. For Geometries 5 and 6, matrix porosity is taken to be that of the altered wallrock (1% for Geometry 5, 5%²⁹ for Geometry 6), since matrix diffusion is confined to this material.

5.3.4.4 Sorption on Matrix Pore Surfaces

With the exception of Cs, data for sorption of all elements is given in the form of linear isotherms; Cs sorption is described by a Freundlich isotherm³⁰ (see Table 3.7.8). Sorption is furthermore assumed to be completely reversible. There is considerable

²⁹ The value of 5% is appropriate to argillic alteration of wallrock (granite or gneiss). High temperature alteration may give lower porosities (4% for granite and 1.5% for gneiss; see Table 3.7.8). However, blocks of crystalline showing *only* high-temperature alteration are not expected.

³⁰ This is because non-linear sorption of Cs is very well characterised; other elements may also be better described by non-linear isotherms, but suitable databases are lacking.

experimental evidence to suggest that, for Cs, some sorption processes are only partially reversible or that the kinetics of desorption is very slow (see, for example, COMANS & HOCKLEY 1992), but this is conservatively ignored in the current assessment. "Realistic-conservative" and "conservative" isotherms are given in Table 3.7.8. The differences in mineralogy between the different rock types (infill, altered and unaltered wallrock) making up the water-conducting features are taken into account in deriving these data (STENHOUSE 1994). However, the sorption parameter values are similar in each case and the data in Table 3.7.8 are applicable to each rock type. A uniform solid density of $\rho = 2.6 \times 10^3 \text{ kg m}^{-3}$ is assumed, as in Project Gewähr 1985.

The transport model given in Subsection 5.3.3.1, in which linear sorption is assumed, is used throughout most of the Kristallin-I assessment (code RANCHMD); a limited comparison is made in Subsection 5.3.5 with results using a model directly incorporating non-linear sorption, described in Subsection 5.3.3.2 (code RANCHMDNL). Where sorption is described by a non-linear Freundlich isotherm (i.e. for Cs) and use is to be made of the model with linear sorption, an appropriate value for $K_d^{(i)}$ must be obtained from the non-linear isotherm.

$K_d^{(i)}$ is related to the concentration-independent retardation factor $R_p^{(i)}$ through Equation 5.3.12. For the model with non-linear sorption, a concentration-dependent retardation factor $R_p^{(i)} = R_p^{(i)}(C_p^{(i)})$ is defined by Equation 5.3.13 and is sketched in Figure 5.3.6. When using the model with linear sorption, it is conservative to choose $K_d^{(i)}$ such that

$$R_p^{(i)} = R_p^{(i)}(C_p^{(i,\max)}), \quad (5.3.26)$$

where $C_p^{(i,\max)}$ is the highest concentration of radionuclide i which would be found at any point and at any time in the geosphere (in practice, this is the maximum concentration at the bentonite-host rock interface, which can be taken from the results of the near-field calculations). It therefore follows that the most appropriate *geosphere* $K_d^{(i)}$ -value for Cs is dependent on the parameter set used in the corresponding *near-field* calculations, particularly the groundwater flowrate through the repository area.

A $K_d^{(i)}$ value for Cs has been calculated based on the Reference-Case flowrate: $3 \text{ m}^3 \text{ y}^{-1}$ for Area West (see Table 3.7.2). The maximum flux from the Reference-Case near field to the geosphere is $3.5 \times 10^{-2} \text{ mol y}^{-1}$ (see Figure 5.2.3). The maximum concentration at the bentonite-host rock interface, $1.2 \times 10^{-5} \text{ M}$, is obtained by dividing this flux by the groundwater flowrate (in litres y^{-1}). Freundlich isotherms for Cs and the stable elemental Cs concentration are given in Table 3.7.8: $C_{\min} = 3.2 \times 10^{-7} \text{ M}$, $N = 0.7$ and $K = 2.0 \text{ mol}^{0.3} \text{ kg}^{-1} \text{ l}^{0.7}$ ("realistic-conservative") and $N = 0.7$ and $K = 0.40 \text{ mol}^{0.3} \text{ kg}^{-1} \text{ l}^{0.7}$ ("conservative"). $K_d^{(i)}$ values for Cs based on these two isotherms are:

– "realistic-conservative": $0.042 \text{ m}^3 \text{ kg}^{-1}$;

– "conservative": $0.0084 \text{ m}^3 \text{ kg}^{-1}$.

These values can be used conservatively³¹ for model-chain calculations with higher flowrates; parameter variations with 10- and 100-fold increases in flowrate are studied using the above "realistic-conservative" $K_d^{(i)}$ value for Cs. For the parameter variation of a 10-fold decrease in flowrate, the model directly incorporating non-linear sorption for Cs (code RANCHMDNL) is used.

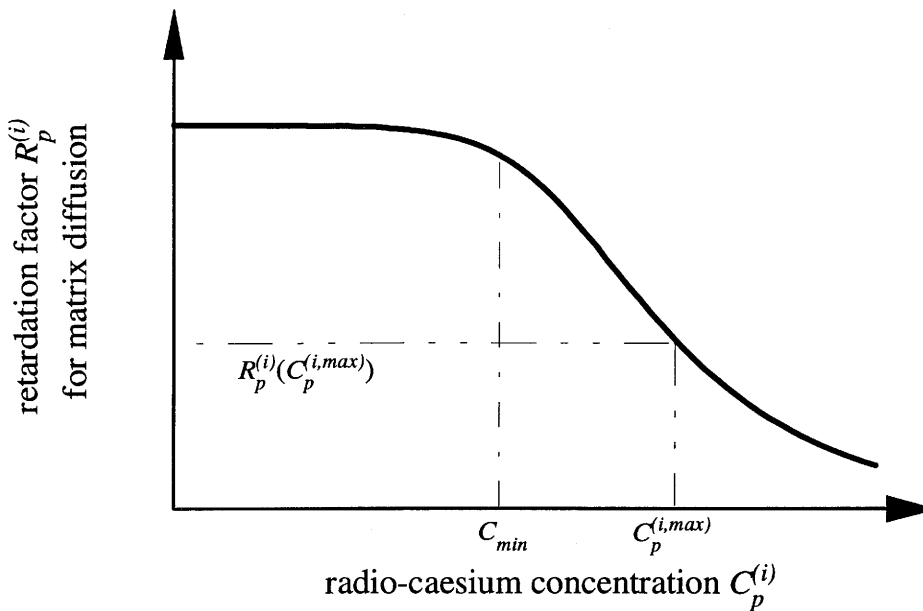


Figure 5.3.6: Retardation factor $R_p^{(i)}$ for matrix diffusion as a function of radio-Cs concentration $C_p^{(i)}$, with sorption modelled by a modified Freundlich isotherm. C_{min} is the natural, stable Cs concentration in the groundwater. $C_p^{(i,max)}$ is the maximum radio-Cs concentration at the point of release to the geosphere.

5.3.5 Parameter Uncertainty

As discussed above, there is a considerable degree of uncertainty associated with many of the geosphere input parameters. In order to study the sensitivity of the model results to these uncertainties, a series of calculations using parameters which are systematically

³¹ The radionuclide concentration at the bentonite-host rock interface tends to zero as the flowrate increases. A low radionuclide concentration gives a high retardation factor. Adopting a single linear sorption isotherm based on high-flowrate results is therefore non-conservative.

varied with respect to the Reference Case are carried out. Data and results for the Reference Case are summarised in Subsection 5.3.5.1. Only maximum calculated geosphere releases (and corresponding doses) are presented, irrespective of time of occurrence. In Chapter 6, where model-chain calculations are presented in more detail, the effect of the geosphere in delaying releases is discussed and results are presented in graphical form as dose vs. time. In Subsection 5.3.5.2, the parameter values used in the sensitivity analysis are given, and their effects described.

5.3.5.1 The Geosphere Reference Case

The geosphere input dataset for the Reference Case is summarised in Table 5.3.4. Model-chain calculations have been carried out for all safety-relevant radionuclides and with each of the geometrical representations of the water-conducting features and the results are described in detail in Subsection 6.2.2.1. Geometry 6 is chosen to model the water-conducting features of the Reference-Case low-permeability domain because this representation is found to yield the highest maximum dose (summed over all safety-relevant radionuclides), as shown in Table 5.3.5 (see Figure 6.2.8 for the full time-dependent results).

Geosphere transport is considered only through the low-permeability domain in the Reference Case. Transport through major water-conducting faults is not considered, both because of the very high degree of uncertainty in the properties of the major water-conducting faults and because transport paths from the repository would not all necessarily include such faults. Colloid transport is also omitted in the Reference Case, because colloid concentrations are expected to be very low and their effect on radionuclide transport negligible. Finally, non-linearity of sorption on matrix pore surfaces is not explicitly modelled (code RANCHMD is used). The effects of transport through major water-conducting faults and of colloid transport are, however, assessed quantitatively in Chapter 6. The effects of non-linear sorption are assessed in Subsection 5.3.5.2 of the current chapter.

Figure 5.3.7(a) illustrates the effect of transport through the geosphere on the fluxes of activation/fission products and of those actinides for which the half-lives are greater than for their parent radionuclides. In these cases, ingrowth during geosphere transport generally makes a negligible contribution to geosphere releases and the steady-state solutions discussed in Subsection 5.3.3.4 provide an upper bound to the ratio of the fluxes out of and into the geosphere. Furthermore, due to the fact that the release from the near field varies only slowly with time (with respect to transit times through the geosphere), the fluxes of many radionuclides conform closely to the steady-state solutions, so that the flux ratio is a function of the transit time to half-life ratio (transit time through the geosphere is defined in Appendix 8) and, weakly, of the Peclet number. The transit times of ^{59}Ni , ^{126}Sn and ^{99}Tc are shown to be sufficient for radionuclide fluxes to be reduced by 2 to 5 orders of magnitude during passage through the geosphere. Fluxes of the isotopes of Am, Cm and Pa are reduced by more than 5 orders of magnitude, and are thus not shown in the figure.

Model Assumption/Parameter	Reference-Case Assumption/Value
Transport through low-permeability domain	Geometry 6 assumed
Transport through major water-conducting faults	Not calculated
Planar / cylindrical geometry	Planar (see Table 5.3.3)
Flow through water-conducting features (per unit length)	$6 \times 10^{-4} \text{ m}^2 \text{ y}^{-1}$ (Corresponds to a flowrate of $3.0 \text{ m}^3 \text{ y}^{-1}$ over a repository area of $1.4 \times 10^5 \text{ m}^2$, with a density of water-conducting features of 0.04 m^{-1} ; see Table 3.7.6)
Trace length of channels per unit area of a plane normal to the flow direction	$2 \times 10^{-3} \text{ m}^{-1}$ (see Table 5.3.2)
Flowpath length	200 m (see Table 3.7.6)
Peclet number	10 (see Subsection 5.3.4.2)
Aperture	10^{-3} m (see Table 5.3.3)
Extent of altered wallrock (matrix accessible to diffusion) from centre of fracture plane	$5 \times 10^{-2} \text{ m}$ (see Table 5.3.3)
Matrix porosity (altered wallrock)	5% (see Table 5.3.3)
Pore diffusion constant	$0.001 \text{ m}^2 \text{ y}^{-1}$ (See Subsection 5.3.4.3.1)
Sorption on matrix pores	Element-dependent "realistic-conservative" values of K_d (see Table 3.7.8 and Subsection 5.3.4.4)

Table 5.3.4: Geosphere model assumptions and parameters for Reference-Case calculations. The calculations are identified by the dataset name SA_60A (see Appendix 4 for a description of this nomenclature). Radionuclide releases from the Reference-Case near field are taken as input. As with the near field, "realistic-conservative" physico-chemical parameters are adopted (see Subsection 5.3.4). Geometry 6 (cataclastic/jointed zones with broad, widely-spaced channels, limited matrix diffusion) is used to describe water-conducting features in the low-permeability domain. Transport through major water-conducting faults is not calculated.

Geometry	maximum dose [mSv y ⁻¹]	time of maximum dose [y]	maximum contributing radionuclide.
1	7×10 ⁻⁷	> 10 ⁷	4N + 3 chain
2	1×10 ⁻⁶	> 10 ⁷	4N + 3 chain
3	1×10 ⁻⁴	2×10 ⁵	¹³⁵ Cs
4	7×10 ⁻⁷	> 10 ⁷	4N + 3 chain
5	3×10 ⁻⁵	2×10 ⁴	¹³⁵ Cs
6	2×10⁻⁴	3×10⁵	¹³⁵Cs

Note: The shaded entries indicate that the dose maxima arise beyond 10⁷ years; in all cases, the maximum contributing radionuclide up to this time is ¹³⁵Cs. The Reference-Case result is shown in bold type

Table 5.3.5: Comparison of maximum annual individual doses, summed over all safety-relevant radionuclides, for the six geometrical representations of the water-conducting features of the low-permeability domain. Doses are calculated using the full performance-assessment model chain and Reference-Case physico-chemical parameters. From this table, Geometry 6 is seen to give the highest annual individual dose and is therefore adopted in the Reference Case.

Complementing this, Figure 5.3.7(b) illustrates the effect of transport through the geosphere on the fluxes of short-lived members of the actinide chains. These reach radioactive equilibrium with their parents provided the transit time through the geosphere is sufficiently long. The quantity Ψ (defined in Appendix 8) is plotted against the transit time to half-life ratio for the radionuclides ²³³U, ²³⁴U, ²²⁹Th, ²³⁰Th, ²²⁶Ra and ²³¹Pa. $\Psi = 0$ when the radionuclide is in radioactive equilibrium with its parent on exiting the geosphere. Figure 5.3.7(b) illustrates that, in the Reference Case, the geosphere transit times of all radionuclides shown are sufficient for them to come into equilibrium with their parents. For this subset of radionuclides, the release from the geosphere to the biosphere is not determined by their near-field release rates, but rather by the release of the parent radionuclides from the geosphere.

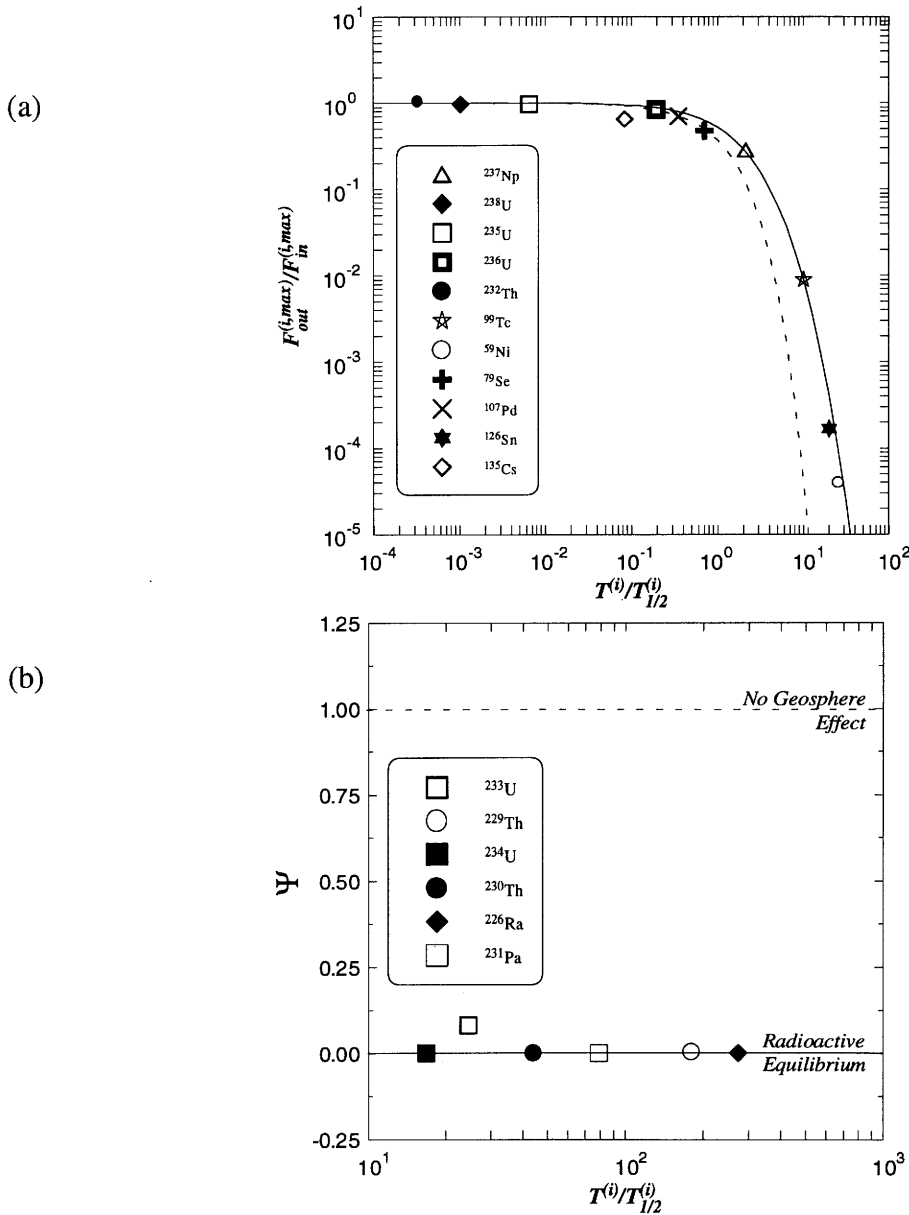


Figure 5.3.7: Comparison of Reference-Case geosphere results with simplified analytical solutions. (a) The ratio of radionuclide flux maxima out of and in to the geosphere $F_{out}^{(i,max)}/F_{in}^{(i,max)}$, plotted as a function of geosphere transit-time to half-life ratio $T^{(i)}/T_{1/2}^{(i)}$. Comparison is made with a steady-state solution for the Peclet number of the Reference-Case ($Pe = 10$, continuous line) and for the case of zero dispersion ($Pe = \infty$, broken line). (b) Daughters of long-lived parent radionuclides emerge from the geosphere in radioactive equilibrium if $T^{(i)}$ is sufficiently large with respect to $T_{1/2}^{(i)}$. $\Psi = 0$ indicates radioactive equilibrium. $\Psi = 1$ indicates that the radionuclide flux from the near field is unchanged by transit through the geosphere. $T^{(i)}$ and Ψ are defined in Appendix 8.

5.3.5.2 Parameter Variations

Parameter variations have been performed using full, time-dependent solutions (codes RANCHMD and RANCHMDNL), to investigate uncertainty in the following:

- the groundwater flowrate q_w through the water-conducting features of the low-permeability domain (see also Subsection 6.2.2.4).
- the flowpath length L through the low-permeability domain,
- the Peclet number Pe ,
- the pore diffusion constant for the matrix D_p ,
- geometry and porosity of diffusion accessible matrix (Geometries 1 - 6 in Figure 5.3.5),
- the depth of (altered) wallrock available to matrix diffusion, y_p , in the specific case of Geometry 6: $y_p = 10^{-2}$ m is investigated as a lower limit to the matrix depth accessible by diffusion, derived on the basis of natural analogue studies (ALEXANDER et al. 1990),
- the sorption constant $K_d^{(i)}$.

The parameter variation studies are carried out for each parameter (or group of related parameters) separately - combinations of unrelated parameters are not investigated. This leads to the identification of 16 distinct datasets (summarised in Table 5.3.6) for which calculations are performed. For the geosphere parameter variation study a subset of the safety-relevant radionuclides is selected. This subset consists of the three activation/fission products giving the highest contributions to dose in the Reference Case (^{79}Se , ^{99}Tc and ^{135}Cs ; see Chapter 6, Figure 6.2.1), together with an example of a long-lived actinide (^{237}Np from the 4N + 1 chain). Results are most conveniently expressed in terms of doses, which provide a yardstick for comparing different radionuclides. Doses are calculated using the Reference-Case biosphere (see Section 5.4).

In Figures 5.3.8 - 5.3.11, maximum annual individual doses for each of the example radionuclides are plotted for all geosphere parameter variations. The effects of the geometrical description of the water-conducting features are shown by the uppermost six bars. The first three bars show maximum doses for geometries in which diffusion is modelled in both altered and unaltered wallrock ("unlimited" matrix diffusion). The second three bars give the corresponding results where diffusion is limited to altered wallrock and fracture infill only ("limited" matrix diffusion). As mentioned above, the highest dose maximum is due to ^{135}Cs with Geometry 6 assumed - cataclastic zones/jointed zones with broad, widely-spaced channels and limited matrix diffusion.

This type of water-conducting feature is adopted in the Reference Case, around which parameter variations are made. Parameter variations affecting the geosphere only are shown by the next 7 bars. Comparison is made with a set of calculations for a hypothetical system in which the Reference-Case near field is coupled directly to the biosphere (results indicated in each case by the full vertical line), with transport through the geosphere not calculated. The latter provides an indication of the "worst possible" geosphere performance, given Reference-Case conditions in the near field and biosphere. The final three bars show the results of flowrate variations, which affect the near field as well as the geosphere; in these cases, comparison is made with the maximum dose in the Reference-Case model-chain calculations (indicated in the figures by the broken, vertical line). The interval between the full and broken vertical lines is a measure of the performance of the Reference-Case geosphere.

The maximum dose is highly sensitive to the choice of geometry for the water-conducting features (see also Figure 6.2.8), varying over more than 9 orders of magnitude for each radionuclide. Particularly for aplitic dykes, results can also be sensitive to whether matrix diffusion is confined to the altered wallrock only, or is modelled in the unaltered wallrock as well. However, having selected Geometry 6 for the Reference Case (cataclastic zones/jointed zones with broad, widely-spaced channels; limited matrix diffusion) because it gives the highest overall dose, the calculated dose maxima are relatively insensitive to all other parameter variations.

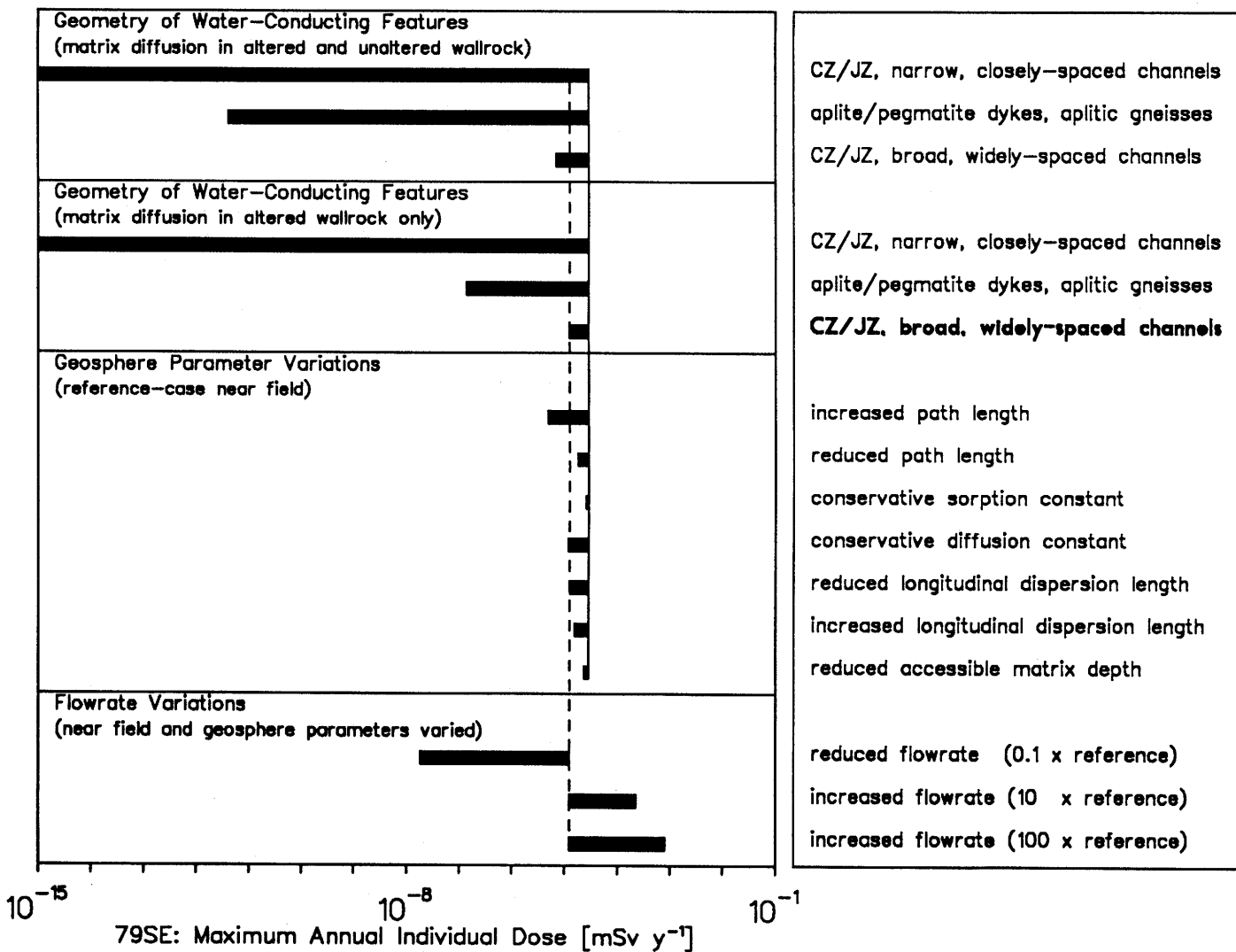
Referring to Figure 5.3.7(a), for ^{79}Se , ^{135}Cs and ^{237}Np transit times through the geosphere are seen to be comparable to the half-lives, differing at most by an order of magnitude. The analytical solutions (also shown in Figure 5.3.7(a)) indicate that the degree to which radioactive decay reduces releases from the geosphere under these circumstances is both small and rather insensitive to either transit time or Peclet number (i.e. the sensitivity only becomes apparent when the transit time to half-life ratio greatly exceeds unity). The transit time is a function of flowpath length, sorption constant, diffusion constant and groundwater flowrate (see Appendix 8). It should be emphasised that this behaviour arises principally because of the conservative assumptions concerning the geometrical description of water-conducting features in the Reference Case. The impact of parameter variations would be quite different if a less pessimistic geometry were selected. ^{99}Tc is more sensitive than the other example radionuclides, since the ratio of transit time to half-life is largest for this radionuclide. Referring again to Figure 5.3.7(a), the reduction in flux across the geosphere is seen to be more sensitive in this case to variations both in transit time and in Peclet number.

The flowrate is the parameter to which the results are most sensitive, since this affects the performance of both the near-field and the geosphere. Thus, the doses for the case in which flowrate is increased to 100 times that of the Reference Case typically exceed by more than an order of magnitude those for the hypothetical case in which geosphere transport is neglected but the Reference-Case flowrate is used for the near field. A 10-fold reduction in flowrate has a pronounced effect, particularly for ^{237}Np and ^{99}Tc , where doses are reduced by 4, and more than 9, orders of magnitude, respectively.

Parameter Variations	Dataset Names
ADVECTION (see Subsection 5.3.4.1)	
Groundwater Flowrate	
10-fold decrease in flowrate through low-permeability domain: $q_w = 6 \times 10^{-5} \text{ m}^2 \text{ y}^{-1}$	EA_60L
10-fold increase in flowrate through low-permeability domain: $q_w = 6 \times 10^{-3} \text{ m}^2 \text{ y}^{-1}$	
100-fold increase in flowrate through low-permeability domain: $q_w = 6 \times 10^{-2} \text{ m}^2 \text{ y}^{-1}$	
Flowpath Length	
Reduced flowpath length through the low-permeability domain: $L = 100 \text{ m}$	SA_60C
Increased flowpath length through low-permeability domain: $L = 500 \text{ m}$	SA_60D
DISPERSION (see Subsection 5.3.4.2)	
Longitudinal Dispersion Length	
Increased dispersion (reduced Peclet number): $Pe = 2$	SA_60G
Reduced dispersion: $Pe = 50$	
MATRIX DIFFUSION (see Subsection 5.3.4.3)	
Diffusion Constant in the Matrix:	
"Conservative" diffusion constant: $D_p = 2 \times 10^{-4} \text{ m}^2 \text{ y}^{-1}$	SA_60F
Geometry and Porosity of Diffusion Accessible Matrix	
Unlimited Matrix Diffusion:	
Fracture Infill + Altered and Unaltered Wallrock	
Cataclastic/jointed zones with narrow, closely-spaced channels	Geometry 1: SA_10A Geometry 2: SA_20A Geometry 3: SA_30A
Aplite/pegmatite dykes and aplitic gneisses	
Cataclastic/jointed zones with broad, widely-spaced channels	
Limited Matrix Diffusion:	
Fracture Infill + Altered Wallrock Only	
Cataclastic/jointed zones with narrow, closely-spaced channels	Geometry 4: SA_40A Geometry 5: SA_50A Geometry 6: SA_60A
Aplite/pegmatite dykes and aplitic gneisses	
Cataclastic/jointed zones with broad, widely-spaced channels	
Depth of Diffusion-Accessible Altered Wallrock	
"Conservative" matrix-diffusion depth within altered wallrock in the case of Geometry 6: $y_p = 10^{-2} \text{ m}$	SA_60I
SORPTION (see Subsection 5.3.4.4)	
Sorption Constant for the Matrix:	
"Conservative" values: see Table 3.7.7	SA_60E

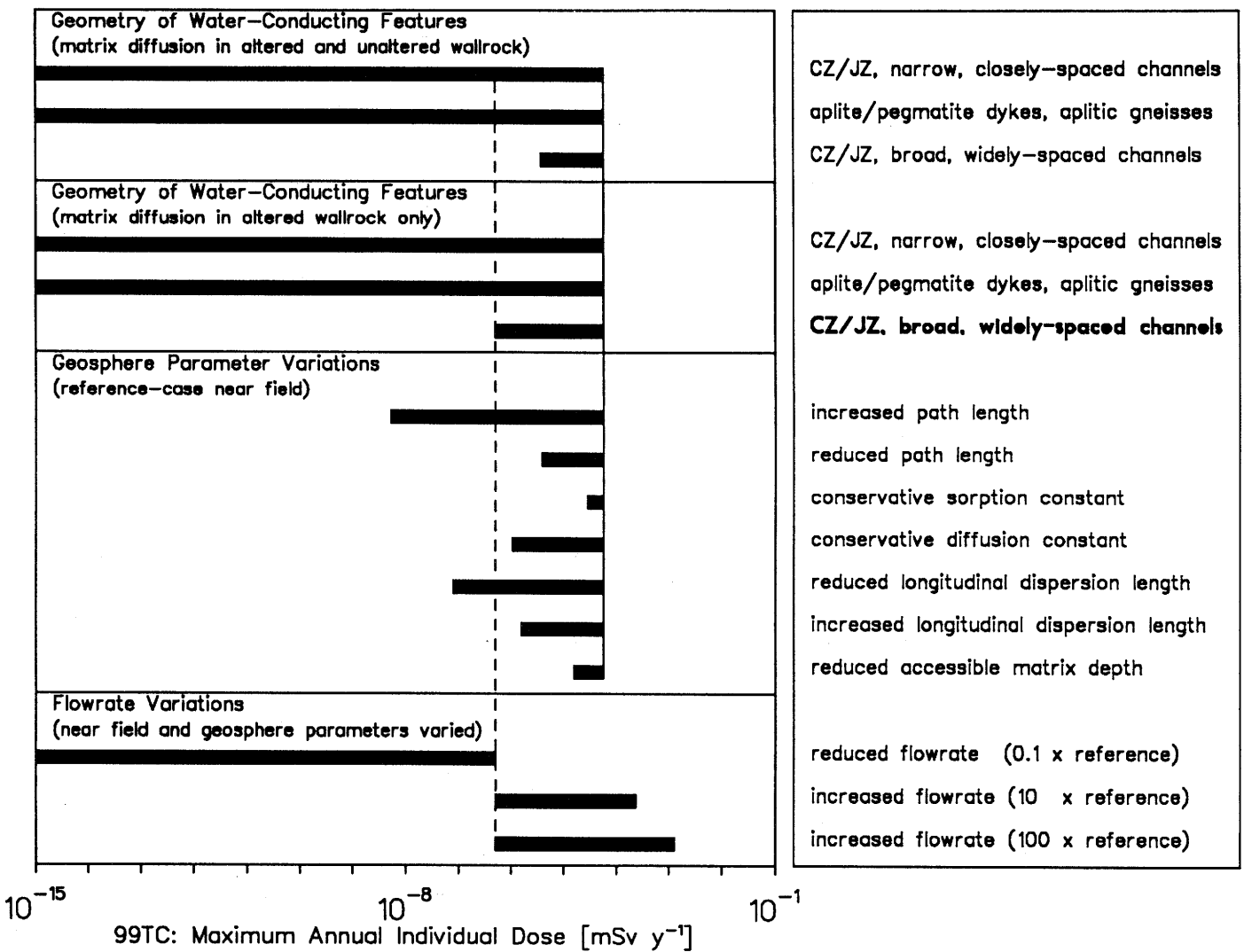
Note: The nomenclature for datasets is discussed in Appendix 4.

Table 5.3.6: Geosphere parameter variations, the geosphere transport processes which they affect and the associated dataset names.



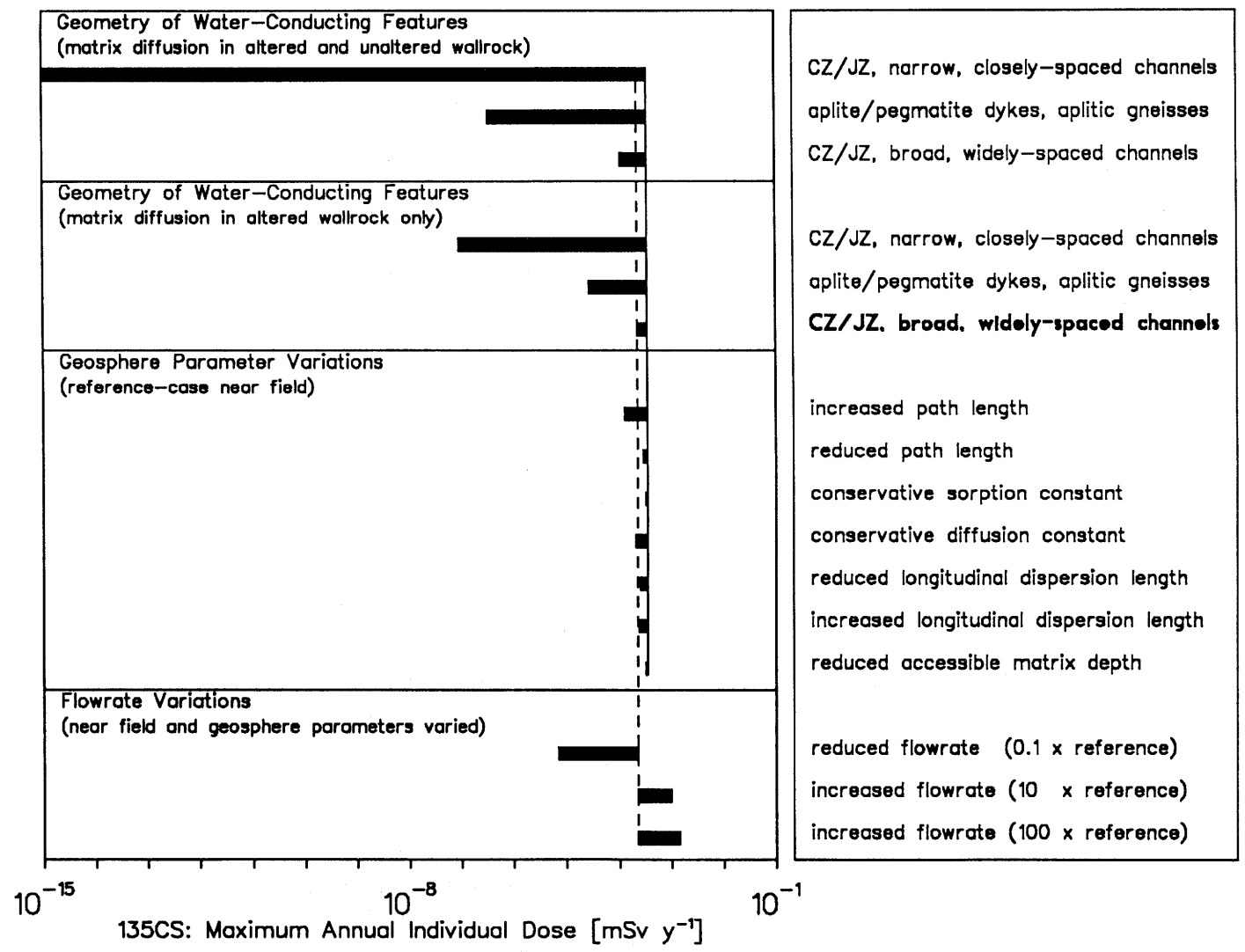
Note: CZ/JZ = cataclastic/jointed zones.

Figure 5.3.8: Maximum annual individual dose from ⁷⁹Se for each of the geosphere parameter variations. (See text for further explanation of this figure).



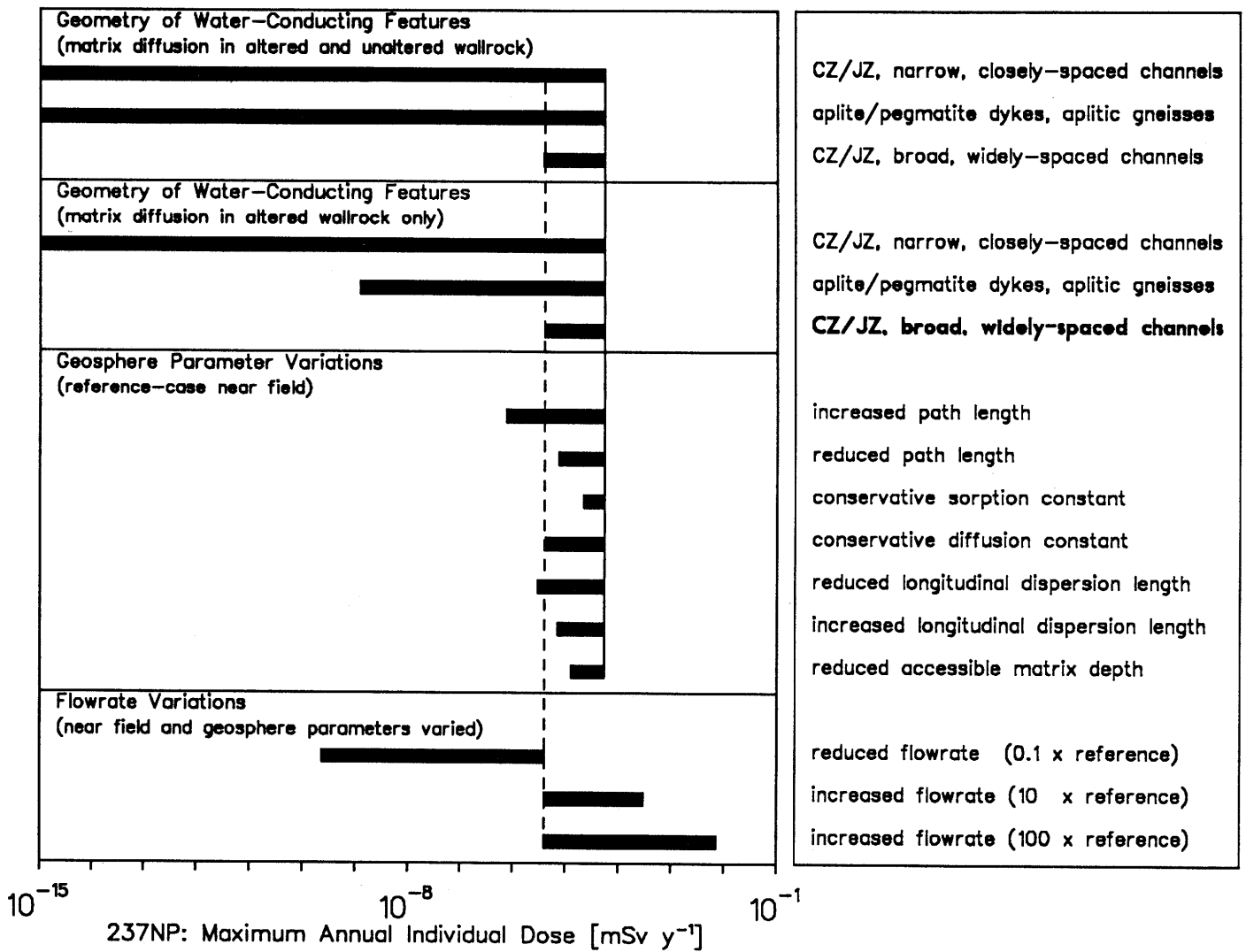
Note: CZ/JZ = cataclastic/jointed zones.

Figure 5.3.9: Maximum annual individual dose from ⁹⁹Tc for each of the geosphere parameter variations. (See text for further explanation of this figure).



Note: CZ/JZ = cataclastic/jointed zones.

Figure 5.3.10: Maximum annual individual dose from ¹³⁵Cs for each of the geosphere parameter variations. (See text for further explanation of this figure).



Note: CZ/JZ = cataclastic/jointed zones.

Figure 5.3.11: Maximum annual individual dose from ²³⁷Np for each of the geosphere parameter variations. (See text for further explanation of this figure).

The transport model described in Subsection 5.3.3.1 (and encoded in RANCHMD), in which linear sorption is assumed, has been used in all calculations so far discussed. However, in the case of Cs, sufficient data are available to define a Freundlich isotherm, which can be incorporated explicitly into transport calculations using the model described in Subsection 5.3.3.2 (and encoded in RANCHMDNL). The time-development of ^{135}Cs flux from the low-permeability domain, calculated using the two approaches to the modelling of sorption, are plotted in Figure 5.3.12 for all six representations of the internal geometry of water-conducting features. For the most conservative geometries (cataclastic zones or jointed zones with broad, widely-spaced channels - Geometries 3 and 6), the results of the two approaches are similar. This is because the geosphere has little effect as a migration barrier for ^{135}Cs , with a geosphere transit time which is less than the radionuclide half-life (see Figure 5.3.7(a)) and, consequently, gives little reduction in maximum radionuclide flux (and concentration) during transport. The linear isotherm is chosen such that it gives the same retardation as the non-linear isotherm when radionuclide concentration is at its maximum (at the point of release to the geosphere; see Subsection 5.3.4.4). Where the geosphere provides an ineffective barrier, radionuclide concentration reaches a similar maximum value at all points along the transport path and, therefore, the non-linearity of sorption will not strongly affect the retardation of the peak of the migrating radionuclide pulse; the effects of sorption non-linearity are confined mainly to the leading and trailing parts of the pulse. For the less conservative geometries, there is a greater flux (and concentration) reduction during transport through the geosphere. Where the effects of non-linear sorption on transport are modelled explicitly, as the concentration falls, both the retardation and transit times increase and the flux is further reduced by decay and dispersion. The model which directly incorporates non-linear sorption therefore gives significantly reduced fluxes from the geosphere in these cases.

5.3.6 Summary of Geosphere Modelling and Performance

A geosphere model has been defined which includes the processes of:

- advection of radionuclides in a network of channels within water-conducting features;
- longitudinal hydrodynamic dispersion;
- diffusion from these channels into the stagnant porewaters of the adjacent porous matrix;
- sorption onto pore surfaces;
- radioactive decay and ingrowth.

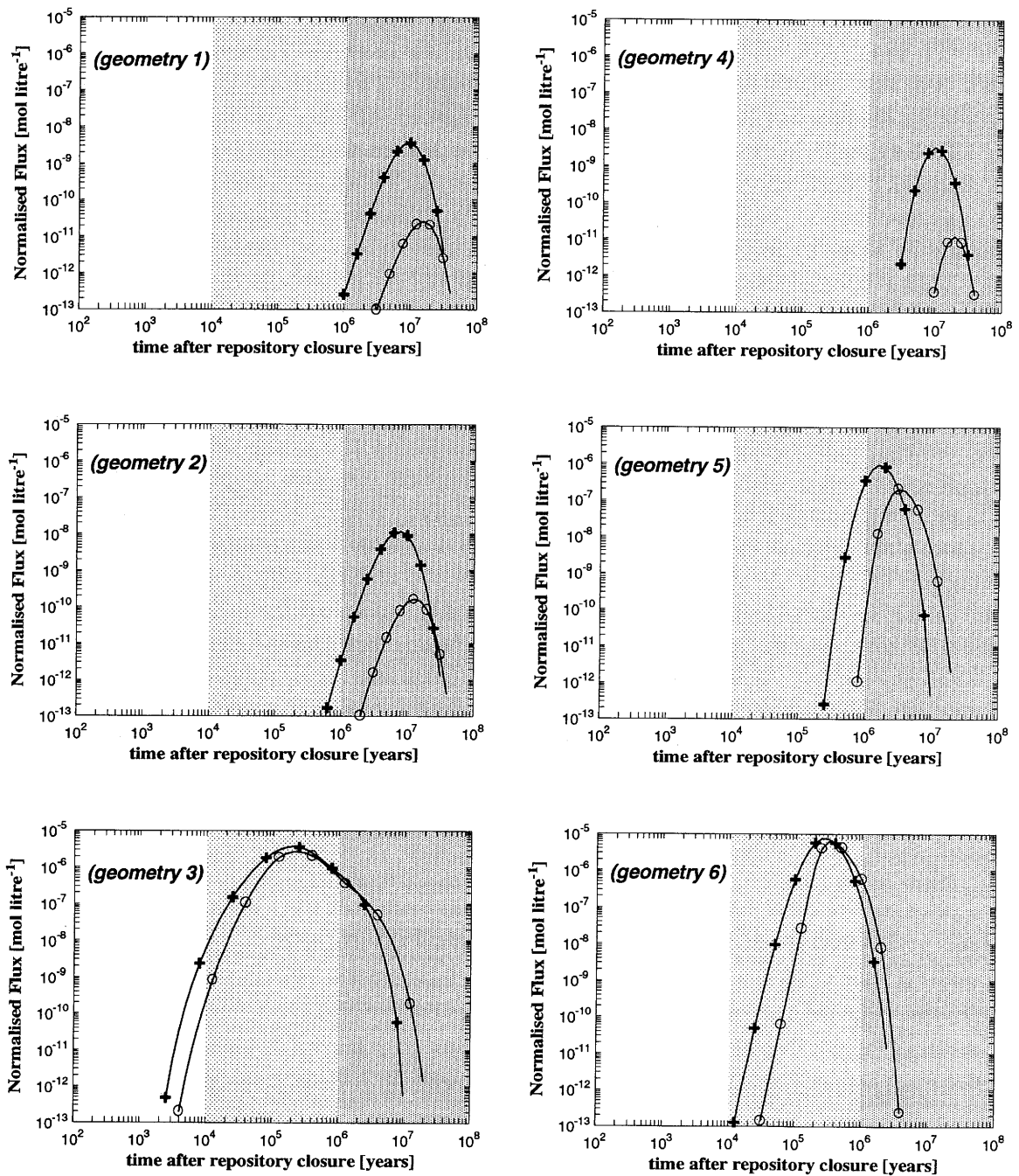


Figure 5.3.12: Time development of the normalised ¹³⁵Cs flux from the geosphere low-permeability domain for each of the six geometric representations of the water-conducting features. The normalised flux is defined here as $F_{out}^{(i)}/q$ (Equation 5.3.8). Results calculated with non-linear sorption incorporated explicitly (—○—) are compared with those calculated with an effective linear isotherm (—■—). For an explanation of the shading used in this plot, see Appendix 1.

Attention focuses on the modelling of radionuclide transport in the low-permeability domain of the crystalline basement, since the other geological units are less well characterised and are thought to provide a smaller barrier potential (see Subsection 6.2.2.2). To facilitate mathematical treatment, a number of simplifications are made, mainly in the description of geometrical features. These include:

- representation of the interconnected network of water-conducting features through which water flow takes place by a single representative conduit of simple geometry. The complexity (variability and interconnectedness) of the actual flowpaths is, to some extent, incorporated in the model as hydrodynamic dispersion;
- neglect of spatial variability in the physico-chemical properties of the water-conducting features.

The results of a set of calculations have been presented which examine the effectiveness of the geosphere as a barrier to migration and the sensitivity of model results to uncertainty in geosphere properties.

Several further issues relating to the geological environment are considered in detail in Chapter 6, in which the results of complete model-chain calculations are presented. Specifically, these are:

- the internal geometry of geosphere water-conducting features;
- the accessibility of altered and unaltered wallrock to matrix diffusion;
- the effects of transport paths which pass along major water-conducting faults;
- the sorption of radionuclides onto groundwater colloids;
- the spatial variability in the flowrate through water-conducting features.

In the present chapter, the uncertainties associated with these issues have been handled by introducing a set of generally conservative assumptions. A Reference Case has been defined, in which a pessimistic geometrical representation of the water-conducting features is adopted and matrix diffusion is limited to the altered wallrock adjacent to individual fractures. Retardation and decay within major water-conducting faults is not considered. The sorption of radionuclides on colloids and the variability of groundwater flowrate through water-conducting features have both been neglected. These two assumptions are potentially non-conservative; both issues are discussed further in Chapter 6 and are subjects of future investigations and model developments.

Further conservatism is introduced via the groundwater flow model (see Subsection 3.5.3): the model neglects the relationship between hydraulic gradient and the transmissivity of water-conducting features and, in the "Sparse Model" for Area West adopted in the Reference Case, assumes that only a few of the first- and second-order faults are hydraulically active, which leads to higher gradients than in the alternative "Full Model".

In spite of the conservatism of most of these assumptions (particularly the very conservative internal geometry assumed for water-conducting features), the geosphere can, for some radionuclides, add significantly to the safety provided by the near-field barriers. Radionuclide fluxes from ^{59}Ni , ^{126}Sn and ^{99}Tc are reduced by 2 to 5 orders of magnitude, while the fluxes of isotopes of Am, Cm and Pa are reduced by still greater amounts. Several radionuclides are in radioactive equilibrium with their parents. However, the chosen representation of the geosphere is ineffective in reducing maximum radionuclide flux of certain other radionuclides, including ^{135}Cs and ^{79}Se , which give important contributions to the total dose (see, however, Chapter 6, where the effect of the geosphere in terms of delaying the arrival in biosphere of the maximum radionuclide fluxes is also discussed).

Parameter variations have been carried out for some key radionuclides. For the Reference-Case geosphere, based on the above assumptions, the model results are insensitive to most parameter variations for the radionuclides ^{79}Se , ^{135}Cs and ^{237}Np (it is, however, likely that the impact of parameter variations would be quite different if a less pessimistic internal geometry for water-conducting features had been selected). ^{99}Tc , for which the Reference-Case geosphere is more effective as a barrier, also shows more sensitivity. Groundwater flowrate through the low-permeability domain is the parameter to which releases are most sensitive, since this parameter affects the performance of both the near field and the geosphere.

5.4 Biosphere Modelling

5.4.1 Introduction

The aim of the biosphere modelling described here is to express the estimated releases of radionuclides from the near field and geosphere on a scale - dose³² - which is accepted as an appropriate measure to discuss when considering radiological hazard. The quantity calculated is not an estimate of the actual doses that might be received by individuals living in the far future (see Subsection 2.4.2); rather, it is an indicator of repository performance. Specifically, it is the quantity required for comparison with Protection Objective 1 of the Swiss regulatory guidelines (see Section 2.3), which specifies an annual limit of 0.1 mSv y⁻¹ to "... an average individual in the population group most likely to be affected by the potential releases from a repository" (HSK & KSA 1993). The use of dose as the end point of safety-assessment calculations is useful since it allows the releases of different radionuclides to be placed on a common scale that accounts for their different radio-toxicity by an established formalism (ICRP 1979-82).

Biosphere modelling involves calculation of the distribution of radionuclides in a region of the surface environment and of doses to a hypothetical individual living in the region and making use of local resources.

The region to be modelled is representative of the area to which radionuclides, released from a repository in the crystalline basement of Northern Switzerland, might eventually be carried by groundwater. The present understanding of the regional hydrogeology of Northern Switzerland (see Section 3.5) indicates that, for a repository anywhere in the areas under consideration in the crystalline basement, the release is most likely to occur somewhere in the upper Rhine valley, where groundwater would mix with recent meteoric and river water in gravel aquifers typical of the valley. The exact location of the entry point for radionuclides into the biosphere depends on the siting of the repository and details of the local hydrogeological regime which are not determined at present. However, given that releases to the biosphere can only occur after the failure of the canisters (conservatively assumed to be at 1000 years post closure) and that the general characteristics of the region do not show significant spatial variability, the precise location and detailed characteristics of the biosphere are not important; indeed, they are expected to change over time. Therefore, in modelling the Reference Scenario, a region broadly representative of a possible discharge zone in the upper Rhine valley is considered. To test the sensitivity of doses to this and other assumptions, a range of alternative biosphere scenarios (see Subsection 4.4.1) are modelled; these consider alternative locations of groundwater discharge and alternative climate states. A conservative model of human behaviour is imposed such that, in most scenarios, doses are received from a wide range of exposure pathways. An exception is the case of a deep well extracting water from the crystalline basement, in which only doses due to drinking the well water are considered.

³² The quantity calculated is annual dose to an average member of the critical group of most exposed individuals, see section 5.4.2.1.

The assumptions of the biosphere model for the Reference Scenario are described in Subsection 5.4.2. The mathematical formulation of the model is summarised in Subsection 5.4.3. Parameter values for the Reference-Case biosphere are presented in Subsection 5.4.4. Results of biosphere modelling, including parameter-sensitivity studies, are presented in Subsection 5.4.5 (results from the modelling of alternative scenarios are presented in Chapter 6). A summary of biosphere modelling and results is presented in Subsection 5.4.6.

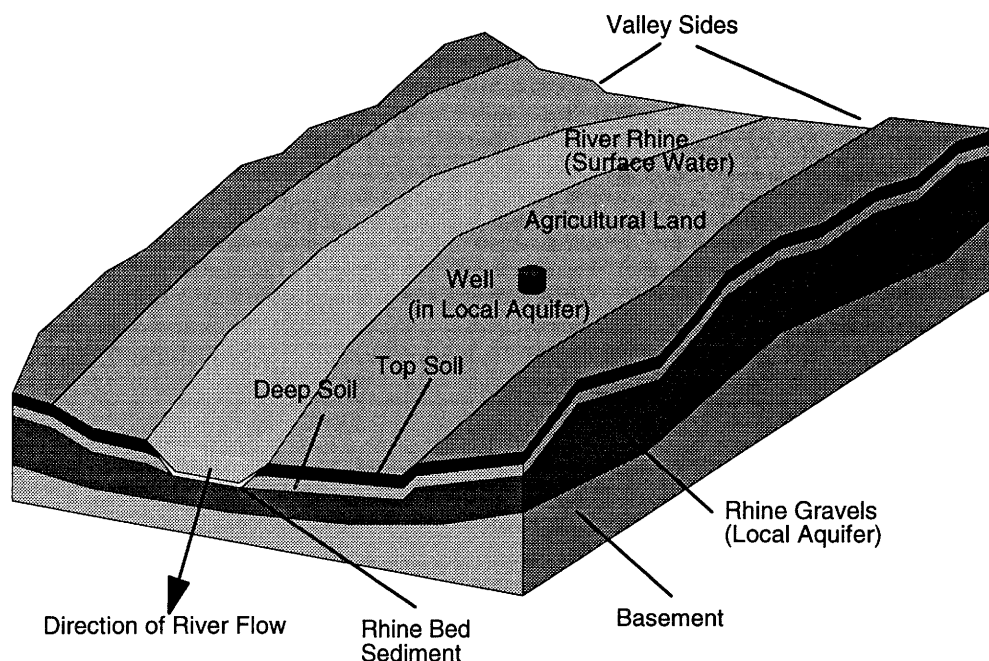
5.4.2 Model Assumptions

Figure 5.4.1 presents a schematic illustration of a section of the Rhine valley, showing the main physical components of the Kristallin-I reference biosphere model: a **local aquifer** in the gravels of the Rhine valley, a **deep soil** layer and a **top soil** layer. The aquatic environment (a section of river) is divided into **surface water** and **aquatic sediment**. The exposure pathways represented in the model are listed in the accompanying table.

5.4.2.1 Features, Events and Processes

The following assumptions are made about the FEPs represented in the biosphere model of the Reference Scenario.

- Contaminated water from the crystalline basement discharges into a gravel aquifer in the Rhine valley.
- The climate and natural environmental characteristics of the region of exfiltration are those of the present day and remain constant throughout the time of the calculation.
- Transport of radionuclides in the biosphere occurs as a result of movements of water (radionuclides in solution) and of movements of solid materials (radionuclides sorbed onto the solid phase in environmental media). The processes considered are:
 - the upward movement of groundwater from the underlying aquifer;
 - the interaction of the aquifer with the river;
 - the interaction of the river with the river bed sediments;
 - irrigation of crops with water from the aquifer or from the river (assuming 50% from each source);



Exposure Pathways to Man			
Ingestion Pathways			Other Pathways
Well water, river water, fish,	meat from cattle, milk from cattle, eggs from poultry,	grain, root vegetables, green vegetables.	External γ -irradiation, dust inhalation.

Figure 5.4.1: Schematic illustration of the reference biosphere region, indicating the main physical features and listing the exposure pathways considered in the calculations of annual individual dose.

- irrigation of crops with water from the aquifer or from the river (assuming 50% from each source);
- the effects of infiltrating meteoric water;
- bioturbation - the effects of soil fauna moving between soil horizons and transporting material in the process;
- the maintenance and evolution of the river, e.g. flooding, dredging, meandering;
- surface run-off, flooding and erosion of soil.
- The area of agricultural land affected by the release is determined by the regional groundwater flow in the gravels.

- The soils are used for agricultural production: arable crops and pasture are grown in a well-mixed rooting zone.
- Livestock in the region ingest radionuclides via fodder as well as by the direct consumption of soil and water from the river or a well in the local aquifer. All foodstuffs for consumption by animals are assumed to be produced in the area of maximum radionuclide concentration.
- Concentration of radionuclides entering the river water and sediments is diluted by mixing with the larger flux of uncontaminated water and sediments.
- Fish in the river accumulate radionuclides from the water.
- Human inhabitants of the region obtain all their dietary requirements from local sources. Vegetables, grain, animal products and fish are consumed.
- Drinking water is assumed to be abstracted from a well in the local gravel aquifer.
- The inhabitants also receive doses due to external irradiation from radionuclides in soil and due to inhalation of soil particulates, which also contain radionuclides.
- Doses are calculated for an adult individual³³ with diet and habits representative of a subsistence farmer dwelling permanently in the contaminated region.
- The quantity calculated by the biosphere model is the effective dose to an individual, defined as the sum of the weighted dose equivalents in specific organs, integrated over 50 years, from the intake of activity into the body in one year, plus the sum of weighted dose equivalents from external irradiation in one year. For convenience, the term *annual individual dose*, or simply *dose*, is used in this report.

Most of the above assumptions also apply to several or all of the alternative scenarios considered. Table 5.4.1 summarises the main points of difference between the Reference and alternative scenarios related to biosphere modelling (see also Table 4.4.1). Apart from the broad differences noted, parameter values are also different in some cases, reflecting, for example, the different agricultural practices in the different biosphere climate states.

³³ The exposed population will include all ages. Whereas doses per unit intake for children and infants are generally greater than doses per unit intake for adults (GREENHALGH et al. 1985), this is compensated for by larger dietary intakes by adults. Thus, for adults and children exposed by various pathways to the same concentrations of safety-relevant radionuclides in environmental media, the doses to children typically differ by not more than a factor of three from, and are generally less than, the doses to adults (BERGSTRÖM & NORDLINDER 1990). If it is assumed that an individual spends their entire life in the region, then the dose to an adult can be thought of as an approximation of the annual average dose over a lifetime.

Scenario	Type and location of geosphere release	Climate state
Reference Scenario	From higher-permeability domain or major water-conducting faults to Rhine valley gravel aquifer.	Temperate - representative of present day and future interglacial periods. Subsistence arable and livestock farming.
Exfiltration to Small Valley (Area East only - included within the Reference Scenario in Chapter 6)	From higher-permeability domain or major water-conducting faults to gravel aquifer in a small valley - only considered for Area East.	Temperate (as in Reference Scenario).
Deep Groundwater Well (e.g. mineral water source)	Extraction of water directly from crystalline basement.	Climate not relevant - drinking water is the only exposure pathway considered.
Alternative Climate-Related Scenarios <ul style="list-style-type: none"> <li data-bbox="167 1104 387 1133">• Dry Climate State <li data-bbox="167 1261 420 1290">• Humid Climate State <li data-bbox="167 1417 462 1447">• Periglacial Climate State <li data-bbox="167 1675 432 1704">• Rhine Gravels Absent 	<p data-bbox="505 1104 795 1133">(as in Reference Scenario)</p> <p data-bbox="505 1261 795 1290">(as in Reference Scenario)</p> <p data-bbox="505 1417 795 1603">Release of radionuclides to the biosphere ceases (at the onset of the periglacial climate) after an initial period modelled as in the Reference Scenario.</p> <p data-bbox="505 1675 795 1794">From higher-permeability domain or major water-conducting faults directly to the river.</p>	<p data-bbox="837 1104 1233 1223">Warm, dry climate, representative of possible (less likely) conditions if glacial cycling ceases. Subsistence arable and livestock farming.</p> <p data-bbox="837 1261 1264 1379">Warm, wet conditions, representative of possible conditions if glacial cycling ceases. Subsistence arable and livestock farming.</p> <p data-bbox="837 1417 1248 1637">Tundra climate - representative of future periglacial periods. Permafrost isolating biosphere from further releases. Local community based on herding and fishing - investigation of the importance of the dust - lichen - reindeer pathway.</p> <p data-bbox="837 1697 1256 1727">Temperate (as in Reference Scenario).</p>

Table 5.4.1: Summary of the biosphere scenarios considered. The basis for the alternatives is discussed in Chapter 4 and results are presented in Chapter 6.

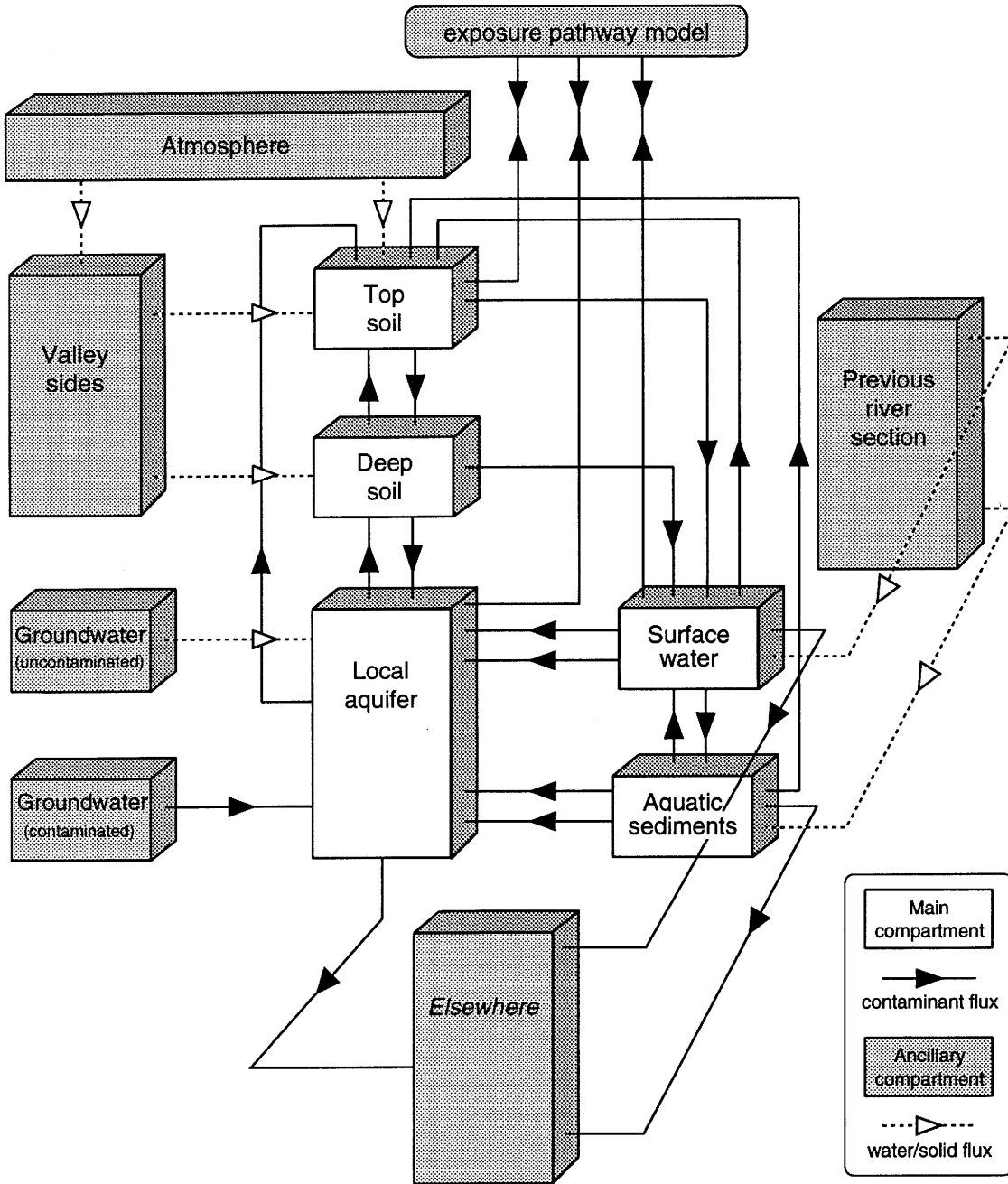
5.4.2.2 Simplifications and Additional Model Assumptions

The population group identified in the Swiss regulatory guidelines, for which dose is to be calculated, is assumed to inhabit a region large enough to supply all basic requirements for a small community. The annual dose received by the average individual depends on the radionuclide concentrations in the various physical compartments of the biosphere (Figure 5.4.1), averaged over the region in which the population group is assumed to live³⁴, and on average concentrations in the water and foodstuffs consumed. Details of spatial distribution of radionuclides are not, therefore, represented. Furthermore, processes operating on short timescales - typically with characteristic time constants of a few years or less, e.g. seasonal effects and episodic flooding, are not considered explicitly.

The following additional simplifications and assumptions are made in biosphere modelling for Kristallin-I:

- A dynamic compartment model (i.e., one in which the variation of compartment inventory is calculated as a function of time) is used to represent the transport and distribution of radionuclides between the environmental features represented (aquifer, soil, river etc., see Figure 5.4.2).
- Average concentrations within the compartments are calculated as the total radionuclide content (time-dependent) divided by the total volume or mass (fixed over the time of the calculations).
- Doses via each pathway are assumed to be directly proportional to the concentration in appropriate compartments, e.g. doses via foodstuff consumption pathways are proportional to the concentration of radionuclides in the top soil compartment.
- The concentrations of shorter-lived radionuclides, not treated explicitly in the dynamic model, are assumed to be in equilibrium with their longer-lived parents (see Appendix 2).

³⁴ The assumed requirements of the community define a *minimum* area over which it is valid to average radionuclide concentrations, i.e. an area that could supply all the dietary needs of the community. However, consideration of the spatial extent of the zone of geosphere discharge may lead to definition of a larger region as being more appropriate. In the Kristallin-I Reference Case, an area of 3.4 km² is considered; this is derived from site-specific studies (BAEYENS et al. 1989) and is the area of land overlying a gravel aquifer unit, typical of the Rhine River valley in Northern Switzerland, in which radionuclides released from the geosphere would be uniformly mixed.



Note: Radionuclides are not actually transferred to and from the exposure pathway model, rather, dose by each pathway considered is proportional to the radionuclide concentration in the top soil, local aquifer or surface water compartments (see subsection 5.4.3.2).

Figure 5.4.2: General arrangement of the compartments for a generic representation of the biosphere. The *Elsewhere* compartment acts as a sink for radionuclides leaving the region of concern.

5.4.3 Mathematical Representation

The *Terrestrial - Aquatic Model of the Environment* (TAME) has been developed to model a wide range of biosphere scenarios representative of possible conditions of exposure arising from underground disposal of radioactive wastes in Switzerland. The mathematical formulation of the model is summarised here; a more detailed description is given in KLOS et al. (1994).

5.4.3.1 Compartment Model

The features of the biosphere depicted in Figure 5.4.1 are translated into the model compartments illustrated in Figure 5.4.2. The transport dynamics of this model are represented by a set of donor-controlled, linear first-order ordinary differential equations of the form:

$$\frac{dN_i}{dt} = \sum_{j \neq i} \lambda_{ji} N_j - N_i \sum_{j \neq i} \lambda_{ij} + \lambda_N M_i - \lambda_N N_i + S_i(t), \quad (5.4.1)$$

where:

- N_i [Bq] is the activity of radionuclide N in compartment i ,
- N_j [Bq] is the activity of radionuclide N in compartment j ,
- M_i [Bq] is the activity of radionuclide M in compartment i (the precursor of radionuclide N in a decay chain),
- $S_i(t)$ [Bq y⁻¹] is an external source term of N to compartment i (i.e. the input to the biosphere from the geosphere per unit time),
- λ_N [y⁻¹] is the decay constant for N ,
- λ_M [y⁻¹] is the decay constant for M (representing radioactive ingrowth),
- λ_{ji} [y⁻¹] is a set of transfer coefficients representing inputs to compartment i from compartments j ($\neq i$),
- λ_{ij} [y⁻¹] is a set of transfer coefficients representing all loss terms from compartment i to compartments j ($\neq i$).

In Equation 5.4.1, the first summation term represents input from the other compartments in the system and the second represents losses to the other compartments. Radioactive ingrowth from the parent in the compartment and radioactive decay are represented by the next two terms and input to the biosphere from the geosphere is the final term.

The application of Equation 5.4.1 to the dynamics of transport requires that the inter-compartment transfer coefficients - the λ_{ij} - be defined in terms of quantities relevant and suitable for the region of interest.

The transfer coefficients, λ_{ij} and λ_{ji} , are given in terms of the amount of contaminant in the source compartment and the amount transferred to the recipient compartment by all processes in unit time, i.e., the fractional transfer rate. If the mass transfer rate from compartment i to compartment j , for a given process p , is $(dN_{ij}/dt)^{(p)}$, then the transfer coefficient can be written

$$\lambda_{ij}^{(p)} = \frac{1}{N_i} \left(\frac{dN_{ij}}{dt} \right)^{(p)} \quad (5.4.2)$$

and, if several processes contribute, then the transfer coefficient λ_{ij} is:

$$\lambda_{ij} = \sum_p \lambda_{ij}^{(p)} \quad (5.4.3)$$

The task of the transport model is to represent the $(dN_{ij}/dt)^{(p)}$ (and hence the λ_{ij}) in terms of observable properties of the biosphere system.

The processes considered are radionuclide transport by water fluxes and by solid material fluxes. If the water flux from compartment i to compartment j is F_{ij} [m^3y^{-1}] and the flux of solid material is M_{ij} [kg y^{-1}], then the components of the transfer coefficient λ_{ij} are:

$$\lambda_{ij}^{(\text{water flux})} = \frac{F_{ij}}{V_i^{\text{liquid}} + k_i m_i^{\text{solid}}}, \quad [\text{y}^{-1}] \quad (5.4.4)$$

and

$$\lambda_{ij}^{(\text{solid flux})} = \frac{k_i M_{ij}}{V_i^{\text{liquid}} + k_i m_i^{\text{solid}}}, \quad [\text{y}^{-1}] \quad (5.4.5)$$

where:

k_i [$\text{m}^3 \text{kg}^{-1}$] is the solid-liquid equilibrium distribution constant (the " K_d ") in the compartment;

V_i^{liquid} [m^3] is the volume of liquid in the compartment;

m_i^{solid} [kg] is the mass of solid material in the compartment.

In terms of the physical dimensions and properties of a compartment, the transfer coefficient is therefore given by

$$\lambda_{ij}^{(\text{water and solid fluxes})} = \frac{1}{l_i A_i} \left[\frac{F_{ij}}{\theta_i + (1 - \varepsilon_i) \rho_i k_i} + \frac{k_i M_{ij}}{\theta_i + (1 - \varepsilon_i) \rho_i k_i} \right], \quad [\text{y}^{-1}] \quad (5.4.6)$$

where the thickness of the compartment l_i and its surface area A_i define the physical volume. The porosity and solid density of the material in the compartment are ε_i [-] and ρ_i [kg m⁻³], respectively; the volumetric moisture content is θ_i [-]. This generic expression is applied to all compartments in the model, with the different properties of the compartments representing different media (e.g. $\varepsilon_i = 0.4$ and $\theta_i = 0.3$ for top soil, $\varepsilon_i \approx 1$ and $\theta_i \approx 1$ for the river).

Diffusion of radionuclides in water between compartments is also included in TAME and the model representation uses a pair of transfer coefficients $\lambda_{ij}^{(\text{diffusion})}$ [y⁻¹] and $\lambda_{ji}^{(\text{diffusion})}$ [y⁻¹] acting between the compartments concerned³⁵. The diffusion constant in pure water for the radionuclides is D_0 [m² y⁻¹] and the internal structure of the material in the compartments is modelled by a *structure factor*, T_i [-], which accounts for the tortuosity of the material. Together with sorption (as modelled above), tortuosity reduces the rate of radionuclide diffusion between the compartments. The characteristic distance over which the diffusion occurs is taken to be the shortest linear dimension of the two compartments (i.e. the minimum of their lengths), so that

$$\lambda_{ij}^{(\text{diffusion})} = \frac{\theta_i}{\theta_i + (1 - \varepsilon_i) \rho_i k_i} \cdot \frac{D_0}{T_i l_i \min(l_i, l_j)}. \quad (5.4.7)$$

The coefficient from j to i is given by an equivalent expression with indices interchanged.

The generic form of the transfer coefficient between compartments i and j is therefore

$$\lambda_{ij} = \frac{1}{\theta_i + (1 - \varepsilon_i) \rho_i k_i} \left(\frac{F_{ij} + k_i M_{ij}}{l_i A_i} + \frac{\theta_i D_0}{T_i l_i \min(l_i, l_j)} \right). \quad (5.4.8)$$

The water and solid fluxes are determined by a mass balance scheme for each biosphere representation. The mass balance schemes for the Kristallin-1 Reference-Case biosphere, are discussed in Subsection 5.4.4.

³⁵ This parameterisation of diffusion is consistent with the representation of the soils as two distinct units in TAME. Such forms are used elsewhere (see for example KLOS & VAN DORP 1994) and are known to both reduce the time taken for dose maxima to be reached as well as increase the maximum dose. However, the influence on the maximum individual doses arising in the Kristallin-I calculations is small because the effect of diffusion appears principally at early times after the start of the release to the biosphere, and then only for the weakly sorbing radionuclides. The releases in Kristallin-I occur far into the future and remain at or near their peak values over considerable periods. The suitability of this form, and the consequences of modelling diffusion in soils in this way, are the subject of several studies in BIOMOVs II (SSI 1993).

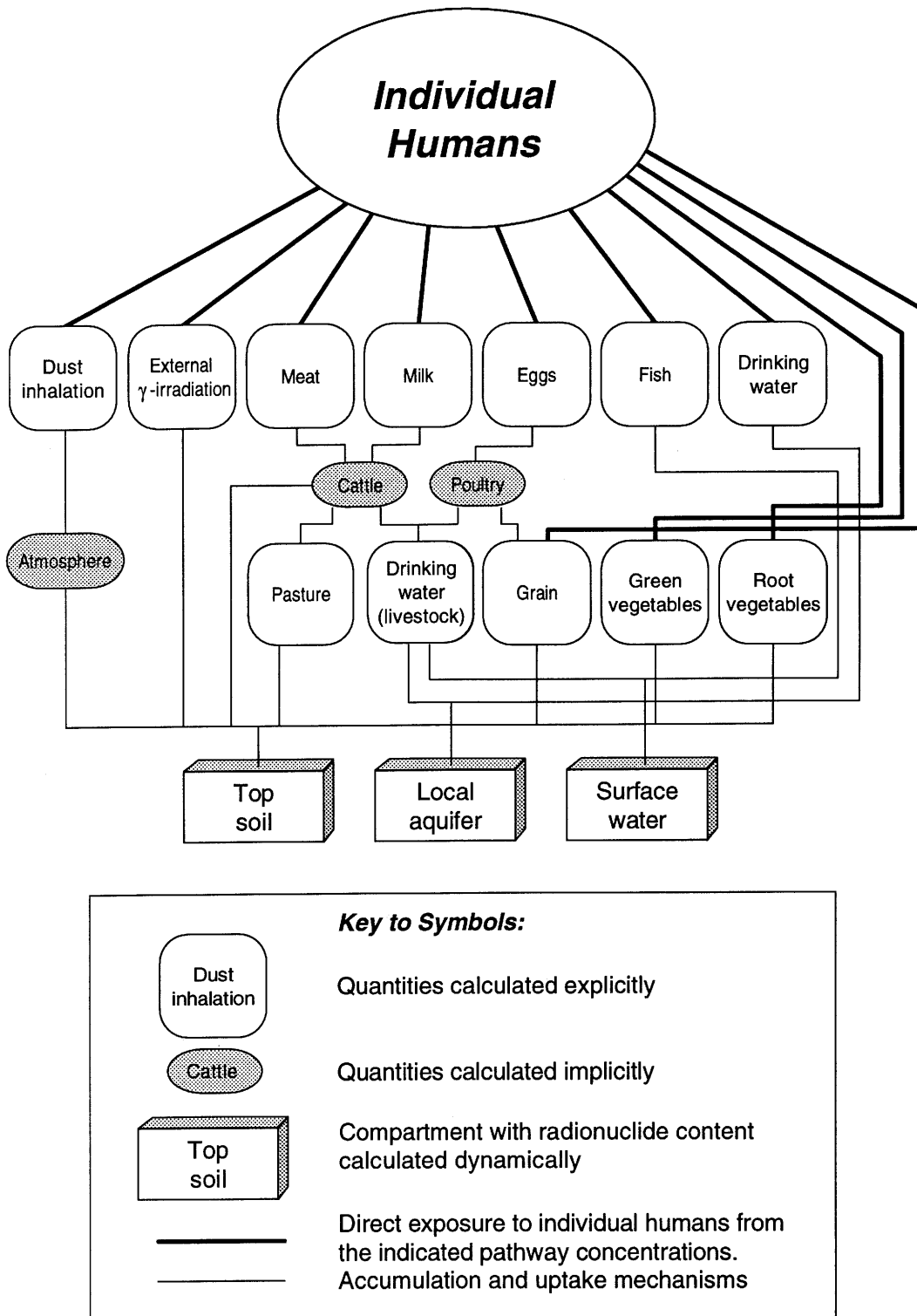


Figure 5.4.3: Schematic representation of the exposure pathways modelled, indicating connections to the compartments in the dynamic part of the model (Figure 5.4.2), which act as sources for dose via ingestion or inhalation of contaminated material, or by direct γ -irradiation.

5.4.3.2 Exposure pathways

Figure 5.4.3 shows a schematic representation of the food chain and radiological exposure pathways considered in the Reference-Case biosphere. The generic form of the steady-state model for the annual individual dose, $D_p^{(N)}(t)$, via exposure pathway p , for radionuclide N is:

$$D_p^{(N)}(t) = \sum_{i, exp} E_p H_{exp}^{(N)} P_{p,i} N_i(t), \quad [\text{mSv y}^{-1}]: \quad (5.4.9)$$

E_p is the annual intake or exposure of the individual via pathway p , e.g., the rate of consumption of meat [kg y^{-1}] or the fraction of time exposed to given airborne dust levels [yy^{-1}].

$H_{exp}^{(N)}$ is the dose per unit intake or exposure for radionuclide N via exposure mechanism exp (ingestion, inhalation or external exposure). In the case of ingestion, or inhalation, the units are [mSv Bq^{-1}] and, in the case of external γ -irradiation due to radionuclides in soil, the units are [$\text{mSv (Bq m}^{-3}\text{)}^{-1}$].

N_i is the activity [Bq] of radionuclide N in biosphere compartment i , as calculated by the solution to Equation 5.4.1.

$P_{p,i}$ is a factor which transforms the radionuclide content of the compartment i into a concentration in pathway p . For example, it could represent factors used to translate the intake of activity in livestock feed [Bq y^{-1}] into a concentration in meat [Bq kg^{-1}], for which the rate of consumption is E_p .

The calculated doses arise from several different pathways, each dependent on the accumulation of radionuclides in one or more of the topsoil, river water or local aquifer compartments. The timescale for uptake in the exposure pathways is short enough for a steady-state (or equilibrium) approach to be valid³⁶. The exact form of Equation 5.4.9 used in the evaluation of annual individual dose in the modelled region depends on the pathways being considered; these are indicated in Figure 5.4.3. A detailed description of the exposure pathway model is given in KLOS et al. (1994).

³⁶ A comparison of Equations 5.4.1 and 5.4.9 illustrates the difference in approach. Effectively, it is assumed that the time dependence of the pathway concentrations arises from the time dependence of the compartment concentrations from which they are derived, since the time to reach equilibrium in the food chain, for example, is less than one year, which is short compared with the time to attain equilibrium in the transport model.

5.4.4 Parameters for the Reference-Case Biosphere

The database given here refers to the Reference-Case biosphere, as defined in Subsection 5.4.2.

The parameters characterising the biosphere transport system are summarised in Table 5.4.2 and the mass balance schemes for water and solid material fluxes in this biosphere representation are shown in Figures 5.4.4 and 5.4.5, with the numerical values used in the calculation of mass balance for the five TAME compartments summarised in Tables 5.4.3 and 5.4.4. The solid-liquid distribution constants for the radionuclides considered in the assessment are given in Table 5.4.5. In this database (TITS et al. 1994), the sorption properties have been classified according to the particle sizes of the solid materials in the compartment.

Data for the exposure pathways are site-independent and are presented in Appendix 7.

5.4.5 Biosphere Results and Sensitivity Analysis

5.4.5.1 Behaviour of the Reference-Case Biosphere Model

Figure 5.4.6(a) shows the results of Reference-Case calculations for the safety-relevant radionuclides (see Appendix 2) that contribute significantly to total dose at any time. Reference-Case models and data for near field, geosphere and biosphere have been used. The results are discussed more fully in Chapter 6. Here, only aspects related to the biosphere model are discussed.

Referring to Equation 5.4.1, steady-state doses could be determined directly by setting dN_i/dt to zero and solving the set of equations for the N_i , with the exposures calculated using the standard expressions. Such an approach would be justified if the time required for the biosphere to reach steady state were small compared to the timescales characterising variations in geosphere release. An advantage of a dynamic biosphere model, as presented in Subsection 5.4.3, is that there is no need to make such an argument. However, in order to illustrate the possible significance of dynamic behaviour in the biosphere model, the time taken for the key radionuclides of the Reference Case to reach steady state in the biosphere has been determined.

Features	Parameter	Value	Units	Reference
Top Soil	solid material in suspension in water	1.0×10^{-3}	kg m^{-3}	(b)
	porosity	0.4	-	(c)
	thickness	0.25	m	(c)
	volumetric moisture content	0.3	-	(c)
	compartment tortuosity	3.9	-	(a)
Deep Soil	solid material in suspension in water	1.0×10^{-3}	kg m^{-3}	(b)
	porosity	0.4	-	(c)
	thickness	1.0	m	(c)
	biomass involved in bioturbation ¹	0.1	kg m^{-2}	(a)
	biomass activity ¹	20	y^{-1}	(a)
	volumetric moisture content	0.3	-	(c)
Local Aquifer	compartment tortuosity	3.9	-	(a)
	solid material in suspension in water	1.0×10^{-3}	kg m^{-3}	(b)
	porosity	0.2	-	(c)
	thickness ²	2.0	m	(c)
	volumetric moisture content	0.2	-	(c)
Surface Water (Rhine)	compartment tortuosity	8.6	-	(a)
	suspended sediment load in river	1.0×10^{-1}	kg m^{-3}	(a)
	depth of river	3.25	m	(b)
	width of river ³	200	m	(b)
River Bed Sediment	length of river section	2.0×10^3	m	(b)
	porosity	0.5	-	(b)
	annual exchange with water column	1	y^{-1}	(b)
	thickness of sediment	0.1	m	(b)
	transfer of sediment to river banks ⁴	0.1	$\text{kg m}^{-2} \text{y}^{-1}$	(a)
	volumetric moisture content	0.5	-	(b)
Miscellaneous	compartment tortuosity	2.9	-	(a)
	recipient compartment for contamination from the geosphere	Local aquifer	-	(a)
	area of agricultural land	3.4×10^6	m^2	(c)
	diffusion constant in pure water	3.8×10^{-2}	$\text{m}^2 \text{y}^{-1}$	(a)
	regional evapotranspiration	0.5	m y^{-1}	(c)
	regional rainfall	1.0	m y^{-1}	(c)
	regional erosion	0.1	$\text{kg m}^{-2} \text{y}^{-1}$	(a)
dry density of solid material (all compartments)	2.65×10^3	kg m^{-3}	(a)	

Notes:

- 1 Bioturbation results in the movement of solid material between the deep soil and the top soil at a rate given by the biomass activity.
- 2 The thickness of the local aquifer is expected to range from 10 m to 20 m. For this study, however, a conservative, lower value is adopted.
- 3 The area modelled in BAEYENS *et al.* (1989) corresponds to a region of the Rhine upstream of a hydro-electric power station. This accounts for the relatively high value for the river width used here. A lower value would not affect the calculated doses, since it is the through-flow in the river that is the important factor.
- 4 This figure corresponds to the mass of sediment dredged from the river bed and applied to the area of farm land; it is chosen to be equal to the erosion rate (KLOS & VAN DORP 1994).

The bold letter in the compartment names (features) denotes the suffix used in the description of the transport processes: T \Rightarrow Top soil, L \Rightarrow Local aquifer, S \Rightarrow aquatic Sediment, etc. See figures 5.4.4 and 5.4.5 and Tables 5.4.3 and 5.4.4, below.

References:

(a) KLOS *et al.* (1994); (b) KLOS & VAN DORP (1994); (c) BAEYENS *et al.* (1989).

Table 5.4.2: Data for the Kristallin-I Reference-Case biosphere.

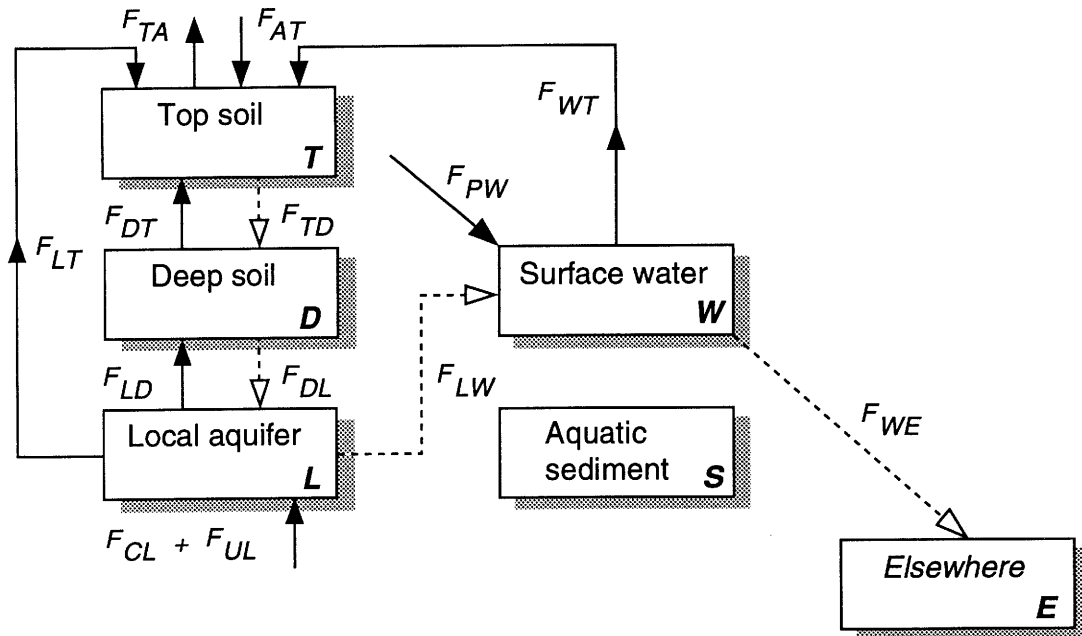


Figure 5.4.4: Water-flux mass balance for the Kristallin-I Reference-Case biosphere. The dashed lines indicate fluxes determined by mass balance. Values for the defined water fluxes are given in the Table 5.4.3.

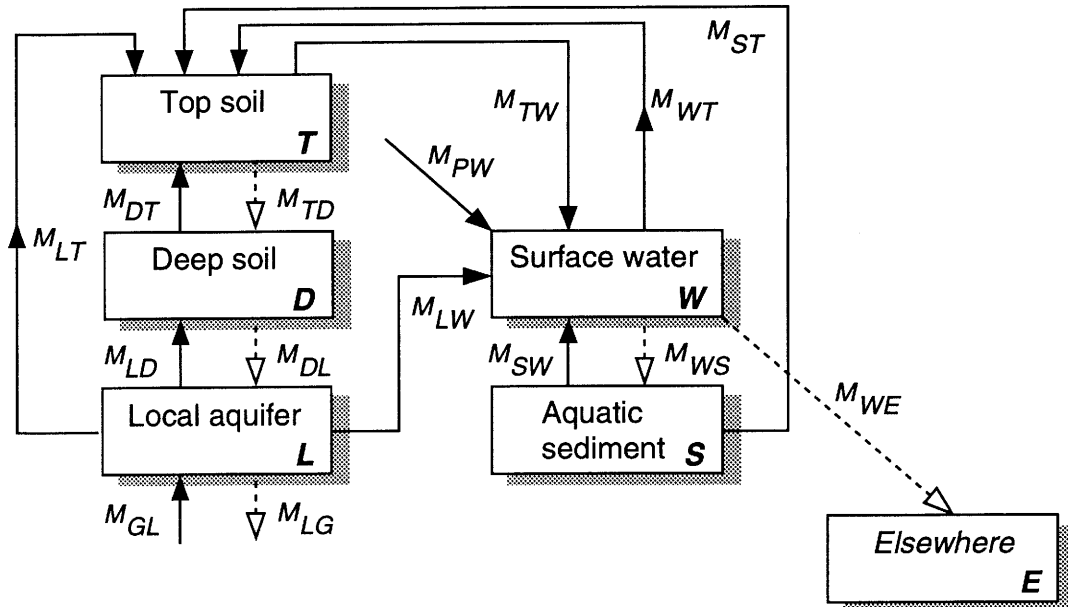


Figure 5.4.5: Solid-material-flux mass balance for the Kristallin-I Reference-Case biosphere. The dashed lines indicate fluxes determined by mass balance. Values for the defined solid material fluxes in the biosphere are given in Table 5.4.4.

Water flux	Symbol	Value	Units	Reference
Regional rainfall ¹	d_{AT}	1.0	m y ⁻¹	(BAEYENS et al. 1989)
Regional evapotranspiration ¹	d_{TA}	0.5	m y ⁻¹	(BAEYENS et al. 1989)
Deep soil → topsoil ¹ (capillary rise)	d_{DT}	0.025	m y ⁻¹	(BAEYENS et al. 1989)
Local aquifer → deep soil ¹ (capillary rise)	d_{LD}	0.025	m y ⁻¹	(BAEYENS et al. 1989)
Irrigation from local aquifer ¹	d_{LT}	0.25	m y ⁻¹	(BAEYENS et al. 1989)
Irrigation from river water ¹	d_{WT}	0.25	m y ⁻¹	(BAEYENS et al. 1989)
Inflow to local aquifer ²	$F_{UL} + F_{CL}$	5.5×10^6	m ³ y ⁻¹	Table 3.7.4
Through flow in the Rhine	F_{PW}	3.2×10^{10}	m ³ y ⁻¹	Table 3.7.4
Percolation: top soil → deep soil	F_{TD}	3.5×10^6	m ³ y ⁻¹	<i>mass balance</i>
Percolation: deep soil → local aquifer	F_{DL}	3.5×10^6	m ³ y ⁻¹	<i>mass balance</i>
Exfiltration: local aquifer → Rhine water	F_{LW}	8.0×10^6	m ³ y ⁻¹	<i>mass balance</i>
Through flow in the Rhine	F_{WE}	3.2×10^{10}	m ³ y ⁻¹	<i>mass balance</i>

Notes:

- 1 The corresponding water flows F_{ij} are obtained by multiplying by the area A_f of farmland: $F_{ij} = d_{ij}A_f$
- 2 Volumetric flow from the geosphere to the biosphere is very small compared to the total flow in the aquifer and is numerically insignificant

Table 5.4.3: Water fluxes defined in the Reference-Case biosphere model (See Figure 5.4.4).

Solid material flux ¹	Symbol	Value	Units	Reference
Top soil → Surface water (erosion of surface material)	M_{TW}	3.4×10^5	kg y ⁻¹	(a)
Deep soil → Top soil ^{2,3}	M_{DT}	7.1×10^6	kg y ⁻¹	(a)
Local aquifer → Deep soil ²	M_{LD}	3.4×10^5	kg y ⁻¹	(a)
Previous river compartment → River water	M_{PW}	3.2×10^9	kg y ⁻¹	(b)
Local aquifer → Top soil Irrigation containing suspended solids	M_{LT}	8.4×10^2	kg y ⁻¹	(b)
River water → Top soil Irrigation containing suspended solids	M_{WT}	8.4×10^4	kg y ⁻¹	(b)
Aquatic sediment → Top soil dredging, flood deposition, etc.	M_{ST}	3.4×10^5	kg y ⁻¹	(a)
Aquatic sediment → River water Turnover of bed sediment	M_{SW}	5.3×10^7	kg y ⁻¹	(b)
Local aquifer → River water Infiltration containing suspended solids	M_{LW}	8.0×10^3	kg y ⁻¹	(b)
Top soil → deep soil	M_{TD}	7.2×10^6	kg y ⁻¹	mass balance
Deep soil → local aquifer	M_{DL}	4.2×10^5	kg y ⁻¹	mass balance
Local aquifer → geosphere	M_{LG}	4.1×10^5	kg y ⁻¹	mass balance
Rhine water → bed sediment	M_{WS}	5.3×10^7	kg y ⁻¹	mass balance
Rhine water downstream flow	M_{WE}	3.2×10^9	kg y ⁻¹	mass balance

Notes:

- 1 Fluxes of solid material transported in suspension between the compartments are given by the product of the water fluxes and the suspended sediment load: $M_{ij} = \alpha_i F_{ij}$. Transport via this mechanism occurs for all compartments linked by water fluxes.
- 2 Erosion acts on the whole surface area of the compartment, so that solid material fluxes caused by erosion are proportional to surface area. The area is the same for the top soil, deep soil and local aquifer compartments (A_p). The deep soil and local aquifer are affected by erosion as a consequence of keeping the volumes of the compartments fixed: removal of material from an overlying compartment of fixed volume requires that a corresponding volume of material is moved from the underlying compartment, which in turn necessitates the inclusion of material from a lower compartment. This continues until the geosphere is reached, which is implicitly assumed to be underlying the entire biosphere model.
- 3 Solid material fluxes also include the effect of bioturbation: the transfer of material from the deep soil to the top soil.

References:

(a) KLOS *et al.* (1994); (b) KLOS & VAN DORP (1994)

Table 5.4.4: Solid-material fluxes defined in the Reference-Case biosphere model (See Figure 5.4.5).

Element	Solid - liquid equilibrium distribution constant [m ³ kg ⁻¹]	
Symbol	Coarse	Fine
Ni	0.1	1
Se	0.01	0.1
Zr	1	10
Tc	0.01	0.1
Pd	0.02	0.2
Sn	0.1	1
Cs	0.1	1
Pb	0.1	1
Po	0.1	1
Ra	0.01	0.1
Ac	1	10
Th	1	10
Pa	1	10
U	1	10
Np	1	10
Pu	1	10
Am	1	10
Cm	1	10

Note:

The soils in the region are of a fine texture and are classified as parabraunerde (see Subsection 3.6.3). The suspended sediments in the Rhine water are also of a fine texture. The regional aquifer and the bed sediments of the river are made up of coarser-grained materials. Details of the derivation and compilation of the K_d database according to the particle size classification are given in TITS et al. (1994).

Table 5.4.5: Solid-liquid equilibrium distribution constants (K_d values) for the modelling of the biosphere in Kristallin-I.

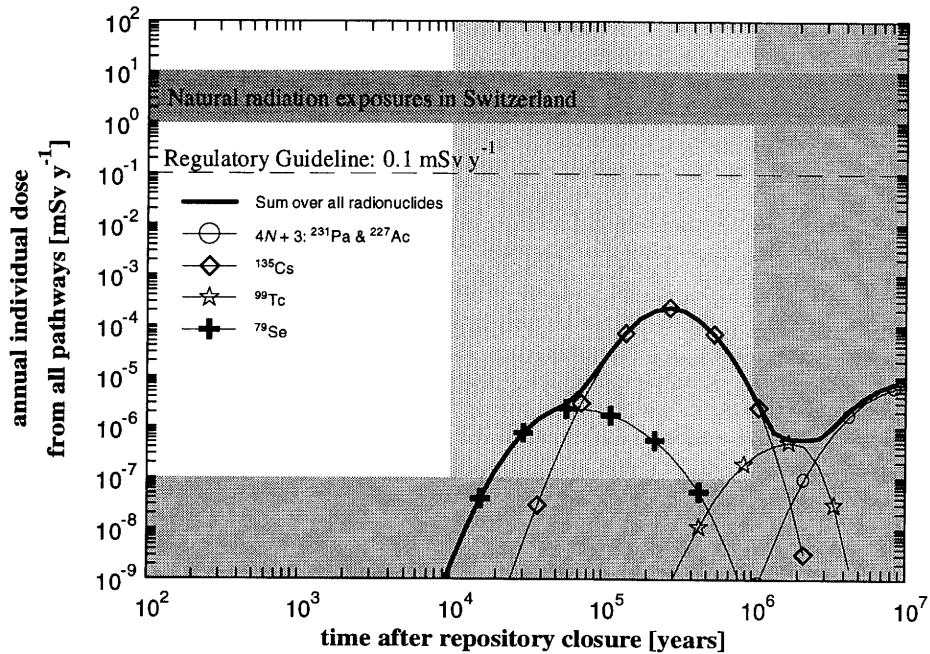
In the results shown in Figure 5.4.6(b), the time-dependent release calculated by the geosphere model is substituted, for each radionuclide, by hypothetical, constant release rates from the geosphere to the local aquifer (set arbitrarily to 10^6 Bq y^{-1}); steady-state conditions are approached as the rate of change of the dose with time tends to zero. The results of this analysis indicate that the time taken to reach steady state is radionuclide-dependent and can, for some radionuclides, exceed 10 000 years (the timescale beyond which significant climate change cannot be excluded; see section 4.3.6.1 and Appendix 1). ^{79}Se and ^{99}Tc reach steady state relatively rapidly, reaching 90% of the steady-state doses within about 250 years. The dose due to ^{135}Cs reaches 90% of the steady-state value in less than 3000 years. However, the releases of ^{79}Se , ^{135}Cs and ^{99}Tc from the geosphere exceed 90% of their maximum values for several tens of thousands of years (and millions of years for the $4N + 3$ chain members). Hence, for these key radionuclides, the time-dependence of the annual individual doses in the Reference-Case calculations are determined by the time-dependence of the geosphere releases, rather than the dynamic behaviour of the biosphere model.

Table 5.4.6 identifies the processes that are considered in calculating the coefficients for radionuclide transfer between the physical compartments of the biosphere model, and also the characteristic times for transport (defined as $\tau_{ij} [\text{y}] = 1/\lambda_{ij}$, where λ_{ij} is given by equation 5.4.8). The table shows these times vary widely for different transfer routes and for different radionuclides. For example, transport from the model river section to a section downstream is very rapid and radionuclide-independent ($\tau_{WE} = 4 \times 10^{-5}$ years), whereas the transfer of radionuclides from the local aquifer to the top soil via irrigation occurs over timescales ranging from 170 to 17 000 years, depending on K_d , the only radionuclide-dependent model parameter. For this, and other transport routes, high K_d values lead to longer characteristic times (and hence longer times to reach steady state in Figure 5.4.6(b)).

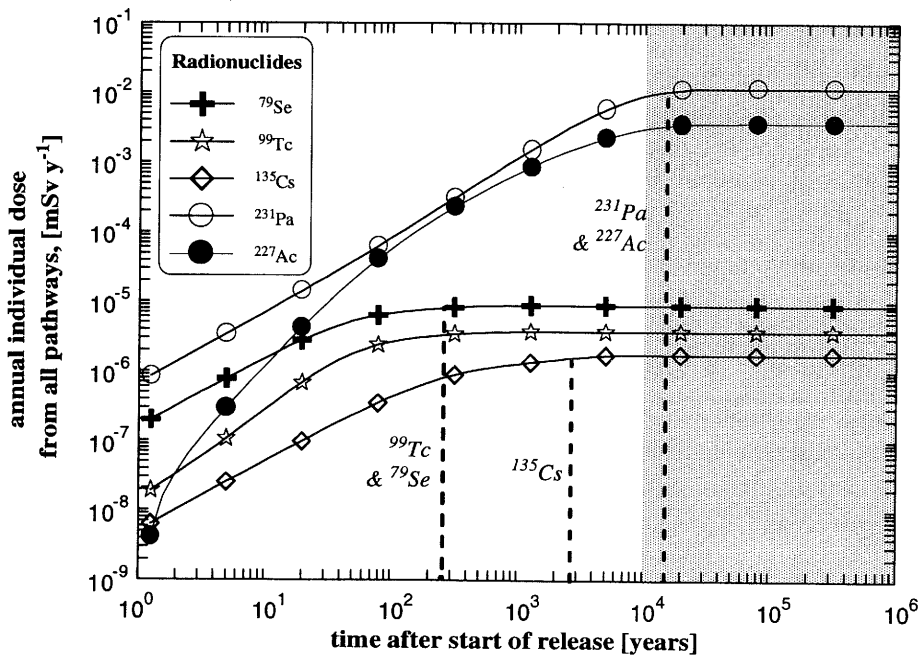
Figure 5.4.7 shows the contributions of each of the exposure pathways for each of the five radionuclides which dominate total dose at different times. In all cases, the pathways contributing most to dose are those from animal products: meat, milk and dairy products. Grain consumption is also significant, but only in the cases of ^{99}Tc and ^{135}Cs does it contribute more than 20% of the dose. The other pathways contribute less than 13% of the dose.

The following subsections illustrate the sensitivity of doses to variation of selected biosphere parameters. The parameters chosen for the investigation are those which have been shown to be important in determining dose in other safety assessments. These are:

- the source of irrigation water,
- the local aquifer thickness,
- rate of erosion, and
- solid-liquid distribution constants (K_{ds}).



(a) Reference-Case results: annual doses calculated with Reference-Case near-field, geosphere and biosphere models and datasets.



(b) Approach to steady state in the biosphere for selected radionuclides, calculated by substituting the Reference-Case geosphere release by a constant release of 10^6 Bq y^{-1} to the local aquifer. The dotted lines indicate the time taken to reach 90% of the maximum dose.

Note: The shaded area on the right of (b) indicates times beyond which significant climatic change cannot be excluded (see Appendix 1).

Figure 5.4.6: Annual individual dose in the Kristallin-I Reference Case and in the hypothetical case of a constant geosphere release.

	from ^{to}	Local aquifer	Deep soil	Topsoil	River water	River sediment	Elsewhere
	Transport processes	Local aquifer	-	capillary rise, pedogenesis	irrigation	exfiltration	diffusion
Deep soil		percolation	-	capillary rise, pedogenesis, bioturbation			
Topsoil			percolation, bioturbation	-	erosion		
River water				irrigation	-	sedimentation	river flow
River sediment		diffusion		dredging	resuspension	-	
⁷⁹ Se & ⁹⁹ Tc (low K_d)	from ^{to}	Local Aquifer	Deep soil	Topsoil	River water	River sediment	Elsewhere
	Local aquifer	-	1.6×10^3	1.7×10^2	1.8×10^1	4.9×10^3	
	Deep soil	1.5×10^2	-	6.5×10^2			
	Topsoil		3.2×10^1	-	4.0×10^3		
	River water			1.5	-	2.5×10^{-1}	4.0×10^{-5}
	River sediment	2.1×10^1		1.6×10^2	1.0	-	
¹³⁵ Cs (intermediate K_d)	from ^{to}	Local	Deep soil	Topsoil	River water	River sediment	Elsewhere
	Local aquifer	-	1.2×10^4	1.7×10^3	1.8×10^2	4.8×10^4	
	Deep soil	1.4×10^3	-	7.5×10^2			
	Topsoil		1.3×10^2	-	4.0×10^3		
	River water			1.5	-	2.7×10^{-2}	4.0×10^{-5}
	River sediment	2.0×10^2		1.6×10^2	1.0	-	
²³¹ Pa & ²²⁷ Ac (high K_d)	from ^{to}	Local Aquifer	Deep soil	Topsoil	River water	River sediment	Elsewhere
	Local aquifer	-	3.4×10^4	1.7×10^4	1.8×10^3	4.8×10^5	
	Deep soil	7.0×10^3	-	7.6×10^2			
	Topsoil		1.8×10^2	-	4.0×10^3		
	River water			1.5	-	4.9×10^{-3}	4.0×10^{-5}
	River sediment	2.0×10^3		1.6×10^2	1.0	-	

Note: The mass-balance schemes shown in Figures 5.4.4 and 5.4.5 and Tables 5.4.3 and 5.4.4 include only the fluxes of water and of solid material between compartments, whereas this table also includes the transport of radionuclides via diffusion (see Equation 5.4.7). This accounts for the entries here for the transport between the river sediment and the local aquifer, for which there are no corresponding data in Tables 5.4.3 and 5.4.4. Exfiltration from the local aquifer is assumed to occur directly to the river water.

Table 5.4.6: Processes considered and characteristic times (in years) for transport between compartments in the Reference-Case biosphere model. These values are the reciprocal of the transfer coefficients, calculated using Equation 5.4.8 with the Reference-Case dataset defined in Tables 5.4.3-5. The blank cells indicate that no transfer is calculated between the compartments.

(a) ^{79}Se		<table border="1"> <thead> <tr> <th><u>Pathway</u></th> <th><u>% contribution</u></th> </tr> </thead> <tbody> <tr><td>Meat (beef)</td><td>88.0</td></tr> <tr><td>Milk and dairy products</td><td>3.9</td></tr> <tr><td>Root vegetables</td><td>2.9</td></tr> <tr><td>Drinking water (well)</td><td>2.4</td></tr> <tr><td>Grain</td><td>2.0</td></tr> <tr><td>Eggs</td><td>0.6</td></tr> <tr><td>Green vegetables</td><td>0.3</td></tr> </tbody> </table>	<u>Pathway</u>	<u>% contribution</u>	Meat (beef)	88.0	Milk and dairy products	3.9	Root vegetables	2.9	Drinking water (well)	2.4	Grain	2.0	Eggs	0.6	Green vegetables	0.3
<u>Pathway</u>	<u>% contribution</u>																	
Meat (beef)	88.0																	
Milk and dairy products	3.9																	
Root vegetables	2.9																	
Drinking water (well)	2.4																	
Grain	2.0																	
Eggs	0.6																	
Green vegetables	0.3																	
(b) ^{99}Tc		<table border="1"> <thead> <tr> <th><u>Pathway</u></th> <th><u>% contribution</u></th> </tr> </thead> <tbody> <tr><td>Milk and dairy products</td><td>63.7</td></tr> <tr><td>Grain</td><td>21.5</td></tr> <tr><td>Root vegetables</td><td>11.1</td></tr> <tr><td>Green vegetables</td><td>1.9</td></tr> <tr><td>Drinking water (well)</td><td>0.9</td></tr> <tr><td>Meat (beef)</td><td>0.7</td></tr> <tr><td>others</td><td>0.2</td></tr> </tbody> </table>	<u>Pathway</u>	<u>% contribution</u>	Milk and dairy products	63.7	Grain	21.5	Root vegetables	11.1	Green vegetables	1.9	Drinking water (well)	0.9	Meat (beef)	0.7	others	0.2
<u>Pathway</u>	<u>% contribution</u>																	
Milk and dairy products	63.7																	
Grain	21.5																	
Root vegetables	11.1																	
Green vegetables	1.9																	
Drinking water (well)	0.9																	
Meat (beef)	0.7																	
others	0.2																	
(c) ^{135}Cs		<table border="1"> <thead> <tr> <th><u>Pathway</u></th> <th><u>% contribution</u></th> </tr> </thead> <tbody> <tr><td>Meat (beef)</td><td>26.0</td></tr> <tr><td>Milk and dairy products</td><td>24.9</td></tr> <tr><td>Grain</td><td>24.7</td></tr> <tr><td>Root vegetables</td><td>12.9</td></tr> <tr><td>Drinking water (well)</td><td>8.7</td></tr> <tr><td>Green vegetables</td><td>2.7</td></tr> <tr><td>others</td><td>0.1</td></tr> </tbody> </table>	<u>Pathway</u>	<u>% contribution</u>	Meat (beef)	26.0	Milk and dairy products	24.9	Grain	24.7	Root vegetables	12.9	Drinking water (well)	8.7	Green vegetables	2.7	others	0.1
<u>Pathway</u>	<u>% contribution</u>																	
Meat (beef)	26.0																	
Milk and dairy products	24.9																	
Grain	24.7																	
Root vegetables	12.9																	
Drinking water (well)	8.7																	
Green vegetables	2.7																	
others	0.1																	
(d) ^{231}Pa		<table border="1"> <thead> <tr> <th><u>Pathway</u></th> <th><u>% contribution</u></th> </tr> </thead> <tbody> <tr><td>Meat (beef)</td><td>43.0</td></tr> <tr><td>Root vegetables</td><td>40.6</td></tr> <tr><td>Grain</td><td>8.6</td></tr> <tr><td>Green vegetables</td><td>4.9</td></tr> <tr><td>Drinking water (well)</td><td>2.0</td></tr> <tr><td>Dust inhalation</td><td>0.7</td></tr> <tr><td>others</td><td>0.1</td></tr> </tbody> </table>	<u>Pathway</u>	<u>% contribution</u>	Meat (beef)	43.0	Root vegetables	40.6	Grain	8.6	Green vegetables	4.9	Drinking water (well)	2.0	Dust inhalation	0.7	others	0.1
<u>Pathway</u>	<u>% contribution</u>																	
Meat (beef)	43.0																	
Root vegetables	40.6																	
Grain	8.6																	
Green vegetables	4.9																	
Drinking water (well)	2.0																	
Dust inhalation	0.7																	
others	0.1																	
(e) ^{227}Ac		<table border="1"> <thead> <tr> <th><u>Pathway</u></th> <th><u>% contribution</u></th> </tr> </thead> <tbody> <tr><td>Meat (beef)</td><td>77.3</td></tr> <tr><td>Drinking water (well)</td><td>8.7</td></tr> <tr><td>Grain</td><td>6.2</td></tr> <tr><td>Dust inhalation</td><td>3.5</td></tr> <tr><td>Root vegetables</td><td>3.2</td></tr> <tr><td>Green vegetables</td><td>0.8</td></tr> <tr><td>others</td><td>0.2</td></tr> </tbody> </table>	<u>Pathway</u>	<u>% contribution</u>	Meat (beef)	77.3	Drinking water (well)	8.7	Grain	6.2	Dust inhalation	3.5	Root vegetables	3.2	Green vegetables	0.8	others	0.2
<u>Pathway</u>	<u>% contribution</u>																	
Meat (beef)	77.3																	
Drinking water (well)	8.7																	
Grain	6.2																	
Dust inhalation	3.5																	
Root vegetables	3.2																	
Green vegetables	0.8																	
others	0.2																	

Figure 5.4.7: Contribution of different exposure pathways to dose for individual radionuclides that contribute most to total dose at different times in the Kristallin-I Reference Case.

5.4.5.2 Sensitivity to the Source of Irrigation Water

In the Reference-Case description of the biosphere, it is conservatively assumed that all crops are irrigated. It is also assumed that pasture land is continuously irrigated: an assumption which is highly conservative. Given the distribution of dose between the exposure pathways discussed above, the contribution of irrigation to exposure is potentially important and has been investigated by two sets of calculations in which the amount of irrigation remains constant, but the source is either the local aquifer or the river Rhine. In the Reference-Case, the irrigation water is assumed to be extracted in equal amounts from both sources. The results of this parameter variation are presented in Figure 5.4.8.

The largest dose arises where the only source of water for irrigation is the aquifer, since the concentration of radionuclides is higher in this source. In the Reference Case, where irrigation water is taken in equal amounts from the river and the aquifer (via a well), the peak dose is lower by up to a factor of two. The dose is a factor of 20 lower when all the irrigation water is drawn from the river. Figure 5.4.9 illustrates the relative significance of the different exposure pathways to the dose from ^{135}Cs , depending on the source of the irrigation water. When the irrigation water is abstracted from the relatively low-concentration source in the river, the importance of the well pathway as a source of drinking water for human consumption increases and the doses from the consumption of meat, milk and crops are greatly reduced compared to the Reference Case.

5.4.5.3 Sensitivity to Local Aquifer Thickness

The thickness of the gravel aquifer at the point of the release from the geosphere is uncertain - in the Reference Case, it is assigned a value of 2 m; values of 0.2 m and 20 m are taken as upper and lower limits in the sensitivity analysis.

This parameter variation investigates the response of the model over a range of thicknesses that can be thought of as being representative of different possibilities in the biosphere at the time of the release. A different aquifer thickness could arise following the removal and redeposition of Rhine valley sediments and thickness will also vary with location.

The calculated total dose maximum is insensitive to this variation, but the time taken to reach peak dose is slightly affected (evaluated using the same constant source used to generate the data shown in Figure 5.4.6(b)). The latter is a function of the storage capacity of the local aquifer. The results of the Reference Case and the case of the 0.2 m thick aquifer are very similar, with the times for all the calculated radionuclides to reach steady state being 3.4×10^4 years in both cases. This increases to 5.3×10^4 years for an aquifer of 20 m thickness.

The limiting case, in which the local aquifer is entirely absent, is investigated as an Alternative Climate-Related Scenario in Chapter 6 (Rhine Gravels Absent), as is the sensitivity of results to the rate of water flow in the aquifer (different climate states with different infiltrating volumes of meteoric water).

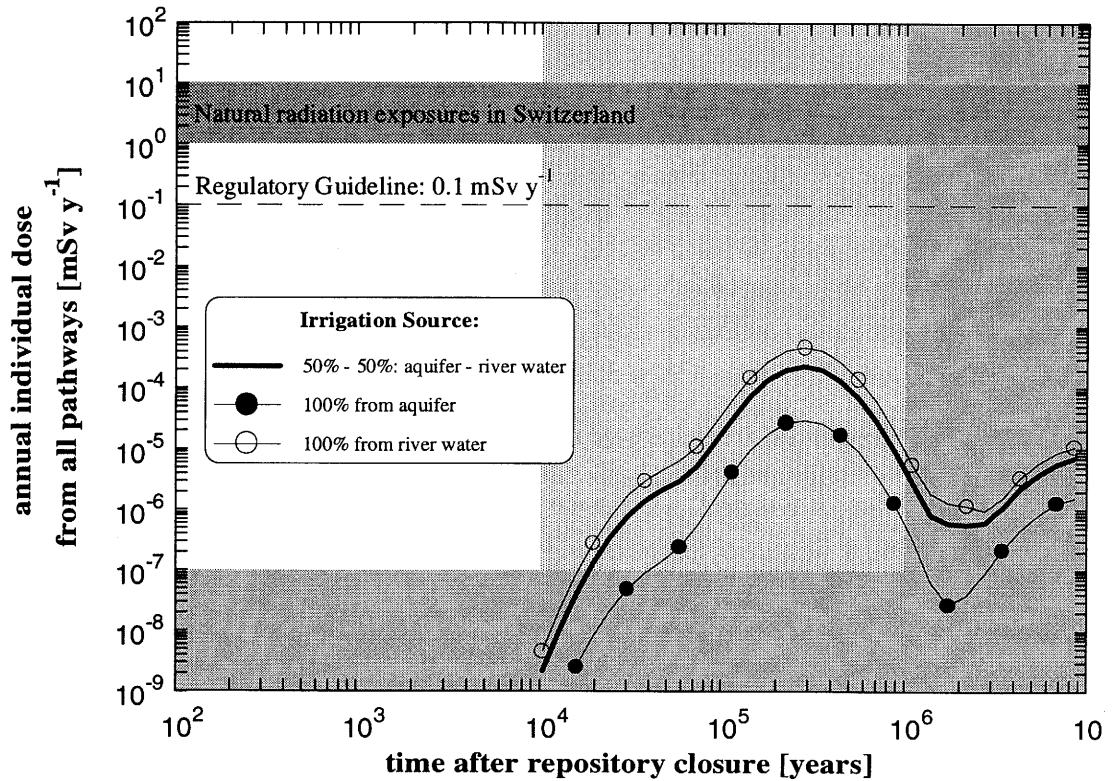


Figure 5.4.8: Sensitivity of calculated dose to the source of irrigation water.

<p>(a) ¹³⁵Cs</p> <p>Irrigation from river</p>		<table border="1"> <thead> <tr> <th>Pathway</th> <th>% contribution</th> </tr> </thead> <tbody> <tr><td>Drinking water (well)</td><td>59.7</td></tr> <tr><td>Meat (beef)</td><td>16.8</td></tr> <tr><td>Milk and dairy products</td><td>16.1</td></tr> <tr><td>Grain</td><td>3.1</td></tr> <tr><td>Root vegetables</td><td>3.0</td></tr> <tr><td>Green vegetables</td><td>1.3</td></tr> <tr><td>others</td><td>0.1</td></tr> </tbody> </table>	Pathway	% contribution	Drinking water (well)	59.7	Meat (beef)	16.8	Milk and dairy products	16.1	Grain	3.1	Root vegetables	3.0	Green vegetables	1.3	others	0.1
Pathway	% contribution																	
Drinking water (well)	59.7																	
Meat (beef)	16.8																	
Milk and dairy products	16.1																	
Grain	3.1																	
Root vegetables	3.0																	
Green vegetables	1.3																	
others	0.1																	
<p>(b) ¹³⁵Cs</p> <p>Irrigation from well</p>		<table border="1"> <thead> <tr> <th>Pathway</th> <th>% contribution</th> </tr> </thead> <tbody> <tr><td>Meat (beef)</td><td>26.8</td></tr> <tr><td>Grain</td><td>26.2</td></tr> <tr><td>Milk and dairy products</td><td>25.7</td></tr> <tr><td>Root vegetables</td><td>13.7</td></tr> <tr><td>Drinking water (well)</td><td>4.6</td></tr> <tr><td>Green vegetables</td><td>2.9</td></tr> <tr><td>others</td><td>0.1</td></tr> </tbody> </table>	Pathway	% contribution	Meat (beef)	26.8	Grain	26.2	Milk and dairy products	25.7	Root vegetables	13.7	Drinking water (well)	4.6	Green vegetables	2.9	others	0.1
Pathway	% contribution																	
Meat (beef)	26.8																	
Grain	26.2																	
Milk and dairy products	25.7																	
Root vegetables	13.7																	
Drinking water (well)	4.6																	
Green vegetables	2.9																	
others	0.1																	

Figure 5.4.9: Variation in the contribution of different exposure pathways for ¹³⁵Cs as a result of changing the source of irrigation water.

5.4.5.4 Sensitivity to Local Erosion Rate

In the Reference Case, the local erosion rate is $0.1 \text{ kg m}^{-2} \text{ y}^{-1}$; this is chosen to correspond to the current uplift-induced regional net erosion rate. The range considered here is 0.01 to $10.0 \text{ kg m}^{-2} \text{ y}^{-1}$; the lower value represents a case of low net erosion corresponding to a case of reduced regional uplift occurring if Alpine orogeny were to cease; the upper value represents a case of maximum uplift assuming Alpine orogeny continues (see section 4.3.5.1).

The evolution with time of total dose summed over radionuclides and pathways is shown in Figure 5.4.10. The principal effect of erosion is to remove contaminated material from the region. Thus, the lower the erosion rate, the higher the doses. The effect is greatest for the more strongly sorbing radionuclides, but the overall influence on the total dose is negligible, despite the three orders of magnitude variation in the erosion rate.

In the PSACOIN intercomparison exercise (NEA 1993), a far more pronounced effect of erosion was shown than that seen here, particularly for highly sorbing radionuclides. The reason for the relatively weak sensitivity to erosion rate in this study is likely to lie in the conservative assumptions regarding the recycling of radionuclides: in particular, in the case of higher erosion rates this is balanced by pedogenesis, i.e. soil development from underlying deep soil and aquifer units which are themselves contaminated. If down-slope erosion processes were represented, i.e. uncontaminated material was introduced to replace eroded material, then greater sensitivity would be observed and the peak radionuclide concentrations in top soil, and hence dose, would be reduced.

5.4.5.5 Sensitivity to Solid-Liquid Distribution Constants (K_d s)

The database of soil-liquid distribution constants (K_d) used in this assessment (TITS et al. 1994) does not provide uncertainty estimates, and so, as a means of estimating the sensitivity of doses to this parameter, a range of ± 1 order of magnitude (compared to the Reference-Case values) is applied in all compartments simultaneously.

Sorption is an important retardation mechanism for radionuclides in the biosphere. The higher the K_d value, the greater fraction associated with the solid phase and the less remaining in solution and available for transport in flowing water. Weakly-sorbed nuclides are transported both in solid and liquid phase, whereas, well-sorbed nuclides are transported almost entirely in solid phase. Thus, at high K_d values, changes in K_d do not greatly affect transport. At lower K_d values, the mobility of the radionuclides is inversely correlated with the K_d value. Thus, the results in Figure 5.4.11 show that doses due to the relatively poorly sorbing ^{79}Se and ^{99}Tc are rather more sensitive to variations of K_d than the more highly sorbing ^{135}Cs and actinides.

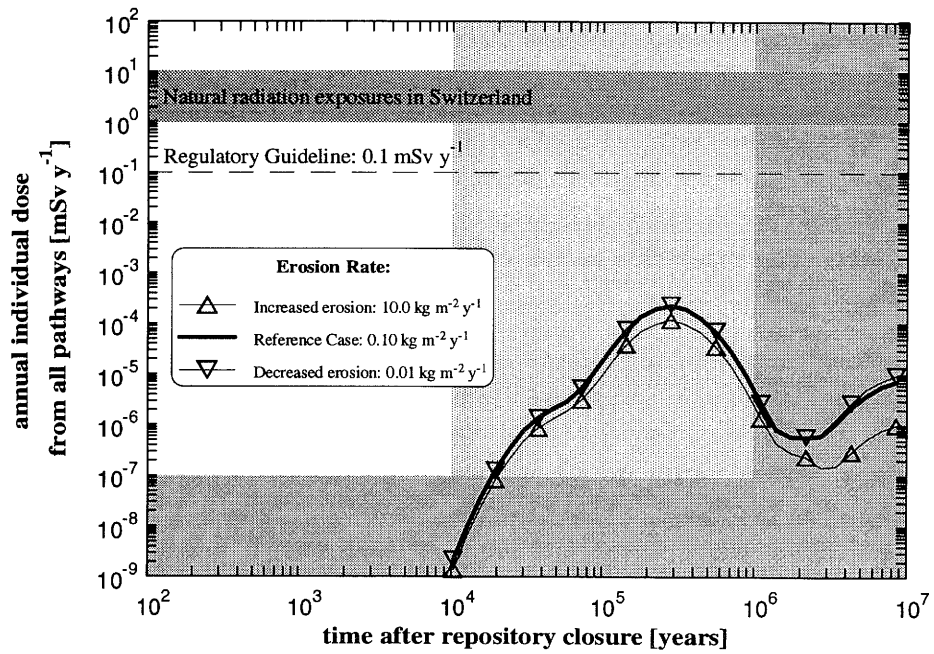


Figure 5.4.10: Sensitivity of calculated dose to variation of the erosion rate.

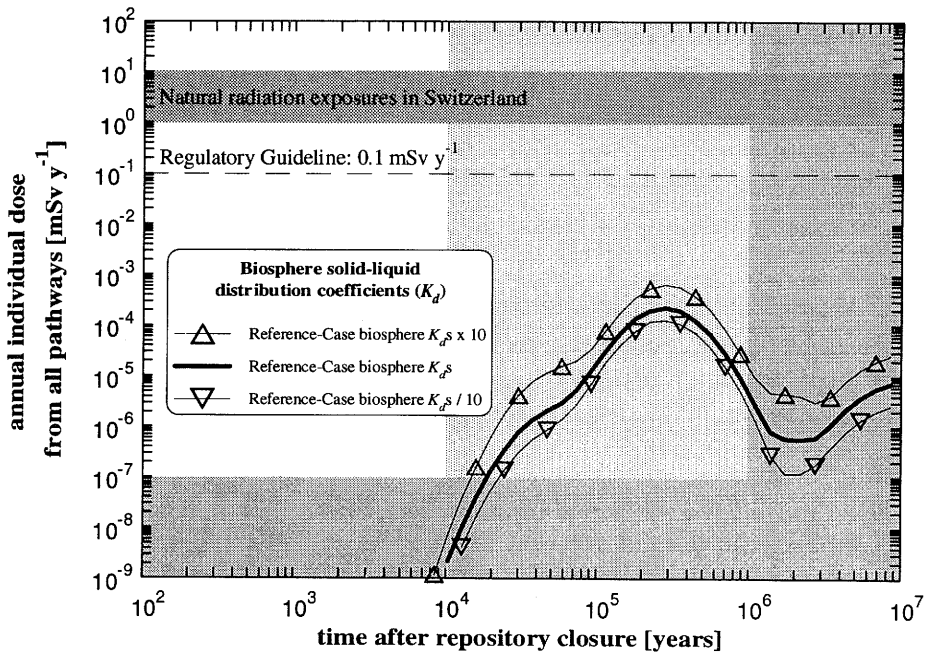


Figure 5.4.11: Sensitivity of calculated dose to variation of the solid-liquid distribution constants.

5.4.6 Summary of Biosphere Modelling

The main assumptions in the conceptual model of the biosphere are:

- The assumed characteristics of the discharge zone and local environment are unchanged in time. That is, activity continues to enter through the same limited zone of discharge, underlying a given area of land, so that radionuclides can potentially accumulate over several thousands of years.
- Humans are assumed to be present in this zone and to behave in such a way as to receive doses through a range of pathways. Specifically, a subsistence agricultural community is postulated, obtaining all its dietary needs and drinking water from local sources, and dwelling permanently in the area.

The physical aspects of radionuclide transport and dispersion in the biosphere are treated by a dynamic compartment model; biological uptake into the food chain and exposure of man are treated by an equilibrium model. By examining the intercompartment transfers in the biosphere model, an understanding of the dynamics of the system can be gained and the timescales of biosphere model dynamics estimated. The timescales over which radionuclides reach steady state in the biosphere tend to be shorter than those characterising release from the geosphere. As a consequence, the time dependence of calculated doses is similar to that of the geosphere releases.

The time invariance assumed for the data describing the biosphere is not realistic. An effect that has not been studied in detail is that significant changes in the characteristics of the biosphere might be expected over timescales which are shorter than those required for some radionuclides to achieve steady-state concentrations in the biosphere. For example, over timescales of the order of 10 000 years, significant alteration in the climate cannot be excluded. This could lead to changes in the transport and accumulation rates in the biosphere. However, such changes, e.g. glacial erosion, are expected to lead to additional dispersion of radionuclides. Hence, lower peak concentrations of radionuclides, and of doses, may be expected for some very immobile radionuclides in the biosphere, if environmental changes are taken into account.

The total calculated dose is, in general, only weakly sensitive to parameter variations tested; several orders of magnitude variation in input parameters are required in order that the outcome of the calculations are affected by a single order of magnitude. This tends to confirm the conclusions from previous studies (e.g., ZACH & SHEPPARD 1992, NEA 1993) that no single parameter in biosphere models dominate the uncertainty in the results. Insensitivity arises because the total dose is summed over a wide range of exposure pathways with different characteristics. Of the parameter variations tested, the source of irrigation water gives the greatest variation in calculated dose. A number of biosphere parameters have not been varied in the results shown here, notably, the area of land and the volumetric water flow in the local aquifer. For the Reference Scenario, these are well defined based on site-specific studies of a typical possible geosphere discharge site in the River Rhine valley (BAEYENS et al. 1989). However, different values of the above parameters are selected in alternative biosphere scenarios, i.e. small valley and alternative climate scenarios, presented in Chapter 6.

6. RESULTS AND THEIR INTERPRETATION

6.1 Introduction

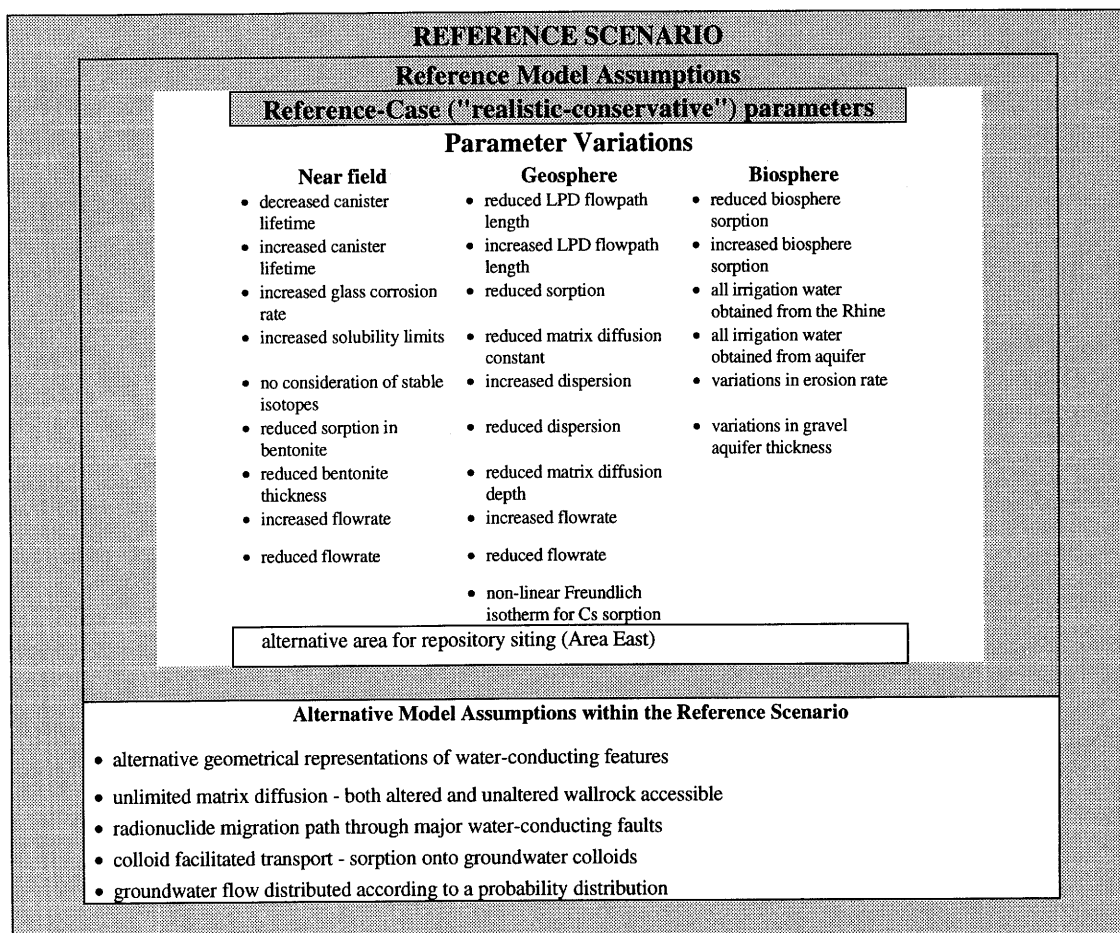
The purpose of this chapter is to evaluate the potential radiological consequences of the repository. Account is taken of uncertainty in the future evolution of the system and in the relevant release, transport and exposure processes. Possible courses of the future evolution of the repository system are identified in the scenario development described in Chapter 4. The scenarios arising from this analysis describe a number of alternative states for the system, the radiological consequences of which are calculated using conservatively constructed models, which ignore some processes that can confidently be expected to have a beneficial effect, but for which detailed models or data are lacking (reserve FEPs; see Subsection 4.4.3). In the biosphere, transitions between alternative climate states are not modelled. Parameter values have also been selected in a partially conservative ("realistic-conservative") way.

The structure of the calculations is summarised in Table 6.1.1. In Chapter 4, a Reference Scenario and a number of alternative scenarios are defined. The Reference Scenario provides the foundation for Reference-Case calculations and a set of parameter variations around the Reference Case, using the models and data presented in Chapter 5.

The Reference-Case parameters are based on a repository located in Area West, which is better characterised than Area East and might provide more favourable conditions for repository siting. However, as a parameter variation, calculations are performed using data appropriate to a repository sited in Area East. Also within the Reference Scenario, calculations using a number of alternative model assumptions for the geosphere are carried out. The Reference Scenario envisages a repository near field evolving according to the design function of the engineered barriers, a geosphere based on current understanding of the geological environment and biosphere based on present-day hydrogeological and climatic conditions. Results for the Reference Scenario, with both Reference Model Assumptions and alternative model assumptions, are given in Section 6.2, together with a discussion of the detailed behaviour of the engineered and geological barriers.

Alternative scenarios are discussed qualitatively in Chapter 4 and a number of these are identified for quantitative consideration (see Table 4.4.1). Those scenarios for which calculations are performed comprise:

- Deep Groundwater Well;
- Tunnel/Shaft Seal Failure;
- Alternative Climate-Related Scenarios.



ALTERNATIVE SCENARIOS

- Deep Groundwater Well
- Tunnel / Shaft Seal Failure
- Alternative Climate-Related Scenarios
 - Dry Climate State - Humid Climate State - Periglacial Climate State
 - Rhine Gravels Absent

ROBUST SCENARIO

- immediate transport from near field to biosphere; reference near-field and biosphere parameters

Parameter Variations

- unlimited groundwater flowrate
- "conservative" glass-corrosion rate, sorption and solubility limits

Note: LPD = low-permeability domain.

Table 6.1.1: Structure of calculations performed in the Kristallin-I safety assessment. The Reference Case (Reference Scenario, Reference Model Assumptions and "realistic-conservative" parameters) is indicated by shading.

The results of these calculations are presented in Section 6.3.

Calculations have also been performed for a "Robust Scenario", which is selected to illustrate the level of safety that can confidently be expected, even given a very pessimistic interpretation of geological uncertainties and geosphere transport processes (see Subsection 4.4.2). This scenario considers the evaluation of the engineered barriers according to their minimum design function and immediate transport of radionuclides released from the near field directly to the biosphere. Results are presented in Section 6.4.

An overview and summary of results in the present chapter is given in Section 6.5.

6.2 The Reference Scenario

6.2.1 Reference Model Assumptions

The assumptions underlying the conceptual models for each component of the reference model chain are described in detail in Chapter 5. These define a near field evolving according to the design function of the engineered barriers and a biosphere based on present-day hydrogeological and climatic conditions, in accordance with the definition of the Reference Scenario (Subsection 4.3.1). For the geological environment, however, a number of alternative model representations may be considered within the Reference Scenario, reflecting uncertainty in the properties of this environment. Key Reference Model Assumptions for the geological environment are:

– Geometry of Water-Conducting Features

Radionuclide transport through the geosphere is modelled for a single type of water-conducting feature, with a unique set of parameters describing its internal geometry - i.e. the variability in geometrical parameters, such as channel width and spacing, is not modelled. Transport from the repository along the flowpath takes place in water-conducting features modelled as cataclastic/jointed zones with broad, widely-spaced channels (Geometry 6)³⁷.

– Limited Matrix Diffusion

Matrix diffusion is limited to the relatively porous altered wallrock adjacent to the fractures. Unaltered wallrock is conservatively considered inaccessible to diffusion.

³⁷

It is not possible to select the most appropriate of the six geometrical representations on the grounds of their likelihood of occurrence. The representation used in the Reference Case is selected because it leads to the highest doses in model-chain calculations, as described in Subsection 6.2.2.1 (in particular, see Figure 6.2.8). Consistent with the methodology discussed in Chapter 4, uncertainty is dealt with by adopting this very conservative approach.

– **Radionuclide Migration Path**

Radionuclides are transported through the low-permeability domain directly (upwards) to the higher-permeability domain and thence to the biosphere. Transport processes in major water-conducting faults are neglected.

– **Colloid Transport**

The processes of radionuclide sorption and transport on groundwater colloids are neglected.

A number of alternatives to these assumptions are described in Subsection 6.2.2 and their consequence evaluated.

6.2.1.1 Reference-Case Calculations

6.2.1.1.1 Parameter Values for the Reference Case

The Reference-Case input datasets are based on a repository located in Area West. The datasets for near-field and geosphere calculations include the "realistic-conservative" parameter values given in Sections 5.2 and 5.3, respectively. The principal input data for the near field and geosphere in the Reference Case are reproduced in Tables 6.2.1 and 6.2.2. For the biosphere, the Reference-Case input dataset is based on the present-day (interglacial) biosphere in the vicinity of the river Rhine (present-day near surface hydrogeology, etc.), with release of radionuclides to the gravel aquifer of the Rhine Valley. The Reference-Case biosphere is discussed in Section 5.4.

Parameter	Units	Reference-Case Value
Time of canister failure	y	10^3 : see Table 3.7.2
Thickness of bentonite, $r_b - r_a$	m	1.38: see Table 3.7.2
Glass corrosion rate, R	$\text{kg m}^{-2} \text{y}^{-1}$	3.8×10^{-4} : see Table 3.7.2
Groundwater flowrate through repository area, Q	$\text{m}^3 \text{y}^{-1}$	3.0: see Table 3.7.2
Element-dependent K_d values for sorption on bentonite	$\text{m}^3 \text{kg}^{-1}$	"Realistic-conservative" values (see Table 3.7.3)
Element-dependent solubility limits, S_E	M	"Realistic-conservative" values (see Table 3.7.3)

Table 6.2.1: Principal near-field parameter values for Reference-Case calculations.

Parameter	Units	Reference-Case Value	Comments
Transport through low-permeability domain	-	Geometry 6	Cataclastic/jointed zones with broad, widely-spaced channels
Transport through major water-conducting faults	-	-	Not calculated
Planar / Cylindrical Geometry	-	Planar	See Table 5.3.3
Flow through water-conducting features (per unit length), q_w	$\text{m}^2 \text{y}^{-1}$	6.3×10^{-4}	Corresponds to a flowrate of $3.0 \text{ m}^3 \text{y}^{-1}$ over a repository area of $1.4 \times 10^5 \text{ m}^2$, with a density of water-conducting features of 0.04 m^{-1} ; see Table 3.7.6 (advection velocity = 11 m y^{-1} ; see Table 5.3.2)
Trace length of channels per unit area of a plane normal to the flow direction, H	m^{-1}	2.4×10^{-3}	See Table 5.3.2
Flowpath length, L	m	200	See Table 3.7.6
Peclet number, Pe	-	10	See Subsection 5.3.4.2
Fracture aperture, $2b^\dagger$	m	10^{-3}	See Table 5.3.3
Extent of altered wallrock (matrix accessible to diffusion) from centre of fracture plane, y_p	m	5×10^{-2}	See Table 5.3.3
Matrix porosity (altered wallrock), ϵ_p	-	5%	See Table 5.3.3
Pore diffusion constant, D_p	$\text{m}^2 \text{y}^{-1}$	0.001	See Subsection 5.3.4.3.1
Element-dependent K_d values for sorption on matrix pores surfaces	$\text{m}^3 \text{kg}^{-1}$	See Table 3.7.8	"Realistic-conservative" values

Note: † Fracture aperture is an insensitive parameter in the modelling of geosphere transport.

Table 6.2.2: Principal geosphere parameter values for Reference-Case calculations.

6.2.1.1.2 Reference-Case Results

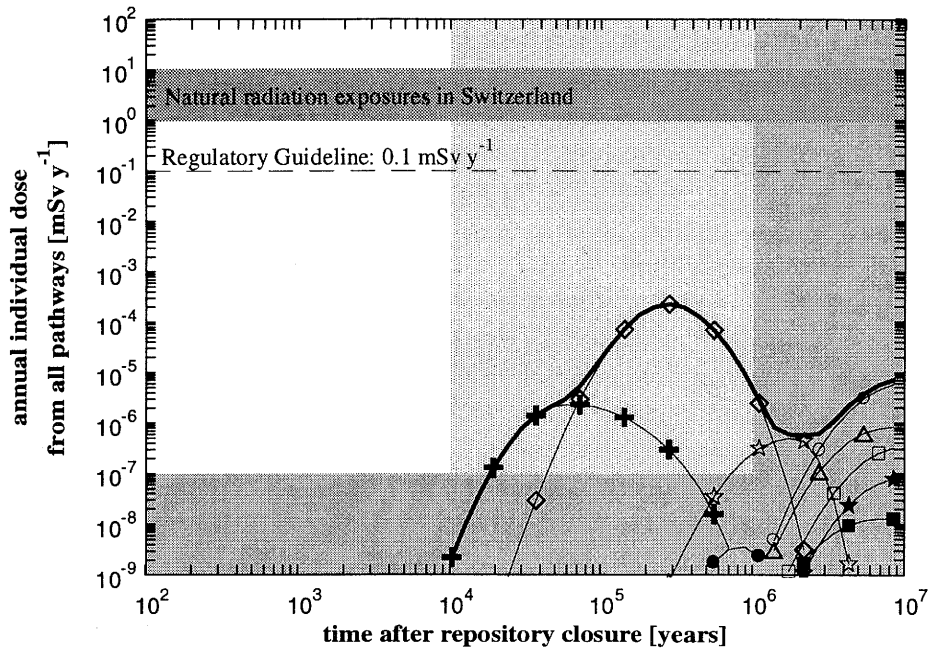
The time development of annual individual dose for the Reference-Case calculations is plotted in Figure 6.2.1(a). Results are shown for safety-relevant radionuclides (contributions are summed in the case of actinide chains and hence doses from the individual members of actinide chains are not shown). The sum over all dose contributions is indicated by the thick black line. The results are summarised in Table 6.2.3.

The peak annual individual dose lies more than two orders of magnitude below the 0.1 mSv y^{-1} dose limit set out in Protection Objective 1 of the Swiss regulatory guidelines (see Section 2.3), which is itself one to two orders of magnitude below the range of annual doses received by the present-day Swiss population ($1 - 10 \text{ mSv y}^{-1}$). This peak occurs more than 200 000 years after repository closure, and is dominated by ^{135}Cs . Radionuclides which dominate the dose at different stages of the dose-history are ^{79}Se at the earliest times (until about 30 000 years after repository closure), ^{135}Cs (which gives the highest of the dose maxima at about 300 000 years) and the members of the $4N + 3$ chain: ^{231}Pa and ^{227}Ac and their short-lived daughters (dose maximum at about 10 million years). Between the decay of ^{135}Cs and the rise of the $4N + 3$ chain doses, ^{99}Tc makes the dominant contribution at around 2 million years. Figure 6.2.1(a) also shows that the $4N + 1$ chain (including ^{237}Np and daughters) gives a slightly higher dose maximum than ^{99}Tc , but the peak dose from this chain is more than an order of magnitude less than that from the $4N + 3$ chain.

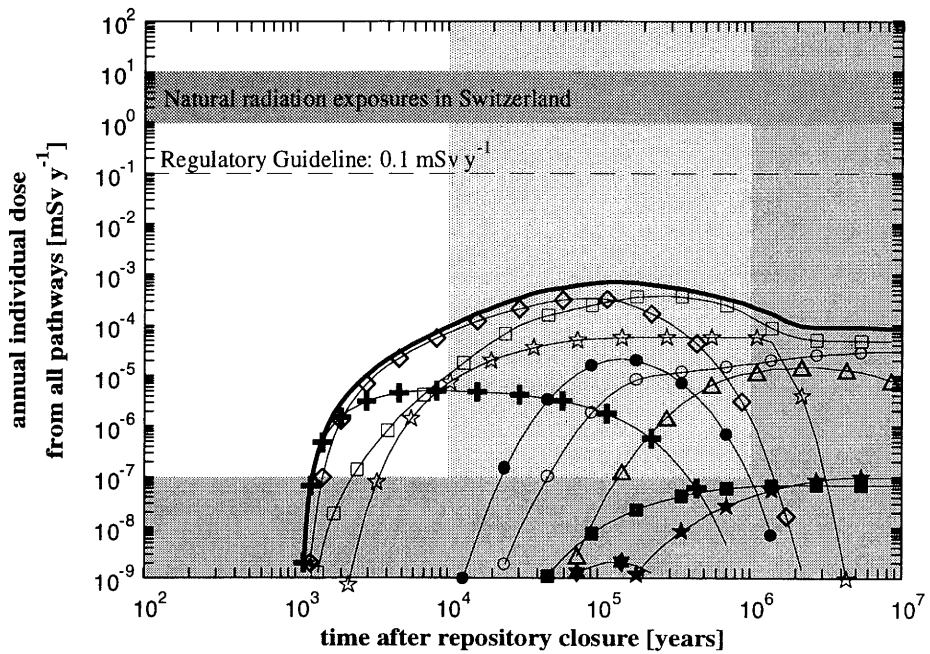
6.2.1.1.3 Retention of Radionuclides in the Near field and Geosphere

In order to illustrate the role played by the geological barriers in the performance of the system, Figure 6.2.1(b) shows the hypothetical dose history which would arise if the radionuclide fluxes from the near field were released directly to the biosphere. A comparison of Figures 6.2.1(a) and (b) shows that the time and magnitude of the maximum dose summed over all radionuclides is similar both with and without transport through the geosphere included in the calculations. However, some of the dose maxima for individual radionuclides and chains are significantly reduced by decay during geosphere transport (for example, the $4N + 2$ chain - ^{246}Cm and its daughters). ^{135}Cs , which is a dominant radionuclide in Figures 6.2.1(a) and (b), is little affected in terms of its dose maximum by geosphere transport (see also Figure 5.3.7 and the discussion thereof). The maximum dose, summed over all calculated radionuclides ($2 \times 10^{-4} \text{ mSv y}^{-1}$), is still more than two orders of magnitude below the regulatory guideline (0.1 mSv y^{-1}), even without credit being taken for transport through the geosphere, reflecting the performance of the near field. Geosphere transport does, however, result in a diminution of the early part of the breakthrough for many radionuclides (see, for example, the $4N + 3$ chain). Where no credit is taken for geosphere transport, doses arise at much earlier times and, for several radionuclides, appear only a few hundred years after canister failure (at 1000 years after emplacement). The behaviour of the geological barriers in the Reference Case has been further discussed in Section 5.3.

The relative performance of the near field and geosphere can be further illustrated by calculating the degree to which the inventory of each radionuclide decays within a particular barrier or barriers, over a time interval from repository closure to a cut-off time set at 10 million years: see Appendix 5. This quantity is denoted by η_N for the near field and by η_F for the near field and geosphere combined. In each case, it is normalised to the sum of initial inventory of the radionuclide (at repository closure) and the amount produced by ingrowth (integrated to the cut-off time). The equations by which η_N and η_F are derived from the radionuclide release rates from the near field and geosphere are given in Appendix 5.



(a) Reference Case



(b) Reference-Case near field and biosphere, direct release to the biosphere (instantaneous transport through the geosphere)

Key to radionuclides.

—	Sum over nuclides.	△	4N + 1 chain	◇	¹³⁵ Cs
○	4N + 3 chain	★	4N chain	●	⁵⁹ Ni
□	4N + 2 chain	●	¹²⁶ Sn	+	⁷⁹ Se
		+	⁹³ Zr	☆	⁹⁹ Tc

Note: (a): dataset SA_60ALA, (b): dataset SA_LA; the nomenclature for datasets is discussed in Appendix 4.

Figure 6.2.1: Time development of the annual individual doses in the Reference Case and in the hypothetical case of direct release of radionuclides from the near field to the biosphere.

Radionuclide	Peak Dose from Radionuclide [mSv y ⁻¹]	Time of Peak Dose from Radionuclide following repository closure [y]	Total Dose at Time of Peak Dose from Radionuclide [mSv y ⁻¹]
⁷⁹ Se	2×10^{-6}	7×10^4	5×10^{-6}
¹³⁵ Cs	2×10^{-4}	3×10^5	2×10^{-4}
⁹⁹ Tc	5×10^{-7}	2×10^6	6×10^{-7}
4N + 3 chain (²³¹ Pa & ²²⁷ Ac)	7×10^{-6}	$> 10^7$	9×10^{-6}

Table 6.2.3: Summary of doses in the Reference Case. Radionuclides given are those for which the dose maximum of the individual radionuclide corresponds to maximum in the total dose, summed over all radionuclides. Even in these cases (with the exception of ¹³⁵Cs) other radionuclides contribute significantly at the time of peak dose. For ⁹⁹Tc and the 4N + 3 chain members, other radionuclides contribute around 20% of the total dose and, for ⁷⁹Se, 60% of the total dose is due to ¹³⁵Cs.

η_N and η_F have been calculated using the results of the Reference Case for those radionuclides with half-lives of less than 3 million years and are given in Table 6.2.4 (longer-lived radionuclides may continue to decay within the barriers following the end of the calculations, which are terminated at 10 million years). With the exception of ¹³⁵Cs, less than 2% of any activation or fission product passes from the near field to the geosphere. In the case of the actinide chains, this figure reduces to 0.25%. When decay within the geosphere is taken into account, again with the exception of ¹³⁵Cs, 0.07% or less of any radionuclide passes into the biosphere.

For ¹³⁵Cs, only 5% decays within the near field alone and 12% in the near field and geosphere combined (compared, for example, with ⁹⁹Tc, of which 98.6% decays within the near field alone and 99.9% in the near field and geosphere combined). ¹³⁵Cs is assigned a very high solubility and sorbs relatively weakly in both bentonite and in the host rock (although accounting for the non-linearity of ¹³⁵Cs sorption can improve the performance of the geosphere significantly for the less pessimistic representations of the geometry of water-conducting features; see Section 5.3). Furthermore, ¹³⁵Cs has a long half-life. It is the combination of these properties, each of which is detrimental to barrier performance, which leads to the less favourable results for this radionuclide in both the near field and geosphere.

The release rates of ¹³⁵Cs from different components of the near field and the distribution of inventory between these components are shown as a function of time in Figure 6.2.2. ¹³⁵Cs is released from the glass over the first 100 000 years following emplacement. The rate of ¹³⁵Cs release from the glass matrix is indicated by the solid curve in Figure 6.2.2(a) and the ¹³⁵Cs contained within the glass is indicated by the

glass diffuses directly into the bentonite, without precipitation at the glass-bentonite interface. The curve *B* in Figure 6.2.2(b) indicates the ^{135}Cs contained within the bentonite, both dissolved in porewater and sorbed on pore surfaces. The broken curve in Figure 6.2.2(a) shows the release rate from the bentonite to the geosphere and the curve labelled *E* indicates the ^{135}Cs which has passed through the bentonite and entered the geosphere (with radioactive decay continuing to be taken into account). The total inventory of ^{135}Cs is shown by the curve *T* in Figure 6.2.2(b). Because of (i) the relatively weak sorption on bentonite and (ii) the high concentration gradients across the bentonite, which arise when the concentration at the inner boundary is not constrained by a solubility limit, diffusion through the bentonite is relatively fast. Most of the ^{135}Cs has passed into the geosphere within one million years; because of the long half-life of ^{135}Cs , little radioactive decay occurs in this time.

Radionuclide	Decay within the Barrier System	
	η_N [%] (Near field)	η_F [%] (Near field and Geosphere)
^{59}Ni	99.73	100.00
^{79}Se	99.90	99.93
^{93}Zr	99.60	100.00
^{99}Tc	98.60	99.93
^{107}Pd	100.00	100.00
^{126}Sn	99.56	100.00
^{135}Cs	5.48	12.33
<hr/>		
^{245}Cm	100.00	100.00
^{241}Am	100.00	100.00
^{237}Np	99.99	100.00
^{233}U	99.97	100.00
^{229}Th	100.00	100.00
<hr/>		
^{246}Cm	100.00	100.00
^{242}Pu	99.75	100.00
<hr/>		
^{243}Am	100.00	100.00
^{239}Pu	100.00	100.00
<hr/>		
^{240}Pu	100.00	100.00

Table 6.2.4: The percentage of the inventory of each radionuclide decaying within the near field (η_N) and the near field and geosphere combined (η_F). In each case, the amount decaying is normalised to the sum of initial inventory of the radionuclide (at repository closure) and the amount produced by ingrowth (integrated to a cut-off time of 10 million years). Radionuclides with half-lives greater than a few million years and their daughters are not included.

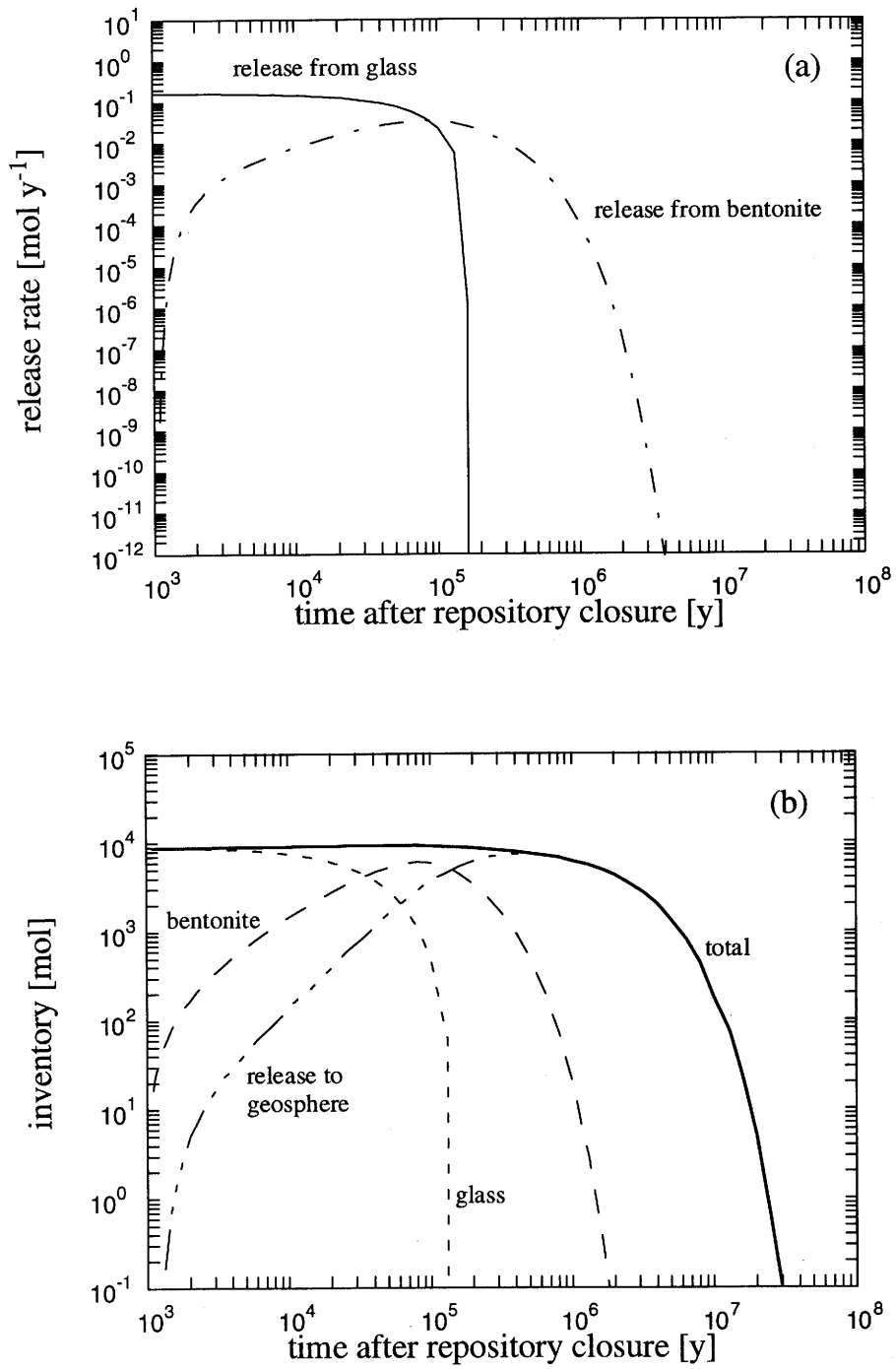
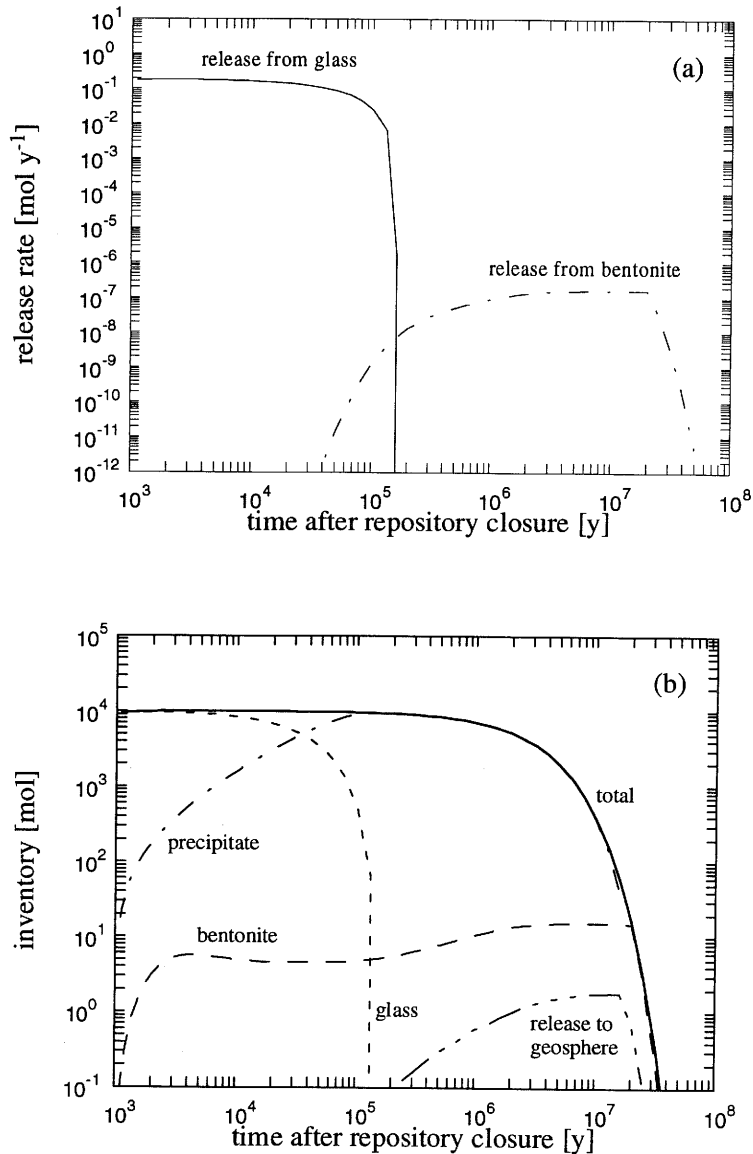


Figure 6.2.2: (a) Release rate of ^{135}Cs from different components of the near field. (b) Distribution of inventory between these components as a function of time.



Note: The small inventory maximum in curve "bentonite" about 3000 years in (b) is an artefact which arises from the (conservative) model assumption that solubility limits apply only at the glass-bentonite interface (see Subsection 5.2.1.1). Radioactive ingrowth of ^{237}Np from its precursors ^{245}Cm and ^{241}Am causes the solubility limit of Np to be exceeded locally within the bentonite. After the precursors decay (i.e. after about 10^4 years), ^{237}Np diffuses from the bentonite, both towards the geosphere and back towards the glass-bentonite interface, resulting in a small decrease in the inventory within the bentonite.

Figure 6.2.3: (a) Release rate of ^{237}Np from different components of the near field. (b) Distribution of inventory between these components as a function of time.

The behaviour of ^{135}Cs contrasts with that of ^{237}Np , 99.99% of which decays in the near field. The distribution of ^{237}Np inventory between different parts of the near-field barrier is shown as a function of time in Figure 6.2.3. Although ^{135}Cs and ^{237}Np have similar half-lives (2.14 million years for ^{237}Np), they differ in that the release of ^{237}Np is solubility limited. In Figure 6.2.3, the curve labelled *P*, which indicates ^{237}Np as a precipitated solid, extends to about 10 million years. This exceeds the half-life of ^{237}Np indicating that significant radioactive decay occurs in this time. Because the concentration at the bentonite inner boundary is constrained by a very low solubility limit, only a very small part of the total ^{237}Np inventory diffuses into the bentonite over this period. Furthermore, ^{237}Np is sorbed strongly on the surfaces of bentonite pores (the sorption constant for ^{237}Np is $5\text{ m}^3\text{ kg}^{-1}$, compared with $10^{-2}\text{ m}^3\text{ kg}^{-1}$ for ^{135}Cs). The result is a very high barrier efficiency for Np, with a small release from the bentonite to the geosphere.

6.2.1.2 Parameter Variations around the Reference Case

The Kristallin-I Reference Case is constructed by simultaneous use of all "realistic-conservative" parameter values. This calculation is thought to yield a moderately conservative result in view of the conservative assumptions in constructing the models and selecting the data. Tables 6.2.5 and 6.2.6 summarise the results of further calculations, made to study the sensitivity of the model-chain components to parameter-value variations (see Chapter 5 for a full description of these calculations). Results are expressed in terms of annual individual dose; in the case of near-field parameter variations, this is a drinking-water dose obtained using a set of simple conversion factors (see Appendix 6). For geosphere parameter variations, the full biosphere model described in Section 5.4 is used to obtain doses. Near-field and geosphere calculations employ a combination of "realistic-conservative" parameter values and variations on these values, with the aim of identifying key parameters. For the biosphere, the values of only a few key parameters are varied. Results are discussed below for two key radionuclides: ^{135}Cs , which makes the largest contribution to the peak annual individual dose in the Reference Case (see Subsection 6.2.1.1, above) and ^{99}Tc , an example of a radionuclide that reaches its elemental solubility limit in the near field.

Important points to note from these studies are:

- **The robustness of the near-field barrier.** It is shown above (see Subsection 6.2.1.1), that release from the Reference-Case near field, even if transferred directly to the biosphere, neglecting retardation and decay in the geosphere, is sufficiently low to meet Protection Objective 1 of the regulatory guidelines (by a margin of more than two orders of magnitude). This result is considered robust, both because of the conservative assumptions incorporated within the near-field model and because of its insensitivity to parameter variations. In particular, the release of ^{135}Cs , the radionuclide that dominates the peak annual individual dose in the Reference Case, is rather insensitive to each of the conservative near-field parameter variations. The adoption of "conservative" parameter values for canister lifetime, glass corrosion rate

or sorption give an increase in maximum release of less than an order of magnitude. Greater sensitivity is displayed to groundwater flowrate, but this sensitivity is principally to a *decrease* in flowrate and, even in this case, either a decrease or an increase in flowrate by a factor of 10 gives less than an order of magnitude change in the release from the near field; the adoption of a set of "conservative" solubility limits has no bearing on the release of this radionuclide.

- **Sensitivity to the selection of solubility limits.** For those radionuclides, the concentrations of which are limited by their solubility limits, the adoption of "conservative" solubility limits may significantly affect their behaviour in the near-field. For example, increasing the solubility limit of ^{99}Tc so that this limit is not reached, gives an increase in maximum release by a factor of about 50. Solubility-limited radionuclides, however, make a smaller contribution to the annual individual dose than ^{135}Cs , except when a very high groundwater flowrate is assumed, in which case the contributions of ^{99}Tc and ^{135}Cs are similar (see Table 6.2.5; sensitivity to geosphere parameter variations).
- **The effectiveness of the geosphere barrier.** The conservative description of the geosphere in the Reference Case (particularly with respect to the selection of a representative internal geometry for water-conducting features), means that the maximum release of ^{135}Cs from the geosphere is less than a factor of 2 less than that from the near field. However, referring to Figure 6.2.1 and the discussion thereof, an important effect of the geosphere, even with this conservative representation, is to delay any release to the human environment for more than 10 000 years. The geosphere provides a more effective barrier for ^{99}Tc (and several other radionuclides), reducing the maximum release rate by two orders of magnitude and delaying releases for around one million years.
- **Insensitivity to variations in geosphere parameter values.** The maximum release of ^{135}Cs from the geosphere is insensitive to each of the conservative geosphere parameter variations (due principally to the conservative representation in the Reference Case - see above). The relatively high sensitivity displayed to groundwater flowrate (particularly to a decrease in flowrate) arises predominantly because the flowrates also affect the near-field release. ^{99}Tc displays a greater sensitivity to geosphere parameter variations. At the highest groundwater flowrate, the geosphere is an ineffective barrier for both radionuclides, with ^{99}Tc and ^{135}Cs giving similar contributions to maximum annual individual dose.
- **Insensitivity to variations in biosphere parameter values.** The response of the biosphere model is insensitive to parameter variations. Commonly, changes of several orders of magnitude in a parameter value with respect to the Reference Case are required to produce a single order of magnitude response in the calculated dose. Exploitation of the local aquifer as a source of water for irrigation and of drinking water for livestock is the most sensitive biosphere process. This sensitivity manifests itself in the response of the biosphere to different climate states - see Subsection 6.3.4.

Results of Near-Field Parameter Variations (from Section 5.2)		
	Maximum near-field release; expressed as drinking water dose [mSv y ⁻¹]	
	¹³⁵ Cs	⁹⁹ Tc
Reference-Case near-field parameters	5×10^{-5}	7×10^{-7}
Reduced canister lifetime: 10^2 y	5×10^{-5}	7×10^{-7}
Increased canister lifetime: 10^5 y	4×10^{-5}	7×10^{-7}
Increased glass corrosion rate $R = 0.04$ kg m ⁻² y ⁻¹	7×10^{-5}	7×10^{-7}
"Conservative" solubilities: see Table 3.7.3	Not solubility limited	3×10^{-5}
"Conservative" K_d values: see Table 3.7.3	1×10^{-4}	8×10^{-7}
Reduced bentonite thickness $r_b - r_a = 0.2$ m	2×10^{-4}	9×10^{-7}
10-fold decrease in flowrate $Q = 0.3$ m ³ y ⁻¹	6×10^{-6}	8×10^{-8}
10-fold increase in flowrate $Q = 30$ m ³ y ⁻¹	1×10^{-4}	6×10^{-6}
Results of Geosphere Parameter Variations (from Section 5.3)		
	Maximum geosphere release; maximum annual individual dose (all pathways) [mSv y ⁻¹]	
	¹³⁵ Cs	⁹⁹ Tc
Reference-Case near-field and geosphere parameters (drinking water dose shown in parentheses for comparison with near-field Reference-Case)	2×10^{-4} (3×10^{-5})	5×10^{-7} (6×10^{-9})
Reduced low-permeability domain flowpath length $L = 100$ m	3×10^{-4}	4×10^{-6}
Increased flowpath length $L = 500$ m	1×10^{-4}	5×10^{-9}
"Conservative" K_d values: see Table 3.7.6	3×10^{-4}	3×10^{-5}
"Conservative" diffusion constant $D_p = 2 \times 10^{-4}$ m ² y ⁻¹	2×10^{-4}	1×10^{-6}
Reduced dispersion $Pe = 50$	3×10^{-4}	8×10^{-8}
"Conservative" matrix diffusion depth $y_p = 10^{-2}$ m	3×10^{-4}	2×10^{-5}
10-fold decrease in flowrate through water conducting features $q_w = 6 \times 10^{-5}$ m ² y ⁻¹ ($Q = 0.3$ m ³ y ⁻¹)	7×10^{-6}	1×10^{-10}
10-fold increase in flowrate through water conducting features $q_w = 6 \times 10^{-3}$ m ² y ⁻¹ ($Q = 30$ m ³ y ⁻¹)	1×10^{-3}	1×10^{-3}
Cs sorption described by modified Freundlich isotherm. RANCHMDNL calculation. Reference- Case geometry for water-conducting features.	2×10^{-4}	Not Applicable

Table 6.2.5: Selected results from calculations investigating sensitivity of near-field and geosphere releases to parameter variations. The Reference-Case calculations, around which variations are made, are based on the Reference Scenario discussed in Chapter 4, together with Reference Model Assumptions and "realistic-conservative" physico/chemical data

described in Chapter 5. Releases have been calculated for a subset of safety-relevant radionuclides; ^{135}Cs and ^{99}Tc are shown here for illustration. ^{135}Cs is chosen since it gives the largest contribution to annual individual dose in the Reference-Case calculations (see Subsection 6.2.1.1). ^{99}Tc provides an example of a radionuclide that is solubility-limited in the near field. Results are expressed in terms of annual individual dose; in the case of near-field parameter variations, this is a drinking-water dose obtained using a set of simple conversion factors (see Appendix 6). For geosphere parameter variations, the full biosphere model described in Section 5.4 is used to obtain doses. Parameter variations which increase release with respect to the Reference Case by a factor of 10 or more are indicated by lighter shading. Those which decrease dose by a factor of 10 or more are indicated by darker shading.

Results of Biosphere Parameter Variations (from Section 5.4)		
	Maximum Annual Individual Dose (all pathways) [mSv y ⁻¹]	
	^{135}Cs	^{99}Tc
Reference-Case near-field, geosphere and biosphere parameters	2×10^{-4}	5×10^{-7}
Biosphere K_d values reduced by a factor 10	1×10^{-4}	8×10^{-8}
Biosphere K_d values increased by a factor 10	6×10^{-4}	4×10^{-6}
All irrigation water obtained from the Rhine	3×10^{-5}	1×10^{-8}
All irrigation water obtained from the aquifer in the Rhine gravel sediments	5×10^{-4}	1×10^{-6}
Regional erosion rate reduced by a factor of 10	2×10^{-4}	5×10^{-7}
Regional erosion rate increased by a factor 100	1×10^{-4}	3×10^{-7}
Gravel aquifer 20 m thick	2×10^{-4}	5×10^{-7}

Table 6.2.6: Selected results from calculations investigating sensitivity of biosphere parameter variations. The Reference-Case sets of calculations, around which variations are made, are based on the Reference Scenario discussed in Chapter 4, together with Reference Model Assumptions and physico/chemical data described in Chapter 5. Parameter variations which decrease dose by a factor of 10 or more are indicated by shading. None of the variations increase dose by more than a factor of 10.

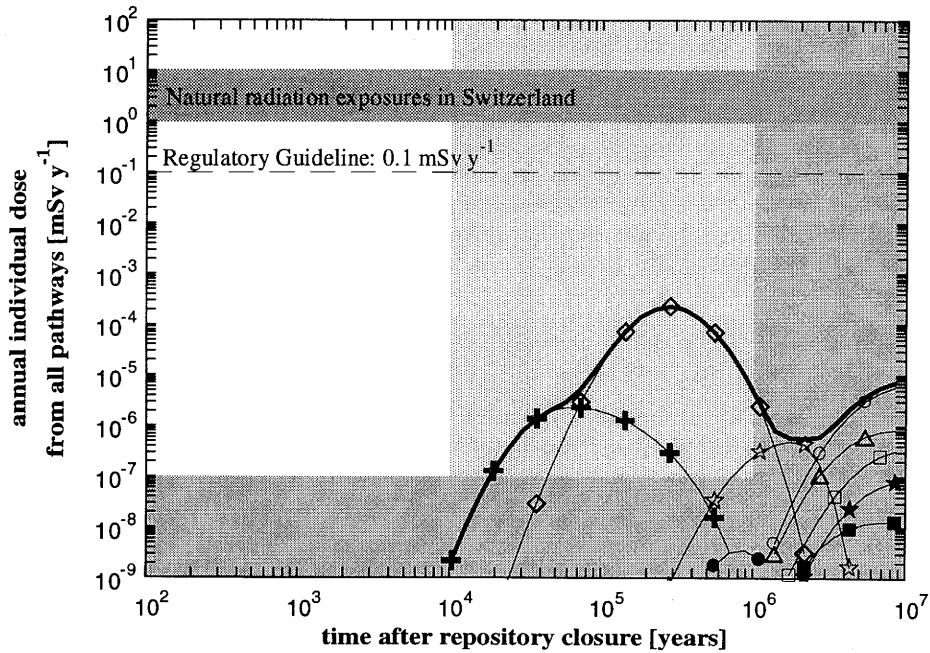
On the basis of near-field calculations alone, solubility limits have been identified as being of key importance in the behaviour of the near field for several long-lived safety-relevant radionuclides. In order to assess the relevance of this conclusion to the performance of the overall repository system, a complete model-chain calculation has been carried out using the "conservative" values for solubility limits, with all remaining data held at the Reference-Case values. The results are compared with those of the Reference Case in Figure 6.2.4.

The peak annual individual dose is little changed by this parameter variation and continues to be dominated by ^{135}Cs , the release of which is not solubility limited. However, other radionuclides, which dominate the dose at earlier and later times, give much higher contributions to dose than in the Reference Case. In particular, the peak doses due to ^{79}Se and the $4N + 1$ chain are significantly increased and are of the same order of magnitude as the ^{135}Cs dose maximum.

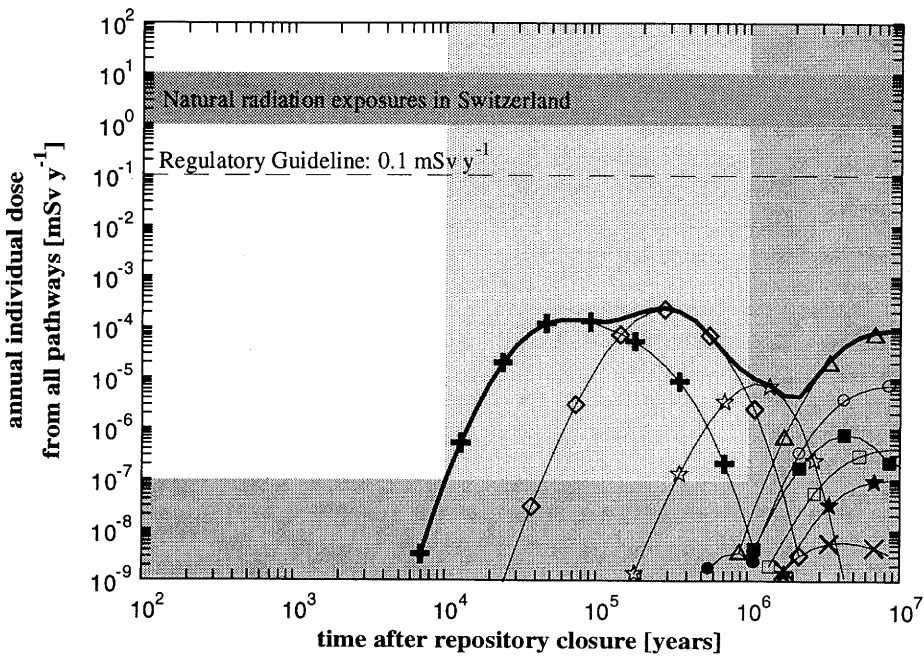
The combination of several "conservative" parameter values is thought to represent an excessive degree of pessimism. However, even when such a combination is made in modelling the near field ("conservative" glass corrosion rate, sorption constants in bentonite and solubility limits, but with a limited, Reference-Case groundwater flowrate at the bentonite-host rock interface; see Table 6.2.7), the highest annual individual dose is still less than the regulatory guideline by more than two orders of magnitude (Figure 6.2.5(a)). Again, the role of the geosphere is demonstrated when this result is compared with the hypothetical case of direct coupling of the near field to the biosphere, with no credit taken for transport through the geosphere (Figure 6.2.5(b)). Accounting for the presence of the geological barriers (with the Reference-Case representation of the geosphere), reduces the maximum calculated dose by more than an order of magnitude, illustrating the advantages of the multi-barrier concept if the performance of the engineered barriers is poorer than expected.

Parameter	"Conservative" Variation
Glass corrosion rate, R	$0.038 \text{ kg m}^{-2} \text{ y}^{-1}$
Element-dependent K_d values for sorption on bentonite	"Conservative" values (see Table 3.7.3)
Element-dependent solubility limits, S_E	"Conservative" values (see Table 3.7.3)

Table 6.2.7: Combination of "conservative" near-field parameter values.



(a) Reference Case



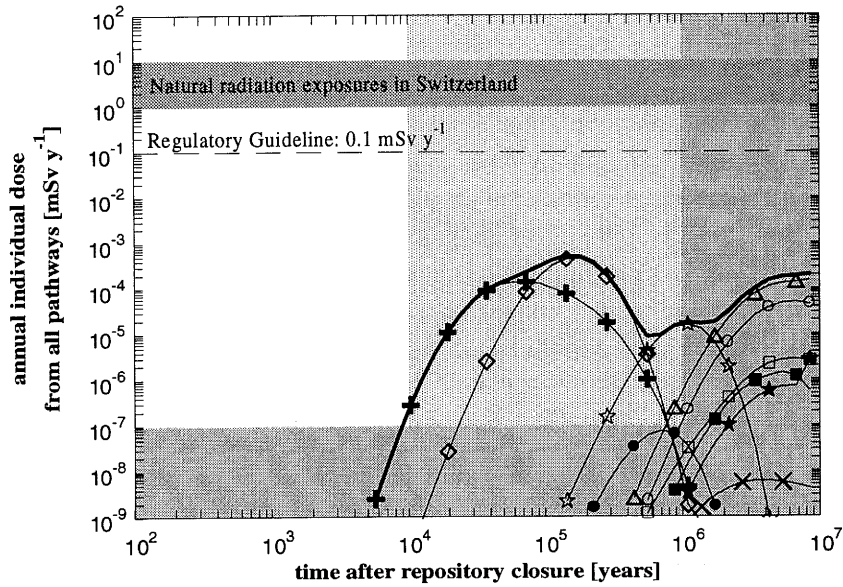
(b) Parameter variation with "conservative" solubility limits

Key to radionuclides.

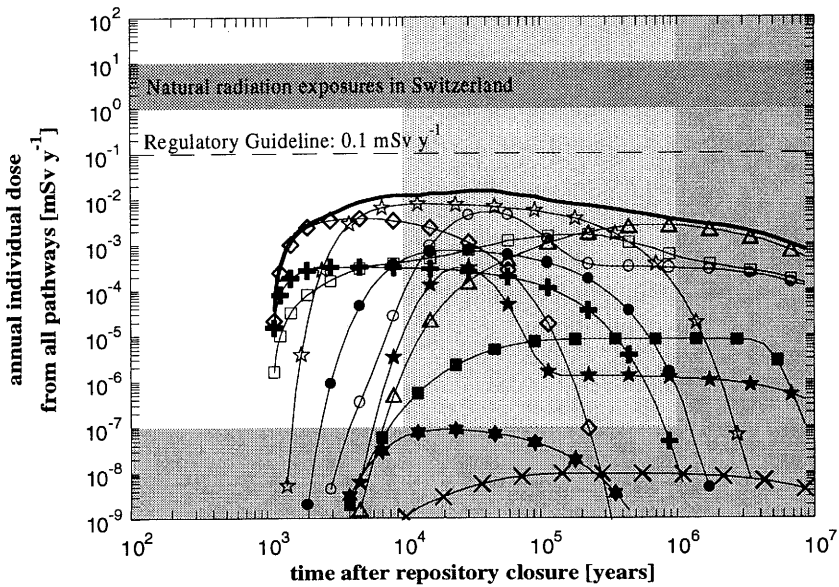
—	Sum over nuclides.	△	4N + 1 chain	★	⁵⁹ Ni	●	¹²⁶ Sn
○	4N + 3 chain	★	4N chain	×	¹⁰⁷ Pd	☆	⁹⁹ Tc
□	4N + 2 chain	◇	¹³⁵ Cs	+	⁷⁹ Se	■	⁹³ Zr

Note: (a): dataset SA_60ALA, (b): dataset 8D_60ALA; the nomenclature for datasets is discussed in Appendix 4.

Figure 6.2.4: Time development of the annual individual doses in the Reference Case and in a parameter variation with "conservative" solubility limits.



(a) Combination of "conservative" near-field parameters (glass corrosion rate, sorption constants and solubility limits). Reference-Case groundwater flowrate at the bentonite-host rock interface, Reference-Case geosphere and biosphere.



(b) Combination of "conservative" near-field parameters (glass corrosion rate, sorption constants and solubility limits). Reference-Case groundwater flowrate at the bentonite-host rock interface. Hypothetical case of direct release from near field to Reference-Case biosphere.

Key to radionuclides.

—	Sum over nuclides.	△	4N + 1 chain	★	⁵⁹ Ni	●	¹²⁶ Sn
○	4N + 3 chain	★	4N chain	×	¹⁰⁷ Pd	☆	⁹⁹ Tc
□	4N + 2 chain	◇	¹³⁵ Cs	+	⁷⁹ Se	■	⁹³ Zr

Note: (a) dataset EB_60ALA, (b) dataset EB_LA; the nomenclature for datasets is discussed in Appendix 4.

Figure 6.2.5: Time development of the annual individual doses in the extreme case of a combination of "conservative" near-field parameters.

6.2.1.3 Alternative Reference Area for Repository Siting

The Reference Case is based on data for Area West, which is better characterised than Area East. For radionuclide transport modelling, the most significant differences between the two areas are the flowrate of groundwater through the repository area and the spacing between the water-conducting features which intersect the repository tunnel system. Differences in groundwater chemistry lead to area-dependent sorption parameters, but these are only relevant to Tc and U. There are also differences in the trace lengths of individual water-conducting features around the tunnel walls (see Tables 3.7.4 and 3.7.5), but these are relatively small. The consequences of the differences between Areas West and East for repository performance are examined in this subsection.

The average flowrate of groundwater through the repository area is assumed to be greater by a factor of 33 in Area East and the density of water-conducting features intersecting repository tunnels is greater by a factor of about 3 (Table 3.7.6a). The higher groundwater flowrate affects the performance of both the engineered and the geological barriers, whereas the higher density of water-conducting features affects the geosphere only. The groundwater flowrate through the water-conducting features (and hence the advection velocity through the geosphere model conduits) is inversely proportional to the density of these features and is therefore greater by about an order of magnitude in Area East (Table 5.3.2). Both near field and geosphere are, therefore, expected to provide less effective barriers to radionuclide migration in Area East. As for Area West, the most likely exfiltration point is in the Rhine valley, with radionuclides released to the gravel aquifer of the Rhine valley. For both areas, therefore, the Reference-Case biosphere is appropriate. There is also the (less likely) possibility of a release occurring to a tributary valley of the Rhine. For this reason, an additional set of biosphere calculations have been carried out to investigate the potential radiological consequences of release in Area East occurring in such a valley.

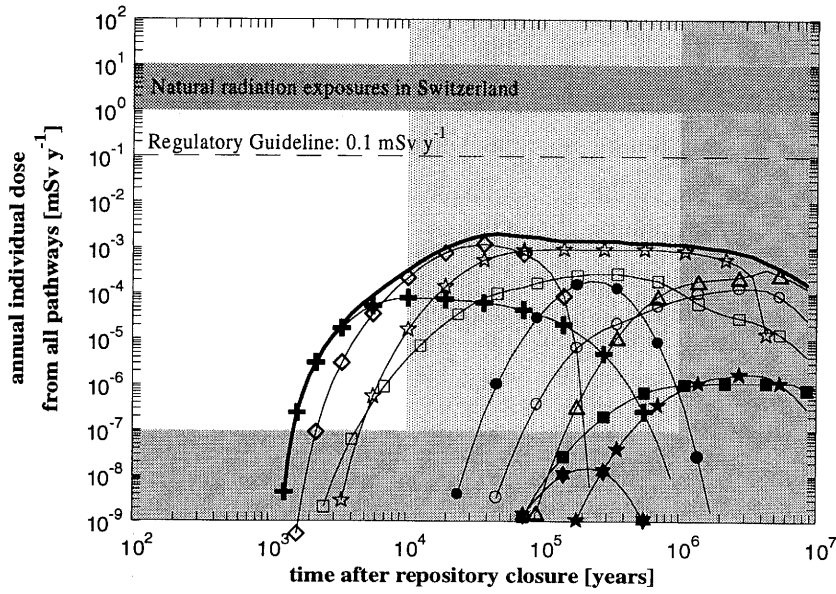
All near-field and geosphere parameters, except those associated with the groundwater flowrate and geosphere sorption, are set to their Reference-Case values. The geosphere advection velocity in these calculations is 150 m y^{-1} for Area East, compared with 11 m y^{-1} for the Area-West Reference Case (see Table 5.3.2). The key differences in the biosphere models of the Rhine valley and the Rhine tributary valley are summarised in Table 6.2.8.

The time development of the annual individual dose for Area East, with radionuclides released to the Rhine gravels, is plotted in Figure 6.2.6(a). The case of release to a tributary valley is shown in Figure 6.2.7. As expected from the discussion of input parameters above, the dose summed over all radionuclides is higher in Area East than in Area West. However, the regulatory guideline dose is at no time reached. The peak annual individual dose is more than an order of magnitude below the regulatory guideline of 0.1 mSv y^{-1} .

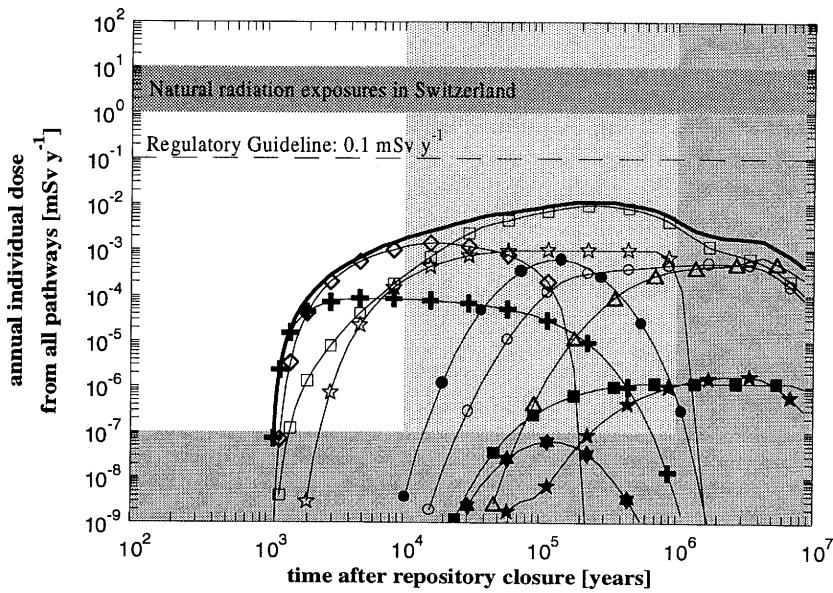
Parameter	Symbol	Units	Rhine Valley (Reference Case)	Tributary Valley
Area of farmland	A_f	m ²	3.4×10^6	2.8×10^5
Thickness of deep soil	l_D	m	1.0	0.75
Thickness of local aquifer	l_L	m	2.0	6.0
Porosity of local aquifer	ϵ_L	-	0.20	0.25
Volumetric moisture content of local aquifer	θ_L	-	0.20	0.25
Depth of water in river	d_w	m	3.25	0.5
Width of river	w_w	m	200	2
Thickness of river bed sediment	d_s	m	0.1	0.02
Through-flow in river	F_{PW}	m ³ y ⁻¹	3.2×10^{10}	2.0×10^7
Through-flow in local aquifer	$F_{UL} + F_{CL}$	m ³ y ⁻¹	5.5×10^6	3.2×10^6

Note: These datasets are taken from earlier biospheres models of sites in northern Switzerland and are used here because they are representative of typical features found in such biospheres. Given the long timescales of this assessment, it is not felt that a more detailed characterisation of present day-conditions at potential release sites is justified.

Table 6.2.8: Comparison of the biosphere parameters values used for the Rhine-valley (Reference-Case) biosphere and the tributary-valley biosphere. Although the river in the tributary valley is much smaller than the Rhine, the initial dilution in the local aquifer is similar (smaller by a factor of less than two). Data for the tributary valley are taken from GROGAN et al. (1990). A full description of the tributary-valley biosphere is given in KLOS & VAN DORP (1994).



(a) Area East: release to the Rhine gravels in the Reference-Case biosphere



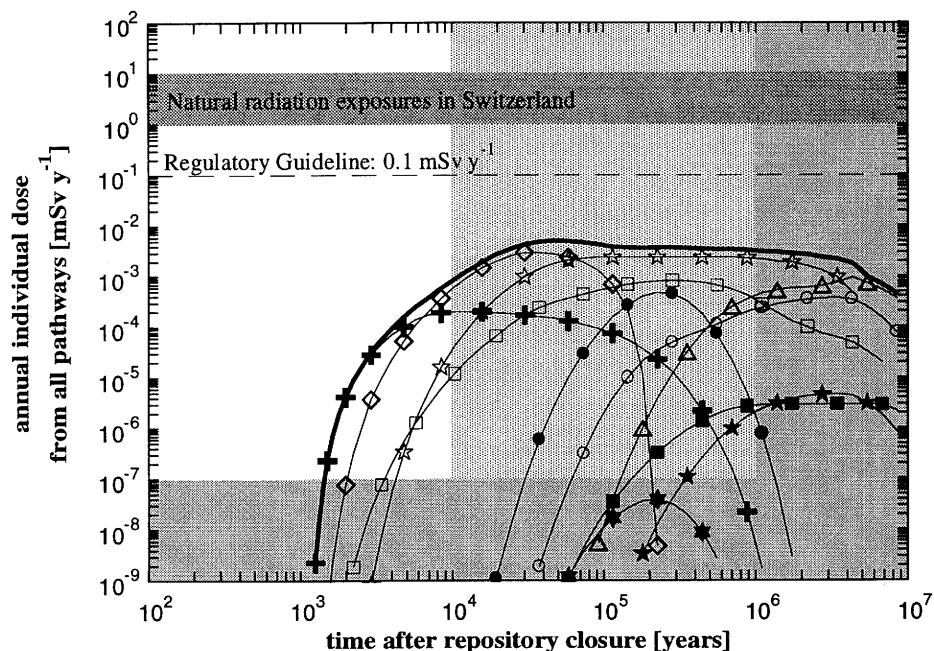
(b) Area East: hypothetical case of direct release from the near field to the Reference-Case biosphere

Key to radionuclides.

—	Sum over nuclides.	△	4N + 1 chain	★	⁵⁹ Ni	●	¹²⁶ Sn
○	4N + 3 chain	★	4N chain	×	¹⁰⁷ Pd	☆	⁹⁹ Tc
□	4N + 2 chain	◇	¹³⁵ Cs	+	⁷⁹ Se	■	⁹³ Zr

Note: (a): dataset SC_60ALA, (b) dataset SC_LA; the nomenclature for datasets is discussed in Appendix 4.

Figure 6.2.6: Time development of the annual individual doses for a repository located in Area East, with release in the Rhine valley; present-day climate and subsistence agriculture.



Note: Dataset SC_60ATA; the nomenclature for datasets is discussed in Appendix 4.

Figure 6.2.7: Time development of the annual individual doses for a repository located in Area East, with release to a tributary valley of the Rhine; present-day climate and subsistence agriculture.

The maximum dose is dominated by ^{135}Cs for releases to both Areas East and West, irrespective of the biosphere representation. Compared to Area West, this maximum is greater by a factor of about 7 in Area East assuming the Reference-Case biosphere (Figure 6.2.6) and by a further factor of about 2 assuming a biosphere based on a tributary valley (Figure 6.2.7). As in Area West, ^{79}Se dominates the total dose at the earliest times (up to about 3000 years after repository closure), followed by ^{135}Cs up to 30 000 years. At still later times, the actinide chains (and particularly the $4N + 2$ chain) give large contributions to the total dose. However, unlike the situation in Area West, from 30 000 years to beyond one million years after closure, the dose is dominated by ^{99}Tc . ^{99}Tc gives doses comparable to those arising earlier from ^{135}Cs , and extending over a far longer time interval. Referring to Table 5.2.3, it can be seen that the release of ^{99}Tc from the near field is much more sensitive to groundwater flowrate than that of ^{135}Cs , which is why ^{99}Tc is more significant in its contribution to total dose in Area East (with a 40 times higher groundwater flowrate) than in Area West.

The role played by the geological barriers in Area East is illustrated by comparing the hypothetical dose history that would arise if the radionuclide fluxes from the near field were released directly to the biosphere with the results obtained when geosphere transport is accounted for (Figure 6.2.6(b)). For Area West, the comparison showed that

that the geosphere results in the diminution of the early part of the breakthrough for many radionuclides. The time and magnitude of the summed dose maximum is little changed if the geosphere is excluded from the calculations, although some of the dose maxima for individual radionuclides and chains are significantly reduced by geosphere transport. In Area East, the diminution in early breakthrough is much less evident, as a result of the higher groundwater flowrate. A clear effect of the Area East geosphere, however, is a reduction in the dose from the $4N + 2$ chain, which gives the highest contribution to the summed dose in the absence of the geosphere. The geosphere reduces the contribution of the $4N + 2$ chain by more than an order of magnitude, taking it below that of ^{99}Tc , which is much less affected by geosphere transport. In general, the geosphere in Area East is rather ineffective as a barrier to the migration of activation/fission products and long-lived members of the actinide chains. For some of the shorter-lived daughters, and particularly ^{210}Pb from ^{226}Ra in the $4N + 2$ chain, the transit time through the geosphere is sufficient with respect to the half-lives to bring them into radioactive equilibrium with their parents and significantly reduce their contribution to dose.

Finally, it should be noted that the regulatory guideline is not exceeded in the less favourable conditions provided by Area East, even when no credit is taken for the geosphere barrier, emphasising the effectiveness of the engineered barriers.

6.2.2 Alternative Model Assumptions

Key Reference Model Assumptions for the geological environment and geosphere transport are listed in Subsection 6.2.1. Alternative assumptions are given in Table 6.2.9 and their consequences are analysed below.

6.2.2.1 Matrix Diffusion and Geometrical Representation of Water-Conducting Features

Groundwater flow in the geosphere takes place in a network of water-conducting features. Three types of features have been identified in the crystalline basement of Northern Switzerland. These are (Figure 3.5.4):

- cataclastic zones and
- jointed zones,

which are geometrically similar - no distinction is made between these two types of water-conducting feature for the purpose of radionuclide transport modelling - and

- fractured aplite/pegmatite dykes and aplitic gneisses.

Reference Model Assumptions (for dataset: SA_60ALA)	Alternative Model Assumptions	
	Dataset Names	Assumptions
Geometrical Representation of Water-Conducting Features:		
All transport takes place in cataclastic/jointed zones with broad, widely-spaced channels.	SA_50ALA	– Transport in aplite/pegmatite dykes and aplitic gneisses.
	SA_40ALA	– Transport in cataclastic/jointed zones with narrow, closely-spaced channels.
Matrix Diffusion:		
Matrix diffusion is limited to the altered wallrock adjacent to the fractures. Unaltered wallrock is inaccessible to diffusion.	SA_30ALA	– Unlimited matrix diffusion - transport in cataclastic/jointed zones with broad, widely-spaced channels.
	SA_20ALA	– Unlimited matrix diffusion - transport in aplite/pegmatite dykes and aplitic gneisses.
	SA_10ALA	– Unlimited matrix diffusion - transport in cataclastic/jointed zones with narrow, closely-spaced channels.
Radionuclide Migration Path:		
Radionuclides are transported through the low-permeability domain directly (upwards) to the higher-permeability domain and thence to the biosphere.	SA_64ALA	– Radionuclides are transported through the low-permeability domain to major water-conducting faults, upwards to the higher-permeability domain and thence to the biosphere.
Colloid Transport:		
Colloid facilitated radionuclide transport is neglected.	SD_60BLA SD_50BLA SD_40BLA SD_30BLA SD_20BLA SD_10BLA	– Radionuclides sorb onto a constant background population of groundwater colloids (all six representative geometries for water-conducting features calculated).
Distribution of Groundwater Flow:		
Water-conducting features are each assigned identical flowrates.	SA_60ALA, XA_60JLA and XB_60KLA.	– Groundwater flow is distributed between water-conducting features according to a probability distribution. Radionuclide flux to the biosphere is obtained from a weighted superposition of Reference-Case results (SA_60ALA) and results with flowrate increased 10-fold (XA_60JLA) and 100-fold (XB_60KLA).

Notes: The nomenclature for datasets (centre column) is discussed in Appendix 4; the Reference-Case dataset name is SA_60ALA.

The alternative assumptions regarding colloid transport and distribution of groundwater flow also affects the near-field calculations - see Subsection 6.2.2.3.

Table 6.2.9: Model Assumptions for the geological environment and for geosphere transport modelling and alternative model assumptions for which further calculations have been made. All calculations lie within the framework of the Reference Scenario.

In order that calculations can be performed which span the variability observed in the internal structure of these water-conducting features, and particularly in the width and separation of channels within fracture infill, three different model representations are defined in Section 5.3: two model representations for cataclastic/jointed zones and a third for fractured aplite/pegmatite dykes and aplitic gneisses (see, in particular, the left-hand side of Figure 5.3.5). These three models correspond to three "extreme cases" of the observed physical dimensions of these structures. The form of the model representations is further constrained by the limitations of the available computer codes, which allow only constant matrix properties and simple geometries; (see Subsection 5.3.4.3.2).

For each of the three representations, two sets of transport model parameters are assigned to (see the right-hand side of Figure 5.3.5): one assuming unlimited matrix diffusion (matrix diffusion in fracture infill and both altered and unaltered wallrock - Geometries 1, 2 and 3) and a second assuming limited matrix diffusion (matrix diffusion confined to the fracture infill and altered wallrock only - Geometries 4, 5 and 6).

Model-chain calculations have been performed for all six geometries and for all safety-relevant radionuclides, using the Reference-Case near field and biosphere. Transport processes in major water-conducting faults are not explicitly modelled. The key parameters for the six representations are given in the Table 6.2.10, together with the dataset names for the calculations. The dataset names allow the parameter values for any calculation to be traced (see Appendix 4). For these calculations, however, all parameters except those associated with the geometrical representation are held at their Reference-Case values.

Figure 6.2.8 shows the time development of annual individual dose, summed over all radionuclides, for each of the geometrical representations. The three graphs on the left-hand side of the figure show the cases in which matrix diffusion is modelled in both altered and unaltered wallrock. It can be seen that, of these three representations, cataclastic zones/jointed zones, in which the channels carrying flowing water are broad and widely-spaced (Geometry 3), gives the highest doses.

On the right-hand side of Figure 6.2.8, the corresponding cases with matrix diffusion limited to altered wallrock only are shown. In general, these display higher doses than their counterparts with unlimited matrix diffusion.

Overall, the highest dose maximum occurs with broad, widely-spaced channels in cataclastic zones/jointed zones with limited matrix diffusion (Geometry 6). For this reason, it is adopted as the Reference Case for Kristallin-I calculations. The corresponding case assuming unlimited matrix diffusion gives a dose curve showing broader peaks, with the doses arising earlier and with only a slightly lower maximum individual dose. However, the earlier breakthrough can be explained in terms of the limitations of the geosphere transport model. As described in Chapter 5, the model allows only for matrix properties that are constant in space (and time). Where unlimited matrix diffusion is assumed, both altered and unaltered wallrock are accessible by diffusion, each of which may, in reality, have a different porosity. In the geosphere model, however, both must

be assigned a single porosity value. This porosity is set conservatively to a low value; generally that of the unaltered wallrock. Where limited matrix diffusion is assumed, only altered wallrock is accessible by diffusion, but the assigned porosity (that of the altered wallrock) is higher. The rate at which radionuclides are transferred from a front migrating along the model conduit is dependent on the *effective* diffusivity - the product of the pore diffusivity and the porosity. This transfer rate is thus lower where unlimited matrix diffusion is assumed, giving rise to earlier radionuclide breakthrough.

A related effect, also due to the limitations of the geosphere transport model, is that the maximum doses arising from individual radionuclides are not always larger when limited, as opposed to unlimited, matrix diffusion is assumed. For example, ^{99}Tc gives a larger maximum dose when unlimited matrix diffusion is assumed. The maximum release from the geosphere is dependent on retardation, which in turn depends on the depth to which radionuclides penetrate the matrix. This depth may be limited either by the total depth of accessible wallrock (particularly for less strongly sorbing or longer-lived radionuclides), or by the extent to which diffusion into the matrix can take place before the radionuclide decays significantly or the concentration gradient reverses due to the radionuclide pulse passing further along the model conduit (for more strongly sorbing or shorter-lived radionuclides). For sorbing radionuclides, the latter is a function of the effective diffusivity and hence the porosity. Although the total depth of the matrix is greater where unlimited matrix diffusion is assumed, the conservative choice of a low porosity can result in a lower depth of matrix penetration than is the case when limited matrix diffusion is assumed for those radionuclides which do not entirely saturate the accessible wallrock.

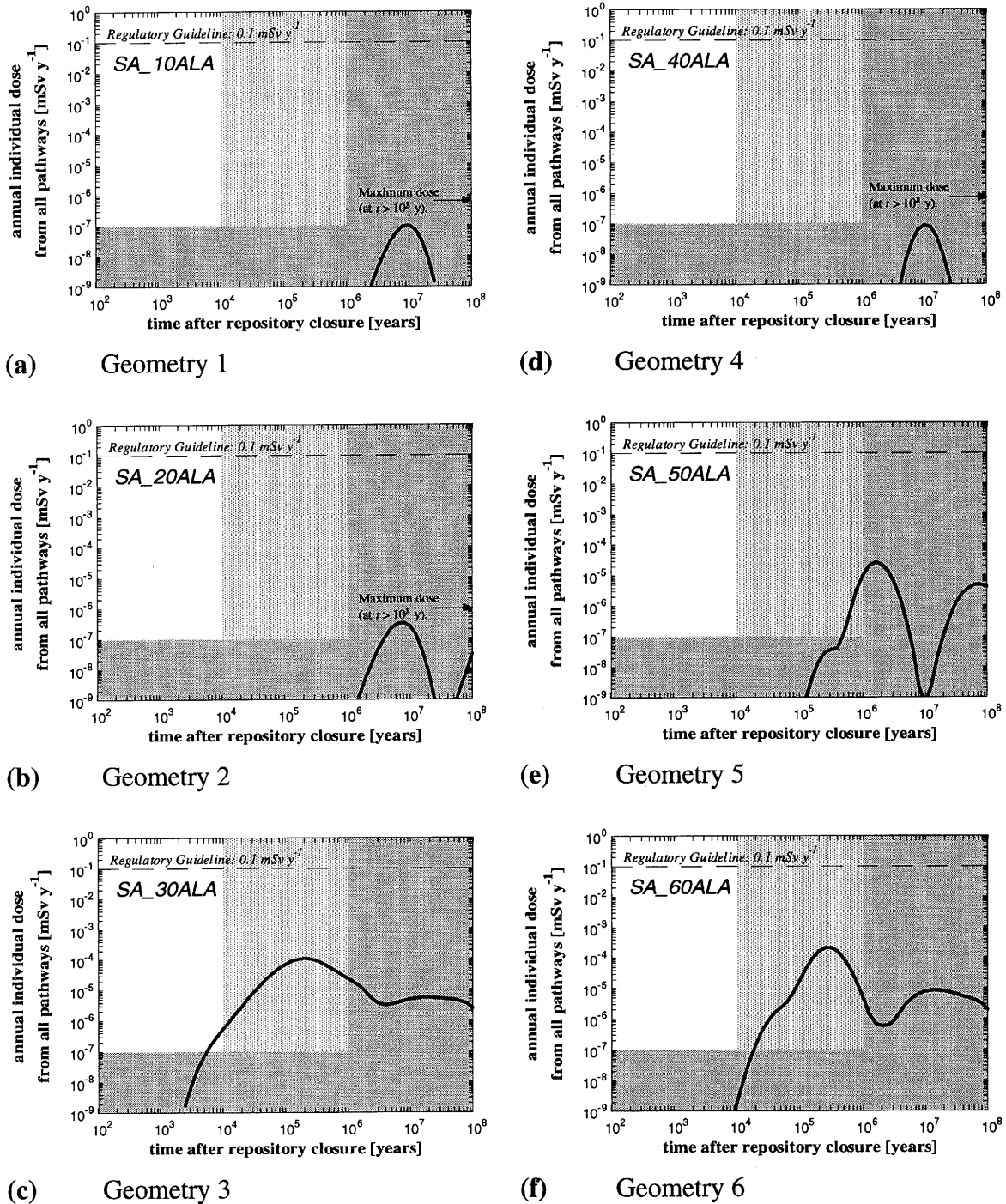
Although the assumption of broad, widely-spaced channels leads to the highest annual individual doses, the alternative interpretations of water-conducting feature geometry may be regarded as equally valid on the basis of available geological data. Figure 6.2.9 illustrates the effect of the different representations on the individual radionuclides in the case of unlimited matrix diffusion in both altered and unaltered wallrock (Geometries 1, 2 and 3). The maximum annual individual doses arising from each of the radionuclides in the calculations is given, irrespective of time of occurrence. As in the discussion of the Reference Case, the role played by the geological barrier is demonstrated by comparison with hypothetical dose maxima that would arise if the radionuclide fluxes from the near field were released directly to the biosphere. In the cases of cataclastic zones/jointed zones with narrow, closely-spaced channels (Geometry 1) and aplite/pegmatite dykes and aplitic gneisses (Geometry 2), the geosphere is highly effective in reducing the doses for most of the radionuclides. Exceptions are the particularly long-lived actinides in the $4N$, $4N + 2$ and $4N + 3$ chains (^{238}U , ^{235}U and ^{232}Th , with half-lives greater than 10^8 years, together with their shorter-lived daughters). Among the activation/fission products, ^{135}Cs is affected least by geosphere transport, but even here the maximum dose is reduced by more than two orders of magnitude. As discussed above, for cataclastic zones/jointed zones with broad, widely-spaced channels (Geometry 3), the geosphere is a far less effective barrier. The difference between this geometry and Geometries 1 and 2 is particularly great for some of the activation/fission products and for the $4N + 1$ chain (^{237}Np and its daughters).

	Unlimited matrix diffusion: altered and unaltered wallrock	Limited matrix diffusion: altered wallrock only
Cataclastic/jointed zones with narrow, closely-spaced channels		
Planar/cylindrical geometry	Cylindrical	
Trace length of channels in the low-permeability domain per unit area of a plane normal to the flow direction	$1.1 \times 10^{-2} \text{ m}^{-1}$	
Extent of accessible matrix (from axis of cylindrical conduit/centre of fracture plane)	$5.0 \times 10^{-2} \text{ m}$	
Matrix porosity	0.25%	3%
Geometry	1	4
Dataset name	SA_10ALA	SA_40ALA
Aplite/pegmatite dykes and aplitic gneisses		
Planar/cylindrical geometry	Planar	
Trace length of channels in the low-permeability domain per unit area of a plane normal to the flow direction	$6.6 \times 10^{-2} \text{ m}^{-1}$	
Extent of accessible matrix (from axis of cylindrical conduit/ centre of fracture plane)	$1.5 \times 10^{-1} \text{ m}$	$2.0 \times 10^{-2} \text{ m}$
Matrix porosity	0.5%	1%
Geometry	2	5
Dataset name	SA_20ALA	SA_50ALA
Cataclastic/jointed zones with broad, widely-spaced channels		
Planar/cylindrical geometry	Planar	
Trace length of channels in the low-permeability domain per unit area of a plane normal to the flow direction	$2.4 \times 10^{-3} \text{ m}^{-1}$	
Extent of accessible matrix (from axis of cylindrical conduit/ centre of fracture plane)	$1.9 \times 10^{-1} \text{ m}$	$5.0 \times 10^{-2} \text{ m}$
Matrix porosity	0.25%	5%
Geometry	3	6
Dataset name	SA_30ALA	SA_60ALA

Notes: Data is taken from Tables 5.3.2 and 5.3.3.

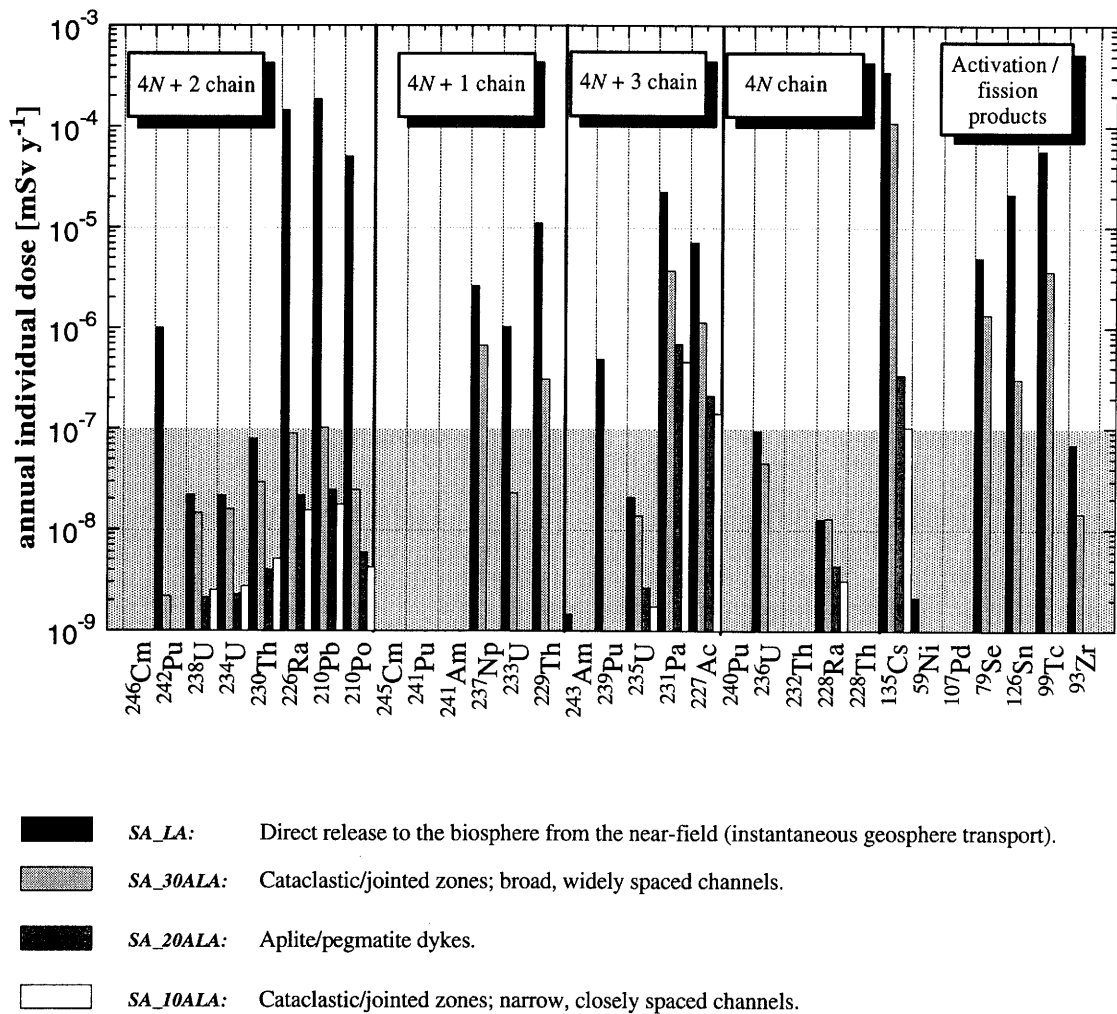
The nomenclature for datasets is discussed in Appendix 4.

Table 6.2.10: Variable parameters and dataset names for model-chain calculations exploring the effects of different representations of the geometry of water-conducting features and of limited matrix diffusion.



Note: The nomenclature for datasets is discussed in Appendix 4.

Figure 6.2.8: Time development of annual individual dose for the six alternative representations of the geometry of water-conducting features. In Geometries 1, 2 and 3, matrix diffusion is modelled in both altered and unaltered wallrock. In Geometries 4, 5 and 6, only altered wallrock is assumed to be available for matrix diffusion. Maximum doses are indicated by arrows in the cases where they arise at times after 10^8 years.



Notes: In the near field and the geosphere, ²¹⁰Pb, ²¹⁰Po, ²⁴¹Pu and ²²⁸Th are assumed to be in secular equilibrium with their immediate precursors. Calculations for ²¹⁰Pb, ²¹⁰Po and ²²⁸Th are only performed in the biosphere. The dose due to ²⁴¹Pu is not calculated, since its parent, ²⁴⁵Cm, decays to insignificance in the near field.

For several radionuclides (higher members of the actinide chains plus ¹⁰⁷Pd), the model-chain calculations give doses less than 10⁻⁹ mSv y⁻¹, even when the release from the near field is input directly to the biosphere.

The nomenclature for datasets is discussed in Appendix 4.

Figure 6.2.9: Comparison of the maximum annual individual doses arising from all the safety-relevant radionuclides for the three different representations of the internal geometry of water-conducting features (with unlimited matrix diffusion). Comparison is also made with the hypothetical case of a direct release of radionuclides from the near field to the biosphere.

As can be seen from the set of curves in Figure 6.2.8, the adoption of cataclastic/jointed zones with broad, widely-spaced channels for the Reference Case is conservative, in that it gives rise to higher annual individual doses than do the other model representations. In reality, it is likely that migrating radionuclides would pass through regions with both narrow, closely-spaced and broad, widely-spaced channels; the former (with a greater volume of matrix available for sorption in the model representation) would be likely to dominate the total transit time of radionuclides through the geosphere, leading to far lower releases than those calculated in the Reference Case.

6.2.2.2 Radionuclide Migration Path

Two alternative assumptions are made concerning the radionuclide migration path through the geosphere (see also Subsection 5.3.1.1):

- radionuclide transport processes in major water-conducting faults are neglected; radionuclides are assumed to be transported instantaneously to the higher-permeability domain on exiting the low-permeability domain;
- radionuclide transport through major water-conducting faults is modelled, taking account of the same processes as in the low-permeability domain, but with modified parameters.

The former assumption is adopted in the Reference-Case calculations. This is both because not all transport paths from the repository would necessarily include the major water-conducting faults and because of the very high degree of uncertainty in the properties of these faults - there is little field data from which their hydraulic properties can be estimated and therefore transport calculations based on the advection velocities given in Table 5.3.2 have to be viewed with caution. However, in order to judge whether a more detailed geological/hydrogeological characterisation of the faults would be valuable, calculations have been performed in which the geosphere transport path is divided into two layers - the first traversing the low-permeability domain and a second along a major water-conducting fault.

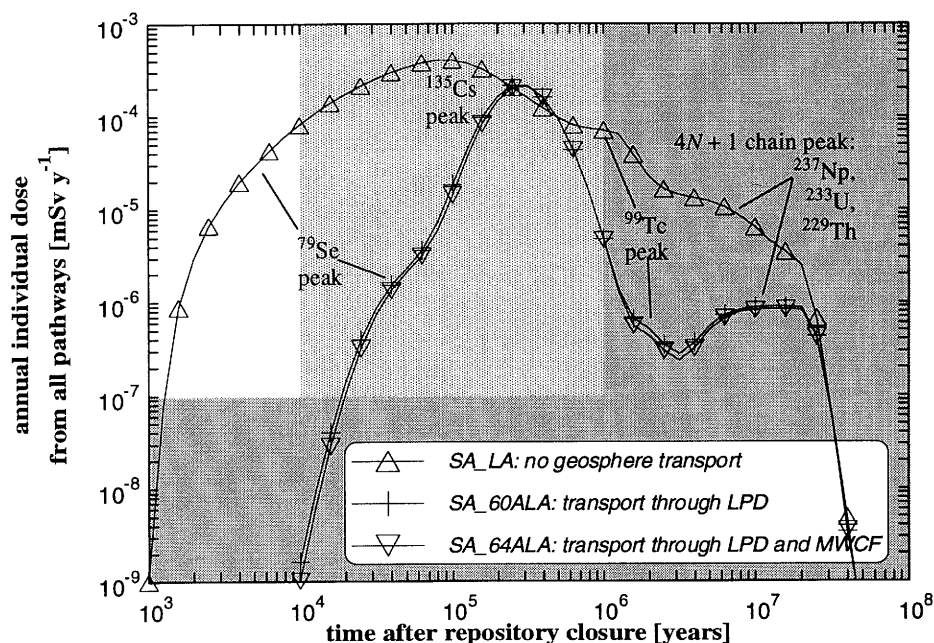
The geosphere data for these calculations are summarised in Table 6.2.11. All parameters, except those associated with the faults, are held at their Reference-Case values. Water-conducting features in the faults are modelled entirely as cataclastic zones/jointed zones with narrow, closely-spaced channels (with limited matrix diffusion). As shown in Figure 6.2.8, this representation is considered to be the least conservative; when applied in the low-permeability domain, it gives a highly effective geosphere barrier. However, it is used here to gauge an upper-limit to the barrier effect which the faults could provide for the given set of hydraulic properties.

Parameter	Low-Permeability Domain	Major Water-Conducting Fault
Geometrical description of water-conducting features	Geometry 6	Geometry 4
Planar / cylindrical geometry	planar	cylindrical
Flow through water-conducting features (per unit length)	$6.3 \times 10^{-4} \text{ m}^2 \text{ y}^{-1}$	$2.1 \text{ m}^2 \text{ y}^{-1}$
Trace length of channels per unit area of a plane normal to the flow direction	$2.4 \times 10^{-3} \text{ m}^{-1}$	$2.7 \times 10^{-2} \text{ m}^{-1}$
Flowpath length	200 m	200 m
Aperture / radius	10^{-3} m	10^{-3} m
Extent of accessible matrix (from axis of cylindrical conduit/ centre of fracture plane):	$5 \times 10^{-2} \text{ m}$	$5 \times 10^{-2} \text{ m}$
Matrix porosity	5%	3%

Table 6.2.11: Selected geosphere parameters for calculations illustrating the effects of explicit consideration of transport processes in major water-conducting faults. (Dataset SA_64ALA).

Figure 6.2.10 shows that, in spite of the non-conservative treatment of water-conducting features within the faults, the assumed high flowrate carried by these features results in rapid transport during which little decay takes place. The faults make a negligible contribution to the geosphere barrier. The figure shows the time development of annual individual dose summed over the three activation/fission products which make the greatest contribution in the Reference Case (^{79}Se , ^{135}Cs and ^{99}Tc) and an example of an actinide chain ($^{237}\text{Np} \rightarrow ^{233}\text{U} \rightarrow ^{229}\text{Th}$ from the $4N + 1$ chain). The Reference Case, in which only transport through the low-permeability domain is calculated, is compared with the case in which transport processes in the faults are also calculated; the results are almost indistinguishable within the resolution of the plot. Again, the role played by the geological barrier is demonstrated by comparison with hypothetical doses which would arise if the radionuclide fluxes from the near field were released directly to the biosphere, showing that retardation in the low-permeability domain, rather than in the faults, accounts for the radionuclide flux reduction across the geosphere.

To further illustrate this point, the ratio of radionuclide flux maxima out of and into the low-permeability domain is compared in Figure 6.2.11 with the ratios for major water-conducting faults. All of the above mentioned radionuclides are shown. The ratios are plotted as a function of transit time to radionuclide half-life ratio (the transit time is based on the steady-state solutions discussed in Appendix 8). The half-life of each radionuclide is shown to exceed the transit time through the faults, so that little decay can occur during transport. By contrast, the flux during transport through the low-permeability domain is reduced by as much as two orders of magnitude in the case of ^{99}Tc .



Note: The nomenclature for datasets is discussed in Appendix 4.
 LPD = low-permeability domain, MWCF = major water-conducting faults.

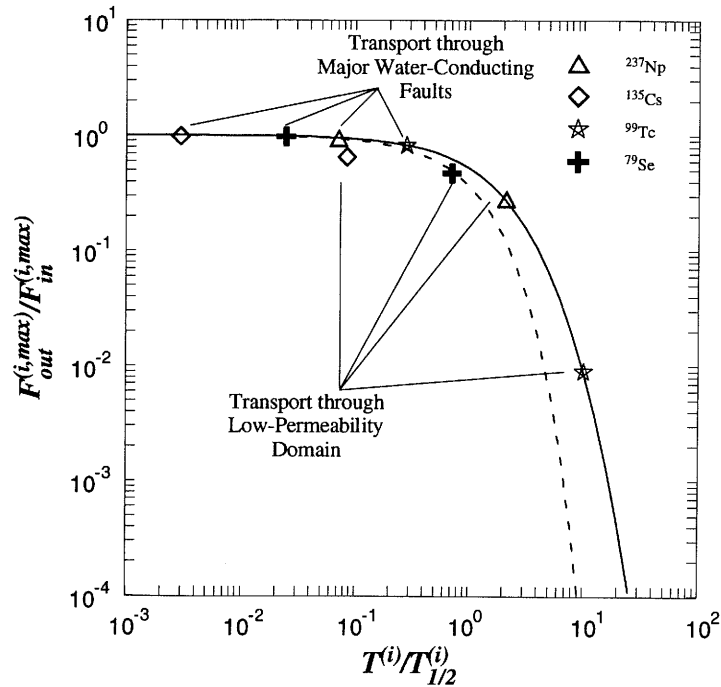
Figure 6.2.10: The effect of explicit consideration of transport in major water-conducting faults. The time development of the annual individual dose for the radionuclides ^{79}Se , ^{99}Tc , ^{135}Cs and the $4N + 1$ chain ($^{237}\text{Np} \rightarrow ^{233}\text{U} \rightarrow ^{229}\text{Th}$) is compared to the results of the Reference Case and a hypothetical case of direct release from near field to biosphere.

6.2.2.3 Sorption on Groundwater Colloids

Colloid-facilitated transport is omitted in the Reference-Case calculations; currently available experimental data and the level of understanding of relevant processes are rather limited, which explains the highly simplistic treatment of colloid transport in the model described in Section 5.3. However, with an appropriate choice of conservative parameters, the model can at least be used to place an upper bound on the consequences of sorption on groundwater colloids.

The process of radionuclide sorption on groundwater colloids enters into the model-chain calculations in two ways (see Subsection 5.3.3.3):

- Through an increased "effective" groundwater flowrate in the near-field calculations. This models the reduction in radionuclide concentration in solution at the bentonite-host rock interface due to sorption on groundwater colloids. The result is an increase in the concentration gradients which drive the diffusion of radionuclides across the bentonite.



Note: Comparison is made with steady-state analytical solutions: steady-state solution for the Peclet number used in the time-dependent calculations ($Pe = 10$, continuous line) and for the case of zero dispersion ($Pe = \infty$, broken line).

Figure 6.2.11: The ratios of radionuclide flux maxima out of and into a geosphere model conduit ($F_{out}^{(i,max)}/F_{in}^{(i,max)}$) as a function of transit time to radionuclide half-life ratio ($T^{(i)}/T_{1/2}^{(i)}$), for transport through the low-permeability domain and for transport through major water-conducting faults. The transit time is based on the steady-state solutions discussed in Appendix 8.

- Through a modified retardation factor and a modified advection velocity in the geosphere calculations. These model the reduction in retardation which is experienced by radionuclides sorbed on colloids, given the highly conservative model assumptions that colloids do not interact with the fracture walls and are excluded from matrix pores.

In general, both the colloid concentration and the degree to which radionuclides sorb on individual colloids affect the total sorption of radionuclides on colloids and hence the conditions under which colloids affect transport. In the simple transport model described in Subsection 5.3.3.3, χ is defined as the colloid concentration (mass of colloids per unit volume of water) and K_c is the sorption constant for the radionuclide on colloids. When $\chi K_c \ll 1$, colloids have no effect on either the effective groundwater flowrate at the bentonite-host rock interface Q' (Equation 5.3.17), or, in the geosphere model itself, on the effective retention factor $R_f^{(i)}$ (Equation 5.3.15), and the effective velocity u' (Equation 5.3.16). Colloids thus have no influence on transport when the condition

velocity u' (Equation 5.3.16). Colloids thus have no influence on transport when the condition $\chi K_c \ll 1$ is satisfied (see also the discussions and conclusions in SMITH 1993a). As mentioned above, there is a high degree of uncertainty in the required data; particularly in the sorption properties of groundwater colloids in the crystalline basement of Northern Switzerland. However, a very conservative assumption for ions of tetravalent Np, U and Th is that their sorption on colloids is quantified by the high sorption constant of $K_c = 10^4 \text{ m}^3 \text{ kg}^{-1}$ and that the colloid population itself can be assigned a concentration of 0.1 ppm ($\chi = 10^{-4} \text{ kg m}^{-3}$), as discussed in Subsection 3.5.4. Under these assumptions, sorption on colloids may affect transport of Np, U and Th; sorption of other species is weaker by an order of magnitude or more and so is not considered further.

Only very limited data are currently available for the interaction of colloids with the walls of the channels along which they are advected (for example, filtration effects: see GRAUER 1990b). Uncertainty is thus replaced by conservatism and interaction is assumed not to occur ($K_a = 0$), although a high degree of attachment might be expected in reality (DEGUELDRE 1994). It is further assumed that colloids are transported with the same advection velocity as is applied to solutes ($u_c = u$). This is a non-conservative assumption; colloids may be advected faster than solutes since they tend to stay in the centre-stream (this phenomenon is employed in hydrodynamic chromatography, discussed in DODDS 1982). The effect, however, is likely to be small, affecting the advection velocity by no more than 30%.

As explained above, both the near field and the geosphere are less effective as migration barriers when the conservative assumptions are made concerning the role of groundwater colloids. This is illustrated in Figure 6.2.12, which shows the results of a series of calculations for the $4N + 1$ chain ($^{237}\text{Np} \rightarrow ^{233}\text{U} \rightarrow ^{229}\text{Th}$), using all six representations of the internal geometry of water-conducting features. The Reference-Case biosphere is used in all the calculations.

Results are compared in Figure 6.2.12 with the corresponding results when colloid transport is neglected (reproduced from Figure 6.2.8). The role played by the geological barrier is demonstrated by a comparison with the results from a set of hypothetical cases, in which radionuclide fluxes from the near field are released directly to the Reference-Case biosphere, but with the effect of the colloids on the near-field outer boundary included. This may be regarded as corresponding to very rapid transport through the geosphere.

Colloid transport has a large effect on the radiological impact for the less conservative water-conducting feature geometries (see, in particular, aplite/pegmatite dykes and aplitic gneisses), although the magnitude of the doses is still extremely small. For the more conservative representations, particularly cataclastic/jointed zones with broad, widely-spaced channels, the effect is much smaller. This is simply explained since, for the $4N + 1$ chain, the effectiveness of the geological barriers is limited, even where sorption on colloids is not considered.

6.2.2.4 Groundwater Flowrate Variability

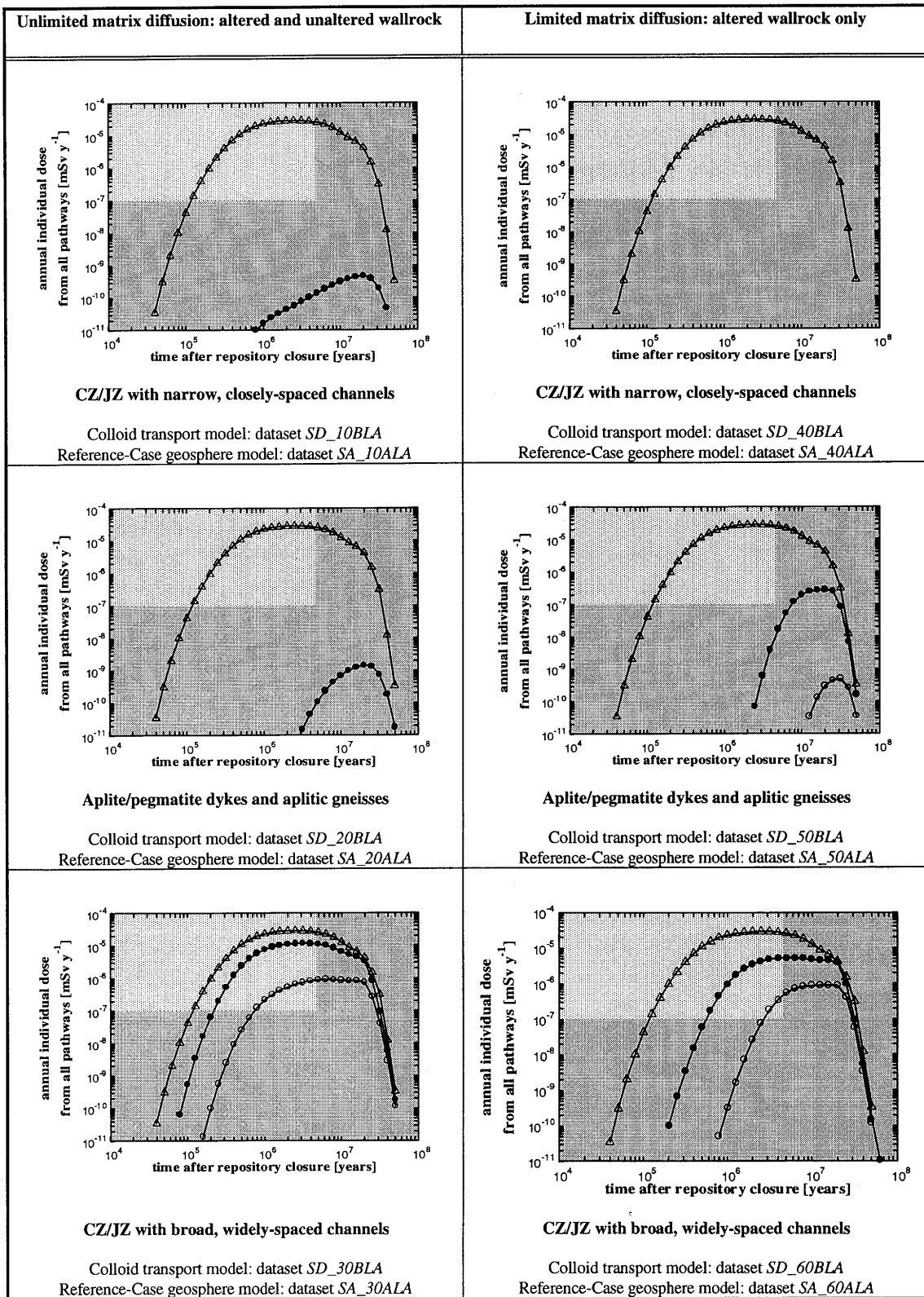
Results are presented in Subsections 5.2.3.7 and 5.3.5.2 (for a subset of the safety-relevant radionuclides), which show the sensitivity of the near field and geosphere to groundwater flowrate. These calculations are simplified in that it is assumed that all water-conducting features which intersect the repository tunnel system carry the same flowrate, although there is uncertainty in its value. Figure 6.2.13 (adapted from Figure 10-4 in THURY et al. 1994), however, shows that, in addition to uncertainty in the flowrate through "representative" water-conducting features, there is variability between the features. This arises from variability in the hydraulic gradient, transmissivity and density of the water-conducting features modelled.

The distribution shown in Figure 6.2.13 is used, in a very simplistic approach, to investigate the effects of groundwater flowrate variability on transport. This approach is not included in the Reference Model Assumptions because of limitations and conservatism in the method used to derive the distribution³⁸.

The water-conducting features (equivalent to the "transmissive elements" of the hydrogeological model) are divided into three groups. One group is assigned a flowrate equal to the geometric mean (as in the Reference Case), while the other two are assigned flowrates 10 and 100 times higher. The number of features assigned to each group is determined from a coarse discretisation of the flowrate distribution, as illustrated in Figure 6.2.13. For example, the 50% of features with flowrates *less than* the geometric mean (based on the results of hydrogeological modelling) are assigned the geometric mean flowrate for the purpose of transport modelling. The groups then consist, respectively, of 50%, 47% and 3% of water-conducting features. This coarse discretisation is conservative in that it overestimates the total water flow, summed over all features. It is assumed that each group carries the radionuclides released from an equal proportion of the repository near field. This assumption implies a limited axial hydraulic conductivity along the emplacement tunnels at the bentonite-host rock interface i.e. along the excavation-disturbed zone.

The discretisation described above can then be used to determine a weighted sum of the dose-histories calculated for each of the three flowrates. The flowrate affects the boundary condition at the bentonite-host rock interface in the near-field calculations and the advection velocity in the geosphere calculations; separate model-chain calculations are therefore required for each of the flowrates. In the calculations, all parameters except those associated with the groundwater flowrate are set to their Reference-Case values. The flowrates for these calculations are given in Table 6.2.12. The final dose-history consists of a sum of 50% of the Reference-Case dose history, 47% of the dose history for a 10-fold flowrate increase and 3% of that for a 100-fold flowrate increase; this is plotted in Figure 6.2.14.

³⁸ In deriving this distribution, no dynamic calculations were performed: hydraulic gradients and transmissivities were assumed to be independent. Since high gradients would, in reality, be expected to coincide with low transmissivities (and vice versa), this assumption is conservative.



○—○ Reference-Case geosphere transport model.

●—● Colloid-facilitated geosphere transport.

▲—▲ Direct release from the near field to the biosphere (instantaneous geosphere transport), including the effect of groundwater colloids on the near field.

Figure 6.2.12:

Notes: In the cases of Geometries 1,2 and 4, there is effectively no release from the geosphere for this actinide chain when calculations are performed using the Reference Model Assumptions for the geosphere. For Geometry 4, this is also true when colloid facilitated transport is included in the geosphere model.

CZ/JZ = Cataclastic zones and jointed zones.

The nomenclature for datasets is discussed in Appendix 4.

Figure 6.2.12: The effect of colloid-facilitated transport, assessed for each of the six: representations of water-conducting feature geometry, for the $4N + 1$ chain ($^{237}\text{Np} \rightarrow ^{233}\text{U} \rightarrow ^{229}\text{Th}$). In each case, the annual individual doses arising from colloid-facilitated transport in the geosphere are compared with the corresponding results when colloid facilitated transport is neglected and when transport through the geosphere is considered instantaneous, but with the effect of colloids on the near-field outer boundary condition included (dataset *SD_LA*).

The clearest difference between the results of this weighted sum and the Reference-Case results of Figure 6.2.1 is in the contribution from the $4N + 2$ chain. ^{226}Ra moves out of equilibrium with its parent at the highest flowrate and gives a greatly enhanced contribution to the total dose. Significantly enhanced contributions arise from the plutonium isotopes ^{239}Pu and ^{242}Pu in the $4N + 3$ and $4N + 2$ chains, respectively, from ^{237}Np in the $4N + 1$ chain and from the activation/fission products ^{126}Sn and ^{99}Tc .

Comparing the total dose summed over all radionuclides with that in the Reference Case, the maximum dose is little changed (less than an order of magnitude). However, relatively high doses arise earlier and persist over a longer time span when groundwater flowrate variability is taken into account.

	Reference Case (dataset <i>SA_60ALA</i>)	10-fold flowrate increase (dataset <i>XA_60JLA</i>)	100-fold flowrate increase (dataset <i>XB_60KLA</i>)
Near-Field flowrate	3.0 m ³ y ⁻¹ through the repository area	30 m ³ y ⁻¹ through the repository area	300 m ³ y ⁻¹ through the repository area
Geosphere flowrate	6.3 × 10 ⁻⁴ m ² y ⁻¹ through water-conducting features (per unit length)	6.3 × 10 ⁻³ m ² y ⁻¹ through water-conducting features (per unit length)	6.3 × 10 ⁻² m ² y ⁻¹ through water-conducting features (per unit length)

Note: The nomenclature for datasets is discussed in Appendix 4.

Table 6.2.12: Groundwater flowrates for calculations used to illustrate the effects of flowrate variability.

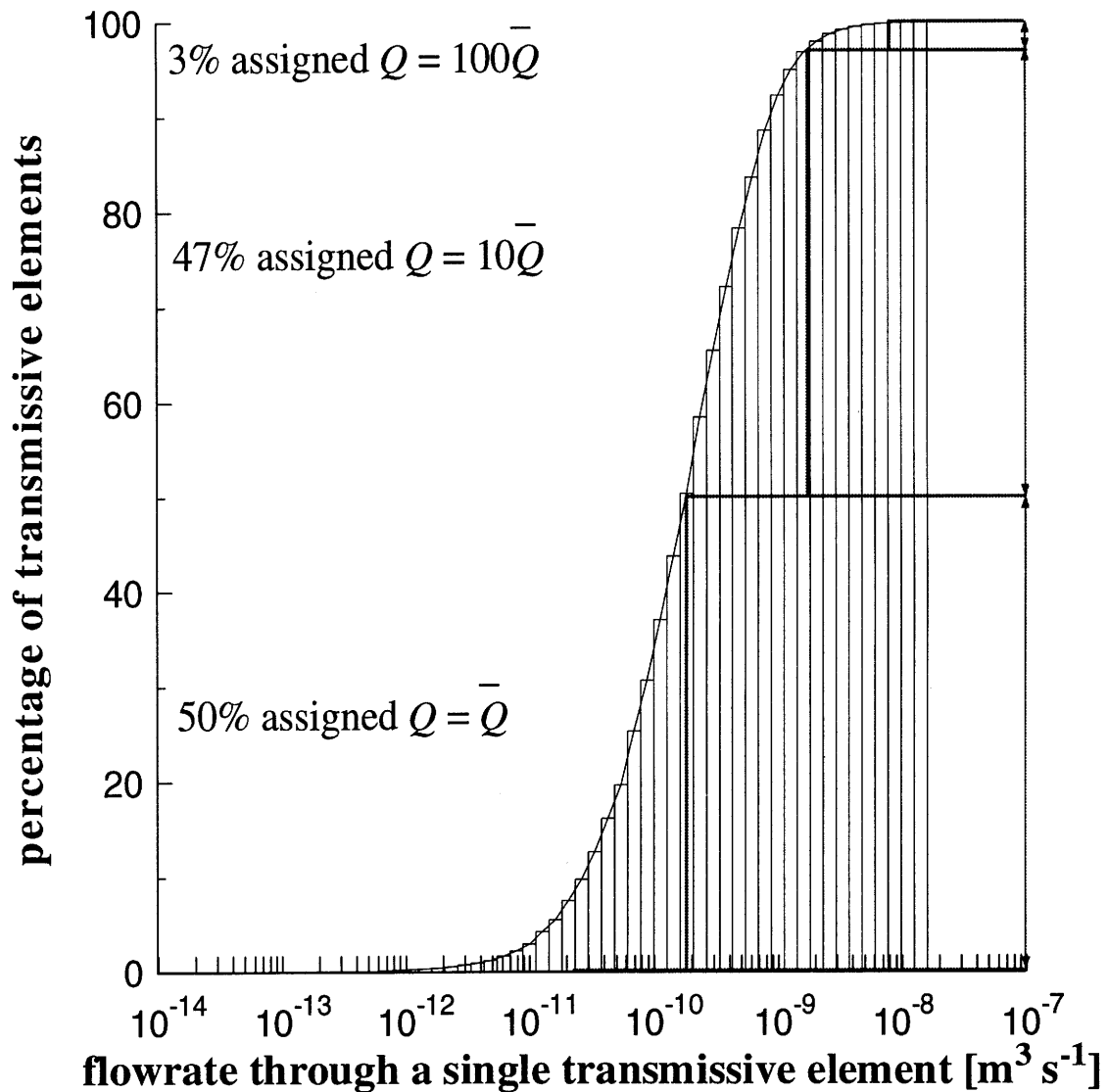
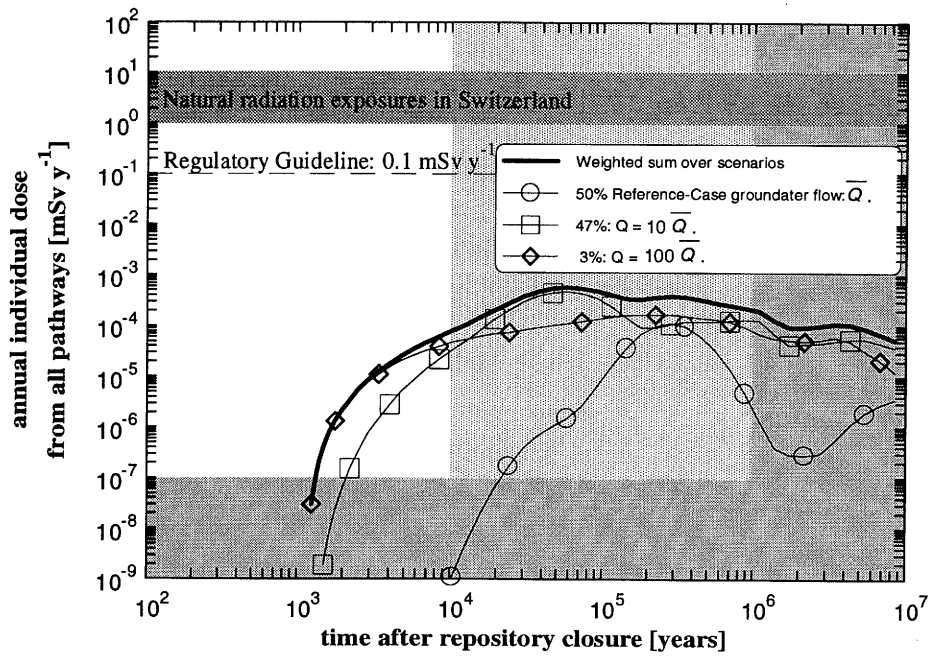
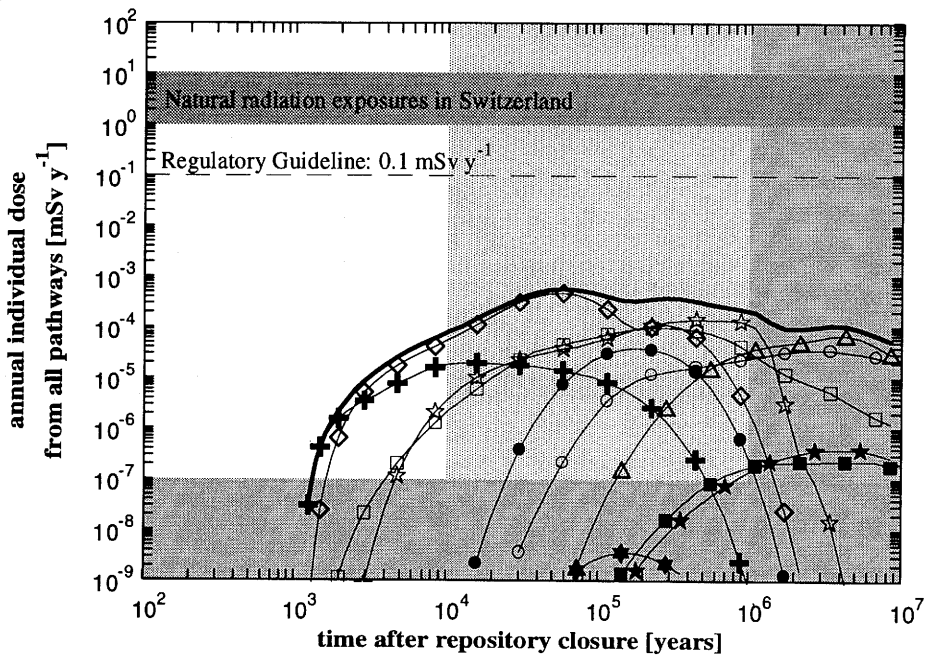


Figure 6.2.13: (adapted from Figure 10-4 in THURY et al. 1994): Cumulative distribution of transmissive-element flowrate for the "sparse" hydrogeological model. (See Subsection 3.5.3). The transmissive elements are equivalent to the water-conducting features of the geosphere model. In order to analyse the consequences of this flowrate variability, water-conducting features are divided into three groups. One group is assigned a flowrate equal to the geometric mean (the Reference Case), while the other two are assigned flowrates 10 and 100 times higher (flowrates for the calculations are given in Table 6.2.12). The groups consist respectively of 50%, 47% and 3% of features. Model-chain calculations are performed for each group separately. A weighted sum of the results gives the final dose history (Figure 6.2.14).



(a) Contributions from each group of water-conducting features to the summed dose-history.



(b) Contributions of individual radionuclides to the weighted summed dose-history.

Key to radionuclides.

—	Sum over nuclides.	△	4N + 1 chain	★	⁵⁹ Ni	●	¹²⁶ Sn
○	4N + 3 chain	★	4N chain	×	¹⁰⁷ Pd	☆	⁹⁹ Tc
□	4N + 2 chain	◇	¹³⁵ Cs	+	⁷⁹ Se	■	⁹³ Zr

Figure 6.2.14: Analysis of the effects of flowrate variability. (See Figure 6.2.13 and text for details).

6.3 Alternative Scenarios

6.3.1 Introduction

Alternative scenarios are discussed qualitatively in Chapter 4 and a number of these are identified for quantitative consideration. Alternative scenarios for which calculations are performed are summarised in Table 6.3.1.

(i) Deep Groundwater Well	
All radionuclides are captured by a deep well.	<i>SA_60AMB</i>
(ii) Tunnel/Shaft Seal Failure	
Radionuclides are transported through the shaft backfill.	<i>XB_00TLA</i>
Radionuclides are transported through the shaft excavation-disturbed zone.	<i>XB_00VLA</i>
(iii) Alternative Climate-Related Scenarios	
Dry Climate State with reduced precipitation and increased evapotranspiration; increased irrigation from aquifer, present-day subsistence agriculture.	<i>SA_60ALD</i>
Humid Climate State with increased precipitation and evapotranspiration; no irrigation, present-day subsistence agriculture.	<i>SA_60ALH</i>
Periglacial Climate State , in which permafrost prevents interaction between deep groundwater and local aquifer (assumed frozen); all water obtained from the river, modified river with reduced flow because of reduced precipitation, reduced evapotranspiration.	<i>SA_60ALC</i>
Rhine Gravels Absent , no local aquifer, present-day subsistence agriculture: - release to the Rhine water; - release to deep soil.	<i>SA_60ARA</i> <i>SA_60ARS</i>

Note: The nomenclature for datasets (right-hand column) is discussed in Appendix 4.

Table 6.3.1: Alternative scenarios considered quantitatively. (Other scenarios are discussed qualitatively in Chapter 4).

6.3.2 Deep Groundwater Well

Wells for extraction of deep groundwater are not uncommon in the region. In this scenario, radionuclides are released from the water-conducting features of the low-permeability domain into the catchment area of a deep well in the higher-permeability domain of the crystalline basement. It is conservatively assumed that all the released radionuclides are captured by the well.

The flux through the repository area in the Reference Case is $3 \text{ m}^3 \text{ y}^{-1}$. This is much less than the $0.5 \text{ m}^3 \text{ min}^{-1}$ ($3 \times 10^5 \text{ m}^3 \text{ y}^{-1}$) pumping rate assumed for the well and implies that nearly all of the water captured by the well originates from elsewhere (e.g.

the higher-permeability domain). The rate of $0.5 \text{ m}^3 \text{ min}^{-1}$ is comparable to the current extraction rate of the deep well at Zurzach ($0.6 \text{ m}^3 \text{ min}^{-1}$; LÖW et al. 1993).

Doses in this scenario are given by

$$D_{\text{water}} = D_{\text{ing}} I_{\text{wat}} \frac{J}{Q_{\text{abs}}}, \quad (6.3.1)$$

where the dose per unit intake D_{ing} [Sv Bq^{-1}] and the rate of ingestion of water I_{wat} [$\text{m}^3 \text{ y}^{-1}$] are the values used also in the Reference-Case calculations (Appendix 7; Tables 7.1 and 7.3). The radionuclide release entering the region of water extraction by the well is J [Bq y^{-1}], taken from the Reference-Case geosphere calculations, and the extraction rate is Q_{abs} [$\text{m}^3 \text{ y}^{-1}$]. Equation 6.3.1 assumes that the water is not filtered and that all radionuclides released from the geosphere are captured by the well.

The results are summarised in Table 6.3.2.

Radio-nuclide	Deep Groundwater Well (dataset SA_60AMB)		Reference Case (dataset SA_60ALA)			Ratio of Doses SA_60AMB/ SA_60ALA
	Maximum Dose [mSv y ⁻¹]	Time of Maximum [y]	Maximum Dose [mSv y ⁻¹]	Time of Maximum [y]	Maximum Pathway	
¹³⁵ Cs	6.1×10^{-4}	2.8×10^5	2.3×10^{-4}	2.8×10^5	Meat	2.7
4N + 2	9.0×10^{-6}	$> 10^7$	4.1×10^{-7}	$> 10^7$	Well water	22.1
4N + 3	7.7×10^{-6}	$> 10^7$	7.1×10^{-6}	$> 10^7$	Meat	1.1
4N + 1	1.8×10^{-6}	$> 10^7$	8.9×10^{-7}	$> 10^7$	Root veg.	2.1
⁷⁹ Se	1.7×10^{-6}	6.5×10^4	2.3×10^{-6}	7.2×10^4	Meat	0.7
4N	4.8×10^{-7}	$> 10^7$	8.8×10^{-8}	$> 1 \times 10^7$	Dust inhal.	5.5
⁹⁹ Tc	1.4×10^{-7}	1.8×10^6	5.1×10^{-7}	1.8×10^6	Milk	0.3
⁹³ Zr	2.2×10^{-8}	1.0×10^7	1.3×10^{-8}	$> 10^7$	Meat	1.7
¹²⁶ Sn	4.0×10^{-9}	8.3×10^5	3.6×10^{-9}	8.8×10^5	Grain	1.1
¹⁰⁷ Pd	5.6×10^{-13}	4.3×10^6	5.9×10^{-14}	4.3×10^6	Grain	9.6
⁵⁹ Ni	3.9×10^{-13}	6.9×10^5	8.6×10^{-14}	7.0×10^5	Grain	4.6

Note: The nomenclature for datasets is discussed in Appendix 4.

Table 6.3.2: Summary of the potential radiological impact of drinking water from a deep well capturing all radionuclides released from the repository. For comparison, results from the Reference Case are also given. The radionuclides are ordered from maximum dose to minimum dose for this alternative scenario. The shaded regions indicate where the dose maxima are below $10^{-7} \text{ mSv y}^{-1}$.

The doses are well below the regulatory guideline for all calculated radionuclides and, as in the Reference Case, the largest dose arises from ^{135}Cs . The table also provides a comparison with the results from the Reference Case. In the Reference Case, the diluting flow in the gravel aquifer is $10.5 \text{ m}^3 \text{ min}^{-1}$ ($5.5 \times 10^6 \text{ m}^3 \text{ y}^{-1}$; Table 5.4.3), giving a dilution 21 times greater than in the deep groundwater well scenario (with a pumping rate of $0.5 \text{ m}^3 \text{ min}^{-1}$). Only the doses from the $4N + 2$ chain reflect this ratio³⁹. This is because the largest contribution to the dose maximum for this chain (from ^{210}Pb) comes via the drinking-water (well) pathway. For the other important contributors to dose, the factor is much less (e.g. 2.7 for ^{135}Cs) and, in some cases, the Reference-Case doses are higher (^{79}Se and ^{99}Tc), in spite of the greater dilution. This occurs because the processes considered in the biosphere model of the Reference Case effectively mean that individual doses arise from contact with a much greater volume of contaminated water than the 0.7 m^3 consumed annually in the drinking-water pathway (see Table A7.1 in Appendix 7); the exposure-pathway model represents not only intake of the radionuclides within drinking water, but also, for example, indirect intake of the radionuclide content of water consumed by livestock - hence the relevance of the meat-consumption pathway.

In order to place the results of the Deep Groundwater Well scenario in perspective, a comparison can be made between the maximum dose calculated for this scenario with that due to the natural actinide content of Swiss mineral water given, for example, in BAERTSCHI & KEIL (1992). Assuming that the entire annual drinking water consumption of $0.7 \text{ m}^3 \text{ y}^{-1}$ is made up of such mineral water, a dose from the natural actinides of about $3 \times 10^{-2} \text{ mSv y}^{-1}$ would arise⁴⁰: higher by a factor of about 50 than that of the Deep Groundwater Well scenario and two orders of magnitude higher than that of the Reference Case.

A final point to note in this analysis concerns the likelihood that such a deep well would capture all radionuclides from the repository. The region of influence of a borehole would need to intersect the radionuclide transport pathways in such a way that all the radionuclides are intercepted, otherwise there would be greater dilution than is assumed here. Some idea of the likelihood of this scenario would be obtained by considering the region of influence of the well compared with the total area from which water could be extracted. This factor is likely to be very small. However, since the doses in this scenario are, in any case, less than the regulatory guideline, there is no requirement to estimate the likelihood of occurrence.

³⁹ The ratio of doses for the $4N + 2$ chain is not exactly equal to the ratio of the dilutions because of the very slight amount of decay during the time taken for the local aquifer concentration to reach its steady-state value in the Reference Case.

⁴⁰ In Appendix 1 (Figure A1.2), the dose arising from the consumption of 0.2 litres of natural mineral water per day ($0.07 \text{ m}^3 \text{ y}^{-1}$) is given as $2.8 \times 10^{-3} \text{ mSv y}^{-1}$.

6.3.3 Tunnel/Shaft Seal Failure

After closure of the repository, all access tunnels and shafts will be backfilled. The shafts will be provided with sealing plugs to prevent the backfill and the surrounding excavation-disturbed zones, which may have significantly higher hydraulic conductivities than the adjacent undisturbed host rock, from providing a rapid transport path from the repository to the biosphere (see Subsection 3.4.5).

In the Reference Scenario of the Kristallin-I safety assessment, it is supposed that the sealing performs as expected for all calculated times, so that release via the shaft can be neglected. In an alternative scenario, it is envisaged that the shaft becomes the dominant migration pathway. No detailed hydrogeological modelling has been carried out for this scenario. Rather, it is conservatively assumed that the repository, including the shaft, offers negligible resistance to water flow (although radionuclide transport processes are considered). Water flow through the system is controlled by how much water the low-permeability host rock can supply to the repository. Because the emplacement tunnels have a much larger surface area than the shaft, it is assumed that water flow from the host rock into the repository tunnel system (including excavation-disturbed zones), is much larger than the flow from the host rock directly into the shaft. The latter is neglected and it is assumed that the entire flow into the tunnel system is channelled through the shaft to the higher-permeability domain and thence to the biosphere.

The repository is located in an exfiltration area and a difference in hydraulic head Δh [m] between the repository tunnel system and the undisturbed host rock would be expected to be not more than about 100 m. If the repository is modelled as a disk of radius R [m], located inside an equivalent porous medium of hydraulic conductivity K [m y^{-1}], the flux into the repository is given approximately by $8K\Delta hR$.⁴¹ Taking the "diameter" of the repository to be in the order of 500 m and $K = 1.3 \times 10^{-3} \text{ m y}^{-1}$ (large-scale hydraulic conductivity for the crystalline low-permeability domain; Table 3.7.4), the total water flow into the repository and through the shaft is $265 \text{ m}^3 \text{ y}^{-1}$. This is in the order of 100 times the groundwater flowrate in the Reference Case ($3 \text{ m}^3 \text{ y}^{-1}$ through the repository area); a flowrate of 100 times the Reference Case ($300 \text{ m}^3 \text{ y}^{-1}$) is assumed in modelling this alternative scenario.

A set of radionuclide transport calculations has been performed for this scenario. The flowpath length along the shaft is constrained by the vertical distance from the repository to the higher-permeability domain of the crystalline basement (which itself is attributed no capacity to retard radionuclide migration). A 200 m flowpath length is therefore assumed, as in the Reference-Case calculations.

⁴¹ An analogy can be used here with electromagnetic theory, in which the capacitance of a disk of conducting material is known to be equal to $8\epsilon_0 R$, where ϵ_0 is the dielectric constant (see, for example, SMYTHE 1968, p.124).

The shaft has a diameter of 6.6 m (NAGRA 1985); its excavation-disturbed zone is assumed to form an annular region around the shaft with a thickness of about one shaft radius. If the dominant migration path is considered to be through the shaft backfill, the area through which migration takes place is therefore 34 m², whereas, if transport through the excavation-disturbed zone dominates, the corresponding area is 103 m². In calculating the consequences of ineffective shaft/tunnel seals, transport through the backfill and through the excavation-disturbed zone are modelled separately. The Darcy velocity is $v = 8.7 \text{ m y}^{-1}$ for migration through the shaft backfill and $v = 2.9 \text{ m y}^{-1}$ for the surrounding excavation-disturbed zone.

The transport path is modelled as an equivalent porous medium⁴² with porosity ε . The transport equation is adapted from Equation (5.3.1), with the advection velocity u replaced by v/ε and the matrix-diffusion term omitted:

$$\frac{\partial C_f^{(i)}}{\partial t} = \frac{1}{\varepsilon R_f^{(i)}} \left[-v \frac{\partial C_f^{(i)}}{\partial z} + a_L \frac{\partial}{\partial z} \left[v \left(\frac{\partial C_f^{(i)}}{\partial z} \right) \right] + \varepsilon R_f^{(i)} \left(\lambda^{(i-1)} C_f^{(i-1)} - \lambda^{(i)} C_f^{(i)} \right) \right] \quad (6.3.2)$$

The effects of sorption are expressed through the retardation factor $R_f^{(i)}$ [-], calculated from the approximation (valid for sorbing radionuclides) that:

$$\varepsilon R_f^{(i)} \approx \rho K_d^{(i)} \quad , \quad (6.3.3)$$

where ρ is the solid density. A value of ε need not, therefore, be specified for the flowpath itself (all material outside the flowpath is considered to lack connected porosity). Sorption properties of the undisturbed host rock (Table 3.7.8) are also applied in the excavation-disturbed zone and in the shaft backfill.

Radionuclide transport along the shaft is assumed to occur immediately following release from the repository. Release from the repository is calculated using the code STRENG; with the exception of the groundwater flowrate, the Reference-Case dataset is used. Transport along the shaft is calculated using RANCHMD; the dataset used is summarised in Table 6.3.3. The biosphere is modelled using the code TAME with the Reference-Case dataset.

The time development of doses calculated for this scenario is shown in Figure 6.3.1(a) (transport through shaft backfill) and Figure 6.3.1(b) (transport through the excavation-disturbed zone). For comparison, Figure 6.3.2 shows the results from the Reference Case (i.e. with transport through the low-permeability domain of the host rock) alongside the results for transport along the shaft backfill and transport through the excavation-disturbed zone. It can be seen that the results of transport through the

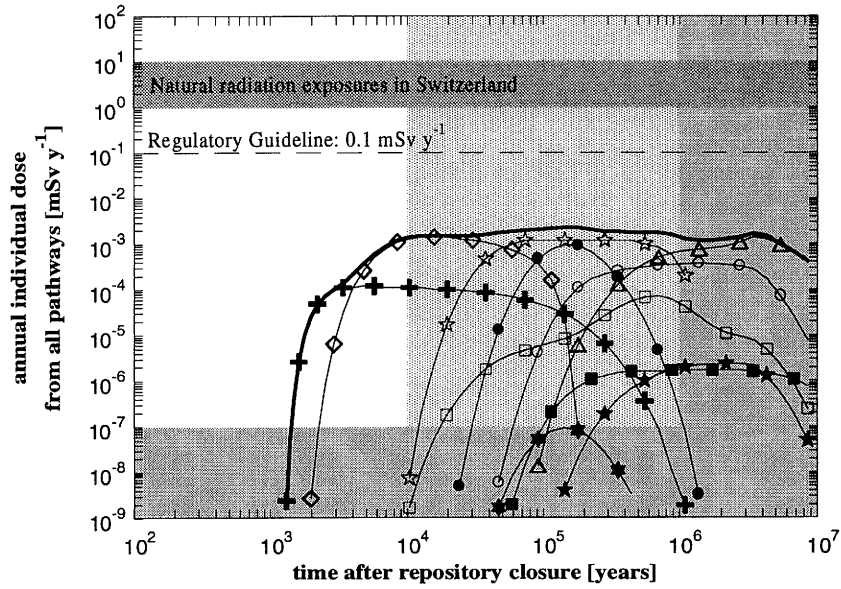
⁴² The treatment of the excavation-disturbed zone as an equivalent porous medium is not conservative. More rapid radionuclide transport would result if the zone were treated as a fractured medium, in the same way as the low-permeability domain of the host rock. However, the required data for such an approach are not currently available.

backfill and through the excavation-disturbed zone are similar. The only difference in the input parameters is the Darcy velocity, which is higher by a factor of about 3 for the backfill. The maximum dose in each case is increased by about an order of magnitude with respect to the Reference Case. In the Reference Case, the largest contributor to dose is ^{135}Cs at times between 100 000 and one million years. Other radionuclides give contributions that are orders of magnitude lower. In the case of shaft-seal failure, different radionuclides dominate the dose at different times, giving a total dose that remains relatively constant from a few thousand years after emplacement to beyond a million years. ^{135}Cs is followed as the dominant radionuclide by ^{99}Tc and, beyond a million years, by the $4N + 1$ actinide chain.

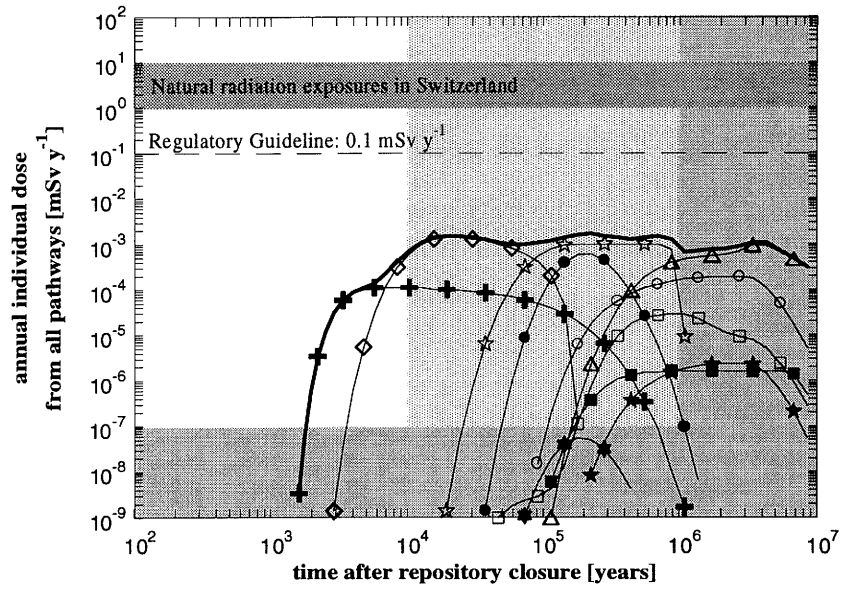
At all calculated times the doses calculated for this alternative scenario are more than an order of magnitude below the regulatory guideline of 0.1 mSv y^{-1} .

Parameter	Transport through Shaft Backfill	Transport through Shaft Excavation-Disturbed Zone
Flowrate through repository area	$300 \text{ m}^3 \text{ y}^{-1}$	
Darcy velocity	8.7 m y^{-1}	2.9 m y^{-1}
Flowpath length	200 m	
K_d values	Element-dependent "realistic-conservative" values (see Table 3.7.6)	

Table 6.3.3: Parameters for modelling transport along either the shaft or the surrounding excavation-disturbed zone (EDZ) for a scenario in which the shaft seals fail. The cases of transport through the shaft backfill and transport through the shaft excavation-disturbed zone are considered separately.



(a) Transport through backfill



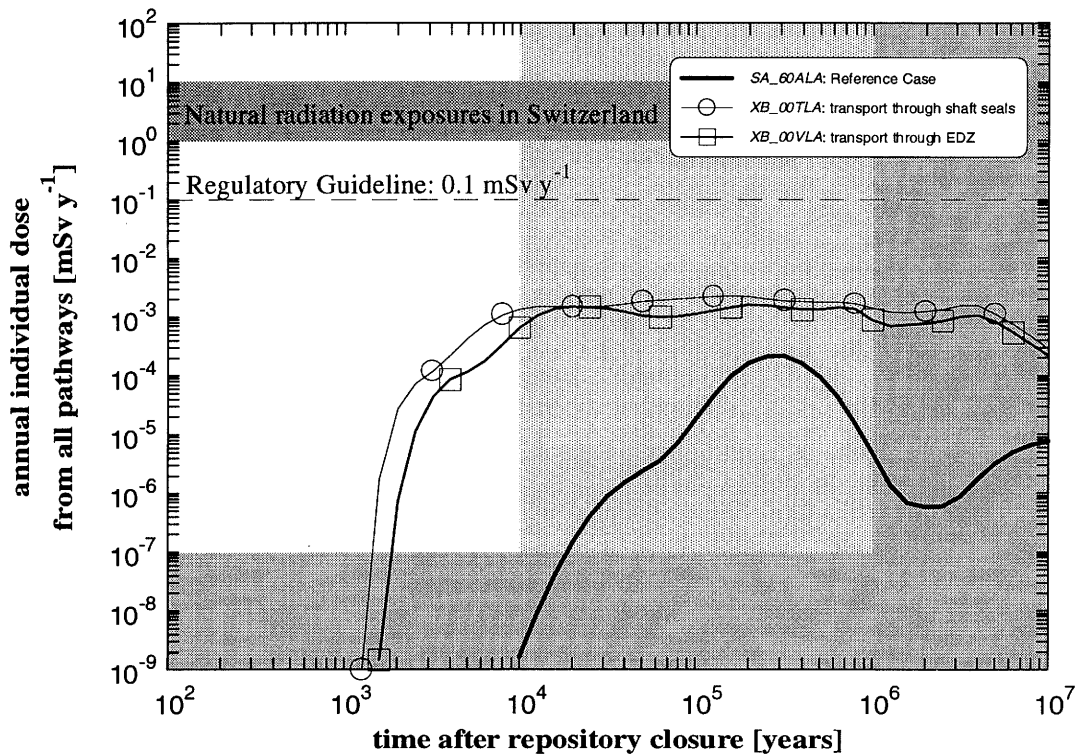
(b) Transport through excavation-disturbed zone

Key to radionuclides.

—●—	Sum over nuclides.	—△—	4N + 1 chain	—★—	⁵⁹ Ni	—●—	¹²⁶ Sn
—○—	4N + 3 chain	—★—	4N chain	—×—	¹⁰⁷ Pd	—☆—	⁹⁹ Tc
—□—	4N + 2 chain	—◇—	¹³⁵ Cs	—+—	⁷⁹ Se	—■—	⁹³ Zr

Note: (a): dataset XB_00TLA, (b): dataset XB_00VLA; the nomenclature for datasets is discussed in Appendix 4.

Figure 6.3.1: Time development of annual individual dose for a scenario in which, rather than migrating through the low-permeability domain of the host rock, radionuclides migrate either (a) along the repository shaft backfill, or (b) through the excavation-disturbed zone surrounding a shaft.



Note: The nomenclature for datasets is discussed in Appendix 4.

Figure 6.3.2: Comparison of the Reference Case, the case of transport through the shaft backfill and transport through the excavation-disturbed zone (EDZ).

6.3.4 Alternative Climate-Related Scenarios

The biosphere in the Reference Scenario is based on the present-day climate with subsistence agriculture. In order to explore the effects of alternative climate states on the radiological consequences of release from the Reference-Case near-field and geosphere, a number of alternative biosphere scenarios have been investigated. These scenarios are discussed qualitatively in Subsection 4.3.6 and are summarised in Table 6.3.4. In most cases, the structure of the biosphere model is used without modification, and only changes in input parameters are required to describe the alternative scenarios. In the case of the Periglacial Climate State (described below), the model representation is changed.

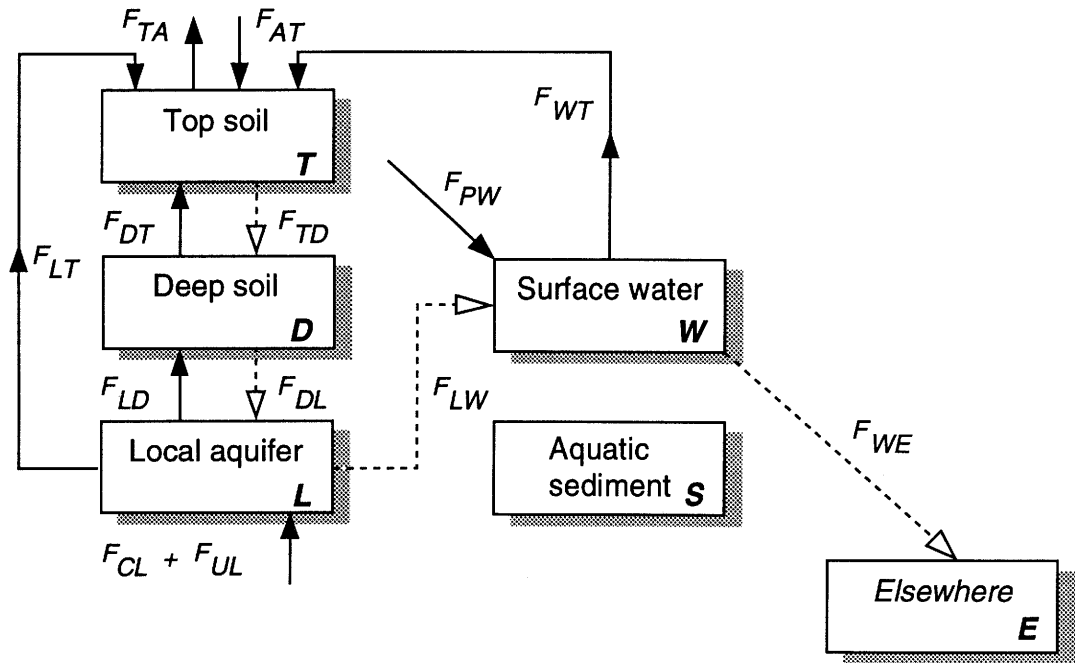
Figure 6.3.3 illustrates the system of water and solid material fluxes used to model the Humid Climate State and Dry Climate State. The representation of the FEPs is the same in these two cases as in Reference Case (see Subsection 5.4.4), but the magnitudes of some of the fluxes differ due to the assumptions summarised in Table 6.3.4. Data for these scenarios are given in Table 6.3.5.

Similarly, Figure 6.3.4 shows the water and solid-material fluxes used to represent of the Periglacial Climate State, with the values for the fluxes given in Table 6.3.6.

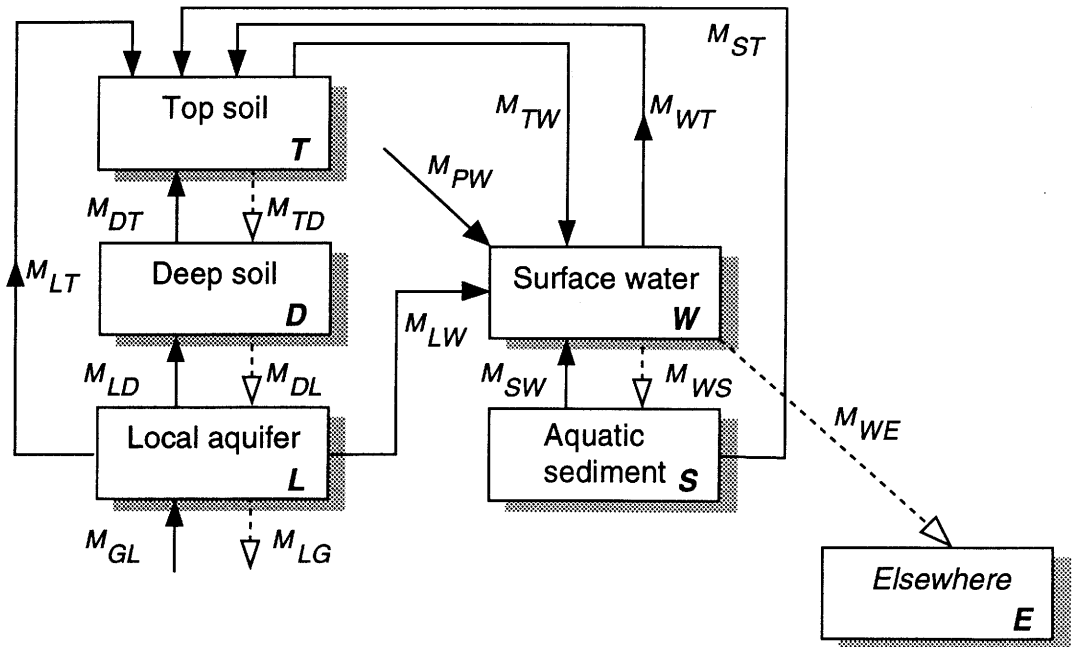
Dataset Name	Description	Modifications to biosphere
SA_60ALD	Dry Climate State , reduced precipitation, increased irrigation from aquifer, increased evapotranspiration. Present-day subsistence agriculture.	data
SA_60ALH	Humid Climate State , increased precipitation, no irrigation, increased evapotranspiration. Present-day subsistence agriculture.	data
SA_60ALC	Periglacial Climate State . Permafrost prevents interaction between crystalline basement and aquifer (assumed frozen). All water obtained from the river - modified river with reduced flow because of reduced precipitation. Reduced evapotranspiration. Modified exposure pathway sub-model: Exposure pathways are: dust inhalation, external γ -irradiation, drinking water (river), freshwater fish, reindeer meat and reindeer milk.	model and data
SA_60ARA	Rhine Gravels Absent . Release to the Rhine water. No local aquifer. Present-day subsistence agriculture.	data
SA_60ARS	Rhine Gravels Absent . Release to deep soil. No local aquifer. Present-day subsistence agriculture.	data

Note: The nomenclature for datasets is discussed in Appendix 4.

Table 6.3.4: Alternative climate-related scenarios. The scenarios are represented by modifying the model and/or data of the Reference-Case biosphere. Detailed descriptions of models and data are given in KLOS et al. (1994) and KLOS & VAN DORP (1994).



(a) Water fluxes between compartments.

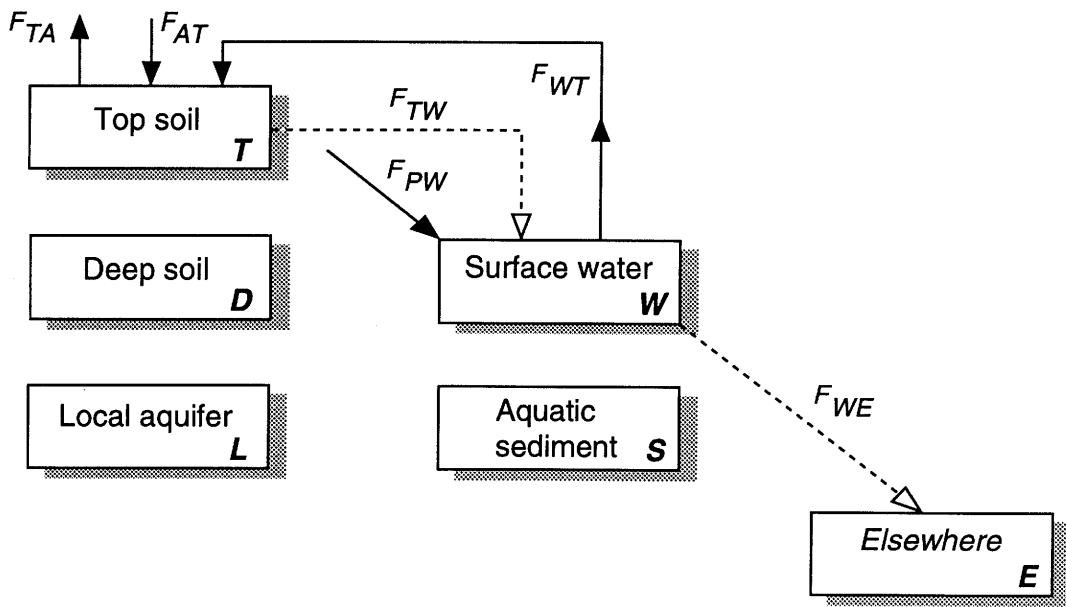


(b) Material fluxes between compartments.

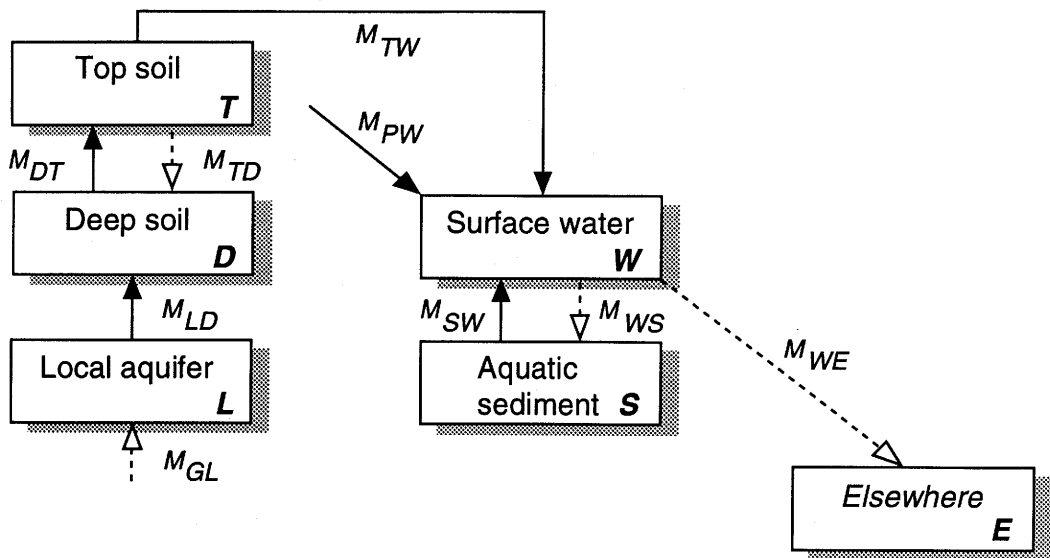
Figure 6.3.3: Schematic representation of the water and solid-material fluxes used to model the Dry Climate State and the Humid Climate State (and the Reference Scenario; see also Figures 5.4.4 and 5.4.5). Fluxes indicated by solid lines are model input, taken from Table 6.3.5. Those indicated by dashed lines are derived from the data in Table 6.3.5 by consideration of mass balance.

Water flux	Symbol	Units	Humid	Dry
Regional rainfall	d_{AT}	m y^{-1}	2.0	0.5
Regional evapotranspiration	d_{TA}	m y^{-1}	1.5	1.5
Deep soil → Top soil	d_{DT}	m y^{-1}	0.05	0.5
Local aquifer → Deep soil	d_{LD}	m y^{-1}	0.05	0.5
Irrigation from local aquifer	d_{LT}	m y^{-1}	0.0	0.6
Irrigation from river water	d_{WT}	m y^{-1}	0.0	0.6
Inflow to local aquifer	$F_{UL} + F_{CL}$	$\text{m}^3 \text{y}^{-1}$	5.5×10^6	2.8×10^6
Through flow in the Rhine	F_{PW}	$\text{m}^3 \text{y}^{-1}$	3.2×10^{10}	1.6×10^{10}
Solid material flux	Symbol	Units	Humid	Dry
Top soil → Surface water	M_{TW}	kg y^{-1}	3.4×10^5	3.4×10^5
Deep soil → Top soil	M_{DT}	kg y^{-1}	7.1×10^6	7.1×10^6
Local aquifer → Deep soil	M_{LD}	kg y^{-1}	3.4×10^5	3.4×10^5
Previous river compartment → River water	M_{PW}	kg y^{-1}	3.2×10^9	1.6×10^9
Local aquifer → Top soil	M_{LT}	kg y^{-1}	0.0	2.0×10^3
River water → Top soil	M_{WT}	kg y^{-1}	0.0	2.0×10^5
Aquatic sediment → Top soil	M_{ST}	kg y^{-1}	3.4×10^5	3.4×10^5
Aquatic sediment → River water	M_{SW}	kg y^{-1}	5.3×10^7	5.3×10^7
Local aquifer → River water	M_{LW}	kg y^{-1}	1.4×10^3	7.2×10^3

Table 6.3.5: Parameter values used in the mass-balance schemes for modelling the Dry Climate State and Humid Climate State. This table can be compared with Tables 5.4.3 and 5.4.4, which give the corresponding data for the Reference Case. The shaded values indicate no change with respect to the Reference Case. (See KLOS & VAN DORP (1994) for a discussion of the parameter values).



(a) Water fluxes between compartments.



(b) Solid material fluxes between compartments.

Figure 6.3.4

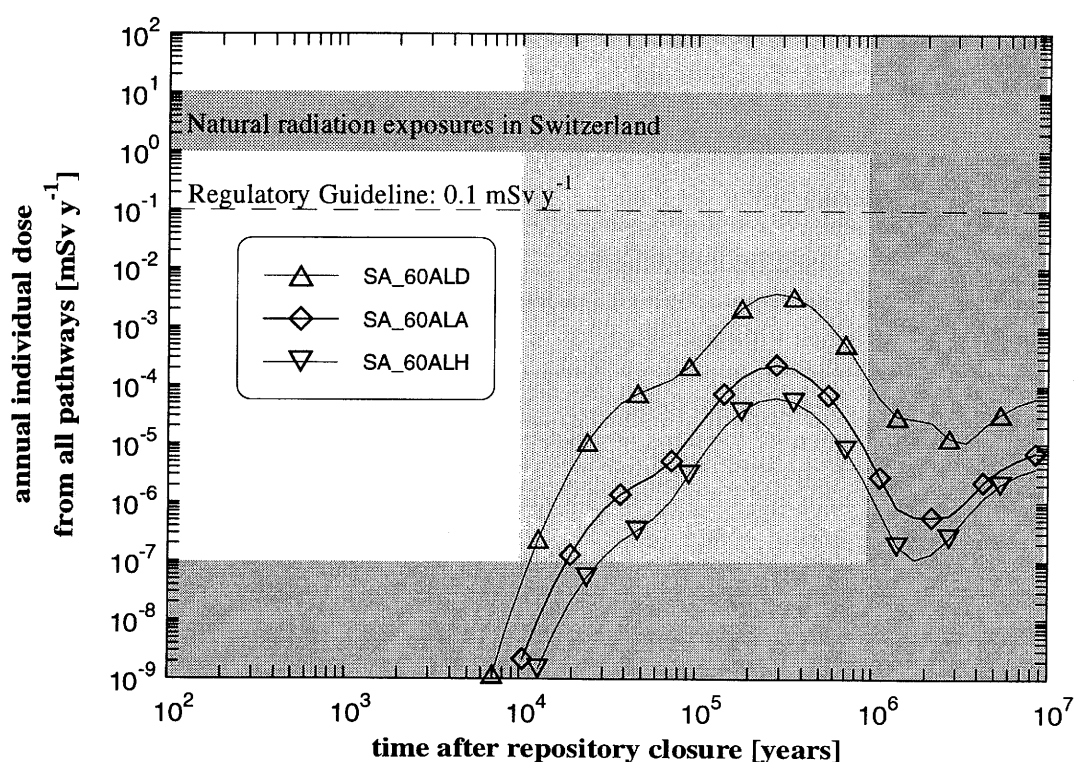
System of compartments and water and solid-material fluxes used to represent the Periglacial Climate State. Fluxes indicated by solid lines are model input, taken from Table 6.3.6. Those indicated by dashed lines are derived from the data in Table 6.3.6 by consideration of mass balance. In this biosphere model, the presence of the permafrost layer substantially inhibits the transport of radionuclides present in the compartments after an initial period of free transport (i.e. an initial period modelled as in the Reference Case). This can be seen by comparing this figure with the mass balance scheme for the inter-glacial climate (Figures 5.4.4 and 5.4.5) or for the Dry Climate State and Humid Climate State (Figure 6.3.3).

Water flux	Symbol	Units	Value
Regional rainfall	d_{AT}	m	0.4
Regional evapotranspiration	d_{TA}	m y^{-1}	0.3
Deep soil → Top soil (capillary rise)	d_{DT}	m y^{-1}	0
Local aquifer → Deep soil (capillary rise)	d_{LD}	m y^{-1}	0
Irrigation from local aquifer	d_{LT}	m y^{-1}	0
Irrigation from river water	d_{WT}	m y^{-1}	0
Inflow to local aquifer	$F_{UL} + F_{CL}$	$\text{m}^3 \text{y}^{-1}$	0
Through flow in the Rhine	F_{PW}	$\text{m}^3 \text{y}^{-1}$	1.0×10^{10}
Solid material flux	Symbol	Units	Value
Top soil → Surface water	M_{TW}	kg y^{-1}	1.3×10^5
Deep soil → Top soil	M_{DT}	kg y^{-1}	6.9×10^6
Local aquifer → Deep soil	M_{LD}	kg y^{-1}	1.3×10^5
Previous river compartment → River water	M_{PW}	kg y^{-1}	1.0×10^9
Local aquifer → Top soil	M_{LT}	kg y^{-1}	0
River water → Top soil	M_{WT}	kg y^{-1}	0
Aquatic sediment → Top soil	M_{ST}	kg y^{-1}	0
Aquatic sediment → River water	M_{SW}	kg y^{-1}	5.3×10^7
Local aquifer → River water	M_{LW}	kg y^{-1}	0

Table 6.3.6: Summary of parameter values used for water and solid-material fluxes in modelling the Periglacial Climate State. This table can be compared with Tables 5.4.3 and 5.4.4, which give corresponding data for the Reference Scenario. The shaded values indicate no change with respect to the Reference Scenario. (See KLOS & VAN DORP (1994) for a discussion of the parameter values).

6.3.4.1 Results for Alternative Climate States

For calculations of warm climatic conditions (Dry Climate State and Humid Climate State), present-day agriculture is assumed, with modifications to the use of near-surface water resources. This gives high importance to irrigation for radionuclide transport in the biosphere (cf. Subsection 5.4.5.2). Figure 6.3.5 compares the results for these alternative scenarios with those from the Reference Case (temperate climate).



Note: Temperate (Reference-Case), Dry and Humid Climate States described by datasets SA_60ALA, SA_60ALD and SA_60ALH, respectively; the nomenclature for datasets is discussed in Appendix 4.

Figure 6.3.5: Comparison of the results of the Reference Case (temperate climate) with those of the Dry Climate State and Humid Climate State.

The Dry Climate State, with greater use of the aquifer for irrigation, gives doses that are around an order of magnitude greater than those of the Reference Case, but are still over an order of magnitude lower than the regulatory guideline. In this scenario, a conservatively high value is assigned to the extraction rate from the aquifer, so that present-day agricultural practices can be maintained and equal irrigation volumes from the river and the aquifer can be assumed (as in the Reference Case); this leads to doses which should be considered as extreme upper limits. The Humid Climate State gives lower doses than the Reference Case, because no irrigation is applied to the farmland and because there is greater throughput in the system due to the higher rainfall.

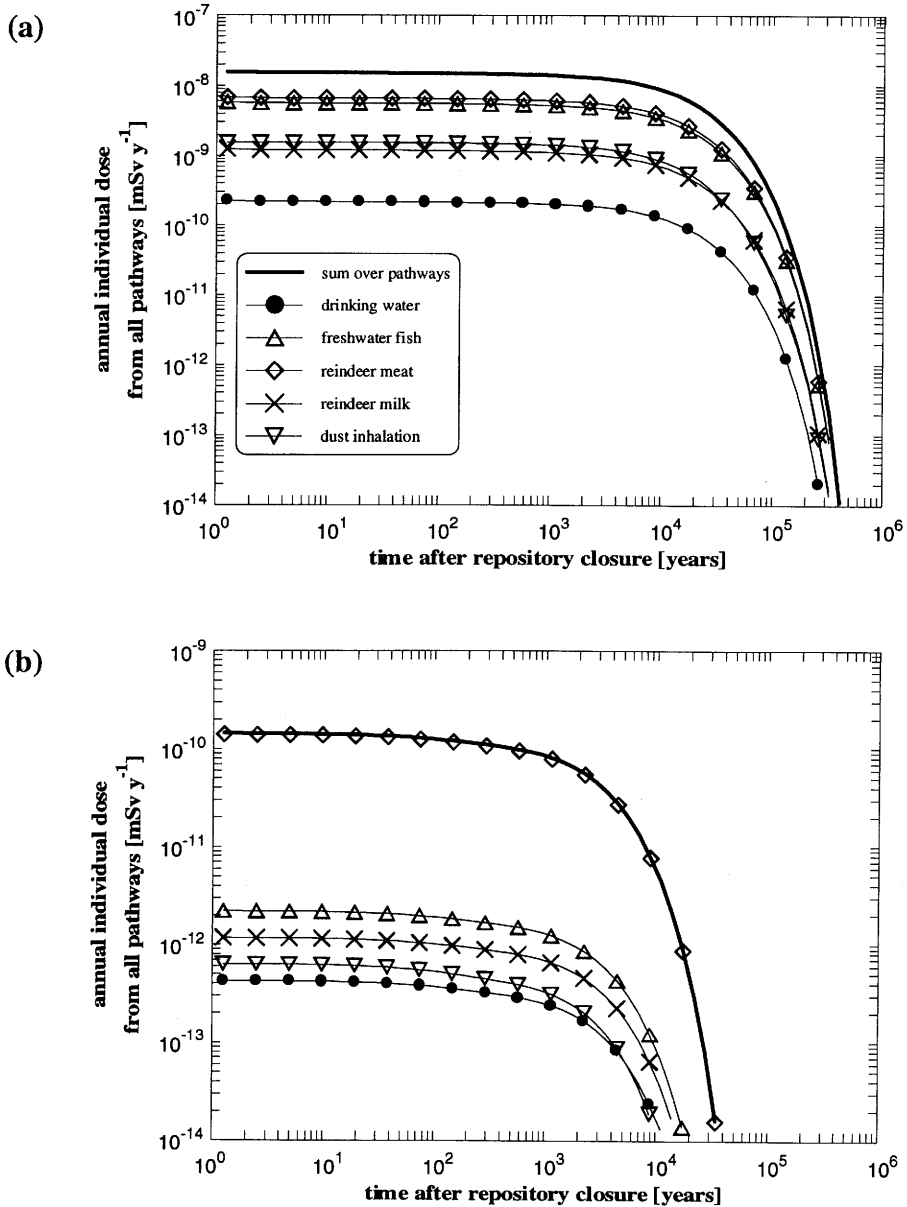
In contrast to the warm climatic conditions, the modelling of the Periglacial Climate State focuses mainly on the alternative exposure pathways (summarised in Table 6.3.4) and, in particular, the dust - lichen - reindeer pathway, which is known to be important in the accumulation of radionuclides in the human food chain (AARKROG 1979). The scenario is modelled by a step transition from temperate to periglacial state; in reality, transitions between states would be gradual. Up to the time of transition, the Reference-Case biosphere model is applied, with a modified biosphere model applied after transition. In the modified biosphere model, it is assumed that a river is present, but that the local aquifer is isolated from the surface biosphere by permafrost so that, after the onset of periglacial conditions, no further releases to any part of the biosphere occur for the duration of the cold conditions. Only the existing radionuclide concentrations in the soils and sediments are further transported within the biosphere. This is known to be non-conservative (see Subsection 4.3.6.6 and, for example, ELSON & WEBBER 1991; McEWEN & DE MARSILY 1991), but does not prevent the analysis of the relative importance of the exposure pathways.

Two radionuclides giving relatively high contributions to dose in the Reference Case, ^{135}Cs and ^{79}Se , are considered in modelling the Periglacial Climate State. The absence of input from the geosphere during periglacial conditions leads to the adoption of the following model. For ^{135}Cs , a time close to the peak of the ^{135}Cs dose curve in the Reference Case (2×10^5 y after repository closure) is chosen for the onset of periglacial conditions. In a separate calculation for ^{79}Se , a time of 2×10^4 y after closure is chosen for this transition in climate. The compartment inventories at these times are then assumed as the initial inventories for calculations of the Periglacial Climate State, with no further input to the system.

The results of each of these calculations are shown in Figure 6.3.6. The doses are several orders of magnitude below those arising in the Reference Case. For both ^{135}Cs and ^{79}Se , the maximum doses in this scenario arise from the initial concentrations of the radionuclides, with the reindeer meat consumption pathway being the most important.

6.3.4.2 Climate-induced Changes in Near-Surface Conditions

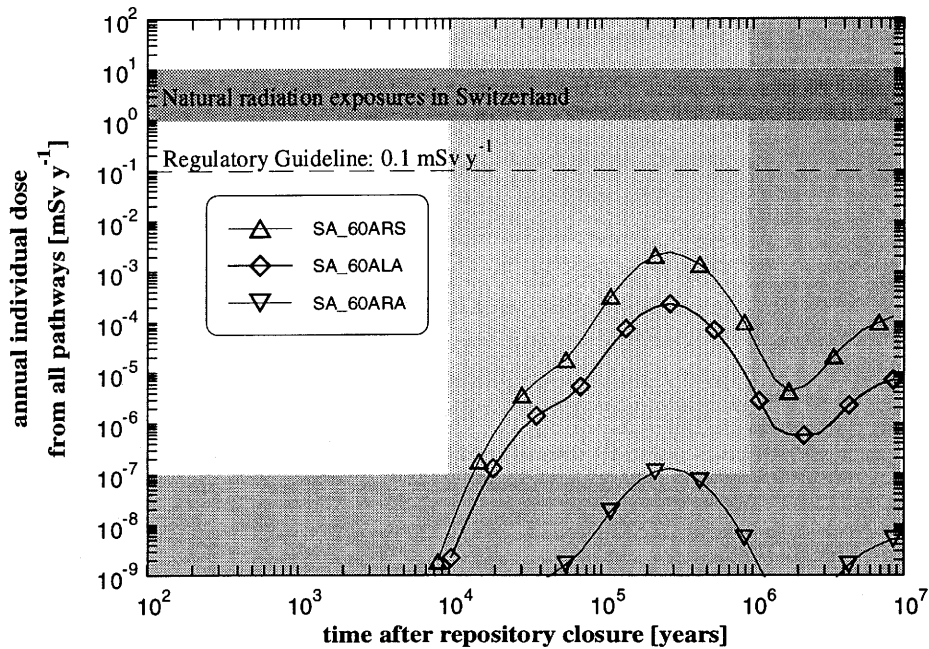
Another potential climatic effect is in the evolution of the near-surface environment of the Rhine valley. The gravel deposits, which lie in the Rhine valley, are likely to be periodically removed due to glacial or fluvial erosion on a timescale in the order of 100 000 years, leaving the Rhine flowing on the exposed crystalline basement. The potential consequences for the release of radionuclides have been modelled, assuming a temperate climate with subsistence agriculture. This biosphere representation differs from that of the Reference Case in that there is no local aquifer underlying the deep soil. The most likely release point would be to the Rhine itself. However, a scenario has also been considered in which, following the removal of the gravel deposits, contaminated groundwater is released to the deep soil rather than to the river. If this were to occur, it is expected that the soils in the region of exfiltration would be of minor importance agriculturally, as they would probably be hydromorphic (close to saturation). The results of this scenario calculation should therefore be considered pessimistic.



Note: Dataset SA_60ALC; the nomenclature for datasets is discussed in Appendix 4.

Figure 6.3.6: Doses arising in the Periglacial Climate State. (a) Dose due to ^{135}Cs , with onset of periglacial conditions at 200 000 years after repository closure (approximately the time of the maximum ^{135}Cs contribution to dose in the Reference Case). (b) Dose due to ^{79}Se , with onset of periglacial conditions at 20 000 years after repository closure.

Parameter values for the modelling of these scenarios are given in KLOS & VAN DORP (1994). Results are compared to those of the Reference Case in Figure 6.3.7. In the case of direct release to the Rhine, doses are very low since the river provides a large and immediate dilution, with subsequent transport to farmland by irrigation using water from this dilute source. In the case of release to the deep soil, doses are higher because there is no initial dilution and because the concentration in the top soil (i.e. the rooting zone of crops) is similar to that in the deep soil. However, the doses in this scenario are still more than an order of magnitude below the regulatory guideline of 0.1 mSv y^{-1} .



Note: Reference-Case: dataset SA_60ALA, Rhine Gravels Absent, release to the river: dataset SA_60ARA, Rhine Gravels Absent, release to deep soil: dataset SA_60ARS; the nomenclature for datasets is discussed in Appendix 4.

Figure 6.3.7: Comparison of the results for the Reference Case, with those for scenarios in which the gravel deposits are removed. The cases of release to the river and release to deep soil are considered.

6.4 The Robust Scenario

A scenario for a robust demonstration of safety is discussed in Subsection 4.4.2. This Robust Scenario is selected to illustrate the level of safety that can confidently be expected, taking account of the effects of uncertainties, particularly in geological conditions, that might affect the evolution and performance of the system of barriers. The effects of uncertainties in the properties and behaviour of the engineered barriers are minimised by the massive nature of the barriers and by the fact that most of the deleterious events and processes that have been identified can be avoided by attention to design, siting and quality control; as in the Reference Scenario, the Robust Scenario considers the evolution of the engineered barriers according to their minimum design function.

There is considerably greater uncertainty pertaining to the characteristics of the geological barriers at the current stage of investigation. This applies particularly to the geometrical characteristics of small-scale water-conducting features and model results have been shown to be highly sensitive to the way in which these characteristics are interpreted. There are also uncertainties in the degree of sorption on matrix pores and the effect of groundwater colloids, which lead to uncertainty in geosphere retardation. The most pessimistic interpretation of these uncertainties is therefore adopted in modelling the Robust Scenario, in which radionuclides released from the near field are assumed to be transported directly to the biosphere. During repository construction, features carrying particularly high water fluxes are likely to be identified and the emplacement of waste packages near such features will be avoided. A limited groundwater flowrate is therefore assumed in the near-field calculation at the bentonite-host rock interface. However, because of uncertainties in the characteristics of the excavation-disturbed zone, the distance over which such features would influence conditions at the interface is unclear. In order to cover this uncertainty, as well as uncertainty in the effect of sorption on groundwater colloids on the radionuclide concentration at the interface, the extreme case of a zero-concentration boundary condition is considered as a parameter variation within the Robust Scenario. As a further variation, a combination of "conservative" values for glass corrosion rate, sorption constants in the bentonite and solubility limits is adopted in the near field, but with a limited, Reference-Case groundwater flowrate at the bentonite-host rock interface. Parameter values for the calculations within the Robust Scenario are listed in Table 6.4.1. The biosphere, which is not considered to form part of the barrier system, is represented in the same way as in the Reference Case.

The Robust Scenario, modelled assuming a limited groundwater flow at the bentonite-host rock interface, is identical to the hypothetical case already considered in Subsection 6.2.1.1.3 in order to illustrate the role played by the geological barrier in the Reference Case (see Figure 6.2.1(b)); the results are reproduced in Figure 6.4.1(a). The dose maximum is dominated by ^{135}Cs and, at later times, by the $4N + 2$ chain; as in the Reference Case, the maximum is about two orders of magnitude below the regulatory guideline, even though no credit is taken for transport through the geosphere.

Results for the parameter variation in which a zero-concentration boundary condition is assumed at the bentonite-host rock interface are shown in Figure 6.4.1(b). In this case, the $4N + 2$ chain makes the largest contribution to the dose maximum, which is less than the regulatory guideline by a factor of approximately 3. The calculated dose maximum due to ^{135}Cs is little changed with respect to the case of limited groundwater flow. However, those due to ^{99}Tc , ^{126}Sn and the $4N + 1$, $4N+2$ and $4N + 3$ chains are all increased, so that their maxima are similar to, or greater than, that of ^{135}Cs .

Near-Field Parameters	Units	Reference Values	Parameter Variations	
Glass corrosion rate, R	$\text{kg m}^{-2} \text{y}^{-1}$	3.8×10^{-4}	3.8×10^{-4}	3.8×10^{-2}
Groundwater flowrate through repository area, Q	$\text{m}^3 \text{y}^{-1}$	3.0	unlimited [†]	3.0
Element-dependent K_d values for sorption on bentonite	$\text{m}^3 \text{kg}^{-1}$	"realistic-conservative" values	"realistic-conservative" values	"conservative" values
Element-dependent solubility limits, S_E	-	"realistic-conservative" values	"realistic-conservative" values	"conservative" values
Geosphere Parameters				
Immediate transport to the Reference-Case biosphere assumed	-	-	-	-

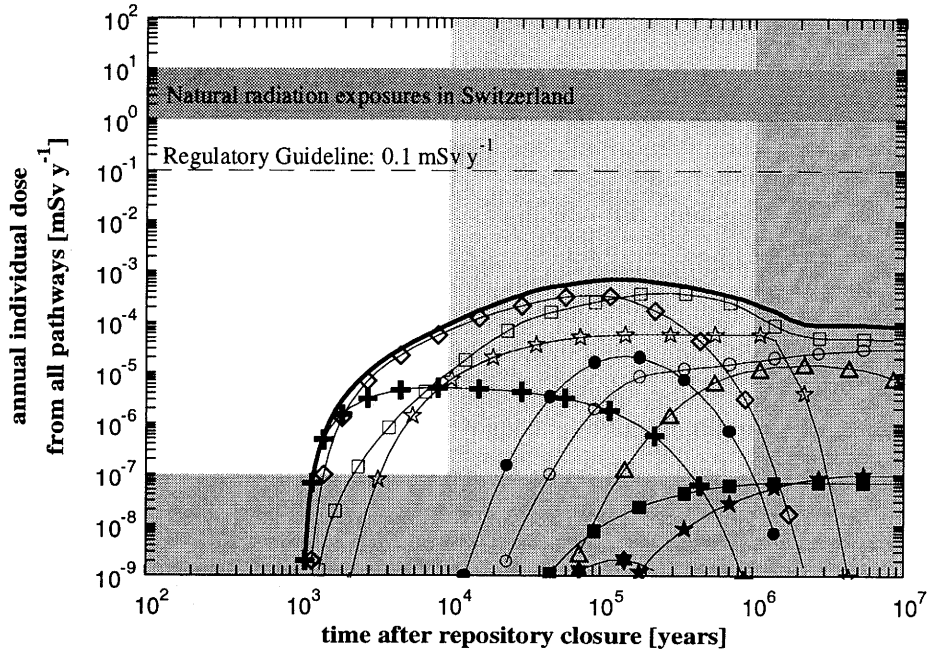
Note: † This parameter variation may account, for example, for irreversible sorption on groundwater colloids, the possibility of which is not included in the model for colloid facilitated transport.

Table 6.4.1: Near-field and geosphere parameters for calculations within the Robust Scenario.

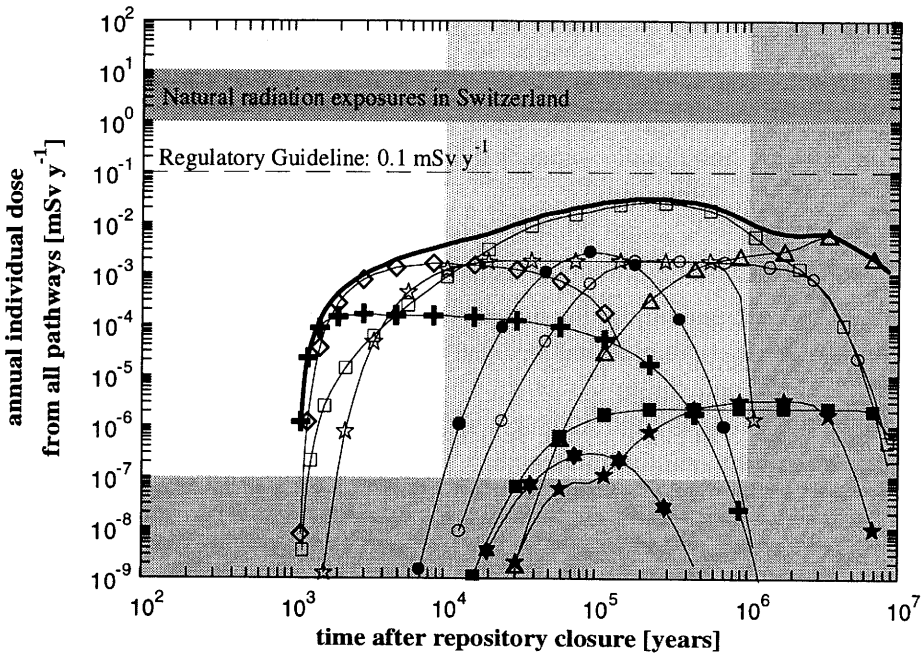
Results for the parameter variation of a combination of "conservative" parameter values in the near field are shown in Figure 6.4.1(c). This is identical to another hypothetical case already considered in Subsection 6.2.1.2 in order to illustrate the role played by the geological barrier in a parameter variation on the Reference Case (see Figure 6.2.5(b)). In this case, the dose maximum is less than the regulatory guideline by a factor of approximately 5. The dose is dominated by ^{135}Cs at the earliest times (up to about 3000 years) and, at later times, by ^{99}Tc and finally the $4N + 1$ chain.

In conclusion, it has been shown that, even taking the most pessimistic interpretation of the geological uncertainties and pessimistic parameter values for modelling the performance of the engineered barriers, the regulatory guideline is not exceeded. Of course it is always possible to construct scenarios whereby the regulatory guideline for dose is exceeded by considering combinations of highly unlikely events or processes effecting both the engineered and geological barriers.

For example, if the bentonite were to cease to function as a colloid filter (as a result, say, of extreme canister sinking, giving a direct contact with the host rock) and, furthermore, if any colloids thus released from the engineered barriers were not filtered by the geological barriers, then calculated doses might exceed the guideline. Scoping calculations, not reported herein), however, indicate that the doses arising from such a "worst case" scenario are still in the order of background radiation levels.

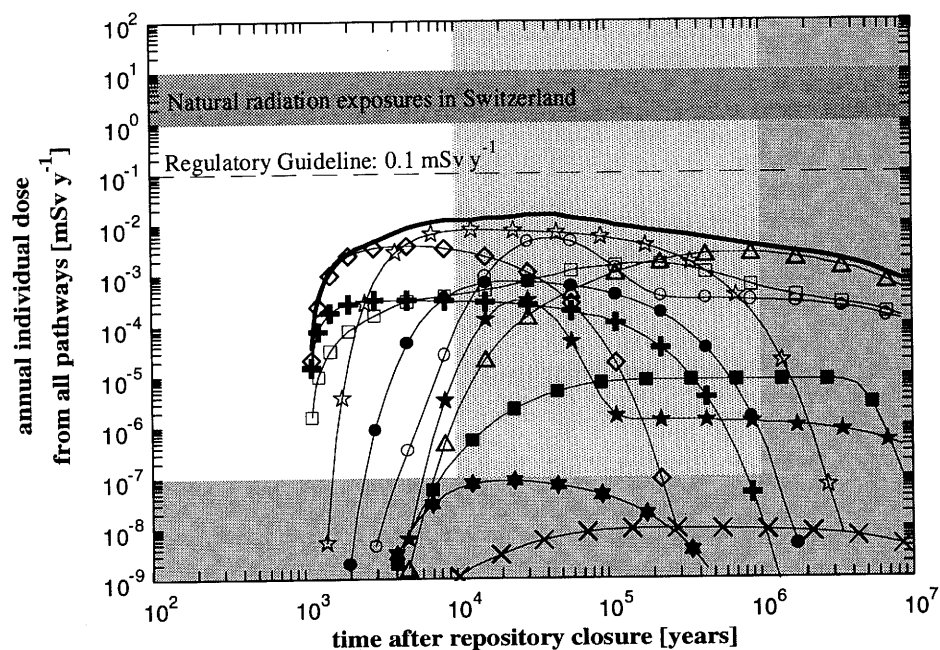


(a) Reference Parameters - limited groundwater flow at the bentonite-host rock interface.

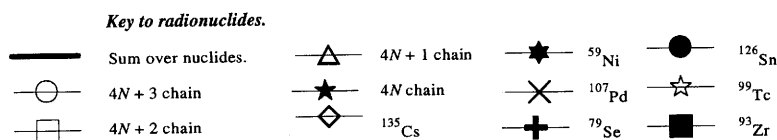


(b) Parameter variation - zero-concentration boundary condition (unlimited groundwater flow) at the bentonite-host rock interface.

Figure 6.4.1: Time development of annual individual doses in the Robust Scenario.



(c) Parameter variation - limited groundwater flow, "conservative" glass corrosion rate sorption constants in the bentonite and solubility limits.



Note: (a): dataset SA_LA, (b): dataset 8A_LA, (c): dataset EB_LA; the nomenclature for datasets is discussed in Appendix 4.

Figure 6.4.1: (Continued). Time development of annual individual doses in the Robust Scenario.

6.5 Summary of Results

In Chapter 6, the radiological impact of the repository has been evaluated by calculations which, due to the conservatism of the models and data selection, are expected to bound maximum expected consequences. The starting point is the Reference Case, based on (i) the Reference Scenario, which envisages a repository with a near field evolving according to the design function of the engineered barriers, a geosphere based on a conservative interpretation of the current understanding of the geological environment and a biosphere based on present-day hydrogeological and climatic conditions, with conservative assumptions regarding human behaviour, (ii) a three-component model chain, incorporating a number of conservative model assumptions which arise from limitations in the available computer codes and from uncertainties in the understanding of the system defined by the Reference Scenario and (iii) a set of "realistic-conservative" physico/chemical parameters appropriate to Area West. The effects of uncertainty both in the future evolution of the system (alternative scenarios) and in the models and data for the calculations have then been explored.

The robustness of the Kristallin-I repository concept (and of the near field in particular) is demonstrated by its effectiveness both in the Reference Case and in calculations that explore the effects of uncertainty in system evolution, models and data.

6.5.1 The Reference Scenario

6.5.1.1 Reference Model Assumptions

6.5.1.1.1 Reference-Case Results

The Reference-Case calculations give a peak annual individual dose lying more than two orders of magnitude below the 0.1 mSv y^{-1} dose limit specified in Protection Objective 1 of the Swiss regulatory guidelines (Section 2.3), which is itself well below the range of typical annual individual doses due to natural sources received by the present-day Swiss population ($1 - 10 \text{ mSv y}^{-1}$). This peak occurs over 100 000 years after repository closure, and is dominated by ^{135}Cs .

The near field provides a highly effective barrier for most radionuclides. With the exception of ^{135}Cs , less than 2% of any activation/fission product passes from the near field to the geosphere. In the case of the actinide chains, this figure is reduced to 0.25%. Both the near field and geosphere provide less effective barriers for ^{135}Cs because of its high solubility and relatively weak sorption. The hypothetical case of a direct release from the near field to the biosphere also shows an overall peak dose dominated by ^{135}Cs , the magnitude of which is little affected by not accounting for transport through the geosphere (see Figure 6.2.1). However, the geosphere is effective in significantly increasing the time before ^{135}Cs is released to the human environment. For several other radionuclides, the geosphere gives both a significant delay of release and a reduction in the magnitude of the resultant doses.

6.5.1.1.2 Results of Parameter Variations

The effects of uncertainty in data for individual models is considered in the parameter variation studies of Chapter 5; results and conclusions are summarised at the start of the present chapter. In general, the model results are insensitive to the values of physico/chemical parameters. Exceptions are the (i) solubility limits, which significantly affect the behaviour of the near field for several radionuclides (though not ^{135}Cs , which dominates the maximum dose in the Reference Case), (ii) groundwater flowrate, which affects the behaviour of both the near-field and the geosphere and (iii) the amount and source of irrigation water applied to farmland and, to a lesser extent, the radionuclide sorption on solid material (K_d values) in the biosphere compartments.

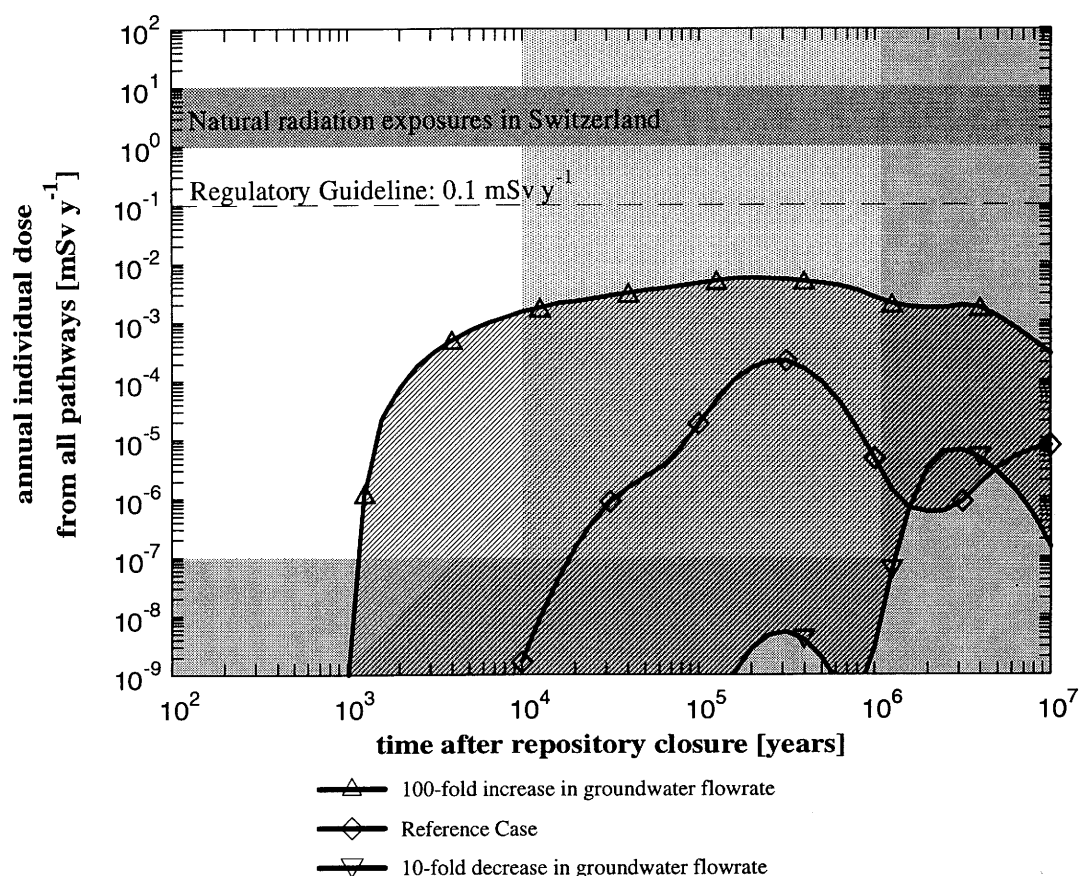


Figure 6.5.1: The effect of varying the assumed groundwater flowrate on radiological impact. Curves shown correspond to the Reference-Case flowrate (the geometric mean from hydrogeological modelling), 0.1 times this value and 100 times this value. The groundwater flowrate affects both the near-field and geosphere models.

The adoption of a highly conservative groundwater flowrate, 100 times greater than that of the Reference-Case value, results in a relatively small increase in the maximum dose due to ^{135}Cs (about an order of magnitude, principally due to the effect on the near field), but has a much larger effect on ^{99}Tc ; the two radionuclides then give similar dose maxima. A 10-fold reduction in flowrate has a pronounced effect on many of the safety-relevant radionuclides. The dose maximum, still dominated by ^{135}Cs , occurs at more than one million years⁴³ after closure and is reduced by more than an order of magnitude with respect to the Reference Case. The range of radiological impact obtained by varying the assumed groundwater flowrate is shown in Figure 6.5.1.

⁴³ The time of the peak dose shows far more sensitivity to variations in parameter values, model assumptions and scenarios than does the magnitude of the peak. However, this factor does not require consideration under the Swiss regulatory guidelines.

Case) have been performed for a repository sited in Area East; these calculations indicate that ^{135}Cs , ^{99}Tc and the $4N + 1$ chain are the dominant contributors to dose and that the dose maximum, summed over all radionuclides, is increased by a factor of between 5 and 30 compared to the Reference Case, depending on whether release takes place in the Rhine valley or in a tributary valley of the Rhine.

6.5.1.2 Alternative Model Assumptions

The results of calculations using alternative geosphere model assumptions are summarised in Table 6.5.1. These assumptions lie within the Reference Scenario (present-day hydrogeological conditions). Near-field and biosphere model assumptions within the Reference Scenario are considered fixed for the purposes of the current assessment. Different assumptions applied in the modelling of the biosphere in order to represent alternative scenarios have been discussed in Section 6.3.

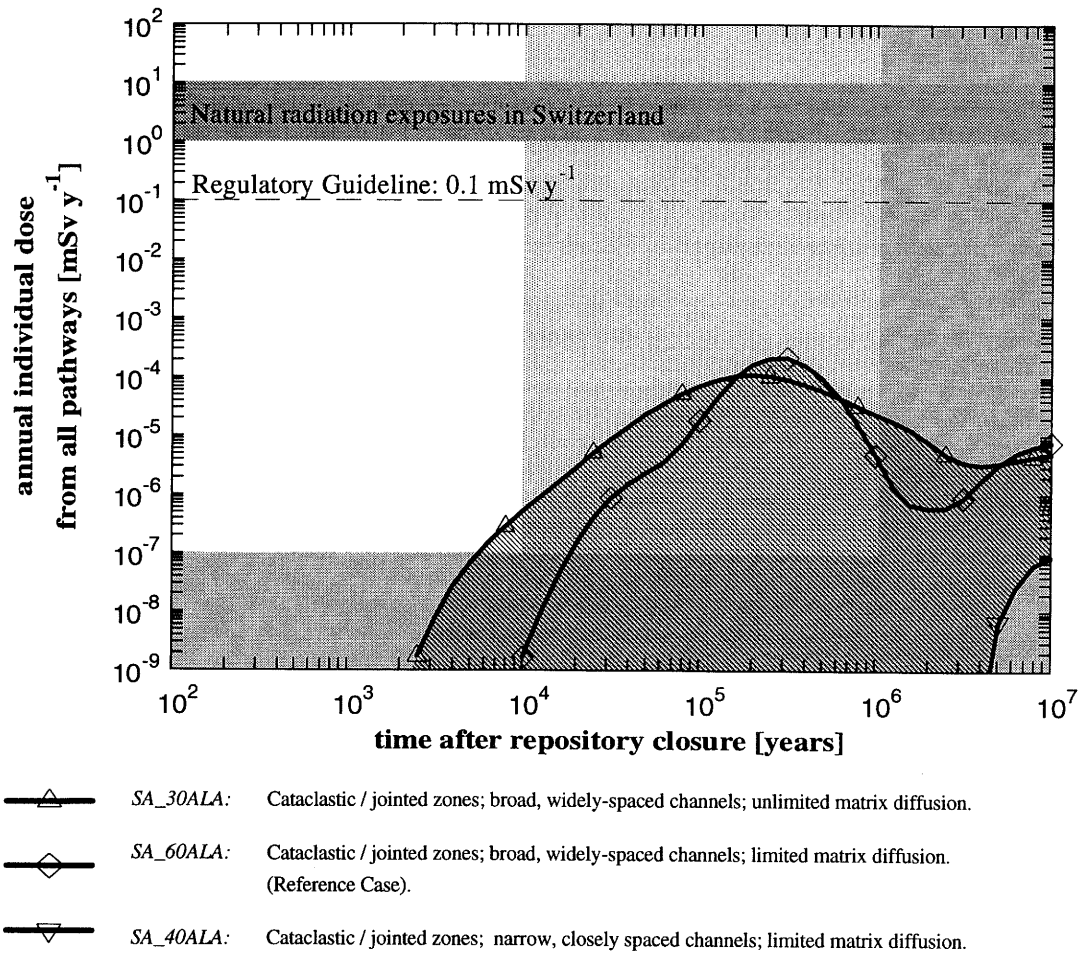
Important points arising from the consideration of alternative model assumptions are as follows:

- The model results exhibit the greatest sensitivity to the selection of a geometrical representation for the internal structure of water-conducting features. Adopting a geometry representing cataclastic or jointed zones with broad, widely-spaced channels gives the highest doses; this is the geometrical representation used in the Reference Case. An alternative assumption of narrow, closely-spaced channels gives a dose maximum more than two orders of magnitude smaller. The range of radiological impact between these two extreme representations is illustrated in Figure 6.5.2, which also shows the smaller effect of considering matrix diffusion in both the altered and unaltered wallrock, rather than in altered wallrock alone.
- The model results are insensitive to the adoption of alternative assumptions concerning radionuclide migration path (whether radionuclides are transported directly from the low-permeability domain to the higher-permeability domain, as in the Reference Case, or indirectly via the major water-conducting faults). The faults provide a very weak barrier effect, with little retardation and decay of radionuclides along their lengths.
- For those radionuclides considered in the study of colloid-facilitated transport (the actinide chain $^{237}\text{Np} \rightarrow ^{233}\text{U} \rightarrow ^{229}\text{Th}$), sorption on groundwater colloids has little effect on the calculated dose where the Reference-Case geometry is assumed for the water-conducting features. For less conservative geometrical representations, the effect of sorption on colloids is much more pronounced.

REFERENCE SCENARIO		Max. Annual Individual Dose [mSv y⁻¹]
Reference Model Assumptions	Alternative Model Assumptions	
Geometry of Water-Conducting Features:		
All transport takes place in cataclastic/jointed zones with broad, widely-spaced channels.	Transport in aplite/pegmatite dykes and aplitic gneisses.	3×10^{-5} (SA_50ALA)
	Transport in cataclastic/jointed zones with narrow, closely-spaced channels.	7×10^{-7} (SA_40ALA)
Matrix Diffusion:		
Matrix diffusion is limited to the altered wallrock adjacent to the fractures. Unaltered wallrock is inaccessible to diffusion.	Unlimited matrix diffusion; transport in: (i) cataclastic/jointed zones with broad, widely-spaced channels;	1×10^{-4} (SA_30ALA)
	(ii) aplite/pegmatite dykes and aplitic gneisses;	1×10^{-6} (SA_20ALA)
	(iii) cataclastic/jointed zones with narrow, closely-spaced channels.	7×10^{-7} (SA_10ALA)
Radionuclide Migration Path:		
Radionuclides are transported through the low-permeability domain directly (upwards) to the higher-permeability domain and thence to the biosphere.	Radionuclides are transported through the low-permeability domain to major water-conducting faults, upwards to the higher-permeability domain and thence to the biosphere.	2×10^{-4} (SA_64ALA)
Colloid Transport:		
Radionuclide sorption on groundwater colloids is neglected. (The maximum dose for the $4N + 1$ chain in the Reference Case is 9×10^{-7} mSv y ⁻¹).	Radionuclides sorb onto a constant background population of groundwater colloids (the effect of this assumption has been evaluated for the $4N+1$ actinide chain; it is likely to be unimportant for the fission/activation products).	$4N + 1$ chain: 5×10^{-6} (SD_60BLA)
Distribution of Groundwater Flow:		
Water-conducting features are all assigned an identical flowrate.	Groundwater flow is distributed between water-conducting features according to a probability distribution. Radionuclide release to the biosphere is obtained from a weighted superposition of Reference-Case results and results with flowrates increased 10- and 100-fold.	6×10^{-4} (weighted superposition of SA_60ALA, XA_60JLA and XB_60KLA)
REFERENCE-CASE RESULT		2×10^{-4} (SA_60ALA)

Note: Dataset names are given in parentheses; the nomenclature for datasets is discussed in Appendix 4.

Table 6.5.1: Alternative model assumptions for geosphere transport and calculated maximum annual individual doses. Alternative assumptions regarding colloid transport and distribution of groundwater flow also affect the near-field calculations (see Subsection 6.2.2). All calculations lie within the framework of the Reference Scenario.



Note: The nomenclature for datasets is discussed in Appendix 4.

Figure 6.5.2: The effect of alternative assumptions regarding the geometrical representation of water-conducting features on radiological impact.

- Accounting for the effect of flowrate variability shows a greater divergence from the Reference Case, with a small number of water-conducting features carrying an increased flow (100 times the Reference-Case value) significantly modifying the calculated dose against time. The radiological impact is uncertain (the analysis used is highly simplistic), but is expected to lie within the range shown in Figure 6.5.1, the upper limit of which corresponds to the assumption that all water-conducting features carry 100 times the Reference-Case water flow.

6.5.2 Alternative Scenarios

Several alternative scenarios are identified for quantitative consideration in Chapter 4; the results of these calculations are summarised in Table 6.5.2. These are (i) a Deep Groundwater Well, (ii) Tunnel/Shaft Seal Failure, (iii) Alternative Climate-Related Scenarios.

For the Deep Groundwater Well scenario, the maximum dose is again dominated by ^{135}Cs and is increased only by a factor of 3 with respect to the Reference Case. In a scenario where it is supposed that the tunnel/shaft seals are ineffective, the maximum dose is increased by a factor of 10 and is dominated by ^{135}Cs , ^{99}Tc and the $4N + 1$ chain at different times. The range of radiological impact is broadest for the climate-related scenarios; example cases of (i) the Dry Climate State (in which higher doses result from a greater use of the aquifer for irrigation - note, however, that the extraction rate from the aquifer is highly conservative) and (ii) Rhine Gravels Absent (complete erosion), with direct release to the river, are shown in Figure 6.5.3.

6.5.3 The Robust Scenario

Calculations have been performed for a Robust Scenario, which is selected to illustrate the level of safety that can confidently be expected, even given the most pessimistic interpretation of geological uncertainties and geosphere transport processes. This scenario postulates that the engineered barriers perform according to their expected minimum design function, but neglects transport processes in the geological barriers, with immediate transport of radionuclides released from the near field to the biosphere. Even in this case, the peak dose is not much higher than that of the Reference Case and is again well below the regulatory guideline; it is dominated by ^{135}Cs and also, at later times, by the $4N + 2$ chain: $^{246}\text{Cm} \rightarrow ^{242}\text{Pu} \rightarrow ^{238}\text{U} \rightarrow ^{234}\text{U} \rightarrow ^{230}\text{Th} \rightarrow ^{226}\text{Ra} (\rightarrow ^{210}\text{Pb} \rightarrow ^{210}\text{Po})^{44}$. Parameter variations have been performed within the Robust Scenario, with (i) an increased water flow around the engineered barriers and (ii) with a highly pessimistic combination of "conservative" values for glass corrosion rate, sorption constants in the bentonite and solubility limits; in no case is the regulatory guideline exceeded.

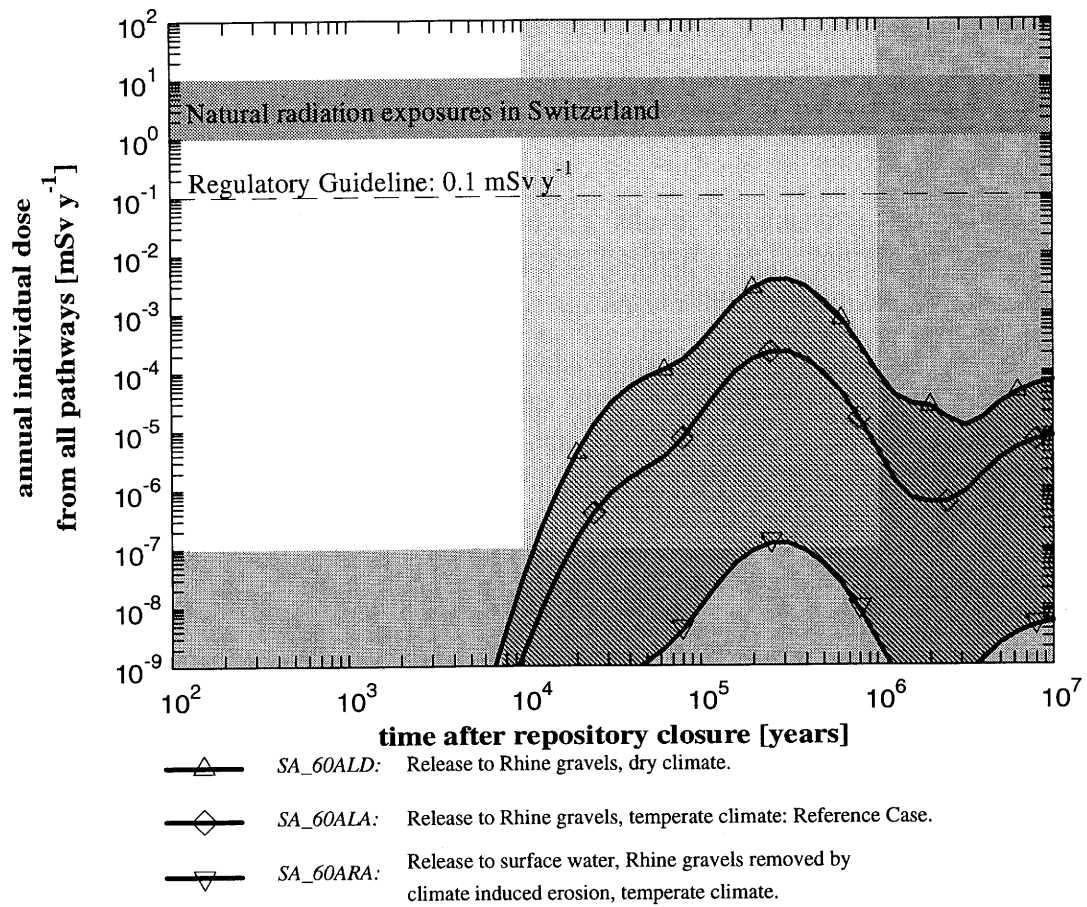
⁴⁴ The $4N+2$ chain members ^{210}Pb and ^{210}Po are modelled only in the biosphere; Appendix 2.

	Maximum Annual Individual Dose [mSv y ⁻¹]
REFERENCE SCENARIO (REFERENCE-CASE RESULT)	2×10^{-4} (SA_60ALA)
ALTERNATIVE SCENARIOS:	
(i) Deep Groundwater Well	
All radionuclides are captured by a deep well.	6×10^{-4} (SA_60AMB)
(ii) Tunnel/Shaft Seal Failure	
Radionuclides are transported through the shaft backfill.	2×10^{-3} (XB_00TLA)
Radionuclides are transported through the shaft excavation-disturbed zone.	2×10^{-3} (XB_00VLA)
(iii) Alternative Climate-Related Scenarios	
Dry Climate State , with reduced precipitation and increased evapotranspiration; increased irrigation from aquifer [†] , present-day subsistence agriculture.	4×10^{-3} (SA_60ALD)
Humid Climate State , with increased precipitation and evapotranspiration; no irrigation, present-day subsistence agriculture.	6×10^{-5} (SA_60ALH)
Periglacial Climate State , in which permafrost prevents interaction with the aquifer (assumed frozen); all water obtained from the river, modified Rhine with reduced flow because of reduced precipitation, reduced evapotranspiration.	1×10^{-10} (SA_60ALC) periglacial conditions at either 2×10^4 years (⁷⁹ Se) or 2×10^5 years (¹³⁵ Cs) after repository closure)
Rhine Gravels Absent , no local aquifer, present-day subsistence agriculture: - release to the Rhine water; - release to deep soil.	1×10^{-7} (SA_60ARA) 2×10^{-3} (SA_60ARS)

Note: † The extraction rate from the aquifer in the Dry Climate State is conservatively high - see Table 6.3.5.

Dataset names are given in parentheses; the nomenclature for datasets is discussed in Appendix 4.

Table 6.5.2: Calculated maximum annual individual doses for the Reference Scenario and alternative scenarios.



Note: The nomenclature for datasets is discussed in Appendix 4.

Figure 6.5.3: The effect on radiological impact of alternative climate-related scenarios.

7. SUMMARY AND CONCLUSIONS

7.1 Introduction

In this chapter, a summary of results and conclusions from the Kristallin-I safety assessment is presented. The chapter is structured according to the aims of the assessment given in Chapter 1, which are:

- to re-evaluate the crystalline basement of Northern Switzerland as a host rock for a high-level radioactive waste repository and, using both moderately conservative arguments and robust arguments, to quantify the levels of safety that can reasonably be expected and can be relied on with confidence:

an overview of overall system performance is given in Section 7.2;

- to improve understanding of the roles of the engineered and geological barriers through quantitative analysis of their performance, including examination of the sensitivity of performance estimates to uncertainties:

an overview of the factors that determine the performance of the engineered and geological barriers and of key uncertainties, including reserves of performance not incorporated in current models is given in Section 7.3;

- to make a detailed examination of the potential performance of the geological barriers, to identify key geological characteristics and to establish desirable ranges for corresponding parameters as input to the identification of sites for additional field work:

a statement of the desired properties of the crystalline host rock to ensure safety is given in Section 7.4;

- to develop and test a more complete safety assessment methodology and tool kit, including a scenario development methodology, new models of specific processes identified as important in Project Gewähr (e.g. colloid facilitated radionuclide transport and non-linear sorption) and new assessment computer codes:

a summary of the main developments in assessment methodology, in modelling tools and in data compared to Project Gewähr 1985 (NAGRA 1985) is given in Section 7.5; a summary of the types of evidence that lead to greater confidence in the results of the assessment is given in Section 7.6.

Finally, a statement of the potential suitability of the crystalline basement of Northern Switzerland as a host rock for a high-level radioactive waste repository is given in Section 7.7.

7.2 Overall System Performance

The current interpretation of the geological situation in Northern Switzerland indicates that the expected conditions in the crystalline basement can provide a suitable environment for a safe repository for vitrified HLW. The peak calculated annual individual dose for the Reference Case is more than two orders of magnitude below the limit of 0.1 mSv y^{-1} established in Protection Objective 1 of the Swiss regulatory guidelines (Section 2.3) and occurs more than 200 000 years after repository closure (Figure 7.2.1). To provide perspective, the calculated doses are compared with typical doses from natural radiation exposures in Switzerland (see also NEALL (ed.) 1994).

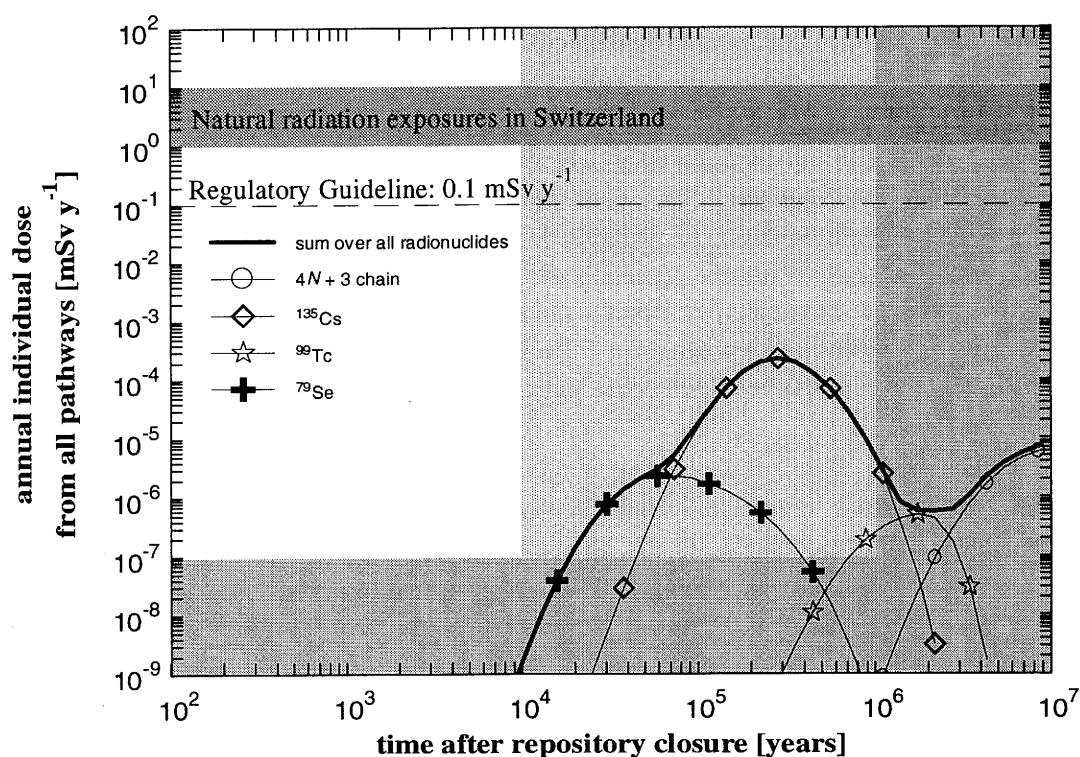


Figure 7.2.1: Results of the Kristallin-I Reference-Case Calculations - annual individual dose as a function of time after repository closure. All the safety-relevant radionuclides are taken into account in calculating the summed dose (thick line). Other lines show results for a subset of safety-relevant radionuclides; those which give the largest contribution to the summed dose at different times. The regulatory guideline of 0.1 mSv y^{-1} is shown, together with the typical range of annual doses from natural background radiation (including radon) in Switzerland. An explanation of the use of shading is given in Appendix 1.

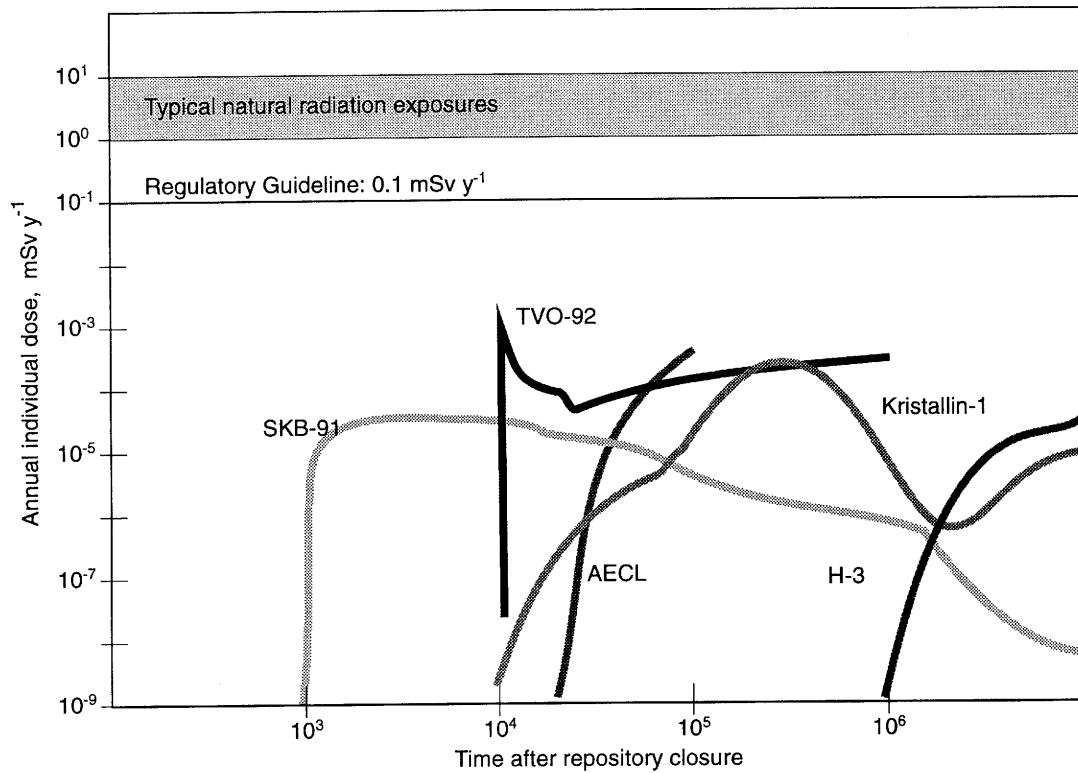
The peak annual dose is dominated by ^{135}Cs . ^{79}Se is the most important radionuclide at early times, between about 10 000 and 60 000 years after closure, but the peak dose due to this radionuclide is more than two orders of magnitude lower than that due to ^{135}Cs . The actinide chains, and especially the 4N+3 chain ($^{243}\text{Am} \rightarrow ^{239}\text{Pu} \rightarrow ^{235}\text{U} \rightarrow ^{231}\text{Pa}$) dominate calculated doses at the longest times calculated, greater than two million years after closure. ^{99}Tc gives the dominant contribution to predicted total doses between about one and three million years after closure.

The calculated doses are considered to be conservative estimates. This is partly because of conservatism in the selection of the data but mainly because (i) a number of key processes that can be expected to give additional safety have been omitted from the Reference Scenario and Reference Case (reserve FEPs, see Subsection 7.3.4) and (ii) the Reference Case includes conservatively selected models of certain key processes.

The modelling approach used is particularly conservative in the case of the geosphere, where an unfavourable geometrical representation of the internal structure of the water-conducting features is adopted. The resulting geosphere representation does little to reduce the peak calculated dose, although it does provide a significant delay in release to the human environment. With this representation, the engineered barriers appear far more important to safety than the geological barriers. However, with only moderately beneficial changes in the representation of the geosphere, the protection level which can be provided by the geosphere becomes apparent and the calculated doses decrease significantly.

The sensitivity of the calculated peak individual dose to parameter variations and alternative model assumptions (with the exception of the choice of geometrical representation for the internal structure of water-conducting features) is rather limited because the behaviour of the dominant radionuclide, ^{135}Cs , is relatively insensitive to these changes; e.g. it is not solubility limited in the near field and has a long half-life so that the peak dose is little affected by retardation. Other radionuclides are more sensitive, but this has only a small impact on peak dose. Of the physico-chemical parameters varied, the groundwater flowrate in the low-permeability domain of the crystalline basement, in which the repository is sited, has the greatest influence on overall system performance, because it affects the performance of both the engineered and the geological barriers. However, even for the highest flowrate considered in the parameter variation study (100 times that of the Reference Case), calculated doses are still below 0.1 mSv y^{-1} .

The results of the Kristallin-I Reference-Case have been compared with those of other assessments of HLW and spent-fuel disposal conducted recently in Canada (GOODWIN et al. 1994), Finland (VIENO et al. 1992), Japan (PNC 1992) and Sweden (SKB 1992). This comparison is illustrated in Figure 7.2.2 (adapted from NEALL (ed.) 1994).



Dominant Radionuclides:

SKB-91	I-129	Cs-135		
TVO-92	I-129	Pa-231 (U-235)		
AECL	I-129			
Kristallin-I	Se-79	Cs-135	Tc-99	Pa-231(U-235)
H-3				Pd-107

Note: Calculations in the AECL and TVO-92 assessments are terminated at 10⁵ years and 10⁶ years after repository closure, respectively.

Figure 7.2.2: Results of the Kristallin-I safety assessment, compared those of other recent assessments. Annual individual doses are shown, summed over all calculated radionuclides, as a function of time for the Kristallin-I Reference Case and for selected calculations from the AECL (Canada), H-3 (Japan), SKB-91 (Sweden) and TVO-92 (Finland) safety assessments. For each assessment, the radionuclides that dominate the total calculated dose at different times are indicated. The figure is adapted from NEALL (ed.) 1994.

A direct comparison must be approached with caution, since the results illustrated each differ somewhat in their meaning, e.g. the AECL result illustrated is the dose calculated with all input parameters set to their median value and the SKB result is the 50 percentile result from a Monte Carlo simulation accounting for uncertainties in the geosphere transport path. The models and data underlying the results are also very different and incorporate different degrees of conservatism. The important point of agreement is that, in all these countries, investigations have concluded that a repository for HLW or spent fuel, that is well engineered and sited in appropriate host rock, will result in doses or radiological risks that are well below the level of regulatory guidelines or limits.

A number of alternative scenarios have been considered in the Kristallin-I safety assessment; this is necessary because of uncertainties in engineered-barrier quality and performance, geological and climatic evolution over the next one million years and possible human activities. Those which are considered sufficiently important to justify quantitative evaluation are:

- alternative biosphere characteristics, arising mainly from uncertainty in climatic conditions in the far future;
- a deep well extracting drinking water directly from the crystalline basement;
- failure of repository tunnel seals and shaft seals.

In all cases, calculated peak doses are well below the regulatory guideline, exceeding that of the Reference Case by no more than about an order of magnitude.

In addition, a Robust Scenario is evaluated, which is selected to illustrate the level of safety that can confidently be expected, even given the most pessimistic interpretation of geological uncertainties and geosphere transport processes. This scenario postulates that the engineered barriers perform according to their expected design function, but neglects all retardation and decay in the geological barriers, with immediate transport of radionuclides released from the near field to the biosphere. The peak dose calculated, even for this case, is not much higher than that of the Reference Case and is again well below the regulatory guideline; dose is dominated by ^{135}Cs and, at later times, by the 4N+2 chain ($^{246}\text{Cm} \rightarrow ^{242}\text{Pu} \rightarrow ^{238}\text{U} \rightarrow ^{234}\text{U} \rightarrow ^{230}\text{Th} \rightarrow ^{226}\text{Ra}$).

7.3 Performance of the Engineered and Geological Barriers

7.3.1 Relative Importance of Engineered Barriers, Geological Barriers and Biosphere

An improved understanding of the role of the engineered and geological barriers has been achieved and the sensitivity of barrier performance to uncertainty in the model assumptions and data has been assessed.

In the Kristallin-I Reference Case, a conservative conceptual model for geosphere transport is adopted appropriate to the current level of uncertainty in the hydrogeological regime and characteristics of the water-conducting features that are expected to provide the paths for radionuclide transport. Under these circumstances, the engineered barriers provide the principal constraints on radionuclide release and transport and the main role of the geological barriers is to provide a suitable environment for engineered barrier longevity and performance; such an environment gives *mechanical protection, adequate geochemical conditions, and sufficiently low groundwater flowrates*. These three broad requirements on the geological environment are currently considered to be the most important.

Future work at a given site, however, will not be limited to investigations of these requirements. A more detailed characterisation of the host rock and properties of the water-conducting features may allow a less conservative approach to geosphere transport modelling. In this case, it may be concluded that the geosphere forms a very efficient, additional safety barrier. A more detailed characterisation of the host rock will also provide information on the spatial and geometrical characteristics of major water-conducting faults in the host rock and will allow the repository layout to be optimised to take best advantage of the natural safety barrier offered by the host rock.

The surface environment, or biosphere, is not usually considered to be part of the barrier system, although, in the Kristallin-I Reference Case, water in near-surface aquifers provide significant dilution of releases and thereby affect calculated individual doses. The actual surface environmental conditions in the far future are largely unpredictable; in particular, it is not possible to predict the patterns of future human behaviour and local resource use that will determine doses received by individuals or populations. Biosphere modelling can be viewed as a procedure to convert estimated releases of radionuclides from the engineered and geological barriers to a common scale - dose - that is accepted as an appropriate quantity to discuss in considering radiological hazard. The dose calculated is an indicator of repository performance and, specifically, it is a quantity calculated for comparison with the Swiss regulatory guideline. The biosphere model is conservatively defined so as not to underestimate doses that are likely to arise for given releases of radionuclides to the surface environment. In particular, the dose is calculated to a representative individual member of a critical group assumed to dwell permanently at the location of maximum radionuclide concentrations and to obtain all foodstuffs from the immediate area.

7.3.2 Performance of the Engineered Barriers

The performance of the engineered barriers is the key component of the current safety concept. The near-field model represents the features and processes most relevant to the performance of these barriers in their geological setting. However, the model represents a conservatively simplified case; some additional processes which, if considered, might significantly improve performance estimates are neglected at present (see Subsection 7.3.4).

The behaviour of the near-field model has been investigated by deterministic parameter sensitivity studies. The near-field Reference Case is based on a set of data that has been selected by expert judgement, based on a review of available data from Swiss and other experimental programmes. The chosen parameter values are considered to be realistic or moderately conservative. Where there is significant data uncertainty, calculations employing more conservative parameters values (representing more pessimistic conditions) have been carried out. Given sufficient longevity of the engineered barriers, good performance of the near field is found to depend primarily on:

- (a) low solubility limits for many safety-relevant radionuclides at the inner boundary of the bentonite:

Other significant features are:

- (b) the low groundwater flowrate at the outer boundary of the bentonite and, to a lesser extent,
- (c) the sorption properties of the bentonite.

The performance is relatively insensitive to variations in canister lifetime and glass matrix corrosion rate over the ranges of parameter values investigated.

It is concluded that, according to currently available models and data, the performance of the engineered barriers is primarily dependent phenomenologically on:

- (a) chemical conditions in the bentonite close to the wastes, which are controlled by the interaction of groundwater with bentonite and the reducing effects of the steel canister corrosion products,
- (b) the fine pore structure of the bentonite, which ensures the filtration of colloids potentially generated within the engineered barriers.

To a lesser extent the performance depends on:

- (c) low hydraulic conductivity and good sorptive properties of the bentonite to ensure slow, diffusive transport of radionuclides away from the wastes and

- (d) low permeability of the host rock, which limits the flux of radionuclides away from the outer boundary of the bentonite.

A large number of phenomena have been considered that have been suggested to have a possible detrimental effect on engineered-barrier performance (see Chapter 4), but, for the majority of these, it is concluded that they cannot have any very significant effect on long-term performance or that they can be avoided by attention to design and quality control. Even using a combination of near-field parameters set to their most conservative values, the performance of the near field is sufficient to ensure that the calculated annual individual dose does not exceed the regulatory guideline. This is also true in the hypothetical case where releases from this pessimistic near-field representation are transferred directly to the biosphere. Hence, only phenomena that would render inappropriate the representation of the engineered barrier by the current near-field model need further consideration. Only three phenomena have been identified which would require a different conceptual model of the engineered barriers:

- **Canister sinking:** the present estimate that sinking of the canister in the bentonite will be insignificant is based on the model of compacted bentonite as a solid with strain-hardening properties. This is supported by short-term experimental measurements. Alternative models could be considered, but the essential understanding and data are lacking at present. However, several emplacement/design alternatives that would prevent or reduce the potential for sinking have been identified (see Subsection 4.3.3.11). These could be considered further if new studies indicate that canister sinking is of concern. This topic will be kept under review.
- **Colloid transport:** it is expected that the saturated bentonite will prevent the transport of colloids away from the wastes. All known processes that might affect the properties of the bentonite under repository conditions have been assessed (see Subsection 3.4.4); this assessment, together with evidence from natural analogues, gives confidence that the essential properties of the bentonite, including the colloid filtration, will be maintained over several million years. This topic will be kept under review because of its central importance to engineered-barrier performance.
- **Human intrusion:** Clearly, direct intrusion by man into the repository (e.g., an exploration borehole, which intercepts an emplacement tunnel or waste canister) could create a condition not covered by the near-field model. Deliberate intrusion into a repository is excluded from consideration in accordance with Swiss regulations (HSK & KSA 1993). Apart from consideration of a deep drinking-water well, inadvertent human actions that might affect repository performance are also excluded from quantitative assessment in Kristallin-I. Siting of the repository in the low-permeability domain of the crystalline basement would be expected to minimise such risks, because of its lack of mineral or other resources (THURY et al. 1994). The potential conflict of interest between the use of the crystalline basement as a repository host rock and its use as a geothermal energy source should be kept under review.

7.3.3 Performance of the Geological Barriers

The geological barriers consist of the block (or blocks) of low-permeability crystalline rock in which the repository is sited, major fault zones that bound such blocks, some of which may be water conducting, and the overlying higher-permeability crystalline rock and sedimentary formations. However, in the present assessment models, possible retardation effects in the higher-permeability domain and in the sediments are neglected, and modelling of radionuclide transport in major water-conducting faults show these can have little impact on overall performance compared to transport in the low-permeability domain.

The low-permeability domain is potentially capable of providing significant attenuation of releases from the engineered barriers. However, the simplified geometrical representation of the internal structure of the water-conducting features in the geosphere model - and, in particular, the width and separation of open channels - is of critical importance to the calculated performance. Variability and uncertainty in the data currently available and the limited range of very simple geometries allowed in the current geosphere transport model have led to the adoption of a highly conservative representation in the Reference-Case geosphere, giving little reduction in the dose maxima of the most important radionuclides. Of the different types of water-conducting features examined, cataclastic zones and jointed zones with broad, widely-spaced channels give the poorest calculated performance; significantly better performances are calculated for other types.

Conservatism is also introduced in the Reference Case by the adoption of a high value for the groundwater flowrate through water-conducting features. In the groundwater flow model, heterogeneity (channelling) within water-conducting features is neglected, as is the correlation between the transmissivity of water-conducting features and the hydraulic gradient. A preliminary study accounting for the latter effect indicates that groundwater flow may be over-estimated by up to a factor of 10 (THURY et al. 1994). In addition, the groundwater flowrate used in the Reference Case is based on a model which considers only a few of the first- and second-order faults to be hydraulically active. This model assumption gives higher gradients (and thus higher flowrates through individual faults) than an alternative assumption in which all such faults are hydraulically active. Transport modelling indicates that a 10-fold reduction in the assumed flowrate can have a pronounced effect in reducing the releases of many radionuclides.

Conclusions from geosphere-transport modelling are as follows:

- The choice of geometrical representation of water-conducting features in the low-permeability domain is critical to calculated performance. Determining which features are most important as potential radionuclide transport paths and accounting for their complex structure with an appropriate model are therefore important tasks which are key areas for future work. The current representation is chosen because it is the most conservative; further characterisation work is therefore expected to lead to a decrease in calculated doses.

- The variability in the groundwater flow between features can be important - a few water-conducting features carrying high water flow can significantly affect the overall performance of the low-permeability domain as presently calculated. It would be useful to determine the frequency of occurrence of such features and to model their interaction with the emplacement tunnels in greater detail.
- The relatively high water fluxes through the major water-conducting faults, even with an optimistic representation of the internal geometry of the small-scale water-conducting features within major faults, means that they provide an insignificant barrier to radionuclide migration compared with that provided by the low-permeability domain.
- Explicit modelling of the non-linear sorption of caesium does not greatly improve the performance of the low-permeability domain in the Reference Case. A reduction of ^{135}Cs flux is, however, predicted when less conservative representations of the internal geometry of water-conducting features are assumed.
- Taking into account the transport of radionuclides sorbed on colloids naturally present in the groundwater of the crystalline basement has little effect on the Reference-Case results. Although the model treatment is relatively simple, conservative parameter values for sorption on colloids and colloid concentration in groundwater were adopted and the calculated results are therefore likely to err on the conservative side. However, the possibility of irreversible sorption on colloids (which may reduce safety margins) has not yet been considered nor has the possibility that the geosphere may act as a filter for colloids (which may increase safety margins); these are also areas which deserve further attention.

In summary, the current view is that the engineered barriers are likely to provide sufficient safety, as demonstrated by the calculations of the hypothetical case of direct release from the near field to the biosphere. However, as further information becomes available, it may be possible to adopt a less conservative representation of the geosphere, thereby increasing supportable safety margins and allowing optimisation of the repository concept.

7.3.4 Reserves of Performance in the Safety Case

There are a number of features, events and processes, which can contribute positively to repository performance, but are not currently represented in the Kristallin-I safety-assessment models. Thus there are reserves of performance in the safety case which could, if required, be mobilised to show even greater levels of safety than indicated by the present safety-assessment calculations. These reserve FEPs are discussed in Subsection 4.4.3. The most significant are thought to be:

- natural concentrations of safety-relevant radionuclides in groundwater, the presence of which would decrease the net fluxes of these radionuclides across the bentonite-host rock interface (for example, uranium isotopes);
- limited extent of the excavation-disturbed zone, which is, in the current model of radionuclide release and transport, assumed to be continuous along the emplacement tunnels and hence provide a conduit for advective radionuclide transport from the bentonite to the water-conducting features of the low-permeability domain;
- variability in the properties of water-conducting features and the connectivity between features (the present assumptions neglect both variability and connectivity; transport is calculated through a single model conduit with a set of conservatively chosen properties, which are constant along the whole transport path - in particular, the most pessimistic internal geometry of water-conducting features is chosen in the Reference Case).

7.4 Preferred Geological Characteristics of a Potential Site

7.4.1 Key Host-Rock Characteristics

From the discussion in Section 7.3, it is possible to identify properties of the host rock that are of key importance to repository performance. Although the repository depth is around 1000 m, only about 100 m of rock closest to the repository is, in the Kristallin-I safety assessment, considered to contribute to the retention of radionuclides. Within the first few metres around the repository, the key geological characteristics affecting the performance and longevity of the engineered barriers are:

- specific groundwater flow (Darcy velocity) around the engineered barriers;
- groundwater chemistry;
- a thick overburden (crystalline and overlying sedimentary rock) and tectonic stability away from major fault zones (to ensure that mechanical integrity is not lost through major rock movements).

Over larger length scales (~100 m), the key characteristics affecting the performance of the geological barriers are:

- specific groundwater flow through the low-permeability host rock;

- density⁴⁵ and geometry of open channels within the water-conducting features of the host rock;
- mineralogy and groundwater chemistry;
- flowpath length in the low-permeability domain of the crystalline basement.

In addition, the overall characteristics of the host rock should be such as not to attract inadvertent human intrusion (for example, no economically viable mineral deposits).

Referring to the objectives of the Kristallin-I safety assessment, a specific aim is to establish desirable ranges for the parameters which delineate these characteristics, providing input for the identification of potential sites for further work. Difficulties arise firstly, because the parameters are interdependent in the way in which they affect repository performance and secondly, because they also depend strongly on the current repository concept, which may well be adapted according to the findings from site characterisation and technical developments in engineered-barrier design. Despite these difficulties, parameter values relevant to different aspects of repository performance are listed below; these provide guidance as to the conditions which are preferred. However, for the above mentioned reasons, the numbers given should be considered as a general guide and not definitive requirements.

7.4.2 Host-Rock Characteristics Providing a Favourable Environment for the Engineered Barriers

In the neighbourhood of the repository (on a scale of a few metres or tens of metres), the following would favour good performance of the engineered barriers over a prolonged period:

- An average specific groundwater flow in the order of 10^{-11} to 10^{-13} m s⁻¹, (corresponding, for example, to a hydraulic conductivity in the range 10^{-9} to 10^{-11} m s⁻¹ for a hydraulic gradient of 1%), although higher flowrates do not necessarily rule out a safe repository. The Reference-Case value in the Kristallin-I study is 10^{-12} m s⁻¹ (2×10^{-5} m y⁻¹; see Table 3.7.6).
- A near-neutral pH and reducing groundwater with low to moderate salinity (ensuring minimum alteration of the bentonite - see also Subsection 3.4.4.5, low solubilities, good sorption and an adequate canister lifetime). The pH of the reference groundwater in the Kristallin-I study is 7.7 (Area West and Area East), the Eh is -18 V (Area West) and -0.03 V (Area East) and the ionic strength has a molality of 0.021 (Area West) and 0.0103 (Area East); see Table 3.5.2.

⁴⁵ The trace length of channels per unit area of a plane normal to the flow direction (the parameter *H* in Table 5.3.2).

An overburden with a thickness in the order of 400 m would protect the engineered barriers from near-surface geological and climatic changes (see Chapter 12 in THURY et al. 1994). Furthermore, temperature and rock-mechanical aspects must be considered in selecting a suitable block of host rock for repository siting.

7.4.3 Host-Rock Characteristics Providing Adequate System Performance, Assuming Poor Performance of the Engineered Barriers

In the Reference Case, where the engineered barriers perform as expected, many radionuclides decay substantially within the engineered barriers. Radionuclides which are less attenuated by the engineered barriers (particularly ^{135}Cs) are also, in general, not greatly attenuated by the geological barriers, although these are not released at a sufficient rate to be problematic. However, in the extremely pessimistic case of a near field described by a combination of conservative parameters, many radionuclides, which would otherwise decay substantially within the engineered barriers, are released to the geological barriers; the Reference-Case representation of the geological barriers may then be highly effective in attenuating these radionuclides. This is true even for a set of host-rock characteristics less favourable than those of the Reference Case. The following characteristics of the low-permeability domain of the crystalline basement, on a scale of about 100 metres around the repository, would ensure significant attenuation of release within the geological barriers:

- A ratio of average specific groundwater flow to density of open channels of $10^{-8} \text{ m}^2 \text{ s}^{-1}$. The Reference-Case value of this ratio is $10^{-9} \text{ m}^2 \text{ s}^{-1}$, corresponding to a specific groundwater flow of $10^{-12} \text{ m s}^{-1}$ ($2 \times 10^{-5} \text{ m y}^{-1}$; see Table 3.7.6) and a density of open channels in the order of 10^{-3} m m^{-2} (for cataclastic zones or jointed zones with broad, widely-spaced channels⁴⁶; see Table 5.3.2). Thus, attenuation would be achieved with either:
 - an average specific groundwater flow of $10^{-11} \text{ m s}^{-1}$ or less, with the currently assumed channel density, or
 - a density of open channels in the order of 10^{-4} m m^{-2} or more, with the currently assumed specific groundwater.

⁴⁶ This corresponds to 1 channel per 100 m^2 for a typical channel width of 10 cm ($2x_1$: see Chapter 5). The assumed density of open channels is smaller than in other recent safety assessments for repositories in crystalline host rock. The density of channels is equivalent to the "specific surface area for matrix diffusion" in the SKB 91 safety assessment (SKB 1992). The value used in the SKB 91 reference case is $10^{-1} \text{ m}^2 \text{ m}^{-3}$, with a conservative parameter variation of $10^{-2} \text{ m}^2 \text{ m}^{-3}$; two or one order of magnitude larger than the Kristallin-I reference case, respectively. However, specific flowrates are also somewhat higher in SKB 91 (the essential parameter is the specific surface area for matrix diffusion divided by the specific flowrate).

- A suitable mineralogy and groundwater chemistry (colloid concentration and salinity) for high radionuclide retardation.

As indicated above, if the engineered barriers perform as expected, geological barriers with these characteristics would provide little further attenuation for those radionuclides least attenuated by the engineered barriers. In order to obtain a significant additional reduction in their dose maxima, either the specific groundwater flowrate would have to be about 10 times lower than in the Reference Case, or the density of open channels would have to be about 10 times higher. For example, with a Reference-Case open-channel density of 10^{-3} m m^{-2} , a specific groundwater flowrate in the order of $10^{-13} \text{ m s}^{-1}$ or less (corresponding, for example, to a hydraulic conductivity of $10^{-11} \text{ m s}^{-1}$ for a hydraulic gradient of 1%) would be required.

Current uncertainties in the geological characteristics of the crystalline basement of Northern Switzerland have led to the adoption of a set of assumptions and data in the Reference Case that errs on the side of conservatism. Additional information from site-specific investigations is likely to enable the conservatism of assumptions concerning the geological characteristics of a potential site to be reduced; the adoption of a set of properties similar to those described above may prove possible.

7.5 Safety Assessment Methods, Tools and Data

7.5.1 Developments in Methods and Tools for the Safety Case

The methodology, conceptual models and codes used in the Kristallin-I assessment are the result of considerable research and development work, carried out since the completion of Project Gewähr 1985; the key new features are summarised below.

- A systematic methodology for managing information on the features, events and processes that determine safety has been developed and successfully tested. This methodology has been used to track information and assumptions, to develop scenarios, to identify key reserve features, events and processes, to identify open questions and to define a set of assessment calculations that should provide sufficient insight into performance and a demonstration of safety.
- The near-field release and transport model now explicitly takes account of radionuclide retention in the bentonite, allowing a better appreciation of the effectiveness of the engineered barrier system. In Project Gewähr 1985, this retention was treated as a reserve process and no credit was taken for its effect in the model-chain calculations, although it was used in the selection of safety-relevant nuclides for these calculations.
- An enhanced and more transparent link between field information and model input parameters is now available. In particular, a better-justified set of model representations of small-scale water-conducting features in crystalline rock has been developed through close interaction between modellers and geologists.

- The geosphere transport model now includes non-linear sorption and can treat colloid-facilitated radionuclide transport.
- A generic biosphere model is now available, which can be adapted to site-specific situations and can better represent biosphere phenomena.

7.5.2 Developments in Supporting Models and Databases

The Kristallin-I assessment also takes advantage of extensive new data, acquired since the completion of Project Gewähr 1985. Where possible, use is made of data which is specific to the crystalline basement of Northern Switzerland. This is particularly true for the geological, geochemical and hydrogeological databases. Information used in Project Gewähr 1985 was based mainly on a single borehole; for Kristallin-I, information from seven deep boreholes has been analysed in detail. The databases are also complemented by an enhanced suite of hydrogeological models. Where data specific to the crystalline basement in Northern Switzerland are unavailable (for example, data quantifying radionuclide sorption in the geosphere), use is made of data from the literature, assessed according to its relevance to the Kristallin-I system. Generic data (for example, element- or radionuclide-specific data for the calculation of annual individual dose from the various exposure pathways of the biosphere model) are obtained from compilations, developed by international technical bodies (for example, in international projects). The key developments in databases and supporting models since the completion of Project Gewähr 1985 are summarised below.

- Supporting rock mechanics and thermal studies, demonstrating, for example, the feasibility of a smaller emplacement-tunnel spacing.
- An updated specification for vitrified waste, which has been assessed and used as a basis for a model radioactive waste inventory. The model inventory also includes components not accounted for in the specification.
- Support for the reference glass-corrosion rate used in Project Gewähr 1985 from the final results of the JSS project (summarised in WERME et al. 1990) and interim results of on-going, long-term corrosion experiments.
- A wider range of detailed models and experimental data, allowing a better assessment of specific near-field processes - for example, various aspects of canister behaviour (mechanical behaviour, hydrogen production, canister sinking).
- A new thermodynamic database that is more rigorously defined, is used in the selection of solubility limits defined for near-field conditions.
- Further investigation of bentonite behaviour (see, for example, Appendix C of OECD 1993), including interaction with cement (e.g. BUCHER et al. 1994).

- An improved model of the structural geology of the crystalline basement, which delineates potential siting sub-regions (Areas West and East) and incorporates a statistical representation of the distribution of major faults within these sub-regions.
- A new suite of hydrogeological models, based on a synthesis of more extensive hydrologic measurements, which takes account of the structural model and regional geochemical and isotopic measurements.
- A detailed characterisation of all water-conducting features observed in the deep boreholes, synthesised into model representations of three classes of such features. These representations are complemented by literature studies which define important sorption and matrix diffusion properties.

7.6 Building Confidence in Kristallin-I Assessment Conclusions

7.6.1 Introduction

The measures adopted to build confidence in the adequacy of the methods, tools and data used in the assessment of repository safety have been outlined in Section 2.7. These measures may be regarded as validation, according to the definition of the term as "Providing confidence that a computer code used in safety assessment is applicable for the specific repository system." (HSK & KSA 1993), and comprise:

- systematic and transparent approaches to model development and consideration of alternative conceptual models, including a full description of the judgements and assumptions made in model development and application;
- use of laboratory and field experiments as well as natural analogues to test the models;
- iteration between model development, safety assessment and collection of experimental data, either in the laboratory or in the field;
- use of natural analogues and palaeohydrogeological models to evaluate uncertainties arising from the temporal and spatial scales of concern;
- ongoing critical peer review through presentations, publications in open literature and participation in international projects and workshops.

This section focuses specifically on the approach to model development and the testing of models using laboratory and field data and natural analogues.

Studies within the Nagra programme prior to Kristallin-I, which employed laboratory and field data to test groundwater flow, geochemical and radionuclide transport models, are summarised in McCOMBIE et al. 1987. In these studies:

- groundwater flow models were tested by comparing predictions with independently collected data (e.g. hydraulic heads and discharge rates) and correlating the predictions with regional hydrochemical and geothermal data;
- predictions of chemical speciation using thermodynamic equilibrium calculations were tested against laboratory experiments and analyses of natural groundwaters;
- for radionuclide transport models, predictions were compared with break-through curves, obtained in experiments carried out over a range of spatial and temporal scales (both laboratory and field test), using a variety of both sorbing and non-sorbing tracers.

Furthermore, Nagra has been involved in several natural analogue study projects, such as the international Poços de Caldas study (summarised in CHAPMAN et al. 1991). The experience gained from these studies supports the understanding of many key processes, although the information can, in many cases, only be used in a qualitative manner. The use of natural analogues has recently been summarised in MILLER et al. 1994, where the following areas are discussed:

- natural analogues of repository materials and their behaviour (for example, waste-form degradation, thermal and chemical stability of buffer materials);
- processes in the engineered and natural barriers (for example, radionuclide transport);
- the application of data derived from natural analogues to repository safety assessments;
- building public confidence.

Recent work which builds confidence in the key assumptions of the Kristallin-I assessment is summarised below. As discussed in Subsection 7.3.2, a good performance of the engineered barriers has been found to depend primarily on:

- the longevity of the engineered system (particularly, that of the bentonite);
- low solubilities at the inner boundary of the bentonite.

These two areas are discussed in more detail in Subsections 7.6.2 and 7.6.3. In regard to the geological barriers, as discussed in Subsection 7.3.3, uncertainties in the data currently available have led to the adoption of a highly conservative representation, with the engineered system providing the principal barriers to radionuclide release and transport. However, as further data become available, the set of assumptions concerning geosphere transport will become less conservative, possibly increasing the calculated performance of the geological barriers. Nagra has carried out a substantial programme of

work to build confidence in its geosphere transport modelling capabilities; this work is discussed below in Subsection 7.6.4.

Work aimed at the testing of other models and underlying assumptions less critical to repository performance includes, for example:

- evaluation of a conservative canister lifetime: there are two components to building confidence in the conservatism of the 1000 year canister lifetime assumed in Kristallin-I:
 - the mechanical strength of the canister - the model used to assess the sufficiency of the canister wall thickness to withstand maximum isostatic loads in the bentonite, has been tested against laboratory experiments on model canisters in the CEC COMPAS exercise (OVE ARUP 1990; ATTINGER & DUIJVESTIJN 1994) (see also Subsection 3.4.3.1),
 - the long-term corrosion rate of the canister - experiments (see, for example, NAGRA 1984, SIMPSON & VALLOTTON 1986) indicate average corrosion rates, which, if extrapolated, would lead to corrosion of only a few millimetres in 1000 years, significant uneven corrosion being ruled out (see Subsection 3.4.3.3); further support for the conservatism of the assumed long-term corrosion rate comes from the study of archaeological analogues (MILLER et al. 1994);
- evaluation of a conservative glass-corrosion rate: the rate assumed in Kristallin-I is supported by the results of relatively long-term (548 days) corrosion experiments (ZWICKY et al. 1992), but taking account of the influence of possible sorption of Si on the canister corrosion products and on the bentonite; the applicability of laboratory tests to leaching of glass under natural conditions is supported by studies of natural basalt glasses, although such results should not be over-interpreted due to the differences in composition between borosilicate and natural glasses (see also Subsection 3.4.2.2);
- testing of the groundwater flow models: independent evidence from measured hydrochemical and isotopic compositions of the groundwater support the conceptual model of regional flow in the crystalline basement of Northern Switzerland from recharge areas in the southern and south eastern Black Forest towards discharge areas along the river Rhine west of Koblenz (Chapter 12 in THURY et al. 1994).

7.6.2 Longevity of the Bentonite

Literature reviews have been carried out (GRAUER 1986; GRAUER 1990a) in order to evaluate the longevity of the bentonite under repository conditions. The alteration of montmorillonite to illite was identified as an important process; alteration to chlorite occurs only in waters with high magnesium concentrations and does not require further discussion. The alteration from montmorillonite to illite requires a supply of potassium ions. If it is assumed that this alteration is controlled by the rate of supply of potassium

from the groundwater (at the Reference-Case groundwater flowrate) and that kinetics does not play a role, then the complete alteration process would take at least 10^8 years (see Subsection 3.4.4.5). Alternatively, if an unlimited supply of potassium is assumed but the kinetics of alteration are taken into account, extrapolation of laboratory experiments also gives very long alteration times (around 1 million years). It should further be noted that illite, with a low permeability and microporous structure, has many of the favourable properties required of a buffer material.

The most likely of the potential interactions between bentonite and canister corrosion products is a reaction forming new iron silicate phases (see Subsection 3.4.4.6). However, given the quantities present in the repository, a complete reaction of this type could alter only a small fraction of the bentonite.

Extensive studies of natural analogues have also shown that, under repository conditions, there will be no drastic change in swelling capability, hydraulic permeability and cation-exchange capacity over periods in excess of 1 million years.

To summarise, there is sufficient evidence to support the assumption that the longevity of the bentonite is ensured over sufficiently long time periods in a suitable environment.

7.6.3 Confidence in the Selection of Solubility Limits

Despite the known low solubility of many of the elements considered, rigorous prediction of their solubility limits under repository conditions is currently not possible. However, understanding of the mechanisms that lead to the observed very low concentrations is sufficiently good to allow bounding estimates of the maximum concentrations under repository near-field conditions to be made.

For the Kristallin-I safety assessment, therefore, a solubility database has been constructed which provides bounding estimates of maximum expected concentrations using state-of-the-art geochemical models, constrained by a subjective appraisal of the uncertainties involved (see BERNER 1994 and Subsection 3.4.6.2). The procedure used involves:

- definition of a reference porewater;
- calculation of the solubility of a range of potentially limiting solid phases;
- use of expert opinion to compile a database from conservatively selected solubility limits.

Confidence in the conservatism of the selected solubility limits is provided by the use of conservative assumptions regarding key features of the reference bentonite porewater and by testing exercises.

The key features of the bentonite porewater are the redox conditions, pH and concentration of complexing ligands (particularly carbonate). In spite of its complexity, the chemistry of the porewater near the canister is expected to remain constant for long periods. This is because of the longevity of the bentonite (as discussed above) and because the system, containing large amounts of bentonite and iron in a stable hydrogeological environment, is strongly buffered. For modelling purposes, an Eh / pH range is selected to cover uncertainties in these parameters and carbonate concentration is set to a maximum expected value, assuming calcite saturation.

Solubility limits for relevant elements in this porewater are calculated for a range of pure solid phases using a standard chemical thermodynamic code (MINEQL/PSI; BERNER 1994) with a carefully selected database⁴⁷ (PEARSON & BERNER 1991; PEARSON et al. 1991). The basic code has been extensively verified (e.g. NORDSTROM et al. 1979) and the specific code / database combination has been tested in intercomparison exercises within the CEC CHEMVAL project (e.g. READ & BROYD 1991).

Having calculated solubility limits for pure solid phases, these must be evaluated by expert opinion in order to assess:

- the completeness and quality of the thermodynamic database;
- the likelihood that such solids would form under repository conditions (for example, many thermodynamically stable minerals form only under high-temperature conditions, whereas less stable - and thus more soluble - phases may persist for geological periods of time);
- other possible reasons for the persistence of non-equilibrium conditions (for example, very slow redox kinetics);
- the possible effects of the formation of impure phases, including co-precipitates: co-precipitation is taken directly into account only for very similar elements (e.g. Cm with Am); otherwise co-precipitated phases are neglected, which, in general, leads to an overestimate of the solubility limits and is therefore conservative (this will be the case for the near field in Kristallin-I, in which secondary minerals, resulting from the corrosion of both the glass and the steel canister, are expected to form various solid solutions capable of incorporating the radionuclides released from the waste form).

In addition to judgement based on experience, documented concentration measurements from relevant laboratory and field systems are taken into consideration in order to make this assessment.

A final step is the comparison of the derived solubility database with those used in other safety assessments (McKINLEY & SAVAGE 1994). Such comparisons need to be interpreted with care, but reasonable consistency of databases for equivalent reference porewaters contributes to confidence.

⁴⁷ Extensions to the database are addressed in BERNER 1994.

7.6.4 Geosphere Transport Modelling

Testing of geosphere transport models has a long history in the Swiss disposal programme; the active participation in international studies such as INTRACOIN (SKI 1984; SKI 1986), INTRAVAL (SKI 1993), HYDROCOIN (SKI 1992) and domestic studies such as the joint Nagra/PNC migration experiment at the Grimsel Test Site (e.g. FRICK et al. 1991; ALEXANDER et al. 1992; FRICK et al. 1992), with supporting laboratory investigations (BRADBURY (ed.) 1989), are an important part of the Swiss programme.

A range of migration tests has been carried out at the Grimsel Test Site, using both sorbing and non-sorbing tracers; the results provide confidence in the dual-porosity concept as an appropriate foundation for a model of transport in fractured porous media.

Experimental conditions have been varied and the measured radionuclide breakthrough successfully reproduced using sets of parameter values which differ only for those parameters relevant to the difference in conditions. For example, in a set of experiments where the rate of water flow through the fracture is varied, the breakthrough curves are reproduced using identical values of, for example, fracture aperture, diffusion constant and porosities. Successful predictions of breakthrough curves for a new experimental set up with reduced migration pathlength are reported in HEER & HADERMANN (1994); the ability to predict the outcome of new experiments provides a most stringent test of the model.

It is concluded that the model provides a satisfactory interpretation of the measured data and no evidence has been found which would indicate that processes relevant to safety assessment and not accounted for in the model are operating (HADERMANN & HEER 1994). This conclusion rests on the ability of the model to:

- reproduce measured data to within limits set by experimental uncertainty;
- reproduce the data using parameters which are physically reasonable (in agreement with general scientific understanding) and are also consistent with (i) observed features of the system (e.g. fracture aperture), (ii) independent experiments (e.g. batch sorption experiments, diffusion experiments) and (iii) further experiments on the same system;
- successfully predict the outcome of new experiments before those experiments are performed.

The key findings with respect to the geosphere transport model employed in the Kristallin-I assessment can thus be summarised as follows:

- During the past few years, significant progress has been made with respect to model testing, especially in the areas of designing experiments and of evaluating their results.

- Although quantity and quality of experimental data has very much increased, no new transport processes have been identified which would be significant for safety assessment. Recent studies show kinetic sorption effects; these are relevant on the short timescales of the experiments, but not on the far longer timescales of concern in a post-closure safety assessment.
- The key mechanism of matrix diffusion has, in many experiments, been identified as important and its existence and effectiveness are much better founded than 10 years ago.
- The observed consistency between sorption values extracted from laboratory batch-sorption and column experiments and migration experiments in the field is a clear indication that sorption values carefully measured in the laboratory can be used as a basis for safety assessment without the need for a safety reduction factor.

Appropriate data for modelling the spatial and temporal scales needed in repository safety assessment are still difficult to obtain, although much progress has been made in the methodology of transforming field observations to transport code input. A more realistic treatment of variability in geosphere properties is needed. The observations from hydrochemistry and isotope chemistry suggest relatively long residence times of the groundwater (see Chapter 7 in THURY et al. 1994), inconsistent with the geosphere transport model (calculated residence time, taking into account the effects of matrix diffusion as well as advection). This indicates that the current dataset for geosphere modelling might be too conservative.

7.7 Suitability of the Crystalline Basement of Northern Switzerland

The overall conclusions from the Kristallin-I assessment studies, with respect to the suitability of the crystalline basement of Northern Switzerland as a host rock for a high-level radioactive waste repository, are summarised below.

- The engineered barriers as designed, emplaced in the low-permeability domain of the crystalline basement as currently characterised, can provide a sufficient level of safety. Even using the conservative models that are appropriate to currently available data, the calculated doses are well below the Swiss regulatory guideline of 0.1 mSv y^{-1} .
- A suite of calculations has been carried out that illustrates the effects of uncertainty in the characteristics of the engineered and geological barrier characteristics and in relevant processes that operate therein. Parameter variations have been performed, both for specific system components and for the whole system, and the effect of alternative model assumptions investigated. Alternative scenarios, covering uncertainty in the long-term evolution of the repository and environment have also been considered. The variations evaluated all lead to doses well below the regulatory guideline.

- The roles of the engineered and geological barriers in providing safety are relatively well understood. Uncertainty in the geological information now available requires a highly conservative representation of radionuclide transport in the geosphere; a robust demonstration of safety relies predominantly on the properties of the engineered barriers. The main role of the host rock in this case is to provide a suitable environment for the engineered barriers, i.e. mechanical protection, adequate geochemical conditions, and sufficiently low groundwater flowrates.
- In future, a more detailed characterisation of the host rock and the properties of its water-conducting features may allow a less conservative approach to geosphere-transport modelling. In this case, it may be concluded that the host rock forms a very efficient additional safety barrier. Such a characterisation will also provide information on the spatial and geometrical characteristics of major faults and will allow the repository layout to be optimised to take advantage of the natural safety barrier offered by the host rock.

Regarding confidence in the methodology and calculations that lead to these conclusions.

- The scenario development procedure provides a structured and documented path by which the safety assessment calculations performed are justified. A number of reserve FEPs has been identified that could, if required, be mobilised to show even greater margins of safety. A number of open questions have also been identified. Most of these can, if necessary, be avoided by attention to detailed engineered-barrier design and siting. An exception is the effect of human intrusion into the repository; in this case, risk-probability arguments may need to be invoked to meet protection objectives.
- The present calculational tools are adequate, although enhancements could still be made. Codes have been tested and verified, including comparison in international exercises. Confidence has been built in the underlying conceptual models by a variety of means, particularly through the testing of models using data from field and laboratory experiments, and from analogue studies. The model input parameters are traceably derived and are defensible by reference to the underlying scientific data.

Overall it is concluded that, whereas considerable work is still to be done on the detailed characterisation of potential sites and optimisation of a repository layout and engineered barriers at a selected site, the crystalline basement of Northern Switzerland continues to offer good prospects as a host rock for high-level radioactive waste repository.

8. REFERENCES

- AARKROG, A. (1979): Environmental Studies on Radioecological Sensitivity and Variability with Emphasis on the Fallout Nuclides ^{90}Sr and ^{137}Cs ; Risø Report R-191, Risø National Laboratory, Roskilde, Denmark.
- AECL (1985): Second Interim Assessment of the Canadian Concept for Nuclear Waste Disposal; AECL-8373, 4 Volumes, Pinawa, Canada.
- ALDER, J.-Cl. & MCGINNES, D. (1994): Model Radioactive Waste Inventory for Swiss Waste Disposal Projects; Nagra Technical Report NTB 93-21, Nagra, Wettingen, Switzerland.
- ALEXANDER, W.R., MACKENZIE, A.B., SCOTT R.D. & MCKINLEY, I.G. (1990): Natural Analogue Studies in Crystalline Rock: The Influence of Water-Bearing Fractures on Radionuclide Immobilisation in a Granitic Rock Repository; Nagra Technical Report NTB 87-08, Nagra, Wettingen, Switzerland.
- ALEXANDER, W.R., BRADBURY, M.H., MCKINLEY, I.G., HEER, W., EIKENBERG, J. & FRICK, U. (1992): The Current Status of the Radionuclide Migration Experiment at the Grimsel Underground Rock Laboratory; Proc. MRS Symp. Scientific Basis for Nuclear Waste Management XV, pp 721-728.
- ANANTATMULA, R.P., DELEGARD, C.H. & FISH, R.L. (1984): Corrosion Behaviour of Low Carbon Steel in Grande Ronde Basalt Groundwater in Presence of a Basalt-Bentonite Packing; Proc. MRS Symp. Scientific Basis for Nuclear Waste Management VII, p 113.
- ANDERSSON, J. (ed.) (1989): The Joint SKI/SKB Scenario Development Project; SKI 89:14, Stockholm, Sweden.
- ANDREWS, R.W. (1993): Review and Evaluation of the Potential Effects of Gas Generation on the Performance of a High-Level Waste Repository in the Crystalline; Nagra Unpublished Report, Nagra, Wettingen, Switzerland.
- ANDREWS, R.W., LaFLEUR, D.W. & PAHAWA, S.B. (1986): Resaturation of Backfilled Tunnels in Granite; Nagra Technical Report NTB 86-27, Nagra, Wettingen, Switzerland.
- ANON (1994): Die letzte Eiszeit wirkt bis heute nach; Horizonte, Nr. 20, March 1994, Schweizerischer Nationalfonds zur Förderung der wissenschaftlichen Forschung, Bern, Switzerland.
- ANTONY, M.S. (1992): Chart of the Nuclides; Centre de Recherches Nucléaire et Université Louis Pasteur, Strasbourg, France.
- ATLAS DER SCHWEIZ (1965-1990): Verlag der Eidgenössischen Landestopographie, Wabern, Bern, Switzerland.

- ATTINGER, R. & DUIJVESTIJN, G. (1994): Mechanical Behaviour of High Level Nuclear Waste Overpacks under Repository Loading and During Welding; Nagra Technical Report NTB 92-14, Nagra, Wettingen, Switzerland.
- AVOGADRO, A. & DE MARSILY, G. (1984): The Role of Colloids in Nuclear Waste Disposal; Proc. MRS Symp. Scientific Basis for Nuclear Waste Management VII, pp 495-505.
- BAECKMANN W. & SCHWENK, W. (1980): Handbuch des Kathodischen Korrosionsschutzes; 2 Auflage, Verlag Chemie.
- BAERTSCHI, P. & KEIL, R. (1992): Urangelhalte von Oberflächen-, Quell-, und Grundwässern der Schweiz; Nagra Technical Report NTB 91-26, Nagra, Wettingen, Switzerland.
- BAEYENS, B., GROGAN, H.A. & VAN DORP, F. (1989): Transport of contaminated groundwater to soil from a radioactive waste repository; PSI-Report Nr. 98, July 1991, PSI, Würenlingen and Villigen, Switzerland; Nagra Technical Report NTB 89-20, Nagra, Wettingen, Switzerland.
- BAG (1992): Radioaktivität der Umwelt in der Schweiz; Bericht für das Jahr 1991, Bundesamt für Gesundheit, Abteilung Strahlenschutz, Bern, Switzerland.
- BAKER, D.A., HOENTZ, G.R. & SOLDAT, J.K. (1976): FOOD - An Interactive Code to Calculate Internal Radioation Doses from Contaminated Food Products; BNWL-SA-5523, Batelle Pacific Northwest Laboratory, U.S.A.
- BARNARD, R.W., WILSON, M.L., DOCKERY, H.A., GAUTHIER, J.H., KAPLAN, P.G., EATON, R.R., BINGHAM, F.W. & ROBEY, T.I.I. (1992): TSPA 1991: An Initial Total System Performance Assessment for Yucca Mountain; Sandia Report SAN91-2795, UC-814.
- BEAR, J. & VERRUJT, A. (1987): Modelling Groundwater Flow and Pollution; D. Reidel Publishing Company.
- BERGER, E. (1987): Konzeptionelle Überlegungen zum Verhalten von Untertagebauten während Erdbeben; Nagra Informiert 9/3, pp 15-20.
- BERGSTRÖM, U. & NORDLINDER, S. (1990): Individual Radiation Doses from Unit Releases of Long-Lived Radionuclides; SKB Technical Report 90-09, Stockholm, Sweden.
- BERNER, U. (1994): Kristallin-I; Estimates of Solubility Limits for Safety Relevant Radionuclides; PSI-Report, PSI, Würenlingen and Villigen, Switzerland; Nagra Technical Report NTB 94-08, Nagra, Wettingen, Switzerland (*in press*).
- BIRCH, L.D. & BACHOFEN, R. (1990): Complexing Agents from Microorganisms; Experientia 46, pp 827-834.

- BÖHRINGER, J., FRITSCHI, M., SCHWANNER, I. & RESELE, G. (1986): Radioökologische Modellierung der Biosphäre am Beispiel des Modellgebietes Oberbauenstock; Nagra Technical Report NTB 85-32, Nagra, Wettingen, Switzerland.
- BÖRGESSON, L., HOEKMARK, H. & KARNLAND, O. (1988): Rheological Properties of Sodium Smectite Clay; SKB Technical Report 88-30, Stockholm, Sweden.
- BOULTON, G.S. & PAYNE, A. (1993): Simulation of the European Ice Sheet through the Last Glacial Cycle and Prediction of Future Glaciation; SKB Technical Report 93-14, SKB, Stockholm, Sweden.
- BRADBURY, M. (ed.) (1989): Laboratory Investigations in Support of the Migration Experiments at the Grimsel Test Site; PSI-Report Nr. 28, April 1989, PSI, Würenlingen and Villigen, Switzerland; Nagra Technical Report NTB 88-23, Nagra, Wettingen, Switzerland.
- BRAINARD, J.R., STRIETELMEIER, B.A., SMITH, P.H., LANGSTON-UNKEFER, P.J., BARR, M.E. & RYAN, R.R. (1992): Actinide Binding and Solubilization by Microbial Siderophores; *Radiochimica Acta*, 58/59, pp 357-363.
- BRENNER, R.P. (1988): Bohrlochversiegelung: Materialeigenschaften von hochverdichtetem Bentonit mit Eignungsbeurteilung; Nagra Technical Report NTB 88-04, Nagra, Wettingen, Switzerland.
- BROOKINS, D.G. (1984): *Geochemical Aspects of Radioactive Waste Disposal*; Springer-Verlag, Berlin, Germany.
- BUCHER, F., KAHR, G., MADSEN, F. & MAYOR, P.A. (1994): Wechselwirkungen von Abgebundenem Zement mit Verdichteten Bentoniten; Nagra Technical Report NTB 93-25, Nagra, Wettingen, Switzerland.
- CARNAHAN, C.C. (1988): Theory and calculation of water distribution in bentonite in a thermal field; Proc. MRS Symp. Scientific Basis for Nuclear Waste Management XII, pp 729-739.
- CEC (1988): Nuclear Science and Technology; PAGIS: Performance Assessment of Geological Isolation Systems for Radioactive Waste, Summary; EUR 11775 EN.
- CHAPMAN, N.A., MCKINLEY, I.G., SHEA, M.E. & SMELLIE, J.A.T. (1991): Poços de Caldas Report No. 15 - Summary and Implications for Radioactive Waste Management; SKB Technical Report 90-24; U.K. DOE WR 90-055; Nagra Technical Report NTB 90-33, Nagra, Wettingen, Switzerland.
- COGEMA (1986): Specifications of Vitrified Residues Produced from Reprocessing at UP2 or UP3-A la Hague Plants, Second Series, COGEMA, July 1986.

- COMANS, R.N. J. & HOCKLEY, D.E. (1992): Kinetics of Cesium Sorption on Illite; *Geochim. Cosmochim. Acta*, Vol. 53, no. 3, pp 157-1164.
- CONCA, J.L., APTED, M. & ARTHUR, R. (1993): Aqueous Diffusion in Repository and Backfill Environments; *Proc. MRS Symp. Scientific Basis for Nuclear Waste Management XVI*, pp 395-402.
- COUTURE, R.A. (1985): Steam Rapidly Reduces the Swelling Pressure of Bentonite; *Nature*; 318, pp 50-52.
- CRANWELL, R.M., GUZOWSKI, R.W., CAMPBELL, J.E. & ORTIZ, N.R. (1982): Risk Methodology for Geologic Disposal of Radioactive Waste: Scenario Selection Procedure; NUREG/CR-1667, SAND80-1429.
- CROFF, A. G. (1980): A Users Manual for the ORIGEN2 Computer Code; ORNL / TM-7175, Oak Ridge National Laboratory, Oak Ridge, U.S.A.
- CURTI, E. (1991): Modelling the Dissolution of Borosilicate Glasses for Radioactive Waste Disposal with the PHREEQE/GLASSOL Code: Theory and Practice; PSI-Report Nr. 86, February 1991, PSI, Würenlingen and Villigen, Switzerland; Nagra Technical Report NTB 91-08, Nagra, Wettingen, Switzerland.
- CURTI, E. (1993): Modelling Bentonite Porewaters for the Swiss High-Level Radioactive Waste Repository; PSI-Report Nr. 93-05, November 1993, PSI, Würenlingen and Villigen, Switzerland; Nagra Technical Report NTB 93-45, Nagra, Wettingen, Switzerland.
- CURTI, E., GODON, N. & VERNAZ, E.Y. (1993): Enhancement of the Glass Corrosion in the Presence of Clay Materials: Testing Experimental Results with an Integrated Glass Dissolution Model; *Mat. Res. Soc. Symp. Proc.* 294, 163-170.
- DAMES & MOORE (1991): Technical Reference Manual for TIME4 Version 1.0 (2 volumes), UK DoE Report HMIP/RR/91.049 and HMIP/RR91.050.
- DeCANNIERE, V., FIORAVANTE, P., GRINDROD, P., HOOKER, P., IMPEY, M. & VOLKAERT, G. (1993): MEGAS: Modelling and experiments on gas migration in repository host rocks; CEC Nuclear Science and Technology Report EUR 14816 EN.
- DEGUELDRE, C. (1994): Colloid Properties in Granite Groundwater Systems; PSI-Report Nr. 94-21, September 1994, PSI, Würenlingen and Villigen, Switzerland; Nagra Technical Report NTB 92-05, Nagra, Wettingen, Switzerland.
- DIEBOLD, P. & MÜLLER, W.H. (1985): Szenarien der geologischen Langzeitsicherheit: Risikoanalyse für ein Endlager für hochaktiver Abfälle in der Nordschweiz; Nagra Technical Report NTB 84-26, Nagra, Wettingen, Switzerland.

- DODDS, J. (1982): La Chromatographie Hydrodynamique; *Analysis*, Vol. 10, 109-119.
- ELSON, J.A. & WEBBER, G.R. (1991): Data to Model the Migration of Radionuclides through the Biosphere during a Glacial Cycle; AECL Technical Report TR/527, Pinawa, Canada.
- FREED, R.L. & PEACOR, D.R. (1989): Variability in Temperature of the Smectite/Illite Reaction in Gulf Sediments; *Clay Minerals* 24, p 171.
- FRICK, U., ALEXANDER, W.R. & DROST, W. (1991): The Radionuclide Migration Experiment at Nagra's Grimsel Underground Test Site - a Comprehensive Program Including Field, Laboratory, and Modeling Studies; Proc. Int. Symp. on the use of Isotope Techniques in Water Resources Development, IAEA-SM-319/27, IAEA, Vienna, Austria.
- FRICK, U., ALEXANDER, W.R., BAEYENS, B., BOSSART, P., BRADBURY, M. H., BÜHLER, C., EIKENBERG, J., FIERZ, T., HOEHN, E., MCKINLEY, I.G. & SMITH, P.A. (1992): Grimsel Test Site: The Radionuclide Migration Experiment - Overview of Investigations 1985 - 1990; PSI-Report Nr. 120, March 1992, PSI, Würenlingen and Villigen, Switzerland; Nagra Technical Report NTB 91-04, Nagra, Wettingen, Switzerland.
- FRICK, U. (1993): Beurteilung der Diffusion im Grundwasser von Kristallingesteinen; Nagra Unpublished Report. Nagra, Wettingen, Switzerland.
- GELHAR, L.W., WELTY, C. & REHFELDT, K.R. (1992): A Critical Review of Data on Field-Scale Dispersion in Aquifers; *Water Resources Research*, Vol. 28, no. 7., pp 1955-1974.
- GOODWIN, B.W. et al. (1994): The Disposal of Canada's Nuclear Fuel Waste: Postclosure Assessment of a Reference System; AECL-10717, COG-93-7, AECL, Pinawa, Canada.
- GRÄFEN, H. & HEITZ, E. (1984): Korrosion und Korrosionsschutz von Endlagerbehältern aus Eisenwerkstoffen unter besonderer Berücksichtigung des schweizerischen Endlagerkonzepts; Nagra Technical Report NTB 84-04, Nagra, Wettingen, Switzerland.
- GRAUER, R. (1983): Gläser zur Verfestigung von hochradioaktivem Abfall: Ihr Verhalten gegenüber Wässern; EIR-Report Nr. 477, February 1983, EIR, Würenlingen, Switzerland; Glasses used in the Solidification of High-Level Radioactive Waste: their Behaviour in Aqueous Solutions; Nagra Technical Report NTB 83-01E, Nagra, Wettingen, Switzerland.
- GRAUER, R. (1985): Synthesis of Recent Investigations on Corrosion Behaviour of Radioactive Waste Glasses; EIR-Report Nr. 538, March 1985, EIR, Würenlingen, Switzerland; Nagra Technical Report NTB 85-27, Nagra, Wettingen, Switzerland.

- GRAUER, R. (1986): Bentonit als Verfüllmaterial im Endlager für hochaktive Abfälle: Chemische Aspekte; EIR-Report Nr. 576, January 1986, EIR, Würenlingen, Switzerland; Bentonite as a Backfill Material in the High-Level Waste Repository: Chemical Aspects; Nagra Technical Report NTB 86-12E, Nagra, Wettingen, Switzerland.
- GRAUER, R. (1990a): The Chemical Behaviour of Montmorillonite in a Repository Backfill - Selected Aspects; PSI-Report Nr. 11, July 1988, EIR, Würenlingen, Switzerland; Nagra Technical Report NTB 88-24E, Nagra, Wettingen, Switzerland.
- GRAUER, R. (1990b): Zur Chemie von Kolloiden: Verfügbare Sorptionsmodelle und zur Frage der Kolloidhaftung; PSI-Report Nr. 65, May 1990, PSI, Würenlingen and Villigen, Switzerland; Nagra Technical Report NTB 90-37, Nagra, Wettingen, Switzerland.
- GRAUER, R. (1991): The Reducibility of Sulphuric Acid and Sulphate in Aqueous Solution; PSI-Report Nr. 109, July 1991, PSI, Würenlingen and Villigen, Switzerland; SKB Technical Report 91-39, SKB, Stockholm, Sweden.
- GRAUER, R. (1993): Zum Verhalten der technischen Barrieren in einem Endlager für hochaktiven Abfall; PSI Unpublished Report, PSI, Würenlingen and Villigen, Switzerland.
- GRAY, M. (1993): Stripa Project 1980-1992: Overview Volume III, Engineered Barriers; Nagra Technical Report NTB 94-43, Nagra, Wettingen, Switzerland.
- GREENHALGH, J.R., FELL, T.P. & ADAMS, N. (1985): Doses from Intakes of Radionuclides by Adults and Young People; NRPB R-162, NRPB Chilton, U.K., available through HMSO, London, U.K.
- GRINDROD, P., ROBINSON, P. & WILLIAMS, M. (1990a): User Guide and Technical Description of RAPIDE: a Package for Radionuclide Decays and Ingrowth Calculations; Nagra Unpublished Report, Nagra, Wettingen, Switzerland.
- GRINDROD, P., WILLIAMS, M., GROGAN, H. & IMPEY, M. (1990b): "STRENG": a Source Term Model for Vitrified High Level Waste; Nagra Technical Report NTB 90-48, Nagra, Wettingen, Switzerland.
- GRINDROD, P., IMPEY, M., SADDIQUE, S. & TAKASE, H. (1994): Saturation and gas migration within clay buffers; Proc. 5rd Int. Conf. on High-Level Radioactive Waste Management, Las Vegas, U.S.A.
- GROGAN, H.A. (1985): Biosphere Modelling for a HLW Repository-Scenario and Parameter Variations; EIR-Report Nr. 561, March 1985, EIR, Würenlingen, Switzerland; Nagra Technical Report NTB 85-48, Nagra, Wettingen, Switzerland.

- GROGAN, H., BAEYENS, B., MÜLLER, H. & VAN DORP, F. (1990): Biosphere Modelling for a Deep Radioactive Waste Repository: Site-Specific Consideration of the Groundwater-Soil Pathway; PSI-Report Nr. 99, July 1991, PSI, Würenlingen and Villigen, Switzerland; Nagra Technical Report NTB 89-21, Nagra, Wettingen, Switzerland.
- HADERMANN, J. & RÖSEL, F. (1985): Radionuclide Chain Transport in Inhomogeneous Crystalline Rocks: Limited Matrix Diffusion and Effective Surface Sorption; EIR-Report Nr.551, February 1985, EIR, Würenlingen, Switzerland; Nagra Technical Report NTB 85-40, Nagra, Wettingen, Switzerland.
- HADERMANN, J. & HEER, W. (1994): The Grimsel Migration Experiment: Integrating Field Experiments, Laboratory Investigations and Modelling; J. Contam. Hydrol. (*to appear 1995*); Proc. Fourth Int. Conf. On the Chemistry and Migration Behaviour of Actinides and Fission Products in the Geosphere, Charleston, U.S.A., pp 765-771.
- HARTLEY, R.W. (1985): Release of Radionuclides to the Geosphere from a Repository for High-Level Waste: Mathematical Model and Results; EIR-Report Nr. 554, February 1985, EIR, Würenlingen, Switzerland; Nagra Technical Report NTB 85-41, Nagra, Wettingen, Switzerland.
- HAWKING, S. (1990): A Brief History of Time; Bantam, Toronto, Canada.
- HEER, W. & HADERMANN, J. (1994): Modelling radionuclide migration field experiments at the Grimsel Test Site; PSI-Report Nr. 94-13, September 1994, PSI, Würenlingen and Villigen, Switzerland; Nagra Technical Report NTB 94-18, Nagra, Wettingen, Switzerland.
- HOFMANN, B.A. (1989): Reduction Spheres in Hematitic Rocks from Northern Switzerland: Implications for the Mobility of some Rare Elements; Nagra Technical Report NTB 89-17, Nagra, Wettingen, Switzerland.
- HOPKIRK, R.J. & WAGNER, W.H. (1986): Thermal Loading in the Near-Field of Repositories for High- and Intermediate-Level Nuclear Waste; Nagra Technical Report NTB 85-54, Nagra, Wettingen, Switzerland.
- HSK (1987): Technischer Bericht zum Gutachten über das Project Gewähr; Swiss Federal Nuclear Safety Inspectorate (HSK), Villigen, Switzerland.
- HSK & KSA (1993): Guideline for Swiss Nuclear Installations: Protection Objectives for the Disposal of Radioactive Wastes; Swiss Federal Nuclear Safety Inspectorate (HSK) and Federal Commission for the Safety of Nuclear Installations (KSA); HSK-R-21/e, HSK, Villigen, Switzerland.
- HYDROLOGISCHES JAHRBUCH DER SCHWEIZ (1979): Landeshydrologie, Bern, Switzerland.

- IAEA (1982): Safety Series No. 57, Generic Models and Parameters for Assessing the Environmental Transfer from Routine Releases - Exposures of Critical Groups; IAEA, Vienna, Austria.
- ICRP (1974): Report of the Task Group on Reference Man; ICRP Publication 23, Pergamon Press, Oxford, U.K.
- ICRP (1979-1982): Limits for Intakes of Radionuclides by Workers; ICRP Publication 30, parts 1, 2 and 3, Pergamon Press, Oxford, U.K.
- ICRP (1983): Radionuclide Transformations Energy and Intensity of Emissions; ICRP Publication 38, Pergamon Press, Oxford, U.K.
- ICRP (1991): 1990 Recommendations of the International Commission on Radiological Protection; ICRP Publication 60, Annals of the ICRP Vol 21 No. 1 - 3. Pergamon Press, Oxford, U.K.
- IMBRIE, J., HAYS, J.D., MARTINSON, G.D. et al. (1984): The orbital theory of Pleistocene climate: support from revised chronology of the marine ^{18}O record; in Milankovitch and Climate, BERGER, A. et al. (eds), Reidel, pp 269-306.
- JAKOB, A. (1992): RANCHMD - Radionuclide Chain Transport with Matrix Diffusion; Nagra Unpublished Report. Nagra, Wettingen, Switzerland.
- JAKOB, A., HADERMANN, J. & ROESEL, F. (1989): Radionuclide Chain Transport with Matrix Diffusion and Non-Linear Sorption, PSI-Report Nr. 54, November 1989, PSI, Würenlingen and Villigen, Switzerland; Nagra Technical Report NTB 90-13, Nagra, Wettingen, Switzerland.
- KBS (1983): Final Storage of Spent Fuel - KBS-3; SKBF/KBS Report (ISSN 0349-6015), Stockholm, Sweden.
- KLIMAATLAS DER SCHWEIZ (1982-1991): Bundesamt für Landestopographie, Wabern, Bern, Switzerland.
- KLOS, R.A. & VAN DORP, F. (1994): Biosphere Datasets for the Kristallin-I Assessment; PSI-Report, PSI, Würenlingen and Villigen, Switzerland; Nagra Technical Report, NTB 93-11, Nagra, Wettingen, Switzerland (*in preparation*).
- KLOS, R.A., MÜLLER-LEMANS, H., VAN DORP, F. & GRIBI, P. (1994): TAME - The Terrestrial-Aquatic Model of the Environment: Model Definition; PSI-Report, PSI, Würenlingen and Villigen, Switzerland; Nagra Technical Report NTB 93-04, Nagra, Wettingen, Switzerland (*in preparation*).
- KREIS, P. (1991): Hydrogen Evolution from Corrosion of Iron and Steel in Low/Intermediate-Level Waste Repositories; Nagra Technical Report NTB 91-21, Nagra, Wettingen, Switzerland.

- LANYON, G.W. & HOCH A.R. (1993): A Comparison of Dynamic and Geometric Calculations of Fluxes around a Repository Tunnel in Crystalline Rock; Nagra Unpublished Report. Nagra, Wettingen, Switzerland.
- LINSLEY, G. (1978): Resuspension of the Transuranium Elements - a Review of Existing Data; NRPB, Chilton, U.K.
- LÖW, S., JOHNS, R. & KLEMENZ, W. (1993): Zur Hydrogeologie der Thermalquellen von Zurzach; Nagra Unpublished Report. Nagra, Wettingen, Switzerland.
- MARSH G.P., BLAND, I.D., TAYLOR, K.J., SHARLAND, S. & TASKER, P. (1986): An Assessment of Carbon Steel Overpacks for Radioactive Waste Disposal; European Communities-Commission, Nuclear Science and Technology Series, EUR 10437.
- McCOMBIE, C., GAUTSCHI, A., THURY, M., HUFSCHMIED, P. & HADERMANN, J. (1987): Swiss Programmes for Validation of Performance Assessment Models by Comparison with Experimental Data; Proceedings of GEOVAL 1987, Stockholm, Sweden, pp 375-399.
- McCOMBIE, C., McKINLEY, I.G. & ZUIDEMA P. (1991): Sufficient Validation: The Value of Robustness in Performance Assessment and System Design. In GEOVAL-1990, Symposium on Validation of Geosphere Flow and Transport Models, pp 598-610. OECD/NEA, Paris, France.
- McCOMBIE, C. & McKINLEY, I.G. (1993): Validation - Another Perspective; Groundwater, 31, pp 530-531.
- McEWEN, T. & DE MARSILY, G. (1991): The Potential Significance of Permafrost to the Behaviour of a Deep Radioactive Waste Repository; SKI 91:08, SKI, Stockholm, Sweden.
- McKINLEY, I. (1985): The Geochemistry of the Near-Field; Nagra Technical Report NTB 84-48, Nagra, Wettingen, Switzerland.
- McKINLEY, I. & HADERMANN, J. (1985): Radionuclide Sorption for Swiss Safety Assessment; Nagra Technical Report NTB 84-40, Nagra, Wettingen, Switzerland.
- McKINLEY, I., WEST, J. & GROGAN, H. (1985): An Analytical Overview of the Consequences of Microbial Activity in a Swiss HLW Repository; Nagra Technical Report NTB 85-43, Nagra, Wettingen, Switzerland.
- McKINLEY, I. (1988): The near-field geochemistry of HLW disposal in an argillaceous host rock; Nagra Technical Report NTB 88-26, Nagra, Wettingen, Switzerland.

- McKINLEY, I.G., ALEXANDER, W.R., McCOMBIE, C. & ZUIDEMA, P. (1992a): Application of Results from Poços de Caldas Project in the Kristallin-I HLW Performance Assessment; Proc. 3rd Int. Conf. on High-Level Radioactive Waste Management, Las Vegas, U.S.A., pp 357-361.
- McKINLEY, I.G., SMITH, P.A. & CURTI, E. (1992b): Can the Kristallin-I Near Field Model be Considered Robust? Proc. 3rd Int. Conf. on High-Level Radioactive Waste Management, Las Vegas, U.S.A., pp 1770-1776.
- McKINLEY, I. & HAGENLOCHER, I. (1993): Quantification of Microbial Activity in a Nuclear Waste Repository; Proceedings of the International Symposium on Subsurface Microbiology (ISSM-93), 19-24 September 1993, Bath, U.K.
- McKINLEY, I.G. & SAVAGE, D. (1994): Comparison of Solubility Databases used for HLW Performance Assessment; J. Contam. Hydrol. (*submitted for publication*), Proc. Fourth Int. Conf. on the Chemistry and Migration Behaviour of Actinides and Fission Products in the Geosphere, Charleston, U.S.A., pp 657-665.
- MEIKE, A. (1989): Transmission Electron Microscope Study of Illite/Smectite Mixed Layers; Nagra Technical Report NTB 89-03, Nagra, Wettingen, Switzerland.
- MILANKOVITCH, M. (1930): Mathematische Klimalehre und astronomische Theorie der Klimaschwankungen; in KÖPPEN, W. & GEIGER, R. (eds.), Handbuch der Klimatologie I, Gebrüder Bornträger, Berlin, Germany.
- MILLER, W., ALEXANDER, W.R., CHAPMAN, N.A., McKINLEY, I.G. & SMELLIE, J.A.T. (1994): Natural Analogue Studies in the Geological Disposal of Radioactive Waste; Nagra Technical Report NTB 93-03, Nagra, Wettingen, Switzerland.
- MITCHELL, J.K., SINGH, A.S. & CAMPANELLA, R.G. (1968): Soil Creep as a Rate Process; ASCE Journal of the Soil Mechanics and Foundations, 7 Divisions, Vol.94, SM 1, pp 231-253.
- MUIR-WOOD, R. & WOO, G. (1992): Tectonic Hazards for Nuclear Waste Repositories in the U.K.; U.K. Department of the Environment Report HMIP/RR/92.070.
- MÜLLER-VONMOOS, M. & KAHR, G. (1983): Mineralogische Untersuchungen von Wyoming Bentonit MX-80 und Montigel; Nagra Technical Report NTB 83-12, Nagra, Wettingen, Switzerland.
- MÜLLER-VONMOOS, M. & KAHR, G. (1985): Langzeitstabilität von Bentonit unter Endlagerbedingungen; Nagra Technical Report NTB 85-25, Nagra, Wettingen, Switzerland.

- MÜLLER-VONMOOS, M., BUCHER, F., KAHR, G., MADSON, F. & MAYOR, P.A. (1991): Untersuchungen zum Verhalten von Bentonit in Kontakt mit Magnetit und Eisen unter Endlagerbedingungen; Nagra Technical Report NTB 91-14, Nagra, Wettingen, Switzerland.
- NAGRA (1984): An Assessment of the Corrosion Resistance of the High-Level Waste Containers Proposed by Nagra; Nagra Technical Report NTB 84-32, Nagra, Wettingen, Switzerland.
- NAGRA (1985): Project Gewähr 1985; Vols. 1-8, Vol. 9 (English Summary); Nagra Gewähr Report Series NGB 85-01/09, Nagra, Wettingen, Switzerland.
- NAGRA (1987): State of the Art Report on Potentially Useful Materials for Sealing Nuclear Waste Repositories; Nagra Technical Report NTB 87-33, Nagra, Wettingen, Switzerland.
- NAGRA (1988a): Untersuchungen zur Standorteignung im Hinblick auf die Endlagerung schwach- und mittelaktiver Abfälle: Berichterstattung über die Untersuchungen der Phase I am potentiellen Standort Oberbauenstock (Gemeinde Bauen, UR); Nagra Technical Report NTB 88-18, Nagra, Wettingen, Switzerland.
- NAGRA (1988b): Untersuchungen zur Standorteignung im Hinblick auf die Endlagerung schwach- und mittelaktiver Abfälle: Berichterstattung über die Untersuchungen der Phase I am potentiellen Standort Piz Pian Grand (Gemeinde Mesocco und Rossa, GR); Nagra Technical Report NTB 88-19, Nagra, Wettingen, Switzerland.
- NAGRA (1988c): Sediment Study - Disposal Options for Long-Lived Radioactive Waste in Swiss Sedimentary Formations - Executive Summary; Nagra Technical Report NTB 88 - 25E, Nagra, Wettingen, Switzerland.
- NAGRA (1991): Sedimentstudie - Zwischenbericht 1990: Zusammenfassende Übersicht der Arbeit von 1988 bis 1990 und Konzept für das weitere Vorgehen; Nagra Technical Report NTB 91-19, Nagra, Wettingen, Switzerland.
- NAGRA (1992): Nukleare Entsorgung Schweiz - Konzept und Realisierungsplan; Nagra Technical Report NTB 92-02, Nagra, Wettingen, Switzerland.
- NAGRA (1993): Beurteilung der Langzeitsicherheit des Endlagers SMA am Standort Wellenberg (Gemeinde Wolfenschiessen, NW); Nagra Technical Report NTB 93-26, Nagra, Wettingen, Switzerland.
- NAGRA (1994): Conclusions from the Regional Investigation Programme for Siting a HLW Repository in the Crystalline Basement in Northern Switzerland; Nagra Technical Report NTB 93-09E, Nagra, Wettingen, Switzerland.
- NEA (1989): Risks Associated with Human Intrusion at Radioactive Waste Disposal Sites; Proc. NEA Workshop, Paris, France.

- NEA (1991a): Disposal of Radioactive Waste: Can Long-Term Safety be Evaluated? A Collective Opinion of the Radioactive Waste Management Committee, OECD Nuclear Energy Agency, and the International Radioactive Waste Management Advisory Committee, International Atomic Energy Agency, endorsed by the Experts for the Community Plan of Action in the Field of Radioactive Waste Management, Commission of the European Communities; OECD/NEA, Paris, France.
- NEA (1991b): Disposal of Radioactive Waste: Review of Safety Assessment Methods. Report of the Performance Assessment Advisory Group of the Radioactive Waste Management Committee: OECD Nuclear Energy Agency; OECD/NEA, Paris, France.
- NEA (1992): Safety Assessment of Radioactive Waste Repositories: Systematic Approaches to Scenario Development. Report of the NEA Working Group on the Identification and Selection of Scenarios for Performance Assessment of Radioactive Waste Disposal; OECD/NEA, Paris, France.
- NEA (1993): The PSACOIN Level 1b Intercomparison; Klos, R.A., Sinclair, J.S., Torres, C., Bergström, U., & Galson, D.A. (eds.); NEA PSAG, Paris: NEA/OECD, France
- NEA (1994): Assessment of Future Human Actions at Radioactive Waste Disposal Sites; Report of NEA Working Group; OECD/NEA Paris, France (*in press*).
- NEALL, F. (ed.) (1994): Kristallin-I Results in Perspective; Nagra Technical Report NTB 93-23, Nagra, Wettingen, Switzerland.
- NERETNIEKS, I. (1985a): Some Aspects of the use of Iron Canisters in Deep Lying Repositories for Nuclear Waste; Nagra Technical Report NTB 85-35, Nagra, Wettingen, Switzerland.
- NERETNIEKS, I. (1985b): Transport in Fractured Rocks; Proc. IAH Int. Cong. Hydrology of Rocks of Low Permeability, Tucson, AZ, U.S.A.
- NERETNIEKS, I. (1993): Some Important Mechanisms and Processes in the Near Field of the Swedish Repository for Spent Nuclear Fuel; Proc. MRS Symp. Scientific Basis for Nuclear Waste Management XVI, pp 675-688.
- NG, Y.C. (1982): A Review of Transfer Factors for Assessing the Dose from Radionuclides in Agricultural Products, Nuclear Safety, 23(1), p 57.
- NORDMAN, M. & VIENO, T. (1989): Consideration of Human Actions in the Finnish Performance Assessments of Nuclear Waste Disposal; Risks Associated with Human Intrusion at Radioactive Waste Disposal Sites, OECD/NEA Paris, France.

- NORDSTROM, D.K., PLUMMER, L.N., WIGLEY, T.M.L., WOLERY, T.J., BALL, J.W., JENNE, E.A., BASSETT, R.L., CRERAR, D.A., FLORENCE, T.M., FRITZ, B., HOFFMAN, M., HOLDREN, G.R. Jr., LAFON, G.M., MATTIGOD, S.V., McDUFF, R.E., MOREL, F., REDDY, M.M., SPOSITO, G. & THRAILKILL, J. (1979): A Comparison of Computerized Chemical Models for Equilibrium Calculations in Aqueous Systems; Chemical modelling in aqueous systems, JENNE, E. A. (ed.), pp 857-892. American Chemical Society (Symposium Series 93), pp 574-584.
- NRPB (1987): Committed Doses to Selected Organs and Committed Effective Doses from Intakes of Radionuclides; NRPB-GS7, NRPB Chilton, U.K, available through HMSO, London, U.K.
- NRPB (1992): Board Statement on Radiological Protection Objectives for the Land-Based Disposal of Solid Radioactive Wastes; Documents of the NRPB, Vol.3, No.3., NRPB Chilton, U.K.
- NUREG (1977): Calculation of Annual Doses to Man from Routine Releases of Reactor Effluents for the Purpose of Evaluating Compliance with 10 CFR Part 50; Appendix 1 in US Nuclear Regulatory Commission Regulatory Guide 1.109, Washington, U.S.A.
- OBAYASHI (1993a): Kristallin-I: Repository layout study based on Rock Mechanics Considerations: Numerical and Engineering Investigation of Tunnel Stability in a Fracture Zone. Nagra Unpublished Report. Nagra, Wettingen, Switzerland.
- OBAYASHI (1993b): Kristallin-I: Repository layout study based on Rock Mechanics Considerations: Preliminary Calculations of Temperature Distributions around an Emplacement Tunnel. Nagra Unpublished Report. Nagra, Wettingen, Switzerland.
- OECD (1993): The Status of Near-Field Modelling; Proceedings of a Technical Workshop - Cadarache, France, 11-13 May 1993.
- OSCARSON, D.W., DIXON, D.A. & GRAY, M.N. (1990): Swelling Capacity and Permeability of an Unprocessed and a Processed Bentonitic Clay; Eng. Geol. 28, p 281.
- OVE ARUP & PARTNERS (1990): COMPAS Project: Stress Analysis of HLW Containers, Intermediate Testwork; CEC Nuclear Science and Technology Report EUR 12593 EN.
- PEARSON, F.J. & BERNER, U. (1991): Nagra Thermochemical Database - I. Core Data; Nagra Technical Report NTB 91-17, Wettingen, Switzerland.
- PEARSON, F.J., BERNER, U. & HUMMEL, W. (1991): Nagra Thermochemical Database - II. Supplemental Data 05/92; Nagra Technical Report NTB 91-18. Nagra, Wettingen, Switzerland.

- PEARSON, F.J. & SCHOLTIS, A. (1993): Chemistry of Reference Waters of the Crystalline Basement of Northern Switzerland for Safety Assessment Studies; Nagra Technical Report NTB 93-07, Nagra, Wettingen, Switzerland.
- PETIT J. -Cl. (1991): Design and Performance Assessment of Radionuclide Waste Forms: What can we Learn from Natural Analogues? Proc. 4th NAWG Meeting, EUR 13014, pp 31-72.
- PNC (1992): H-3 - First Progress Report of Research and Development on Geological Disposal for High Level Radioactive Waste; PNC TN1410 93-059, PNC, Tokyo, Japan.
- POPPER, K. R. (1959): The Logic of Scientific Discovery; Hutchinson, London, U.K.
- PRIJ, J.V., WEERS, A.W., GLASBERG, P. & SLOT, A.F.M. (1989): The Role of Human Intrusion in the Dutch Safety Study; Risks Associated with Human Intrusion at Radioactive Waste Disposal Sites, OECD/NEA Paris, France.
- PUSCH, R. (1980a): Swelling Pressure of Highly Compacted Bentonite; KBS TR 80-13, Stockholm, Sweden.
- PUSCH, R. (1980b): Permeability of Highly Compacted Bentonite; KBS TR 80-16, Stockholm, Sweden.
- PUSCH, R. (1983): Use of Clays as Buffers in Radioactive Repositories; KBS TR 83-46, Stockholm, Sweden.
- PUSCH, R. (1985): Final Report of the Buffer Mass Test: Volume III: Chemical and Physical Stability of the Buffer Materials; Nagra Technical Report NTB 85-60, Nagra, Wettingen, Switzerland.
- PUSCH, R., RANHAGEN, L. & NILSSON, K. (1985): Gas migration through MX-80 bentonite; Nagra Technical Report NTB 85-36, Nagra, Wettingen, Switzerland.
- PUSCH, R., BÖRGESSION, L. & RAMQUIST, G. (1987): Final Report of the Borehole, Shaft and Tunnel Sealing Test: Volume I: Borehole Plugging; Nagra Technical Report NTB 87-25, Nagra, Wettingen, Switzerland.
- PUSCH, R. & KARNLAND, O. (1988): Geologic Evidence of Smectite Longevity. The Sardinian and Gotland Cases; SKB Technical Report 88-26, Stockholm, Sweden.
- PUSCH, R. & KARNLAND, O. (1990): Preliminary Report on Longevity of Montmorillonite Clay under Repository-Related Conditions; SKB Technical Report 90-44, Stockholm, Sweden.

- PUSCH, R., KARNLAND, O., LAJUDIE, A. & ATABEK, R. (1992): Hydrothermal Field Experiment Simulating Steel Canister Embedded in Expansive Clay - Physical Behaviour of the Clay; Proc. MRS Symp. Scientific Basis for Nuclear Waste Management XV, pp 547-556.
- READ, D. & BROYD, T.W. (1991): The CHEMVAL International Exercise: a Geochemical Benchmark within the MIRAGE Project - Second Phase; Radioactive Waste Management and Disposal, CECILLE, L. (ed.), EUR 13389, Elsevier Applied Science, pp 574-584.
- ROSSELET, A. (1984): Kriechverhalten unlegierter Stahlwerkstoff für Endlager-Behälter: Auswertung der Literaturangaben; Nagra Technical Report NTB 84-35, Nagra, Wetztingen, Switzerland.
- RYAN, J.N. & GSCHWEND, P.M. (1990): Colloid Mobilization in two Atlantic Coastal Plain Aquifers: Field Studies; Water Resour. Res., 26(2), pp 307-322.
- RYBACH, L., EUGSTER, W. & GRIESSER, J.-C. (1987): Die geothermischen Verhältnisse in der Nordschweiz; Eclogae geol. Helv. 80/2, pp 521-534.
- RYBACH, L. (1992a): Die Bedeutung des Hot Dry Rock Verfahrens für die Schweiz; Schweizer Ingenieur und Architekt; Sonderdruck aus Heft 6.
- RYBACH L. (1992b): Geothermal Potential of the Swiss Molasse Basin; Eclogae geol. Helv. 85/3: pp 733-744.
- SAOTOME, E., HARA, K., FUJITA, T. & SASAKI, N. (1991): Study of Mechanical Stability of Engineered Barrier System for Deep Geological Isolation of High-Level Radioactive Waste; Proc. 11th Int. Conf. on Structural Mechanics in Reactor Technology, Japan.
- SCHMASSMANN, H., KULLIN, M. & SCHNEEMANN, K. (1992): Hydrochemische Synthese Nordschweiz. Buntsandstein-, Perm- und Kristallin-Aquifere; Nagra Technical Report NTB 91-30, Nagra, Wetztingen, Switzerland.
- SCHENK, R. (1988): Untersuchungen über die Wasserstoffbildung durch Eisenkorrosion unter Endlagerbedingungen; Nagra Technical Report NTB 86-24, Nagra, Wetztingen, Switzerland.
- SCHMIDT, W., SITZ, P. & KESSLER, J. (1994): Physikalische und chemische Eigenschaften von Bentonit als Verfüll- und Versiegelungsmaterial bei der Endlagerung Radioaktiver Abfälle - Literaturstudie; Nagra Technical Report NTB 93-37, Nagra, Wetztingen, Switzerland (*in preparation*).
- SCHÖTZIG, U. & SCHRADER, H. (1993): Halbwertszeiten und Photonen-Emissionswahrscheinlichkeiten von häufig verwendeten Radionukliden. 4, erweiterte Auflage. PTB-Ra-16/4.

- SHARLAND, S. (1991): Discussion on Post Emplacement Environment; Proceedings from the Technical Workshop on Near-Field Performance Assessment for High-Level Waste, October 15-17 1990, Madrid, Spain, pp 23-24.
- SIMPSON, J.P. & VALLOTTON, P.H. (1986): Experiments on Container Material for Swiss High-Level Waste Disposal Projects - Part III; Nagra Technical Report NTB 86-25, Nagra, Wettingen, Switzerland.
- SIMPSON, J.P. (1989): Experiments on Container Material for Swiss High-Level Waste Disposal Projects - Part IV; Nagra Technical Report NTB 89-19, Nagra, Wettingen, Switzerland.
- SKB (1992): SKB 91: Final Disposal of Spent Nuclear Fuel: Importance of the Bedrock for Safety; SKB Technical Report 92-20, SKB, Stockholm, Sweden.
- SKI (1984): INTRACOIN, Final Report Level 1: Code Verification; SKI 84:3, Stockholm, Sweden.
- SKI (1986): INTRACOIN, Final Report Levels 2 and 3: Model Validation and Uncertainty Analysis; SKI 86:2, Stockholm, Sweden.
- SKI, HSK & SSI (1990): Regulatory Guidance for Radioactive Waste Disposal – an Advisory Document; SKI 90:15, Stockholm, Sweden.
- SKI (1991a): Geogas - a Carrier or a Tracer ? SKI Report 51, Stockholm, Sweden.
- SKI (1991b): Geogas in Crystalline Bedrock; SKI Report 52, Stockholm, Sweden.
- SKI (1991c): SKI Project-90; SKI 91:23, 2 Volumes, Stockholm, Sweden.
- SKI (1992): The International HYDROCOIN Project, Summary Report; OECD/NEA and SKI, Paris, France.
- SKI (1993): The International INTRAVAL Project, Phase 1, Summary Report; OECD/NEA and SKI; Paris, France.
- SMITH, P.A. (1993a): A Model for Colloid Facilitated Transport through Fractured Media; PSI Report Nr. 93-04, July 1993, PSI, Würenlingen and Villigen, Switzerland; Nagra Technical Report NTB 93-32, Nagra, Wettingen, Switzerland.
- SMITH, P.A. (1993b): Quantifying the Performance of the Geosphere as a Barrier to the Migration of Radionuclides. Nagra Unpublished Report. Nagra, Wettingen, Switzerland.
- SMYTHE, W.R. (1968): Static and Dynamic Electricity; Third Ed., McGraw-Hill, New York.
- SSI (1991): Proceedings of the BIOMOVS Symposium on the Validity of Environmental Transfer Models; October 8-10 1990, Stockholm, Sweden.

- SSI (1993): BIOMOVIS II Progress Report No. 4; November 1993, SSI, Stockholm, Sweden.
- STÄUBLE, J. (1993): Hydrogeologische Charakterisierung der Schottergrundwässer im unteren Aaretal und Rheintal. Nagra Unpublished Report. Nagra, Wettingen, Switzerland.
- STEAG & MOTOR-COLUMBUS (1985): Behälter aus Stahlguss für die Endlagerung verglaster hoch-radioaktiver Abfälle; Nagra Technical Report NTB 84-31, Nagra, Wettingen, Switzerland.
- STENHOUSE, M.J. (1994): Sorption Databases for Crystalline, Marl and Bentonite for Performance Assessment; Nagra Technical Report NTB 93-06, Nagra, Wettingen, Switzerland (*in preparation*).
- STUDER, J., AMMANN, W., MEIER, P., MÜLLER, Ch., GLAUSER, E. & GSS. (1984): Verfüllen und Versiegeln von Stollen, Schächten und Bohrlöchern - Band 1: Bericht, Band 2: Anhänge; Nagra Technical Report NTB 84-33, Nagra, Wettingen, Switzerland.
- SUMERLING, T.J. (Ed.) (1992): Dry Run 3: A Trial Assessment of Underground Disposal of Radioactive Wastes Based on Probabilistic Risk Analysis: Overview; U. K. DoE Report DOE/HMIP/RR92.039 (and 9 supporting volumes).
- SUMERLING, T. J., ZUIDEMA, P., GROGAN, H.A. & VAN DORP, F. (1993): Scenario Development for Safety Demonstration for Deep Geological Disposal in Switzerland; Proc. 4th Int. Conf. on High-Level Radioactive Waste Management, Las Vegas, U.S.A.
- SUMERLING, T.J. & GROGAN, H.A. (1994): Scenario Development for Kristallin-I; Nagra Technical Report NTB 93-13, Nagra, Wettingen, Switzerland (*in preparation*).
- SVENSSON, L. (1979): Dose Conversion Factors for External Photon Radiation; FOA Rapport C40060-A3, Försvarets Forskningsanstalt, Huvudavdelning 4, Sunbyberg, Sweden.
- THORNE, M.C. (1992): Dry Run 3; Volume 8, Uncertainty and Bias Audit, U.K. DOE Report DoE/HMIP/RR/92.040.
- THURY, M. (1980): Erläuterungen zum Nagra-Tiefbohrprogramm als vorbereitende Handlung im Hinblick auf das Projekt Gewähr; Nagra Technical Report NTB 80-07, Nagra, Wettingen, Switzerland.
- THURY, M., GAUTSCHI, A., MÜLLER, W.H., NAEF, H., PEARSON, F.J., VOBORNY, O., VOMVORIS, S. & WILSON, W. (1994): Geologie und Hydrogeologie des Kristallins der Nordschweiz; Nagra Technical Report NTB 93-01. Nagra, Wettingen, Switzerland.

- TITS, J., KLOS, R.A. & VAN DORP, F. (1994): The Swiss Biosphere K_d Database; PSI-Report, PSI, Würenlingen and Villigen, Switzerland; Nagra Technical Report NTB 94-05, Nagra, Wettingen, Switzerland (*in preparation*).
- TRAVIS, C.C. & ETNIER, E.L. (1981): A Survey of Sorption Relationships for Reactive Solutes; Soil. J. Environ. Qual., Vol. 10, p 8.
- VERNAZ, E.Y. & DUSSOSSOY, L.L. (1992): Current State of the Knowledge of Nuclear Waste Glass Corrosion Mechanisms: the Case of R7T7 Glass; Appl. Geochem. Suppl. Issue No. 1, 13-22.
- VIENO, T., HAUTOJÄRVI, A., KOSKINEN, L. & NORDMAN, H. (1992): TVO-92 Safety Analysis of Spent Fuel Disposal; TVO Report YJT-92-33E, TVO, Helsinki, Finland.
- VOMVORIS, S., VOBORNY, O., LANYON, W. & ANDREWS, R.W. (1993): Methodology for deriving Hydrogeological Input Parameters for Safety Analysis Models and Application to fractured Rocks in Switzerland; Nagra Technical Report NTB 93-14, Nagra, Wettingen, Switzerland (*in preparation*).
- VSE, GKBP, UeW & NAGRA (1978): Die Nukleare Entsorgung in der Schweiz; Verband Schweizerische Elektrizitätswerke - VSE, Gruppe der Kernkraftwerk-betreiber und Projektanten - GKBP, Konferenz der Überlandwerke - UeW, Nationale Genossenschaft für die Lagerung radioaktiver Abfälle - Nagra.
- WANNER, H. (1986): Modelling Interaction of Deep Groundwaters in Bentonite and Radionuclide Speciation; EIR-Report Nr. 589, April 1986, EIR, Würenlingen, Switzerland; Nagra Technical Report NTB 86-21, Nagra, Wettingen, Switzerland.
- WERME, L., BJÖRNER, I.K., BART, G., ZWICKY, H.U., GRAMBOW, B., LUTZE, W., EWING, R.C. & MAGRABI, C. (1990): Chemical Corrosion of Highly Radioactive Borosilicate Nuclear Waste Glass under Simulated Repository Conditions; J. Mater. Res., Vol. 5, No. 5, pp 1130-1146.
- WHITTLE, A.J. & ARISTORENAS, G. (1991): Settlement of canisters in compacted bentonite. Nagra Unpublished Report. Nagra, Wettingen, Switzerland.
- WIPP Performance Assessment Division (1992): Preliminary Comparison with 40 CFR Part 191, Subpart B for the Waste Isolation Pilot Plant, December 1992; (5 volumes) SAND91-0700-4. UC-814, Sandia National Laboratory, U. S. A.
- ZACH, R. & SHEPPARD, R.C. (1992): The Food Chain and Dose Submodel, CALDOS, for the Assessment of Canada's Nuclear Fuel Waste Management Concept; AECL-10165, COG-91-195, Pinawa, Canada.
- ZWICKY, H.U., GRABER, T. & KEIL, R. (1992): Versuche zur Bestimmung der Langzeitkorrosionsrate von Alkaliborosilicatglas: Zwischenbericht; PSI Unpublished Report, PSI, Würenlingen and Villigen, Switzerland.

APPENDIX 1 CONVENTIONS FOR PRESENTATION OF GRAPHICAL RESULTS

Results presented in this report may be divided into two categories. These are, first, results used to assess the performance of the disposal system in the context of regulatory guidelines and, second, results used to illustrate important aspects of the behaviour of individual model elements. The two categories are illustrated below, with a description of the conventions used to express the meaningfulness of the output from the models. In particular, the timescales and ranges of radiological impact require clear definition so that they are used in context, and do not give a misleading impression of the confidence in the calculated results.

(i) Results demonstrating the radiological impact of the disposal system

As an example of the first category, Figure A1.1 shows the results of the Reference-Case calculations (see Section 6.2). The shaded areas and lines have specific meanings and these are described below.

– Natural radiation exposures in Switzerland

Natural radiation exposures in Switzerland lie in the range 1 to 150 mSv y⁻¹ (BAG 1992), where the higher end of the range is due to unusually high exposures to radon daughters. More typically, doses are in the range 1 to 10 mSv y⁻¹ (including radon); this range is shown for comparison with the results of the calculations and with the regulatory guideline. Graphical presentations are assigned an upper limit of one order of magnitude above this range (100 mSv y⁻¹).

– Regulatory Guideline

The regulatory guidelines of HSK R-21 require that "*the release of radionuclides from a sealed repository subsequent upon processes reasonably expected to happen, shall at no time give rise to individual doses which exceed 0.1 mSv per year*" although exceptions can be made for unlikely processes and events (see Section 2.3).

– Level of Insignificant Dose

The level of insignificant dose is set at 10⁻⁷ mSv y⁻¹, which is one million times smaller than the regulatory guideline of 0.1 mSv y⁻¹. A dose of 10⁻⁷ mSv y⁻¹ to an individual corresponds to a risk of death due to radiation-induced fatal cancer of the exposed person, or of serious hereditary effects, of 6×10⁻¹² y⁻¹. This estimate is based on the ICRP recommended risk factors of 0.05 Sv⁻¹ for fatal cancer and 0.01 Sv⁻¹ for serious hereditary effects in all generations (ICRP 1991), i.e., a total factor of 0.06 Sv⁻¹, which is the risk factor advised as appropriate in assessing risks from underground disposal of solid radioactive wastes by the UK National Radiological Protection Board (NRPB 1992).

Many results in the Kristallin-I safety assessment show radiological impacts below this level; in order to illustrate the behaviour of the models representing the disposal system, the lower limit on the plots has been extended to 10^{-9} mSv y^{-1} . However, such numbers have no meaning in terms of radiological significance.

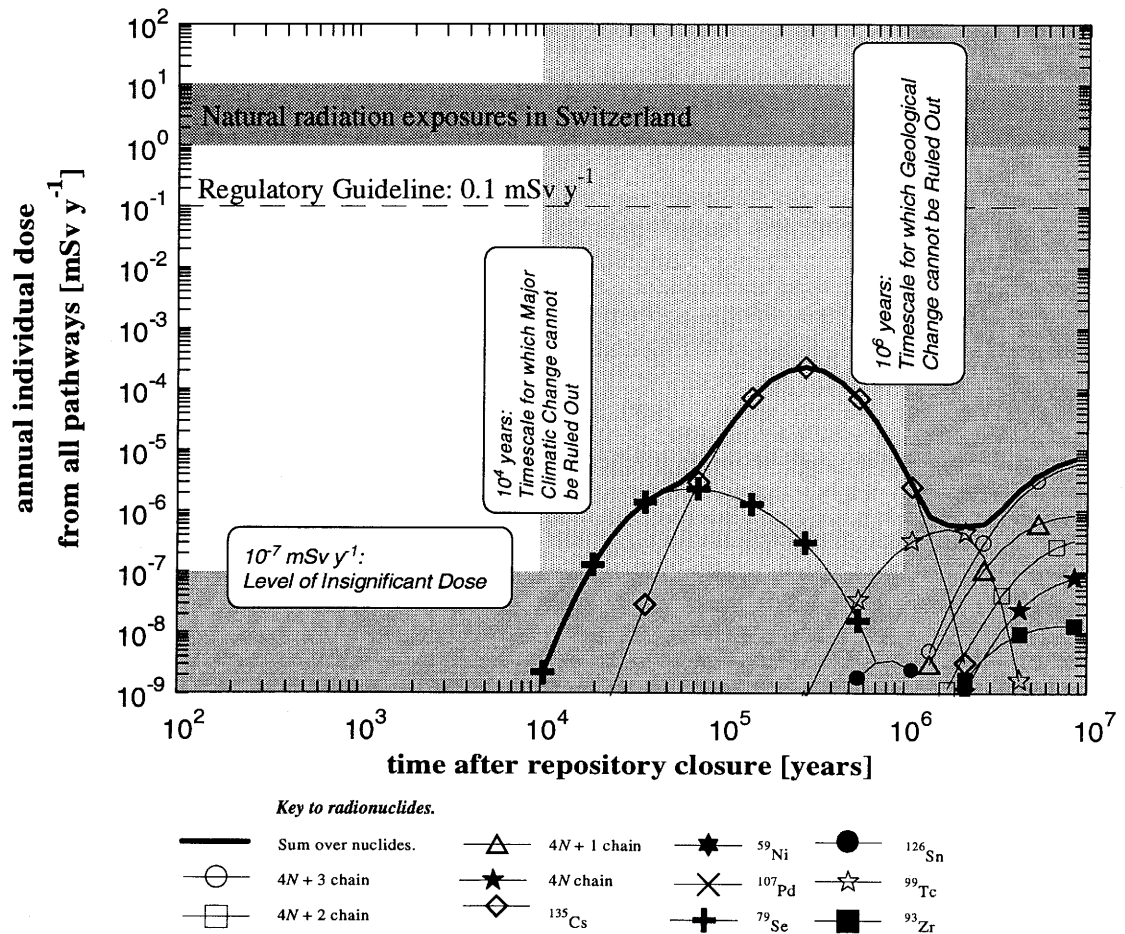


Figure A1.1: *Regions of Significance* for graphical results in the Kristallin-I assessment. Reference-Case results, showing the contributions of the actinide chains and activation/fission products to the overall radiological impact of the disposal.

– **Time after repository closure**

Time is measured from repository closure. In the Reference-Case calculations, the canisters are assumed to fail at 10^3 years post closure (with 10^2 years and 10^5 years as parameter variations). The lower limit of all plots is taken to be either 10^2 years or 10^3 years post closure.

– **Timescale for climatic change**

Changes in the surface environment (and especially human activity) occur over relatively short timescales and are inherently unpredictable. The reference biosphere model used in Kristallin-I is based on current conditions and provides an indication of the significance of any radionuclide releases in terms of radiological consequences. The uncertainty in such a model will increase with time, especially over timescales where a major climatic change cannot be excluded (about 10^4 years - a timescale typical of glacial cycles). The conversion of releases to doses using the biosphere model must be considered particularly uncertain after this time (shown by shading in Figure A1.1) as illustrated by the alternative biosphere scenarios modelled.

– **Timescale for geological change**

The main components of the safety barriers, the engineered barriers and the low-permeability domain of the host rock, lie at considerable depth and hence will be relatively unaffected by surface changes. Nevertheless, increasing uncertainty in the representation of gradual geological evolution will result in a decrease with time of the ability of the models to simulate (or bound) performance. The model representations of the near field and geosphere are considered to be acceptable for periods of up to about 10^6 years. Beyond this time, the results presented must be considered as qualitative indications of trends (hence the darker shading in Figure A1.1).

– **Comparison with doses due to other human activities**

Figure A1.2 indicates that calculated doses due to the release of radionuclides from the repository (in the Reference Case) are liable to be much smaller than those due to everyday human activities, in which the associated doses are generally disregarded. It should be noted, however, that the system of dosimetry by which the values shown are calculated (ICRP 1979-82) was derived primarily for use in control of radiation sources. The health risks associated with the different exposure pathways plotted in Figure A1.2 are different in kind and the comparison should be made with caution (see Chapter 5 in NEALL (ed.) 1994).

(ii) Results illustrating model behaviour

In addition to lying below the "level of insignificant dose", defined above, dose maxima for individual radionuclides frequently lie beyond the timescales for climatic and geological change. Indeed, some of the model runs give peak consequences beyond 10^7 years, while others give maximum doses below 10^{-7} mSv y^{-1} . In cases where the intention is purely to illustrate important aspects of the behaviour of individual model elements, the time limits for graphical presentation of results may be extended to 10^8 years; the shading conventions outlined above in (i) are followed in order to emphasise how the results should be interpreted.

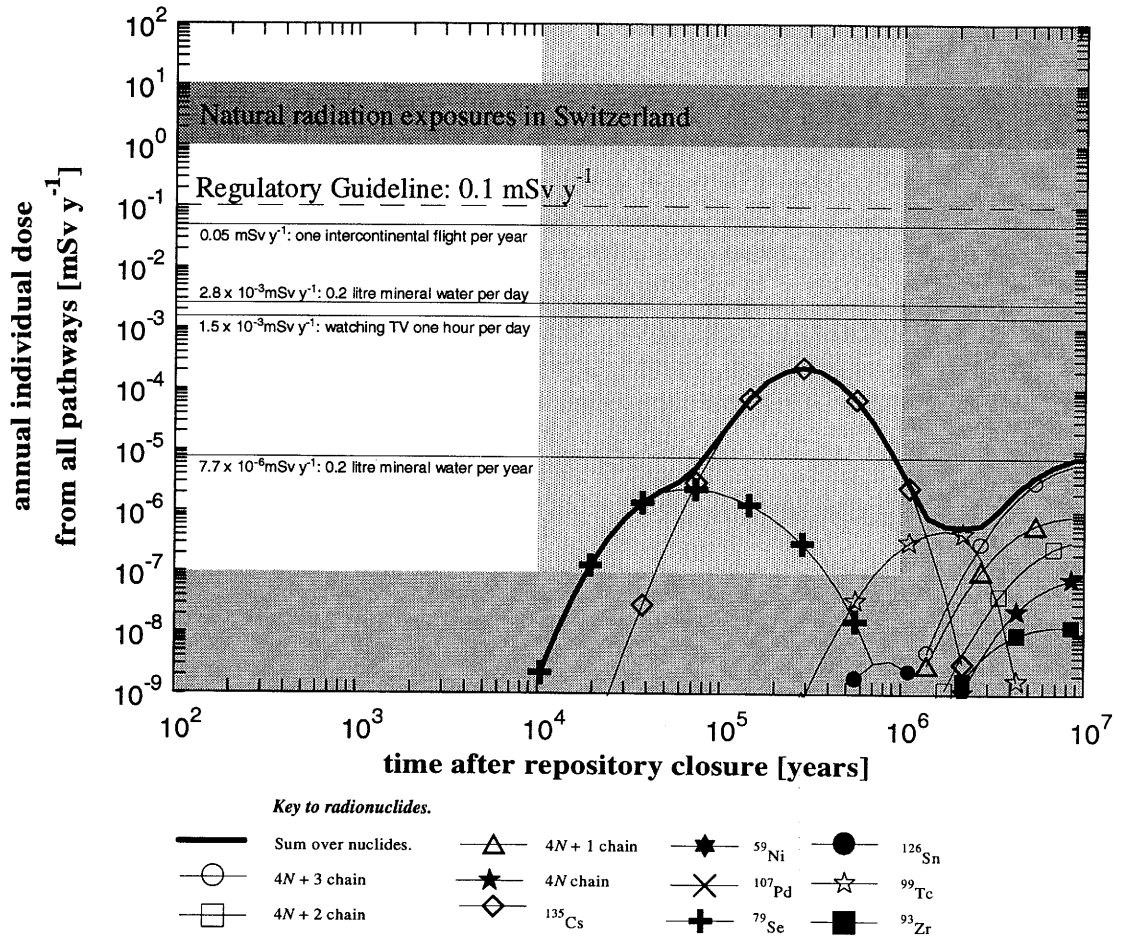


Figure A1.2: Results of the Kristallin-I Reference-Case calculations; annual individual dose as a function of time after repository closure. The regulatory guideline of 0.1 mSv y^{-1} is shown, together with the range of natural background radiation in Switzerland and the calculated radiation exposure from a range of common activities.

APPENDIX 2 SELECTION OF SAFETY-RELEVANT RADIONUCLIDES

For safety assessment, it is necessary to consider all radionuclides with potential to give rise to significant radiation doses following disposal of waste in the repository, or the parents of such radionuclides. The number of radionuclides present in the inventory is prohibitively large for detailed model-chain calculations to be performed for all of them. A set of radionuclides for consideration in the Kristallin-I assessment has therefore been selected by means of a simple screening analysis which takes account of:

- the design lifetime of the waste canister;
- a rate of glass dissolution;
- dilution in a near-surface aquifer;
- drinking of contaminated aquifer water.

Transport processes in the engineered and geological barriers, further dilution/concentration processes in the surface environment and other dose pathways are neglected. Although the radionuclide selection procedure described below may discard some radionuclides that could, if included, give calculated doses of similar order to those of some selected radionuclides in the results presented in this report, it is unlikely that any radionuclides that would contribute significantly to total dose have been omitted.

The drinking water dose $D^{(i)}(t)$ [mSv y^{-1}] due to a radionuclide i at time t [y], with $t = 0$ defined as the time of canister failure (1000 years after repository closure in the Reference Case), is thus calculated by the expression:

$$D^{(i)}(t) = A^{(i)}(t) R_f N [W/(F_{UL} + F_{CL})] D_{ing}^{(i)},$$

where:

- $A^{(i)}(t)$ [Bq] is the average activity of radionuclide i per canister at time t . The reference inventory per canister, calculated at 4 years after unloading of fuel from the reactor, is provided by the MIRA database (ALDER & MCGINNES 1994). The inventory at $t = 0$, 1040 years after unloading and 1000 years after repository closure, is calculated from this reference inventory using the code RAPIDE (GRINDROD et al. 1990a);
- R_f is the fractional rate of glass corrosion, set at $3/1.55 \times 10^5 y^{-1}$, where $1.55 \times 10^5 y$ is the time for complete glass dissolution in the Reference Case (see Table 5.2.2) and the initial rate is assumed three times higher than the average;
- N is 2693, the total number of canisters;

- $F_{UL}+F_{CL}$ is the water flow in a near-surface aquifer, taken as $5.5 \times 10^6 \text{ m}^3 \text{ y}^{-1}$ (see Table 5.4.3);
- W is the total annual drinking water intake by an individual set at $0.73 \text{ m}^3 \text{ y}^{-1}$ (see Table A7.1);
- $D_{ing}(i)$ is the committed effective dose equivalent per unit ingestion of radionuclide i , according to NRPB 1987 [mSv Bq^{-1}].

Table A2.1 gives the dose index, defined as the ratio of $D^{(i)}(0)$, the drinking water dose at the time of canister failure, to the Swiss regulatory dose limit of 0.1 mSv y^{-1} , calculated for the activation/fission products. It is assumed that only radionuclides for which the calculated dose index greater than 10^{-3} (or long-lived parents of such radionuclides) are relevant to long-term radiological safety; these radionuclides are indicated in the table by shading.

In addition to these radionuclides, ^{59}Ni and ^{107}Pd are selected in spite of their lower dose indices, in order that the Kristallin-I assessment covers all radionuclides calculated in the "base case" of Project Gewähr 1985 (see Figure 8-1 in Volume 5 of NAGRA 1985). The following radionuclides and chains are thus selected for detailed consideration in the Kristallin-I safety assessment:

activation/fission products: ^{59}Ni , ^{79}Se , $^{93}\text{Zr} \rightarrow ^{93\text{m}}\text{Nb}$, ^{99}Tc , ^{107}Pd , $^{126}\text{Sn} \rightarrow ^{126\text{m}}\text{Sb} \rightarrow ^{126}\text{Sb}$, ^{135}Cs

actinide decay chains: $4N + 3$, $4N + 2$, $4N + 1$ and $4N$

The selected radionuclides, including those contained within the $4N + 3$, $4N + 2$, $4N + 1$ and $4N$ decay chains, are shown in Table A2.2. Decay-chain branches with very low branching ratios are neglected. In addition, in the near-field and geosphere release and transport calculations, those radionuclides with half-lives that are very short (with respect to the timescales over which release and transport occur) are not calculated explicitly, but are assumed to be in equilibrium with their parents. In the biosphere, all radionuclides with half-lives of around one year or greater are modelled explicitly⁴⁷. The radiological effects of the shorter-lived radionuclides are accounted for in the dose sub-model by adding the dose per unit intake of the daughter to that of the immediate pre-cursor (this corresponds to the assumption of equilibrium between daughter and parent).

⁴⁷ In the case of ^{93}Zr , the contribution of the daughter $^{93\text{m}}\text{Nb}$ was erroneously neglected in the calculations for Kristallin-I. Subsequent calculations of the Reference Case have been carried out (i), in which $^{93\text{m}}\text{Nb}$ is assumed to be in equilibrium with ^{93}Zr and (ii), in which $^{93\text{m}}\text{Nb}$ is calculated explicitly in the biosphere. In the former case, the maximum individual dose for ^{93}Zr and its daughter is increased by a factor of around 1.2 and, in the latter case, it is increased by around 1.8. As ^{93}Zr is only a minor contributor to dose in all the Kristallin-I calculations, this oversight has no consequences for the safety case.

This decay-chain simplification scheme (Table A2.2) is similar to those adopted in other post-closure repository safety assessments, e.g. SKI Project 90 and SKB 91 (SKI 1991c; SKB 1992). A potential source of bias, identified in Subsection 4.3.4.1, arises in the treatment of ^{222}Rn in the $4N + 2$ chain, which is assumed to be in equilibrium with its parent throughout the assessment model chain. ^{222}Rn is the immediate daughter of ^{226}Ra and is a noble gas with a half-life of about 4 days; it decays through a series of very short-lived radionuclides (half-lives 27 minutes or less) to ^{210}Pb (half-life 21 years). In the near field and geosphere, ^{222}Rn may emanate from the sites of ^{226}Ra atoms sorbed on the solid phase, and dissolve in adjacent porewater. Hence, the concentration of ^{222}Rn in porewater will be large with respect to that of dissolved ^{226}Ra ; this effect is observed in natural systems (see, for example NEALL (ed.) 1994). However, the dissolved ^{222}Rn cannot move far in advance of the parent ^{226}Ra , because of its short half-life and the slow groundwater flowrate; thus, the effect on transport is negligible. In the biosphere, if ^{226}Ra is present in the soil, then a fraction of the ^{222}Rn produced would escape to the atmosphere and be rapidly dispersed; hence, explicit consideration of ^{222}Rn would lead to a reduction in calculated doses due to ^{210}Pb and ^{210}Po through food-chain pathways, because of the lower concentrations retained in the soil. However, there is a potential for significant doses from ^{222}Rn and its short-lived daughters in conditions of limited air circulation. This is especially true in buildings, in which ^{222}Rn emanating from ^{226}Ra in underlying soil and rocks, or in building materials, may accumulate. It is currently estimated that the net bias due to the assumption of ^{222}Rn equilibrium in biosphere modelling is small, but this is an issue that deserves attention in future assessment calculations.

Radionuclide	Half-life [y]	Ding(i) [Sv/Bq]	Inventory per Canister [Bq]	Dose Index [-]
¹⁰ Be	1.60×10 ⁶	1.10×10 ⁻⁰	2.20×10 ⁵	1.67×10 ⁻⁸
¹⁴ C	5.73×10 ³	5.60×10 ⁻¹⁰	3.97×10 ⁷	1.54×10 ⁻⁶
⁴¹ Ca	1.40×10 ⁵	3.80×10 ⁻¹⁰	9.15×10 ⁶	2.41×10 ⁻⁷
⁵⁹ Ni	7.50×10 ⁴	5.60×10 ⁻¹¹	1.88×10 ⁹	7.29×10 ⁻⁶
⁶³ Ni	9.60×10 ¹	1.50×10 ⁻¹⁰	1.41×10 ⁸	1.46×10 ⁻⁶
⁷⁹ Se	6.50×10⁴	2.30×10⁻⁹	2.18×10¹⁰	3.46×10⁻³
⁹⁰ Sr	2.91×10 ¹	3.30×10 ⁻⁸	6.63×10 ⁴	1.51×10 ⁻⁷
⁹⁰ Y	7.30×10 ⁻³	2.70×10 ⁻⁹	6.64×10 ⁴	1.24×10 ⁻⁸
⁹³ Zr	1.53×10⁶	4.20×10⁻¹⁰	9.20×10¹⁰	2.67×10⁻³
^{93m} Nb	1.36×10¹	1.00×10⁻⁹	9.20×10¹⁰	6.36×10⁻³
⁹⁴ Nb	2.03×10 ⁴	1.80×10 ⁻⁸	9.65×10 ⁷	1.20×10 ⁻⁴
⁹³ Mo	3.50×10 ³	3.00×10 ⁻¹⁰	3.01×10 ⁷	6.25×10 ⁻⁷
⁹⁹ Tc	2.13×10⁵	3.50×10⁻¹⁰	6.48×10¹¹	1.57×10⁻²
¹⁰⁷ Pd	6.50×10 ⁶	3.80×10 ⁻¹¹	5.20×10 ⁹	1.37×10 ⁻⁵
¹⁰⁸ Ag	4.51×10 ⁻⁶	2.40×10 ⁻¹²	1.93×10 ⁵	3.21×10 ⁻¹¹
^{108m} Ag	1.27×10 ²	2.00×10 ⁻⁹	2.17×10 ⁶	3.00×10 ⁻⁷
^{121m} Sn	5.50×10 ¹	3.70×10 ⁻¹⁰	1.97×10 ⁴	5.03×10 ⁻¹⁰
¹²¹ Sn	3.09×10 ⁻³	2.40×10 ⁻¹⁰	1.53×10 ⁴	2.53×10 ⁻¹⁰
¹²⁶ Sn	1.00×10⁵	4.70×10⁻⁹	3.67×10¹⁰	1.19×10⁻²
^{126m} Sb	3.61×10⁻⁵	2.50×10⁻¹¹	3.67×10¹⁰	6.35×10⁻⁵
¹²⁶ Sb	3.39×10⁻²	2.90×10⁻⁹	5.14×10⁹	1.03×10⁻³
¹²⁹ I	1.57×10 ⁷	6.60×10 ⁻⁸	1.60×10 ⁶	7.31×10 ⁻⁶
¹³⁵ Cs	2.30×10⁶	1.70×10⁻⁹	1.90×10¹⁰	2.23×10⁻³
¹³⁷ Cs	3.00×10 ¹	1.20×10 ⁻⁸	1.93×10 ⁵	1.60×10 ⁻⁷
^{137m} Ba	4.85×10 ⁻⁶	6.90×10 ⁻¹³	1.83×10 ⁵	8.72×10 ⁻¹²
¹⁴⁷ Sm	1.06×10 ¹¹	4.80×10 ⁻⁸	2.49×10 ⁵	8.28×10 ⁻⁷
¹⁵¹ Sm	9.00×10 ¹	9.20×10 ⁻¹¹	6.17×10 ⁹	3.93×10 ⁻⁵
¹⁵² Gd	1.08×10 ¹⁴	4.30×10 ⁻⁸	8.96×10 ⁻³	2.67×10 ⁻¹⁴
^{166m} Ho	1.20×10 ³	2.20×10 ⁻⁹	1.04×10 ⁸	1.59×10 ⁻⁵

Table A2.1: Dose index, defined as the ratio of drinking water dose to the regulatory guideline of 0.1 mSv y⁻¹, calculated for the activation/fission products. Those radionuclides which, when short-lived daughters are included, give a dose index exceeding 10⁻³, are indicated by shading. The inventory per canister is calculated at 1000

Table A2-1: (Continued) years after emplacement (1040 years after unloading of spent fuel from the reactors). The reference inventory per canister at 4 years after unloading is provided by the MIRA database (ALDER & MCGINNES 1994). The inventory at 1000 years after emplacement is calculated from this reference inventory, accounting for decay and ingrowth, using the code RAPIDE (GRINDROD et al. 1990a). Parents and daughters in secular equilibrium are grouped together in the table and shown without separating lines.

Naming Convention	Members Decay Relationship
activation/fission products	$^{135}\text{Cs}, ^{126}\text{Sn}, ^{107}\text{Pd}, ^{99}\text{Tc}, ^{93}\text{Zr}, ^{79}\text{Se}, ^{59}\text{Ni}$
4N + 3 chain	$^{243}\text{Am} \rightarrow (^{239}\text{Np}) \rightarrow ^{239}\text{Pu} \rightarrow ^{235}\text{U} \rightarrow (^{231}\text{Th}) \rightarrow ^{231}\text{Pa} \rightarrow ^{227}\text{Ac} \rightarrow (^{227}\text{Th}) \rightarrow (^{223}\text{Ra})$
4N + 2 chain	$^{246}\text{Cm} \rightarrow ^{242}\text{Pu} \rightarrow ^{238}\text{U} \rightarrow (^{234}\text{Th}) \rightarrow ^{234}\text{U} \rightarrow ^{230}\text{Th} \rightarrow ^{226}\text{Ra} \rightarrow (^{222}\text{Rn}) \rightarrow ^{210}\text{Pb} \rightarrow (^{210}\text{Bi}) \rightarrow ^{210}\text{Po}$
4N + 1 chain	$^{245}\text{Cm} \rightarrow ^{241}\text{Pu} \rightarrow ^{241}\text{Am} \rightarrow ^{237}\text{Np} \rightarrow (^{233}\text{Pa}) \rightarrow ^{233}\text{U} \rightarrow ^{229}\text{Th} \rightarrow (^{225}\text{Ra}) \rightarrow (^{225}\text{Ac})$
4N chain	$^{240}\text{Pu} \rightarrow ^{236}\text{U} \rightarrow ^{232}\text{Th} \rightarrow ^{228}\text{Ra} \rightarrow ^{228}\text{Th} \rightarrow (^{224}\text{Ra})$

Table A2.2: The radionuclides selected for consideration in the Kristallin-I assessment. Naming conventions for the actinide chains is also shown. Decay-chain branches with very low branching ratios are neglected. Those radionuclides given in italics are assumed to be in radioactive equilibrium in the near-field and geosphere models, but are calculated explicitly in the biosphere. The radionuclides given in brackets are assumed to be in equilibrium throughout the assessment model chain (see text for explanation).

APPENDIX 3 QUALITY ASSURANCE AND TRACEABILITY

1. Overview

In the Kristallin-I safety assessment, a number of procedures are adopted to ensure that the quality of the conclusions can be defended.

a) Procedures relevant to the definition of calculations to be performed and to the establishment of appropriate models, data and computational tools for these calculations are itemised below:

- **defining the calculations:** a formal scenario analysis was carried out, to ensure the transparency and traceability of the process of defining the cases to be considered (see Chapter 4);
- **building confidence in models and data (validation):** a series of measures were used to build confidence, including a systematic and transparent approach to model development, with a full description of the judgements and assumptions made (see Chapter 5) and use of laboratory tests, field tests and natural analogues to test models and data (see Section 7.6);
- **code verification:** a number of tests have been applied to each code, to ensure that the calculations associated with a particular model are correct solutions of the specified equations, with the specified boundary conditions (see "code verification", below);
- **code maintenance:** modifications to the codes are documented in log-books, with each new version distinguished by an identification number appended to the code name (see "code maintenance", below);

b) The quality-assurance procedure applied to the calculations themselves consists of the following components:

- **file handling:** a formalised file-handling system for safety-assessment calculations has been adopted to ensure traceability of results, including the automatic generation of a record of all data files and codes (with version numbers) used (see "organisation of the calculations", below);
- **traceability of data:** it is ensured that, in all cases, the sources of parameter values used in calculations are traceable to the original data through careful referencing of bibliographical sources and a detailed description of manipulations performed to derive parameter values;

– **consistency checks**

- **input data:** consistency between source data and input parameters is further facilitated by common tables in the synthesis report of geological investigations (THURY et al. 1994) and the safety analysis report (Tables 3.7.4 and 3.7.5);
 - **results:** computational results are tested by means of comparison with results from other computer codes and analytical solutions of simplified systems.
- c) The methods, models and data used in the Kristallin-I safety assessment are summarised in the present report, which is itself based on a wide range of supporting publications, including many in the Nagra technical report series. Quality these documents is ensured principally by means of:
- **peer review:** formal review of key documentation was carried out by both internal and external experts.

The topics of code verification, code maintenance and organisation of the calculations (file handling) include several aspects which are specific to the Kristallin-I assessment and are discussed in the following sections.

2. Code Verification

The Kristallin-I model chain is based on three distinct computer codes:

- Radionuclide release and transport in the near field, STRENG;
- Radionuclide transport in the geosphere, RANCHMD;
- Radionuclide distribution in the biosphere and exposure pathways, TAME (incorporating the BIOPATH equation solving routines - ACTIVI).

For a small number of calculations, variations on these codes were employed. For example, the code RANCHMDNL was used to model the effects of non-linear sorption in the geosphere and a version of the TAME exposure pathway sub-model, TAME_1D, was used to model pathways in the Periglacial Climate State. In modelling the Deep Groundwater Well scenario, where a detailed biosphere model was not required, dose calculations were carried out on a spreadsheet.

Each of the computer codes has been verified; tests have been carried out to ensure that the codes give correct solutions of the specified equations, with the specified boundary conditions. The verification procedures for each code are briefly discussed below.

In the case of STRENG, comparison can be made with an analytical solution in the case of a single radionuclide, for which the solubility limit is not reached (GRINDROD et al. 1990b). Close agreement has been found between the results of the numerical calculations using STRENG and the analytical solution.

A version of the code RANCHMD has been made available to the NEA Databank for distribution to a wide community of users. A small number of minor problems have since been reported and corrected in the version of the code used in the Kristallin-I assessment. Major components of the code were also tested against the INTRACOIN benchmarks (SKI 1984; SKI 1986). Following this successful application, a version of the code incorporating non-linear sorption, RANCHMDNL, was developed (JAKOB et al. 1989).

In the case of TAME, a series of studies comparing the performance of TAME with earlier Swiss biosphere codes has been undertaken. The intercomparison shows that, with the system solved by TAME simplified to emulate those solved by the earlier codes, the results are identical (KLOS et al. 1994). The correct functioning of the code component used for the solution of the compartment model equations has been demonstrated in the PSACOIN Level 1b exercise (NEA 1993).

3. Code Maintenance

Modifications, improvements and bug-fixes in the codes are documented in log-books as well as in detailed comments added to the codes themselves in the appropriate subroutines. Versions of the codes are distinguished by major and minor variant names, e.g. STRENG_1.2 - major version 1, modification 2; TAME_1B - major variant 1, second version, TAME_1D - major variant 1, fourth version.

All codes use an advanced version of the FORTRAN 77 standard and have been successfully implemented on a variety of platforms, including DOS, VMS and UNIX.

4. Organisation of the Calculations

Input data and results from calculations using each of the model-chain codes is stored in the directory structure shown in Figure A3.1. The directory structure is set up in a way that facilitates traceability of the data flow as results from one calculation provide input data for others at the next stage along the model chain.

Each model is assigned its own directory, with associated subdirectories. Source codes, executable and command files are stored at the highest level in this hierarchy, with, at the next level, subdirectories named "data" and "results" defining the storage locations of all input and output files for a particular model. At the lowest level of subdirectories, all files for a particular set of calculations are stored, i.e. calculations using a specific set of radionuclide-independent parameters to describe the near field, geosphere or biosphere.

Directory Structure	Kristallin I Command	Summary
	<p>S_NEAR sec_a chains</p> <p>FAR sec_a sa_60a chains cm246</p> <p>REL sa_60ala cm246 g_1 sa_60a</p> <p>TAME_1B sa_60ala cm246 BIO_ sa_60ala cm246 DOSE_1B sa_60ala cm246</p>	<p>Performs <i>STRENG</i> runs for all radionuclide chains for near-field calculations using the SEC_A dataset.</p> <p>Performs the <i>RANCHMD</i> runs for the geosphere dataset SA_60A extracting the data for ²⁴⁶Cm from the <i>STRENG</i> output files.</p> <p>Releases the geosphere fluxes from SA_60A to the biosphere representation SA_60ALA.</p> <p>Sets up run details: Transport in the biosphere: Calculates doses arising from radionuclide distribution in the biosphere.</p>

Figure A3.1: Kristallin-I directory structure and commands. The case illustrated shows the sequence of commands and flow of data in a calculation of the transport of ²⁴⁶Cm and its daughters (the 4N+2 chain) from the repository to the biosphere and subsequent doses. Radionuclide-independent data for the total system is encoded in the dataset name SA_60ALA.

Subdirectories at this lowest level are referred to by dataset names. The naming convention for datasets is described in Appendix 4. Within a particular directory, there is a one to one correspondence between the dataset names for input files and output files. Thus, a set of STRENG calculations associated with the dataset name SEC_A will draw on input data from files located in [streng.data.sec_a] and direct the output to [streng.results.sec_a]. At the lowest level of subdirectory, files are named according to their function using a suitable file extension (for example, files with names *.bio in the TAME directory contain biosphere description data). Files containing radionuclide-specific data are named after the radionuclide itself, or, in the case of files containing data for a decay chain, after the first member of the chain considered in the calculation. Thus, files with names of the form CM246.* contain data for ²⁴⁶Cm and its daughters

(the $4N+2$ chain). However, for the near-field model, all chains are calculated simultaneously because shared solubilities between isotopes of the same element in different chains must be taken into account. Near-field files for decay chains have names of the form CHAINS.*. In the case of the biosphere model, files with radionuclide-independent data are simply given the dataset name for the subdirectory in which they are located: the files SA_60ALA.* contain radionuclide-independent data for the dataset SA_60ALA (the Reference Case - see Chapter 6).

The directory structure shown in Figure A3.1 illustrates how the number of datasets to be considered is relatively small for the near field (the STRENG directory), but increases along the model chain. This is because one particular representation of the near field may provide data for several sets of geosphere calculations. As shown in Figure A3.1, the results calculated using near-field dataset SEC_A provide data for geosphere calculations of datasets SA_10A to SA_60A. In turn, SA_60A provides data for the biosphere component of the complete model-chain calculations SA_60ALA to SA_60ARS. Note that the each geosphere dataset name contains within it the dataset name of the corresponding near-field calculation (the near-field dataset name SEC_A corresponds to SA_ in the geosphere name). Similarly, both near-field and geosphere information is encoded within biosphere dataset names.

To perform the STRENG calculation for the release and transport of radionuclides in the near field, the command **S_NEAR** is used, along with two parameters to identify the input files to be used. The first is the dataset name, which specifies the location of radionuclide-independent data, since that information is common to all input files in the named subdirectory. The second is the name of the files containing the radionuclide-specific data. Thus, the command **S_NEAR SEC_A CHAINS** initiates a STRENG calculation of near-field release for all radionuclide chains in a near field described by the dataset SEC_A.

The command **FAR** is used to perform a geosphere calculation with code RANCHMD. This time, four parameters must be supplied. The first is a dataset name specifying the near-field radionuclide-independent data. The second is a dataset name for the geosphere radionuclide-independent data. The third is the name of the files containing results from the particular near-field calculation which is to be used as geosphere input. The fourth is the name of the files containing radionuclide-specific data for the geosphere itself. In the case of calculations for single radionuclides (the activation/fission products), the third and fourth parameters may be identical. Decay chains, however, are calculated separately for the geosphere and simultaneously for the near field, as explained above. Thus the command **FAR SEC_A SA_60A CHAINS CM246** initiates a RANCHMD calculation of geosphere transport for ^{246}Cm and its daughters (the $4N+2$ chain) in a geosphere described by the dataset SA_60A.

The biosphere calculations are carried out in four stages.

- The **REL** command, which again requires four parameters, transfers data for biosphere modelling (geosphere releases) from the geosphere directory to the biosphere directory. The first parameter is a dataset name for the biosphere radionuclide-independent data. The second is the name of the files containing the radionuclide-specific data (the same name is used for geosphere and biosphere data since chains are handled separately). The third indicates whether the geosphere has been modelled in a single calculation (the crystalline low-permeability domain only - indicated by a parameter **G_1**) or in two consecutive calculations (first, the low-permeability domain and second, major water-conducting faults - indicated by **G_2**). The fourth is a dataset name for the geosphere radionuclide-independent data.
- The command **TAME_1B** sets up the transport characteristics for the biosphere representation and radionuclide chain.
- The command **BIO_** runs the BIOPATH-ACTIVI routines, using the files generated by **REL** and **TAME_1B**, in order to calculate the time-evolution of radionuclide concentrations in the biosphere.
- The command **DOSE-1B** is used to calculate the doses arising from the distribution of radionuclides concentrations.

As data passes through the directory structure, its progress is recorded automatically on a "log-file". Figure A3.2 shows an example of a log-file, generated by the sequence of calculations in Figure A3.1.

Each time a code is run, a record is automatically generated containing the code name, version number and time of execution. In addition, the dataset name and the name of the files containing radionuclide-specific data are recorded. The log-file of the near-field calculation which provides input to a geosphere calculation is added to the log-file generated by the geosphere calculation itself. Similarly, this log-file is appended to that of the subsequent biosphere calculation. Log-files are appended to tabular and graphical representations of the results and are located at the lowest level of the directory structure, below the "results" subdirectory of each model. They enable the location (in terms of both position in the directory structure and of the time at which they were read) of all input files and output files for a particular sequence of runs to be traced. At an early stage in the development of this system, these log-files proved useful in the quick identification of model runs where incorrect data files were passed between the code modules.

```

+-----+
| The Paul Scherrer Institut: Full Assessment |
| Model Executive: Version 1b Stardent: March 92 |
+-----+
| STRENG 1.2: Aug 1992 |
+-----+
parent radionuclide: chains
  scenario name: sec_a
  run at: 17:04:25
  on: Sep 2 1992
+-----+
| The Paul Scherrer Institut: Full Assessment |
| Model Executive: Version 1b Stardent March 92. |
+-----+
| RANCH MD vsn 2C **** STARDENT |
+-----+
parent radionuclide: CM246
  scenario name: SA_60A
  run at: 10:13:48
  on: Jan 26 1993
+-----+
| The Paul Scherrer Institut: Full Assessment |
| Model Executive: Version 1a: January 1992. |
+-----+
| TAME 1b Biosphere Release: March 1992. |
+-----+
parent radionuclide: CM246
  scenario name: SA_60ALA
  run at: 16:51:21
  on: 4-FEB-93
+-----+
| The Paul Scherrer Institut: Full Assessment |
| Model Executive: Version 1a: January 1992. |
+-----+
| TAME 1b transfer coefficients: October 1992. |
+-----+
parent radionuclide: CM246
  scenario name: SA_60ALA
  run at: 17:05:51
  on: 15-MAR-93
+-----+
| The Paul Scherrer Institut: Full Assessment |
| Model Executive: Version 1a: January 1992. |
+-----+
| TAME 1b doses calculations: October 1992 |
+-----+
parent radionuclide: CM246
  scenario name: SA_60ALA
  run at: 17:06:37
  on: 15-MAR-93

```

Figure A3.2: The Kristallin-I log-file. A record of the sequence of model calculations performed corresponding to the sequence of commands shown in Figure A3.1. Near-field, geosphere and biosphere calculations are performed for ^{246}Cm and its daughters (the $4N+2$ chain). The dataset names *SEC_A*, *SA_60A* and *SA_60ALA* enable the data used at each stage of the model chain to be located in the Kristallin-I directory structure.

APPENDIX 4 NAMING CONVENTIONS FOR DATASETS

A directory structure is described in Appendix 3 for the storage of input and output data for the model-chain calculations. The data are stored in files at the lowest level in a hierarchy of subdirectories. These lowest-level subdirectories are referred to by dataset names. These subdirectories are grouped according to whether they contain files of input or output data and, at a higher level, according to whether the data are associated with near-field, geosphere or biosphere calculations. A near-field subdirectory at the lowest level with a particular dataset name contains files for all calculations which use a common set of radionuclide-independent parameters to describe the near field (radionuclide-specific data are stored in separate files within the subdirectory). The near-field dataset name is chosen so that it uniquely identifies the radionuclide-independent parameters for the associated calculations. A particular geosphere subdirectory contains files for all calculations which use a common set of radionuclide-independent parameters to describe not only the geosphere itself, but also the near field which supplies the radionuclide release to the geosphere. The geosphere dataset name is therefore chosen so that it uniquely identifies the radionuclide-independent parameters of both the near field and the geosphere itself. Similarly, near-field, geosphere and biosphere data are encoded in a dataset name for a complete model-chain calculation.

Geosphere dataset names have the general format:

NF_{*mn*}G.

Dataset names for a complete model chain are of the form

NF_{*mn*}GBS,

which encodes radionuclide-independent data for the **Near Field**, **Geosphere** (calculations *m* - for the low-permeability domain - and *n* - for major water-conducting faults) and **BioSphere**.

Near Field

NF is a two-character abbreviation of the (longer) near-field dataset name. The Reference-Case near field is identified by the name *SEC_A*, which is abbreviated to *SA_* in the dataset names for the geosphere and the complete model chain. The Reference Case employs a "realistic-conservative" combination of near-field physico/chemical parameters. In addition, a number of individual parameter variations have been carried out and are discussed in Chapter 5. Though all safety-relevant radionuclides were calculated in the Reference Case, not all the radionuclides were

considered in all the parameter variations. The groups of radionuclides calculated for each dataset (near field, geosphere and biosphere) are identified by a number, interpreted using Table A4.1. The near-field datasets are summarised in Table A4.2 (excluding individual near-field parameter variations for which no geosphere or biosphere calculations were performed). The table gives the dataset names (in full and abbreviated form), the radionuclide group calculated, a brief comment on the purpose and/or distinguishing features of the calculations and a code identifying the combination of parameters used. This code is interpreted using the "job matrix" in Table A4.3. Taking the Reference Case as an example, the parameter combination used is denoted as [1=C, 2=C, 3=C, 4=F, 5=C]. Using Table A4.3, this is interpreted as :

1. glass corrosion rate of $1.2 \times 10^{-11} \text{ kg m}^{-3} \text{ s}^{-1}$;
2. groundwater flowrate through repository area of $3 \text{ m}^3 \text{ y}^{-1}$ (Area West) or $111 \text{ m}^3 \text{ y}^{-1}$ (Area East);
3. "realistic-conservative" set of K_d values;
4. "realistic-conservative" set of solubilities;
5. stable isotopes considered.

Geosphere

The part of the dataset name related to the geosphere consists of two integers and a letter. The integers denote the geometrical representation of water-conducting features within the crystalline low-permeability domain and major water-conducting faults respectively. A zero as the second integer indicates that transport through the major water-conducting faults is not calculated. The letter denotes the set of all other radionuclide-independent geosphere parameters. Transport in the Reference Case geosphere, denoted by the identifier *60_A*, takes place in the low-permeability domain along cataclastic zones/jointed zones with fractures containing broad, widely-spaced channels and with matrix diffusion into the adjacent altered wallrock only (water-conducting feature geometry 6 - refer to Section 5.3). Transport in the major water-conducting faults is not calculated and a "realistic-conservative" combination of geosphere parameters is used. As with the near field, a number of individual parameter variations have been carried out. These are identified and summarised in Table A4.4. A job matrix for the geosphere is given in Table A4.5.

radio-nuclide group	purpose	decay chain members	
①	full assessment runs	4N + 3 chain: 4N + 2 chain: 4N + 1 chain: 4N chain: activation/ fission products:	$^{243}\text{Am} \rightarrow ^{239}\text{Pu} \rightarrow ^{235}\text{U} \rightarrow ^{231}\text{Pa} \rightarrow (^{227}\text{Ac})$ $^{246}\text{Cm} \rightarrow ^{242}\text{Pu} \rightarrow ^{238}\text{U} \rightarrow ^{234}\text{U} \rightarrow ^{230}\text{Th} \rightarrow ^{226}\text{Ra} \rightarrow (^{210}\text{Pb} \rightarrow ^{210}\text{Po})$ $^{245}\text{Cm} \rightarrow (^{241}\text{Pu}) \rightarrow ^{241}\text{Am} \rightarrow ^{237}\text{Np} \rightarrow ^{233}\text{U} \rightarrow ^{229}\text{Th}$ $^{240}\text{Pu} \rightarrow ^{236}\text{U} \rightarrow ^{232}\text{Th} \rightarrow (^{228}\text{Ra} \rightarrow ^{228}\text{Th})$ $^{135}\text{Cs}, ^{126}\text{Sn}, ^{107}\text{Pd}, ^{99}\text{Tc}, ^{93}\text{Zr}, ^{79}\text{Se}, ^{59}\text{Ni}$
②	geosphere sensitivity analysis	4N + 1 chain: activation/ fission products:	$^{237}\text{Np} \rightarrow ^{233}\text{U} \rightarrow ^{229}\text{Th}$ $^{135}\text{Cs}, ^{99}\text{Tc}, ^{79}\text{Se}$
③	biosphere sensitivity analysis	4N + 3 chain: activation/ fission products:	$^{243}\text{Am} \rightarrow ^{239}\text{Pu} \rightarrow ^{235}\text{U} \rightarrow ^{231}\text{Pa} \rightarrow (^{227}\text{Ac})$ $^{135}\text{Cs}, ^{99}\text{Tc}, ^{79}\text{Se}$
④	colloid facilitated transport	4N + 1 chain:	$^{237}\text{Np} \rightarrow ^{233}\text{U} \rightarrow ^{229}\text{Th}$

Table A4.1: Summary of the radionuclides considered in the Kristallin-I assessment runs. The radiological impact of the intermediate radionuclides in these chains was taken into account by adding the dose per unit intakes of the short-lived daughters to the immediate precursor radionuclide (see Appendix 2). All radionuclides with half-lives of the order of one year or more were explicitly calculated in the biosphere (chain members in brackets) although these were not included in the near-field and geosphere calculations. Release fluxes of these radionuclides to the biosphere were assumed to be in equilibrium with the immediate precursors.

Parameter Combination					Dataset Name (with abbreviated form)		Radio-nuclide Group	Comments
1	2	3	4	5				
C	C	C	F	C	<i>SEC_A</i>	(<i>SA_</i>)	①	Combination of "realistic-conservative" physico-chemical parameters for Area West. The Reference Case near field.
C	A	C	F	C	<i>EIGHTH_A</i>	(<i>8A_</i>)	①	Combination of "realistic-conservative" parameter values; zero-concentration boundary condition
B	A	B	C	C	<i>SEC_B</i>	(<i>SB_</i>)	①	Combination of "conservative" parameter values; zero-concentration boundary condition.
B	C	B	C	C	<i>ELEVEN_B</i>	(<i>EB_</i>)	①	Combination of "conservative" parameter values; mixing-tank boundary condition with reference-case flowrate.
C	C	C	F	C	<i>SEC_C</i>	(<i>SC_</i>)	①	Groundwater flowrate for Area East.
C	E	C	F	C	<i>SEC_D</i>	(<i>SD_</i>)	④	Sorption of radionuclides on groundwater colloids reduces the near-field outer-boundary concentration - equivalent to an increased flowrate.
C	C	C	C	C	<i>EIGHTH_D</i>	(<i>8D_</i>)	①	"Conservative" solubility limits applied.
C	F	C	F	C	<i>ELEVEN_A</i>	(<i>EA_</i>)	①	Groundwater flowrate reduced by a factor 10 with respect to Reference Case.
C	B	C	F	C	<i>SIXTH_A</i>	(<i>XA_</i>)	①	Groundwater flowrate increased by a factor 10 with respect to Reference Case.
C	D	C	F	C	<i>SIXTH_B</i>	(<i>XB_</i>)	①	Groundwater flowrate increased by a factor 100 with respect to Reference Case.

Table A4.2: Dataset names for near-field calculations. The Reference-Case near field is indicated by shading. The radionuclide groups are explained in Table A4.1. Each parameter is assigned a number (1-5). The value that a parameter takes is assigned a letter (A-F). The parameter combinations are interpreted using the job matrix in Table A4.3. Only near-field datasets which provide input data for geosphere and/or biosphere calculations (i.e. not near-field parameter variation) are shown.

Parameter	Units	A	B	C	D	E	F
1: Glass corrosion rate	kg m ⁻² y ⁻¹		3.8×10 ⁻²	3.8×10 ⁻⁴			
2: Flowrate through repository area (Area West)	m ³ y ⁻¹	unlimited	30	3.0 (111 for Area East)	300	6.0	0.3
3: <i>K_d</i> values	-		"conservative"	"realistic-conservative"			
4: Solubility limits	-			"conservative"			"realistic-conservative"
5: Stable isotopes	-		ignored	considered			

Table A4.3: Job matrix for the Kristallin-I near-field calculations. Each parameter is assigned a number (1-5). The letter (A-F) assigned to a particular parameter value corresponds to that in the parameter combinations of Table A4.2.

Biosphere

In the two character identifier for the biosphere datasets, the first letter corresponds to the release type, and the second identifies the characteristics of the biosphere. The Reference-Case biosphere, denoted by the identifier *LA*, corresponds to the present-day biosphere in the vicinity of the Rhine (*A* ⇒ present-day near-surface hydrology, agricultural practices, etc.) with the release of radionuclides to the gravels of the Rhine valley (*L*). Further information is given in Section 5.4. The influence of different potential climate states was considered, as were a number of individual parameter variations, and these are identified and summarised in Table A4.6.

Table A4.6 also summarises all datasets modelled through to dose. These include the release to a biosphere in which the Rhine gravels have been removed by fluvial or glacial processes (scenarios *Rx*). Soils in the region were assumed to lie directly above the higher-permeability domain of the crystalline basement and the release was assumed to be to the Rhine water, which would flow in the lowest part of the valley. Additionally, a very pessimistic scenario was considered where the geosphere water-conducting features carrying the contaminated water were assumed to discharge directly to the deep soil horizon (because the removal of the gravel terraces means that no near-surface aquifer is present).

Release to Area East was again modelled as the discharge of groundwaters to a regional aquifer in Rhine gravels, but, in addition to the Reference-Case biosphere, a tributary valley of the Rhine (*TA*) was considered. Finally, the extraction of groundwater from a deep groundwater well (*MB*) was considered.

Parameter Combination								Dataset Name	Radio-nuclide Group	Comments
1	2	3	4	5	6	7	8			
A	C	C	C	C	C	C	C	SA_10A	①	Cataclastic zones or jointed zones with narrow, closely-spaced channels, unlimited matrix diffusion.
B	C	C	C	C	C	C	C	SA_20A	①	Fractured aplite/pegmatite dykes and aplitic gneisses, unlimited matrix diffusion.
C	C	C	C	C	C	C	C	SA_30A	①	Cataclastic zones or jointed zones with broad, widely-spaced channels, unlimited matrix diffusion.
D	C	C	C	C	C	C	C	SA_40A	①	Cataclastic zones or jointed zones with narrow, closely-spaced channels, limited matrix diffusion.
E	C	C	C	C	C	C	C	SA_50A	①	Fractured aplite/pegmatite dykes and aplitic gneisses, limited matrix diffusion.
F	C	C	C	C	C	C	C	SA_60A	①	Cataclastic zones or jointed zones with broad, widely-spaced channels, limited matrix diffusion.
F	C	C	C	C	C	C	C	8D_60A	①	Reference-case geosphere; "conservative" solubility limits in near field.
F	C	C	C	C	C	C	C	SC_60A	①	Groundwater flowrate for Area East.
A	B	C	C	C	C	C	C	SD_10B	④	Colloid transport, geometry 1.
B	B	C	C	C	C	C	C	SD_20B	④	Colloid transport, geometry 2.
C	B	C	C	C	C	C	C	SD_30B	④	Colloid transport, geometry 3.
D	B	C	C	C	C	C	C	SD_40B	④	Colloid transport, geometry 4.
E	B	C	C	C	C	C	C	SD_50B	④	Colloid transport, geometry 5.
F	B	C	C	C	C	C	C	SD_60B	④	Colloid transport, geometry 6.
F	C	C	C	C	C	C	C	SA_64A	②	Transport path divided between (i) low-permeability domain and (ii) major water-conducting faults.
D	C	C	C	C	C	C	C			
F	C	B	C	C	C	C	C	SA_60C	②	Reduced flowpath length.
F	C	D	C	C	C	C	C	SA_60D	②	Increased flowpath length.
F	C	C	B	C	C	C	C	SA_60E	②	"Conservative" (low) sorption on matrix pores.
F	C	C	C	B	C	C	C	SA_60F	②	"Conservative" (low) diffusion coefficient.
F	C	C	C	C	D	C	C	SA_60G	②	Reduced Peclet number - high longitudinal dispersion.
F	C	C	C	C	B	C	C	SA_60H	②	Increased Peclet number - reduced longitudinal dispersion.
F	C	C	C	C	C	B	C	SA_60I	②	"Conservative" (1 cm) matrix depth accessible to diffusion.
F	C	C	C	C	C	C	D	EA_60L	①	Decreased flowrate - 10 times less than that of Reference Case.
F	C	C	C	C	C	C	B	XA_60J	①	Increased flowrate - 10 times that of Reference Case.
F	C	C	C	C	C	C	A	XB_60K	①	Increased flowrate - 100 times that of Reference Case.

Table A4.4: Datasets for geosphere calculations. The Reference-Case geosphere is indicated by shading. The radionuclide groups are given in Table A4.1. Each parameter is assigned a number (1-8). The value that a parameter takes is assigned a letter (A-F). The parameter combinations are interpreted using the job matrix in Table A4.5.

Parameter	Units	A	B	C	D	E	F
1: Geometry of water-conducting features		1	2	3	4	5	6
2: Colloid concentration	kg m ⁻³		10 ⁻⁴	0			
3: Flowpath length	m		100	200	500		
4: K_d values	-		conservative	realistic-conservative			
5: Diffusion constant	m ² y ⁻¹		2×10 ⁻⁴	10 ⁻³			
6: Peclet number	-		50	10	2		
7: Accessible matrix depth	-		conservative	realistic-conservative			
8: Flowrate through repository area	m ³ y ⁻¹	300	30	3 (111 for Area East)	0.3		

Table A4.5: Job Matrix for the Kristallin-I geosphere calculations. Each parameter is assigned a number (1-8). The letter (A-F) assigned to a particular parameter value corresponds to that in the parameter combinations of Table A4.4. The K_d values are dependent on groundwater chemistry and are, for some radionuclides, different in the two areas West and East. A conservative depth of matrix accessible to diffusion is taken to be 1 cm. In the "realistic-conservative" case, the only constraint on the extent of accessible matrix is that imposed by the geometrical representation of the water-conducting features. For major water-conducting faults, a single flowrate is used throughout.

The Reference Scenario		
Reference Model Assumptions		
Reference-Case Parameters		
Dataset Names	Radio-nuclides	Purpose and/or Distinguishing Features
SA_60ALA SA_LA	① ①	Reference Case Hypothetical case of direct release from NF to BIOS; used to illustrate the role of GS
Near-Field Parameter Variations (see Section 5.2 for a description of near-field parameter variations for which no model-chain calculations were performed)		
Dataset Names	Radio-nuclides	Purpose and/or Distinguishing Features
SD_60ALA EB_60ALA	① ①	"Conservative" solubility limits Combination of "conservative" parameters (glass corrosion rate, sorption constants, solubility limits)
EB_LA	①	Hypothetical case of direct release from NF to BIOS; used to illustrate the role of GS
Geosphere Parameter Variations		
Dataset Names	Radio-nuclides	Purpose and/or Distinguishing Features
SA_60CLA SA_60DLA SA_60ELA SA_60FLA SA_60GLA SA_60HLA SA_60ILA	② ② ② ② ② ② ②	Reduced migration path length Increased migration path length "Conservative" GS sorption constants Reduced diffusion coefficient for matrix diffusion Reduced Peclet number: increased longitudinal dispersion Increased Peclet number: reduced longitudinal dispersion Reduced depth of diffusion-accessible matrix
Parameter Variations affecting Near Field and Geosphere		
Dataset Names	Radio-nuclides	Purpose and/or Distinguishing Features
EA_60LLA XA_60JLA XB_60KLA	① ① ①	10-fold decrease in groundwater flowrate 10-fold increase in groundwater flowrate 100-fold increase in groundwater flowrate

Key to abbreviations:

<i>CZ</i>	<i>Cataclastic zones</i>	<i>JZ</i>	<i>Jointed zones</i>	<i>MD</i>	<i>Matrix diffusion</i>
<i>NF</i>	<i>Near Field</i>	<i>GS</i>	<i>Geosphere</i>	<i>BIOS</i>	<i>Biosphere</i>
<i>GW</i>	<i>groundwater</i>	<i>EDZ</i>	<i>Excavation-disturbed zone</i>		
<i>MWCF</i>	<i>Major water-conducting fault</i>				

Table A4.6: Summary of calculations performed in the Kristallin-I assessment. Near-field parameter variations, for which no geosphere and/or biosphere calculations have been carried out, are excluded from the table. The radionuclide groups are given in Table A4.1.

The Reference Scenario		
Reference Model Assumptions		
Biosphere Parameter Variations		
Dataset Names	Radio-nuclides	Purpose and/or Distinguishing Features
SA_60ALI	③	Increased sorption
SA_60ALR	③	Decreased sorption
SA_60ALW	③	All irrigation from Rhine
SA_60ALQ	③	All irrigation from local aquifer
SA_60ALL	③	Decreased regional erosion
SA_60ALG	③	Increased regional erosion
SA_60ALT	③	Thicker local aquifer
SA_60ALN	③	Thinner local aquifer
Alternative Reference Area for Repository Siting		
Dataset Names	Radio-nuclides	Purpose and/or Distinguishing Features
SC_60ALA	①	Area East - release to Reference-Case BIOS
SC_60ATA	①	Area-East - exfiltration to a small valley
SC_LA	①	Hypothetical case of direct release from NF to BIOS; used to illustrate the role of GS
Alternative Model Assumptions		
Geometrical Representation of Water-Conducting Features		
Dataset Names	Radio-nuclides	Purpose and/or Distinguishing Features
SA_10ALA	①	CZ / JZ with narrow, closely-spaced channels, MD in altered and unaltered rock
SA_20ALA	①	Fractures aplite / pegmatite dykes and aplitic gneisses, MD in altered and unaltered rock
SA_30ALA	①	CZ / JZ with broad, widely-spaced channels, MD in altered and unaltered rock
SA_40ALA	①	CZ / JZ with narrow, closely-spaced channels, MD limited to altered rock
SA_50ALA	①	Fractures aplite / pegmatite dykes and aplitic gneisses, MD limited to altered rock
SA_60ALA	①	CZ / JZ with broad, widely-spaced channels, MD limited to altered rock
Radionuclide Transport Path		
Dataset Names	Radio-nuclides	Purpose and/or Distinguishing Features
SA_64ALA	②	Radionuclide transport in GS through both the low-permeability domain and MWCF
Colloid Transport		
Dataset Names	Radio-nuclides	Purpose and/or Distinguishing Features
SD_10ALA	④	CZ / JZ with narrow, closely-spaced channels, MD in altered and unaltered rock
SD_20ALA	④	Fractures aplite / pegmatite dykes and aplitic gneisses, MD in altered and unaltered rock
SD_30ALA	④	CZ / JZ with broad, widely-spaced channels, MD in altered and unaltered rock
SD_40ALA	④	CZ / JZ with narrow, closely-spaced channels, MD limited to altered rock
SD_50ALA	④	Fractures aplite / pegmatite dykes and aplitic gneisses, MD limited to altered rock
SD_60ALA	④	CZ / JZ with broad, widely-spaced channels, MD limited to altered rock
SD_LA	④	Hypothetical case of direct release from NF to BIOS; used to illustrate the role of GS

Table A4.6: (Continued). Summary of calculations performed in the Kristallin-I assessment. The radionuclide groups are given in Table A4.1.

Alternative Scenarios		
Dataset Names	Radio-nuclides	Purpose and/or Distinguishing Features
SA_60AMB	①	Deep groundwater well
XB_00TLA	①	Tunnel / shaft seal failure - radionuclide transport along shaft backfill
XB_00VLA	①	Tunnel / shaft seal failure - radionuclide transport along shaft EDZ
SA_60ALD	①	Dry climate state
SA_60ALH	①	Humid climate state
SA_60ALC	②	Periglacial climate state
SA_60ARA	①	Rhine gravels absent - release to Rhine water
SA_60ARS	①	Rhine gravels absent - release to deep soil

Robust Scenario		
Dataset Names	Radio-nuclides	Purpose and/or Distinguishing Features
SA_LA	①	Reference-Case NF and BIOS, no account taken for retardation and decay in GS
8A_LA	①	Unlimited flowrate around NF, no account taken for retardation and decay in GS
EB_LA	①	Combination of "conservative" NF parameters (glass corrosion rate, sorption constants, solubility limits), no account taken for retardation and decay in GS

Table A4.6: (Continued). Summary of the calculations performed in the Kristallin-I assessment. The radionuclide groups are given in Table A4.1.

APPENDIX 5 QUANTIFICATION OF NEAR-FIELD AND GEOSPHERE PERFORMANCE

The relative performance of the near field and geosphere can be quantified in terms of the amount of each radionuclide which decays within a particular barrier or barriers. This quantity is denoted by η_N for the near field and by η_F for the near field and geosphere combined. In each case, it is normalised to the sum of initial inventory of the radionuclide and the amount produced by ingrowth.

Only radionuclides that have half-lives of less than 3×10^6 years are considered⁴⁸. For a radionuclide chain $1 \rightarrow 2 \rightarrow \dots(i-1) \rightarrow i \rightarrow \dots$, the amount of radionuclide I decaying to radionuclide 2 in the near field (i.e. the amount of 2 produced by ingrowth) is equal to the initial inventory of radionuclide I *minus* the integrated release of radionuclide I from the near field (integrated to 10^7 years):

$$I_1 - \int_0^{10^7} \Lambda^{(1)} dt, \quad (\text{A5.1})$$

where I_I [mol] is the inventory of radionuclide I at time $t = 0$ and $\Lambda^{(I)}$ [mol y⁻¹] is its release rate from the near field. The amount of radionuclide 2 decaying within the near field is equal to the initial inventory of radionuclide 2 *plus* the amount of radionuclide 2 produced by ingrowth (Equation A5.1) *minus* the integrated release of radionuclide 2 from the near field :

$$I_2 + I_1 - \int_0^{10^7} \Lambda^{(1)} dt - \int_0^{10^7} \Lambda^{(2)} dt = \sum_{j=1}^2 \left(I_j - \int_0^{10^7} \Lambda^{(j)} dt \right). \quad (\text{A5.2})$$

More generally, the amount of radionuclide i produced by ingrowth in the near field is given by:

$$\sum_{j=1}^{i-1} \left(I_j - \int_0^{10^7} \Lambda^{(j)} dt \right) \quad (\text{A5.3})$$

and the amount of radionuclide i decaying within the near field by:

⁴⁸ Consideration is restricted to those radionuclides which are expected to have decayed to insignificant levels by the end of the calculation; those with half lives of less than 3×10^6 years. 10^7 years has been chosen as a cut-off time for Reference-Case model-chain calculations, (see Appendix 1). Radionuclides with half-lives in the order of 10^7 years or greater may continue to decay within the barrier system beyond the time at which calculations are terminated (unless they have passed out of the system entirely).

$$\sum_{j=1}^i \left(I_j - \int_0^{10^7} \Lambda^{(j)} dt \right). \quad (\text{A5.4})$$

η_N , the amount of radionuclide i decaying within the near field, normalised to the sum of initial inventory of the radionuclide and the amount produced by ingrowth, is thus given by:

$$\eta_N^{(i)} = \frac{\sum_{j=1}^i \left(I_j - \int_0^{10^7} \Lambda^{(j)} dt \right)}{I_i + \sum_{j=1}^{i-1} \left(I_j - \int_0^{10^7} \Lambda^{(j)} dt \right)}. \quad (\text{A5.5})$$

Similarly, for the near-field and geosphere barriers combined,

$$\eta_F^{(i)} = \frac{\sum_{j=1}^i \left(I_j - \int_0^{10^7} \Theta^{(j)} dt \right)}{I_i + \sum_{j=1}^{i-1} \left(I_j - \int_0^{10^7} \Theta^{(j)} dt \right)}, \quad (\text{A5.6})$$

where $\Theta^{(j)}$ [mol y^{-1}] is the release rate of radionuclide j from the geosphere.

APPENDIX 6 DOSE CONVERSION FACTORS FOR NEAR-FIELD CALCULATIONS

In presenting the results of parameter variations in the near field (Section 5.2), it is useful to express the results for different radionuclides on a radiologically comparable scale. Near-field releases have therefore been converted to annual individual doses using a set of simple conversion factors based on the drinking-water dose per unit activity released directly to a gravel aquifer in the Rhine River valley. These dose-conversion factors are given in this appendix.

For a release rate of 1 mol y^{-1} , the corresponding conversion factor is given by:

$$1 \text{ Sv y}^{-1} = 1 \text{ mol y}^{-1} \times N_{av} \cdot \lambda \cdot [W/(F_{UL}+F_{CL})] \cdot D_{ing} ,$$

where:

- N_{av} is Avogadro's Number ($6.02 \times 10^{23} \text{ atoms mol}^{-1}$);
- λ [s^{-1}] is the decay constant;
- $F_{UL}+F_{CL}$ is the water flow in the gravel aquifer, taken as $5.5 \times 10^6 \text{ m}^3 \text{ y}^{-1}$ (see Table 5.4.3);
- W is the total annual drinking water intake by an individual set at $0.73 \text{ m}^3 \text{ y}^{-1}$ (see Table A7.1);
- D_{ing} is the committed effective dose equivalent per unit ingestion, according to NRPB (1987) [Sv Bq^{-1}].

The resulting dose-conversion factors are presented in Table A6.1.

radionuclide	half-life [y]	D_{ing} [Sv Bq ⁻¹]	dose-conversion factor [mSv mol ⁻¹]
²⁴⁵ Cm	8.50×10^3	1.02×10^{-6}	2.11×10^2
²⁴¹ Am	4.32×10^2	9.80×10^{-7}	3.99×10^3
²³⁷ Np	2.14×10^6	1.10×10^{-6}	9.04×10^{-1}
²³³ U	1.59×10^5	7.10×10^{-8}	7.88×10^{-1}
²²⁹ Th	7.34×10^3	1.07×10^{-6}	2.56×10^2
²⁴³ Am	7.38×10^3	9.81×10^{-7}	2.34×10^2
²³⁹ Pu	2.41×10^4	9.50×10^{-7}	6.94×10^1
²³⁵ U	7.04×10^8	6.64×10^{-8}	1.66×10^{-4}
²³¹ Pa	3.28×10^4	6.87×10^{-6}	3.69×10^2
²⁴⁶ Cm	4.73×10^3	1.00×10^{-6}	3.72×10^2
²⁴² Pu	3.76×10^5	9.00×10^{-7}	4.21
²³⁸ U	4.47×10^9	6.65×10^{-8}	2.62×10^{-5}
²³⁴ U	2.45×10^5	7.00×10^{-8}	5.03×10^{-1}
²³⁰ Th	7.54×10^4	1.40×10^{-7}	3.26
²²⁶ Ra	1.60×10^3	2.13×10^{-6}	2.34×10^3
²⁴⁰ Pu	6.54×10^3	9.50×10^{-7}	2.56×10^2
²³⁶ U	2.34×10^7	6.60×10^{-8}	4.96×10^{-3}
²³² Th	1.41×10^{10}	1.27×10^{-6}	1.59×10^{-4}
⁵⁹ Ni	7.50×10^4	5.60×10^{-11}	1.31×10^{-3}
⁷⁹ Se	6.50×10^4	2.30×10^{-9}	6.22×10^{-2}
⁹⁰ Sr	2.85×10^1	3.30×10^{-8}	2.03×10^3
⁹³ Zr	1.53×10^6	1.37×10^{-9}	1.57×10^{-3}
⁹⁹ Tc	2.13×10^5	3.50×10^{-10}	2.89×10^{-3}
¹⁰⁷ Pd	6.50×10^6	3.80×10^{-11}	1.03×10^{-5}
¹²⁶ Sn	1.00×10^5	5.13×10^{-9}	9.02×10^{-2}
¹³⁵ Cs	2.30×10^6	1.70×10^{-9}	1.30×10^{-3}
¹³⁷ Cs	3.02×10^1	1.20×10^{-8}	6.99×10^2

Notes: ⁹⁰Sr and ²³⁷Cs are considered in the calculations for a reduced canister lifetime - see Subsection 5.2.3.1.

Table A6.1: Conversion factors based on the drinking-water dose per unit activity released directly to a gravel aquifer in the valley of the Rhine. D_{ing} is the committed effective dose equivalent per unit ingestion and includes the short-lived daughter radionuclides omitted from the chains.

APPENDIX 7 GENERIC BIOSPHERE DATA

A large number of the data used for biosphere modelling are generic in the sense that they can be taken as applying to a range of sites and environmental conditions, especially bearing in mind the difficulty of defining conditions in the future (see Subsection 2.4.2). The data are not necessarily appropriate to all conditions and may need to be reviewed before application in specific cases. The following data are used in Kristallin-I and are taken from a database that has been developed to model doses for environmental conditions broadly as might occur in Switzerland.

The following data are presented:

- human diet and habits (Table A7.1);
- agricultural practices (Table A7.1);
- food-chain transfer and distribution factors (Table A7.2);
- half-life and dosimetric data (Table A7.3).

	Parameter	Value	Units	Reference
Basic human requirements and behaviour	food energy intake	4.6×10^6	kJ y^{-1}	[KLOS et al. 1994]
	annual breathing rate	8.4×10^3	$\text{m}^3 \text{y}^{-1}$	[ICRP 1974]
	fluid intake	1.1	$\text{m}^3 \text{y}^{-1}$	[NAGRA 1985]
	fraction of drinking water from well ¹	1.0	-	pessimistic assumption
	occupancy at high airborne dust level ²	0.034	yy^{-1}	assumed value
	occupancy at normal airborne dust level ²	0.966	yy^{-1}	assumed value
Annual consumption and exposure rates	eggs	200	y^{-1}	[KLOS et al. 1994]
	milk	0.3	$\text{m}^3 \text{y}^{-1}$	[KLOS et al. 1994]
	water	0.7	$\text{m}^3 \text{y}^{-1}$	[NAGRA 1985]
	fish	2.0	kg y^{-1}	[KLOS et al. 1994]
	root vegetables	235	kg y^{-1}	[KLOS et al. 1994]
	grain	148	kg y^{-1}	[KLOS et al. 1994]
	green vegetables	62	kg y^{-1}	[KLOS et al. 1994]
	meat	95	kg y^{-1}	[KLOS et al. 1994]
	normal airborne dust loading ²	5.0×10^{-8}	kg m^{-3}	[LINSLEY 1978]
high airborne dust loading ²	1.0×10^{-5}	kg m^{-3}	[LINSLEY 1978]	
Cattle	cattle stocking density	2.0×10^{-4}	m^{-2}	[KLOS et al. 1994]
	daily water consumption	0.03	$\text{m}^3 \text{day}^{-1}$	[KLOS et al. 1994]
	daily pasture consumption (dry weight)	20	kg day^{-1}	[KLOS et al. 1994]
	fraction of drinking water obtained from well	1.0	-	pessimistic assumption
Poultry	daily water consumption	2.0×10^{-4}	$\text{m}^3 \text{day}^{-1}$	[KLOS et al. 1994]
	daily grain consumption	0.07	kg day^{-1}	[KLOS et al. 1994]
	fraction of drinking water obtained from well	1.0	-	pessimistic assumption
Crop yields ³	grain	0.4	kg m^{-2}	[KLOS et al. 1994]
	green vegetables	3.0	kg m^{-2}	[KLOS et al. 1994]
	root vegetables	3.5	kg m^{-2}	[KLOS et al. 1994]
	pasture (dry weight)	1.66	kg m^{-2}	[KLOS et al. 1994]
Crop spray-irrigation interception factors	grain	1.0	$\text{m}^2 \text{kg}^{-2}$	[BÖHRINGER et al. 1986]
	green vegetables	0.13	$\text{m}^2 \text{kg}^{-2}$	[BÖHRINGER et al. 1986]
	root vegetables	0.11	$\text{m}^2 \text{kg}^{-2}$	[BÖHRINGER et al. 1986]
	pasture	0.24	$\text{m}^2 \text{kg}^{-2}$	[BÖHRINGER et al. 1986]
Fractional weight of soil consumed with crop	grain (human)	9.0×10^{-5}	kg kg^{-1}	[KLOS et al. 1994]
	green vegetables (human)	2.0×10^{-4}	kg kg^{-1}	[KLOS et al. 1994]
	root vegetables (human)	0.0	kg kg^{-1}	[KLOS et al. 1994]
	pasture (wet soil/dry pasture - cattle)	1.0×10^{-2}	kg kg^{-1}	[KLOS et al. 1994]

Notes:

- ¹ *Water could also be taken from the river Rhine, but the concentrations would be higher in the aquifer. The water is **not** assumed to be filtered to remove suspended particles.*
- ² *High airborne dust levels are associated with occupational activities such as ploughing. In deriving this value, 12 days per year is assumed for occupancy at the increased dust levels, the remainder of the time is assumed to be at lower dust levels found under normal conditions.*
- ³ *Yields here refer to the annual weight of produce of each crop type. Harvesting rates are once per year for all crops for human consumption. The cropping rate of pasture is determined by the cattle stocking density and the consumption rate, as well as the pasture growth rate*

Table A7.1: (Previous page). Parameter values characterising the human behaviour and practices in the Reference-Case biosphere.

Parameter	Units	Ni	Se	Zr	Tc	Pd	Sn
distribution factor for fish	$(\text{Bq kg}^{-1}) (\text{Bq m}^{-3})^{-1}$	0.1	0.2	0.2	1.5×10^{-2}	0.1	3.0
distribution factor for meat	$(\text{Bq kg}^{-1}) (\text{Bq day}^{-1})^{-1}$	2.0×10^{-3}	0.32	2.0×10^{-2}	10^{-3}	2.0×10^{-3}	4.0×10^{-4}
distribution factor for milk	$(\text{Bq kg}^{-1}) (\text{Bq day}^{-1})^{-1}$	1.0×10^{-3}	4.0×10^{-3}	3.0×10^{-5}	2.5×10^{-2}	1.0×10^{-3}	1.2×10^{-3}
distribution factor for eggs	$(\text{Bq egg}^{-1}) (\text{Bq day}^{-1})^{-1}$	5.2×10^{-2}	0.48	1.0×10^{-4}	9.8×10^{-2}	5.2×10^{-2}	4.6×10^{-2}
transfer factor for pasture	$(\text{Bq kg}^{-1} \text{ fresh weight}) (\text{Bq kg}^{-1} \text{ dry soil})^{-1}$	5.0×10^{-2}	0.25	2.0×10^{-2}	2.5	5.0×10^{-2}	0.1
transfer factor for grain	$(\text{Bq kg}^{-1} \text{ fresh weight}) (\text{Bq kg}^{-1} \text{ dry soil})^{-1}$	4.2×10^{-2}	3.6×10^{-2}	2.7×10^{-2}	4.5	$5.0 \times 10^{-2} \dagger$	0.36
transfer factor for green vegetables	$(\text{Bq kg}^{-1} \text{ fresh weight}) (\text{Bq kg}^{-1} \text{ dry soil})^{-1}$	1.7×10^{-2}	3.5×10^{-2}	3.4×10^{-3}	1.0	1.7×10^{-2}	4.6×10^{-2}
transfer factor for root vegetables	$(\text{Bq kg}^{-1} \text{ fresh weight}) (\text{Bq kg}^{-1} \text{ dry soil})^{-1}$	1.6×10^{-2}	3.8×10^{-2}	2.1×10^{-3}	1.5	1.6×10^{-2}	6.0×10^{-2}
Parameter	Units	Cs	Pb	Po	Ra	Ac	Th
distribution factor for fish	$(\text{Bq kg}^{-1}) (\text{Bq m}^{-3})^{-1}$	1.0	0.1	0.5 $\dagger\dagger$	2.5×10^{-2}	1.0×10^{-7}	3.0×10^{-2}
distribution factor for meat	$(\text{Bq kg}^{-1}) (\text{Bq day}^{-1})^{-1}$	2.6×10^{-2}	4.0×10^{-4}	$4.0 \times 10^{-3*}$	9.0×10^{-4}	6.0×10^{-2}	2.0×10^{-4}
distribution factor for milk	$(\text{Bq kg}^{-1}) (\text{Bq day}^{-1})^{-1}$	7.1×10^{-3}	2.6×10^{-4}	$3.0 \times 10^{-4*}$	4.0×10^{-4}	5.0×10^{-6}	5.0×10^{-6}
distribution factor for eggs	$(\text{Bq egg}^{-1}) (\text{Bq day}^{-1})^{-1}$	2.5×10^{-2}	4.6×10^{-2}	$5.0 \times 10^{-5**}$	4.6×10^{-2}	5.0×10^{-2}	5.0×10^{-2}
transfer factor for pasture	$(\text{Bq kg}^{-1} \text{ fresh weight}) (\text{Bq kg}^{-1} \text{ dry soil})^{-1}$	2.0×10^{-2}	4.5×10^{-3}	$2.0 \times 10^{-4} \ddagger$	4.0×10^{-3}	5.0×10^{-4}	9.5×10^{-4}
transfer factor for grain	$(\text{Bq kg}^{-1} \text{ crop weight}) (\text{Bq kg}^{-1} \text{ dry soil})^{-1}$	1.3×10^{-2}	1.7×10^{-2}	$2.0 \times 10^{-4} \ddagger$	1.4×10^{-2}	1.8×10^{-4}	7.1×10^{-4}
transfer factor for green vegetables	$(\text{Bq kg}^{-1} \text{ fresh weight}) (\text{Bq kg}^{-1} \text{ dry soil})^{-1}$	1.3×10^{-2}	1.8×10^{-3}	$2.0 \times 10^{-4} \ddagger$	1.6×10^{-3}	2.0×10^{-4}	3.8×10^{-4}
transfer factor for root vegetables	$(\text{Bq kg}^{-1} \text{ fresh weight}) (\text{Bq kg}^{-1} \text{ dry soil})^{-1}$	8.0×10^{-3}	2.7×10^{-3}	$2.0 \times 10^{-4} \ddagger$	3.0×10^{-3}	3.0×10^{-4}	5.7×10^{-4}
Parameter	Units	Pa	U	Np	Pu	Am	Cm
distribution factor for fish	$(\text{Bq kg}^{-1}) (\text{Bq m}^{-3})^{-1}$	1.0×10^{-2}	2.0×10^{-3}	1.0×10^{-2}	5.0×10^{-3}	2.5×10^{-2}	2.5×10^{-2}
distribution factor for meat	$(\text{Bq kg}^{-1}) (\text{Bq day}^{-1})^{-1}$	8.0×10^{-2}	3.4×10^{-4}	2.0×10^{-4}	2.0×10^{-6}	2.0×10^{-4}	2.0×10^{-4}
distribution factor for milk	$(\text{Bq kg}^{-1}) (\text{Bq day}^{-1})^{-1}$	5.0×10^{-6}	3.7×10^{-4}	5.0×10^{-6}	1.0×10^{-7}	4.1×10^{-7}	5.0×10^{-6}
distribution factor for eggs	$(\text{Bq egg}^{-1}) (\text{Bq day}^{-1})^{-1}$	5.0×10^{-2}	5.1×10^{-2}	4.4×10^{-4}	3.9×10^{-4}	4.4×10^{-4}	4.4×10^{-4}
transfer factor for pasture	$(\text{Bq kg}^{-1} \text{ fresh weight}) (\text{Bq kg}^{-1} \text{ dry soil})^{-1}$	9.4×10^{-3}	9.5×10^{-4}	$2.4 \times 10^{-3} \dagger$	$9.5 \times 10^{-5} \dagger$	5.0×10^{-4}	5.0×10^{-4}
transfer factor for grain	$(\text{Bq kg}^{-1} \text{ fresh weight}) (\text{Bq kg}^{-1} \text{ dry soil})^{-1}$	1.7×10^{-2}	1.3×10^{-3}	$1.5 \times 10^{-2} \dagger$	1.8×10^{-3}	2.2×10^{-5}	1.1×10^{-3}
transfer factor for green vegetables	$(\text{Bq kg}^{-1} \text{ fresh weight}) (\text{Bq kg}^{-1} \text{ dry soil})^{-1}$	2.7×10^{-2}	3.8×10^{-4}	$2.7 \times 10^{-3} \dagger$	1.4×10^{-4}	2.0×10^{-4}	2.0×10^{-4}
transfer factor for root vegetables	$(\text{Bq kg}^{-1} \text{ fresh weight}) (\text{Bq kg}^{-1} \text{ dry soil})^{-1}$	6.0×10^{-2}	5.7×10^{-4}	$6.0 \times 10^{-2} \dagger$	3.0×10^{-4}	3.0×10^{-4}	3.0×10^{-4}

Notes: All data values taken from Project Gewähr, 1985 except:

† From GROGAN (1985);

‡ From IAEA (1982);

* From NG (1982);

** From BAKER et al. (1976);

†† From NUREG (1977).

Table A7.2: Uptake and accumulation factors in the TAME exposure pathway model.

Radio-nuclide	Half-life [years]*	Dose per unit intake on ingestion [Sv Bq ⁻¹] [†]	Dose per unit intake on inhalation [Sv Bq ⁻¹] [†]	γ-ray exposure factor [Sv (Bq m ⁻³) ⁻¹ year ⁻¹] [‡]
⁵⁹ Ni	7.50×10 ⁴	5.6×10 ⁻¹¹	3.6×10 ⁻¹⁰	-
⁷⁹ Se	6.50×10 ⁴	2.3×10 ⁻⁹	2.4×10 ⁻⁹	-
⁹³ Zr	1.53×10 ⁶	4.2×10 ⁻¹⁰	2.2×10 ⁻⁸	-
⁹⁹ Tc	2.13×10 ⁵	3.5×10 ⁻¹⁰	2.0×10 ⁻⁹	-
¹⁰⁷ Pd	6.50×10 ⁶	3.8×10 ⁻¹¹	3.4×10 ⁻⁹	-
¹²⁶ Sn	1.00×10 ⁵	5.1×10 ⁻⁹	2.4×10 ⁻⁸	2.7×10 ⁻¹¹
¹³⁵ Cs	2.30×10 ⁶	1.7×10 ⁻⁹	1.1×10 ⁻⁹	-
²⁴⁰ Pu	6.54×10 ³	9.5×10 ⁻⁷	1.1×10 ⁻⁴	-
²³⁶ U	2.34×10 ⁷	6.6×10 ⁻⁸	3.3×10 ⁻⁵	-
²³² Th	1.40×10 ¹⁰	7.4×10 ⁻⁷	3.1×10 ⁻⁴	1.3×10 ⁻¹³
²²⁸ Ra	5.75	3.3×10 ⁻⁷	1.1×10 ⁻⁶	-
²²⁸ Th	1.91	1.9×10 ⁻⁷	8.2×10 ⁻⁵	1.8 10 ⁻¹²
²⁴³ Am	7.38×10 ³	9.8×10 ⁻⁷	1.2×10 ⁻⁴	2.6×10 ⁻¹¹
²³⁹ Pu	2.41×10 ⁴	9.5×10 ⁻⁷	1.1×10 ⁻⁴	5.8×10 ⁻¹⁴
²³⁵ U	7.04×10 ⁸	6.6×10 ⁻⁸	3.3×10 ⁻⁵	9.5×10 ⁻¹¹
²³¹ Pa	3.28×10 ⁴	2.9×10 ⁻⁶	2.3×10 ⁻⁴	1.6×10 ⁻¹¹
²²⁷ Ac	2.18×10 ¹	4.0×10 ⁻⁶	3.5×10 ⁻⁴	-
²⁴⁵ Cm	8.50×10 ³	1.0×10 ⁻⁶	1.2×10 ⁻⁴	2.8×10 ⁻¹¹
²⁴¹ Pu	1.44×10 ¹	1.9×10 ⁻⁸	2.2×10 ⁻⁶	-
²⁴¹ Am	4.32×10 ²	9.8 10 ⁻⁷	1.2×10 ⁻⁴	9.5×10 ⁻¹²
²³⁷ Np	2.14×10 ⁶	1.1×10 ⁻⁶	1.3×10 ⁻⁴	1.6×10 ⁻¹¹
²³³ U	1.59×10 ⁵	7.1×10 ⁻⁸	3.6×10 ⁻⁵	5.3×10 ⁻¹³
²²⁹ Th	7.34×10 ³	1.1×10 ⁻⁶	4.7×10 ⁻⁴	1.8×10 ⁻¹¹
²⁴⁶ Cm	4.73×10 ³	1.0×10 ⁻⁶	1.2×10 ⁻⁴	-
²⁴² Pu	3.76×10 ⁵	9.0×10 ⁻⁷	1.1×10 ⁻⁴	-
²³⁸ U	4.47×10 ⁹	6.7×10 ⁻⁸	3.1×10 ⁻⁵	-
²³⁴ U	2.45×10 ⁵	7.0×10 ⁻⁸	3.5×10 ⁻⁵	2.7×10 ⁻¹³
²³⁰ Th	7.70×10 ⁴	1.4×10 ⁻⁷	7.0×10 ⁻⁵	3.0×10 ⁻¹³
²²⁶ Ra	1.60×10 ³	3.0×10 ⁻⁷	2.1×10 ⁻⁶	5.5×10 ⁻¹²
²¹⁰ Pb	2.23×10 ¹	1.4×10 ⁻⁶	3.5×10 ⁻⁶	6.2×10 ⁻¹³
²¹⁰ Po	3.79×10 ⁻¹	4.3×10 ⁻⁷	2.2×10 ⁻⁶	5.5×10 ⁻¹⁴

Notes: * Data taken from ALDER & MCGINNES (1994), except ²³⁰Th, value taken from NAGRA (1985) (See Chapter 3).

† Data taken from NRPB (1987).

‡ Data taken from SVENSSON (1979).

The decay product of ⁹³Zr has not been included in these calculations. This omission, though undesirable, would increase the maximum dose from ⁹³Zr by less than a factor of 2.

Table A7.3: Radionuclide half-life and dosimetric data.

APPENDIX 8 SIMPLIFIED ANALYTICAL SOLUTIONS FOR GEOSPHERE TRANSPORT

The governing equations of the dual-porosity model for geosphere transport are presented in Subsection 5.3.2 and their solution discussed in Subsection 5.3.3. The full, time-dependent equations are solved numerically using codes RANCHMD (linear sorption) and RANCHMDNL (non-linear sorption). However, analytical solutions of special cases of the governing equations are also available. Because of their transparency, these are useful in interpreting the more general numerical solutions and exploring the sensitivity of the system to parameter variations. Two such solutions are:

- a steady-state solution, applicable where the release from the near field is slowly varying with respect to the transit time through the geosphere and radioactive ingrowth is negligible;
- equilibrium between radioactive decay and ingrowth of decay-chain daughters, applicable where the transit time through the geosphere is sufficiently long with respect to half-life for equilibrium to be attained.

Steady-State Solution

An analytical steady-state solution has been derived for the case of linear sorption on matrix pores (and colloids) (SMITH 1993b). If the boundary condition given by Equation 5.3.7 is replaced by:

$$\lim_{z \rightarrow \infty} C_f^{(i)}(z, t) = 0 \quad \forall t \quad (\text{A8.1})$$

and radioactive ingrowth is not considered, then:

$$\frac{F_{out}^{(i)}}{F_{in}^{(i)}} = \exp \left\{ \frac{Pe}{2} \left[1 - \sqrt{1 + \frac{4}{Pe} \frac{LR_{eff}^{(i)}}{u'} \lambda^{(i)}} \right] \right\}. \quad (\text{A8.2})$$

$Pe = L/a_L$ is the Peclet number and $R_{eff}^{(i)}$ [-] is an effective retardation factor, incorporating the effects of matrix diffusion, such that:

$$\frac{R_{eff}^{(i)}}{R_f^{(i)}} = 1 + \varepsilon_p \frac{R_p^{(i)}}{R_f^{(i)}} \begin{cases} \frac{1}{b\sqrt{\mu}} \tanh[y_p \sqrt{\mu}] & \text{planar geometry} \\ \frac{2}{r_0 \sqrt{\mu}} \left[\frac{I_1(r_p \sqrt{\mu}) K_1(r_0 \sqrt{\mu}) - I_1(r_0 \sqrt{\mu}) K_1(r_p \sqrt{\mu})}{I_1(r_p \sqrt{\mu}) K_0(r_0 \sqrt{\mu}) + I_0(r_0 \sqrt{\mu}) K_1(r_p \sqrt{\mu})} \right] & \text{cylindrical geometry} \end{cases} \quad (\text{A8.3})$$

where:

$$\mu = \frac{\lambda^{(i)} R_p^{(i)}}{D_p}. \quad (\text{A8.4})$$

$R_f^{(i)}$, u' and $R_p^{(i)}$ are given by Equations 5.3.15, 5.3.16 and 5.3.12. $I_n(\zeta)$ and $K_n(\zeta)$ are n th order modified Bessel functions, respectively of the first and second kinds.

A transit time $T^{(i)}$ for a radionuclide through the geosphere is defined from this steady-state solution as

$$T^{(i)} = \frac{LR_{eff}^{(i)}}{u'}. \quad (\text{A8.5})$$

From Equation A8.2, $F_{out}^{(i)} \cong F_{in}^{(i)}$ when $\lambda^{(i)}T^{(i)} \ll 1$, i.e. when the transit time through the geosphere layer is very much less than the radionuclide half-life. When this condition is fulfilled, decay is insignificant during passage through the geosphere and the radionuclide flux exiting the layer is the same as that entering. The analytical solution is appropriate when the release from the near field is of long duration with respect to the radionuclide half-life, and may be considered to give a conservative upper bound to the performance of the geosphere barrier (assuming negligible effects resulting from the difference in downstream boundary conditions given by Equations 5.3.7 and A8.1).

Radioactive Equilibrium

Provided that the amount of the radionuclide stored within a channel is small compared to that stored in the adjacent matrix, the concentration within the channel (and, referring to Equation 5.3.8, the flux through the channel), will be determined by the equilibrium concentration (in solution) in the matrix. In the matrix, radioactive equilibrium is defined to exist where the following condition is fulfilled:

$$R_p^{(i)} C_p^{(i)} \lambda^{(i)} = R_p^{(i-1)} C_p^{(i-1)} \lambda^{(i-1)} \quad (\text{A8.6})$$

or

$$\frac{\varepsilon_p C_p^{(i)} + \rho(1 - \varepsilon_p) S_p^{(i)}}{T_{1/2}^{(i)}} = \frac{\varepsilon_p C_p^{(i-1)} + \rho(1 - \varepsilon_p) S_p^{(i-1)}}{T_{1/2}^{(i-1)}}$$

The numerators on the left and right-hand sides represent respectively the amount of radionuclide i and the amount of its parent radionuclide $i - 1$ in a unit volume of the matrix. $S_p^{(i)}$ [mol kg⁻¹] and $S_p^{(i-1)}$ [mol kg⁻¹] are the amounts sorbed onto a unit mass of solid material and $T_{1/2}^{(i)}$ and $T_{1/2}^{(i-1)}$ are the half-lives.

$$S_p^{(i)} = K_p^{(i)} C_p^{(i)}. \quad (\text{A8.7})$$

The fluxes from the geosphere of the radionuclide and its parent are related by the equation:

$$YF_{out}^{(i)} = F_{out}^{(i-1)}, \quad (\text{A8.8})$$

where:

$$Y = \frac{T_{1/2}^{(i-1)} [\epsilon_p + (1 - \epsilon_p) \rho K_d^{(i)}]}{T_{1/2}^{(i)} [\epsilon_p + (1 - \epsilon_p) \rho K_d^{(i-1)}]} \quad [-]. \quad (\text{A8.9})$$

Defining a further dimensionless quantity:

$$\Psi = \frac{\left(YF_{out}^{(i)} / F_{out}^{(i-1)} \right) - 1}{\left(YF_{in}^{(i)} / F_{out}^{(i-1)} \right) - 1} \quad [-]. \quad (\text{A8.10})$$

$\Psi = 0$ when the radionuclide is in radioactive equilibrium with its parent on exiting the geosphere. This will occur when the transit time is sufficiently long for the initial inventory of the radionuclide to decay to insignificance with respect to ingrowth from the parent. For small transit times, where there is insufficient time for significant ingrowth to occur and the radionuclide decays little during passage through the geosphere, $\Psi \rightarrow 1$.

APPENDIX 9 THE EFFECT OF A NON-UNIFORM FLOW AROUND THE BENTONITE

The text of this appendix is adapted from an unpublished communication from Dr. Peter Robinson, Intera Information Technologies, Henley-on-Thames, U.K.

This appendix demonstrates, for a simplified example case, that non-uniformity in the groundwater flow around the outer-boundary of the bentonite in the near-field model (see Subsection 5.2.1.2) gives only a second order effect on the total diffusive flux from the near field. The notation of Section 5.2 is followed.

The effect of perturbing the groundwater flowrate, Q , by the introduction of some dependence on the angle θ is considered. The following simplifications are made:

- a single, solubility-limited element is considered;
- steady-state conditions are assumed;
- retardation due to sorption in the bentonite is neglected;
- radioactive decay is neglected.

With these simplifications, from Equation 5.2.10, the steady-state diffusion equation is simply:

$$\frac{1}{r} \frac{\partial}{\partial r} \left(r \frac{\partial C}{\partial r} \right) + \frac{1}{r^2} \frac{\partial^2 C}{\partial \theta^2} = 0 \quad (\text{A9.1})$$

and, from Equations 5.2.13 and 5.2.14, the boundary conditions are:

$$C(r_a, \theta) = S_E \quad (\text{A9.2})$$

and

$$\left[Q(\theta)C + A_{ben}D_e \frac{\partial C}{\partial r} \right] \Bigg|_{r=r_b} = 0, \quad (\text{A9.3})$$

where

$$Q(\theta) = Q_0(1 + \varepsilon p(\theta)). \quad (\text{A9.4})$$

Here, ε is small and the integral of perturbation, $p(\theta)$, is zero, so that the total flow is unchanged from the original case.

To solve these equations, C can be written as

$$C = C_0 + \varepsilon C_1 + \varepsilon^2 C_2 + \dots \quad (\text{A9.5})$$

Each individual term must obey the diffusion equation and the boundary conditions become:

$$C_0(r_a, \theta) = S_E, \quad (\text{A9.6})$$

$$C_j(r_a, \theta) = 0 \quad \text{for } j > 0 \quad (\text{A9.7})$$

and:

$$\left[Q_0 C_0 + A_{ben} D_e \frac{\partial C_0}{\partial r} \right] \Bigg|_{r=r_b} = 0, \quad (\text{A9.8})$$

$$\left[Q_0 C_j + A_{ben} D_e \frac{\partial C_j}{\partial r} \right] \Bigg|_{r=r_b} = -Q_0 C_{j-1} p(\theta) \quad \text{for } j > 0. \quad (\text{A9.9})$$

For the purposes of calculating the total flux, it is the integral of $\frac{\partial C}{\partial r}$ around the outer boundary which is of relevance. Thus only \bar{C}_j , denoting the average over θ of C_j , need be considered. Noting that C_0 is independent of θ and that $p(\theta)$ integrates to zero:

$$\bar{C}_0(r_a) = S_E, \quad (\text{A9.10})$$

$$\bar{C}_1(r_a) = 0 \quad (\text{A9.11})$$

and

$$\left[Q_0 \bar{C}_0 + A_{ben} D_e \frac{\partial \bar{C}_0}{\partial r} \right] \Bigg|_{r=r_b} = 0, \quad (\text{A9.12})$$

$$\left[Q_0 \bar{C}_1 + A_{ben} D_e \frac{\partial \bar{C}_1}{\partial r} \right] \Bigg|_{r=r_b} = 0. \quad (\text{A9.13})$$

From this, it is clear that C_0 is the original solution (no dependence on θ) and that \bar{C}_1 is identical to zero. Note that C_1 itself is non-zero and so \bar{C}_2 will be non-zero. Thus the first order perturbation in Q has caused only a second order perturbation in C and hence in the total near-field flux.